UNIVERSIDADE DE LISBOA

FACULDADE DE FARMÁCIA

DESIGN AND SYNTHESIS OF SMALL MOLECULE MODULATORS OF P53

CARLOS JORGE AZEVEDO COSTA RIBEIRO

Orientadores: Doutora Maria Manuel Duque Vieira Marques dos Santos

Prof. Doutor Rui Ferreira Alves Moreira

Prof.ª Doutora Cecília Maria Pereira Rodrigues

Tese especialmente elaborada para obtenção do grau de Doutor em Farmácia, especialidade de Química Farmacêutica e Terapêutica

2015

UNIVERSIDADE DE LISBOA

FACULDADE DE FARMÁCIA

DESIGN AND SYNTHESIS OF SMALL MOLECULE MODULATORS OF P53

CARLOS JORGE AZEVEDO COSTA RIBEIRO

Orientadores: Doutora Maria Manuel Duque Vieira Marques dos Santos
Prof. Doutor Rui Ferreira Alves Moreira
Prof.ª Doutora Cecília Maria Pereira Rodrigues

Tese especialmente elaborada para obtenção do grau de Doutor em Farmácia, especialidade de Química Farmacêutica e Terapêutica

JÚRI:

PRESIDENTE: Doutora Matilde da Luz dos Santos Duque da Fonseca e Castro

VOGAIS:

- Doutor Jorge António Ribeiro Salvador
- Doutora Maria Emília da Silva Pereira de Sousa
- Doutora Maria Alexandra Núncio de Carvalho Ramos Fernandes
- Doutora Maria Matilde Soares Duarte Marques
- Doutora Rita Alexandra do Nascimento Cardoso Guedes
- Doutora Joana São José Dias Amaral
- Doutora Maria Manuel Duque Vieira Marques dos Santos

Este trabalho foi financiado pela Fundação para a Ciência e a Tecnologia através da bolsa de doutoramento SFRH/BD/69258/2010 e dos projectos PTDC/QUI-QUI/111664/2009, PTDC/SAU-FAR/110848/2009, PTDC/SAU-ORG/119842/2010 e Pest-OE/SAU/UI4013/2014.

2015

List of Publications

- In the Scope of the PhD Thesis:

1. C. J. A. Ribeiro, R. Moreira, M. M. M. Santos, Synthesis of a Spiroisoxazoline Oxindole by 1,3-Dipolar Cycloaddition. In: Comprehensive Organic Chemistry Experiments for the Laboratory Classroom Book, Royal Society of Chemistry (accepted).
2. J. J. Badillo, C. J. A. Ribeiro, M. M. Olmstead, A. K. Franz, Titanium(IV)-Catalyzed Stereoselective Synthesis of Spirooxindole-1-Pyrrolines. *Org. Lett.* **2014**, 16: p. 6270−6273
3. C. J. A. Ribeiro, J. D. Amaral, C. M. P. Rodrigues, R. Moreira, M. M. M. Santos, Synthesis and Evaluation of Spiroisoxazoline Oxindoles as Anticancer Agents. *Bioorg. Med. Chem*. **2014**, *22*(1): p. 77−84
4. C. J. A. Ribeiro, S. P. Kumar, R. Moreira, M. M. M. Santos, Efficient Synthesis of Spiroisoxazoline Oxindoles. *Tetrahedron Lett.* **2012**, *53*(3): p. 281−284.

- Other publications:

1. C. J. A. Ribeiro, S. P. Kumar, J. Gut, L. M. Gonçalves, P. J. Rosenthal, R. Moreira, M. M. M. Santos, Squaric Acid/4-Aminoquinoline Conjugates: Novel Potent Antiplasmodial Agents. *Eur. J. Med. Chem.* **2013**, 69: p. 365−72.

Oral Communications in Scientific Conferences

1. C. J. A. Ribeiro, J. D. Amaral, C. M. P. Rodrigues, R. Moreira, M. M. M. Santos. "Synthesis and Biological Evaluation of Spiroisoxazoline and Spirooxadiazoline Oxindoles as Anticancer Agents". Flash Poster Presentation. EFMC-YMCS 2014. 1st EFMC Young Medicinal Chemist Symposium. Lisbon, Portugal. 12/09/2014.
2. C. J. A. Ribeiro, J. D. Amaral, C. M. P. Rodrigues, R. Moreira, M. M. M. Santos. "Synthesis and Biological Evaluation of Spiroisoxazoline Oxindoles as Anticancer Agents". 4rd Portuguese Young Chemists Meeting. Coimbra, Portugal. 29-30/04-01/05/2014.
3. C. J. A. Ribeiro, J. D. Amaral, C. M. P. Rodrigues, R. Moreira, M. M. M. Santos. "Spiroisoxazoline Oxindoles: a New Class of p53-MDM2 Interaction Inhibitors". 4th iMed.UL Post-Graduate Students Meeting. Lisbon, Portugal. 20/12/2012.
4. C. J. A. Ribeiro. "Synthesis and Biological Evaluation of New Spiroisoxazoline Oxindoles as Potential Anticancer Agents". Poster Selected for Oral Presentation. 32nd

Edition of the European School of Medicinal Chemistry (ESMEC). Urbino, Italy. 2-7/07/2012.

5. C. J. A. Ribeiro, R. Moreira, M. M. M. Santos. "Efficient Synthesis of New Spiroisoxazoline Oxindoles". 3rd Portuguese Young Chemists Meeting. Porto, Portugal. 9-11/05/2012.

6. C. J. A. Ribeiro, R. Moreira, M. M. M. Santos. "Structural Characterization of a Novel Spiroisoxazoline Oxindole". Flash Presentation. Modern Methods of Structure Elucidation (MMSE). Lisbon, Portugal. 14-18/11/2011.

Poster Communications in Scientific Conferences

1. C. J. A. Ribeiro, J. D. Amaral, C. M. P. Rodrigues, R. Moreira, M. M. M. Santos. "Synthesis and Biological Evaluation of Spiroisoxazoline and Spirooxadiazoline Oxindoles as Anticancer Agents". EFMC-YMCS 2014. 1st EFMC Young Medicinal Chemist Symposium. Lisbon, Portugal. 12/09/2014.

2. C. J. A. Ribeiro, J. D. Amaral, C. M. P. Rodrigues, R. Moreira, M. M. M. Santos. "Spiroisoxazoline and Spirooxadiazoline Oxindoles as Anticancer Agents". EFMC-ISMC 2014, 23nd International Symposium on Medicinal Chemistry. Lisbon, Portugal. 07-11/09/2014.

3. C. J. A. Ribeiro, J. D. Amaral, C. M. P. Rodrigues, R. Moreira, M. M. M. Santos. "Spiroisoxazoline Oxindoles: Novel Small-Molecule Inhibitors of the p53-MDM2 Interaction". COST Action CM1106: Chemical Approaches to Targeting Drug Resistance in Cancer Stem Cells. 2nd Working Group Meeting. Warsaw, Poland. 19-20/09/2013.

4. C. J. A. Ribeiro, S. P. Kumar, J. Gut, L. M. Gonçalves, P. J. Rosenthal, R. Moreira, M. M. M. Santos. "Synthesis of novel antiplasmodial agents containing squaramide and 4-amino-7-chloroquinoline moieties". 10th Portuguese National Meeting of Organic Chemistry/1st Portuguese-Brazilian Organic Chemistry Symposium. Lisbon, Portugal. 4-6/09/2013.

5. C. J. A. Ribeiro, J. D. Amaral, C. M. P. Rodrigues, R. Moreira, M. M. M. Santos. "Spiroisoxazoline Oxindoles: New p53-MDM2 Interaction Inhibitors". 4th Frontiers in Medicinal Chemistry. San Francisco, USA. 23-26/06/2013.

6. C. J. A. Ribeiro, J. D. Amaral, C. M. P. Rodrigues, R. Moreira, M. M. M. Santos. "Evaluation of New Spiro-Oxindoles as Anticancer Agents". 3rd Portuguese Meeting on Medicinal Chemistry. Aveiro, Portugal. 28-30/11/2012.

7. C. J. A. Ribeiro, J. D. Amaral, C. M. P. Rodrigues, R. Moreira, M. M. M. Santos. "Synthesis and Biological Evaluation of New Spiroisoxazoline Oxindoles as Potential

Anticancer Agents". EFMC-ISMC 2012, 22nd International Symposium on Medicinal Chemistry. Berlin, Germany. 2-6/09/2012.

8. C. J. A. Ribeiro. "Synthesis and Biological Evaluation of New Spiroisoxazoline Oxindoles as Potential Anticancer Agents". 32nd Edition of the European School of Medicinal Chemistry (ESMEC). Urbino, Italy. 2-7/07/2012.
9. C. J. A. Ribeiro, R. Moreira, M. M. M. Santos, "Simple and Efficient Synthesis of Spiroisoxazoline Oxindoles, Using Zinc as Dehydrochlorinating Agent". 3rd iMed.UL Post-Graduate Students Meeting. Lisbon, Portugal. 11/12/2011.
10. C. J. A. Ribeiro, R. Moreira, M. M. M. Santos. "Synthesis of Spiroisoxazoline oxindoles from Methyleneindolinones and Nitrile oxides". XXII National Meeting of SPQ - 100 years of Chemistry in Portugal, Braga, Portugal. 03-06/07/2011.

Table of Contents

Chapter 1. State of the Art **1**

1.1. p53 activation in Health and Disease ... 3
1.2. Reactivation of p53 as a Therapeutic Strategy ... 4
1.2.1. Targeting p53-MDM2 Interaction ... 5
1.2.1.1. Cis-imidazolines (Nutlins). Road to RG7112 ... 8
1.2.1.2. Spirooxindoles ... 10
1.2.1.2a. Spiropyrrolidine Oxindoles. Road to MI-77301 ... 10
1.2.1.2b. Spirothiazolidine Oxindoles ... 13
1.2.1.3. Pyrrolidine-2-carboxamides. Road to RG7388. ... 15
1.2.1.4. Piperidinones and Morpholinones. Road to AMG232. ... 16
1.2.1.5. Other MDM2 Inhibitors in Clinical Trials ... 19
1.2.1.6. Benzodiazepinediones ... 19
1.2.1.7. Isoindolinones ... 21
1.2.1.8. Chromenotriazolopyrimidines ... 23
1.2.1.9. 3-Imidazoyl Indoles and Other Indolyl Derivatives ... 25
1.2.1.10. Other Compounds ... 26
1.2.2. Inhibition of E3 Ligase Activity of MDM2 ... 28
1.2.3. MDMX and Dual MDM2/MDMX Inhibitors ... 29
1.2.4. Targeting Upstream Regulators ... 31
1.2.5. Sirtuins Inhibitors ... 33
1.2.6. S100B Inhibitors ... 34
1.2.7. p53-Targeting Compounds ... 35
1.2.8. Mutant p53 Reactivation ... 35
1.3. Concluding Remarks ... 38

Chapter 2. Scope and General Goals **39**

2.1. Synthesis of Spirooxindole Derivatives ... 41
2.2. Biological Studies ... 42
2.3. Stability Assessment ... 43
2.4. Thesis Layout ... 43

Chapter 3. Spiroisoxazoline Oxindoles: Synthetic Methodology Optimization **45**

3.1. Introduction ... 47
3.2. Synthesis of Intermediates ... 48
3.3. Synthesis of Spiroisoxazoline Oxindoles and Optimization ... 49
3.4. Regio and Stereoselectivity Considerations ... 52
3.5. Concluding Remarks ... 55

Chapter 4. Spiroisoxazoline Oxindoles: Increasing Synthetic Scope and Biological Evaluation 57

4.1. Introduction 59
4.2. Synthesis of Intermediates 61
4.3. Synthesis of Spiroisoxazoline Oxindole Derivatives 62
4.4. Regio and Stereoselectivity Considerations 64
4.5. Biological Studies 64
4.5.1. Assessment of Cell Viability 64
4.5.2. Evaluation of Compounds Ability to Block the Intracellular p53-MDM2 Interaction 66
4.5.3. Evaluation of Apoptosis 68
4.6. Stability 68
4.7. Concluding Remarks 69

Chapter 5. Spiroisoxazoline Oxindoles: Enantioselective Approach 71

5.1. Enatioselective Approaches towards Spiroisoxazoline Oxindoles 73
5.1.1. Introduction 73
5.1.2. Synthesis of intermediate **121n**. 74
5.1.3. Attempts to Enanteoselectively Synthesize Compound **119ac** 75
5.2. Enatioselective Approaches towards Spiropyrroline Oxindoles 81
5.2.1. Introduction 81
5.2.2. Synthesis of Intermediate **121p**. 81
5.2.3. Attempts to Enantioselectively Synthesize compound **163** 82
5.3. Concluding Remarks 84

Chapter 6. Spirooxadiazoline Oxindoles: Synthesis and Biological Evaluation 85

6.1. Introduction 87
6.2. Synthesis of Intermediates 88
6.3. Synthesis of Spiro[indoline-3,5'-[1,2,4]oxadiazoline]-2-ones 89
6.4. Biological Studies 90
6.4.1. Assessment of Cell Viability 90
6.4.2. Evaluation of Compounds Ability to Block the Intracellular p53-MDM2 Interaction 93
6.4.3. Evaluation of Apoptosis 94
6.5. Stability 95
6.6. Concluding Remarks 95

Chapter 7. Spirotriazoline Oxindoles: Synthesis and Biological Evaluation **97**

7.1. Introduction 99
7.2. Synthesis of Intermediates 101
7.3. Synthesis of 2',4'-Dihydrospiro[indoline-3,3'-[1,2,4]triazol]-2-ones 103
7.4. Synthesis of Spiropyrazoline Oxindole **167f** 103
7.5. Biological Studies 104
7.5.1. Assessment of Cell Viability and SAR Study 104
7.5.2. Evaluation of Compounds Ability to Block the Intracellular p53-MDM2 Interaction 108
7.5.3. Evaluation of Apoptosis 109
7.6. Stability 110
7.7. Concluding Remarks 111

Chapter 8. General Conclusions and Future Perspectives **113**

Chapter 9. Experimental Section **117**

9.1. Experimental Section: Chemistry 119
9.1.2. General Procedure for the Synthesis of 3-Methylene indoline-2-ones. 121
9.1.2.1. Method A. Wittig Reaction. 121
9.1.2.2. Method B. Aldolic Condensation. 121
9.1.3. Synthesis of Indolin-2,3-diones and 5-Bromoindolin-2-one. 126
9.1.4. General Procedure for the Synthesis of 3-Imino-indoline-2-ones. 128
9.1.5. General Procedure for the Synthesis of Aldoximes. 134
9.1.6. General Procedure for the Synthesis of Chlorooximes. 135
9.1.6.1. Aromatic Derivatives 135
9.1.6.2. Ester Derivatives 137
9.1.7. General Procedure for the Synthesis of Hydrazones 138
9.1.8. General procedure for the synthesis of Hydrazonoyl Chlorides. 141
9.1.9. General Procedure for the Synthesis of 4'H-Spiro[indoline-3,5'-isoxazol]-2-ones. 144
9.1.9.1. Method A (Et_3N). 144
9.1.9.2. Method B (Zn) 146
9.1.9.3. Method C (synthesis directly from aldoxime). 151
9.1.10. Synthesis of 4'-ethyl 5'-methyl (3*S*,4'*R*,5'*S*)-N-acetyl-5-fluoro-2'-(4-methoxyphenyl)-2-oxo-4',5'-dihydrospiro[indoline-3,3'-pyrrole]-4',5'-dicarboxylate (***epi*-163**). 160
9.1.11. General Procedure for the Synthesis of Spiro[indoline-3,5'-[1,2,4]oxadiazoline]-2-ones. 161
9.1.12. General Procedure for the Synthesis of 2',4'-Dihydrospiro[indoline-3,3'-[1,2,4]triazol]-2-ones. 176
9.2. Experimental Section: Biology. 192
9.2.1. *In vitro* Anti-proliferative Assays. 192

9.2.2. Western Blot Analysis. 193
9.2.3. Evaluation of Caspase-3/7 Activity 194
9.2.4. Bimolecular Fluorescence Complementation (BiFC) Assay. 194
9.3. Experimental section: Stability. 195
9.3.1. HPLC Analysis. 195
9.3.2. Stability in pH 7.4 Phosphate Buffer 195
9.3.3. Stability in Human Plasma. 195
9.3.4. Stability in Rat Microsomes. 195
9.4. Experimental Section: Docking Studies 196

Chapter 10. References 197

Figure Index

Figure 1.1. Simplified p53 activation and response upon acute DNA damage. 4

Figure 1.2. Cellular regulation of p53 by MDM2. 5

Figure 1.3. The p53-MDM2 interaction representation (PDB 1YCR) 6

Figure 1.4. Nutlins optimization to RG7112. Right upper quadrant: crystal structure of compound **3** bound to MDM2 (PDB 4IPF) 9

Figure 1.5. Nutlin and derivatives. 9

Figure 1.6. Spiropyrrolidines optimization to MI-106. Docking pose of compound **13** in MDM2 (PDB 3LBL). 12

Figure 1.7. Spiropyrrolidines and others spiro-heterocyclic-oxindole derivatives. 13

Figure 1.8. Spiropyrrolidines and spirothiazolidines derivatives. 14

Figure 1.9. Pyrrolidine-2-carboxamide optimization to RG7388. Right upper quadrant: crystal structure of compound 26 bound to MDM2 (PDB 4JRG) 15

Figure 1.10. Piperidinone optimization to AMG232. 18

Figure 1.11. Piperidinone and morpholinone derivatives. Right lower quadrant: crystal structure of compound **34** bound to MDM2 (PDB 4OAS) 19

Figure 1.12. Benzodiazepinediones scaffold optimization. Right upper quadrant: crystal structure of compound **40** bound to MDM2 (PDB 1T4E) 21

Figure 1.13. Examples of benzodiazepinediones derivatizations. 21

Figure 1.14. Isoindolinone scaffold optimization 23

Figure 1.15. Oxazoloisoindolinone derivative **52**. 23

Figure 1.16. Chromenotriazolopyridines scaffold optimization. Right upper quadrant: crystal structure of compound **53** bound to MDM2 (PDB 3JZK) 24

Figure 1.17. Indolyl derivatives. Right upper quadrant: structure of compound **56** bound to MDM2 (PDB 1YCR). 25

Figure 1.18. p53-MDM2 interaction inhibitors 27

Figure 1.19. MDM2 E3 Ligase activity inhibitors 29

Figure 1.20. MDMX and dual MDM2/MDMX inhibitors 30

Figure 1.21. Compounds that target upstream regulators of p53 activating pathway. 32

Figure 1.22. SIRT1and/or SIRT2 inhibitors. 34

Figure 1.23. p53-S100B interaction inhibitors. 34

Figure 1.24. RITA. 35

Figure 1.25. Compounds targeting mutant p53. 37

Figure 1.26. Different strategies for targeting wild-type and mutant p53 by small molecules. 38

Figure 3.1. Spiroisoxazoline oxindoles obtained by 1,3-dipolar cycloaddition described in literature. 54

Figure 3.2. X-ray crystallography structure of spiroisoxazoline oxindole **119a**. 54

Figure 4.1. Examples of spirooxindoles with biological activity 59

Figure 4.2. Number of publications per year in the last 15 years for the topic: (A) spirooxindole(s) and (B) p53-MDM2 interaction inhibitor(s)..... 60

Figure 4.3. Examples of spirooxindoles with anticancerl activity 60

Figure 4.4. p53 and MDM2 are linked to different non-fluorescent fragments of a fluorescent reporter protein..... 67

Figure 4.5. Compound **119z** decreases p53-MDM2 interaction by BiFC. 67

Figure 4.6. Compound **119aa** and **119ac** induces caspase-3 activation and PARP cleavage 68

Figure 5.1. Examples of catalysts, ligands and counterions employed. 78

Figure 5.2. X-ray crystallography of 163 and *epi*-163 [339]..... 83

Figure 6.1. Compound **165ab** decreases p53-MDM2 interaction by BiFC. 94

Figure 6.2. Compound **165ab** and **165ad** induce PARP cleavage and compound **165ad** induce caspase 3/7 activity..... 95

Figure 7.1. **A.** Best docking pose for **119ac** (depicted in stick model and colored in green) and MI-77301 (**13**, depicted in stick model and colored in white) in the p53 binding pocket (grey surface) of MDM2 (4WT2). **B.** Schematic representation of the moieties that mimic (**13**) or potentially mimic (**119ac**) p53 Phe19, Trp23, Leu26 100

Figure 7.2. A. Best docking pose for **168h** (depicted in stick model and colored in green) and MI-77301 (**13**, depicted in stick model and colored in white) in the p53 binding pocket (grey surface) of MDM2 (4WT2). **B.** Schematic representation of the moieties that mimic (**13**) or potentially mimic (**168h**) p53 Phe19, Trp23, Leu26..... 108

Figure 7.3. Compound **168h** decreases p53-MDM2 interaction by BiFC 109

Figure 7.4. Compound **168h** induce PARP cleavage and caspase 3/7 activity.. 110

Table Index

Table 1.1. Cell-free and cell-based *in vitro* assays. 7

Table 1.2. Other inhibitors or potential inhibitors of p53-MDM2 interaction..... 26

Table 1.3. Therapy strategies when p53 is mutated in cancers. 36

Table 3.1. Cycloadditions attempts, using primary nitro compound **123a** as precursors of nitrile oxides. 48

Table 3.2. Intermediates synthesized..... 49

Table 3.3. Optimization attempts of the 1,3-dipolar cycloaddition reaction using clorooxime **121a** 50

Table 3.4. Optimization of the 1,3-dipolar cycloaddition reaction using chlorooxime **123b**..... 51

Table 3.5. Cycloaddition reaction scope: Using different dipolarophiles with chlorooxime **123b**. 51

Table 3.6. Cycloaddition reaction scope: Using three equivalents of chlorooxime and zinc..... 52

Table 3.7. NMR chemical shifts (ppm) for representative spirooxindoles derivatives 54

Table 4.1. Synthesis of 3-methylene indolin-2-ones. 61

Table 4.2. Synthesis of aldoximes 62

Table 4.3. New spiroisoxazoline oxindole synthesized..... 63

Table 4.4. Synthesis of compound **119q**. 64

Table 4.5. *In vitro* antiproliferative activities in HepG2 cell line..... 65

Table 4.6. *In vitro* antiproliferative activities 66

Table 5.1. Cycloaddition reaction between **121n** and **123e**..... 76

Table 5.2. Cycloaddition reaction between **121k** and **123e**..... 77

Table 5.3. Cycloaddition reaction between **121k** and **123e**..... 78

Table 5.4. Cycloaddition reaction between **121k** and **123e**..... 79

Table 5.5. *In vitro* antiproliferative activities 80

Table 5.6. Synthesis of enantioenriched spiropyrroline ***epi*-163**. 82

Table 6.1. Synthesis of 3-imino-indolin-2-ones. 88

Table 6.2. Synthesis of hydroximoyl chlorides. 89

Table 6.3. *In vitro* antiproliferative activities in HCT116 $p53^{(+/+)}$ cell line. 91

Table 6.4. *In vitro* antiproliferative activities in HCT116 $p53^{(-/-)}$, HepG2 and SW620 cell lines... 92

Table 7.1. Synthesis of hydrazones. 101

Table 7.2. Synthesis of hydrazonyl chlorides..... 102

Table 7.3. Spiropyrazoline oxindoles reported in literature 105

Table 7.4. *In vitro* antiproliferative activities. 106

Table 7.5. *In vitro* antiproliferative activities. 107

Scheme Index

Scheme 2.1. Different spirooxindole scaffolds synthesized during the PhD. 42

Scheme 3.1. Retrosynthesis of spiroisoxazoline oxindoles derivatives highlighting the final step between 3-methylene indolin-2-ones (**121**) and chlorooximes (**123**) 47

Scheme 3.2. Synthesis of ester 3-methylene indolin-2-ones. 49

Scheme 3.3. Synthesis of chlorooximes. 49

Scheme 3.4. Possible regioisomers formed as a result of 1,3-dipolar cycloaddition between **121a** and **120a**. 53

Scheme 4.1. Synthesis of 3-methylene indolin-2-one. 61

Scheme 4.2. Synthesis of aldoximes 62

Scheme 4.3. Synthesis of spiroisoxazoline oxindoles 63

Scheme 5.1. Example of chiral Lewis acid-catalysed cycloaddion reaction with nitrile oxides (Sibi *et al*). 74

Scheme 5.2. Synthesis of alkylidene oxindole **121n**. 74

Scheme 5.3. Asymmetric Synthesis of Spiroisoxazoline oxindoles by Liang *et al*. 80

Scheme 5.4. Titanium-catalysed stereoselective synthesis of spirooxazoline oxindole **162** 81

Scheme 5.5. Titanium-catalysed stereoselective synthesis of spiropyrazole oxindole **163** 81

Scheme 5.6. Synthesis of 3-methylene indolin-2-one **121p** 81

Scheme 5.7. Proposed mechanism for Lewis acid catalyzed formation of **163**. 83

Scheme 6.1. Optimization Strategy 87

Scheme 6.2. Retrosynthesis of spirooxadiazoline oxindoles derivatives, highlighting the final step between 3-imino indolin-2-ones (**165**) and chlorooximes (**123**) 87

Scheme 6.3. Synthesis of 3-imino-indolin-2-ones 88

Scheme 6.4. Synthesis of hydroximoyl chlorides 89

Scheme 6.5. Synthesis of spirooxadiazoline oxindoles. 89

Scheme 6.6. Possible regioisomers formed as a result of 1,3-dipolar cycloaddition between **166** and **120**. 90

Scheme 7.1. Optimization strategy first from spiroisoxazoline to spiropyrazoline (**A**) and then to spirotriazoline (**B**) oxindoles. 99

Scheme 7.2. Retrosynthesis of spirotriazoline oxindoles derivatives, highlighting the final between imino indolin-2-ones (**166**) and nitrile imines (**169**). 100

Scheme 7.3. Synthesis of 3-imino-indoline-2-one 101

Scheme 7.4. Synthesis of hydrazones 101

Scheme 7.5. Synthesis of hydrazonyl chlorides 102

Scheme 7.6. Synthesis of spirotriazoline oxindoles 102

Scheme 7.7. Possible regioisomers formed as a result of 1,3-dipolar cycloaddition between **166** and **169**. 103

Scheme 7.8. Synthesis of spiropyrazoline oxindole **167f** 103

Acknowledgments

First of all I would like to thank Fundação para a Ciência e a Tecnologia for financial support (SFRH/BD/69258/2010) and the three supervisors that embarked in this journey with me: Dr. Maria M. M. Santos, Professor Rui Moreira and Professor Cecília M. P. Rodrigues.

I would like to thank the Liquid Chromatography and Mass Spectrometry Laboratory of the Faculty of Pharmacy of Lisbon University, especially João Fereira for the elemental analyses and LRMS; and the FT-ICR and Advanced Proteomics Laboratory from Faculty of Sciences of Lisbon University for HRMS analyses.

I also acknowledge Sara Silva (iMed.ULisboa) and Dr. Rita Guedes (iMed.ULisboa) for the docking studies.

I would like to thank Lídia Gonçalves (iMed.ULisboa) for the MTT antiproliferative assays and for all the know how behind biological assays transmitted.

I also thank Dr Joana Amaral for all the help in the biology department, especially for performing the western blotting assays. I want to extend this acknowledgement to all the colleagues from the Cellular Function and Therapeutic Targeting group (iMed.ULisboa) that help me in all the logistics that biology assays entail.

I would like to thank Dr. Annaliese K. Franz for accepting me in her lab in University of California – Davis for a period of three months. I want to thank all Franz group, and especially Joseph Badillo and Nicholas Ball-Jones, for all the help in the lab, and for open my mind on how to approach science. And also for remind me once again that Portuguese hospitality is overrated.

I would like to thank the entire medicinal chemistry group (from 2011-2015) for all the help, the stories, the camaraderie, and good times. I want to special acknowledge the post docs that are in reality the lab supervisors.

Since the PhD work represents most of the time period that I lived in Lisbon, I want to especially acknowledge the people that disrupted the coworker bubble and arose into friendship domain outside Faculty. Therefore, I want to especially mention two folks that are going to stay with me for a very long time: Catarina Charneira and Marta Figueiras; the former for representing the exception of what I think about people that live bellow Douro River and the latter for corroborating that there is something special about people from the North. In addition I want to thank my tango partner Mariana “Marisol” Reis for all the adventures, Marta Carrasco for turning out to be a very good surprise, the newbie Sara

Silva, Ana Rita “pompetinha” Duarte for all the songs (or not!), and Ana da Ress for all the scientific and life discussions throughout the years.

Outside Lisbon bubble I want to acknowledge my longtime friends (you know who you are!), with a special shout out to Isabel Duarte that represents what I think a scientist should aspired to be.

Finalmente quero agradecer à minha família, em particular ao Guedes e à Rosinha, pelo apoio incondicional, mesmo quando as coisas deixaram de correr como deviam. Um muito obrigado!

ABBREVIATIONS

1-NMI	1-Methylimidazole
5-HT6	5-hydroxytryptamine receptor 6
A549	Human lung carcinoma cell line
ARF (or p14ARF)	Alternate reading frame protein product of the CDKN2A locus
ATM	Ataxia-telangiectasia mutated
ATR	Ataxia telangiectasia and RAD3-related
BDP	1,4-benzodiazepine-2,5-dione
BiFC	Bimolecular fluorescence complementation assay
Boc	tert-Butyloxycarbonyl
Box	Bisoxazoline
BrdU	Bromo-2'-deoxyuridine
casp-3	caspase 3
CCK-8	Cell Counting Kit-8
CDK	cyclin-dependent kinase
CHK1	Checkpoint kinase 1
CHK2	Checkpoint kinase 2
CK2	casein kinase 2
Compds	Compounds
CRL	Cullin-RING ubiquitin E3 ligase
CRM1	Chromosomal maintenance 1
D. A.	Dihydrochlorinating agent
DABCO	1,4-diazabicyclo[2.2.2]octane
DCE	Dichloroethane
DCM	Dichloromehane
Del	Deleted
DIEA	N,N-Diisopropylethylamine
DMAP	4-Dimethylaminopyridine
DMF	Dimethylformamide
DMSO	Dimethyl sulfoxide
DNA	Deoxyribonucleic acid
dr	Diasteriomeric ratio
E2F1	E2F transcription factor 1
EdU	5-Ethynyl-2'-deoxyuridine
ee	Enantiomeric excess
ELISA	Enzyme-linked immunosorbent assay
er	Enantiomeric ratio
ESI	Electrospray Ionization
Et	Ethyl
EtOAc	Ethyl Acetate
FACT	Facilitates chromatin transcription
FP	Fluorescence polarization
Fro	Human anaplastic thyroid carcinoma cell line
G1 phase	Growth 1/Gap 1 phase
GC	Guanine-cytosine
GI_{50}	Concentration for 50% of maximal inhibition of cell proliferation
Gln	Glutamine
HCT116 $p53^{(-/-)}$	Human colorectal cancer cell line with null p53
HCT116 $p53^{(+/+)}$	Human colorectal cancer cell line with wild-type p53

HDAC	Histone deacetylase
HDACi	Histone deacetylase inhibitor
HIC-1	Hypermethylated in cancer 1
His	Histidine
HPLC	High-performance liquid chromatography
HRMS	High-resolution mass stectrometry
HSP90	Heat shock protein 90
HTRF	Homogeneous time resolved fluorescence
HTS	High-throughput screening
Hz	Hertz
$hNa_v1.7$	Voltage-gated sodium channel
IC_{50}	Concentration for 50% of maximal inhibition
Ile	Isoleucin
ipr	Isopropyl
IR	Infra-red
JAR	Human choriocarcinoma cell line
Kat-4	Human thyroid tumor cell line
Ki	Inhibition constant
LCVA	Luminescent cell viability assay
Leu	Leucine
LNCaP	Human prostatic adenocarcinoma cell line
Lys	Lysine
LRMS	Low resolution mass spectrometry
M phase	Mitotic phase
M. S.	Molecular sieves
M.W.	Microwave
MCF-7	Human breast adenocarcinoma cell line
MDA-MB-231	Human breast adenocarcinoma cell line
MDM2	Murine double minute-2
MDM4	Murine double minute-4
Me	Methyl
MHM	Human osteosarcoma cell line
mp	Melting point
mRNA	Messenger ribonucleic acid
MTS	(3-(4,5-dimethylthiazol-2-yl)-5-(3-carboxymethoxyphenyl)-2-(4-sulfophenyl)-2H-tetrazolium)
MTT	3-(4,5-dimethylthiazol-2-yl)-2,5-diphenyltetrazolium bromide
Mut	Mutated
NaBArF	sodium tetrakis[3,5-bis(trifluoromethyl)-phenyl]borate
NADPH	Nicotinamide adenine dinucleotide phosphate
NAE	NEDD8-activating enzyme
NCS	N-Chlorosuccinimide
NF-κB	Nuclear factor kappa-light-chain-enhancer of activated B cells
NMR	Nuclear magnetic resonance
NMR-AIDA	NMR-based antagonist induced dissociation assay
NOE	Nuclear Overhauser Effect
Otf	Triflate
PARP	poly ADP ribose polymerase
PDB	Protein data bank
Ph	Phenyl
Phe	Phenylalanine
PK	Pharmacokinetic

PLK-4	Serine/threonine-protein kinase 4 also known as polo-like kinase 4
PMP	para-methoxyphenyl
PPA	Phenyl phosphinic acid
py	Pyridine
Pybox	bis(oxazolinyl)pyridine
R,R-TUC	3,5-Bis(trifluoromethyl)phenyl]-3-[(1R,2R)-(-)-2-(dimethylamino)cyclohexyl]thiourea
RITA	Reactivation of p53 and induction of tumor cell apoptosis
RNA	Ribonucleic acid
rRNA	Ribosomal ribonucleic acid
r.t.	Room temperature
S phase	Synthesis phase
S. M.	Starting material
S100B	S100 calcium-binding protein B
SAR	Structure-activity relationship
SEM	Standard Error of the Mean
Ser	Serine
SI	Selectivity index
SINE	Selective inhibitor of nuclear export
SIRT	Sirtuin
SJSA-1	Human osteosarcoma cell line
SPR	Surface plasmon resonance
SRB	Sulforhodamine B
TDZ	1,4 thienodiazepine-2,5-diones
TEA	Triethylamine
temp.	Temperature
ThermoFluor	Thermal denaturation screening assay
THF	Tetrahydrofuran
TLC	Thin layer chromatography
TR-FRET	Time-resolved fluorescence energy transfer
Trp	Tryptophan
U-2OS	Human osteosarcoma cell line
U937	Human lung lymphoblast cell line
Weri1	Retinoblastoma cell line
WST-8	Water soluble tetrazolium-8: 2-(2-methoxy-4-nitrophenyl)-3-(4-nitrophenyl)-5-(2,4-disulfophenyl)-2H-tetrazolium
Wt	Wild-type
XPO1	Exportin-1

ABSTRACT

Among the tumor suppressor genes, p53 is one of the most studied. It is widely regarded as the "guardian of the genome", playing a pivotal part in the preservation of genomic integrity by regulating cell cycle, apoptosis, DNA repair, senescence and angiogenesis, and consequently has a major role in carcinogenesis. The function played by p53 in tumor suppression is further highlighted by the fact that direct inactivation of this gene occurs in more than 50% of malignancies. In addition, in tumors that retain wild type p53 status, its function is usually inactivated by overexpression of negative regulators, primarily murine double minute-2 (MDM2), mainly through *MDM2* gene amplification or by activity loss of MDM2 inhibitor ARF. Hence, restoring p53 function in cancer cells represents a valuable anticancer approach. Several strategies are being developed, and in particular targeting p53-MDM2 interaction has emerged as a promising viable approach when dealing with cancers that retain wild type p53 function. These two proteins regulate each other through an autoregulatory feedback loop: activation of p53 stimulates the transcription of MDM2, which in turn binds to the *N*-terminal transactivation domain of p53, disabling its transcriptional function. p53-MDM2 interaction inhibitors share common structural features: a rigid heterocyclic scaffold with three lipophilic groups that mimic the three pivotal p53 Phe19, Trp23 and Leu26 that interact with MDM2. Seven compounds have already entered clinical trials.

The main goal of this PhD thesis was to develop new anticancer agents containing a spirooxindole scaffold with different spiro five-membered rings: isoxazoline, oxadiazoline, and triazolines. The spirocycle can potentially function as the rigid heterocyclic scaffold, from which three lipophilic groups are projected to mimic the three pivotal p53 amino acids.

This work followed three major strategies: synthesis of spirooxindole derivatives by 1,3 dipolar cycloaddition; biological evaluation of the compounds synthesized; and stability assessment.

Overall this PhD thesis contributed with three new families of spirooxindoles with *in vitro* anti-cancer activity. The most active derivative possessed a GI_{50} of 1.72 µM in HCT116 $p53^{(+/+)}$ cell line. Furthermore their ability to disrupt the interaction between p53 and MDM2 was confirmed by implementing a cell-base *in vitro* bimolecular fluorescence complementation assay (BiFC) and the apoptotic outcome verified by immunoblotting analysis and luminescent caspase 3/7 activity assay.

KEYWORDS: spirooxindoles, anticancer drugs, protein-protein interaction, p53, MDM2.

RESUMO

A proteína p53 foi descoberta há mais de 35 anos e é actualmente um dos mais estudados supressores tumorais, sendo designada até por "guardião do genoma". A p53 desempenha um papel crucial na célula: regulação do ciclo celular, apoptose, reparação do DNA, senescência e angiogénese e, consequentemente, tem um papel decisivo na carcinogénese. Este papel central da p53 como supressor tumoral é incontestável, como observado no aumento da predisposição para o desenvolvimento de tumores em indivíduos com a síndrome Li-Fraumeni, caracterizados por serem detentores de uma mutação no gene da p53 (*TP53*) e em ratos sem o gene que codifica esta proteína (*Trp*-null). Actualmente acredita-se que em virtualmente todos os cancros se verifica algum tipo de perda da função supressora tumoral da p53. Em cerca de 50 % dos tumores, esta perda é directa, isto é, é devido à presença de uma mutação no gene *Tp53* ou ocorre indirectamente, por inactivação das vias de sinalização celular da p53. Em tumores que retêm o fenótipo selvagem da p53, normalmente ocorre aumento da expressão de reguladores negativos da p53, como por exemplo a MDM2 e MDM4.

Em condições normais, os níveis de expressão da p53 são mantidos em valores baixos. Contudo em resposta a sinais de stress, como por exemplo a danos genotóxicos, a p53 é estabilizada e activada por meio de modificações pós-tradução. Como esta proteína é um factor de transcrição, a sua activação levará a um aumento da expressão de determinados genes-alvo que culminará numa resposta apropriada, incluindo prevenção da tumorigénese. Em contraste a inactivação da função celular da p53 pode levar à proliferação de células danificadas, podendo resultar no aparecimento e desenvolvimento de tumores.

Devido à importância da inactivação da via da p53 para o desenvolvimento tumoral, conceber estratégias que visam a reactivação desta proteína é de grande interesse, especialmente se permitirem um efeito apoptótico selectivo em células cancerígenas. Estas estratégias podem ser agrupadas em duas categorias: direccionadas para cancros detentores de uma versão mutada da p53 ou para cancros que conservam a sua forma nativa. No primeiro grupo, o objectivo será focado em estratégias que permitam o correcto enrolamento da p53 mutada com o intuito de restaurar a sua função. No segundo grupo, o objectivo é inibir a função de reguladores negativos da p53. A segunda categoria compreende diversas estratégias, incluindo: inibidores das sirtuínas, inibidores da S100B, inibidores da actividade E2 ligase da MDM2, inibidores da proteína MDM4, compostos que promovem a disrupção do nucléolo, agentes intercalantes e inibidores da exportação nuclear de proteínas. Contudo, a estratégia que tem suscitado mais interesse nos últimos 10 anos corresponde à inibição da interacção

entre a p53 e a MDM2. Estas duas proteínas auto-regulam-se: a activação da p53 estimula a transcrição da MDM2 e esta proteína, por sua vez, liga-se ao terminal N da p53 desactivando a sua função transcricional. A proteína MDM2 também promove a exportação da p53 do núcleo e favorece a sua degradação mediada pelo proteasoma, através da função de E3 ubiquitina ligase. Estes eventos conduzem a uma diminuição dos níveis de p53 que, por sua vez, promovem uma diminuição da expressão da MDM2, permitindo assim que a proteína p53 possa ser novamente activada. A estrutura cristalográfica da p53 ligada à MDM2 revelou que esta interacção ocorre numa pequena fenda hidrofóbica superficial na proteína MDM2. Os resíduos mais importantes da p53 que contribuem para esta interacção são a Phe19, o Trp23 e a Leu26. Portanto, quando se desenham inibidores da interacção p53-MDM2 é necessário que estes sejam capazes de mimetizar os três aminoácidos da p53 supracitados. Diversas famílias de compostos já foram descritas na literatura capazes de inibir esta interacção, sendo as mais importantes: cis-imidazolinas, spiropirrolidina oxindoles, pirrolina-2-carboxamidas, piperidinonas, benzodiazepinedionas e isoindolinonas. Sete compostos inibidores da interacção p53-MDM2 encontram-se em ensaios clínicos.

Compostos com um núcleo spirooxindole são encontrados em produtos naturais e apresentam diversas actividades biológicas. Em particular, já se encontram descritos na literatura compostos spiropirrolidina oxindoles com diversas actividades cancerígenas, como por exemplo inibidores da polimerização dos microtúbulos e, consequente, paragem da mitose e inibidores da interacção p53-MDM2. Deste segundo grupo, o composto MI-77301 encontra-se em ensaios clínicos.

O objectivo principal desta tese de doutoramento consistiu em desenvolver novos agentes anticancerígenos detentores de um esqueleto spirooxindole fundido com diferentes anéis de cinco membros: isoxazoline, oxadiazolina e triazolina. Diferentes grupos essencialmente hidrofóbicos foram introduzidos no esqueleto central, numa tentativa de encontrar aqueles que melhor mimetizam os três aminoácidos da p53. Para cada uma destas famílias foram descritos os métodos sintéticos envolvidos e a respectiva avaliação biológica *in vitro* dos derivados sintetizados. Os compostos foram sintetizados por cicloadição 1,3-dipolar entre 3-imino ou 3-metileno indolina-2-onas e dipolos 1,3 gerados *in situ* por desidrohalogenação de cloretos de hidroximoílo e cloretos de hidrazonoílo. Para o primeiro núcleo sintetizado – spiroisoxazoline oxindoles – são ainda descritas tentativas de síntese enanteosselectiva do composto mais activo. Esta parte do trabalho foi realizada num período de três meses no grupo da Dr. Annaliese K. Franz na Universidade da Califórnia – Davis (EUA). Em paralelo, neste período na Califórnia, foi também desenvolvida uma metodologia de síntese enanteosselectiva de um derivado spiropirrolina oxindole.

Os estudos *in vitro* permitiram avaliar e demonstrar a potencialidade dos compostos como agentes anticancerígenos, através da realização de ensaios anti-proliferativos em diversas linhas celulares cancerígenas: par isogénico HCT116 $p53^{(+/+)}$ e $p53^{(-/-)}$ de cancro colorrectal humano, carcinoma hepatocelular humano HepG2, adenocarcinoma colorrectal humano SW620, cancros da mama MCF-7 e MDA-MB-231 e uma linha celular epitelial embrionária humana de rim. A capacidade dos compostos interferirem com a interacção entre a p53 e a MDM2 foi também avaliada e confirmada *in vitro* através da implementação de um método de fluorescência de complementação biomolecular (BiFC) realizado em células. A capacidade dos compostos induzirem a apoptose foi avaliada por ensaios de Western blotting e luminescência, onde se verificou um aumento da actividade das caspases e um aumento da clivagem do seu substrato PARP.

Por último, foram efectuados ensaios de estabilidade química em tampão fosfato pH 7.4, em plasma e em microssomas de rato, para dois compostos de cada família. Estes ensaios servirão para ajudar na escolha dos compostos a seguir para ensaios *in vivo* numa futura continuação do trabalho.

Foram sintetizados trinta e três compostos da primeira família (spiroisoxazoline oxindoles). O derivado mais activo possui um GI_{50} de 26.50 µM em HCT116 $p53^{(+/+)}$. Com a segunda família de compostos (spirooxadiazoline oxindoles) conseguiu-se aumentar a actividade para 1.72 µM, na mesma linha celular. Nesta série de compostos foram sintetizados trinta e dois derivados, dos quais nove revelaram possuir um GI_{50} inferior a 10 µM. Na terceira família sintetizada (spirotriazolina oxindoles) foi possível encontrar cinco derivados com GI_{50} abaixo dos 10 µM na linha celular MCF-7 (p53 fenótipo selvagem). Curiosamente outros cinco derivados revelaram ser selectivos para a linha celular tumoral MDA-MD-231 (p53 mutada). Desta série foram sintetizados vinte e sete derivados. Estudos preliminares de *docking* molecular corroboraram a possibilidade destes compostos conseguirem mimetizar os três resíduos da p53.

PALAVRAS-CHAVE: spirooxindoles, compostos anticancerígenos, interacção proteína-proteína, p53, MDM2

Chapter 1

STATE OF THE ART

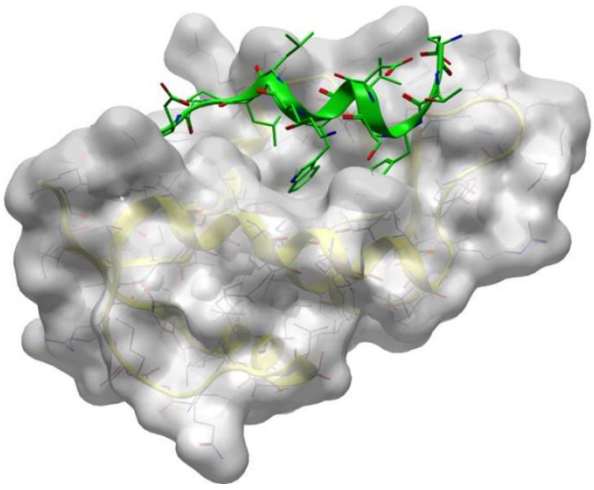

Tumor suppressor p53 was discovered over 35 years ago and since then it emerged as a key protein of scientific interest, and became widely regarded as the "guardian of the genome" [1]. p53 plays a pivotal role in the regulation of cell cycle, apoptosis, DNA repair, senescence and angiogenesis, and consequently has a major function in carcinogenesis. The central role of p53 as tumor suppressor is undeniable, as observed by the increased predisposition to cancer in individuals with Li-Fraumeni syndrome, who inherit a mutant p53 gene *TP53*, and in *Trp*-null mice [2]. Additionally, it is now believed that in virtually all cancers, loss of p53 function occurs, either directly due to the presence of a mutated form of *TP53*, or by inactivation of the p53 signal transduction pathways. In tumors that retain wild type p53 status, corresponding to 50% of all cancers, its function is usually inactivated by overexpression of negative regulators, primarily murine double minute-2 (MDM2) and MDM4 (also known as MDMX) [3].

1.1. p53 ACTIVATION IN HEALTH AND DISEASE

The cellular levels of the p53 protein are tightly regulated. In normal cells, and under physiological conditions, steady-state values of p53 are maintained at very low levels by its negative regulators, mainly MDM2 and MDM4. However, under cellular stress, such as DNA damage, hypoxia or oncogene activation, a range of differential posttranslational modifications of p53 are triggered that lead to p53 stabilization and activation, by promoting its release from repression and by inhibiting its degradation. For instance, upon acute DNA damage, p53 stabilization is mostly achieved by phosphorylation mediated by upstream kinases such as ATM/ATR and/or CHK1/CHK2 (Figure 1.1). Activated p53 binds to DNA and promotes the transcription of several target genes, culminating in a proper cellular response that is dictated by the nature of the stress, cell type and environment milieu. Under low levels of stress, p53 induces a transient G1 cell cycle arrest, while cells attempt to repair their genome. However, if the damage is too severe, activation of the p53 pathway results in cell death by apoptosis or senescence. By contrast, loss of p53 tumor suppressor activity allows the proliferation of cells that are damaged under stress conditions, potentially leading to uncontrolled proliferation that can result in tumor development [4-6].

Canonical p53 responses that lead to cellular functions of cell cycle arrest, senescence and apoptosis are extensively studied specially when triggered upon acute DNA damage. However, recently more attention is given to understanding p53 signaling in a tumor context, since distinct stresses and different responses that can facilitate/trigger tumor suppression have been described. These interesting p53 responses include: inhibition of oncogenic metabolic reprogramming, activation of autophagy, communication endorsement within the tumor microenvironment, inhibition of stem cell self-renewal and

differentiated cells reprogramming into stem cells, and limiting invasion and metastasis [2, 7].

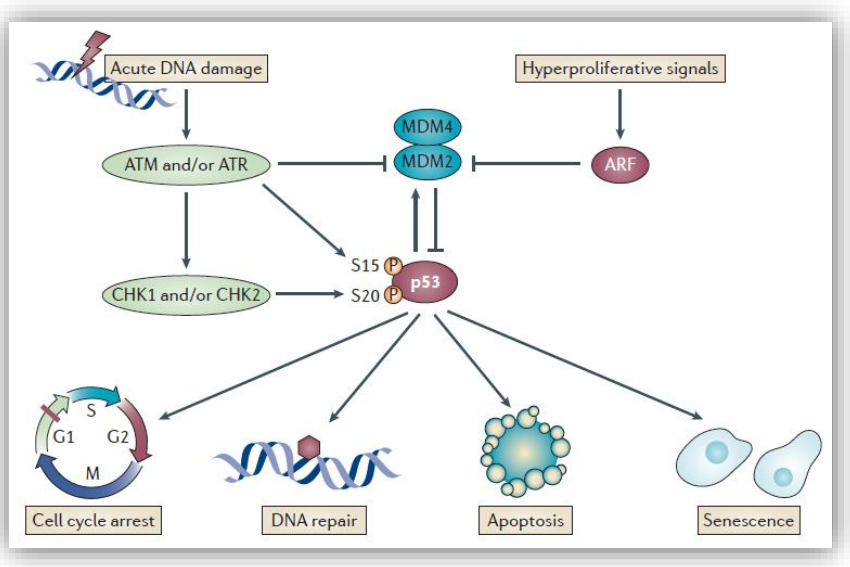

Figure 1.1. Simplified p53 activation and response upon acute DNA damage (adapted from [2]).

1.2. REACTIVATION OF P53 AS A THERAPEUTIC STRATEGY

It is well documented that the loss of p53 can induce tumor formation in mice, whereas its restoration leads universally to a rapid regression of established *in situ* tumors, showcasing the anticancer therapeutic potential of p53 reactivation. Furthermore, the key question for p53 reactivation strategy is whether or not this event will result in a selective effect on tumor cells as opposed to healthy tissues. It seems that a simple overexpression of p53 in cells is not sufficient to activate the p53 pathway. The restored p53 protein needs to be properly activated and for that the transformed environment of tumor cells appears to be required [8, 9]. For instance, studies using p53-MDM2 interaction inhibitors showed that in fact, in normal cells, the activation of p53 induces preferentially cell cycle arrest and not cell death, revealing therefore a more selective apoptotic effect on tumor cells. The effect of p53 activation by this type of inhibitor in normal tissues has immense interest from a therapeutic perspective due to the possibility of using it in monotherapy, as well as a normal cells protector in combination with more aggressive agents [10, 11].

Throughout the last ten years, great advance was made in devising strategies to modulate p53, giving rise to several review papers on the subject [3, 11-24]. Pharmacological p53 reactivation strategies for cancer therapy can be clustered in two major approaches based on p53 status. In tumors that retain wild-type p53 but have defects in p53 regulatory pathways, the main goal is to inhibit the function of negative regulators of p53 activation outcome. When p53 is mutated in tumors, the most common strategy consists in refolding the protein into a wild-type conformation to restore its function. In

this chapter, it will be given emphasis to small-molecules that use the former strategy and in particular to the interaction between p53 and its inhibitor MDM2. However other strategies are also being pursued to restore p53 function in cancer cells such as using peptides, stapled peptides and other oligomers as inhibitors on p53-MDM2/X interaction [20] and adenovirus-mediated p53 cancer gene therapy [25].

1.2.1. TARGETING P53-MDM2 INTERACTION

Increased levels of p53 repressor MDM2 are present in many cancers, mainly through *MDM2* gene amplification or by activity loss of MDM2 inhibitor ARF. Therefore, targeting the p53-MDM2 interaction to reactivate p53 has emerged as a promising new cancer therapeutic strategy, in the last fifteen years or so, with already *in vitro* an *in vivo* established proof-of-concept [10, 26-45]. These two proteins regulate each other through an autoregulatory feedback loop [46]. Activation of p53 stimulates the transcription of MDM2, which in turn binds to the *N*-terminal transactivation domain of p53, disabling its transcriptional function. MDM2 also promotes the nuclear export of p53 and p53 proteasome-mediated degradation through its E3 ubiquitin ligase activity by promoting mono and polyubiquitination, respectively, at several lysine residues (Figure 1.2). These events result in decreased levels of p53 that will therefore reduce MDM2 expression, allowing p53 protein to potentially be activated again [44, 47].

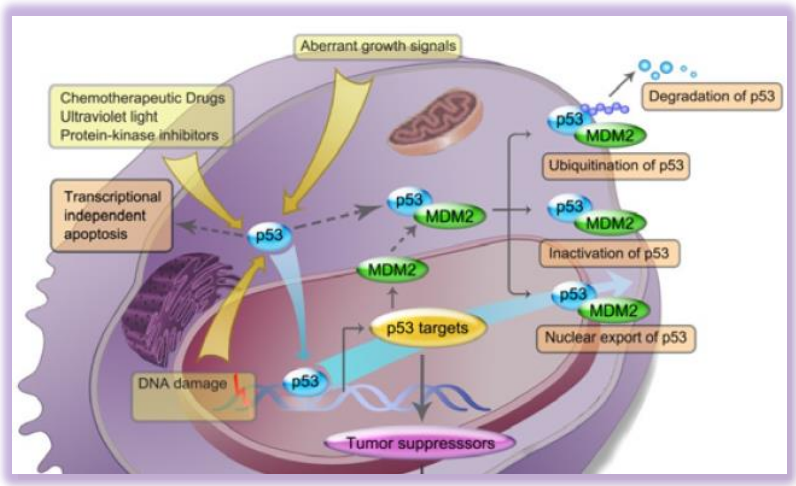

Figure 1.2. Cellular regulation of p53 by MDM2 (adapted from [39]).

The crystal structure of the p53 binding domain of MDM2 (109-residue amino-terminal) with a short peptide of the p53 transactivaction domain (15-residues) has been solved and published, providing detailed information about the interaction between these two proteins [48]. The co-crystal revealed that MDM2 has a deep hydrophobic cleft on which the p53 peptide binds as an amphipathic alpha helix. In the bound conformation, the p53 amphipathic α-residues 19-26 of the transactivation domain projects residues Phe19,

Trp23 and Leu26 into the deep hydrophobic cleft of the MDM2 protein, representing the critical residues for binding between this two proteins to occur (Figure 1.3). In the crystal structure, Phe19 and Trp23 align in the deeper portion of the cleft. Phe19, through its backbone amine, forms one hydrogen bond with the backbone carbonyl Gln72 at the entrance of the cleft, while establishing hydrophobic interactions with Gly58 and Ile61 of MDM2. Trp23 occupies the deepest part of the binging pocket, forming a solvent protected hydrogen bond between the NH from its indole side chain and Leu54 of MDM2, and makes hydrophobic interactions with Gly58 and Ile61 of MDM2. Leu26 is the final residue of the alpha helix to be projected into the hydrophobic pocket. Furthermore, the interaction is strengthened by additional van der Waals contacts provided by p53 Leu22 [39, 48].

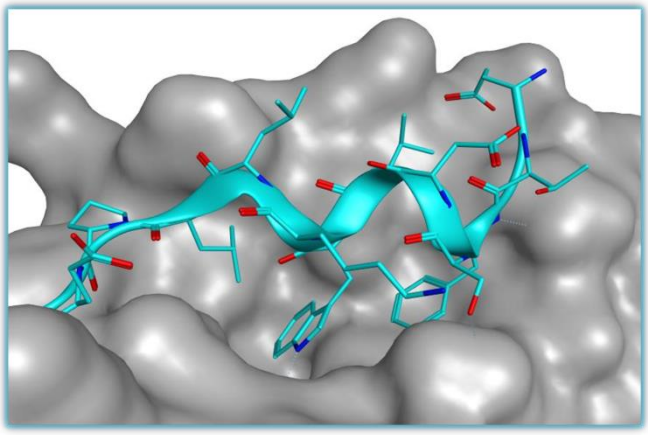

Figure 1.3. The p53-MDM2 interaction representation (PDB 1YCR). Phe19, Trp23 and Leu26 from a small amphipathic p53 derived α-helix (blue) are projected into the MDM2 pocket (grey surface).

After publication of the crystal structure of p53 bound to MDM2, several efforts were made to design more potent peptide derivatives. The search for small molecules that could interfere with the protein-protein interaction only flourished after the publication of a co-crystal structure of a small-molecule in MDM2 pocket. To date more than 20 different chemical classes have been described as inhibitors of p53-MDM2 interaction. Recently, several molecules entered, and are still in, clinical trials, revealing the continuous relevance and efforts in finding new and improved derivatives/ scaffolds.

In this chapter, a detailed understanding of the medicinal chemistry and optimization approach is going to be given especially to scaffolds that provided molecules that entered clinical trials [45, 49]: *cis*-imidazolines, spiropyrrolidine oxindoles, pyrrolidine-2-carboxamides and piperidinones, as well as other relevant families, such as morpholinones, benzodiazepinediones, isoindolinones, chromenotriazolopyridines and imidazole-indoles.

To facilitate the comprehension of this section, it is depicted in table 1.1 all *in vitro* cell-free and cell-based methods used to determine the IC_{50}s presented, as well as the cell lines employed and their p53 status. In general, the description will be given as follows for cell-based assays: "assay" "cell line" $IC_{50=}$ "value" (e.g. compound **3**, MTT SJSA-1 $IC_{50=}$ 0.3 μM, Figure 1.4).

Table 1.1. Cell-free and cell-based *in vitro* assays.

CELL-FREE BINDING ASSAYS:	
SPR	Surface plasmon resonance
HTRF	Homogeneous time resolved fluorescence
FP	Fluorescence polarization
NMR-AIDA	NMR-based antagonist induced dissociation assay
ThermoFluor	Thermal denaturation screening assay
TR-FRET	Time-resolved fluorescence energy transfer
ELISA	Enzyme-linked immunosorbent assay
CELL-BASED ASSAYS:	
BrdU	Bromo-2'-deoxyuridine
EdU	5-Ethynyl-2'-deoxyuridine
LCVA	Luminescent cell viability assay
MTT	Tetrazolium salt
SRB	Sulforhodamine B
WST-8	Water soluble tetrazolium salt
CELL LINES:	
A549	Human lung carcinoma – wild-type p53
Fro	Human anaplastic thyroid carcinoma – null p53
HCT116 *p53*$^{(+/+)}$	Human colorectal cancer – wild-type p53
JAR	Human choriocarcinoma – wild-type p53
Kat-4	Human thyroid tumor – mutant p53
LNCaP	Human prostatic adenocarcinoma – wild-type p53
MCF-7	Human breast adenocarcinoma – wild-type p53
MDA-MB-231	Human breast adenocarcinoma – mutant p53
MHM	Human osteosarcoma – wild-type p53
SJSA-1	Human osteosarcoma – wild-type p53
U-2OS	Human osteosarcoma – wild-type p53
U937	Human lung lymphoblast – wild-type p53

1.2.1.1. *CIS*-IMIDAZOLINES (NUTLINS). ROAD TO RG7112

The Nutlin scaffold, consisting of a tetrasubstituted imidazoline unit, was first discovered by high-throughput screening (HTS) of a diverse library of synthetic compounds, using a surface plasmon resonance (SPR) assay, followed by structure-based optimization (Hoffman-La Roche). Three compounds arose from this study in 2004. It also provided the first crystallographic structure published of a small-molecule (Nutlin-2: **1**, Figure 1.4) in complex with MDM2 [50]. The *para*-bromophenyl ring at position 4 occupies $Leu26_{(p53)}$ pocket while the other *para*-bromophenyl substituent at position 5 inserts deeply into the $Trp23_{(p53)}$ pocket with the bromo atom enhancing the binding by filling a small cavity not normally occupied by the indole ring of p53 Trp23. The $Phe19_{(p53)}$ pocket is occupied by the ethyl ether side chain of the third aromatic ring while its *para*-methoxy group mimics the p53 Leu22. The *N*1 chain functions mainly as a "solubility-tag" but also contributes to activity by possibly establishing polar interactions between the hydroxyl group and Gln72 side chain [50, 51]. The most potent of these three compounds is the enantiopure Nutlin-3a (**2**, SPR IC_{50} of 0.09 µM, MTT IC_{50}= 1 - 2 µM in wild-type p53 cancer cell lines). Nutlin-3a usage in monotherapy and in combination with other anti-cancer drugs and radiation has already been extensively published, serving as proof-of-concept for Nutlins and establishing p53-MDM2 interaction as a promising and valuable target [52-57].

Since biological and pharmacokinetic (PK) properties achieved by Nutlin-3a were still suboptimal for clinical development, further research was performed. The strategy mainly focused on probing different *N*1 side chains in an attempt to enhance PK properties and MDM2 binding and on removing stability liabilities found in the previous compounds: oxidation of the main core to imidazole, and metabolization of the *para*-methoxyphenyl group to phenol. They were amended by adding methyl groups to position 4 and 5 of the imidazoline ring, and by replacing the methoxy with *tert*-butyl group, respectively [58]. One of the best compounds, RG7112 (**3**, HTRF IC_{50}= 18 nM, MTT IC_{50}= 0.18 - 2.2 µM in wild-type p53 cancer cell lines) entered clinical trials [59]. RG7112 shows good selectivity over mutated p53 cancer cells (MTT IC_{50}= 5.7 - 20.3 µM), and it is able to activate the p53 signaling pathway in wild-type p53 cells, leading to cell cycle arrest and apoptosis. Furthermore a daily dose of 100 mg/kg is capable of promoting partly regression of SJSA-1 and MHM tumor xenograft mice models [45, 60].

Hu *et al* published in 2011 [61] and 2012 [62] novel derivatives based on the imidazoline scaffold, mainly by varying the *N*1 side chain of Nutlin-3. Compound **4** (FP IC_{50}= 0.59 µM, MTT HCT116 $p53^{+/+}$ IC_{50}= 3.73 µM, Figure 1.5) was one of the most potent compounds obtained, however not representing an improvement of potency when

compared with Nutlin-3a. Nevertheless, these publications helped once again to establish that changing *N*1 side chain interferes mainly with PK properties but also with potency.

Several analogs are disclosed in patents from Hoffman-La Roche, possessing the same imidazoline core and others structure variations such as imidazopyridinones (**5**) [29, 38, 63, 64]. Miyazaki *et al* also published a new series of dihydroimidazothiazole derivatives based on Nutlin-3a structure, such as DS-5272 (**6**, HTRF IC_{50}= 2.4 µM, LCVA SJSA-1 IC_{50}= 0.2 µM) [65, 66].

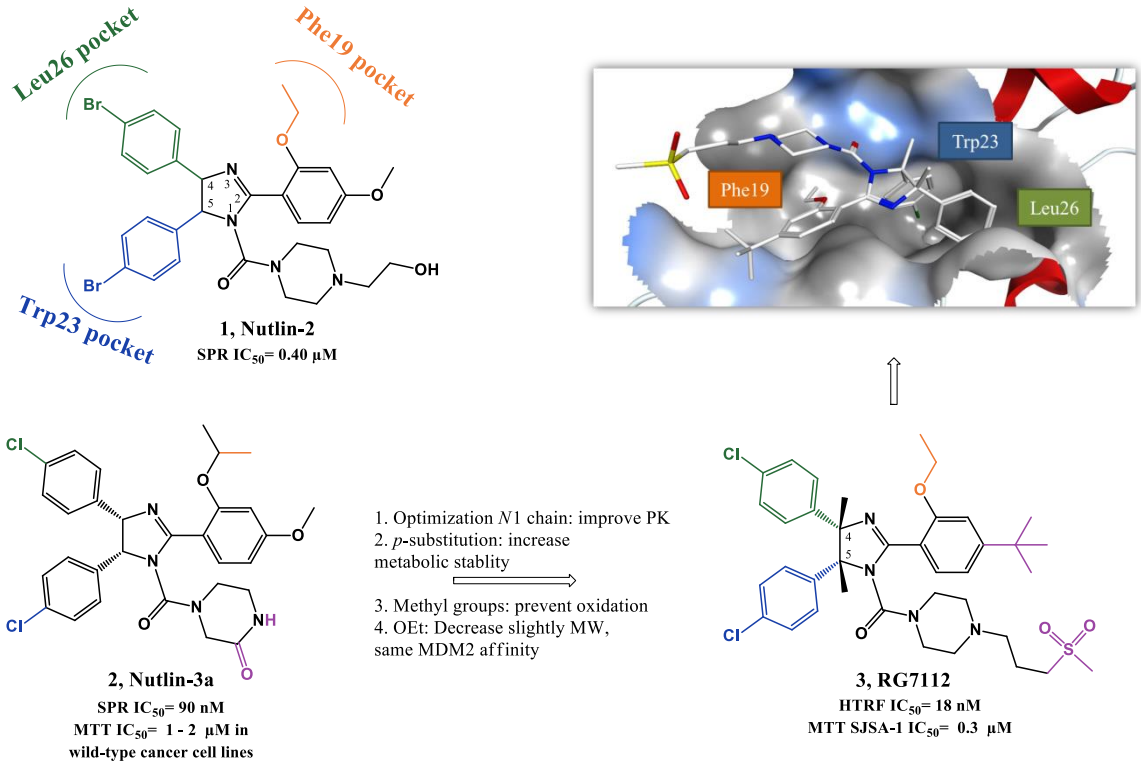

Figure 1.4. Nutlins optimization to RG7112. Right upper quadrant: crystal structure of compound **3** bound to MDM2 (PDB 4IPF). MDM2 surface is colored in blue for hydrophilic areas and grey for hydrophobic areas. Compound **3** is depicted in stick model and is colored according to element type: white for carbon atoms, blue for nitrogen atoms, red for oxygen atoms, yellow for the sulfur atom, and green for chlorine atoms.

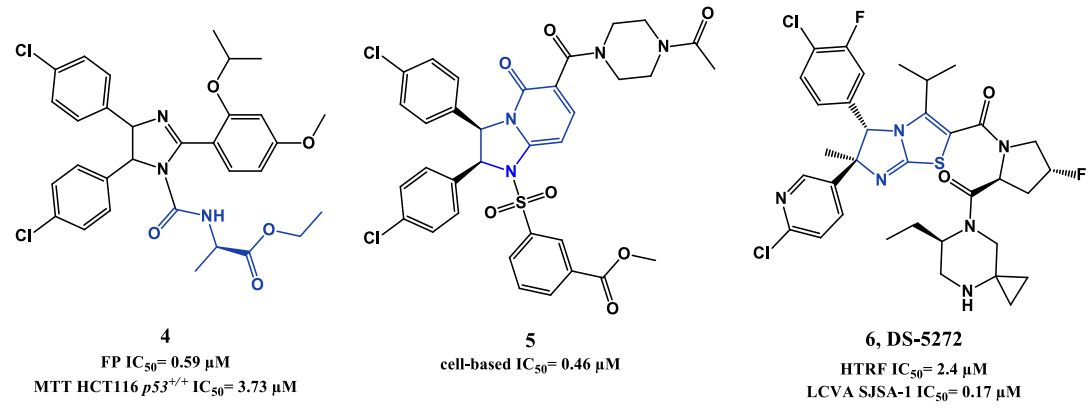

Figure 1.5. Nutlin and derivatives.

1.2.1.2. SPIROOXINDOLES

1.2.1.2a. Spiropyrrolidine oxindoles. Road to MI-77301

Taking in consideration that p53 Trp23 side chain (indole group) seems to be critical for p53-MDM2 interaction, by burring deeply inside p53 hydrophobic pocket and by establishing a hydrogen bond (NH) to MDM2 backbone (carbonyl), the oxindole moiety was believed to perfectly mimic this residue. Moreover since many natural anticancer products, such spirotryprostatin A and alstonisine, have a spirooxindole main core, it was rationalized and later corroborated by *in silico* studies that the spiropyrrolidine ring could provide the necessary rigidity to the spirooxindole scaffold, from which two extra hydrophobic groups could be projected in the required orientation to mimic the other two residues of p53. From this structure-based design an initial lead compound arose in 2005 (**7**, Figure 1.6) with a FP Ki of 8.46 μM (Wang group, University of Michigan). Computational modeling suggested that interaction optimization could be achieved by varying the isobutyl substituent and by introducing small substituents in the *meta*-position of the phenyl ring (room in Leu26$_{(p53)}$ and Phe19$_{(p53)}$ pocket respectively still available). Therefore, structure-activity relationship (SAR) studies led to MI-43 (**8**, FP Ki= 86 nM, WST-8 LNCaP IC_{50}= 0.83 μM). This compound also showed good selectivity over normal cells and cancer cells with deleted p53 [67].

Further virtual investigation into the interaction of compound **8** and p53 with MDM2, suggested that a possible fourth residue (Leu22) could be mimicked. Leu22$_{(p53)}$ pocket is partially exposed to solvent and therefore mimicking this residue could result not only in an increase of potency but also in PK improvement, since it could allow the presence of polar groups. A second round of SAR studies was devised, having mainly this observation in consideration, leading to MI-63 (**9**) with a 2-morpholin-4-yl-ethylamine group. Docking studies revealed that not only this side chain could mimic Leu22 but the morpholine oxygen could possibly interact by H bond with Lys90 in MDM2 (mimicking p53 Glu17). Furthermore the introduction of a fluor atom in the phenyl group, a frequently effective strategy to increase metabolic stability, augmented the potency (FP Ki of 3 nM, WST-8 LNCaP IC_{50}= 0.28 μM) [68, 69]. However, due to the fact that compound **9** had only a modest oral bioavailability, additional investigations, especially on the polar morpholinyl substituent were performed. It was found that changing to a butyl-1,2-diol significantly improved PK (MI-219: **10**, FP Ki of 13.1 nM, WST-8 SJSA-1 IC_{50}= 0.7 μM and MI-147: **11**, FP Ki of 0.6 nM, WST-8 SJSA-1 IC_{50}= 0.2 μM) [70]. Nevertheless these new derivatives still required high oral doses (200-300 mg/kg) to achieve tumor growth inhibition in mice xenograft models, and most important a complete tumor regression was still elusive [71]. More recently this last goal was attained with MI-888 (**12**, FP Ki of 0.44 nM, WST-8 SJSA-1 IC_{50}= 0.08 μM) [72] and MI-77301/SAR405838 (**13**, FP Ki of 0.88

nM, WST-8 SJSA-1 IC_{50}= 0.092 μM) [73]. These compounds were synthesized in a new series of optimizations that continued to focus on the 5' pyrrolidine tail chain, especially by introducing conformational constrain, while attempting to increase metabolic stability [72].

Recently it was discovered that some of these spiropyrrolidine oxindoles can suffer reversible ring-opening and cyclization of the pyrrolidine ring in protic solution, giving rise to different stereoisomers with different binding affinities to MDM2 [74]. Therefore a second generation of spirooxindoles emerged in 2015 that possess symmetrical substituents at C2' position of the pyrrolidine ring that allow a rapid and irreversible conversion to the most active diastereoisomer (MI-1061: **14**, FP Ki of 0.16 nM, WST-8 SJSA-1 IC_{50}= 0.10 μM) [75]. Compounds **12** and **13** from the first generation were already synthesized having in consideration the desired stereochemistry. Interestingly the best diastereomer revealed a different and better binding to MDM2 with the neopentyl and phenyl ring occupying now $Phe19_{(p53)}$ and $Leu26_{(p53)}$ pockets respectively (Figure 1.6, represented for compound **11**). Furthermore their side chain carbonyl is capable of stablish an H bond with the imidazole side chain of His96 and terminal hydroxyl group with Lys94 side chain [73].

Compound **13** advanced into clinical trials in 2012 sponsored by Sanofi. It displays more than 100-fold selectivity over cell lines with mutated or deleted p53, activating a p53-dependent pathway leading to cell-cycle arrest and/or apoptosis in cancer cells *in vitro* and *in vivo* xenograft tumor models. A complete tumor regression was achieved at 100 mg/kg with a daily dose for 9 days and at 200 mg/kg with a single oral dose in SJSA-1 mice xenograft [73].

In 2014, Hoffmann-La Roche published two other papers describing further optimizations of spiro[oxindole-3,3'-pyrrolidines], having in consideration the beneficial PK and potency improvement obtained when a phenyl derivative group is attached to the amide side chain as in their p53-MDM2 inhibitor RG7388 (see section 1.2.1.3). RO8994 (**15,** HTRF IC_{50} of 5 nM, SJSA-1 IC_{50}= 13 nM, Figure 1.7) emerged in a SAR study focused especially in additional modifications to this side chain [76, 77]. Compounds RO2468 (**16,** HTRF IC_{50} of 6 nM, MTT SJSA-1 IC_{50}= 3 nM), and RO5353 (**17,** HTRF IC_{50} of 7 nM, MTT SJSA-1 IC_{50}= 2 nM) were based on RO8994, and represent a bioisosteric substitution study of the 6-chlorooxindole moiety. Although with *in vitro* and *in vivo* activity comparable with RO8994, these compounds showed improve selectivity between wt p53 cell lines and mut p53 cell lines [78].

Several patents emerged from Hoffmann-La Roche throughout the last 10 years covering spiro[oxindole-3,3'-pyrrolidines] and others spiro-heterocyclic-oxindole based compounds (e.g. **18**, **19** and **20**) [38, 41, 64].

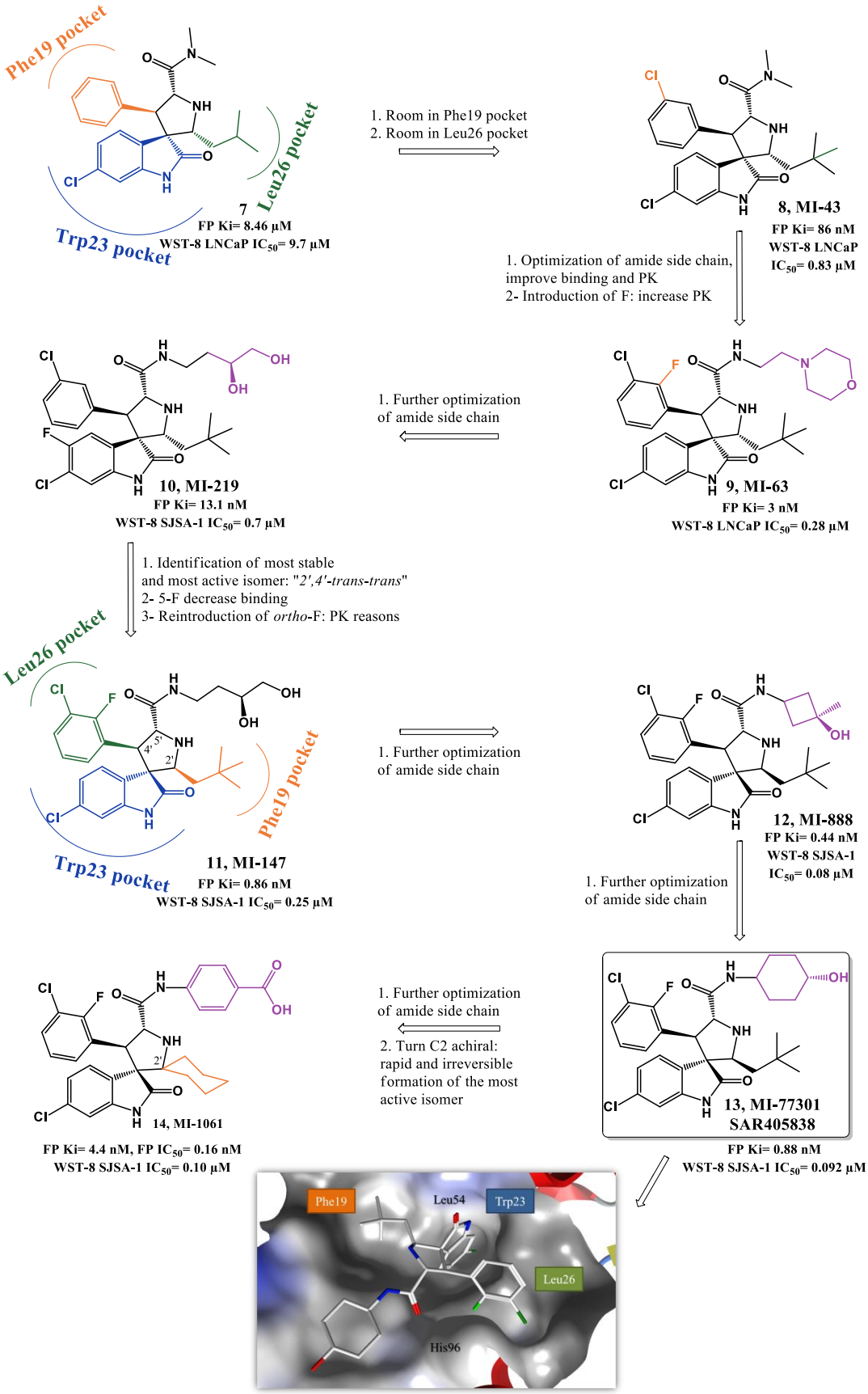

Figure 1.6. Spiropyrrolidines optimization to MI-106. Docking pose of compound **13** in MDM2 (PDB 3LBL). MDM2 surface is colored in blue for hydrophilic areas and grey for hydrophobic areas. Compound **13** is depicted in stick model and is colored according to element type: white for carbon atoms, blue for nitrogen atoms, red for oxygen atoms, bright green for fluorine, and dark green for chlorine atoms.

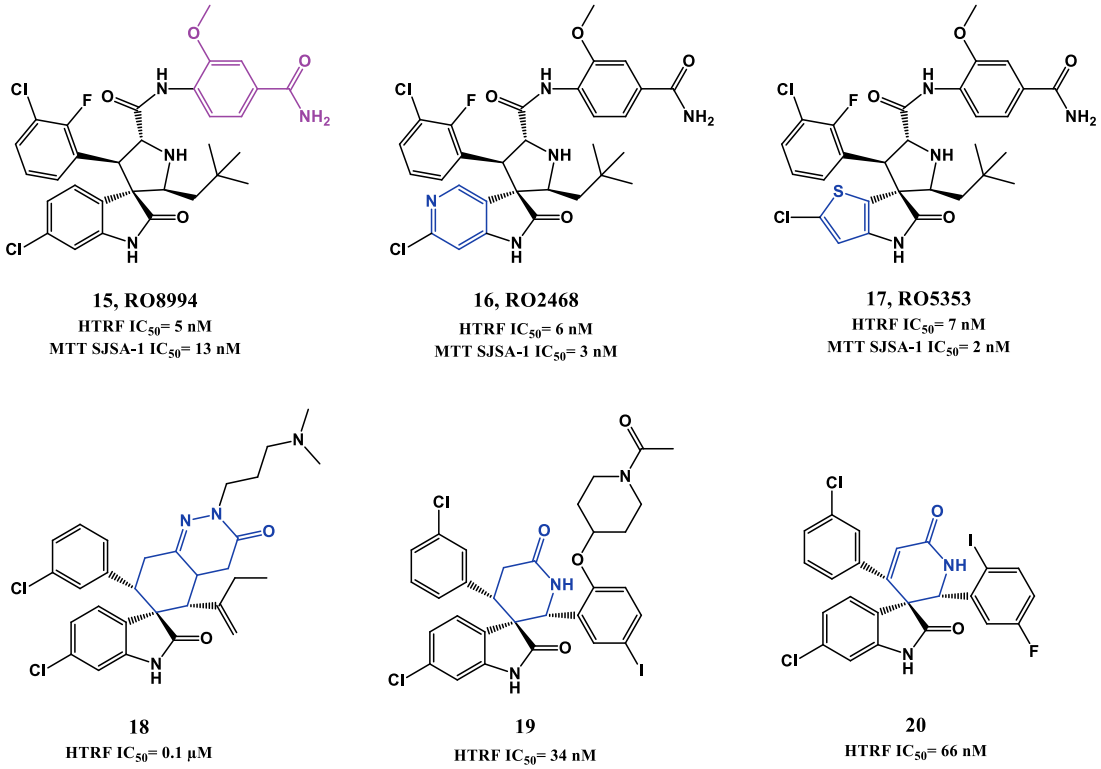

Figure 1.7. Spiropyrrolidines and others spiro-heterocyclic-oxindole derivatives.

Kumar *et al* published this year a new family of spiro[oxindole-3,2'-pyrrolidines] [79]. They focused in breast cancer, providing good evidence that the best compound modulates p53 *in vitro* and *in vivo*. However, the compounds did not show selectivity between breast cancer cell lines with wt p53 (MCF-7) and mut p53 (MDA-MB-231), and although it was observed an increase in MDM2 levels, no studies were focused in the p53-MDM2 interaction (**21**, MTT MCF-7 IC_{50}= 6.5 µM, Figure 1.8). Also this year, Ivanenkov *et al* reported dispiros with spiropyrrolidine oxindole moiety that can potentially interfere with p53-MDM2 interaction by *in silico* comparison with known MDM2 antagonists (**22**, MTT MCF-7 IC_{50}= 4.88 µM) [80].

1.2.1.2b. Spirothiazolidine oxindoles

In 2010, Gomez-Monterrey *et al* synthesized a series of spiro[oxindole-3,3'-thiazolidines], with ISA27 emerging as the most potent derivative in cell lines (**23**, MTT U937 IC_{50}= 0.87 µM, Figure 1.8). Destabilization of p53-MDM2 interaction by compound **23** was established first by NMR analysis (AIDA method) [81], and later complemented by an in depth *in vitro* validation in human glioblastoma multiforme [82]. A second round of SAR studies was focused on opening ISA27 imidazole ring in an attempt to increase structural diversity and introduce extra potential binding points. Therefore, it could allow a better fitting to p53 pocket, since ISA27 most likely only mimic two of the three pivotal p53 amino acids [83]. SM13 (**24**, MTT MCF-7 IC_{50}= 0.04 µM) emerged from this study.

Docking studies suggested that 3-cyclohexylcarboxy moiety occupies the Trp23$_{(p53)}$ pocket, and ethyl ester side chain the Phe19$_{(p53)}$ pocket. Leu26$_{(p53)}$ pocket is only slightly occupied by the oxindole ring, but the authors suggested that this drawback seems to be somewhat compensated by extra hydrophobic interactions gained through the *N*1-methyl group. *In vitro* inhibition of p53-MDM2 interaction was evaluated for both compounds using an ELISA binding assay. At 5 µM ISA27 (**23**) and SM13 (**24**) inhibited 25% and 30% of the interaction respectively (nutlin-3 inhibited 19%). However, both compounds were also effective in cancer cell lines with mutated p53. A detailed study to clarify the mechanism of action of SM13 suggested that besides inhibiting p53-MDM2 interaction, this compound acts in a manner strictly dependent on p53. No apoptosis induction was observed in FRO cells (null p53) and only activation of p53-dependent mitochondrial apoptotic pathway was observed in Kat-4 (mut p53) due to its lack of p53 transcriptional activity [84].

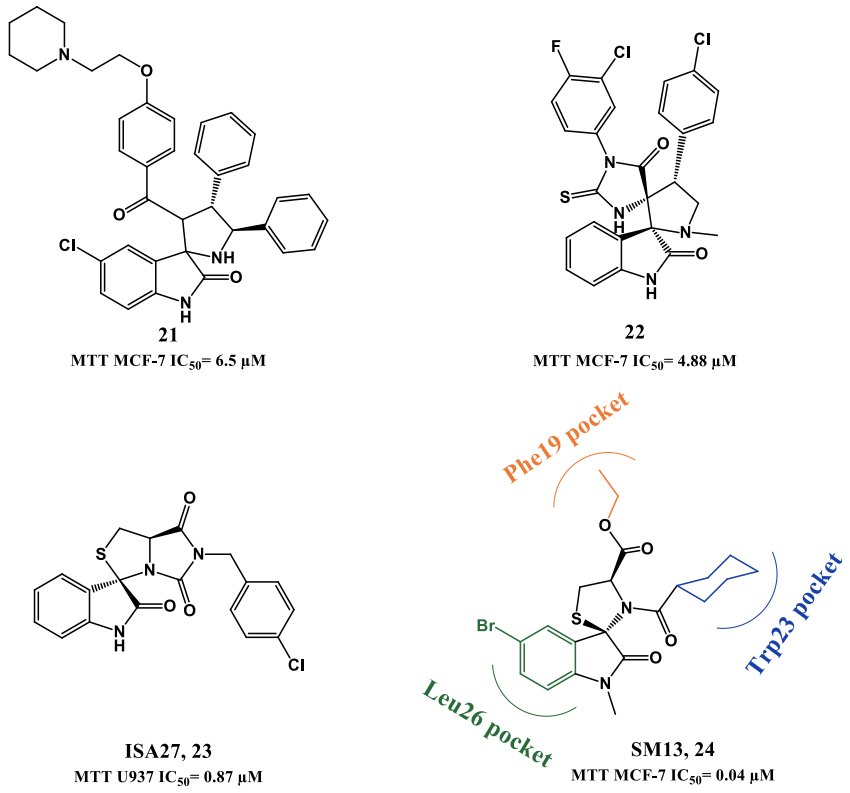

Figure 1.8. Spiropyrrolidines and spirothiazolidines derivatives.

1.2.1.3. PYRROLIDINE-2-CARBOXAMIDES. ROAD TO RG7388.

RG7388 from Hoffman-La Roche (**25**, Figure 1.9) was design based on the spiropyrrolidine oxindole MI-219 structure (**10**) and on the notion that an aromatic moiety would be better to mimic Leu26 of p53. They reported that the presence of a nitrile group favored the necessary "trans-trans" configuration (between rings A and B, and ring A and neopentyl group, Figure 1.9) to obtain the proper configuration and the better interaction with MDM2. As referred previously, Wang group later also described that a different configuration for MI-219 was preferred to obtain more potent spiropyrrolidine oxindoles. Optimization to RG7388 was mainly focused on the amide side chain of compound **26** (HTRF IC_{50}= 74 nM, MTT SJSA-1 IC_{50}= 2.1 µM), with best PK properties and potency obtained with a methoxy *para*-benzoic acid moiety (**25**, HTRF IC_{50}= 6 nM, MTT SJSA-1 IC_{50}= 10 nM). Furthermore, the addition of fluor to both phenyl rings also contributed to increase binding to MDM2. RG7388 exhibits more than 100-fold selectivity over cell lines with mutated p53, and activates the p53 pathway. It promoted tumor regression at 25 mg/kg with daily doses in SJSA-1 mice xenograft [85, 86] and is currently in clinical trials.

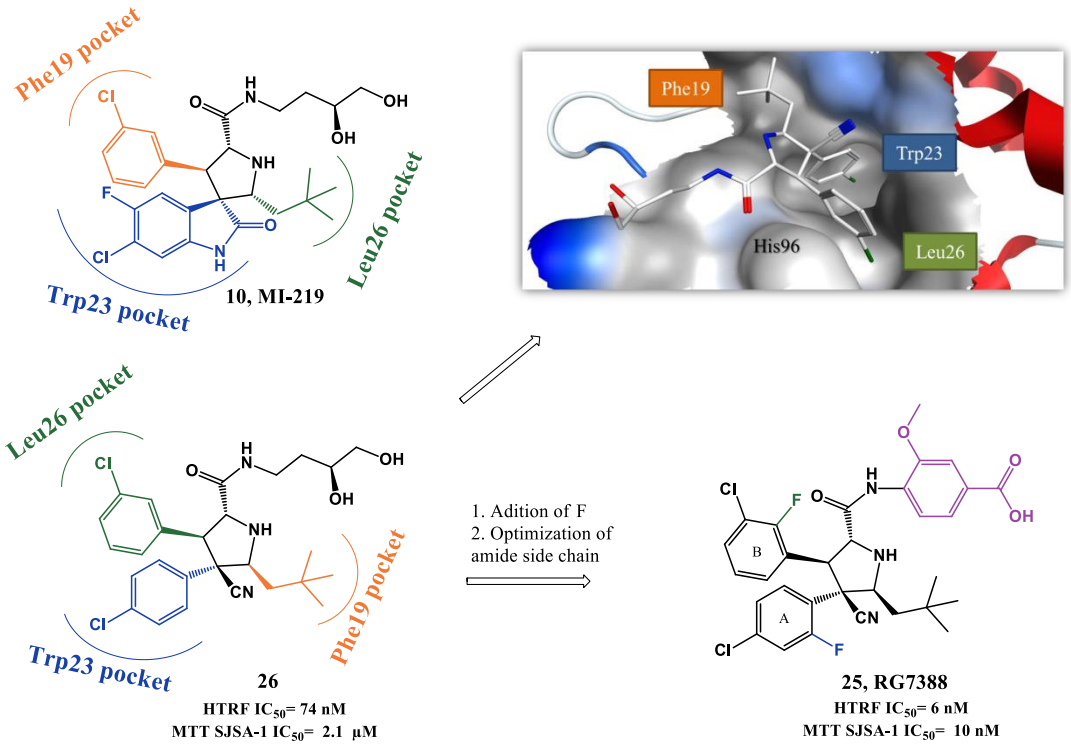

Figure 1.9. Pyrrolidine-2-carboxamide optimization to RG7388. Right upper quadrant: crystal structure of compound **26** bound to MDM2 (PDB 4JRG). MDM2 surface is colored in blue for hydrophilic areas and grey for hydrophobic areas. Compound **26** is depicted in stick model and is colored according to element type: white for carbon atoms, blue for nitrogen atoms, red for oxygen atoms, and green for chlorine atoms.

1.2.1.4. PIPERIDINONES AND MORPHOLINONES. ROAD TO AMG232.

Applying a structure-based design, focusing particularly in the knowledge that most inhibitors have the common feature of possessing two vicinal aromatic groups attached to a rigid heterocyclic core, Amgen design several new scaffolds. The most potent compounds synthesized possessed a morpholinone core (**27**, HTRF IC_{50}= 2.0 µM, Figure 1.10) [87] and were first published in 2012 [88]. Co-crystal structure of **27** with MDM2 showed that 6- and 5-*p*-bromophenyl rings occupy $Phe19_{(p53)}$ and $Trp23_{(p53)}$ pockets, respectively. Unfortunately the benzyl group was not projected into $Leu26_{(p53)}$ pocket, remaining unoccupied. Instead it interacted with Phe55 residue in a shallow hydrophobic shelf region. Having in consideration that mimicking Leu26 is also vital to develop potent MDM2 inhibitors, they redesign the two haloaryl rings in an attempt to mimic instead the residues Leu26 and Trp23, as observed for previously described *cis*-imidazolines and spiropyrrolidine oxindoles [58, 73]. That was accomplished by shifting the *p*-halogen to *m*-halogen at C6 phenyl ring to mimic Leu26, leading to a 180º rotation of morpholinone in the p53 pocket. Phe19 could be filled by introducing a proper *N*-alkyl substituent to the scaffold (**28,** HTRF IC_{50}= 1.8 µM). Additionally SAR study at C2 position revealed that acetic acid moiety increased potency by establishing an electrostatic interaction with His96 residue of MDM2 (**29**, HTRF IC_{50}= 0.3 µM, EdU SJSA-1 IC_{50}= 15.7 µM). However due to the fact that the proximity of this carboxylic acid to morpholinone oxygen could possibly generate electrostatic repulsion and consequently destabilize the right binding conformation, the latter was substituted with a methylene group. This alteration created more potent derivatives, detaining now a piperidinone core. Studies of stereochemistry configuration revealed that stereoisomer **30** was the most potent one (HTRF IC_{50}= 34 nM, EdU SJSA-1 IC_{50}= 3.35 µM) [87, 89].

The next SAR studies focused primarily in conformational controls to make sure that the best conformation was favored. In the best binding pose, the *N*-substituent needs to adopt a *syn* ("downward") orientation in regards to *p*-chlorophenyl group to properly occupy the $Phe19_{(p53)}$ pocket. However, since the alternative *anti* conformation is more stable, it was envisaged that introducing a "directing" group at the alpha-carbon to the piperidinone nitrogen could proper direct the desire group into the pocket. Another important orientation aspect observed in the binding conformation is the necessity of C5 and C6 aryl groups to adopt a *gauche*-like orientation instead of the more stable *anti*-like orientation. For that, introducing another substituent at C3 position could create a 1,3-steric repulsion to the *anti*-like orientation, favoring the desired one (**31,** HTRF IC_{50}= 2.2 nM, EdU SJSA-1 IC_{50}= 190 nM) [88, 90].

In an attempt to increase PK properties further SAR studies were performed in the *N*-alkyl chain, especially by introducing polar functional groups, leading to AM-8553 (**32**, HTRF IC_{50}= 1.1 nM, EdU SJSA-1 IC_{50}= 68 nM) [88, 91]. This compound was able to inhibit tumor growth and even promoting partial tumor regression, but still was unable to

produce the desired complete tumor regression in SJSA-1 xenograft tumor model [92]. Therefore, further optimization was pursuit. Analyzing the co-crystal structure of **32** with MDM2 it was identified a shallow hydrophobic cleft near $Phe19_{(p53)}$ pocket, designated "glycine shelf" by the authors (MDM2 Gly58 lies in the center), that could be filled in an attempt to enhance binding. Therefore more SAR studies were performed in the *N*-side chain to promote the new interaction envisioned, while still allowing a proper binding to $Phe19_{(p53)}$ pocket and maintaining good PK properties [93]. Several derivatives were synthesized including sulfonamides, that led to the most potent piperidone published so far (**33**, HTRF IC_{50}= 0.091 nM, EdU SJSA-1 IC_{50}= 0.48 nM, Figure 1.11) [94]. However due to the fact that most of these new derivatives with sulfonamides were less metabolically stable than **32**, other derivatizations were tested, leading to compound **34 (**HTRF IC_{50}= 0.1 nM, EdU SJSA-1 IC_{50}= 3 nM, Figure 1.10) and AMG232 (**35**, HTRF IC_{50}= 0.6 nM, EdU SJSA-1 IC_{50}= 9.1 nM) [93]. Nevertheless it is noteworthy to point out that even a simple *N*-group can give rise to potent derivatives (**36**, HTRF IC_{50}= 9 nM, EdU SJSA-1 IC_{50}= 0.38 µM, Figure 1.11) [95]. Compound **35** entered clinical trials in 2012. Although compound **34** was more active than **35** it offered poorer PK properties in *in vivo* studies.

Binding of **35** with MDM2 was extrapolated from the cocrystal structure of **34** with MDM2 (Figure 1.11). As expected the three pivotal p53 amino acids Phe19, Trp23 and Leu26 are being mirrored by isopropyl, C6 aryl group and C5 aryl group, respectively. Two substituents interact with His96: C5 aryl engages in a π-π stacking, while carboxylate function forms a hydrogen bond with its imidazole side chain. In addition, sulfone group projects the terminal isopropyl to the glycine shelf region. Compound **35** was able to induce complete tumor regression in 10 out of 12 SJSA-1 xenograft mice (60 mg/Kg administered orally once daily) [93, 96]. Additional SAR studies were performed mainly by searching for new replacements for the carboxylate moiety that still allowed the interaction with His96 and possibly enhance potency. It led to AM-6761 (**37**, HTRF IC_{50}= 0.1 nM, EdU SJSA-1 IC_{50}= 16 nM) with potency similar to **35**. Interestingly these two derivatives have different metabolic profile that can be of interest to explore. Compound **37** is primarily metabolized by oxidative pathways, while compound **35** is metabolized mainly by glucuronidation of the carboxylate moiety [97]. Further optimization led to AM-7209 (**38**, HTRF IC_{50}< 0.1 nM, EdU SJSA-1 IC_{50}= 1.6 nM) [98].

Alongside with the synthesis of piperidones, Amgen continued to optimize morpholinone derivatives, leading to AM-8735 (**39**, HTRF IC_{50}= 0.4 nM, EdU SJSA-1 IC_{50}= 25 nM) [99].

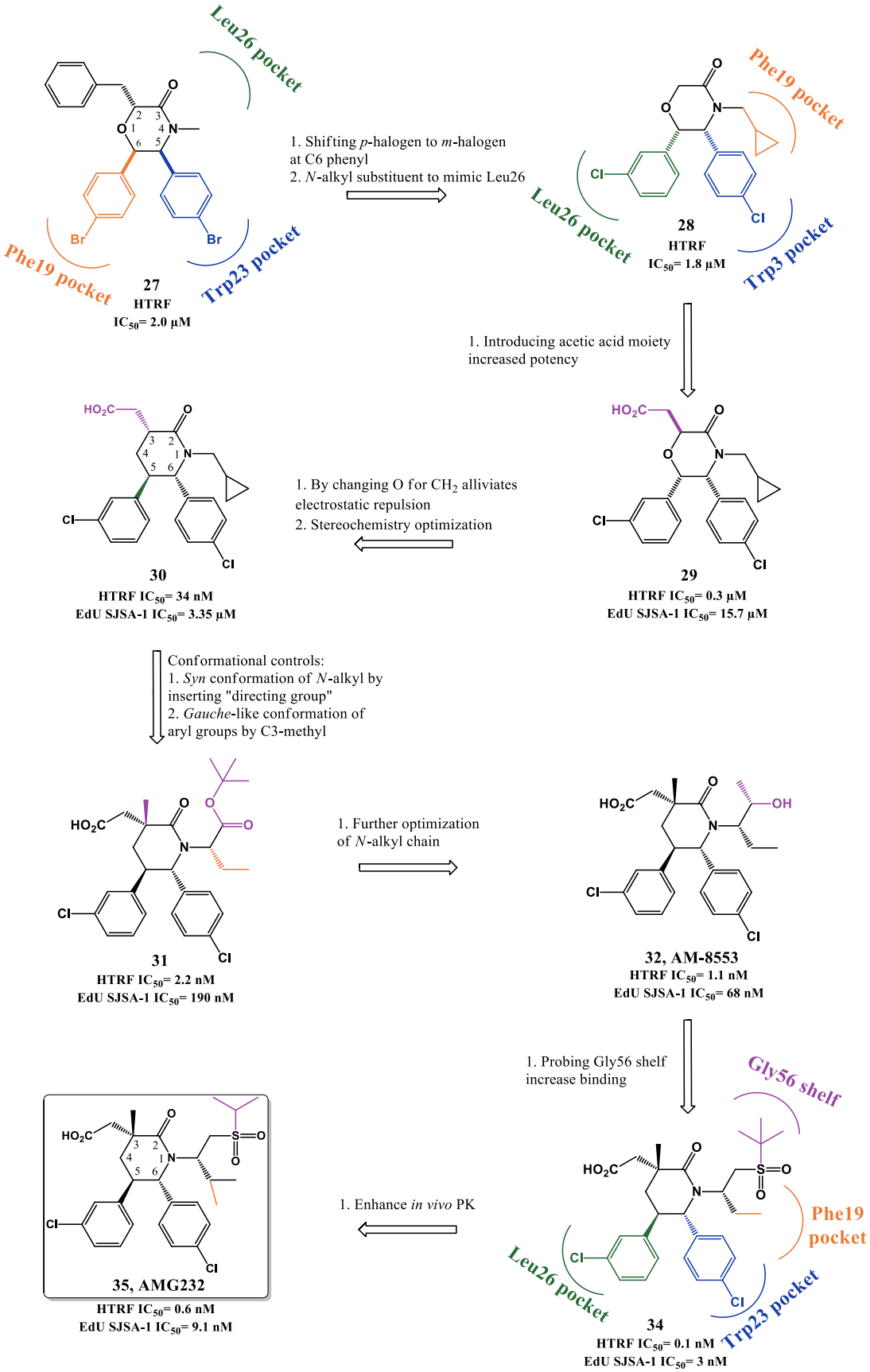

Figure 1.10. Piperidinone optimization to AMG232.

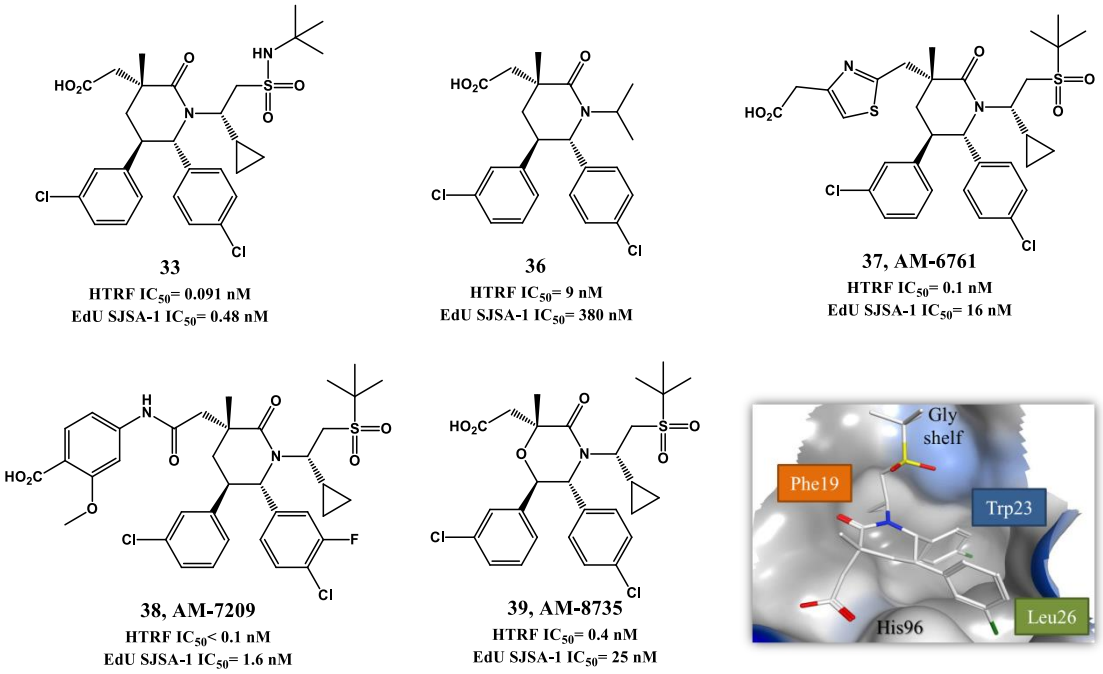

Figure 1.11. Piperidinone and morpholinone derivatives. Right lower quadrant: crystal structure of compound **34** bound to MDM2 (PDB 4OAS). MDM2 surface is colored in blue for hydrophilic areas and grey for hydrophobic areas. Compound **34** is depicted in stick model and is colored according to element type: white for carbon atoms, blue for the nitrogen atom, red for oxygen atoms, yellow for the sulfur atom, and green for chlorine atoms.

1.2.1.5. OTHER MDM2 INHIBITORS IN CLINICAL TRIALS

Other three compounds advanced into clinical trials, but no structural information is available: MK-8242, CGM097 and DS-3032b developed by Merck, Novartis International and Daiichi Sankyo, respectively.

1.2.1.6. BENZODIAZEPINEDIONES

p53-MDM2 interaction inhibitors bearing a 1,4-benzodiazepine-2,5-dione scaffold (BDP) were first reported as a result of a miniaturized affinity-based screening assay, termed ThermoFluor, of a library of 338 000 compounds [100]. Selected compounds from this first screen were further tested employing a fluorescence polarization (FP) assay to detect specific p53-MDM2 interaction inhibitors. The confirmation of this class of compounds as feasible MDM2 inhibitors evoked a more detailed study in which a library of 22 000 BDP compounds was synthetized and screened using the two method described above [101]. A first SAR study gave rise to the lead compound **40** (FP IC_{50} of 0.42 µM, BrdU JAR IC_{50}= 30 µM, Figure 1.12) in 2005 (Johnsons & Johnsons).

BDP:MDM2 co-crystal structure elucidated the interaction: 1,4-diazepine core gives the necessary rigidity from which the two chlorophenyl groups mimic perfectly Leu26 and Trp23 of p53, while the 7-iodophenyl group inserts in the $Phe19_{(p53)}$ pocket [100, 102]. Although this last group does not inserts as deeply as p53 Phe19 in the pocket,

it was later rationalized that this interaction is enhanced because iodine atom makes contacts to the carbonyl group of backbone Gln72 with a strength comparable to a weak hydrogen bond [103]. The initial observation that BDP iodophenyl and p53 Phe19 were not superimposable, gave rise to a rational design of a novel 1,4-diazepine scaffold. In this new scaffold an increased flexibility was introduced to the fused phenyl-diazepine rings in an attempt to ameliorate the Phe19 mimetic effect, while maintaining the orientation of the two chlorophenyl groups. Unfortunately, although this approach produced new active compounds, the FP IC_{50} values attained were higher in comparison to the original series (best compound: **41**, FP IC_{50} of 3.6 µM) [104]

Due to poor PK properties of compound **40**, modifications were made to try to improve solubility and permeability. It was rationalized that the inclusion of substituents in *N*1 might be tolerated since it is primarily solvent-exposed in the co-crystal structure, and also changing the carboxylic acid could convey better PK properties to the scaffold. Several solubilizing groups were inserted to *N*1 and ultimately pentanoic acid group was selected for further PK optimization. In this study it was found that the acid group was important to activity, possibly by establishing a hydrogen bond to MDM2 Ser17, and most importantly by placing the chlorophenyl group in the correct orientation through steric repulsion. This repulsion orientation was maintained when carboxylate was substituted with methyl group, while increasing cell permeability (**42**, FP IC_{50}= 0.70 µM, BrdU MCF-7 IC_{50}= 7 µM) [105].

Searching for more potent BDP led to compound **43** bearing an *ortho* amino group in the *N*-benzylic ring (FP IC_{50} of 0.55 µM, BrdU MCF7 IC_{50}= 0.8 µM) responsible for an additional hydrogen bond established with the carbonyl of MDM2 Val93 [106, 107]. Compound **43** was found later to have a synergistic outcome in association with doxorubicin, allowing the visualization of doxorubicin-mediated *in vivo* activity in a xenograft model at doses that are inactive in a monotherapy treatment [108].

More recently, two new scaffolds based on the principle of bioisosterism of BDP have been reported: 1,4 thienodiazepine-2,5-diones (TDZ) [109] and thio-benzodiazepines (Figure 1.13) [110, 111]. For TDZ it has only been reported a cell-free binding screening, emerging compound **44** as lead compound with a FP Ki of 40 µM [109]. The synthesis and biological evaluation of thio-benzodiazepines showed that the simple replacement of the oxygen by a sulfur atom increased potency in a FP binding assay, but not in cell-based evaluation. In this SAR study compound **45** emerged as a potential lead compound for future optimization with a FP Ki of 5.34 µM and MTT U-2OS IC_{50} of 1.06 µM [110]. Continuation of this work showed compounds with better affinity to MDM2, but without cell-based assay improvement [111]. Last year new benzodiazepine analogues were reported, but without showing potency improvement (best derivative, **46**, FP Ki= 0.2 µM, MTT U-2OS IC_{50}= 3.12 µM) [112]. Furthermore, these new scaffolds derivatives did not show selectivity towards cells with wild-type p53 as observed for 1,4-benzodiazepine-2,5-

dione derivatives (e. g. compound **43** is 10 times more selective, MCF-7 vs MDA-MB-231 [107]).

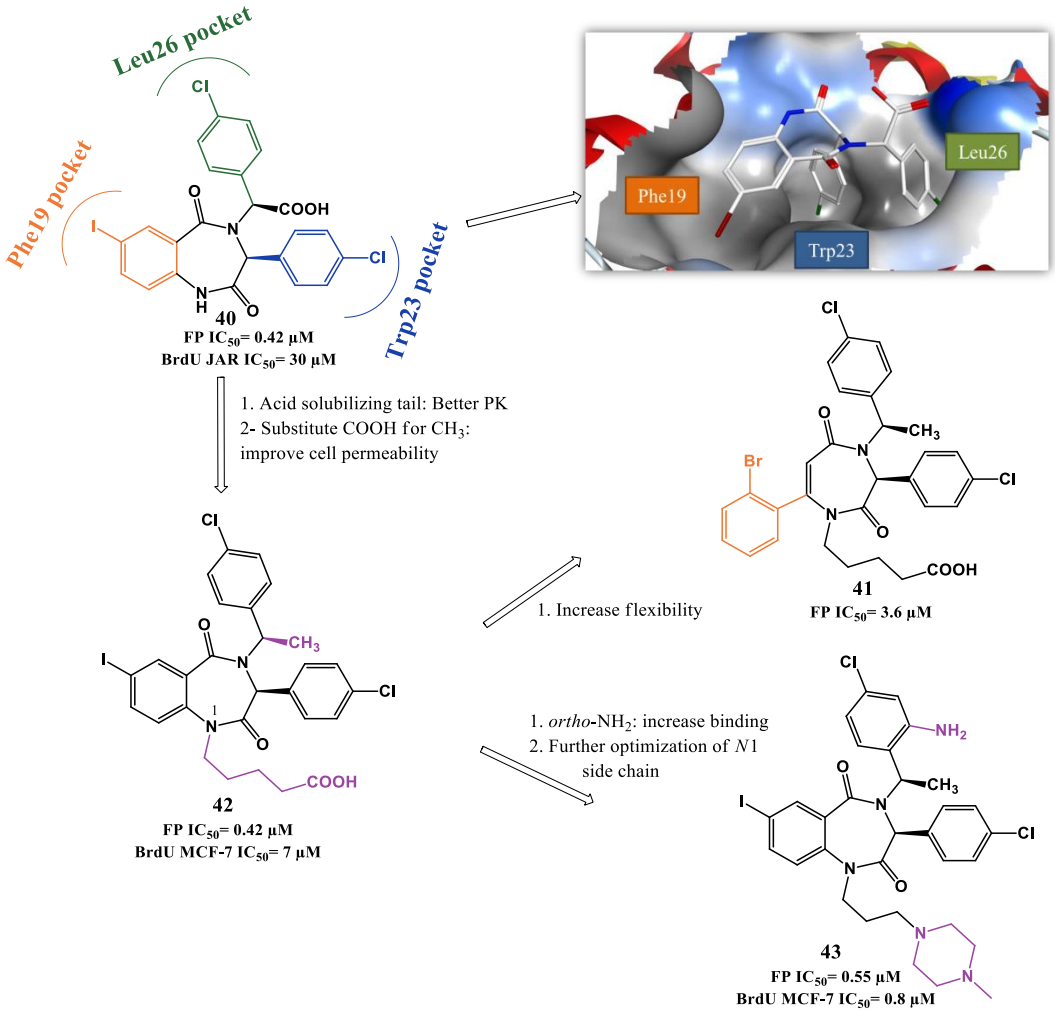

Figure 1.12. Benzodiazepinediones scaffold optimization. Right upper quadrant: crystal structure of compound **40** bound to MDM2 (PDB 1T4E). MDM2 surface is colored in blue for hydrophilic areas and grey for hydrophobic areas. Compound **40** is depicted in stick model and is colored according to element type: white for carbon atoms, blue for nitrogen atoms, red for oxygen atoms, dark red for the iodine atom, and green for chlorine atoms.

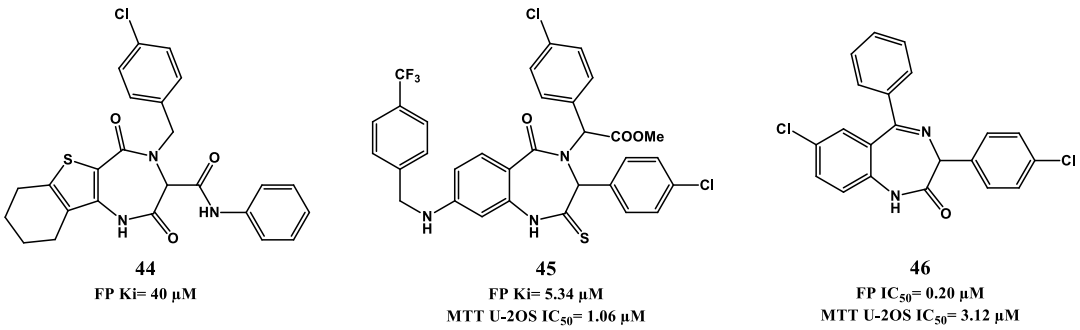

Figure 1.13. Examples of benzodiazepinediones derivatizations.

1.2.1.7. ISOINDOLINONES

Hardcastle *et al* described inhibitors of the p53-MDM2 interaction based on an isoindolinone scaffold. Compounds bearing this template were first identified (**47a,b**, Figure 1.14) as modest inhibitors of the p53–MDM2 interaction (IC_{50} ~ 200 μM) in an *in vitro* p53-MDM2 binding assay screening study. In a first optimization approach, a small compound library focused on the isoindolinone core was synthesized guided by *in silico* ligand-design, using published MDM2 crystal structure. Compound **48** emerged as a lead compound with an IC_{50} of 5.3 μM in a cell-free ELISA binding assay. It was also shown that compound **48** induced a dose-dependent increase of p53 transcriptional activity in SJSA-1 cancer cell line [113, 114]. In this first study, it was suggested that the introduction of different substituents into the isoindolinone template allowed different orientations of the inhibitors in the hydrophobic MDM2 pocket making consequently SAR studies more difficult to interpret. This statement was later corroborated by NMR experiments in which it was identified four different binding modes in twelve isoindolinone compounds analyzed differing only in one group attached to the isoindolinone scaffold [115].

Having in consideration the different binding modes and structure information gained by the NMR experiments, compound **49** (ELISA IC_{50}= 15.9 μM) was selected as lead compound for further optimization. The binding mode model of this compound suggested that introducing rigidity to the alkoxy side chain and adding substituents to the *N*-benzyl moiety could favor interaction with MDM2, giving rise to compound **50** (ELISA IC_{50}= 0.17 μM, SRB SJSA-1 IC_{50}= 5.2 μM) [116, 117]. In the last study published by this group attempts of increasing potency were made through modifications in the aromatic ring of the isoindolinone core, revealing that the introduction of a 4-chloro in isoindolinone ring improved binding [**51(-)**, IC_{50}= 0.044 μM, SRB SJSA-1 IC_{50}= 3.7 μM] [118]. Furthermore opposing to compound **50**, compound **51** showed selectivity (3- to 4-fold) towards cells with wild-type p53.

Recently, Santos group (iMed.ULisboa) reported that oxazoloisoindolinones, a more rigid isoindolinone derivatives, are potential inhibitors of p53-MDM2 interaction in a yeast-based assay (**52**, SRB HCT116 $p53^{+/+}$ IC_{50}= 9.7 μM, Figure 1.15). Compound **52** is capable of inducing a p53-dependent activation *in vitro* leading to apoptosis [119].

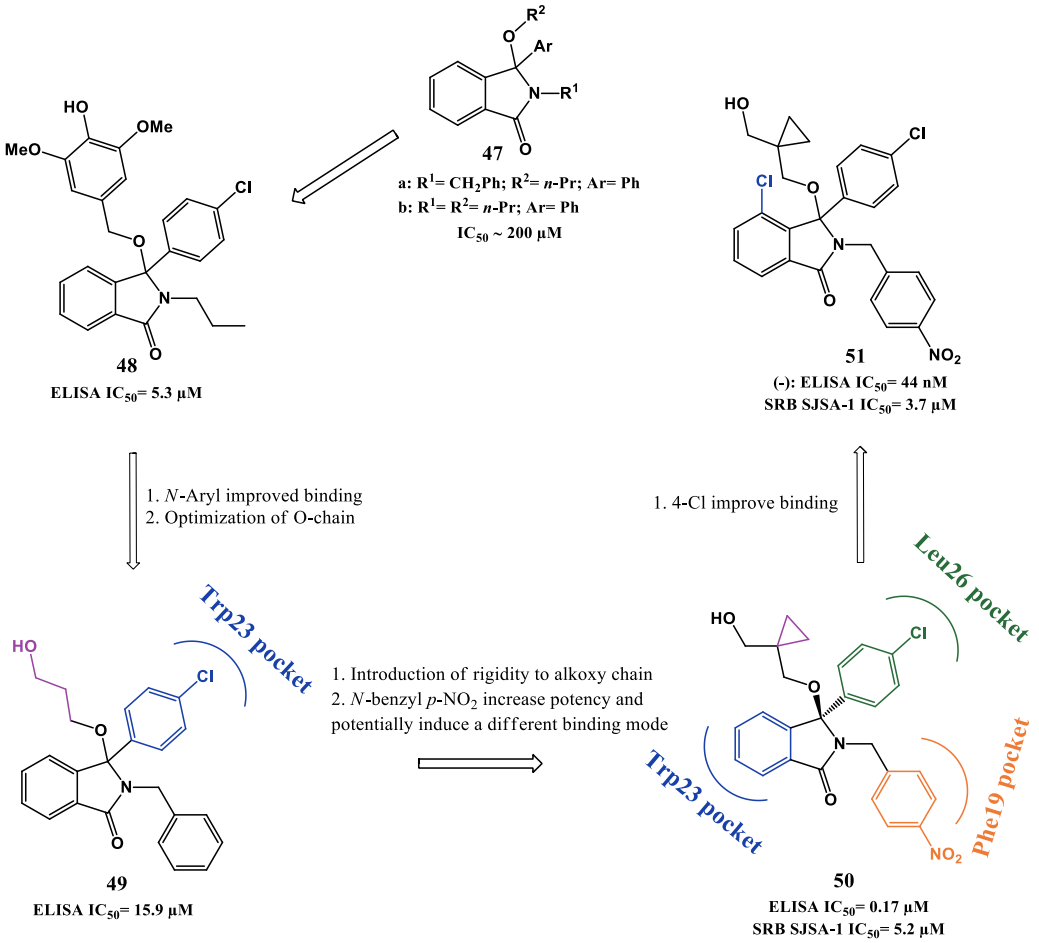

Figure 1.14. Isoindolinone scaffold optimization. Representations of binding modes were determined from chemical shift data and molecular docking [115, 116].

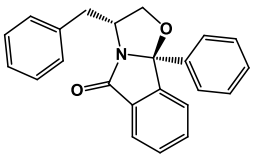

52
SRB HCT116 $p53^{+/+}$
IC_{50}= 9.7 µM

Figure 1.15. Oxazoloisoindolinone derivative **52**.

1.2.1.8. CHROMENOTRIAZOLOPYRIMIDINES

Chromenotriazolopyrimidines were found by Amgen to be inhibitors of p53-MDM2 in a HTRF-based high throughput screen of about 1.4 million compounds, and their binding to MDM2 confirmed by SPR. From this screening emerged hit compound **53** (Figure 1.16) [120]. Only *syn*-(6R,7S) isomer was found to be active (HTRF IC_{50}= 1.23 µM). Cocrystallization of **53** with MDM2 showed that the chromenotriazolopyrimidine is a fairly rigid scaffold from which two *para*-bromophenyl groups at C-6 and C-7 in a *syn* relationship interact with MDM2 in $Trp23_{(p53)}$ and $Leu26_{(p53)}$ pockets, respectively. Furthermore the C-7 aromatic group also establishes a weak π-stacking interaction with

His96 side chain of MDM2. The third key p53 amino acid Phe19 is mimicked by chromene D ring.

It was observed that these compounds were chemically unstable and individual diastereoisomers tended to equilibrate, forming mixtures consisting mostly of the more stable *anti* diastereoisomers. This problem was surpassed by *N*11-methylation, which prevented racemization without affecting the potency. Optimization of the lead compound was attempted by introducing variability to the three phenyl rings involved in the binding. Introduction of a methoxy group in position 1 gave the best cell-free activity (**54**, HTRF IC_{50}= 0.20 µM). However, it is believed that this improved activity is product of the molecule core torsion due to *N*-methyl and C1-methoxy proximity that allows a better pocket fitting rather than a improve interaction to the protein by the methoxy group [120].

To enhance PK properties, especially problems observed with metabolic stability hypothesized due to rapid *N*-demethylation and consequent tautomeric isomerization, SAR studies were performed at the *N*-substituent. It lead to compound **55** (HTRF IC_{50}= 0.35 µM, SJSA-1 p21 IC_{50}= 12 µM), with increase metabolic stability [121] .

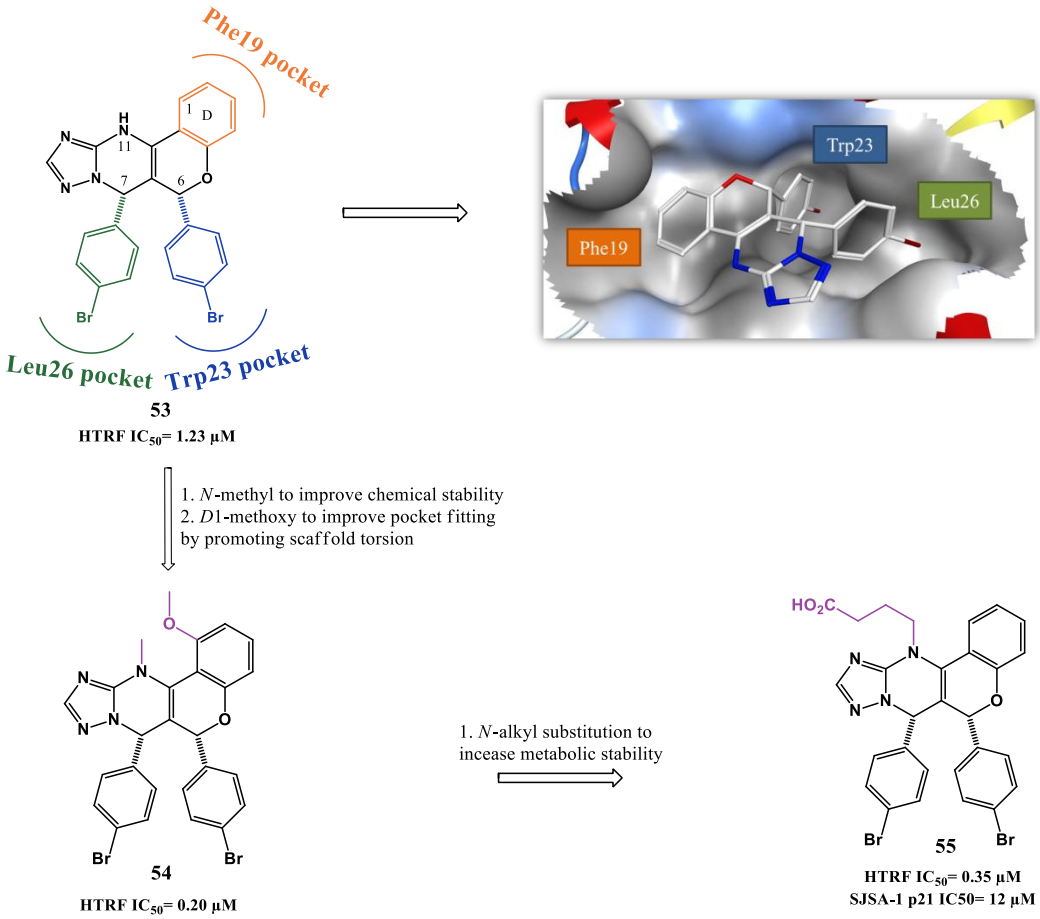

Figure 1.16. Chromenotriazolopyrimidines scaffold optimization. Right upper quadrant: crystal structure of compound **53** bound to MDM2 (PDB 3JZK). MDM2 surface is colored in blue for hydrophilic areas and grey for hydrophobic areas. Compound **53** is depicted in stick model and is colored according to element type: white for carbon atoms, blue for the nitrogen atom, red for the oxygen atom, and dark red for bromine atoms.

1.2.1.9. 3-IMIDAZOYL INDOLES AND OTHER INDOLYL DERIVATIVES

Compounds detaining an imidazole-indole scaffold were simultaneously and independently developed by Novartis and University of Pittsburgh, with the latter publishing in 2010 [122, 123]. In this family two compounds have emerged, WK23 (**56**, FP IC_{50}= 1.71 μM, Figure 1.17) and WK298 (**57**, FP IC_{50}= 0.19 μM). The two molecules only differ by the substituent attached to position 2 of the 6-chloroindole moiety and consequently the central core that mimics p53 is the same. As already observed for other MDM2 inhibitors, co-crystal structure reveal that 6-chloroindole ring mimics the p53 Trp23 with the 6-chloro substituent enhancing the interaction by penetrating deeply in the pocket. Moreover, the indole nitrogen atom forms hydrogen bond with Leu54. *Para*-chlorobenzyl group fills Leu26 pocket and phenyl group interacts with $Phe19_{(p53)}$ pocket. The additional tail in **57** enhances not only PK properties but also protects $Phe19_{(p53)}$ pocket from solvent [123].

The recognizing that an indole/oxindole moiety function as an excellent Trp23 mimetic moiety gave rise to several other potential good compounds (e.g. **58**, FP KI= 400 nM and **59**, HTRF IC_{50}= 1.16 nM) [64, 124].

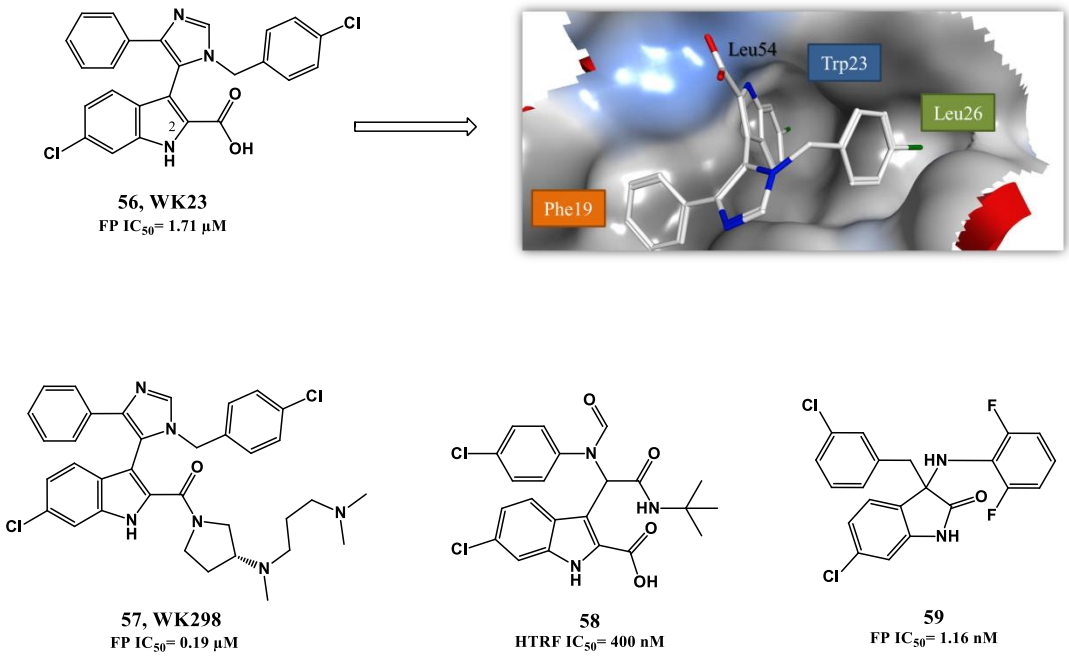

Figure 1.17. Indolyl derivatives. Right upper quadrant: structure of compound **56** bound to MDM2 (PDB 1YCR). MDM2 surface is colored in blue for hydrophilic areas and grey for hydrophobic areas. Compound **56** is depicted in stick model and is colored according to element type: white for carbon atoms, blue for nitrogen atoms, red for oxygen atoms, and green for chlorine atoms.

1.2.1.10. OTHER COMPOUNDS

Several other inhibitors or potential inhibitors of p53-MDM2 interaction have been reported throughout the years (Table 1.2, Figure 1.18).

Table 1.2. Other inhibitors or potential inhibitors of p53-MDM2 interaction

COMPOUNDS	CELL-FREE ASSAY (IC_{50})	CELL-BASED ASSAY (IC_{50})	REF.
- **Chalcones**	ELISA IC_{50}= 49 µM	-	[125-127]
- **Dihydroisoquinolinones** (**60**)	TR-FRET IC_{50}= 2.3 nM	SJSA-1 IC_{50}= 1.2 µM	[128]
- **Terphenyl derivatives** (**61**)	ELISA Ki= 0.18 µM	-	[129, 130]
- **Benzothiazole-hydrazone** (**62**, NSC333003)	ELISA IC_{50}= 13 µM	-	[131]
- **Pyrrolidones** (**63**)	FP IC_{50}= 0.09 µM	-	[132, 133]
- **Pyrrolo[3,4-*c*]pyrazoles** (**64**)	FP IC_{50}= 83 nM	MTT A549 IC_{50}= 5.82 µM	[134, 135]
- **Piperidines** (**65**)	FP IC_{50}= 41 nM	MTT SJSA-1 IC_{50}= 1 µM	[136-138]
- **3-benzylideneindolin-2-ones** (**66**)	FP Ki= 93 nM	MTT HCT116 $p53^{(+/+)}$ IC_{50}= 13.42 µM	[139]
- **Bisarylsulfonamides** (**67**)	ELISA IC_{50}= 3.5 µM	-	[34, 140]
- **Norcamphanes** (**68**)	-	-	[141]
- **8-hidroxiquinoline** NSC66811(**69**)	FP Ki= 0.12 µM	-	[142]
- **Pyridine derivative** (**70**)	FP Ki= 0.11 µM		[143]
- **Diphenylthiophenes** (**71**)	FP IC_{50}= 2.08 µM	SRB HCT116 $p53^{(+/+)}$ IC_{50}= 0.24 µM	[144]
- **Pyrazoles** (**72**)	FP IC_{50}= 6.56 µM	-	[145, 146]
- **Pyrrolidine-pyrimidines** (**73**)	FP IC_{50}= 5.2 µM	-	[147]
- **Imidazoles** (**74**)	TR-FRET IC_{50}= 2 nM	SJSA-1 IC_{50}= 0.5 µM	[148]
- **Natural products**:			[149]
- **Chlorofusin**	ELISA IC_{50}= 4.6 µM	-	[150-152]
- **(-)-hexylitaconic acid**	ELISA IC_{50}= 233.4 µM	-	[153]
- **Hoiamide D**	HTR-FRET IC_{50}= 4.5 µM	-	[154]
- **Siladenoserinol A**	ELISA IC_{50}= 2.0 µM	-	[155]
- **Xanthones**	-	-	[156, 157]
- **Ganoderic acids**	Only virtual screening results reported		[158]

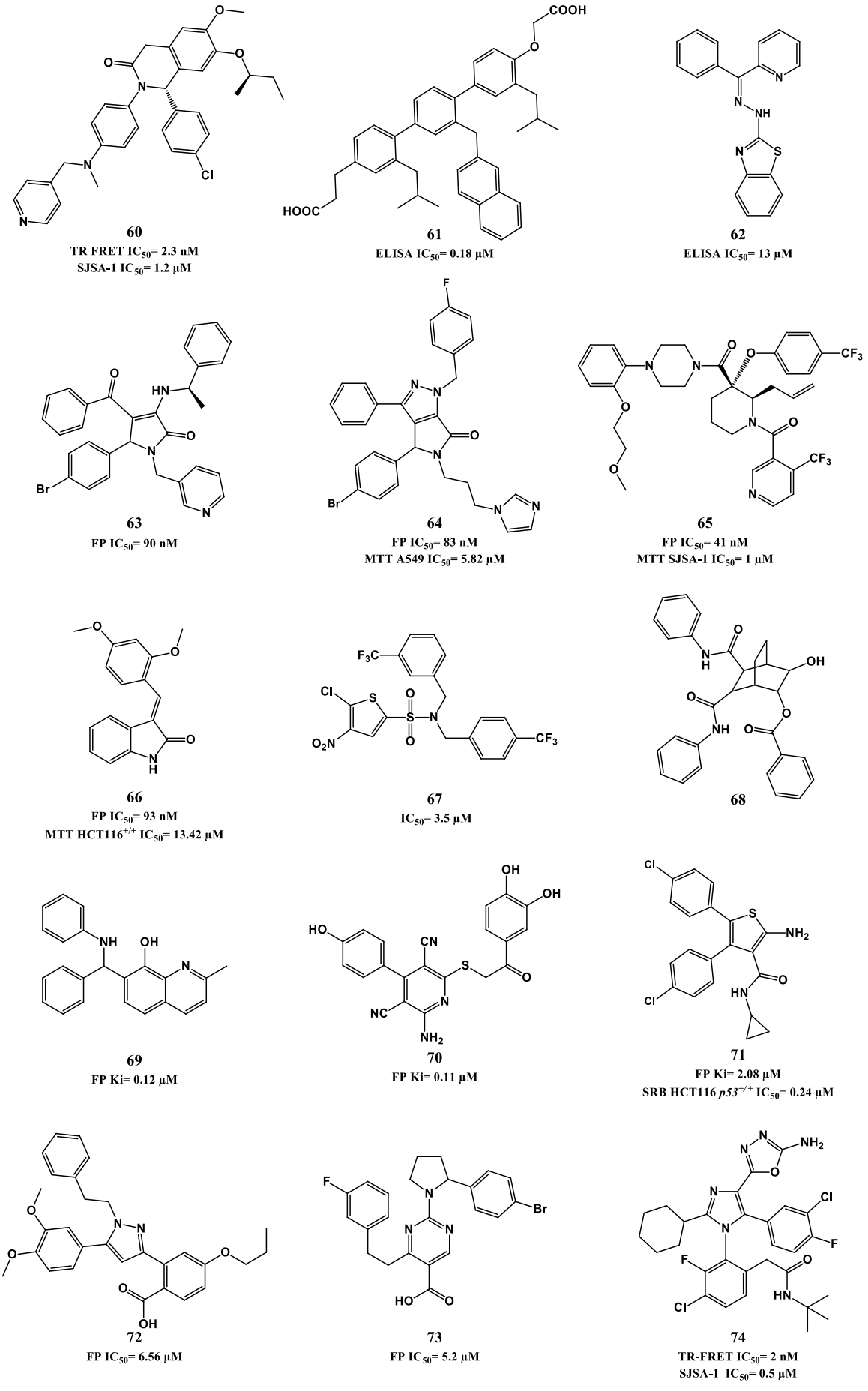

Figure 1.18. p53-MDM2 interaction inhibitors.

1.2.2. INHIBITION OF E3 LIGASE ACTIVITY OF MDM2

Proteasome-mediated degradation is an important mechanism that allows cells to renew their intracellular proteins and preserve protein homeostasis. Consequently a deregulation in this process can favor the stabilization of oncoproteins or favor the degradation of tumor suppressors, leading to cancer development [159, 160]. Targeting specific proteins for ubiquitin-mediated proteasome degradation is carried out by E3 ubiquitin ligases and, as already described previously for p53, that labeling is mainly credited to MDM2. Therefore targeting directly the E3 ligase activity of MDM2 can be of interest [161].

Lai *et al* published in 2002 the first compounds inhibitors of MDM2 E3 ligase activity, discovered in an *in vitro* biochemical enzyme assay (e.g. **75**, IC_{50}= 3.2 µM, figure 1.19) [162]. Later a new family of compounds was described by Weissman group [163-165]. Their first compounds (5-deazaflavins, HLI98C-E) were obtained in a high-throughput screening for E3 ligase inhibitors and later optimized mainly due to PK shortages giving rise to HLI373 (**76**). They also described sempervirine (**77**) a natural product as a MDM2 E3 ligase inhibitor [166]. Furthermore natural products extracts screenings gave rise to several other hits (e.g. **78**) [167, 168]. In a cell-based ubiquitination assay, compounds MEL23 and MEL24 (**79**) were found to inhibit MDM2 and p53 ubiquitination in cells, through inhibition of E3 ligase activity of MDM2-MDMX complex. It is believed that this complex has a better ligase activity for p53 than MDM2 alone [169].

Unlike p53-MDM2 interaction inhibitors, this mechanism of action leads initially to increase levels of both p53 and MDM2 without promoting their interaction disruption. Therefore one problem that can be envisioned by this mechanism of action is that p53 transcriptional activity can be somewhat impaired or at least not complete. Nevertheless endogenous MDM2 inhibitor p14ARF also prevents ubiquitination without disrupting the interaction, and it is still capable of promoting p53 stabilization and activation, validating the potential of this target. From all compounds mentioned, only **75** was found to inhibit MDM2-mediated p53 ubiquitination without interfering with MDM2 autoubiquitination. This can represent an advantage and potentially attenuates the previous concern of an inadequate p53 activation that can be attributed to this approach.

Serdemetan (JNJ-26854165, **80**) is a tryptamine derivative developed by Johnson&Johnson and it was initially suggested that it blocked p53-MDM2 complex binding to the proteasome, preventing p53 degradation. However, more recent additional evidences suggest that others mechanisms of action are also taking place [170, 171]. Serdemetan is capable of inducing p53-mediated apoptosis, but activates p53-independent pathways, such as E2F1-mediated apoptosis as well. Interestingly, this compound induces p21 proteasome degradation, enhancing therefore its apoptotic effect [172]. In several

cancer cell lines (wt and mut p53), this compound showed a range of IC_{50} from 0.25 to 3 μM [173]. This compound is in clinical trials.

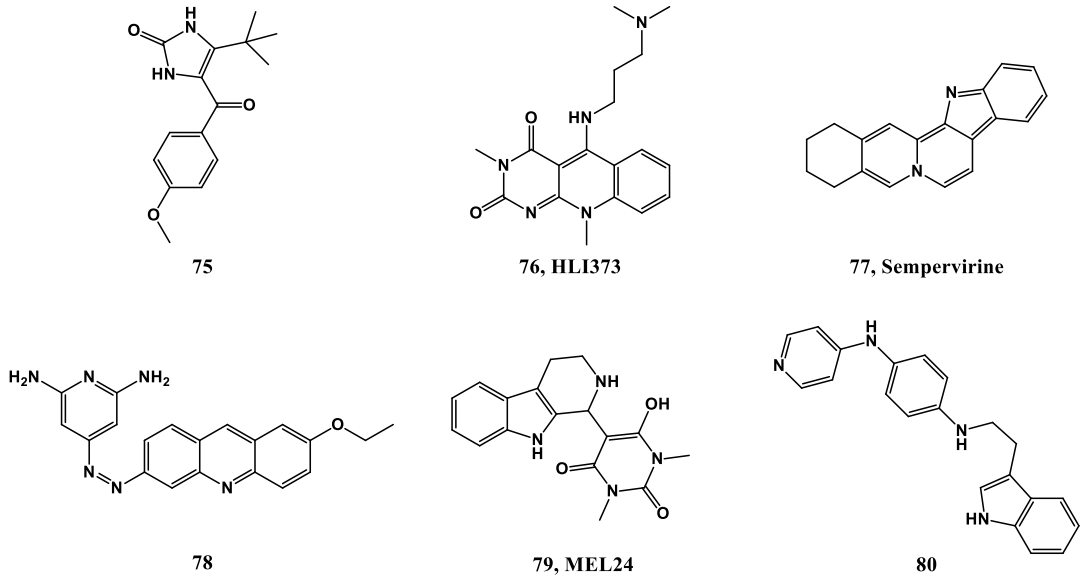

Figure 1.19. MDM2 E3 Ligase activity inhibitors.

1.2.3. MDMX AND DUAL MDM2/MDMX INHIBITORS

Although MDM2 is the foremost negative regulator of p53, MDMX has been recognized more recently as a critical discrete p53 modulator, and in fact its overexpression is observed in several cancers [174, 175]. MDMX is structurally related to MDM2, but lacks its p53 ubiquitin-mediated degradation signal. However it is able to control p53 activity mostly by inhibiting p53 transcription function. In addition, MDMX protein levels are regulated by MDM2 ubiquitin-mediated degradation [176]. Since inhibiting p53-MDM2 interaction increase MDM2 levels by autoregulatory feedback loop, and therefore can facilitate MDMX degradation, the problem of MDMX presence could be lessened when targeting this interaction. However, although reduced MDMX levels are observed in many cancers after treatment with nutlin-3a, the effectiveness of the inhibitor can still be compromised, especially in tumors overexpressing MDMX [177].

The first small molecule inhibitor of MDMX (SJ-172550, **81**, Figure 1.20) was only published in 2010 by Reed *et al*. This compound was found to bind reversibly to MDMX in the p53 binding pocket, and showed cytotoxicity in MDMX-amplified retinoblastoma cell line Weri1 [178]. Further investigation revealed that compound **81**, through reversible covalent binding, seemingly locks MDMX into a conformation that is unable to bind p53. This complex mechanism of action was revealed to be dependent on several factors, limiting this compound as a feasible lead compound [179].

Compounds XI-006 (NSC207895) and XI-011 (NSC146109, **82**) were identified in a HTS assay as activators of p53-dependent transcription [180]. Their mechanism of action

was later unveiled to involve inhibition of MDMX expression, by repressing *MDMX* promoter and subsequent down-regulation of its mRNA [27, 181]. Recently it was also suggested that XI-011 was capable of disrupting the p53-MDMX interaction [182].

Although initially some reports demonstrated the beneficial aspect of inhibiting MDMX alone, specially due to its lower toxicity to normal tissues [177], it is now recognized that a full p53 activation outcome is favored and more likely to be achieved with dual inhibition of MDM2 and MDMX. Compounds possessing an imidazo-indole scaffold revealed to be dual inhibitors (e.g. WK298, **57**, MDM2 FP IC_{50}= 0.19 µM; MDMX FP IC_{50}= 19.7 µM, Figure 1.17), and represents the first co-crystal structure of MDMX with an inhibitor published [123]. As expected, the main aspects that need to be addressed for an adequate inhibition of both proteins lies in the three subpockets $Phe19_{(p53)}$, $Trp23_{(p53)}$ and $Leu26_{(p53)}$. The difficulty of dual inhibition seems to be attributed mainly to $Leu26_{(p53)}$ pocket, which is quite different in the two proteins, and may be the reason for a much weaker binding observed for most of the known MDM2 inhibitors. From this observation it can be assumed that the common feature of possessing a chorophenyl group, although ideal for MDM2, is not optimal for mimicking p53 Leu26 interaction with MDMX.

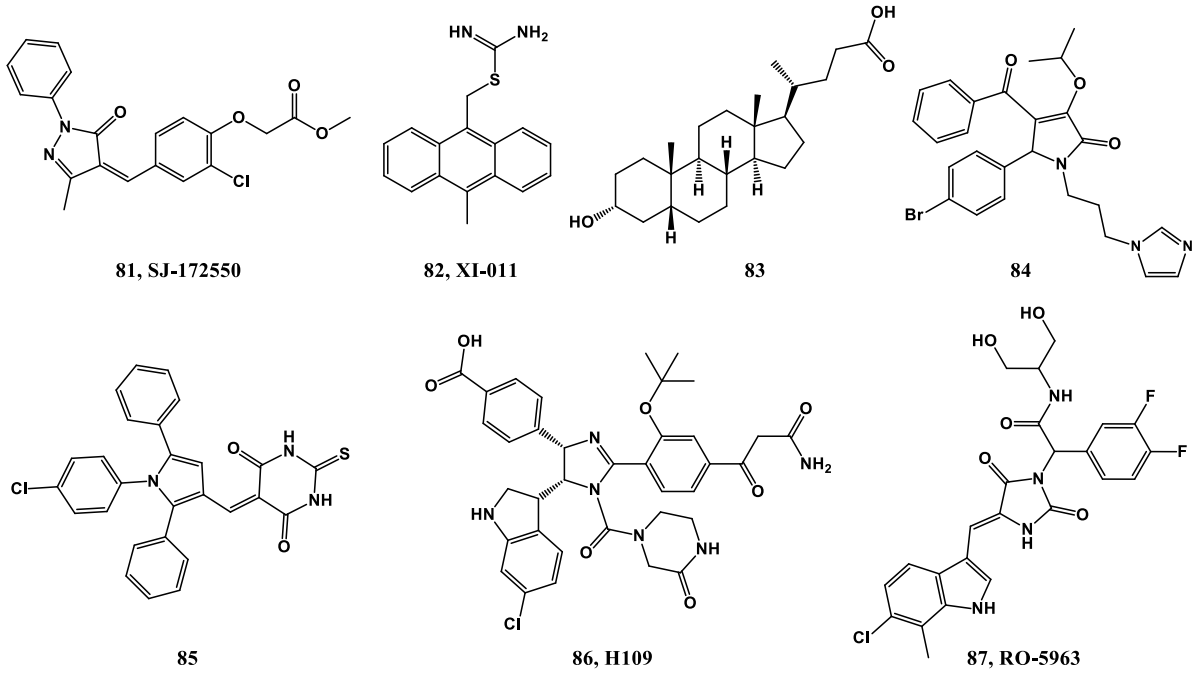

Figure 1.20. MDMX and dual MDM2/MDMX inhibitors.

Other compounds have since emerged, such as endogenous steroidal bile acid lithocolic acid (**83**, MDM2 FP IC_{50}= 66.0 µM; MDMX FP IC_{50}= 15.4 µM, Figure 1.20) [183], pyrrolidones (**84**, MDM2 FP IC_{50}= 0.26 µM; MDMX FP IC_{50}= 2.68 µM) [132], triaryl-pyrroles (**85**, MDM2 FP IC_{50}= 0.11 µM; MDMX FP IC_{50}= 4.2 µM) [184],

imidazolines (HI109: **86**, MDM2 FP IC_{50}= 6 nM; MDMX FP IC_{50}= 27 nM) [185], and indolyl hydantoins (RO-5963: **87**, MDM2 TR-FRET IC_{50}= 17 nM; MDMX TR-FRET IC_{50}= 25 nM). RO-5963 disrupts both p53-MDM2 and p53-MDMX and promotes the formation of homo and/or heterodimeric protein complexes that are held together by two molecules of the inhibitor. This compound was able to restore p53-transcription activity in several p53 wild type cell lines, including MDMX-overexpressing cell lines resistant to nutlin-3a [186].

1.2.4. TARGETING UPSTREAM REGULATORS

Instead of inhibiting MDM2 and/or MDMX directly, other strategies can be focused on upstream factors that regulate their stability, expression and activity. One of the early events that lead to p53 signaling pathway activation is nucleolar disruption triggered in response to cellular stress [187]. This nucleolar disturbance promotes the release of free ribosomal proteins such as L5 and L11, that can sequester MDM2, leading consequently to p53 activation [188]. Moreover, nucleolus is responsible for ribosome biogenesis, and since this process is upregulated in cancer cells due to their increase of protein demand, targeting nucleolar activity can be useful [189]. Indeed, low nongenotoxic doses of actinomicyn D [190], and compound BMH-21 (**88**, Figure 1.21) promote activation of p53-dependent apoptotic signaling. They bind to GC-rich regions of DNA, in particular rDNA, impairing RNA polymerase I (Pol I) function. Consequently it will lead to perturbations of ribosomal RNA biosynthesis, while triggering nucleolar segregation and the chain of events previously described. Moreover, unlike actinomicyn D, BMH-21 showed selectivity by inducing a cancer-specific activation of p53 [191, 192]. This selectivity is also achieved by compound CX-5461 (**89**) that inhibits Pol I transcription initiation step [193, 194]. The cyclin-dependent kinase (CDK) inhibitor roscovitine (**90**) also inhibits rRNA processing, disrupts the nucleolus and can promote down-regulation of MDM2 at protein and mRNA level [195, 196]. Several others DNA-targeting compounds can also activate p53. For example, by intercalating with DNA, curaxins (e.g. CBLC-137: **91** [197]), increase the affinity of chromatin towards FACT (Facilitates Chromatin Transcription), trapping it. The depletion of FACT causes transcription suppression leading to inhibition of NF-κB pathway that normally is up-regulated in cancer environment. It also leads to p53 activation by promoting phosphorylation at Ser392 by FACT-associated casein kinase 2 (CK2) that prevents its MDM2-mediated degradation [198].

p53 activation can also be achieved by targeting nucleus export processes. Exportin-1 protein (XPO1, also known as CRM1) is responsible for exporting from the nucleus several vital cell signaling modulators, including p53. An increase of nuclear export versus import will render these modulators in the cytoplasmatic compartment, preventing their transcription activities, and potentially leading, for instance, to

inactivation of apoptosis. Therefore inhibiting XPO1 can potentially restore tumor suppressor functions. The first inhibitor of XPO1, leptomycin B (**92**), was capable of inducing apoptosis, but revealed to be toxic in *in vivo* studies. Since then semi-synthetic derivatives, more potent and less toxic were synthesized [199], as well as other compounds, such as CBS9106 (**93**) that decreases XPO1 protein through proteasomal degradation [200]. The small molecule XPO1 inhibitor selinexor (KPT-330: **94**), among others selective inhibitors of nuclear export (SINEs) are currently in clinical trials [201].

MLN4924 (**95**) is a small molecule inhibitor of the NEDD8-activating enzyme (NAE) that entered phase I clinical trials. By inhibiting NAE, it prevents ubiquitination and proteasomal degradation mediated by cullin-RING ubiquitin E3 ligases (CRLs) on several substrates. The overall network of effects is still not clear, but CRLs are implicated in p53 ubiquitination [202] and indeed p53 up-regulation is observed [203, 204]. Recently it was found that the previous described XPO1 inhibitor CBS9106 induced XPO1 degradation through CRL and neddylation pathway, opening new insights about the potentialities of interfering with this pathway [205].

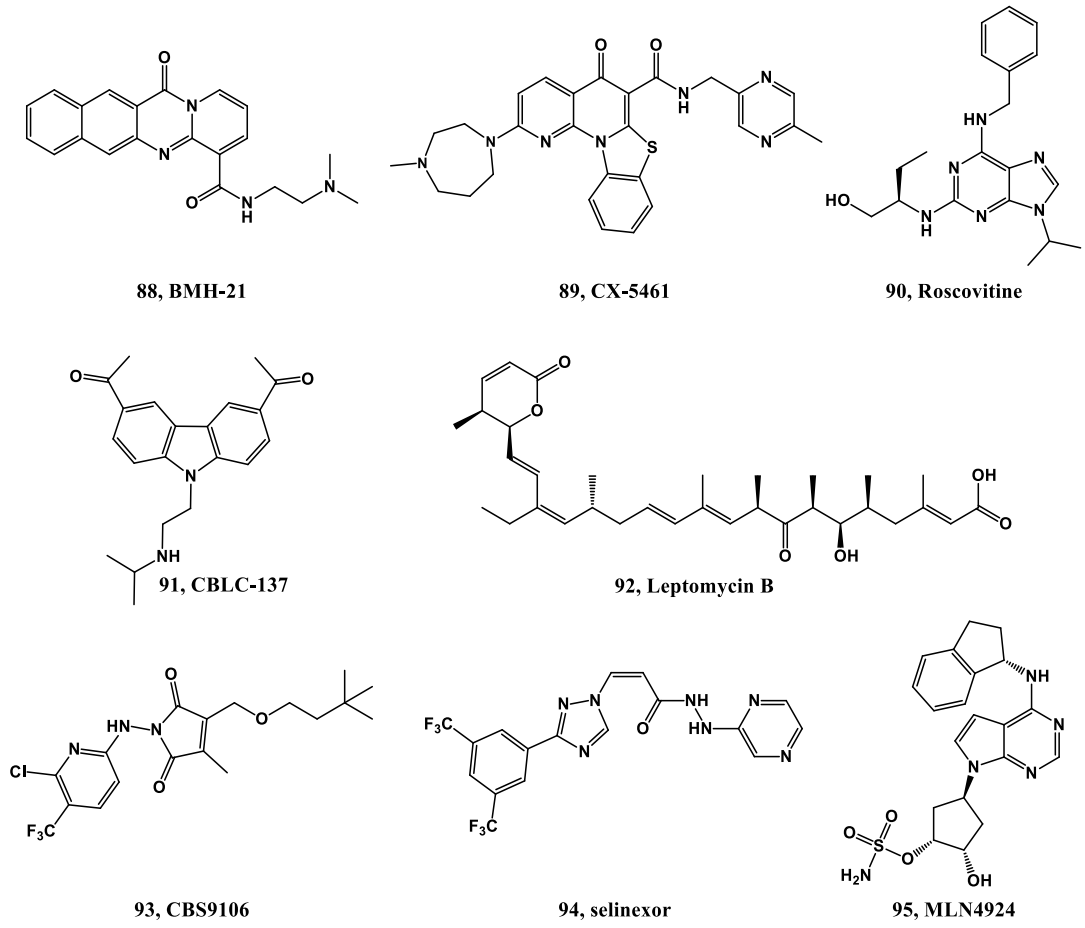

Figure 1.21. Compounds that target upstream regulators of p53 activating pathway.

It is necessary to have in consideration that all of these compounds described in this section act on targets that will not only affect the p53 signaling pathway, but also several others. Consequently some of them are also active in cancers with impaired p53 function.

1.2.5. SIRTUINS INHIBITORS

As already discussed, wild-type p53 in a cancer environment is often deactivated by overexpression of its suppressors, namely MDM2 and MDMX. Other relevant suppressors are histone deacetylases (HDACs), and in particular SIRT1 that can be highly expressed in cancer cells due to loss of its repressor HIC-1, keeping p53 in a deacetylated status. This status can be prooncogenic because acetylation of p53 leads to its activation by: (*i*) promoting p53 stabilization via preventing ubiquitination at the same sites; (*ii*) inhibiting MDM2/MDMX repressive complex formation on target gene promoters; and assembling cofactors that endorse p53 transcriptional activation. Therefore, deacetylated p53 in cancer cells will primarily favor MDM2-mediated degradation by ubiquitination, impairing p53 activity [206, 207].

Throughout the years several sirtuin deacetylase inhibitors were described in the literature, most of them inhibitors of both SIRT1 and SIRT2 isoforms: sirtinol (**96**, Figure 1.22), salermide (**97**) and their derivatives [208-211]; cambinol (**98**) and analogues [212-215]. Splitomicin (**99**) and analogues [216-219], and EX527 (**100**) and derivatives [220, 221] are more selective towards SIRT2 and SIRT1, respectively. Tenovins were the first compounds inhibitors of SIRT1 and SIRT2, with a well-documented proof-of-concept anticancer activity, including *in vivo* efficacy (tenovin-6: **101**), fully validating these targets as promising anticancer strategy [222]. Later, inauhzin was reported to be a better inhibitor than tenovins and specific towards SIRT1 (**102**, WST-8 HCT116 $p53^{(+/+)}$ IC_{50}= 2.0 μM), and also more selective between cancer and normal cells [223].

Although as mentioned targeting SIRT1 already proved to be valuable in some cancers, its role is still quite questioned, since depending on the malignancy it can be found overexpressed or reduced. For instance SIRT1 deacetylation of p53 and of oncogene *β*-catenin can represent tumor promoter and tumor suppressor effects, respectively. Furthermore SIRT2, initially found to be less important, is also being implicated in cancer development. Therefore the benefit of using a sirtuin inhibitor (specific isoform or dual inhibitor) will be dependent on the type of targeted tissue and cancer [224, 225].

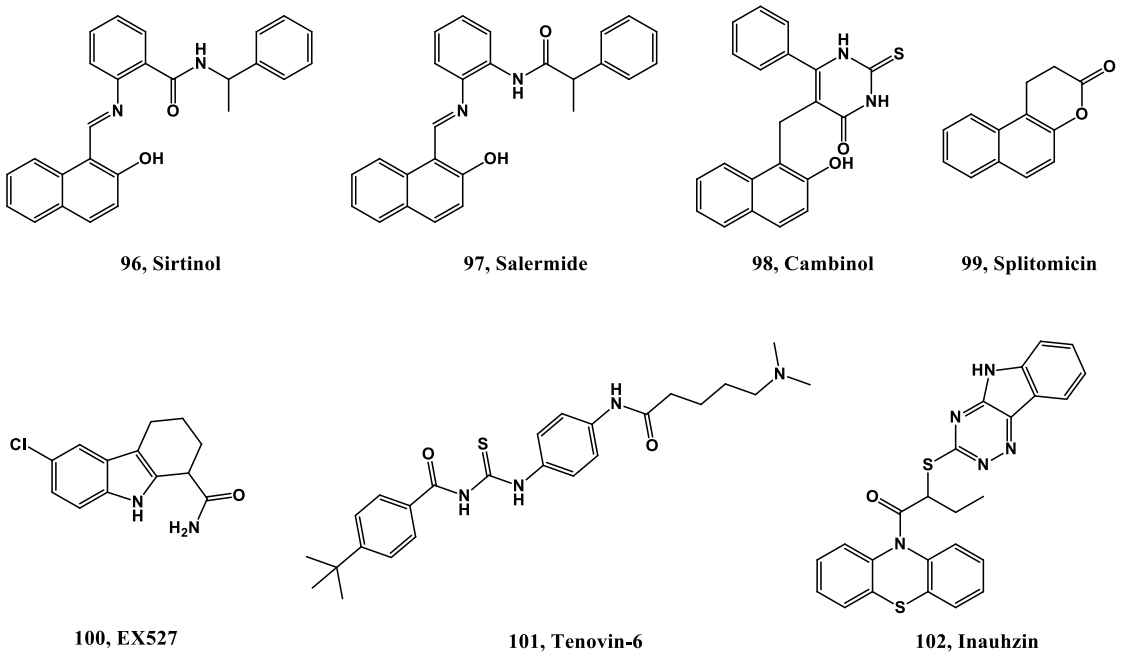

Figure 1.22. SIRT1and/or SIRT2 inhibitors.

1.2.6. S100B INHIBITORS

The calcium-binding protein S100B is overexpressed in malignant melanoma, representing a reliable cancer biomarker. S100B binds directly to p53 in a calcium-dependent manner, leading to reduction of p53 levels by blocking activating phosphorylation sites in the C-terminal, disrupting its oligomerization, and promoting its degradation. Since p53 remains wild-type in melanoma, targeting this interaction can be useful to restore p53 function [226, 227]. Several inhibitors that targets S100B have already emerged such as: pentamidine (SBi1: **103**, Figure 1.23) [228], SBi523 (**104**) [229], **105** [230] and SC1982 (**106**) [231].

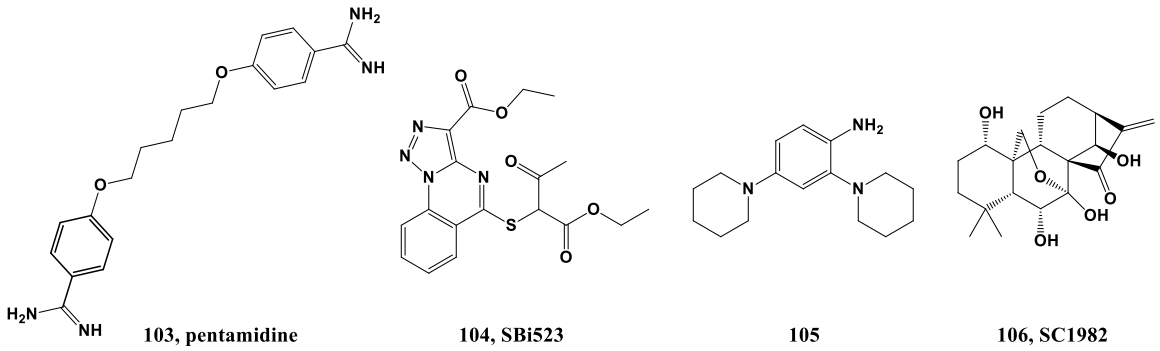

Figure 1.23. p53-S100B interaction inhibitors.

1.2.7. p53-Targeting Compounds

In 2004, as a result of a chemical library screening, a compound named RITA (Reactivation of p53 and Induction of Tumor Cell Apoptosis, **107**, Figure 1.24) was identified to suppress selectively HCT116 cell line expressing wild-type p53 over the p53 null counterpart cell line. Opposing to p53-MDM2 interaction, it was proposed that RITA binds to the p53 *N*-terminal domain, inducing a conformational change that prevents its binding to MDM2, thus restoring p53-transcriptional activity [232, 233]. Interestingly, more recently RITA's mechanism of action was extended to cell lines presenting mutated p53. Presumably the binding to mutated p53 might affect the core domain folding in a way that potentially restore its DNA binding ability [234]. This dual targeting increases the application scope of RITA turning it into a very promising lead compound to rescue p53 regardless of the nature of its inactivation [235]. In addition, RITA can promote down-regulation of MDMX selectively in wild-type cancer cells through a pathway independent of MDM2 [236]. Novel analogues slightly more active and selective have been already synthesized [237, 238].

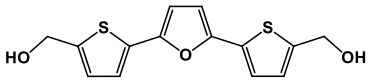

107

Figure 1.24. RITA.

1.2.8. Mutant p53 Reactivation

All strategies described so far are focused on restoring p53 function in a cancer cell environment that retains wild-type p53, but somehow impaired. However, p53 function perturbations are also observed in cancers as a result of point mutations to the *TP53* gene, representing the most frequent mutated gene observed in human cancers. Although in some cases such event can lead to loss of p53 protein expression, as a result of frameshift or nonsense mutations, more frequently it leads to a single amino acid substitution in the protein (missense mutations). These replacements take place more frequently within the DNA binding domain leading to loss or attenuation of wild-type p53 function. p53 mutants can generically be categorized into two groups: *contact mutants*, in which the amino acid replacement affects p53 ability to bind to DNA without significantly affecting its conformation; and *conformational mutants*, in which the substitution promotes a disruption of the normal p53 tertiary structure. However, the signaling outcome cannot be oversimplified in two possible outcomes, since different mutations can lead to different degrees of inhibition/ loss of p53 function, as well as to the acquisition of gain of function. This gain of function can further promote tumorigenesis, potentially leading to a more aggressive cancer profile. Gain of function by mutant p53 can be a consequence of the

activation of others signaling pathways, through interaction with other proteins, such as p53 family members p63 and p73, and indirectly affecting gene expression. The intricacy of this mutant p53 signaling disturbance effect is further amplified by the fact that different expression of its targets can be met in different tissues, potentially generating the variety of cancer phenotypes observed, even for the same point mutation [239, 240].

TABLE 1.3. Therapy strategies when p53 is mutated in cancers.

- **RESTORING WILD-TYPE P53 FUNCTION**		**REF.**
·PhiKan083 ·PhiKan5196 ·PK7088 (**108**)	- Target Y220C p53 mutation. This mutation creates a druggable surface crevice that destabilizes the protein.	[241] [242] [243]
·PRIMA-1 ·PRIMA ^{MET} (APR-246, **109**)	- They are converted into compounds capable of forming adducts with mutant p53 cysteine residues. APR-246 is also able to restore mutant p63 function among others p53 homologues.	[244, 245]
·MIRA-1 (**110**) ·STIMA-1 (**111**)	- Probably act by reacting with thiols and amino groups in p53	[246] [247]
·Stictic acid (**112**)	- Predicted to bind to p53 L1/S3 pocket in the core domain. This pocket might also be targeted by PRIMA active products, MIRA and STIMA.	[248]
·CP-31398 (**113**)	- Reactivate mutant p53 and inhibits p53 ubiquitination and degradation.	[249, 250]
·SCH529074 (**114**)	- Binds to p53 core domain and it is believed to acts as chaperone, not binding covalently to p53. It also inhibits MDM2-mediated ubiquitination.	[251]
·NSC319726 (ZMC1, **115**)	- Functions as zinc metallochaperones, providing an optimal concentration of zinc to p53, promoting proper folding of p53-R175H.	[252, 253]
- **PROMOTION OF MUTANT P53 DEGRADATION**		
·Vorinostat (SAHA, **116**)	- SAHA is a histone deacetylase inhibitor and can destabilize the complex formed between HSP90 and mut p53. This complex inhibits E3 ubiquitin ligases MDM2 and CHIP, causing mut p53 stabilization.	[254]
- **INTERFERENCE WITH THE INTERACTION BETWEEN MUTANT P53 AND OTHER PROTEINS**		
·RETRA (**117**) ·NSC176327 (**118**)	- Promote the release of p73 protein from the blocking complex with mutant p53. NSC176327 is a derivative of ellipticine.	[255] [256]

A variety of small-molecule therapy strategies can be devised when dealing with mutant p53, such as: (*i*) reactivation of wild-type p53 function; (*ii*) interference with the interaction between mutant p53 and other proteins; (*iii*) promotion of mutant p53 degradation; and (*iv*) downstream interference in the mutant p53 signaling pathways (Table 1.3, Figure 1.25). The mechanism of action for most of the compounds cited is still not

fully understood. Most of them also show p53-independent activity and cytotoxicity in cancers with wild-type p53 [20, 239, 240]. Compound APR-246 is in clinical trials and vorinostat is already being used in the clinic for treatment of cutaneous T cell lymphoma [257].

One of the main problems when dealing with chemotherapy is its toxicity to normal cells. Therefore finding drugs that can distinguish cancer cells from normal cells is very appealing. It was already mentioned in the beginning of this chapter that non-genotoxic strategies that focus on reactivating p53 can represent a step further in this direction, due to the fact that the outcome of p53 activation relies, among other factors, in the intracellular environment that *per se* is different in cancer and normal cells. In the case of tumors with mutated p53, p53 status represents an inherent difference between these two types of cells and therefore p53-based cyclotherapy can be a very useful strategy. In this approach, first it is given a pretreatment with a low dose of wild-type p53 activating molecule that can trigger a transient cell cycle arrest in normal cells, without affecting cancer cells. Then, by adding a conventional anticancer agent that targets S and M phase, cancer cells will selectively be triggered into an apoptotic outcome [258].

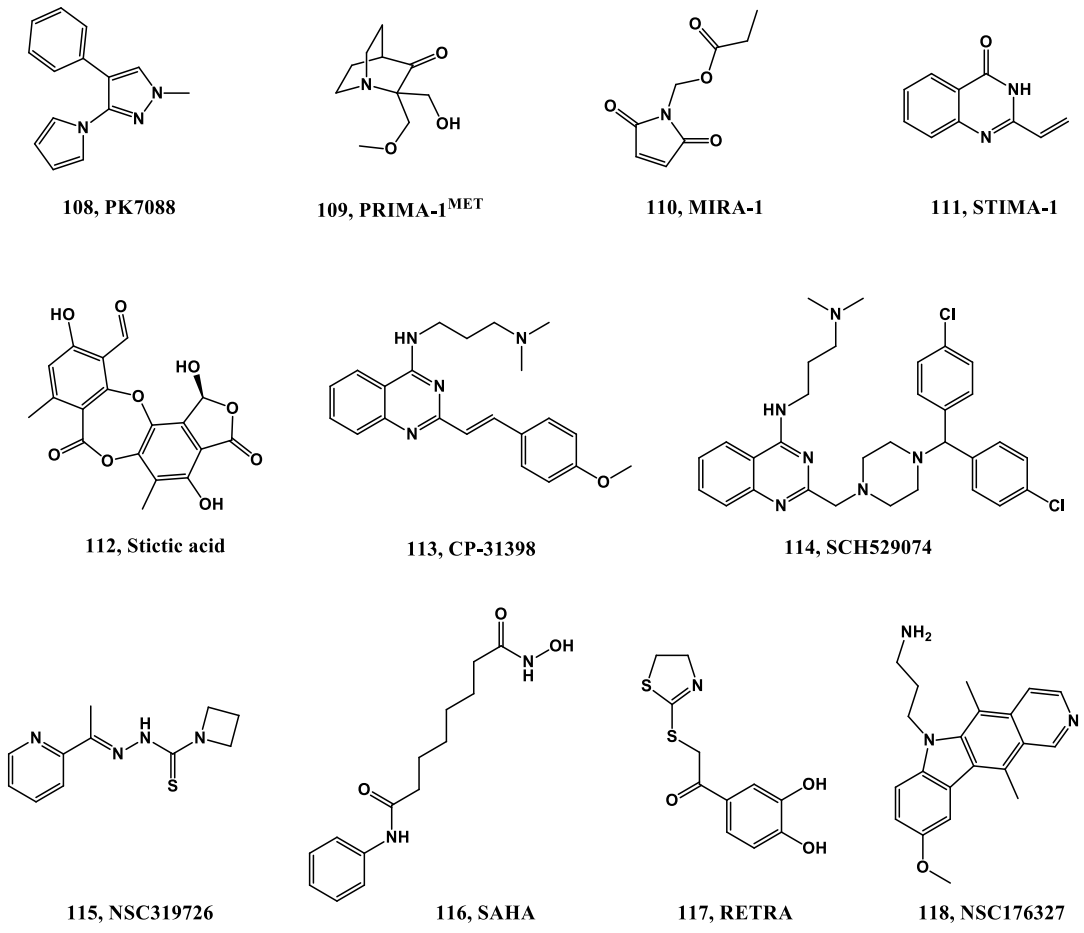

Figure 1.25. Compounds targeting mutant p53.

1.3. Concluding Remarks

Due to the unquestionable contribution of p53 to the preservation of genomic integrity, it is not surprising that tumor pathogenesis and development involves some sort of p53 impairment. Hence, restoring p53 function in cancer cells represents a valuable anticancer approach. Several strategies are being developed (Figure 1.26) and in particular targeting p53-MDM2 interaction has emerged as a promising approach, when dealing with cancers that retain wild type p53 function. Seven compounds have already entered clinical trials.

p53-MDM2 interaction inhibitors share common structural features: a rigid heterocyclic scaffold, from which three lipophilic groups are projected into p53 pocket in MDM2, mimicking the three pivotal Phe19, Trp23 and Leu26. Furthermore, all the interactions are primarily hydrophobic, with potency increasing essentially by introduction of halide-substituted aromatic groups, and PK requirements achieved by inclusion of solvent exposure polar groups that can also contribute to potency.

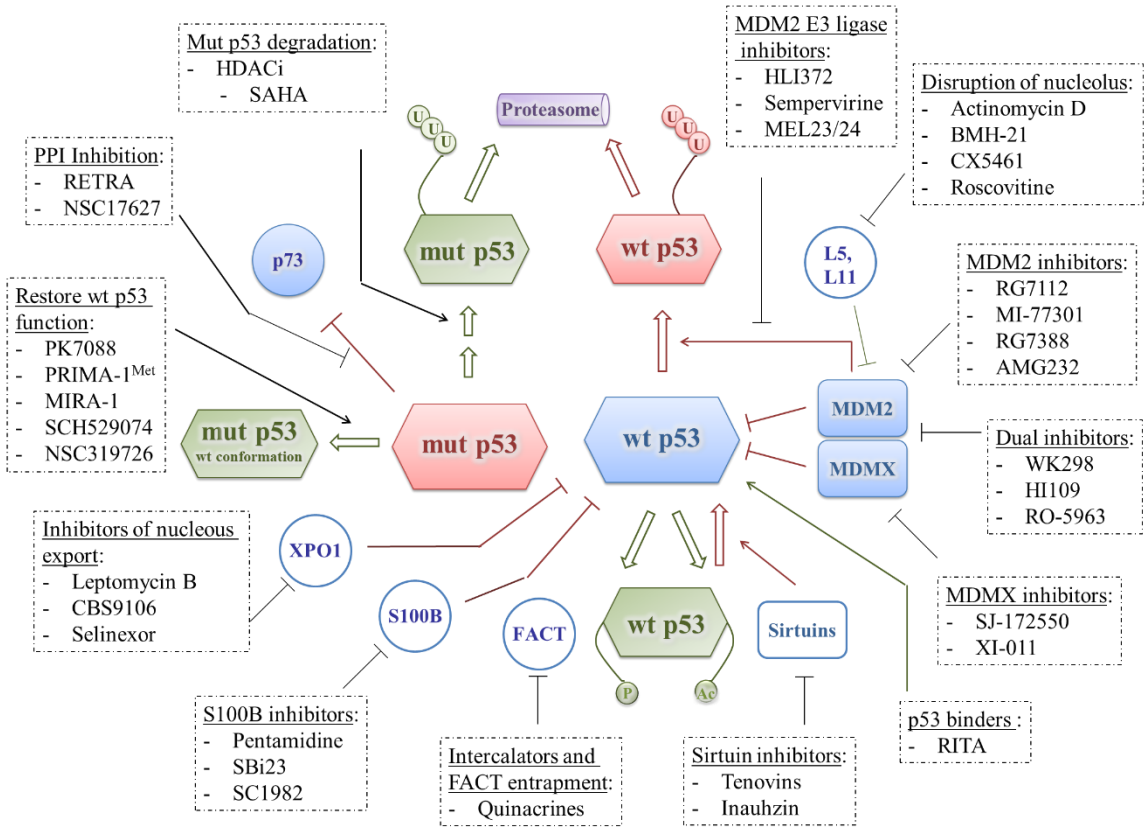

Figure 1.26. Different strategies for targeting wild-type and mutant p53 by small molecules. Red and green events can be seen as procarcinogenic and anticarcinogenic, respectively.

Chapter 2

SCOPE AND GENERAL GOALS

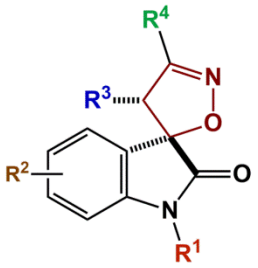

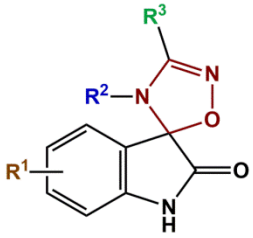

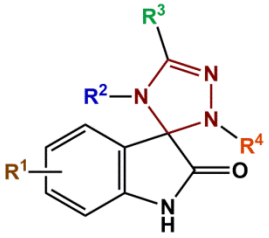

A spirooxindole framework is present in many natural products and in medicinal agents with diverse biological activities [259]. In particular, spiropyrrolidine oxindoles already revealed to possess anticancer activity by different mechanisms of action, with the most studied being the inhibition of p53-MDM2 interaction [73]. As discussed in the introduction, a rigid heterocyclic scaffold, from which three lipophilic groups are projected are the main features of this type of inhibitors. The main goal of this PhD thesis was to develop new anticancer agents containing a spirooxindole scaffold with different spiro five-membered rings: isoxazoline, oxadiazoline, and triazolines.

The PhD thesis carried out the following three major strategies:

2.1. Synthesis of spirooxindole derivatives;

2.2. Biological evaluation of the compounds synthesized;

2.3. Stability assessment.

2.1. SYNTHESIS OF SPIROOXINDOLE DERIVATIVES

The spirooxindoles were obtained by 1,3-dipolar cycloaddition between alkene and imine oxindoles and 1,3-dipoles generated *in situ*. To introduce variability to the five-membered ring, different 1,3-dipoles were also probed (Scheme 2.1):

- **Spiroisoxazolines**: 1,3-dipolar cycloaddition between 3-methylene indolin-2-ones and nitrile oxides;

- **Spirooxadiazolines**: 1,3-dipolar cycloaddition between 3-imino indolin-2-ones and nitrile oxides;

- **Spirotriazolines**: 1,3 dipolar cycloaddition between 3-imino indolin-2-ones and nitrile imines.

In order to obtain compounds with better anticancer activity, molecular diversity was introduced by attaching different groups to the spirooxindole moiety. These modifications were mainly focused in hydrophobic moieties, since the p53-MDM2 interaction is primarily hydrophobic.

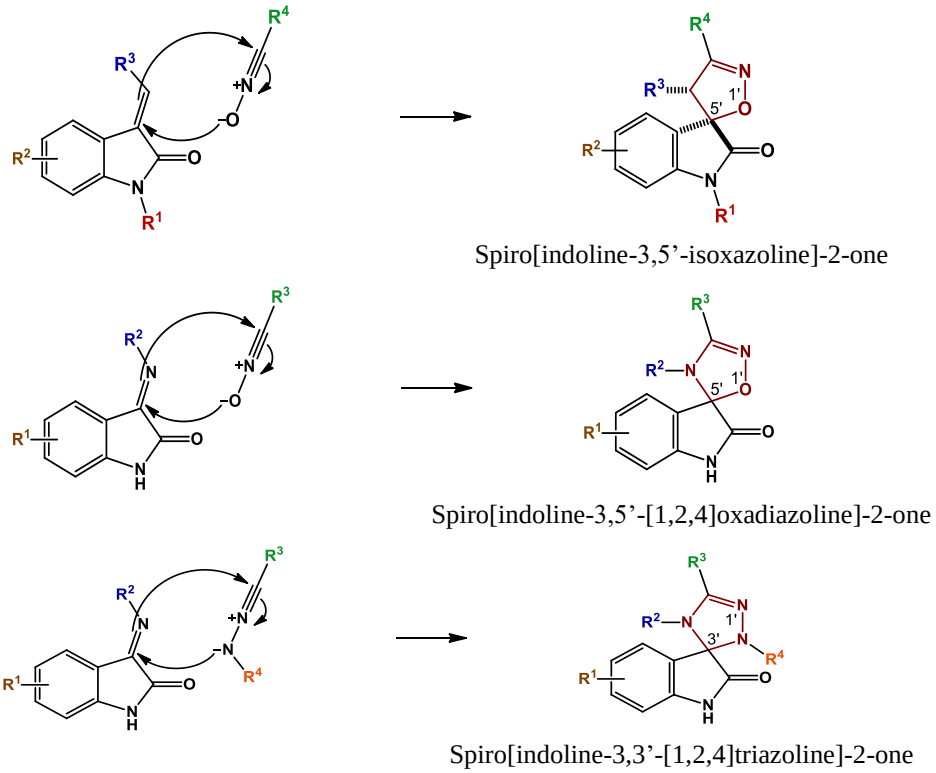

Scheme 2.1. Different spirooxindole scaffolds synthesized during the PhD.

2.2. BIOLOGICAL STUDIES

In vitro studies are required for proof-of-concept. The biological evaluation had two main goals: to prove that spiro compounds are cytotoxic and that their cytotoxicity occurs through an apoptotic outcome, mediated by activation of the p53 signaling pathway in cancer cell lines. Furthermore, it was also assessed if this activation involves disruption of the interaction between p53 and MDM2.

- *Assessment of cell viability in cancer cell lines*. The antiproliferative activity of the compounds was evaluated by MTS or MTT assays in several cell lines with different p53 status. These assays will indicate if spiro compounds have anticancer activity. Furthermore, SAR study led to new sets of synthesis and biological assessment in an attempt to obtain compounds with improved activity. Only the most active compounds continued for further biological evaluation.

- *Evaluation of compounds ability to block the intracellular p53-MDM2 interaction.* This assessment was achieved by implementing a bimolecular fluorescence complementation assay (BiFC) developed in the group of Professor Cecília Rodrigues [260]. This assay uses expression plasmids encoding p53 and MDM2 fused to the two

halves of the fluorescent protein Venus in HCT116 *p53*$^{(-/-)}$ cell line. This assay allows the direct visualization of the p53-MDM2 interaction in living cells.

- *Evaluation of compounds ability to induce apoptosis in cancer cell lines.* To evaluate apoptosis, immunoblotting analysis and caspase 3/7 activity assays were performed in whole-cell lysates obtained after 24 h of incubation with the compounds. With these experiments, it is expected to observe in wild-type p53 cells a dose-dependent increase of cleaved PARP and a dose-dependent induction of caspase activity

2.3. STABILITY ASSESSMENT

Stability of the most promissing compounds was assessed. These determinations are important to give a preliminary idea of the compounds PK properties and consequently to guide the selection of the best candidate to advance into *in vivo* studies. Chemical stability and blood compartment enzimatic stability were evaluated by incubating the compounds in pH 7.4 phosphate buffer and human plasma at 37ºC, respectively. Metabolic stability was assessed by determination of the compounds half-lives in rat pooled liver microsomes at 37ºC with NADPH regenerating system. All these measurements were analyzed by HPLC.

2.4. THESIS LAYOUT

Chapters three to five are dedicated to the synthesis and biological evaluation of spiroisoxazoline oxindoles. Chapter three presents the first studies performed to optimize the methodology to obtain the spiroisoxazoline oxindole scaffold. These studies were developed for spiroisoxazoline oxindole derivatives containing ester groups in position R^3 (Scheme 2.1). In chapter four, the synthetic scope was increased, in order to obtain spiroisoxazoline oxindole derivatives with alquilic and aromatic groups in this position. Furthermore, it is also presented the biological and stability assessment. Chapter five presents the attempts to synthesize enantioselectively the most active derivative. These experiments were carried out in Franz group at University of California – Davis during a PhD short scientific mission (3 months) financed by FCT. This chapter also describes experiments developed for the enantioselective synthesis of a spiropyrroline oxindole derivative performed in parallel to the main objectives of the PhD. Chapter six and seven are dedicated to the synthesis, biological evaluation and stability assessment of the spirooxadiazoline and spirotriazoline oxindole libraries, respectively. General conclusions and future perspectives are described in chapter eight.

Chapter 3

SPIROISOXAZOLINE OXINDOLES:

SYNTHETIC METHODOLOGY OPTIMIZATION

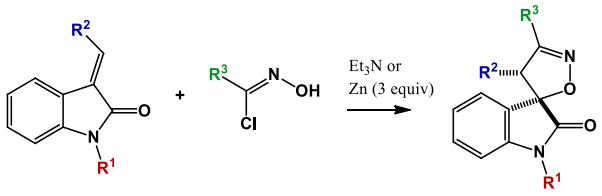

This chapter describes the synthesis of spiroisoxazoline oxindoles containing ester groups at position 4' and aromatic or ester groups at position 3' of the isoxazoline ring. The compounds were synthesized in yields up to 94% by 1,3-dipolar cycloaddition of 3-methylene indolin-2-ones and chlorooximes in the presence of triethylamine or zinc.

- Carlos J. A. Ribeiro, S. Praveen Kumar, Rui Moreira, Maria M. M. Santos, *Efficient synthesis of spiroisoxazoline oxindoles.* Tetrahedron Lett., **2012**. 53(3): p. 281-284

- Carlos J. A. Ribeiro, Rui Moreira, Maria M. M. Santos. Synthesis of a spiroisoxazoline oxindole by 1,3-dipolar cycloaddition. In: Comprehensive Organic Chemistry Experiments for the Laboratory Classroom Book, Royal Society of Chemistry (accepted).

3.1. INTRODUCTION

The most common approach to prepare isoxazoline derivatives is by 1,3-dipolar cycloaddition between nitrile oxides and alkene dipolarophiles. Nitrile oxides are generally generated *in situ* in the presence of the dipolarophile in order to avoid dimerization. That can be achieved by dehydration of primary nitroalkanes or by dehydrohalogenation of hydroximoyl halides [261, 262]. Translating to the intended scaffold, spiroisoxazoline oxindoles (**119**, Scheme 3.1) can be synthesized by 1,3-dipolar cycloaddition between nitrile oxides (**120**) and 3-methylene indolin-2-ones (**121**).

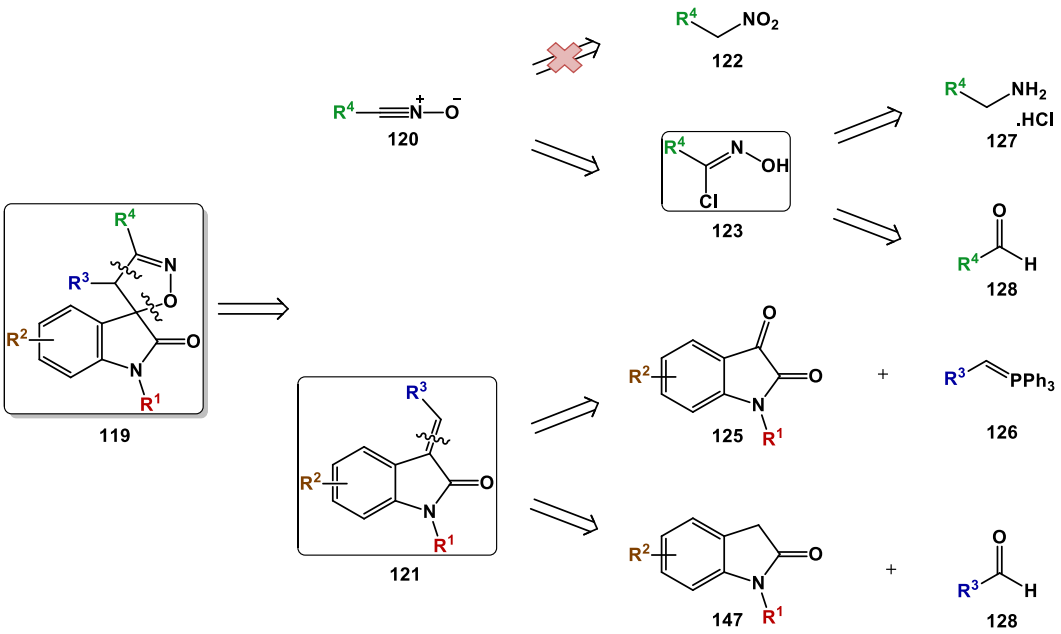

Scheme 3.1- Retrosynthesis of spiroisoxazoline oxindoles derivatives, highlighting the final step between 3-methylene indolin-2-ones (**121**) and chlorooximes (**123**).

During the master thesis work [263], attempts were made to obtain the desired spiro compounds by dehydration of primary nitro compounds (**122**). However, after employing unproductively several well-known dehydration methods described in literature (Table 3.1) [264-269], the focus was redirected to chlorooximes (**123**).

This chapter describes the methodology developed to obtain spiroisoxazoline oxindoles with ester groups in R^3 position. This endeavor started with compound **119a** (R^1= CH_3, R^2= H, R^3= CO_2Et), which was synthesized in a very low yield in the previous work [263].

Table 3.1. Cycloadditions attempts, using primary nitro compound **122a** as precursors of nitrile oxides.

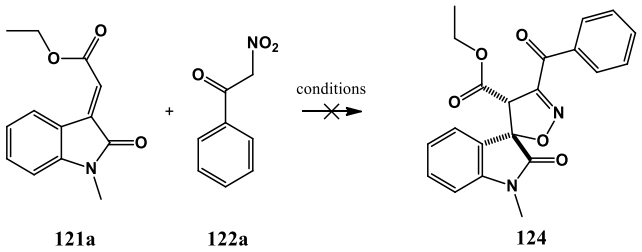

121a **122a** **124**

Entry[a]	**dehydration agent**	**solvent**	**time (h)**	**T (ºC)**
1	DABCO	$CHCl_3$	9	60
2	DABCO	$CHCl_3$	0.5	120
3	DABCO	Toluene	0.5	160
4	DABCO	Toluene	0.5	160
5	1-NMI	$CHCl_3$	21.5	60
6	1-NMI	$CHCl_3$	0.5	120
7	1-NMI	Toluene	0,5	160
8	PhNCO/ TEA	Toluene	49	90
9	Boc_2O/ DMAP	Toluene	19	90
10	$POCl_3$/ TEA	Toluene	22	rt

[a] Entries 1, 5: the reaction was proceeded in a sealed vessel. Conditions: **121a** (1.0 equiv), **122a** (2.0 equiv), base (0.5 equiv) [265]. Entries 2-3, 6-7: Conditions: **121a** (1.0 equiv), **122a** (2.0-2.5 equiv), base (2.0 equiv), M.W. (300 W, sealed vessel). Entry 4: Conditions: **121a** (1.0 equiv), **122a** (2.0 equiv), DABCO (0.5 equiv), $ZnCl_2$ (1.0 equiv), M.W. (300 W, sealed vessel). Entry 8: Conditions: **121a** and **122a** (1.0 equiv), PhNCO (2.6 equiv) and TEA (0.3 equiv) [267, 268]. Entry 9: Conditions: **121a** and **122a** (1.0 equiv), DMAP (0.2 equiv) and Boc_2O (2.5 equiv) [267]. Entry 10: Conditions: **121a** and **122a** (1.0 equiv), $POCl_3$ (2.0 equiv) and TEA (6.0 equiv) [269].

3.2. SYNTHESIS OF INTERMEDIATES

3-methylene indolin-2-ones containing an ester group (**121,** R^3= ester group) were prepared by Wittig reaction between indolin-2,3-diones (**125**) and phosphonium ylides (**126**), and were obtained in very good yields (92-98 %) [270]. In addition, *N*-methyl indolin-2,3-dione was synthesized by methylation of indoline-2,3-dione with iodomethane in the presence of K_2CO_3 (96 % yield) [271] (Scheme 3.2, Table 3.2). All four starting 3-methylene indolin-2-one derivatives were synthetized as *E*-isomers as described in literature [270, 272-274], and that was confirmed by ^{1}H NMR, by tracking the chemical shift of H-4, which is highly sensitive to the substitution at C-8 and to the *E–Z* configuration [272]. Using **121a** as example, H-4 signal appeared deshielded when compared to the starting indolin-2,3-dione (8.56 versus 7.61 ppm respectively), corroborating the *E* configuration.

Chlorooximidoacetates (**123**, R^4= ester groups) were prepared by addition of $NaNO_3$ and HCl to a aqueous solution of the corresponding glycine ester hydrochloride (**127**) and were obtained in moderate yields (51-58 % yield) [275]. The aromatic derivatives (**123**, R^4= aromatic group) were synthesized starting from the corresponding

aromatic aldehyde **128**. By reacting with hydroxylamine it was formed first the aldoxime (**129**) *in situ* and then the halogenation reaction was achieved by employing NCS in the presence of catalytic pyridine (71-85 % yield) [276] (Scheme 3.3, Table 3.2).

The ^{1}H NMR spectra of the intermediates are in accordance with literature [274-283].

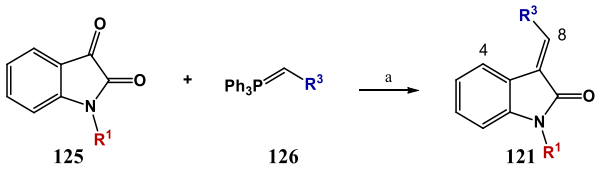

Scheme 3.2- Synthesis of ester 3-methylene indolin-2-ones.
(a) toluene, 80 ºC, 5-6 h

Ester chlorooximes:

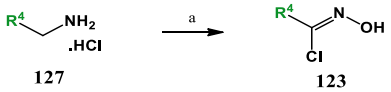

Aromatic chlorooximes:

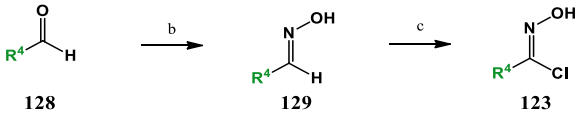

Scheme 3.3. Synthesis of chlorooximes. (a) HCl, $NaNO_2$, H_2O, -5 ºC, 1 h; (b) $NH_3OH{\cdot}HCl$, Na_2CO_3 H_2O, reflux, 2-5 h; (c) NCS, pyridine, $CHCl_3$, r.t., 24h.

Table 3.2. Intermediates synthesized.

Compound	R^1	R^3	Yield (%)
121a	Me	Et	92
121b	H	Et	97
121c	Me	Me	93
121d	H	Me	98

Compound	R^4	Yield (%)
123a	CO_2Et	58
123b	Ph	85
123c	CO_2Me	51
123d	*p*-OMePh	71

3.3. SYNTHESIS OF SPIROISOXAZOLINE OXINDOLES AND OPTIMIZATION

Classically the dehydrohalogenation and cycloaddition are achieved by slow addition of one equivalent of a tertiary amine base, normally triethylamine (Et_3N), to a solution or suspension of the chlorooxime and dipolarophile in an inert organic solvent such as diethyl ether at low temperature [284].

Applying the protocol described in the literature by El-Ahl [285], spiroisoxazoline oxindole **119a** was isolated after recrystallization in a very low yield (Table 3.3, entry 1).

In order to improve the yield, several reaction conditions were tested. It was found that changing the reagents addition sequence order (entry 1 and 3 versus 2 and 4) and increasing the number of equivalents of the chlorooxime (entries 3, 4 and 5) led only to a slight increase in the yield of **119a**. The use of sodium hydride or zinc to form the nitrile oxide (entries 6 and 7) also only improved very slightly the yield of product. In addition, changing the solvent ($CHCl_3$, toluene, THF) and the base (DIEA, DABCO) did not increase the reaction yield either [263].

Table 3.3. Optimization attempts of the 1,3-dipolar cycloaddition reaction using clorooxime **121a**.

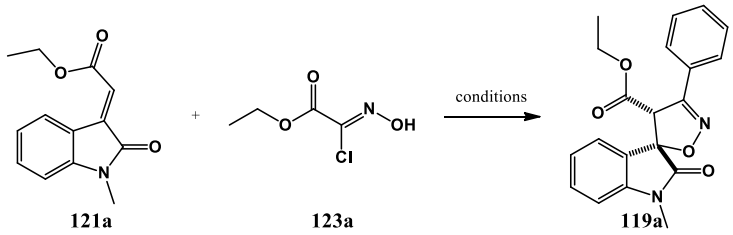

121a **123a** **119a**

entry	dipole equiv	dehydrochlorinating agent (D. A.) [d]	solvent	Time (h)[e]	Yield (%)[f]
1[a]	1	Et_3N	Et_2O	5	16
2[b]	1	Et_3N	Et_2O	5	16
3[a]	2	Et_3N	Et_2O	5	20
4[b]	2	Et_3N	Et_2O	5	22
5[b]	3	Et_3N	Et_2O	5	25
6[b]	1	NaH	THF	5	18
7[c]	1	Zn	Et_2O	48	20

[a] Slow addition of Et_3N solution (1.0-2.0 equiv) for 30 min (for each equiv) to a solution of **121a** (1.0 equiv) and **123a** (1.0-2.0 equiv) at 0ºC [285]; [b] Slow addition of **123a** solution (1.0-3.0 equiv) for 30 min (for each equiv) to a solution of **121a** (1.0 equiv) and base (1.0-3.0 equiv) at 0ºC; [c] A mixture of the three components, **121a** (1.0 equiv), **123a** (1.0 equiv), and Zn (1.0 equiv) was stirred at r.t.; [d] All dehydrochlorinating agents (D. A.) were used in the same number of equiv as chlorooxime **123a**; [e] Reaction time after addition of all reagents and D. A. at r.t.; [f] After column chromatography.

It can be rationalized that the low yields obtained for all conditions are presumably a consequence of the rapid dimerization of the 1,3-dipole generated *in situ*. The dimerization reaction is extremely fast at room temperature for low aliphatic nitrile oxides, while for most aromatic derivatives the half-life are of several hours [284]. Therefore, it was decided to study the reaction with aromatic chlorooximes to evaluate if the observed low yields could be averted. Interestingly, cycloaddition between **121a** and chlorooxime **123b** occurred even without the presence of a dehydrochlorinating agent (D. A.) (Table 3.4, entry 1), although in low yield (11 %). The use of Et_3N, NaH or Zn improved almost 3 times the yield of **123b** (entries 2-4). In this case, increasing the number of equivalents of chlorooxime **123b** to 3 equivalents was sufficient to increase significantly the yield of **119b**, from 33 % to 80 % (entry 6 versus 2).

Table 3.4. Optimization of the 1,3-dipolar cycloaddition reaction using chlorooxime **123b**.

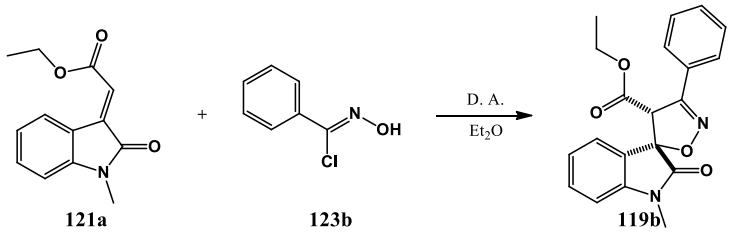

121a **123b** **119b**

entry	dipole equiv	dehydrochlorinating agent (D. A.)[c]	time (h)[d]	S. M. recovery (%)[e]	yield (%)[e]
1[a]	1	-	15	88	11
2[a]	1	Et_3N	15	67	33
3[a]	1	NaH	15	65	32
4[b]	1	Zn	15	61	35
5[a]	2	Et_3N	15	31	68
6[a]	3	Et_3N	15	16	80

[a] Slow addition of **123b** solution (1.0-3.0 equiv) for 30 min (for each equiv) to a solution of **121a** (1.0 equiv) and base (1.0-3.0 equiv) at 0 ºC; [b] A mixture of the three components, **121a** (1.0 equiv), **123b** (1.0 equiv), and Zn (1.0 equiv) was stirred at r.t.; [c] All dehydrochlorinating agents (D. A.) were used in the same number of equiv as chlorooxime **123a**; [d] Reaction time after addition of the chlorooxime at r.t.; [e] After column chromatography. S. M.: starting material.

This methodology was then applied to 3-methylene indolin-2-ones **121b-d** (Table 3.5). Using three equivalents of *N*-hydroxybenzimidoyl chloride (**123b**) in the presence of three equivalents of Et_3N, compounds **119c-e** were obtained in 89-94 % yields. For the *N*-deprotected 3-methylene indolinones, a mixture of Et_2O:THF (1:1) was used as the solvent to improve the solubility of the starting material.

Table 3.5. Cycloaddition reaction scope: Using different dipolarophiles with chlorooxime **123b**.

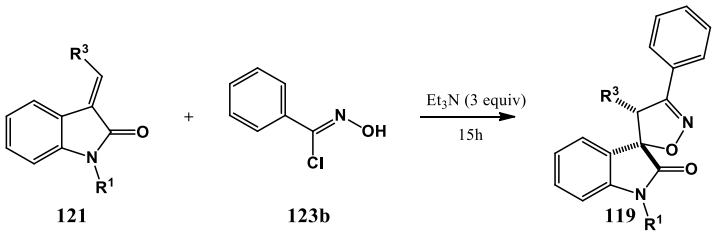

121 **123b** **119**

entry	R^1	R^3	product	solvent	yield (%)[a]
1	Me	CO_2Et	**119b**	Et_2O	80
2	Me	CO_2Me	**119c**	Et_2O	94
3	H	CO_2Et	**119d**	Et_2O/THF	89
4	H	CO_2Me	**119e**	Et_2O/THF	92

[a] After column chromatography.

The absence of a base reduces significantly the rate of dehydrochlorination, and that was clearly evident when zinc was used as dehydrochlorinating agent for chlorooximidoacetate **123a** (Table 3.3, entry 7 versus 1, 2 and 6). As a consequence, nitrile oxide dimerization is also likely to occur more slowly in the presence of zinc. In fact,

increasing the equivalents of chlorooxime in the presence of zinc, the yield of **119a** increased from 20 to 79 % (Table 3.3 - entry 7 versus Table 3.6 - entry 1).

Applying this method, several spiroisoxazoline oxindoles derivatives were synthesize in 71-92 % yields from different chlorooximes **123a-d** and 3-methylene indolin-2-ones **121a-d** (Table 3.6).

Table 3.6. Cycloaddition reaction scope: Using three equivalents of chlorooxime and zinc.

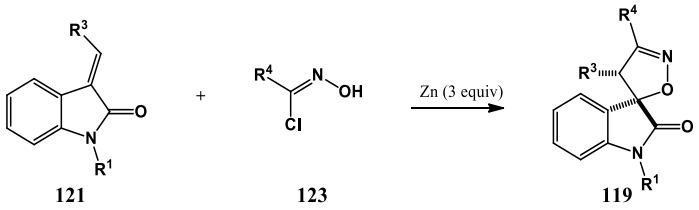

121 123 119

Entry	R^1	R^3	R^4	product	solvent	t (h)	yield (%)[a]
1	Me	CO_2Et	CO_2Et	**119a**	Et_2O	36	79
2	Me	CO_2Et	Ph	**119b**	Et_2O	15	92
3	Me	CO_2Me	CO_2Et	**119f**	Et_2O	48	72
4	Me	CO_2Et	CO_2Me	**119g**	Et_2O	36	74
5	H	CO_2Et	CO_2Et	**119h**	Et_2O/THF	36	77
6	H	CO_2Me	CO_2Et	**119i**	Et_2O/THF	48	76
7	H	CO_2Et	CO_2Me	**119j**	Et_2O/THF	36	71
8	H	CO_2Et	*p*OMePh	**119k**	Et_2O/THF	15	87
9	Me	CO_2Et	*p*OMePh	**119l**	Et_2O	15	89

[a] After column chromatography.

3.4. REGIO AND STEREOSELECTIVITY CONSIDERATIONS

1,3-dipolar cycloaddition reactions between a nitrile oxide and a alkene can generate two regioisomeric isoxazolines, with regioselectivity dependent upon electronic and steric effects. The electronic nature of the dipolarophile substituents to the regioselectivity outcome is particularly important for 1,2-dissubtituted dipolarophiles. However, as a generalization, the oxygen of the nitrile oxide tends to bond to the most highly substituted end of the alkene [284, 286]. Applying this consideration to spiroisoxazoline oxindole cycloaddition reaction it was expected and later observed that the regioisomer obtained would be the spiro[indoline-3,5'-isoxazoline]-2-one (Scheme 3.4, exemplified for compound **119a**). Furthermore searching through literature for similar spiroisoxazoline oxindole structures obtained by 1,3-dipolar cycloaddition between 3-methylene indolin-2-ones (mostly 3-substituted alkenes derivatives [285, 287-289]) and nitrile oxides also corroborate the exclusive (**130** [287], **131** [288], Figure 3.1) or almost exclusive (> 20:1 **132** [290]) formation of this regioisomer. The only exception was described by El-Ahl in which the 1,3 dipolar cycloaddition was reported to give regioselectively (> 95 %) the spiro[indoline-3,4'-isoxazoline]-2-one (**133**, [285]).

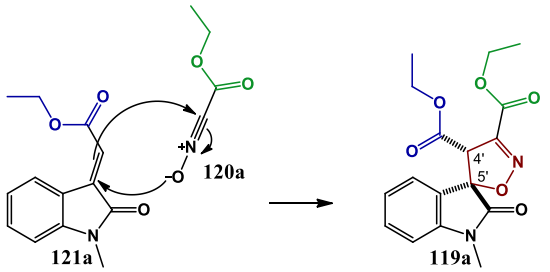

Spiro[indoline-3,5'-isoxazoline]-2-one

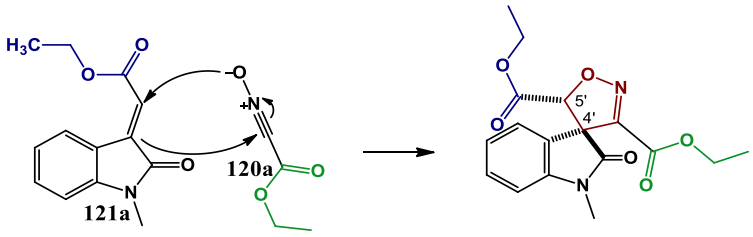

Spiro[indoline-3,4'-isoxazoline]-2-one

Scheme 3.4- Possible regioisomers formed as a result of 1,3-dipolar cycloaddition between **121a** and **120a**.

By NMR studies and X-ray crystallography (Figure 3.2) it was confirmed that the regioisomer obtained was the expected spiro[indoline-3,5'-isoxazoline]-2-one. In the NMR the most enlightening signals correspond to the proton of the isoxazoline ring (H-4') and its carbon (C-4') and to the spiro carbon. For all cases the presence of vicinal oxygen instead of a carbon makes these signals appear downfield. For example the spiro carbon chemical shift obtained for compound **119a** was 88.47 ppm. This value is in the normal range obtained for spiro[indoline-3,5'-isoxazoline]-2-ones (87.61 – 89.81 ppm [287], Table 3.7; 86.68 – 89.0 ppm [290]). The same rationalization can also be made for C-4' (59.46 ppm) and H-4' (4.76 ppm). As mentioned, this reaction is regiospecific and therefore the NMR signals for the spiro[indoline-3,4'-isoxazoline]-2-one are not reported in literature (El-Ahl did not report ^{13}C NMR values). Just to have an idea of the expected difference observed for both regioisomers it is reported in Table 3.7 the values for the structurally similar spiroisoxazolidine oxindoles (**134**) [270]. As expected the spiro carbon signal appears much more shielded for the 5-regioisomer **134a** (83.0 – 83.7 as opposed to 66.3 – 68.9 ppm).

Furthermore the additional isoxazoline carbon (C=N) appeared at 149.48 ppm in the ^{13}C NMR spectrum (147.8 – 149.1 ppm [287]).

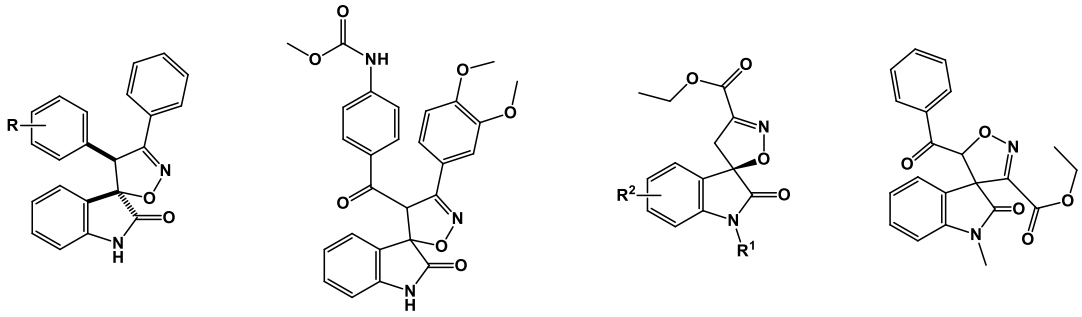

130 131 132 133

Figure 3.1- Spiroisoxazoline oxindoles obtained by 1,3-dipolar cycloaddition described in literature.

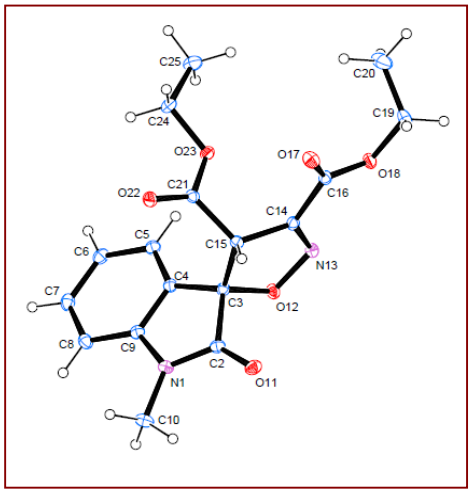

Figure 3.2- X-ray crystallography structure of spiroisoxazoline oxindole **119a** [263].

Table 3.7. NMR chemical shifts (ppm) for representative spirooxindoles derivatives.

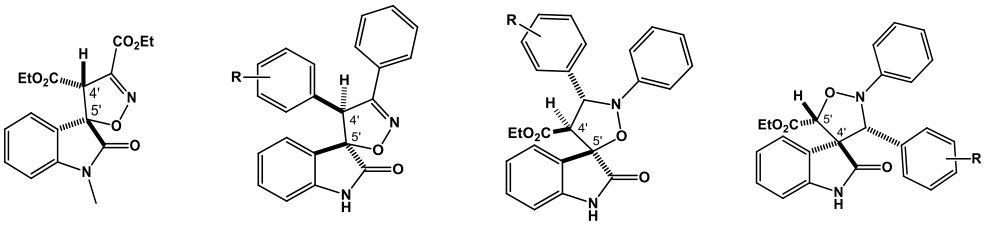

	119a	**130**	**134a**	**134b**
Cspiro	88.47	87.61 – 89.81	83.0 – 83.7	66.3 – 68.9
H-4'	4.76	4.96 – 5.40	4.16 – 4.24	-
C-4'	59.46	55.62 – 64.91	64.3 – 64.8	-
H-5'	-	-	-	5.30 – 5.45
C-5'	-	-	-	81.9 – 84.7

As observed for compound **119a**, in all the other reactions described the regioisomer purified was the spiro[indoline-3,5'-isoxazoline]-2-one, as confirmed by ^{1}H NMR (δ H-4' 4.76 – 4.93 ppm) and ^{13}C NMR (δ Cspiro 86.7 – 88.9 ppm). Furthermore, the isoxazoline C=N chemical shift appeared at 149.26 – 154.65 ppm.

In addition, since pericyclic reactions occur through a concerted mechanism, the relationship between substituents in the starting materials needs to be preserved in the final product. Therefore in **119a** the oxindole phenyl group will be in the same direction as CO_2Et and consequently H-4' and oxindole carbonyl will be projected to the other side, as observed by X-ray crystallography (Figure 3.2).

All compounds were further characterized by melting point, IR and mass spectrometry (chapter 9).

3.5. CONCLUDING REMARKS

In conclusion, twelve spiro[indoline-3,5'-isoxazoline]-2-ones were synthesized, containing ester groups at position 4' and aromatic or ester groups at position 3', in yields up to 94%. In addition, this work represents the first time that zinc is being used as the dehydrochlorinating agent in 1,3-dipolar cycloaddition reactions. This methodology can be applied to chlorooximes with an aryl or ester side chains and does not require the slow addition of base to avoid nitrile oxide dimerization.

Chapter 4

SPIROISOXAZOLINE OXINDOLES:

INCREASING SYNTHETIC SCOPE AND BIOLOGICAL EVALUATION

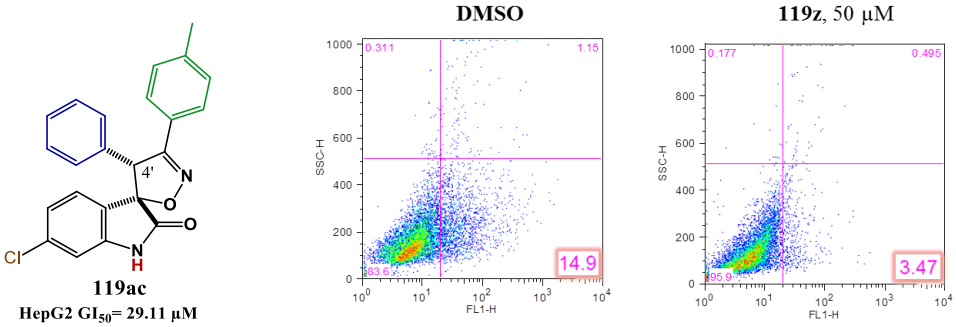

This chapter reports the synthesis of additional twenty one spiroisoxazoline oxindoles, this time with aromatic side chain at C-4' position. It also reports the evaluation of all thirty three derivatives synthesized as anticancer agents, and in particular as potential p53-MDM2 interaction inhibitors. Seven compounds showed an antiproliferative profile superior to the p53-MDM2 interaction inhibitor nutlin-3, and induced cell death by apoptosis (shown for compounds **119aa** and **119ac**). Moreover, proof-of-concept was demonstrated by inhibition of the interaction between p53 and MDM2 in a live-cell bimolecular fluorescence complementation assay for compound **119z**.

- Carlos J. A. Ribeiro, Joana D. Amaral, Cecília M. P. Rodrigues, Rui Moreira, Maria M. M. Santos, *Synthesis and evaluation of spiroisoxazoline oxindoles as anticancer agents*. Bioorg. Med. Chem., **2014**. 22: p. 577-584

4.1. INTRODUCTION

Heterocycles possessing a spirooxindole framework are found in many natural products and medicinal agents with diverse biological activities (Figure 4.1) [259, 291, 292]. The attractiveness of this type of scaffold in organic and medicinal chemistry is evident by the increasing number of publications in the subject throughout the years (Figure 4.2, A). One reason behind its popularity can be attributed to the fact that a centrally situated spiro carbon imposes conformational restriction to the structure. As a result it creates a specific three-dimensionality that can be beneficial to maintain the molecule in the desired conformation for ligand-target binding, and therefore potentially promoting an increase in potency and/ or specificity [291]. Furthermore, reducing molecular flexibility also potentially contributes to better PK properties [293].

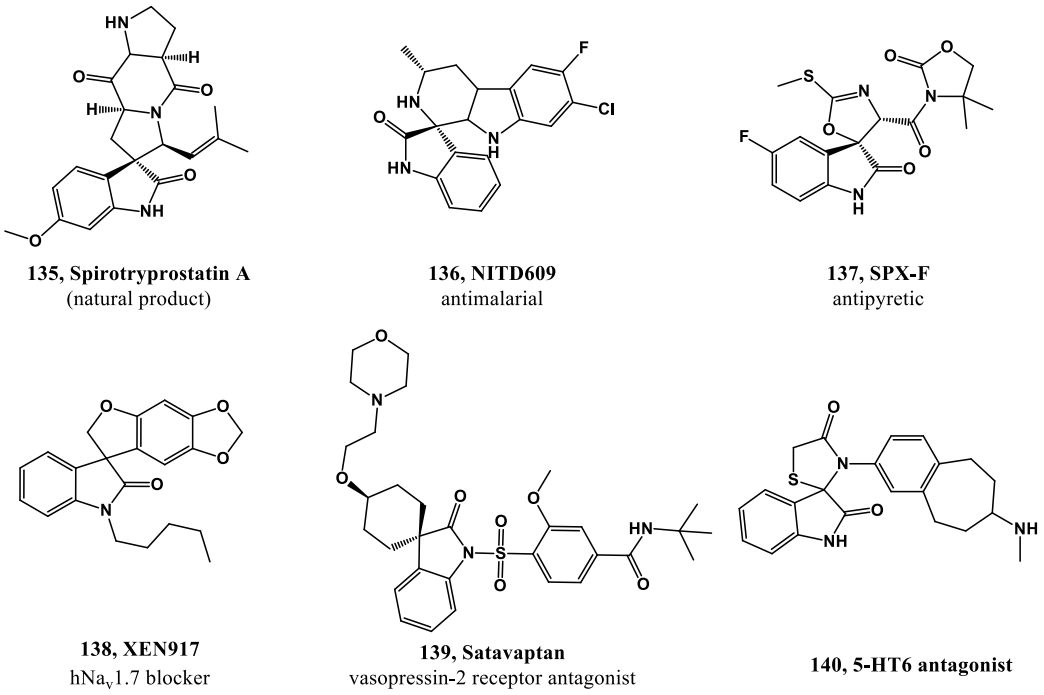

Figure 4.1. Examples of spirooxindoles with biological activity.

Among their biological effects, the most frequently reported in literature is their antiproliferative activity against cancer cell lines (Figure 4.3) [294]. For some of these compounds additional information about their mechanism of action is given. For instance, CFI-400945 (**145**) is a PLK4 inhibitor. PLK4 represents a new potential anticancer strategy, since it is found up-regulated in about 80% of cancers and is involved in centriole duplication during the cell cycle, cytokinesis and maintenance of chromosomal stability and can promote cancer cell invasion [295]. Compound **(-)-146** interferes with microtubule polymerization and arrests mitosis [296] and compounds **13** and **24** modulate p53. As discussed in chapter 1, spiro[indoline-3,3'-pyrrolidine]-2-one oxindole derivatives are potent inhibitors of the interaction between p53-MDM2, with compound MI-77301 (**13**)

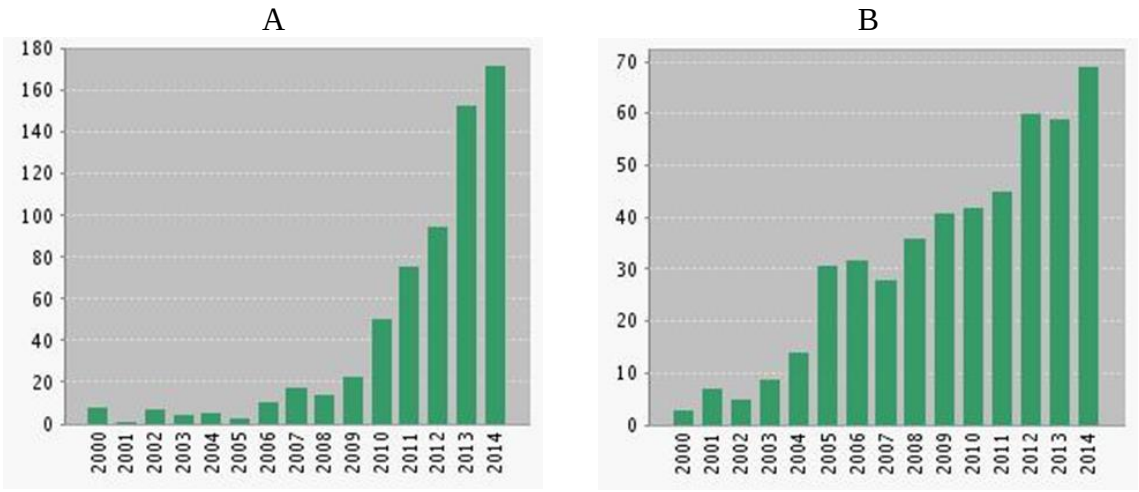

Figure 4.2. Number of publications per year in the last 15 years for the topic: (A) spirooxindole(s) and (B) p53-MDM2 interaction inhibitor(s).

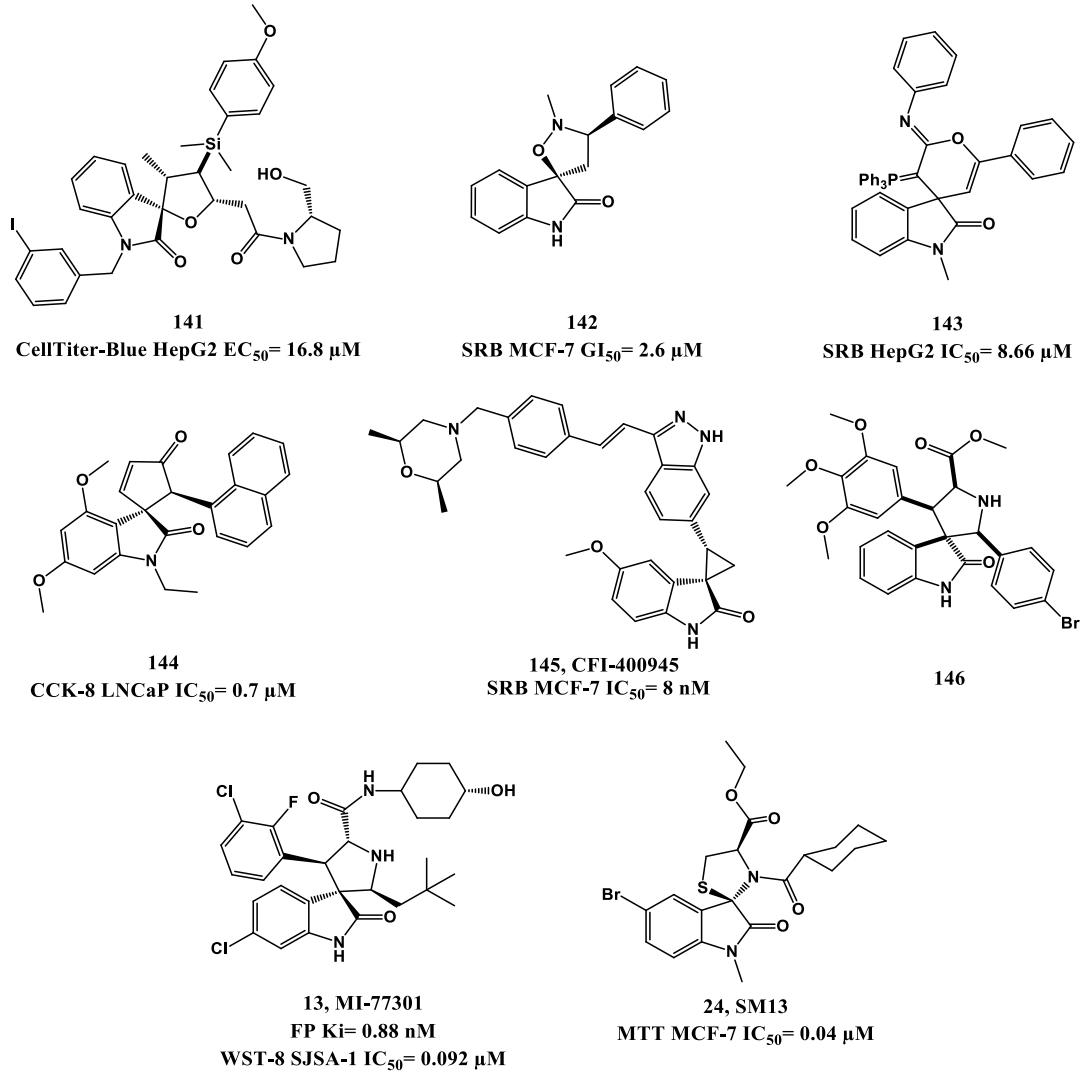

Figure 4.3. Examples of spirooxindoles with anticancer activity.

already in clinical trials. In this last decade, after publication of the first co-crystal structure of an inhibitor bound to MDM2 in 2004, it is observed an increase interest in this target as p53 reactivating anti-cancer strategy (Figure 4.2, B).

This chapter describes the anti-cancer activity for spirooxindoles with an isoxazoline fused ring. Due to structural similarities to spiropyrrolidines their potentiality as p53-MDM2 interaction inhibition will also be analyzed. The oxindole moiety could potentially mimic the indole side chain of Trp23 of p53 and the spiroisoxazoline ring would act as the rigid heterocyclic scaffold. In addition, due to the fact that mimicking p53 entails three hydrophobic moieties, it was synthesized primarily derivatives with three aromatic side chains attached to the isoxazoline moiety.

4.2. Synthesis of Intermediates

3-methylene indolin-2-ones (**121**) possessing aromatic and alquilic substituents at R^3 were synthesized by aldolic condensation of substituted indolin-2-ones (**147**) with different aldehydes (**128**) in the presence of catalytic piperidine (76-99 % yield) [297] (Scheme 4.1, Table 4.1).

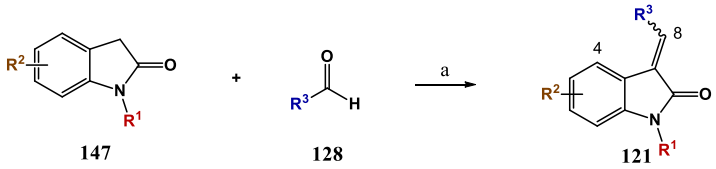

Scheme 4.1. Synthesis of 3-methylene indolin-2-one.
(a) piperidine, EtOH, reflux, 3-5h.

Table 4.1. Synthesis of 3-methylene indolin-2-ones.

Compd	R^1	R^2	R^3	Yield (%)	Compd	R^1	R^2	R^3	Yield (%)
121e	H	H	Ph	99	**121j**	H	7-Cl	Ph	99
121f	H	H	*p*-OMePh	76	**121k**	H	6-Cl	Ph	95
121g	Me	H	*p*-OMePh	89	**121l**	H	6-Cl	*p*-OMePh	99
121h	H	H	Propyl	96	**121m**	H	6-Br	Ph	93
121i	H	5-NO_2	Ph	93					

The benzylidene indolin-2-ones may exist as either *Z* or *E* isomer depending on the substituents at C-8 and C-4. Furthermore, isomer *E* tends to be favored in great extent in benzylidene indolin-2-ones without substituents at C-4 [297-299], as observed for all derivatives synthesized. Exemplifying with compound **121g**, *ortho*-arylidine signal of the minor *Z* isomer appears deshielded (8.40 ppm) in comparison to the major *E* isomer (7.65 ppm), due to the presence of the oxindole carbonyl. The same rationalizations can be made

to H-8 chemical shift. However, it is noteworthy mentioning that *E–Z* isomerization is observed over time in the solvent employed [296, 300, 301].

Aldoximes (**129**) were synthesized from the corresponding aldehyde (**128**) by reaction with hydroxylamine hydrochloride in the presence of Na_2CO_3 (87-98% yield) [276] (Table 4.2, Scheme 4.2).

The ^{1}H NMR spectra of the intermediates are in accordance with literature [301-312].

Table 4.2. Synthesis of aldoximes

Compound	R^4	Yield (%)
129a	Ph	97
129b	*p*-OMePh	89
129c	*o*-OMePh	97
129d	*p*-MePh	87
129e	*p*-NO_2Ph	98

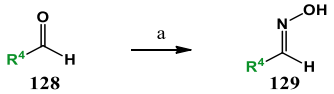

Scheme 4.2. Synthesis of aldoximes
(a) $NH_3OH{\cdot}HCl$, Na_2CO_3, H_2O, reflux, 24h.

4.3. SYNTHESIS OF SPIROISOXAZOLINE OXINDOLE DERIVATIVES

In the last chapter it was described the optimization of the 1,3-dipolar cycloaddition reaction, revealing that when ester chlorooximes were used, the best protocol involved 3 equivalents of chlorooxime and Zn (Scheme 4.3, step a). Therefore, derivatives **119m** and **119n** were additionally prepared using this procedure (Table 4.3). When aromatic chlorooximes were employed, spirooxindoles were obtained in high yields in the presence of Zn or Et_3N (e.g. **119b**, 80 and 92 %, respectively, Table 3.4, entry 6; Table 3.6, entry 2). However, this was observed when R^3 was an ester group. Reaction yields for compounds **119o** and **119p** revealed that electron-donating group at R^3 of the dipolarophile decreased considerably its reactivity to the 1,3-dipole (34 % and 22 % yield, respectively).

Due to the fact that hydroximoyl chlorides are unstable, it was decided to try to consecutively generate *in situ* both chlorooxime and nitrile oxide. Applying the protocol developed by Risitano *et al* [287], in which the hydroximoyl chloride is first generated *in situ* and then cycloaddition occurs after addition of compound **121** and Et_3N, compound **119q** was synthesized in 22 % yield (Table 4.4, entry 1). Increasing the number of chlorooxime equivalents improved the yield to 53 % (entry 2). Repeating the same protocol, but using metallic zinc as dehydrohalogenating agent instead, reduced the yield to 42 % (entry 3). Therefore, the following spiroisoxazoline oxindoles (**119r-ag**) were prepared using the best condition in yields of 43-76 % (Scheme 4.3, step b and c, Table 4.3).

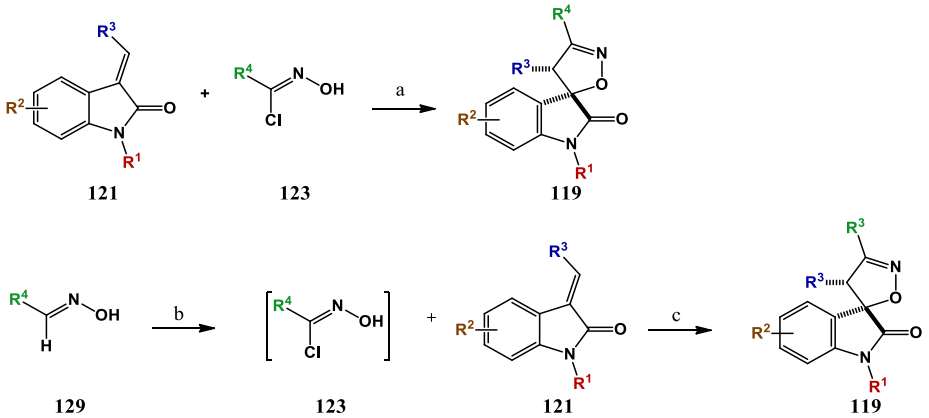

Scheme 4.3- Synthesis of spiroisoxazoline oxindoles. (a) Zn, ether or ether:THF (1:1), r.t., 36 h; (b) NCS, pyridine, $CHCl_3$, r.t., 24 h (c) Et_3N, $CHCl_3$, reflux, 26 h.

Table 4.3. New spiroisoxazoline oxindole synthesized.

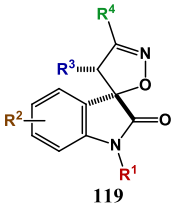

Compd	R^1	R^2	R^3	R^4	yield (%)[a]
119m	H	H	Ph	CO_2Et	42
119n	H	H	*p*-OCH_3Ph	CO_2Et	38
119o	H	H	Propyl	Ph	34
119p	CH_3	H	*p*-OCH_3Ph	Ph	22
119q	H	H	Ph	Ph	53
119r	H	H	Ph	*p*-NO_2Ph	57
119s	H	H	Ph	*p*-OCH_3Ph	70
119t	H	H	*p*-OCH_3Ph	Ph	57
119u	H	H	*p*-OCH_3Ph	*p*-OCH_3Ph	72
119v	H	5-NO_2	Ph	Ph	52
119w	H	5-NO_2	Ph	*p*-OCH_3Ph	72
119x	H	7-Cl	Ph	*p*-NO_2Ph	46
119y	H	7-Cl	Ph	*p*-OCH_3Ph	66
119z	H	6-Cl	Ph	Ph	55
119aa	H	6-Cl	Ph	*p*-OCH_3Ph	49
119ab	H	6-Cl	Ph	*p*-NO_2Ph	43
119ac	H	6-Cl	Ph	*p*-CH_3Ph	71
119ad	H	6-Cl	Ph	*o*-OCH_3Ph	76
119ae	H	6-Cl	*p*-OCH_3Ph	*p*-OCH_3Ph	70
119af	H	6-Br	Ph	Ph	44
119ag	H	6-Br	Ph	*p*-OCH_3Ph	73

[a] For compounds **119m-p** the yields correspond to step a (Scheme 4.3). For compounds **119o-ag** the yields correspond to step b and c (Scheme 4.3).

Table 4.4. Synthesis of compound **119q**.

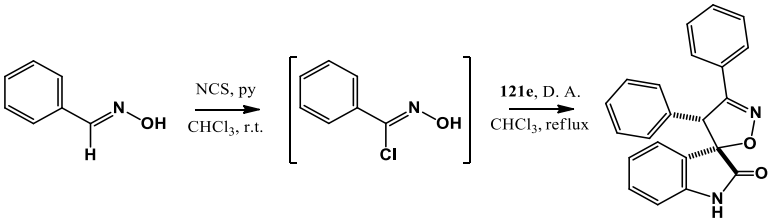

129a **123b** **119q**

Entry	dipole equiv	dehydrochlorinating agent (D.A.)[a]	time (h)[b]	yield (%)
1	1	Et_3N	15	22
2	3	Et_3N	15	53
3	3	Zn	15	42

[a] Dehydrochlorinating agents (D.A.) were used in the same number of equiv as aldoxime **129a**. [b] Reaction time after addition of the D.A.

4.4. REGIO AND STEREOSELECTIVITY CONSIDERATIONS

As discussed in chapter 3, the final compounds correspond to the spiro[indoline-3,5'-isoxazoline]-2-one regioisomer. The chemical shift of the spiro carbon and the isoxazoline C=N appeared at 88.41 – 91.14 ppm and 154.90 – 160.54 ppm, respectively. The relative configuration was established by NMR comparisons with others spiroisoxazoline oxindoles [287], and with the X-ray crystallography structure of compound **119a** (Figure 3.2). Furthermore, NOE effect was observed in compound **119ad** between the H-4 of the oxindole and the *ortho* protons of the phenyl at C-4' of the isoxazoline ring, revealing spatially proximity and corroborating the established configuration. The compounds were further characterized by melting point, IR and their purity assessed by elemental analysis (chapter 9).

4.5. BIOLOGICAL STUDIES

4.5.1. Assessment of cell viability

The antiproliferative activity of the 33 spiroisoxazoline oxindoles was evaluated in a human hepatocellular carcinoma cell line (HepG2) with wild type p53 (Table 4.5). As expected all compounds with ester groups in position R^3 and/or R^4 (**119a-n**) were inactive (GI_{50}> 100 µM, Table 4.5). In addition, compound **119q** with no substituents in the three phenyl rings was also not active. However, any substituent introduced at position R^2 and/or to the phenyl ring at R^4 gave rise to active compounds (**119r-s**, **119v-ad**, and **119af-ag**). Introducing a *p*-methoxyphenyl group at position R^3 abrogates antiproliferative activity, despite the pattern of substituents in other positions (**119p**, **119t-u** and **119ae**).

Table 4.5. *In vitro* antiproliferative activities in HepG2 cell line.

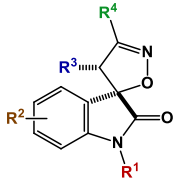

119

Compd	R^1	R^2	R^3	R^4	HepG2 GI_{50}, μM[a]
119a	CH_3	H	CO_2Et	CO_2Et	>100
119b	CH_3	H	CO_2Et	Ph	>100
119c	CH_3	H	CO_2Me	Ph	>100
119d	H	H	CO_2Et	Ph	>100
119e	H	H	CO_2Me	Ph	>100
119f	H	H	CO_2Me	CO_2Et	>100
119g	CH_3	H	CO_2Et	CO_2Me	>100
119h	CH_3	H	CO_2Et	CO_2Et	>100
119i	H	H	CO_2Me	CO_2Et	>100
119j	H	H	CO_2Et	CO_2Me	>100
119k	H	H	CO_2Et	*p*-OCH_3Ph	>100
119l	CH_3	H	CO_2Et	*p*-OCH_3Ph	>100
119m	H	H	Ph	CO_2Et	>100
119n	H	H	*p*-OCH_3Ph	CO_2Et	>100
119o	H	H	Propyl	Ph	>100
119p	CH_3	H	*p*-OCH_3Ph	Ph	>100
119q	H	H	Ph	Ph	>100
119r	H	H	Ph	*p*-NO_2Ph	52.14±1.09
119s	H	H	Ph	*p*-OCH_3Ph	77.77±1.05
119t	H	H	*p*-OCH_3Ph	Ph	>100
119u	H	H	*p*-OCH_3Ph	*p*-OCH_3Ph	>100
119v	H	5-NO_2	Ph	Ph	83.59±1.04
119w	H	5-NO_2	Ph	*p*-OCH_3Ph	53.10±1.14
119x	H	7-Cl	Ph	*p*-NO_2Ph	55.48±1.11
119y	H	7-Cl	Ph	*p*-OCH_3Ph	55.79±1.11
119z	H	6-Cl	Ph	Ph	37.07±1.08
119aa	H	6-Cl	Ph	*p*-OCH_3Ph	38.14±1.08
119ab	H	6-Cl	Ph	*p*-NO_2Ph	33.84±1.11
119ac	H	6-Cl	Ph	*p*-CH_3Ph	29.11±1.09
119ad	H	6-Cl	Ph	*o*-OCH_3Ph	35.70±1.07
119ae	H	6-Cl	*p*-OCH_3Ph	*p*-OCH_3Ph	>100
119af	H	6-Br	Ph	Ph	32.84±1.07
119ag	H	6-Br	Ph	*p*-OCH_3Ph	31.69±1.10
Nutlin-3					51.31±1.04

[a] GI_{50} determined by the MTS method. Each value is the mean (GI_{50} ± SEM) of three independent experiments.

The most active compounds were obtained when a halogen was introduced at position 6 (Cl or Br) of the oxindole moiety (**119z-ad**, and **119af-ag**). In fact, spiropyrrolidine oxindole derivatives already published with co-crystal structure bound to MDM2 (e.g. [123]) revealed that the oxindole moiety can perfectly mimic the indole side chain of Trp23 of p53. Furthermore, the strength of this interaction is increased by introducing a halogen at position 6 that can fill a small pocket not occupied by indole, corroborating these findings. Different substituents at the phenyl ring at R^4 in *para* position (methoxy, nitro and methyl) and *ortho*-methoxy are well tolerated, not affecting substantially their potency. The best activity was found for compound **119ac** (GI_{50}= 29.1 μM).

To investigate if cytotoxicity is mediated by p53, all compounds more active than the positive control nutlin-3 (GI_{50}< 50 μM) were tested in three other cell lines with different p53 status: an isogenic pair of wild type p53 and null human colorectal cancer cell lines [HCT116 $p53^{(+/+)}$ and $p53^{(-/-)}$]; and a p53 mutant human colorectal adenocarcinoma cell line (SW620) (Table 4.6). All compounds showed only a marginal increase in potency in cell lines harboring wild type p53, revealing that p53 non-related effects are also contributing to cytotoxicity.

Table 4.6. *In vitro* antiproliferative activities.

Compd	HepG2 GI_{50}, μM[a]	HCT$p53^{(+/+)}$ GI_{50}, μM[a]	HCT$p53^{(-/-)}$ GI_{50}, μM[a]	SW620 GI_{50}, μM[a]
119z	37.07±1.08	39.80±1.10	48.22±1.13	48.86±1.08
119aa	38.14±1.08	34.72±1.14	40.14±1.17	53.20±1.10
119ab	33.84±1.11	32.37±1.12	38.97±1.14	33.52±1.07
119ac	29.11±1.09	26.56±1.07	30.64±1.12	31.56±1.05
119ad	35.70±1.07	30.51±1.08	35.56±1.10	36.74±1.04
119af	32.84±1.07	35.01±1.07	40,55±1.11	39.65±1.07
119ag	31.69±1.10	33.38±1.13	39.03±1.18	40.36±1.09
Nutlin-3	51.31±1.04	39.65±1.12	52.34±1.15	57.04±1.04

[a] GI_{50} determined by MTS method. Each value is the mean (GI_{50} ± SEM) of three independent experiments.

4.5.2. Evaluation of compounds ability to block the intracellular p53-MDM2 interaction

Due to similar response profile obtained for nutlin-3 in results assessed after 24 hours (Table 4.6), further investigation was performed to evaluate if the compounds can in fact inhibit p53-MDM2 interaction.

By applying a Venus-based bimolecular fluorescence complementation system methodology (BiFC [260], Figure 4.4), it was demonstrated that compound **119z** can inhibit p53-MDM2 interaction in the same extent as nutlin-3 (Figure 4.5). With this assay, it is possible to directly visualize and quantify the p53-MDM2 interaction in live cells by

flow cytometry, since the fluorescence observed is proportional to the protein dimers present.

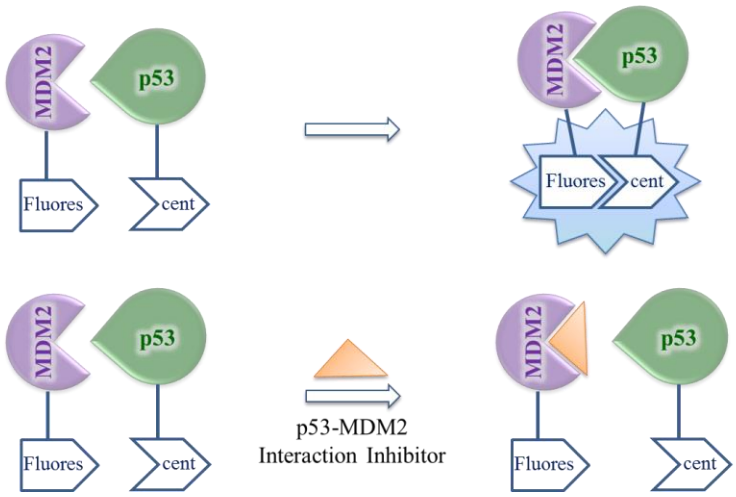

Figure 4.4. p53 and MDM2 are linked to different non-fluorescent fragments of a fluorescent reporter protein. Upon interaction between p53 and MDM2, the functional fluorophore is reconstituted. Therefore, the presence of an inhibitor of the p53-MDM2 interaction will lead to a decrease of dimers present inside the cell and consequently to a decrease in the fluorescence observed.

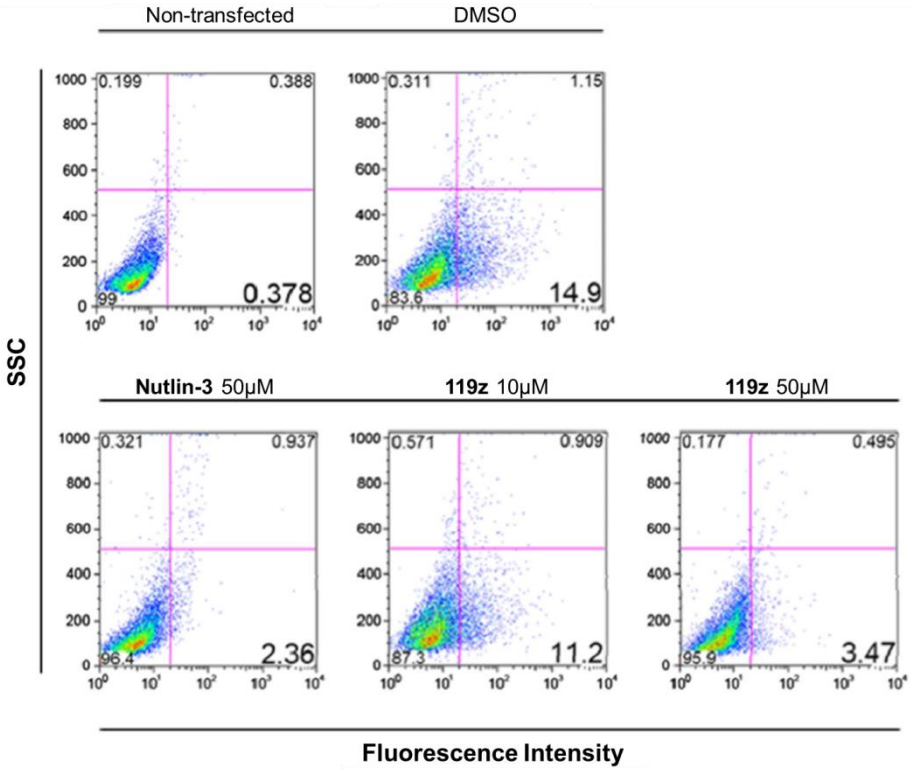

Figure 4.5. Compound **119z** decreases p53-MDM2 interaction by BiFC. HCT116 *p53*$^{(-/-)}$ cells were co-transfected with V1-p53/MDM2-V2 BiFC combination plasmids for 24 h. Vehicle, nutlin-3 (50 μM) and compound **119z** (10 and 50 μM) were included in the culture medium 4 h after transfection. Representative flow cytometry profiles of the disruption of V1-p53/MDM2-V2 complementation (n=3).

4.5.3. Evaluation of apoptosis

Inhibition of p53-MDM2 interaction will restore p53 in cancer cell lines leading to its activation, and consequently induce a p53-mediated signaling pathway that will culminate in cell death by apoptosis. The activation of caspase-3 upon cleavage by upstream proteases and subsequent cleavage of caspase-3 substrate PARP are considered reliable markers of the apoptotic process [313]. In accordance, compounds **119aa** and **119ac** induced a dose-dependent increase of cleaved PARP and active caspase-3 as detected by Western blotting (Figure 4.6).

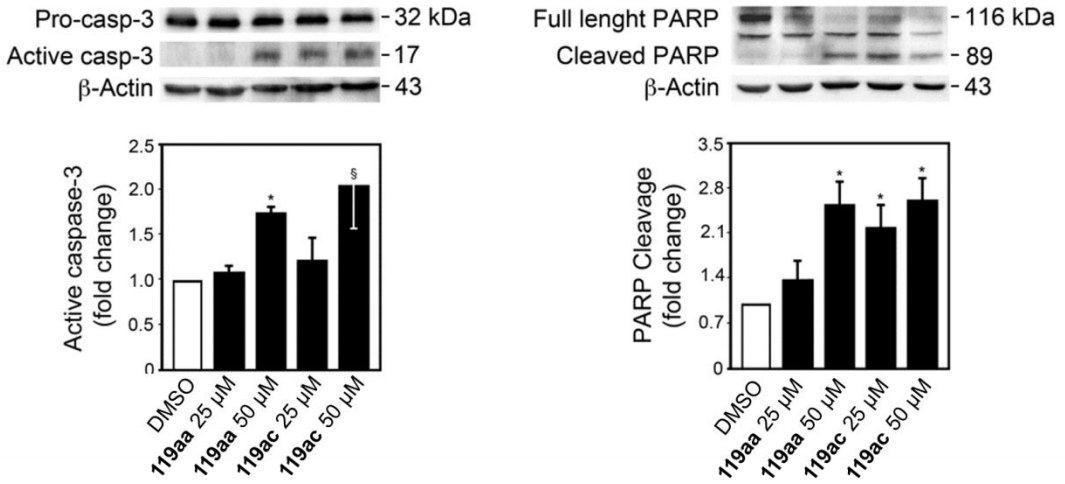

Figure 4.6. Compounds **119aa** and **119ac** induce caspase-3 activation and PARP cleavage. HCT116 *p53*$^{(+/+)}$ cells were incubated with vehicle or 25 and 50 μM of compounds **119aa** and **119ac**, for 24 h. Representative immunoblots of caspase-3 processing (*left*) and PARP cleavage (*right*) analyzed in whole cell extracts. Blots were normalized to endogenous *β*-actin. Data represent mean ± SEM of three independent experiments. **p* < 0.01 and §p < 0.05 from control.

4.6. Stability

Chemical stability in pH 7.4 phosphate buffer and metabolic stability in human plasma and rat liver microsomes at 37 ºC were evaluated for compounds **119aa** and **119ag**. Both compounds were stable in phosphate buffer and plasma for the duration of the assays (three days). Compounds **119aa** and **119ag** exhibited degradation when incubated in rat microsomes with NADPH regenerating system, with half-lives of 3.15±0.07 h and 3.62±0.06 h, respectively, indicating moderate susceptibility towards co-factor dependent microsomal enzymes.

4.7. CONCLUDING REMARKS

Thirty three compounds were synthesized with different substituents attached to the spiroisoxazoline oxindole scaffold to assess their anticancer effect. Screening the compounds in a HepG2 cell line revealed that compounds with chloro or bromo at position 6 of the oxindole aromatic ring were more active than nutlin-3. In addition, compound **119z** showed inhibition of p53-MDM2 interaction in a cell-based bimolecular fluorescence complementation assay, and compounds **119aa** and **119ac** were able to induce apoptosis, as detected by Western blotting. Moreover, compounds **119aa** and **119ag** showed good stability in pH 7.4 phosphate buffer and plasma, and moderate susceptibility towards NADPH-dependent rat microsomal enzymes. The profile of inhibitory activity in cell lines with different p53 status was comparable to that of nutlin-3, revealing also p53-independent effects.

Chapter 5

SPIROISOXAZOLINE OXINDOLES:

ENANTIOSELECTIVE APPROACH

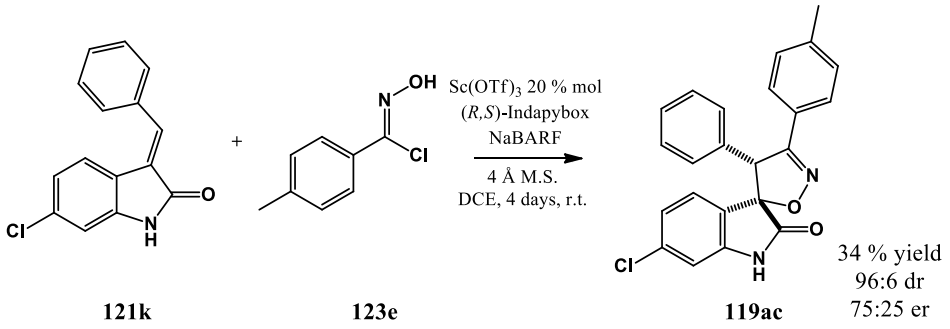

This chapter describes the attempts to enantioselectively synthesize spiroisoxazoline oxindole **119ac** (Section 5.1). The maximum selectivity of 50 % enantiomeric excess was obtained with $Sc(OTf)_3$ (20 mol %), indapybox and NaBArF (1:1.1:1 equiv) in DCE, r.t., 4 days. In parallel with this work, spiropyrroline oxindole *epi*-**163** was also synthesized by cyclization between alkylidene oxindole **121p** and 5-methoxyoxazole **161** (Section 5.2). By employing a chiral scandium(III)-indapybox/BArF complex an enantioenriched *epi*-**163** was obtained.

Joseph J. Badillo, Carlos J. A. Ribeiro, Marilyn M. Olmstead, Annaliese K. Franz, *Titanium(IV)-Catalyzed Stereoselective Synthesis of Spirooxindole-1-Pyrrolines*. Org. Lett., **2014**, 16: p. 6270−6273.

5.1. ENATIOSELECTIVE APPROACHES TOWARDS SPIROISOXAZOLINE OXINDOLES

5.1.1. Introduction

1,3-dipolar cycloaddition between nitrile oxides and alkenes represent a versatile synthetic strategy for the construction of isoxazolines. These heterocyclic moieties not only are present in several biologically active substances, but are also useful precursor to a variety of chiral chain compounds, such as *β*-hydroxy ketones and *γ*-aminoalcohols, due to the easy cleavage of the oxygen-nitrogen bond in the ring [261]. Therefore it is of great importance to synthesize these compounds with a specific chirality. However asymmetric 1,3-dipolar cycloaddition with nitrile oxides are underdeveloped when compared to other dipoles, in particular to its allyl anion type 1,3-dipole counterpart nitrones. Several factors can contribute to this observation [284, 314-316]:

(*a*) Steric interaction between the incoming nitrile oxide and dipolarophile is relatively small. The forming ring in the transition state is roughly planar, with the two nearest atoms (O and N) bearing no substituents while the most distant atom (C) bears only a single substituent that is projected away from the dipolarophile. For instance, in the bent structure of nitrones the N atom is substituted and it can be attached two substituents to the C atom;

(*b*) Instability of the 1,3-dipole and its propensity to dimerize especially in great extent in the absence of reactive dipolarophiles;

(*c*) When hydroximoyl chlorides are involved, it normally requires the use of tertiary amines to generate the 1,3-dipole *in situ* and that can interfere with Lewis acids;

(*d*) Due to the high donor ability of the oxygen atom, nitrile oxides are strong Lewis bases and therefore can form highly stable and/or deactivated dipole-Lewis acid complexes.

All these factors hampered the development of asymmetric 1,3-dipolar cycloadditions with nitrile oxides, especially involving chiral Lewis acids. The most developed approach employs chiral reagents, mostly chiral dipolarophiles, and normally requires the incorporation of chiral auxiliary moieties. As expected, chiral nitrile oxides are less used, due to the linearity of the dipole and the distance between the inducing group and the created stereocenters.

The first successful metal coordinated 1,3-dipolar cycloaddition involving nitrile oxides was published by Kanemasa *et al* in 1994 [316]. They reported the use of EtMgBr (1.0 equiv) to obtain regio and esterocontrol in the nitrile oxide cycloadditions to allylic alcohols. After this publication, several reports were published with moderate success [317-321] and normally requiring high catalyst loading (stoichiometric quantities). It was

only in 2004 that catalyzed chiral metal quantities were employed with high success (Scheme 5.1) [322].

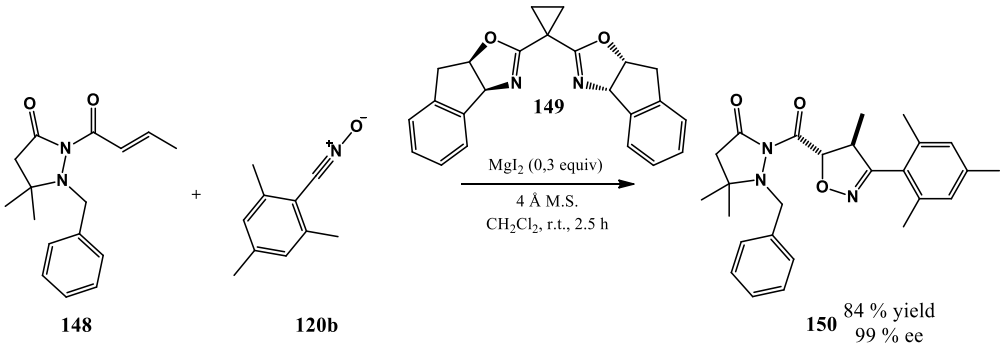

Scheme 5.1. Example of chiral Lewis acid-catalyzed cycloaddition reaction with nitrile oxides (Sibi *et al*).

At the time that the work presented in this chapter took place only few additional examples were described [323-328]. Furthermore in most cases it was used electron-deficient dipolarophiles that detained an α-chiral center, such as allylic alcohols or bared chiral auxiliary moieties such as oxazolidinone or pyrazolidinone, that facilitated the asymmetric cycloaddition.

5.1.2. Synthesis of intermediate 121n.

Alkylidene oxindole **121k** was synthesized by aldolic condensation between 6-chlorooxindole and benzaldehyde in the presence of piperidine, as described in chapter 4 [297]. Acylation of **121k** was achieved by using acetic anhydride in the presence of pyridine and *N*,*N*-dimethyl-aminopyridine (Scheme 5.2). The overall yield was of 88 %.

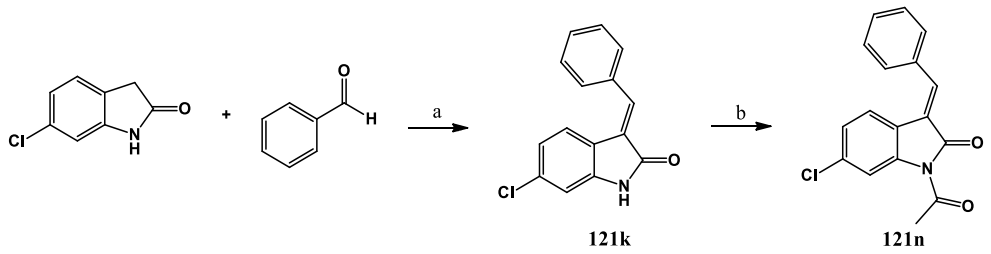

Scheme 5.2. Synthesis of alkylidene oxindole **121n**. (a) piperidine, EtOH, reflux, 8h. (b) Ac_2O, DMAP, pyridine, THF, 2h.

5.1.3. Attempts to enantioselectively synthesize compound 119ac

The goal was to enantioselectively synthesize both enantiomers of the best spiroisoxazoline oxindole (**119ac**) obtained in the previous chapter to assess their cytotoxicity. These experiments were performed in the Franz group at University of California – Davis.

The conditions utilized in chapter 4 for the synthesis of compound **119ac** were not ideal for asymmetric catalysis: Et_3N as dehydrohalogenating agent and high temperature (70 ºC). Therefore the initial changes were to perform the reaction at room temperature and to use molecular sieves instead of base as dehydrohalogenating agent [327]. These changes were made to diminish possible interference with catalyst/ligand and to slow down the generation of nitrile oxide *in situ*, in order to decrease the uncatalysed background reaction. Since the goal was to perform the reaction at room temperature the solvent was also changed to the less toxic dichloromethane. In addition, to potentially increase the interaction between dipolarophile and the metal an additional binding point was introduced in the molecule (*N*-acyl group) [329]. As revealed in the previous chapter, arylidine-oxindole dipolarophiles are less reactive than the ester counterparts, constituting an additional concern. And in fact in these conditions the yield was only of 16 % (Table 5.1, entry 1).

Franz group already had a substantial know-how in asymmetric synthesis of spirooxindoles and other oxindole derivatives [330-338] that helped guiding the choices tested. The study started by testing different metals (entry 2-7) as catalyst (20 mol %), with (*R,S*)-Indapybox (**151**, Figure 5.1) and sodium tetrakis[3,5-bis(trifluoromethyl)-phenyl]borate (NaBArF, **152**) as ligand and counterion respectively. In all cases, racemic mixtures or less than 10% enantiomeric excess (ee) were obtained. It was also tested a bivalent metal ($CuCl_2$), in this case with the bidentate ligand **153**, without obtaining better enantiomeric ratio (er), although promoting a yield increase to 35% (entry 8). Due to the constantly low yields achieved, different approaches were also tested, such as using Bronsted acid phenylphosphinic acid (**154**) and thioureas. With the non-chiral thiourea **155** (entry 9) the yield did not increase, but with (*R*,*R*)-TUC (**156**) the yield increased to 34% (entry 10), however without showing significant ee improvement. As expected with the use of an acid (entry 11) the yield decreased due probably to the fact that its presence can hinder the dehydrohalogenation step.

In the conditions used for entries 2, 3, 5 and 6 it was observed deacylation of the starting material **121n** and/or the spirooxindole **119ah**. Interestingly it was found that the ee for the deacylated product **119ac** was higher than **119ah**, revealing most likely that the deacylation occurred prior to 1,3-dipolar cycloaddition. Therefore the next conditions tested were focused on alkylidene **121k** (Table 5.2, entry 2-10). The best result was obtained with $Sc(OTf)_3$ (entry 2), in which the diastereomeric ratio (dr) improved to 90:10

Table 5.1. Cycloaddition reaction between **121n** and **123e**.

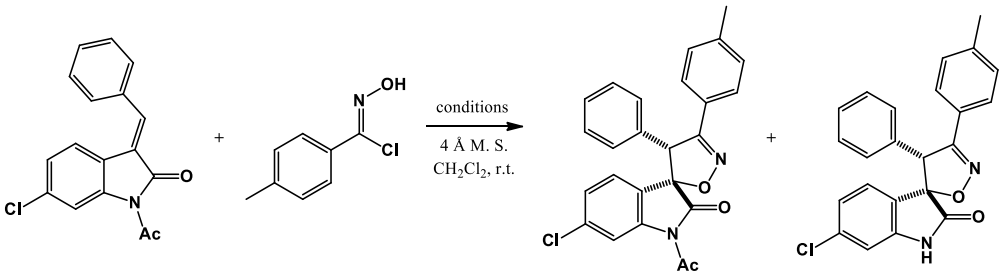

121n **123e** **119ah** **119ac**

Ent.	Catalyst[a]	Ligand[a]	Counterion[a]	Time	Yield (%)	Product	er[e]
1	-	-	-	3 days	16[b]	**1ah**	50:50
2	$Sc(OTf)_3$	(*R*,*S*)-Indapybox	NaBArF	3 days	<16[c]	**1ah**	52:48
						1ac	70:30
3	$ScCl_3THF_3$	(*R*,*S*)-Indapybox	NaBArF	3 days	<16[c]	**1ah**	51:49
						1ac	69:31
4	$In(OTf)_3$	(*R*,*S*)-Indapybox	NaBArF	4 days	22[d]		55:45
5	$Y(OTf)_3$	(*R*,*S*)-Indapybox	NaBArF	4 days	<10[d]	**1ah**	-
						1ac	54:45
6	$La(OTf)_3$	(*R*,*S*)-Indapybox	NaBArF	4 days	28[d]	**1ah**	50:50
						1ac	66:34
7	$BiCl_3$	(*R*,*S*)-Indapybox	NaBArF	4 days	27[d]	**1ah**	53:47
8	$CuCl_2$	(*S*)-Phenylbox	-	4 days	35[d]	**1ah**	52:48
9	Thiourea **155**	-	-	4 days	14[d]	**1ah**	50:50
10	(*R*,*R*)-TUC **156**	-	-	4 days	34[d]	**1ah**	54:46
11	PPA (**154**)	-	-	4 days	15[d]	**1ah**	50:50

[a] All reactions performed under argon with 3.0 equiv of **123e** and, when applicable, in a 1:1.1:1 ratio of catalyst, ligand, and counterion for 1h at a 20 mol % catalyst loading; [b] Isolated yields; [c] Yields by TLC comparison to entry 1; [d] Yields determined by ^1H NMR analysis of unpurified reaction mixture; [e] Determined using chiral-phase HPLC. M. S.: molecular sieves. PPA: Phenyl phosphinic acid.

and the er to 70:30 when compared to the uncatalysed reaction (entry 1). Intriguingly, when thiourea **156** was tested (entry 11) complete loss of stereoselectivity occurred. The alkaloid (-)-cinchonine ((-)-**157**) was also tested (entry 12) but did not affect the er outcome. Divalent catalysts with bidentate ligands were also unsuccessfully used, albeit a slight increase in dr was detected (entry 17-19). Maintaining the best catalyst employed ($Sc(OTf)_3$) it was then decided to test different ligands (entry 16-17, **158-159**) and counterions (entry 18-19). In all conditions loss of ee was observed.

Efforts were also made towards increasing the reaction yield. The most apparent problem seemed to be the lack of base to generate properly the 1,3-dipole. Since tertiary amines such as Et_3N was discourage, it was decided to experiment a bulky base that can act as a proton scavenger but lacks capacity to interfere with the Lewis acid, such as 2,6-ditertbutyl 4-methylpyridine (**160**). Increasing the equivalents of this base augmented the yield (Table 5.3 entry 2-3 versus entry 1), improving also the dr when 3 equivalents were

Table 5.2. Cycloaddition reaction between **121k** and **123e**.

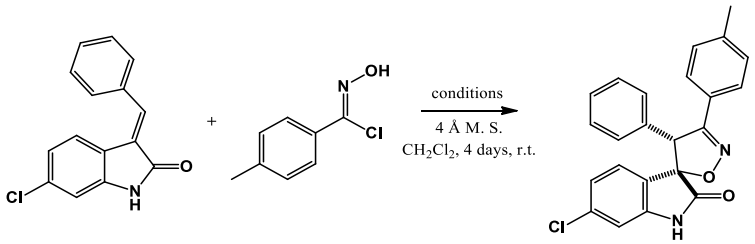

121k **123e** **119ac**

Ent.	Catalyst[a]	Ligand[a]	Counterion[a]	Yield (%)[b]	dr[b]	er[c]
1	-	-	-	20	78:22	50:50
2	$Sc(OTf)_3$	(*R*,*S*)-Indapybox	NaBArF	25	90:10	70:30
3	$ScCl_3THF_3$	(*R*,*S*)-Indapybox	NaBArF	25	78:22	64:36
4	$ScCl_3{\cdot}6H_3O$	(*R*,*S*)-Indapybox	NaBArF	19	78:22	63:37
5	$ScCl_3$	(*R*,*S*)-Indapybox	NaBArF	34	86:14	70:30
6	$La(OTf)_3$	(*R*,*S*)-Indapybox	NaBArF	39	84:26	52:48
7	$Y(OTf)_3$	(*R*,*S*)-Indapybox	NaBArF	30	90:10	51:49
8	$BiCl_3$	(*R*,*S*)-Indapybox	NaBArF	20	65:35	52:48
9	$RuCl_3$	(*R*,*S*)-Indapybox	NaBArF	27	78:22	52:48
10	$NiNO_3{\cdot}6H_3O$	(*R*,*S*)-Indapybox	NaBArF	16	67:33	52:48
11	(*R*,*R*)-TUC	-	-	28	50:50	50:50
12	(+)-cinchonine	-	-	22	80:20	50:50
13	$CuCl_2$	(*S*)-Ph-box	-	31	95:5	50:50
14	$MgBr_2$	(*S*)-Ph-box	-	32	95:5	50:50
15	$Zn(OTf)_2$	(*S*)-Ph-box	-	34	91:9	50:50
16	$Sc(OTf)_3$	(*4R,5S*)-Methyl Phepybox	NaBArF	27	86:14	47:53
17	$Sc(OTf)_3$	(*S*)-iPr-pybox	NaBArF	27	90:10	48:52
18	$Sc(OTf)_3$	(*R*,*S*)-Indapybox	$LiClO_4$	37	90:10	57:43
19	$Sc(OTf)_3$	(*R*,*S*)-Indapybox	$NaSbF_6$	35	90:10	58:42

[a] All reactions performed under argon with 3.0 equiv of **123e** and, when applicable, in a 1:1.1:1 ratio of catalyst, ligand, and counterion for 1h at a 20 mol % catalyst loading; [b] Determined by ^{1}H NMR analysis of partially purified reaction mixture; [c] Determined using chiral-phase HPLC. M. S.: molecular sieves.

employed. However, when the same conditions were applied with $Sc(OTf)_3$ (entry 5-6), it was observed that only catalytic quantities of the base were tolerated without reducing the ee. This observation was probably due to an increase in the background reaction. At the same time different solvent were tested (entry 7-12). The only solvent that promoted a slight increase in er was ether (67:33, entry 9 versus 62:38, entry 6), although it also promoted a slight decrease in dr.

In an attempt to reduce the extent of the background reaction two approaches were devised: (*a*) slow addition of the chlorooxime/nitrile oxide over time, and (*b*) increasing catalyst loading. First the 3 equivalents of chlorooxime were added in three consecutive days (entry 13) without improving the er, but increasing the yield to 62%. Adding slowly the nitrile oxide freshly prepared by stirring the chlorooxime with amberlyst 15 over time (Table 5.4, entry 2-3 versus entry 1) increased the er to a maximum of 70:30 for an addition

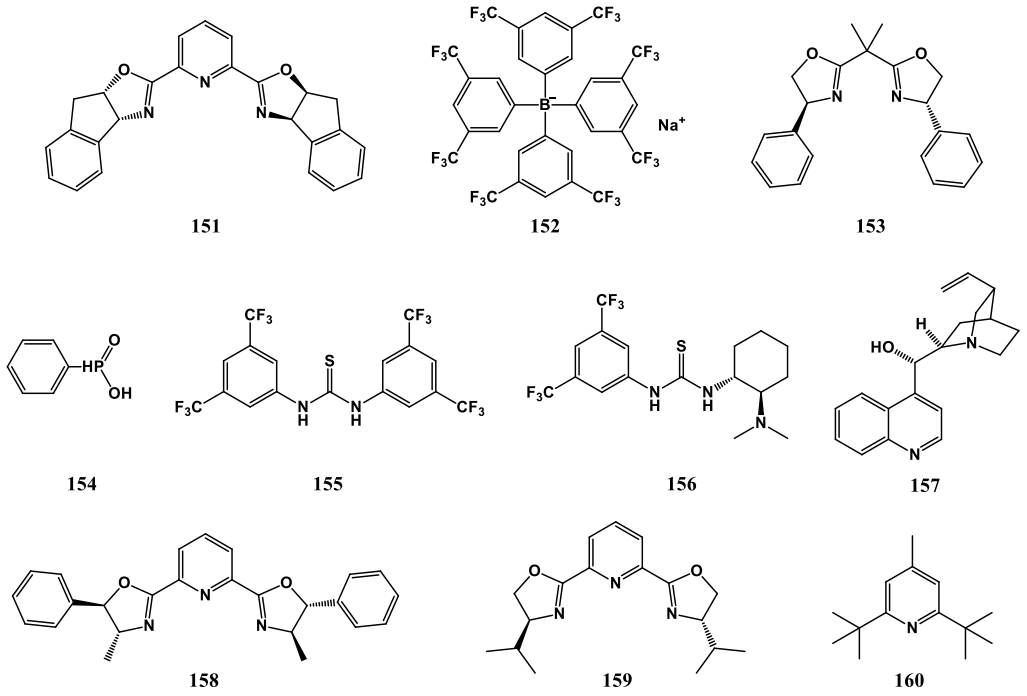

Figure 5.1. Examples of catalysts, ligands and counterions employed.

Table 5.3. Cycloaddition reaction between **121k** and **123e**.

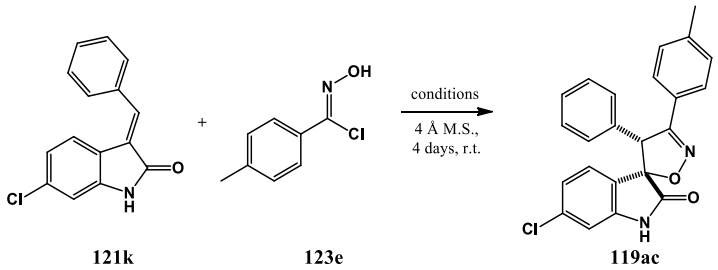

Ent.	Catalyst[a]	Solvent	Base[b] (equiv)	Yield (%)[d]	dr[d]	er[e]
1	-	DCM	-	20	78:22	50:50
2	-	DCM	0.2	29	78:22	50:50
3	-	DCM	3.0	65	90:10	50:50
4	$Sc(OTf)_3$	DCM	-	25	90:10	70:30
5	$Sc(OTf)_3$	DCM	0.3	45	90:10	70:30
6	$Sc(OTf)_3$	DCM	3.0	50	90:10	62:38
7	$Sc(OTf)_3$	Toluene	3.0	28	87:13	61:39
8	$Sc(OTf)_3$	MeCN	3.0	33	86:14	62:38
9	$Sc(OTf)_3$	Et_2O	3.0	24	86:14	67:33
10	$Sc(OTf)_3$	Hexanes	3.0	15	81:29	62:38
11	$Sc(OTf)_3$	MeOH	3.0	21	78:22	51:49
12	$Sc(OTf)_3$	THF	3.0	30	83:17	60:40
13	$Sc(OTf)_3$	DCM	1+1+1[c]	62	94:6	64:36
14	$Yb(OTf)_3 \cdot H_2O$	DCM	3.0	62	93:7	51:49
15	$In(OTf)_3$	DCM	3.0	85	93:7	51:49

[a] All reactions performed under argon with 3.0 equiv of **123e** and, when applicable, in a 1:1.1:1 ratio of catalyst, (*R*,*S*)-Indapybox, and NaBArF for 1h at a 20 mol % catalyst loading; [b] 2,6-ditertbutyl 4-methylpyridine; [c] 1 equiv of **123e** and base added in three consecutive days; [d] Determined by ^1H NMR analysis of partially purified reaction mixture; [e] Determined using chiral-phase HPLC. M.S.: molecular sieves.

Table 5.4. Cycloaddition reaction between **121k** and **123e**.

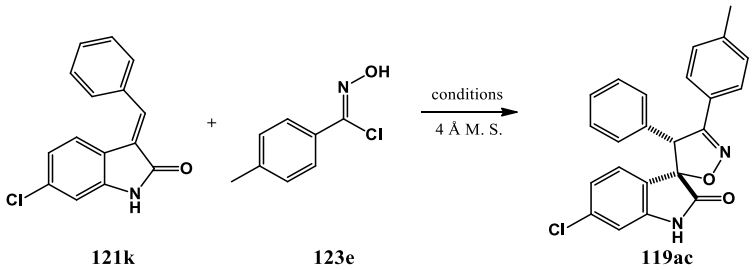

121k **123e** **119ac**

Ent.	% Catalyst loading[a]	Solvent	Addition time[b]	Time (days)	Temp.	Yield (%)[d]	dr[d]	er[f]
1	20	DCM	0	1	r.t.	25	90:10	51:49
2	20	DCM	0.5 h	1	r.t.	25	90:10	65:35
3	20	DCM	6 h	1	r.t.	20	90:10	70:30
4	20	DCM	11 h[c]	1	r.t.	15	90:10	70:30
5	20	Et_2O	6 h	1	r.t.	19	90:10	70:30
6	20	DCM	-	4	r.t.	25	90:10	70:30
7	20	DCM	-	4	r.t.	45[e]	90:10	70:30
8	40	DCM	-	4	r.t.	44[e]	96:4	72:28
9	100	DCM	-	4	r.t.	35[e]	96:4	75:25
10	20	DCE	-	4	r.t.	34	96:4	75:25
11	20	DCE	-	4	50 ºC	39	95:5	67:33
12	20	$CHCl_3$	-	4	r.t.	35	96:4	67:33
13	20	bromobenzene	-	4	r.t.	31	91:9	62:38
14	20	chlorobenzene	-	4	r.t.	29	97:3	61:39
15	20	2-bromo benzotrifluoride	-	4	r.t.	36	95:5	58:42
16	20	2,6-*bis*(trifluoromethyl) bromobenzene	-	4	r.t.	13	95:5	65:35
17	20	*o*-bromobenzene	-	4	r.t.	30	96:4	61:39
18	20	2-bromo-*m*-xylene		4	r.t.	23	96:4	68:32
19	20	Ethylene glycol monoethyl ether	-	4	r.t.	28	96:4	56:44

[a] All reactions performed under argon with 3.0 equiv of **123e** and in a 1:1.1:1 ratio of $Sc(OTf)_3$, (*R*,*S*)-Indapybox, and NaBArF for 1h; [b] Chorooxime and amberlyst 15 (2x m/m) were stirred for 1h prior to addition; [c] Ambertyst 15 (4x m/m); [d] Determined by ^1H NMR analysis of partially purified reaction mixture; [e] 2,6-ditertbutyl 4-methylpyridine (0.3 equiv) was also employed; [f] Determined using chiral-phase HPLC. M.S.: molecular sieves.

time of 6 h. Further increment in the addition time did not improve the er (entry 4). As expected adding the 3 equivalents of nitrile oxide altogether abolished the metal-catalyzed cycloaddition reaction (entry 1). Although these experiments corroborate once again the necessity to deliver slowly the 1,3-dipole to the dipolarophile, it did not improve the previous best result of 70:30 er. Increasing the catalyst loading (entry 8-9) improved both dr and er, but even when the quantities were stoichiometric the er was only of 75:25.

One strategy to increase the efficacy of asymmetric catalysis is to reduce the temperature. However in this case, since the yields were already very low and the reaction time long, it was decided to test the less common, but sometimes effective increase of temperature. To allow increasing the temperature to 50ºC the solvent was changed to

dichloroethane, and interestingly, although the yield did not improve in higher temperature (entry 5), at room temperature the yield, dr and er (75:25) increased (entry 10 versus entry 6). Since DCM and DCE gave the best er results, a series of halogenated solvents were tested (entries 12-18). Unfortunately none revealed to be a better choice.

The best condition that gave 75:25 er was employed to synthesize both enantiomeric enriched mixtures by using (*R*,*S*)-indapybox and (*S*,*R*)-indapybox ligands. The enantioenriched mixtures were tested in HCT116 $p53^{(+/+)}$ (Table 5.5), revealing that one enantiomer is more potent than the other. However since enantioselective synthesis was not achieved, no further evaluation was performed.

Table 5.5. *In vitro* antiproliferative activities

Compound	HCT116 $p53^{(+/+)}$ GI_{50}, μM[a]
1ac (50:50 er)	32.49±1.47
1ac (25:75 er)	41.71±0.89
1ac (75:25 er)	27.97±1.50

[a] IC_{50} determined by the MTS method after 72h. Each value is the mean (IC_{50} ± SD) of three independent experiments performed in duplicate.

Interestingly last year Liang *et al* were able to synthesize spiroisoxazoline oxindoles enantioselectively using 10 mol % of L1−$Ni(ClO_4)_2·6H_2O$ (1:1) with 4 Å molecular sieves and a small amount of H_2O in DCE at 35 °C for 24 h (Scheme 5.3).

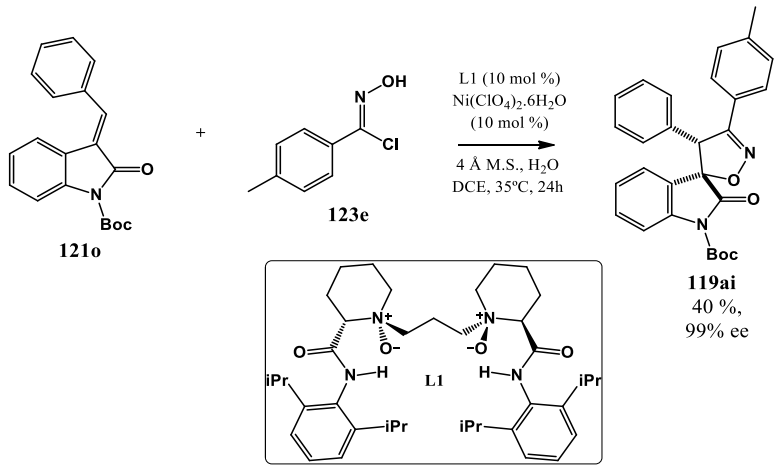

Scheme 5.3. Asymmetric Synthesis of Spiroisoxazoline oxindoles by Liang *et al*.

5.2. ENATIOSELECTIVE APPROACHES TOWARDS SPIROPYRROLINE OXINDOLES

5.2.1. Introduction

It was previously shown in the Franz group that 5-methoxy-2-aryloxazoles cyclize onto indolin-2,3-diones to form spirooxazoline oxindoles in excellent yields and with high diastereoselectivity [335] (Scheme 5.4). Interestingly when these conditions were applied to the addition of 5-methoxy-2-aryloxazole **161** to alkylidene oxindole **121p,** spiropyrroline oxindole **163** was obtained in 90 % yield and with 91:9 dr in just 10 minutes (Scheme 5.5). Obviously since a catalyst was tested without a chiral ligand, the compound was obtained in a racemic mixture. The goal of the work presented in this section was to synthesize enantioenriched compound **163** by employing scandium catalysts.

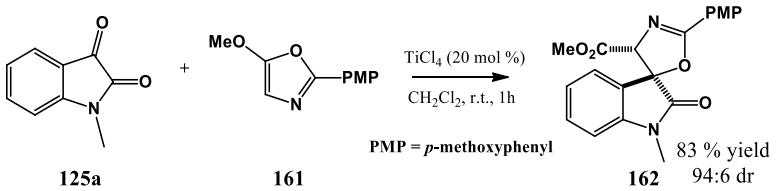

Scheme 5.4. Titanium-catalyzed stereoselective synthesis of spirooxazoline oxindole **162**.

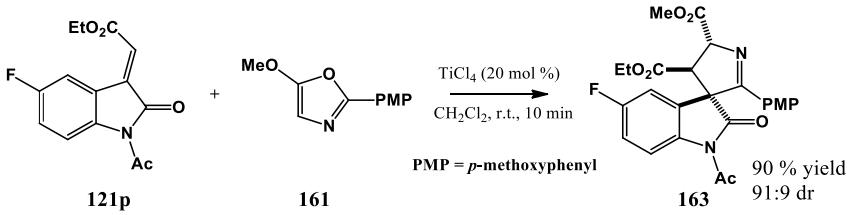

Scheme 5.5. Titanium-catalyzed stereoselective synthesis of spiropyrazole oxindole **163**.

5.2.2. Synthesis of intermediate 121p.

Alkylidene-oxindole **121q** was synthesized by Wittig reaction between 5-fluoroindolin-2,3-dione (**125a**) and phosphonium ylide **128a**. Acylation of **121q** was achieved by using acetic anhydride in the presence of pyridine and *N*,*N*-dimethyl-aminopyridine (Scheme 5.6). The overall yield was of 50 %.

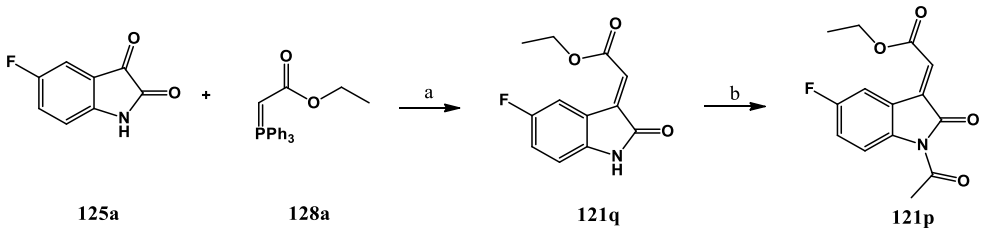

Scheme 5.6. Synthesis of 3-methylene indolin-2-one **121p**. (a) THF, reflux, 10 h. (b) Ac_2O, DMAP, pyridine, THF, 2h.

5.2.3. Attempts to enantioselectively synthesize compound 163

Changing the catalyst from $TiCl_4$ to $Sc(OTf)_3$ maintained the same stereoselectivity, while decreasing the reaction rate (Table 5.6, entry 1). Several conditions were then tested with $ScCl_3THF_3$ or $Sc(OTf)_3$ with (*R,S*)-indapybox and NaBArF. With $ScCl_3THF_3$ the reaction rate was higher than with $Sc(OTf)_3$, however lower dr was obtained (entry 2-6 versus entry 9-13), even when solvent and temperature were changed. The use of NaBArF to promote formation of a cationic scandium complex proved to be essential for enhancing the reaction rate in the presence of ligand (entry 7 versus entry 2), although as expected it was unable to promote the reaction by itself (entry 8). Using $Sc(OTf)_3$, (*R,S*)-indapybox, and NaBArF the best result was obtained in toluene at room temperature (entry 11). Changing the counterion (entry 14-15) and the ligand (entry 16-17) reduced the stereoselectivity.

Table 5.6. Synthesis of enantioenriched spiropyrroline ***epi*-163**.

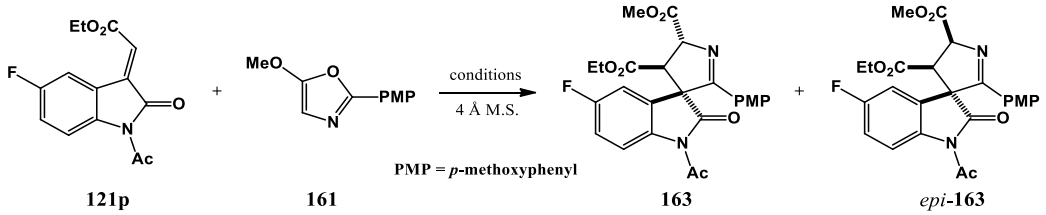

121p **161** **163** *epi*-**163**

Ent.	Catalyst[a]	Ligand[a]	Counter ion[a]	Solvent	Time	Temp. (ºC)	Yield (%)[c]	dr 163: *epi*-163[c]	er[d]
1	$Sc(OTf)_3$[b]	-	-	DCM	5h	r.t.	complete	90:10	50:50
2	$ScCl_3THF_3$	Indapybox	NaBArF	DCM	15min	r.t.	complete	30:70	28:72
3	$ScCl_3THF_3$	Indapybox	NaBArF	DCM	1h	0ºC	complete	30:70	18:82
4	$ScCl_3THF_3$	Indapybox	NaBArF	DCM	12h	-20ºC	complete	30:70	17:83
5	$ScCl_3THF_3$	Indapybox	NaBArF	Toluene	12h	0ºC	complete	30:70	16:84
6	$ScCl_3THF_3$	Indapybox	NaBArF	MeCN	12h	0ºC	complete	30:70	22:78
7	$ScCl_3THF_3$	Indapybox	-	DCM	4 days	r.t.	87	30:70	22:78
8	-	-	NaBArF	DCM	4 days	r.t.	-	-	-
9	$Sc(OTf)_3$	Indapybox	NaBArF	DCM	3 days	r.t.	complete	9:91	22:78
10	$Sc(OTf)_3$	Indapybox	NaBArF	Pentane	4 days	r.t.	complete	13:87	23:77
11	$Sc(OTf)_3$	Indapybox	NaBArF	Toluene	12h	r.t.	complete	9:91	14:86
12	$Sc(OTf)_3$	Indapybox	NaBArF	Toluene	24h	0ºC	complete	9:91	14:86
13	$Sc(OTf)_3$	Indapybox	NaBArF	Toluene	24h	-20ºC	complete	5:95	17:83
14	$Sc(OTf)_3$	Indapybox	$NaSbF_6$	Toluene	4 days	r.t.	14	15:85	12:88
15	$Sc(OTf)_3$	Indapybox	$LiClO_4$	Toluene	4 days	r.t.	4	19:81	17:83
16	$Sc(OTf)_3$	(*S*)-iPrpybox	NaBArF	Toluene	4 days	r.t.	45	22:78	62:38
17	$Sc(OTf)_3$	(*4R,5S*)-Me Phepybox	NaBArF	Toluene	4 days	r.t.	36	30:70	56:46
18	$CuCl_2$	(*S*)-Phbox	-	Toluene	4 days	r.t.	-	-	-
19	$In(OTf)_3$	Indapybox	NaBArF	Toluene	4 days	r.t.	7	30:70	23:77

[a] All reactions performed under argon with 2.0 equiv of **161** and, when applicable, in a 1:1.1:1 ratio of catalyst, ligand, and counterion for 1h at a 20 mol % catalyst loading; indapybox: (*R,S*); [b] Run with 5 mol % of catalyst; [c] Determined by ^1H NMR analysis of unpurified reaction mixture; [d] Determined using chiral-phase HPLC for the major isomer. M.S.: molecular sieves.

Applying the best condition the spirooxindole was then isolated with 99% yield. It was notable that these conditions afforded a reversal in the diastereoinduction to afford pyrroline *epi*-**163** (dr = 91:9) with the 4',5'-syn isomer as the major product. The relative stereochemistry was determined by X-ray crystallographic analysis to be 3,4'-trans/4',5'-trans isomer (a racemic mixture of 3*S*,4'*R*,5'*R* and 3*R*,4'*S*,5'*S* notated 3*S**,4'*R**,5'*R** for compound **163**, and 3*S*,4'*R*,5'*S* to ***epi*-163** (Figure 5.2). The reversal in diastereoselectivity is directly attributed to the addition of the ligand because the Sc-catalyzed reaction in the absence of ligand still affords **163** with high 4',5'-anti diastereoselectivity.

A proposed mechanism for the formation of **163** (in the absence of a chiral ligand) is shown in Scheme 5.7. Lewis acid activation of alkylidene **121p** followed by oxazole conjugate addition would give rise to enolate-bound oxocarbenium intermediate **164**. Subsequent cyclization and oxazole ring opening affords spirocycle **163**.

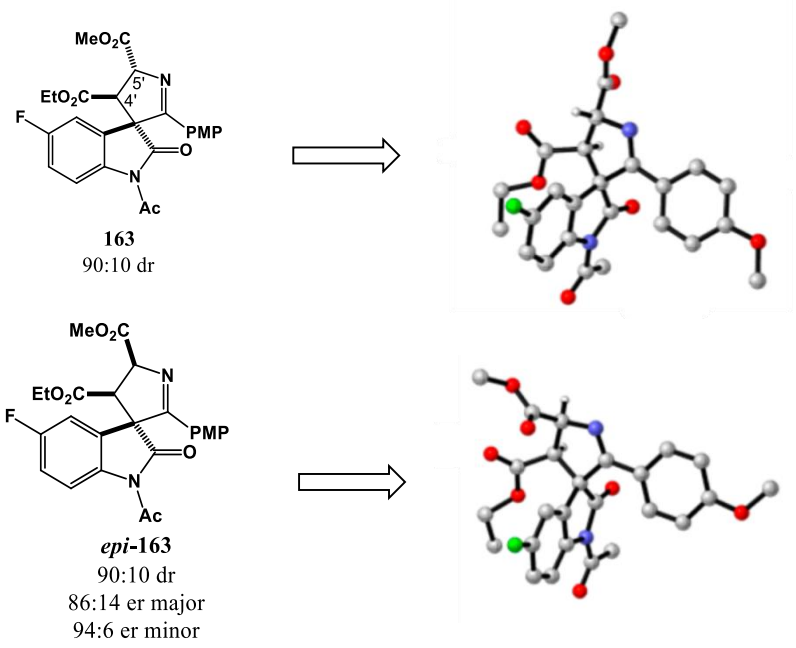

Figure 5.2. X-ray crystallography of **163** and *epi*-**163** [339].

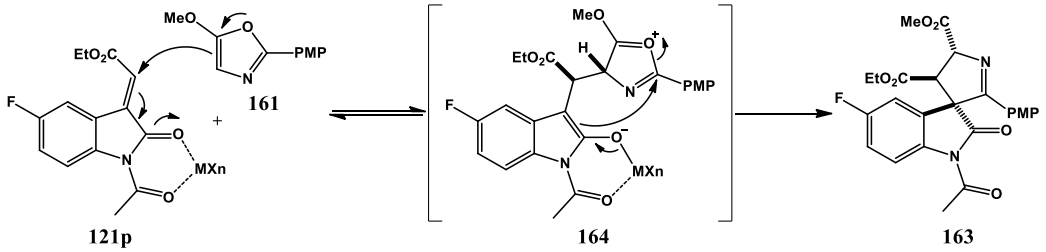

Scheme 5.7. Proposed mechanism for Lewis acid catalyzed formation of **163**.

5.3. CONCLUDING REMARKS

Attempts to synthesize enantioenriched spiroisoxazoline oxindole **119ac** were described. The best result was obtained when $Sc(OTf)_3$ (20 mol %), indapybox and NaBArF (1:1.1:1 equiv) were used in DCE (r.t., 4 days), affording an ee of 50 %. The enantioenriched mixtures were tested *in vitro*, revealing that one enantiomer is more potent in HCT116 $p53^{(+/+)}$cell line.

It was also presented a methodology for the synthesis of spirocyclic pyrroline oxindole ***epi*-163** upon cyclization of 5-alkoxy-2-aryloxazoles to alkylidene oxindoles. This strategy forges a quaternary spirocenter with excellent levels of stereocontrol. Using a chiral scandium(III) − indapybox/BArF complex provides efficient access to the enantio-enriched spiropyrroline. The addition of the ligand reverses the diastereoselection relative to conditions performed without the ligand for either the $Sc(OTf)_3$ or $TiCl_4$ catalyst.

Chapter 6

SPIROOXADIAZOLINE OXINDOLES:

SYNTHESIS AND BIOLOGICAL EVALUATION

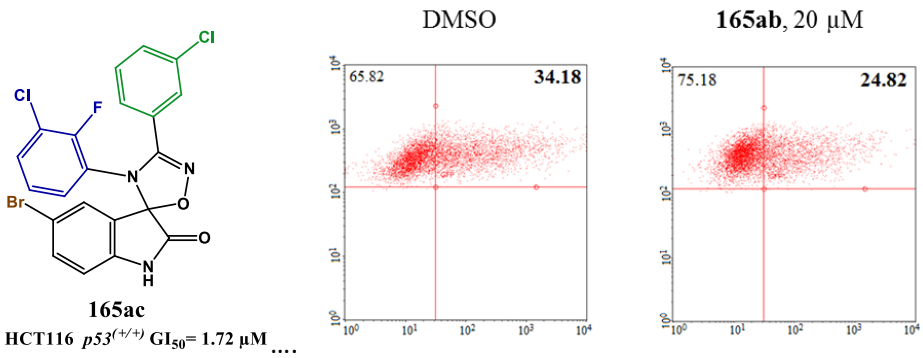

This chapter reports the synthesis and biological evaluation of thirty two spirooxadiazoline oxindoles as anticancer agents. Nine compounds showed an antiproliferative activity below 10 µM, with four compounds more active than the positive control nutlin-3a in HCT116 *p53*$^{(+/+)}$ cell line. Moreover, proof-of-concept was demonstrated by inhibition of the interaction between p53 and MDM2 in a live-cell bimolecular fluorescence complementation assay for compound **165ab**. Furthermore, the induction of apoptosis was confirmed for compound **165ab** and **165ad** in HCT116 *p53*$^{(+/+)}$ cell line.

- Carlos J. A. Ribeiro, Joana D. Amaral, Cecília M. P. Rodrigues, Rui Moreira, Maria M. M. Santos, *Spirooxadiazoline oxindoles with promising in vitro antitumor activities*, in preparation

6.1. INTRODUCTION

The moderate anticancer activity of spiroisoxazoline derivatives (discussed in chapter four), and the apparent lack of selectivity for the p53 pathway, prompt the search for potentially more active spirooxindoles with five-membered fused ring. It was decided to explore the substitution effect of the chiral C-4', with tetrahedral molecular geometry, to the non-chiral with trigonal planar geometry N-4' (Scheme 6.1). This simple alteration abolishes a chiral center and reorients spatially the R^2 substituent.

Therefore, this chapter will be dedicated to the synthesis (Scheme 6.2) and biological evaluation of spirooxadiazoline oxindoles **165**. As for spiroisoxazoline oxindoles, it was synthesized primarily derivatives with three aromatic side chains attached to the oxadiazoline moiety, in an attempt to mimic the three pivotal p53 amino acids that interact with MDM2.

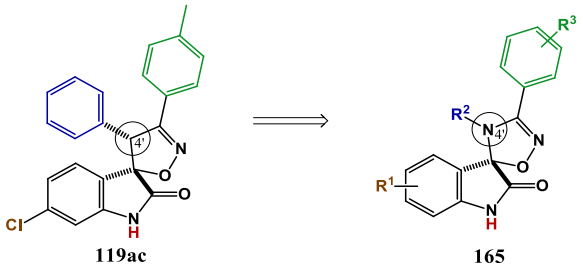

Scheme 6.1. Optimization Strategy

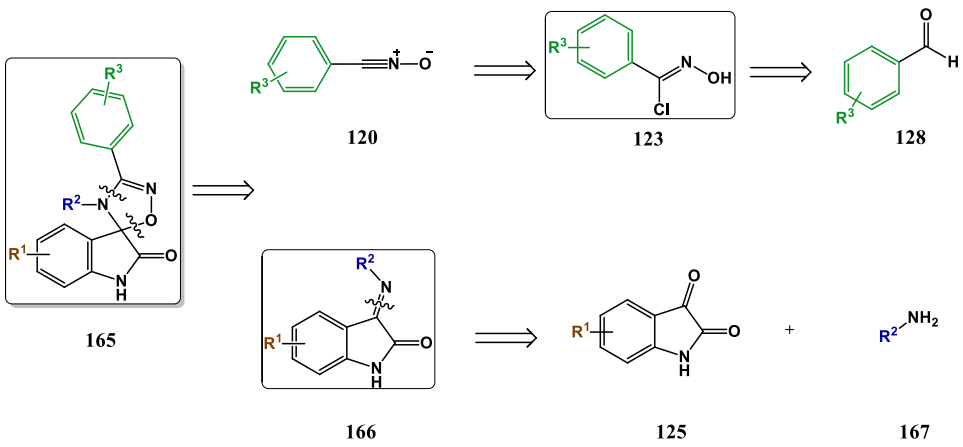

Scheme 6.2. Retrosynthesis of spirooxadiazoline oxindoles derivatives, highlighting the final step between 3-imino indolin-2-ones (**165**) and chlorooximes (**123**).

6.2. SYNTHESIS OF INTERMEDIATES

3-Imino-indolin-2-ones (**166**) were synthesized by reacting indolin-2,3-diones (**125**) with different primary amines, mainly anilines (**167**) in the presence of acetic acid in yields of 54-93 % (Scheme 6.3, Table 6.1) [340]. Furthermore 6-chloroindolin-2,3-dione was synthesized from the corresponding oxindole. First, 3,3-dibromo-6-chloroindolin-2-one was obtained by heating the starting 6-chloroindolin-2-one with copper(II) bromide, and then by refluxing in aqueous methanol the intended compound was isolated (55 % yield) [341, 342].

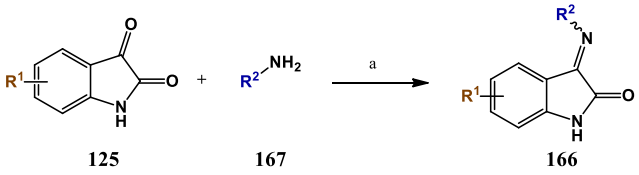

125 167 166

Scheme 6.3. Synthesis of 3-imino-indolin-2-ones (a) CH_3COOH, EtOH, reflux, 3-72h

Table 6.1. Synthesis of 3-imino-indolin-2-ones.

Compd	R^1	R^2	Yield (%)	Compd	R^1	R^2	Yield (%)
166a	H	Ph	69	**166k**	5-Br	4-ClPh	86
166b	H	3-ClPh	87	**166l**	5-Br	3-Cl,4-FPh	82
166c	H	4-ClPh	81	**166m**	5-Br	2-F,3-ClPh	85
166d	H	3-Cl,4-FPh	90	**166n**	5-Br	3-Br	86
166e	H	4-F	61	**166o**	5-Cl	*tert*-butyl	54
166f	5-Cl	Ph	84	**166p**	6-Cl	Ph	75
166g	5-Cl	3-ClPh	68	**166q**	6-Cl	3-ClPh	82
166h	5-Cl	4-ClPh	83	**166r**	6-Cl	4-ClPh	80
166i	5-Br	Ph	80	**166s**	7-Cl	Ph	87
166j	5-Br	3-ClPh	93	**166t**	7-Br	Ph	80

As observed for 3-methylene indolin-2-ones, 3-imino-indole-2-ones derivatives were also synthesized predominantly as *E* isomers, as confirmed by ^{1}H-NMR and in accordance to literature [340, 343, 344]. For example, the signal for H-4 of the *E*-isomer of derivative **166b** appears considerably shifted upfield (6.67 ppm) in comparison to both H-4 signals of the parent indolin-2,3-dione (7.63 ppm) and the minor *Z*-isomer (7.61 ppm).

As described in chapter three, additional aromatic chlorooxime **123** were synthesized starting from the aromatic aldehyde **128** with *in situ* formation of the corresponding aldoxime **129** [276] (Scheme 6.4, Table 6.2).

The ^{1}H NMR spectra of the intermediates are in accordance with literature [345-349].

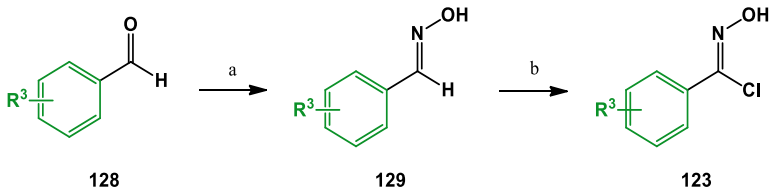

Scheme 6.4. Synthesis of hydroximoyl chlorides. (a) $NH_3OH{\cdot}HCl$, H_2O, Na_2CO_3, reflux; (b) NCS, pyridine, $CHCl_3$, r.t.

Table 6.2. Synthesis of hydroximoyl chlorides.

Compound	R^3	Yield (%)	Compound	R^3	Yield (%)
123e	4-MePh	83	**123h**	3-BrPh	88
123f	3-ClPh	90	**123i**	2-F,3-ClPh	91
123g	4-ClPh	82			

6.3. SYNTHESIS OF SPIRO[INDOLINE-3,5'-[1,2,4]OXADIAZOLINE]-2-ONES

Spirooxadiazoline oxindoles (**165**) were obtained by 1,3-dipolar cycloaddition between 3-imino-indolin-2-ones (**166**) and nitrile oxides generated *in situ* by dehydrohalogenation of hydroximoyl chlorides (**123**) (Scheme 6.5, Table 6.3).

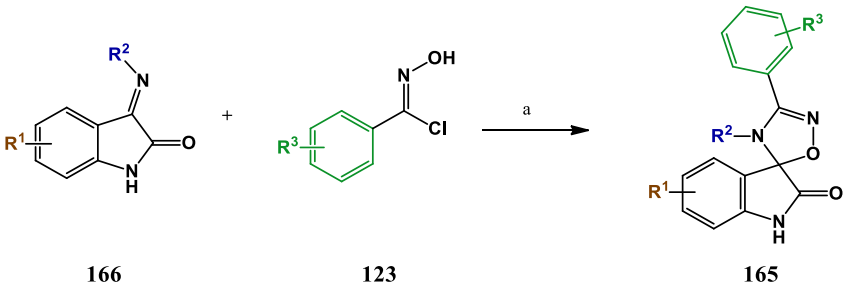

Scheme 6.5. Synthesis of spirooxadiazoline oxindoles. (a) Et_3N, CH_2Cl_2, 5-12 h, r.t.

As expected, based on the previous results with spiroisoxazoline oxindoles, the regioisomer isolated was the spiro[indoline-3,5'-[1,2,4]oxadiazoline]-2-one (Scheme 6.6). The ^{13}C NMR spectrum showed that spiro carbon signal appeared at 98.34 – 99.15 ppm, as described for other spirooxadiazoline oxindoles found in literature (98.4 – 98.9 ppm) [350]. For the alternative regioisomer, it would be expected a much more shielded value for the spiro carbon, as observed for spiropyrazoline oxindoles, in which the spiro carbon is linked to three carbons and one nitrogen (75.44 - 78.17 ppm [351]). In addition, the chemical shift of oxadiazoline C=N appeared at 154.44 – 156.34 ppm (155.4 – 157.0 ppm [350]). The compounds were further characterized by melting point, IR and their purity assessed by elemental analysis (chapter 9).

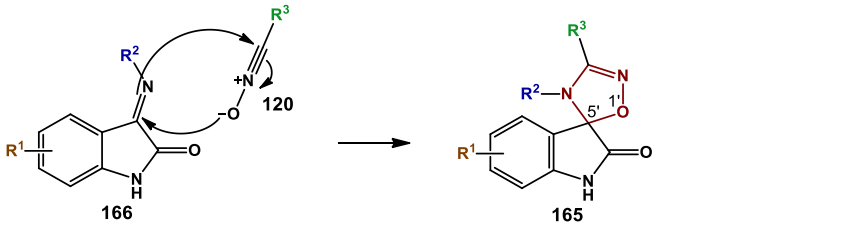

Spiro[indoline-3,5'-[1,2,4]oxadiazoline]-2-one

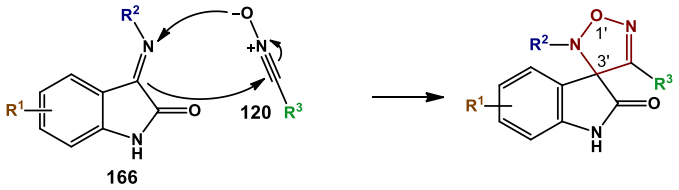

Spiro[indoline-3,3'-[1,2,5]oxadiazoline]-2-one

Scheme 6.6. Possible regioisomers formed as a result of 1,3-dipolar cycloaddition between **166** and **120**.

6.4. BIOLOGICAL STUDIES

6.4.1. Assessment of cell viability

It was decided to primarily address two previous underexplored substitutions: (*a*) probing the phenyl ring A (Table 6.3) that previously was limited to *p*-OMe group, and (*b*) expand halogen substitutions outside the oxindole ring, since two vicinal halophenyl groups attached to a rigid heterocyclic core are a common feature among the published p53-MDM2 interaction disruptors. Therefore, the SAR study started by probing the phenyl ring A with halogens in *meta* and *para* position without any substituents in the other phenyl rings. The three compounds synthesized (**165a-c**) exhibited GI_{50} higher than 50 µM, but informed that *p*-chloro substitution doubled the potency when compared to *p*-fluor (**165a**). Then compounds with two chloro atoms (one in ring A and the other in ring B) were tested. All 4 derivatives synthesized (**165d-g**) were found to be equipotent and more active than the previous monohalogenated derivatives.

In the spiroisoxazoline study (chapter 4) the most active compounds detained a halogen at position 6 of the oxindole, which is in agreement with potent spiropyrrolidine oxindoles described in literature [72]. In addition, other publications describing different spirooxindoles reported that a 5-halogen can sometimes be beneficial to increase anticancer activity [79, 83]. Therefore the next derivatizations were focused at these two positions. By probing $R^{2'}$ and R^3, different spirooxadiazolines with 5-chlorooxindole (**165h-n**) and 6-chlorooxindole (**165p-w**) moieties were synthesized. In both cases, a

Table 6.3. *In vitro* antiproliferative activities in HCT116 *p53*$^{(+/+)}$ cell line.

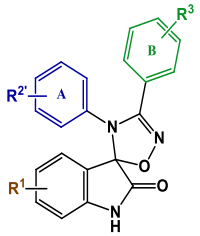

165

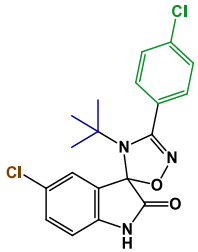

165o

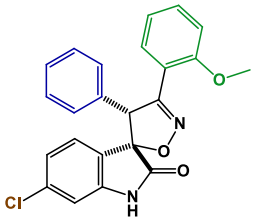

119ad

Compd	R^1	$R^{2'}$	R^3	Yield (%)	HCT116 *p53*$^{(+/+)}$ GI_{50}, μM[a]
165a	H	4-F	H	80	99.55±0.80
165b	H	3-Cl	H	82	70.07±3.23
165c	H	4-Cl	H	87	54.54±0.10
165d	H	3-Cl	3-Cl	85	32.63±0.40
165e	H	3-Cl	4-Cl	80	33.73±0.14
165f	H	4-Cl	3-Cl	84	38.38±2.37
165g	H	4-Cl	4-Cl	85	31.19±2.46
165h	5-Cl	H	H	76	39.10±2.01
165i	5-Cl	3-Cl	H	56	26.42±0.27
165j	5-Cl	3-Cl	3-Cl	54	4.56±0.16
165k	5-Cl	3-Cl	4-Cl	58	25.63±1.05
165l	5-Cl	4-Cl	H	69	27.09±2.49
165m	5-Cl	4-Cl	3-Cl	66	21.34±1.02
165n	5-Cl	4-Cl	4-Cl	64	17.63±0.46
165o				55	48.22±0.01
165p	6-Cl	H	H	81	28.35±3.95
165q	6-Cl	H	4-Me	70	50.56±4.41
165r	6-Cl	H	4-Cl	82	26.51±0.13
165s	6-Cl	3-Cl	3-Cl	75	6.59±0.03
165t	6-Cl	3-Cl	4-Cl	78	20.15±1.02
165u	6-Cl	4-Cl	H	80	31.76±1.92
165v	6-Cl	4-Cl	3-Cl	80	28.66±2.13
165w	6-Cl	4-Cl	4-Cl	79	13.18±0.37
165x	5-Br	H	H	73	13.53±4.54
165y	5-Br	4-Cl	H	68	21.94±2.41
165z	5-Br	3-Cl	H	62	4.72±0.16
165aa	5-Br	3-Cl	4-Cl	60	7.74±0.12
165ab	5-Br	3-Cl	3-Cl	61	2.04±0.03
165ac	5-Br	3-Br	3-Br	67	3.20±0.11
165ad	5-Br	3-Cl,4-F	3-Cl	55	6.61±0.18
165ae	5-Br	2-F,3-Cl	3-Cl	57	1.72±0.08
165af	5-Br	3-Cl	2-F,3-Cl	61	3.22±0.28
119ad					34.60±2.44
Nutlin-3a					3.99±1.21

[a] GI_{50} determined by the MTS method after 72h. Each value is the mean (GI_{50} ± SD) of three independent experiments performed in duplicate.

Table 6.4. *In vitro* antiproliferative activities in HCT116 *p53*$^{(-/-)}$, HepG2 and SW620 cell lines

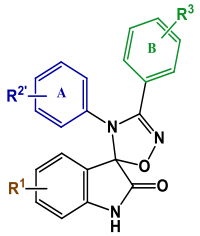

165

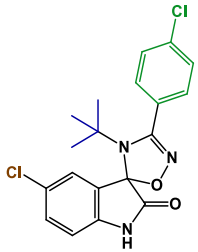

165o

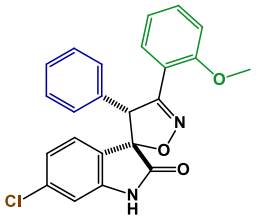

119ad

Compd	HCT116 *p53*$^{(-/-)}$ GI_{50}, μM[a]	HepG2 GI_{50}, μM[a]	SW620 GI_{50}, μM[a]	Compd	HCT116 *p53*$^{(-/-)}$ GI_{50}, μM[a]	HepG2 GI_{50}, μM[a]	SW620 GI_{50}, μM[a]
165d	34.55±3.69	-	-	**165t**	22.49±1.34	-	-
165e	37.11±2.40	-	-	**165u**	31.96±2.07	-	-
165f	39.81±2.84	-	-	**165v**	30.25±2.35	-	-
165g	33.96±2.99	-	-	**165w**	13.96±1.15	-	-
165h	44.74±1.85	-	-	**165x**	14.43±4.49	-	-
165i	41.57±2.04	-	-	**165y**	25.77±0.58	-	-
165j	6.85±0.75	3.29±0.26	3.89±0.38	**165z**	7.50±1.26	3.51±0.37	4.21±0.26
165k	28.95±0.56	-	-	**165aa**	12.26±1.39	4.09±0.37	7.99±0.37
165l	27.00±2.66	-	-	**165ab**	2.90±0.23	2.08±0.00	2.05±0.305
165m	21.79±1.41	-	-	**165ac**	5.98±0.57	2.20±0.23	3.74±0.37
165n	18.05±0.85	-	-	**165ad**	7.22±0.49	4.03±0.45	6.96±0.19
165o	52.45±1.59	-	-	**165ae**	2.03±0.40	1.15±0.18	2.00±0.18
165p	35.52±6.67	-	-	**165af**	4.44±0.81	2.46±0.06	3.47±0.04
165r	30.65±1.32	-	-	**119ad**	37.99±2.70	-	-
165s	7.77±0.76	4.40±0.36	6.69±0.76	**Nutlin-3a**	47.81±1.88	-	-

[a] GI_{50} determined by the MTS method after 72h. Each value is the mean (GI_{50} ± SD) of three independent experiments performed in duplicate.

second chloro (at phenyl ring A) maintained or slightly increased the potency (**165i** and **165l** versus **165h**; **165u** versus **165p**). Adding an additional chloro, at R^3, an increase in potency was observed when both halogens (ring A and B) were in *meta* or in *para* position, with the former representing an impressive 8.6-fold and 4.3-fold increase in potency when compared to the non-halogenated counterparts (**165j**, GI_{50}= 4.56 µM versus **165h**, GI_{50}= 39.10 µM and **165s**, GI_{50}= 6.59 µM versus **165p**, GI_{50}= 28.35 µM). Compound **165o** is the only derivative with a non-aromatic side chain at *N*-4', and was found to decrease activity, representing the least active compound of the 5-chlorooxindole derivatives series.

It was then decided to test the effect of changing the chloro substituent in the oxindole moiety to bromo. As the best compound so far contained a 5-chlorooxindole (**165j**), the next set of compounds was focused in this position (**165x-ab**). Interestingly all compounds revealed to be more active than the 5-chlorooxindole equivalents, with three compounds reaching activities below 10 µM in HCT116 $p53^{(+/+)}$. As expected the best compound (**165ab**, GI_{50}= 2.04 µM) possesses two chloros (rings A and B) in *meta* position, representing a 2.2-fold increase in comparison to **165j**. Changing all the chloro atoms to bromo, slightly decreased the activity (**165ac**). The next step was to introduce fluor atoms into phenyl rings A and B (**165ad-af**), revealing that only 2-F,3-Cl in ring A promoted a slight increase in potency (**165ae**, GI_{50}= 1.72 µM), as expected by comparison to spiropyrrolidine oxindoles.

In addition, four derivatives revealed more potent than the positive control nutlin 3a (**165ab-ac**, **165ae-af**). All compounds with GI_{50} lower than 50 µM were tested in HCT116 $p53^{(-/-)}$ (Table 6.4) and the derivatives with GI_{50} lower than 10 µM were additionally tested in two other cell lines (HepG2 and SW620). As observed for the previous spiroisoxazoline oxindoles studied, the compounds showed only a marginal increase in potency in cell lines harboring wild type p53, revealing that p53 non-related effects are also relevant to the observed cytotoxic outcome.

6.4.2. Evaluation of compounds ability to block the intracellular p53-MDM2 interaction

By applying a Venus-based bimolecular fluorescence complementation system methodology (BiFC [260], Figure 4.4, pg 67) it was demonstrated that compound **165ab** can inhibit p53-MDM2 interaction in the same extent as the positive control Nutlin-3a at concentrations of 10 and 20 µM (Figure 6.1).

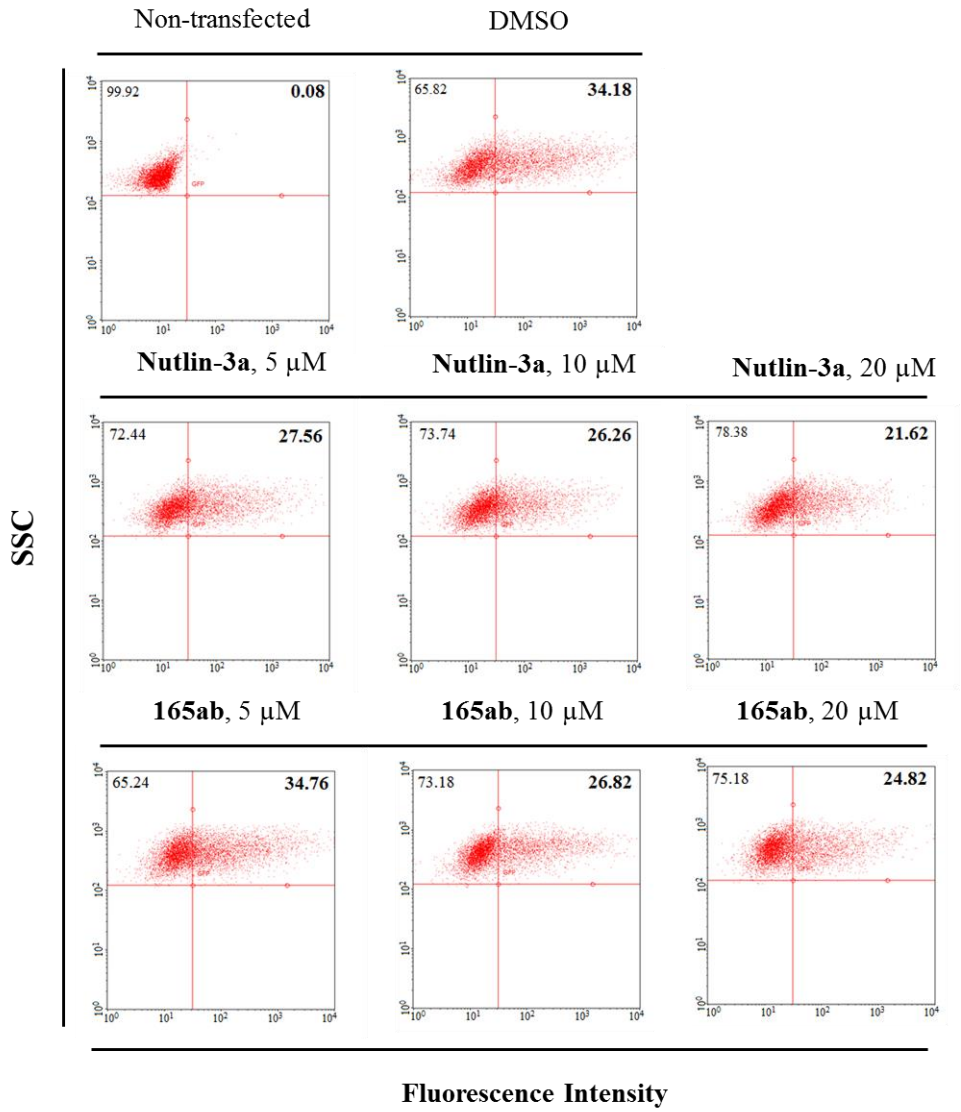

Figure 6.1. Compound 165ab decreases p53-MDM2 interaction by BiFC. HCT116 *p53*$^{(-/-)}$ cells were co-transfected with V1-p53/MDM2-V2 BiFC combination plasmids for 24 h. Vehicle, nutlin-3a (5, 10, and 20 µM) and compound **165ab** (5, 10, and 20 µM) were included in the culture medium 4 h after transfection. Representative flow cytometry profiles of the disruption of V1-p53/MDM2-V2 complementation (n=3).

6.4.3. Evaluation of apoptosis

Inhibition of p53-MDM2 interaction will restore p53 in cancer cell lines leading to its activation, and consequently induce a p53-mediated signaling pathway that will culminate in cell death by apoptosis. Caspase activation and cleavage of caspase-3 substrate PARP are considered reliable markers of the apoptotic process [313]. Compounds **165ab** and **165ad** induced a dose-dependent increase of cleaved PARP as detected by Western blotting (Figure 6.2, left) and compound **165ad** induced a dose-dependent activation of caspases 3 and 7 in a luminescent caspase 3/7 assay (Figure 6.2, right).

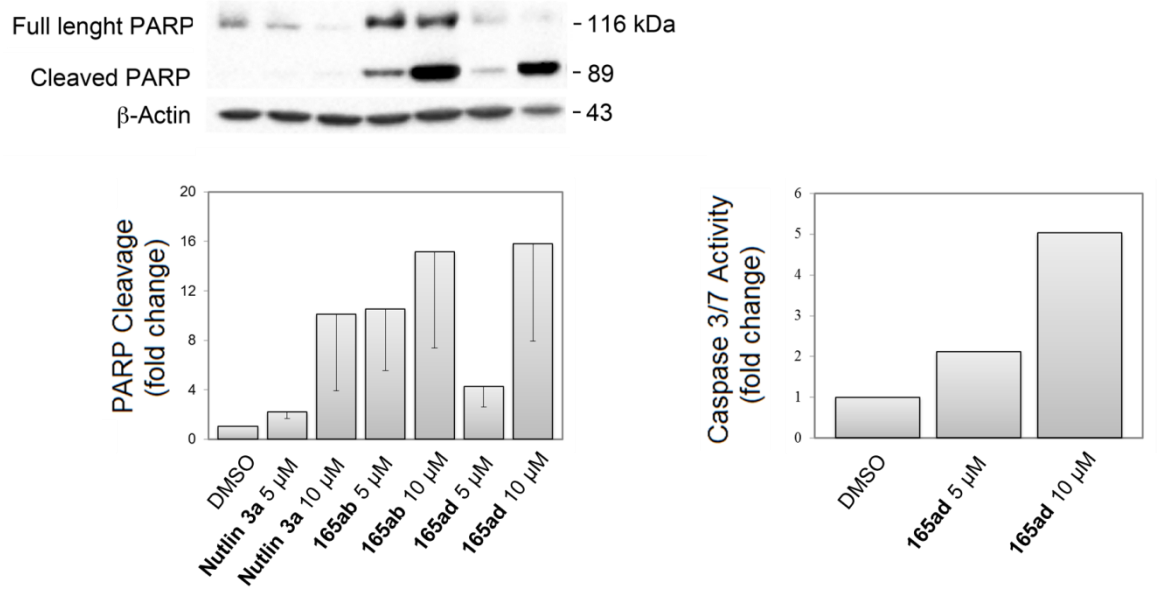

Figure 6.2. Compounds **165ab** and **165ad** induce PARP cleavage and compound **165ad** induce caspase 3/7 activity. HCT116 *p53*$^{(+/+)}$ cells were incubated with vehicle or 5 and 10 μM of compounds **165ab**, **165ad**, and nutlin-3a for 24 h. Representative immunoblots of PARP cleavage analyzed in whole cell extracts (left). Blots were normalized to endogenous *β*-actin. Data represent mean ± SEM of three independent experiments. Caspase-3 and -7 activities were measured using the Caspase-Glo 3/7 assay (Promega) in cell lysates (right).

6.5. Stability

Chemical stability in pH 7.4 phosphate buffer and metabolic stability in human plasma and rat liver microsomes at 37 ºC were evaluated for compounds **165x** and **165ae**. Both compounds were stable in phosphate buffer for the duration of the assays (3 days). They showed good stability in plasma, as shown by the detection of 75.3±7.0 % (**165x**) and 62.5±3.8 % (**165ae**) after 72 h incubation. Compounds **165x** and **165ae** exhibited degradation when incubated in rat microsomes with NADPH regenerating system, with half-lives of 14.8±0.3 min and 33.5±2.6 min, respectively, indicating great susceptibility towards co-factor dependent microsomal enzymes.

6.6. Concluding Remarks

Thirty two compounds were synthesized with different substituents attached to the spirooxadiazoline oxindole scaffold. Screening the compounds in HCT116 *p53*$^{(+/+)}$ cell line revealed that nine derivatives displayed potency below 10 μM, and four derivatives were more potent than the positive control nutlin-3a (GI_{50} bellow 3.99 μM). The best compounds possessed halogen in positions 5 or 6 of the oxindole and *meta*-halogens in rings A and B. The best compound (**165ae**) showed a GI_{50} of 1.72 μM, representing an 15.4-fold increase in potency when compared to the most active spiroisoxazoline oxindole (**119ac**, HCT116 *p53*$^{(+/+)}$ GI_{50}= 26.56 μM).

In addition, compound **165ab** showed inhibition of p53-MDM2 interaction in a cell-based bimolecular fluorescence complementation assay. Compound **165ab** and **165ad** also induced apoptosis, as verified by the dose dependent increase of PARP cleavage by immunoblotting analysis. A dose-dependent activation of caspases 3 and 7 in a luminescent caspase 3/7 assay was also observed for compound **165ad**. Moreover, compounds **165x** and **165ae** showed good stability in pH 7.4 phosphate buffer and plasma, and great susceptibility towards NADPH-dependent rat microsomal enzymes. The inhibitory activity profile in cell lines with different p53 status revealed also p53-independent effects.

Chapter 7

SPIROTRIAZOLINE OXINDOLES:

SYNTHESIS AND BIOLOGICAL EVALUATION

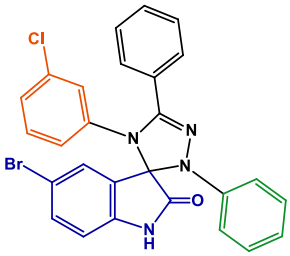

168k

MDA-MB-231 GI_{50}= 3.5 µM
MCF7 GI_{50}= 21.4 µM
Hek293T GI_{50}= 21.6 µM
HCT $p53^{(+/+)}$ GI_{50}= 15.7 µM

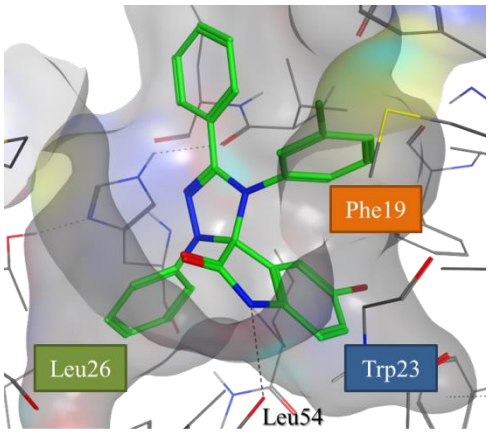

This chapter reports the synthesis and biological evaluation of twenty seven spirotriazoline oxindoles and one spiropyrazoline oxindole as anticancer agents. Five compounds showed an antiproliferative activity below 10 µM in MCF-7 cell line. Interestingly, other five derivatives were at least 2-fold more active in MDA-MB-231 than MCF-7, with compound **168k** showing a selectivity index of 6.1. In addition three compounds showed selectivity toward cancer cell lines over Hek293T. Docking studies suggested that spirotriazolines oxindoles can disrupt the p53-MDM2 interaction. This was demonstrated for compound **168h** in the live-cell bimolecular fluorescence complementation assay. Compound **168h** was also able to induce apoptosis in HCT116 $p53^{(+/+)}$ cell line.

- Carlos J. A. Ribeiro, Joana D. Amaral, Lídia M. Gonçalves, Cecília M. P. Rodrigues, Rui Moreira, Maria M. M. Santos, *Synthesis and evaluation of spirotriazolines oxindoles as anticancer agents*, in preparation.

7.1. INTRODUCTION

Santos group (iMed.ULisboa) published in 2014 a study about the *in vitro* anticancer properties of spiropyrazoline oxindoles (**167**, Scheme 7.1) against two breast cancer cell lines, one non-invasive estrogen receptor (ER) positive (MCF-7, wt p53), and one invasive ER-negative (MDA-MB-231, mut p53), both derived from a metastatic adenocarcinoma [351]. This work was envisioned after the study presented in chapter 4, in an attempt to increase anticancer potency by introducing a fourth substituent to the main scaffold (Scheme 7.1A). To achieve that, the isoxazoline oxygen was substituted by *N*-phenyl group.

Since spiroisoxazoline oxindoles (**119**) disrupt p53-MDM2 interaction, as observed in the BiFC assay, preliminary *in silico* studies were performed to assess their interaction with MDM2. It was suggested that, although they still could potentially mimic the three pivotal p53 residues, the optimal Trp23 mimicry by the 6-oxindole is lost due to the spatial orientation of the three groups (Figure 7.1). Instead, oxindole is projected into Phe19$_{(p53)}$ pocket, while phenyl A and B are projected into Trp23$_{(p53)}$ and Leu26$_{(p53)}$ pockets, respectively. However, an additional *N*-phenyl could potentially reorient the ligand in the p53 pocket. In fact, two spiropyrazoline oxindole derivatives were found to be selective toward MCF-7 (GI_{50} < 12 μM) over MDA-MB-231 and also over the non-tumor derived cell line Hek 293T (**167c** and **167e**, Table 7.3, page 105). Therefore it was decided to apply the same strategy as in chapter six: assess the biological effect of changing CH-4' (pyrazoline) to *N*-4' (triazoline) (Scheme 7.1B).

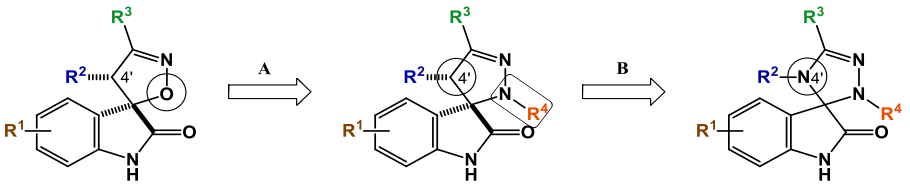

Scheme 7.1. Optimization strategy: first from spiroisoxazoline to spiropyrazoline (A) and then to spirotriazoline (B) oxindoles.

The synthetic strategy employed to synthesize spirotriazolines oxindoles (**168**) is depicted in the scheme 7.2. The final spirocyclization step was achieved by 1,3-dipolar cycloaddition between 3-imino methylene indolin-2-one (**166**) and nitrile imines (**169**) generated *in situ* from hydrazonyl chlorides (**170**).

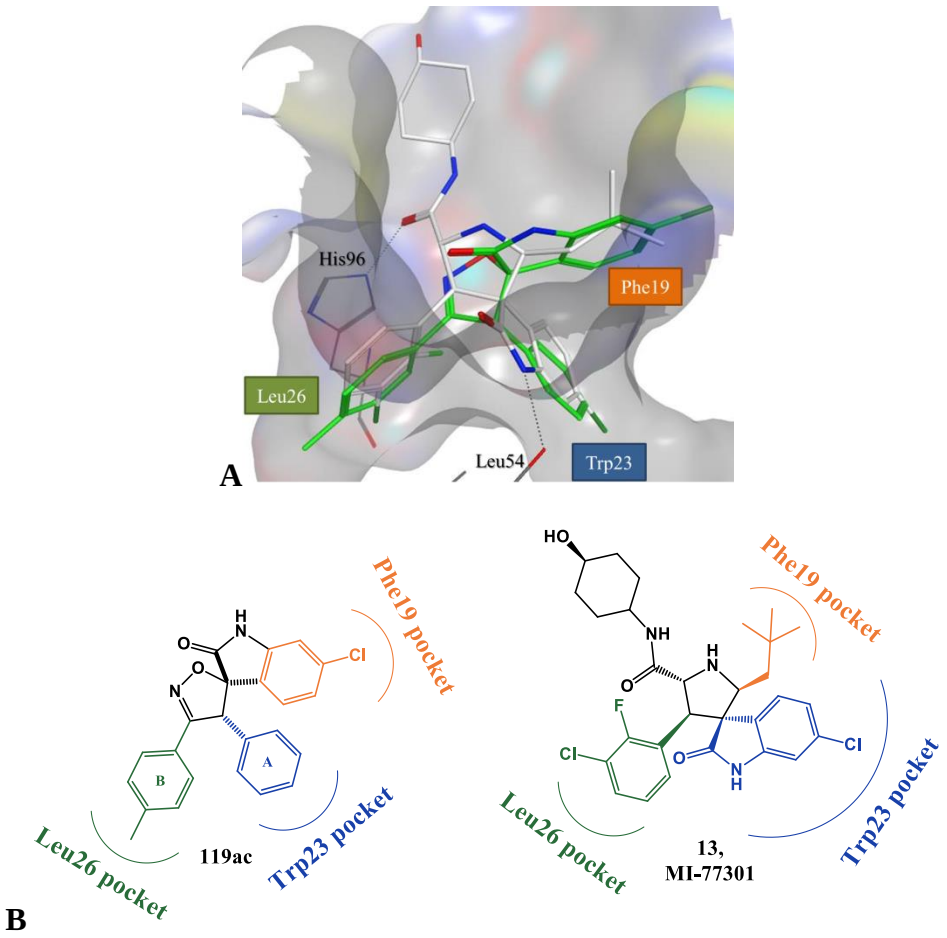

Figure 7.1. A. Best docking pose for **119ac** (depicted in stick model and colored in green) and MI-77301 (**13**, depicted in stick model and colored in white) in the p53 binding pocket (grey surface) of MDM2 (4WT2). **B.** Schematic representation of the moieties that mimic (**13**) or potentially mimic (**119ac**) p53 Phe19, Trp23, Leu26.

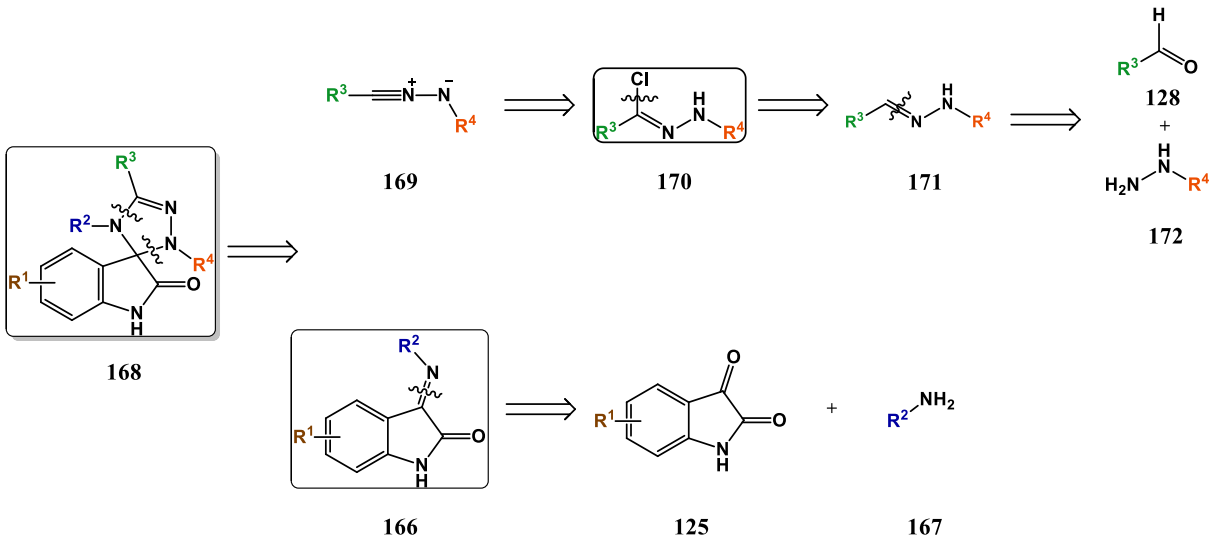

Scheme 7.2. Retrosynthesis of spirotriazoline oxindole derivatives, highlighting the final step between imino indolin-2-ones (**166**) and hydrazonyl chlorides (**170**).

7.2. Synthesis of Intermediates

3-imino-indolin-2-ones (**166**, Scheme 7.3) were synthesized using the previously described methodology (Section 6.2).

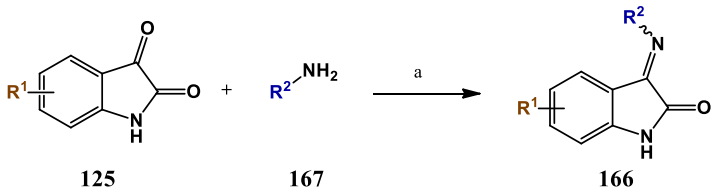

125 **167** **166**

Scheme 7.3. Synthesis of 3-imino-indoline-2-one. (a) CH_3COOH, EtOH, reflux, 3-72h

Hydrazones (**171**) were prepared by reacting phenylhydrazines (**172**) with benzaldehyde derivatives (**128**) in aqueous ethanol 20% [352], and were obtained in very good yields (81-99 %) (Scheme 7.4, Table 7.1).

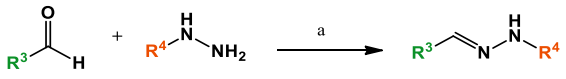

128 **172** **171**

Scheme 7.4. Synthesis of hydrazones. (a) aqueous ethanol 20%, r.t., 2-3h.

Table 7.1. Synthesis of hydrazones.

Compd	R^3	R^4	Yield (%)	Compd	R^3	R^4	Yield (%)
171a	Ph	Ph	81	**171f**	Ph	3-ClPh	84
171b	3-ClPh	Ph	99	**171g**	Ph	4-ClPh	92
171c	4-ClPh	Ph	95	**171h**	3-ClPh	2-ClPh	90
171d	4-OMePh	Ph	86	**171i**	3-ClPh	3-ClPh	88
171e	Ph	2-ClPh	92				

Hydrazonyl chlorides (**170**) were synthesized by reacting *N*-chlorosuccinimide-dimethyl sulphide complex (**173**) prepared *in situ* with the appropriate *N*-arylhydrazones (**171**) at -78 ºC (Scheme 7.5, Table 7.2), and were obtained in good yields (62-88 %) [353, 354].

The ^{1}H NMR spectra of the intermediates are in accordance with literature [354-358].

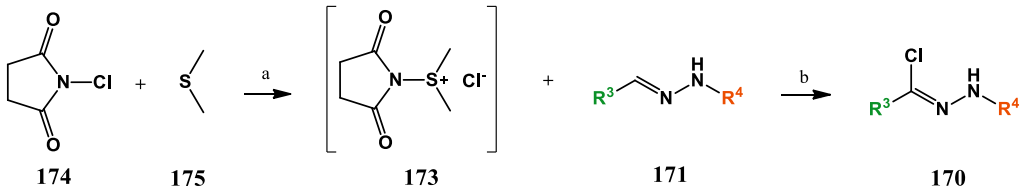

Scheme 7.5. Synthesis of hydrazonyl chlorides, (a) 0 ºC, 15 min; (b) -78ºC, 1 h, then allowed to warm up to r.t.

Table 7.2. Synthesis of hydrazonyl chlorides.

Compd	R^3	R^4	Yield (%)	Compd	R^3	R^4	Yield (%)
170a	Ph	Ph	81	**170f**	Ph	3-ClPh	80
170b	3-ClPh	Ph	71	**170g**	Ph	4-ClPh	88
170c	4-ClPh	Ph	67	**170h**	3-ClPh	2-ClPh	73
170d	4-OMePh	Ph	62	**170i**	3-ClPh	3-ClPh	73
170e	Ph	2-ClPh	84				

7.3. Synthesis of 2',4'-dihydrospiro[indoline-3,3'-[1,2,4]triazol]-2-ones

Spirotriazoline oxindoles were obtained by 1,3-dipolar cycloaddition between 3-imino-indolin-2-ones (**166**) and nitrile imines (**169**) generated *in situ* by dehydrohalogenation of hydrazonyl chlorides (**170**) (Scheme 7.6, Table 7.4 and 7.5). They were synthesized in good yields (60-95 %).

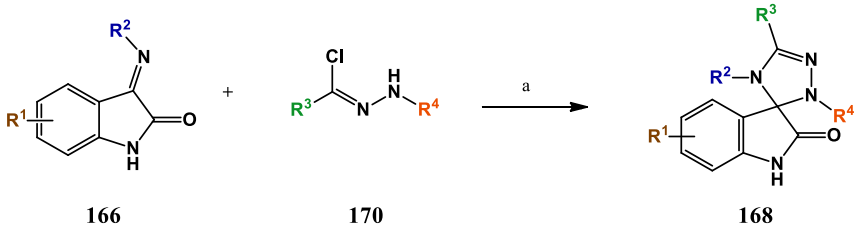

Scheme 7.6. Synthesis of spirotriazoline oxindoles. (a) Et_3N, CH_2Cl_2, 24 h, r.t.

The regioisomer obtained was the spiro[indoline-3,3'-[1,2,4]triazoline]-2-one (Scheme 7.7). The ^{13}C NMR spectrum showed that spiro carbon signal appeared at 87.88 – 89.83 ppm, as described in the literature for spirotriazoline oxindoles (88.42 – 88.59 ppm) [359]. In the alternative regioisomer the signal would appear shifted upfield, as observed for the spiro carbon of spiropyrazoline oxindoles, in which it is linked to three carbons and one nitrogen (75.44 - 78.17 ppm [351]). Additionally the triazoline C=N chemical shift appeared at 146.77 – 152.73 ppm (147.45 – 148.60 ppm [359]). The compounds were further characterized by melting point, IR and their purity assessed by elemental analysis (Chapter 9).

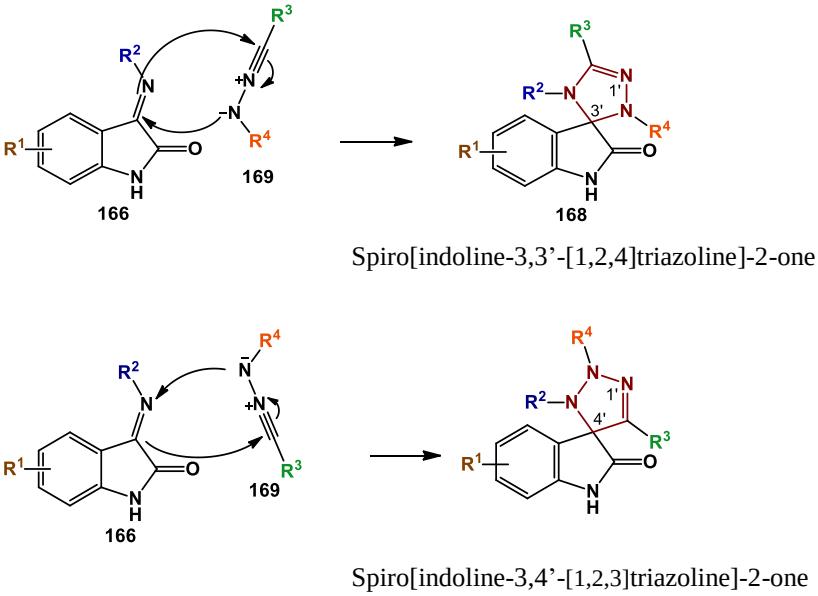

Scheme 7.7. Possible regioisomers formed as a result of 1,3-dipolar cycloaddition between **166** and **169**.

7.3. SYNTHESIS OF SPIROPYRAZOLINE OXINDOLE 167F

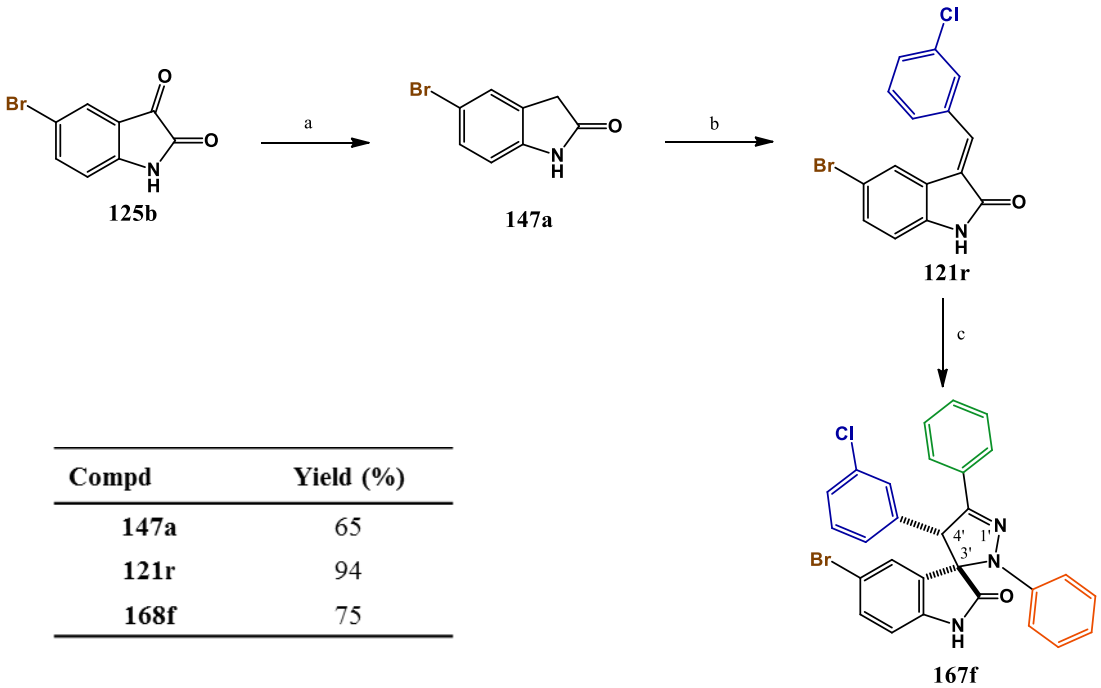

Compd	Yield (%)
147a	65
121r	94
168f	75

Scheme 7.8. Synthesis of spiropyrazoline oxindole **167f**. (a) $TiCl_4$, Zn, THF, 2h, reflux, then at r.t. **125b**, 10 min (b) 3-chlorobenzaldehyde, piperidine, EtOH, reflux, 5h; (c) **170a**, Et_3N, CH_2Cl_2, 24 h, r.t.

Spiropyrazoline oxindole **167f** was prepared by reacting 3-methylene indolin-2-one **121r** with hydrazonyl chloride **170a**, and was obtained in 65 % yield (Scheme 7.8). Compound **121r** was synthesized by aldolic condensation between 5-bromoindolin-2-one (**147a**) and 3-chlorobenzaldehyde and the former by reduction of 5-bromoindolin-2,3-dione with $TiCl_4$/Zn. The regioisomer formed was established to be the spiro[indoline-3,3'-pyrazoline]-2-one by NMR comparisons to spiropyrrolidine derivatives described in literature [351, 354]. In particular, the chemical shift of the spiro carbon appeared at 77.22 ppm (75.44 – 78.17 ppm [351]) and the H-4' and C-4' at 5.45 ppm (4.43 – 5.47 ppm [351]) and 62.34 ppm (60.73 – 63.22 ppm [351]), respectively. Additionally the pyrazoline C=N chemical shift appeared at 149.40 ppm (148.93 – 149.63 ppm [351]). The relative stereochemistry was established by comparison with published X-ray crystallography structure [360]. The compound was further characterized by melting point and IR and its purity assessed by elemental analysis (Chapter 9).

7.4. BIOLOGICAL STUDIES

7.4.1. Assessment of cell viability and SAR study

In the spiropyrazoline oxindole series published by Santos group [351], the two most promising compounds (**167c** and **167e**, Table 7.3) displayed more than 8-fold selectivity towards MCF-7 cell line, over MDA-MB-231 and Hek 293T cell lines. Therefore, it was decided to start the spirotriazoline oxindole study by synthesizing and evaluating derivatives with the same halogen pattern in the oxindole moiety (Cl and Br in position 5 or 7 in the oxindole) and without substituents in phenyl rings A, B and C (Table 7.4). This first study revealed that three out of the four evaluated spirotriazolines with published spiropyrazoline equivalents showed significant increase in potency in MCF-7 cell line. The non-halogenated derivative (**168a**) was at least 2.8-fold more potent than its spiropyrazoline equivalent (**167a**, Table 7.3), and the 5-chloro and 7-chloroxindole derivatives were 2-fold more potent (**168e**, **168l**, Table 7.4 versus **57b**, **57d**, Table 7.3). Compound **168h** (R^1= 5-Br) represents the only exception, by promoting a 3.2-fold decrease in potency in MCF-7 cell line when compared to its spiropyrazoline counterpart (**167c**). However, surprisingly it was at least 14.9-fold more potent in MDA-MB-231 cell line, revealing that by simply changing CH (**167c**) for N (**168h**) it was possible to go from a compound at least 13.7-fold more selective towards MCF-7 cell line to a derivative 3.4 more selective toward MDA-MB-231 cell line. In addition, in the spirotriazoline series, a 2.0-fold decrease in potency in both cells lines was observed when 7-chloro was changed to 7-bromo (**168m** versus **168l**, Table 7.4).

Table 7.3. Spiropyrazoline oxindoles reported in literature

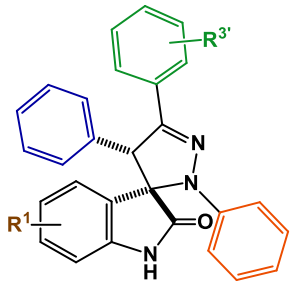

167

Compd	R^1	$R^{3'}$	MCF-7 GI_{50}, µM	MDA-MB-231 GI_{50}, µM	Hek 293T GI_{50}, µM
167a	H	H	>100	-	-
167b	5-Cl	H	37.7±14.1	-	-
167c	5-Br	H	7.3±3.3	>100	>100
167d	7-Cl	H	22.4±3.5	16.9.±1.2	>100
167e	7-Cl	4-OMe	11.5±1.6	>100	>100

Although a certain degree of selectivity was lost with compound **168h**, its remarkable MDA-MB-231 GI_{50} of 6.7 µM spurred the synthesis of new derivatives with 5-bromoxindole moiety, starting by probing *meta* and *para* position of ring A (**168i-k**). It was also synthesized compounds with the same substituents in ring A, but without halogen in the oxindole (**168b-d**) to assess their independently contribution to activity. In general any additional halogen to one or both positions tested led to an activity improvement. Interestingly, comparing 5-Br to 5-H derivatives revealed that their activity was quite similar (<1.8-fold difference) in MCF-7 cell line. In MDA-MD-231 cell line, 5-bromo derivatives were substantially more active, with derivative **168j** ($R^{2'}$= 3-Cl, 4-F) showing a 7.0-fold increase in potency (**168j** versus **168d**). The most active compound in MDA-MD-231 cell line was **168k** (R^1= 5-Br and $R^{2'}$= 3-Cl) with a GI_{50} of 3.5 µM, representing a 1.9-fold activity improvement and better selectivity between cancer cell lines in comparison to **168h**. Maintaining the same substituent in ring A (3-Cl) and changing the halogen in R^1 from bromo to chloro, decreased the activity in MDA-MD-231, while increasing activity in MCF-7, both by at least a factor of two (**168f** versus **168k**). Furthermore *tert*-butyl group instead of phenyl ring A decreased activity in all cell lines tested (**168g** versus **168e**).

Then it was decided to investigate different substitutions at ring B and C (Table 7.5). Two compounds were selected as starting point for this endeavor: the most active compound in MDA-MB-231 cell line (**168k**) and the non-toxic derivative (Hek293T GI_{50} > 100 µM) with selectivity between breast cancer cell lines (**168b**). With the exception of compound **168p**, introducing chloro atoms in different positions in one or both rings doubled the potency in MCF-7 cell line (**168n-o**, **168q-u**, **and 50w-aa**). The most active

Table 7.4. *In vitro* antiproliferative activities.

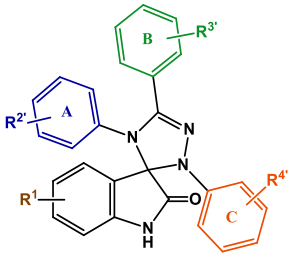

168

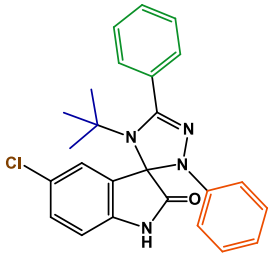

168g

Compd	R^1	$R^{2'}$	$R^{3'}$	$R^{4'}$	Yield (%)	MCF-7 GI_{50}, μM[b]	MDA-MB-231 GI_{50}, μM[b]	Hek 293T GI_{50}, μM[b]	HCT116 *p53*$^{(+/+)}$ GI_{50}, μM[a]	HCT116 *p53*$^{(-/-)}$ GI_{50}, μM[a]	SI[c]	SI[d]
168a	H	H	H	H	81	36.2±3.3	23.4±4.3	-	32.6±1.5	30.4±0.4		
168b	H	4-Cl	H	H	84	24.1±4.8	10.7±1.0	>100	15.0±1.5	18.5±1.2	2.3	>9.3
168c	H	3-Cl	H	H	90	13.7±0.4	12.5±1.1	25.7±5.6	19.9±1.4	22.1±2.0		>2.1
168d	H	3-Cl,4-F	H	H	70	19.5±0.7	32.3±4.0	-	17.5±0.3	18.8±0.3		
168e	5-Cl	H	H	H	87	19.1±0.8	11.7±0.6	32.6±9.3	21.6±0.6	22.1±3.2		2.8
168f	5-Cl	3-Cl	H	H	89	9.8±1.5	8.9±1.9	>100	16.3±0.2	17.9±0.6		>11.2
168g					79	30.8±1.2	32.3±4.0	-	39.2±1.5	41.9±2.9		
168h	5-Br	H	H	H	95	23.0±1.7	6.7±0.4	56.3±11.3	22.2±0.5	22.5±4.4	3.4	8.4
168i	5-Br	4-Cl	H	H	93	16.8±1.0	5.2±1.0	21.6±6.8	16.3±1.2	18.2±0.9	3.2	4.2
168j	5-Br	3-Cl, 4-F	H	H	90	11.0±2.4	4.6±0.3	16.6±3.7	13.5±1.0	15.9±1.3	2.4	3.6
168k	5-Br	3-Cl	H	H	92	21.4±2.2	3.5±1.0	21.6±6.8	15.7±1.4	17.8±2.0	6.1	6.2
168l	7-Cl	H	H	H	91	10.8±0.9	8.9±0.6	>100	23.7±0.6	20.1±1.7		>11.2
168m	7-Br	H	H	H	94	21.8±1.6	23.7±4.5	-	20.7±1.9	17.3±0.1		
Nutlin-3a									4.0±1.2	47.8±1.9		

[a] GI_{50} determined by the MTT method after 72h. Each value is the mean (GI_{50} ± SD) of three independent experiments; [b] GI_{50} determined by the MTS method after 72h. Each value is the mean (GI_{50} ± SD) of three independent experiments performed in duplicate. [c] Selectivity index towards MDA-MB-231 between cancer cell lines, expressed by the ratio MDA-MB-231 GI_{50}/ MCF-7 GI_{50}; [d] Selectivity index towards MDA-MB-231 over Hek 293T, expressed by the ratio MDA-MB-231 GI_{50}/ Hek 293T GI_{50}.

Table 7.5. *In vitro* antiproliferative activities.

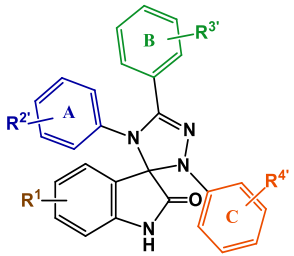

168

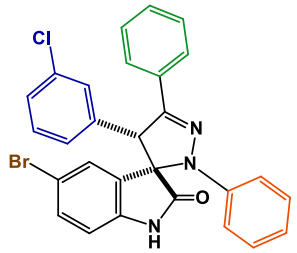

167f

Compd	R^1	$R^{2'}$	$R^{3'}$	$R^{4'}$	Yield (%)	MCF7 GI_{50}, μM[a]	MDA-MB-231 GI_{50}, μM[a]	Hek293T GI_{50}, μM[a]	HCT116 *p53*$^{(+/+)}$ GI_{50}, μM[b]	HCT116 *p53*$^{(-/-)}$ GI_{50}, μM[b]	SI[c]	SI[d]
168b	H	4-Cl	H	H		24.1±4.8	10.7±1.0	>100	15.0±1.5	18.5±1.2	2.3	>9.3
168n	H	4-Cl	3-Cl	H	89	13.1±2.4	11.6±1.3	20.5±5.3	17.4±2.4	16.1±1.6		
168o	H	4-Cl	4-Cl	H	86	10.9±2.0	8.2±0.8	22.7±5.3	16.8±2.2	18.5±1.6		>2.8
168p	H	4-Cl	H	2-Cl	76	28.4±5.0	24.8±0.8	69.8±12.8	32.9±3.6	37.9±3.0		>2.8
168q	H	4-Cl	H	3-Cl	91	14.2±2.4	15.7±2.4	15.4±2.6	19.8±1.4	18.5±0.9		
168r	H	4-Cl	H	4-Cl	84	10.1±0.5	9.0±1.2	15.8±4.4	18.5±0.9	18.7±0.5		
168s	H	4-Cl	3-Cl	2-Cl	86	13.1±0.5	14.5±0.5	35.0±12.2	25.3±1.3	34.6±2.9		>2.8
168k	5-Br	3-Cl	H	H		21.4±2.2	3.5±1.0	22±7	15.7±1.4	17.8±2.0	6.1	6.2
168t	5-Br	3-Cl	3-Cl	H	85	8.0±1.4	10.2±1.3	12.5±1.1	12.6±1.2	13.0±1.4		
168u	5-Br	3-Cl	4-Cl	H	82	10.1±0.9	14.6±2.1	20.3±6.5	10.8±1.2	10.8±0.9		
168v	5-Br	3-Cl	4-OMe	H	60	12.3±1.5	14.1±1.1	25.9±5.8	22.2±1.4	25.8±1.2		
168w	5-Br	3-Cl	H	2-Cl	63	10.2±0.8	11.7±1.7	20.9±3.0	21.5±2.1	31.6±1.5		
168x	5-Br	3-Cl	H	3-Cl	88	9.8±0.9	10.7±3.1	16.9±3.4	12.0±1.1	13.1±1.4		
168y	5-Br	3-Cl	H	4-Cl	89	11.4±0.9	15.0±4.4	16.2±2.4	15.0±1.3	17.2±1.8		
168z	5-Br	3-Cl	3-Cl	2-Cl	80	9.5±3.1	7.6±2.4	21.4±7.4	13.9±1.1	17.7±1.3		>2.8
168aa	5-Br	3-Cl	3-Cl	3-Cl	88	6.9±0.7	7.0±1.9	9.0±1.7	10.2±1.7	9.0±0.8		
167f						10.0±0.7	12.6±0.3	17.5±3.3	11.4±1.1	12.4±1.3		

[a] GI_{50} determined by the MTT method after 72h. Each value is the mean (GI_{50} ± SD) of three independent experiments; [b] GI_{50} determined by the MTS method after 72h. Each value is the mean (GI_{50} ± SD) of three independent experiments performed in duplicate. [c] Selectivity index towards MDA-MB-231 between cancer cell lines, expressed by the ratio MDA-MB-231 GI_{50}/ MCF-7 GI_{50}; [d] Selectivity index towards MDA-MB-231 over Hek 293T, expressed by the ratio MDA-MB-231 GI_{50}/ Hek 293T GI_{50}.

compound obtained for this cell line was **50aa** (GI_{50}= 6.9 μM). Unfortunately these new substitutions did not improve activity in MDA-MB-231, and in fact for all 5-bromooxindole derivatives at least a 2-fold decrease in activity was observed. The same pattern of response was also achieved for compound **168v** ($R^{3'}$= OMe). Finally the spiropyrazoline equivalent of compound **168k** was also synthesized and evaluated (**167f**). It was found to be 3.6-fold less active in MDA-MD-231 cell line, but 2.2-fold more potent in MCF-7 cell line.

All derivatives were also tested in the isogenic pair HCT116, with compound **168aa** revealing to be the most active (HCT116 $p53^{(+/+)}$ GI_{50}= 10.2 μM; HCT116 $p53^{(-/-)}$ GI_{50}= 9.0 μM). Unfortunately, for all compounds, lack of selectivity between both HCT116 cell lines was observed.

7.4.2. Evaluation of compounds ability to block the intracellular p53-MDM2 interaction

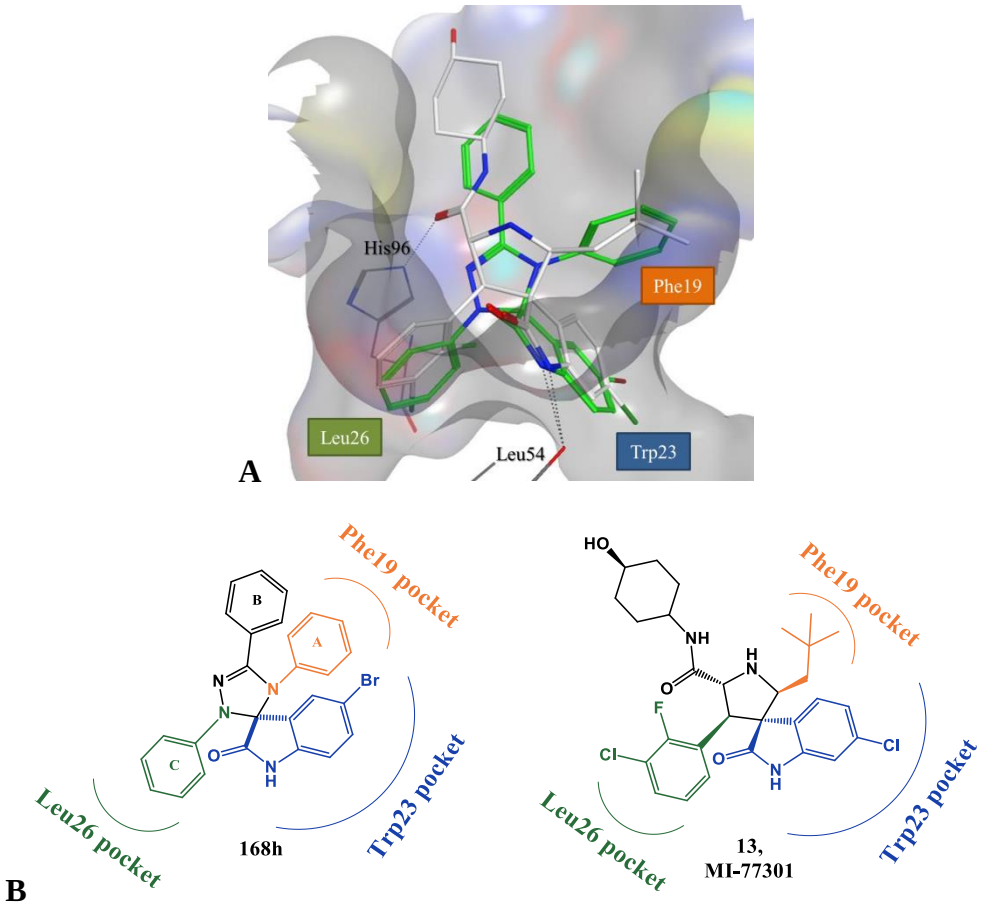

Figure 7.2. A. Best docking pose for **168h (**depicted in stick model and colored in green) and MI-77301 (**13**, depicted in stick model and colored in white) in the p53 binding pocket (grey surface) of MDM2 (4WT2). **B.** Schematic representation of the moieties that mimic (**13**) or potentially mimic (**168h**) p53 Phe19, Trp23, Leu26.

As hypothesized in the beginning of this chapter, adding an extra phenyl ring could potentially reorient the spirooxindole in the MDM2 p53 binding pocket (Figure 7.2). In the best docking pose, the oxindole moiety of **168h** occupies the Trp23$_{(p53)}$ pocket, with the NH establishing an H-bond with MDM2 Leu54, as in spiropyrrolidine oxindole **13**. Furthermore, phenyl A and C are projected into Phe19$_{(p53)}$ and Leu26$_{(p53)}$ pockets, respectively. Therefore, although this series of compounds did not show selectivity between HCT116 *p53* cell lines, and in fact five derivatives showed selectivity towards MDA-MB-231, the docking suggestions fomented further biological investigation. By applying the Venus-based bimolecular fluorescence complementation system methodology (BiFC [260], Figure 4.4, pg 67), it was demonstrated that compound **168h** can inhibit p53-MDM2 interaction in the same extent as the positive control Nutlin-3a (Figure 7.3).

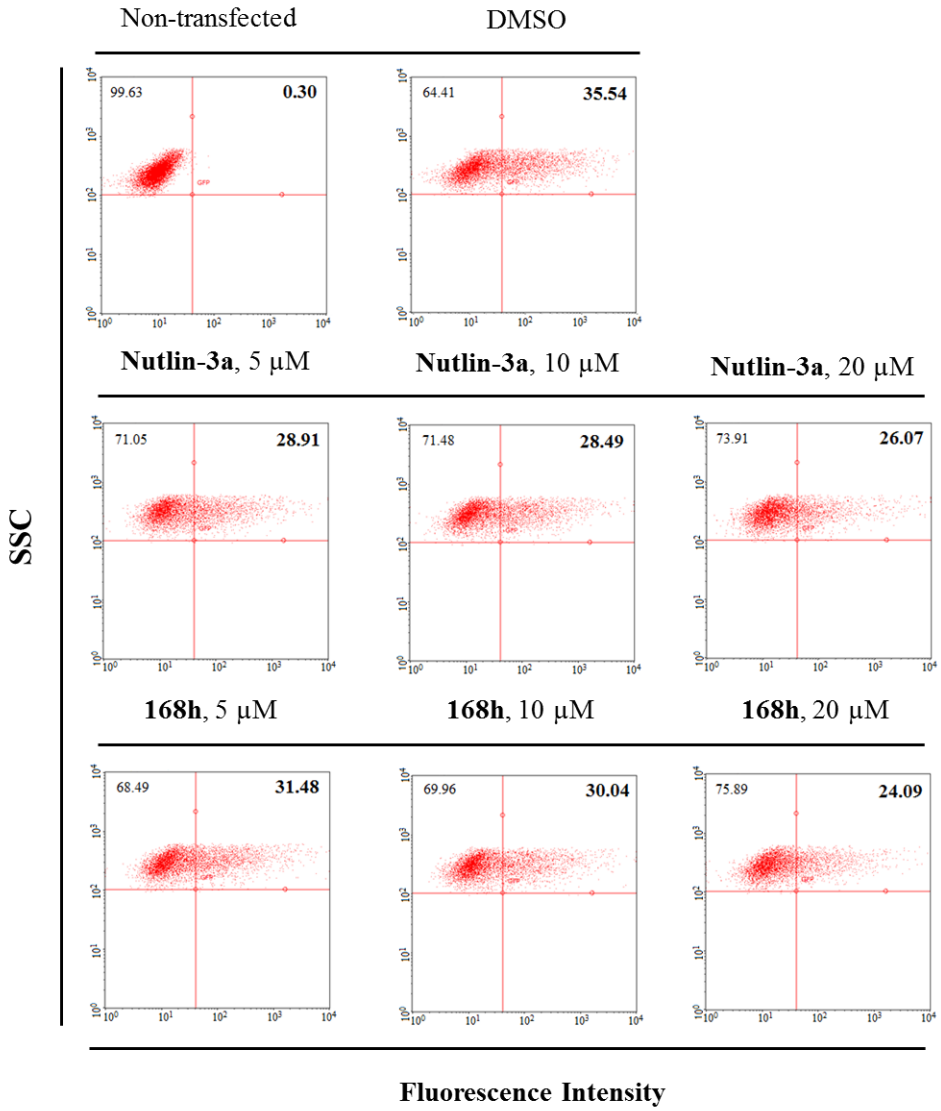

Figure 7.3. Compound 168h decreases p53-MDM2 interaction by BiFC. HCT116 *p53*$^{(-/-)}$ cells were co-transfected with V1-p53/MDM2-V2 BiFC combination plasmids for 24 h. Vehicle, nutlin-3a (5, 10, and 20 µM) and compound **168h** (5, 10, and 20 µM) were included in the culture medium 4 h after transfection. Representative flow cytometry profiles of the disruption of V1-p53/MDM2-V2 complementation (n=3).

7.4.2. Evaluation of apoptosis

Inhibition of p53-MDM2 interaction will restore p53 in cancer cell lines leading to its activation, and consequently induce a p53-mediated signaling pathway that will culminate in cell death by apoptosis. Caspase activation and cleavage of caspase-3 substrate PARP are considered reliable markers of the apoptotic process [313]. Compound **168h** induced a dose-dependent increase of cleaved PARP as detected by Western blotting (Figure 7.4, left) and induce a dose-dependent activation of caspases 3 and 7 in a luminescent Caspase 3/7 assay (Figure 7.4, right).

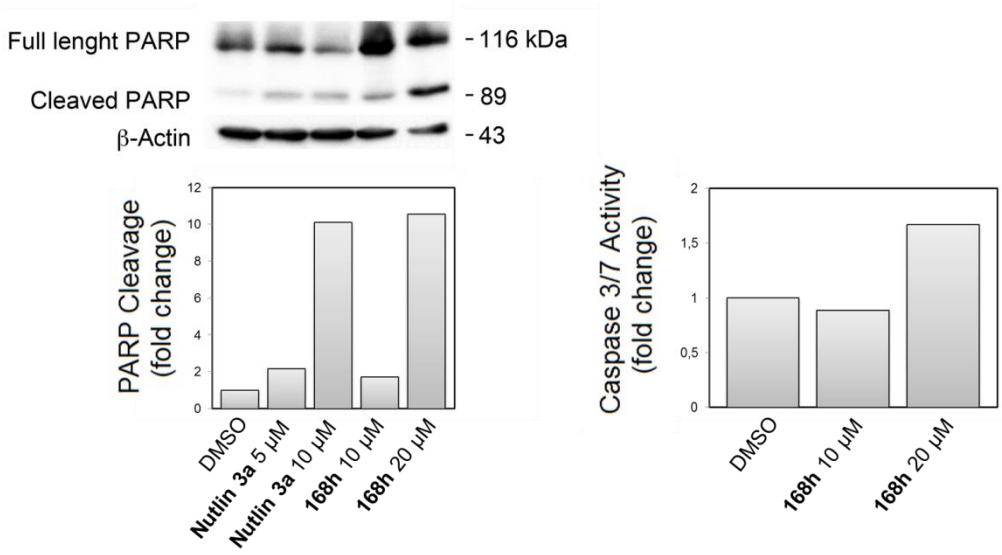

Figure 7.4. Compound **168h** induce PARP cleavage and caspase 3/7 activity. HCT116 *p53*$^{(+/+)}$ cells were incubated with vehicle or 10 and 20 μM of compounds **168h** and 5 and 10 μM of nutlin-3a for 24 h. Immunoblots of PARP cleavage analyzed in whole cell extracts (*left*). Blots were normalized to endogenous β-actin. Caspase-3 and -7 activities were measured using the Caspase-Glo 3/7 assay (Promega) in cell lysates (right).

7.5. Stability

Chemical stability in pH 7.4 phosphate buffer and metabolic stability in human plasma and rat liver microsomes at 37 ºC were evaluated for compounds **168h** and **168z**. Both compounds were stable in plasma for the duration of the assays (three days). Compounds **168h** and **168z** exhibited degradation when incubated in rat microsomes with NADPH regenerating system, with half-lives of 18.9±1.8 min and 6.12±0.5 min, respectively, indicating great susceptibility towards co-factor dependent microsomal enzymes.

7.6. CONCLUDING REMARKS

Twenty seven compounds were synthesized with different substituents attached to the spirotriazoline oxindole scaffold. Screening the compounds in MCF-7 cell line revealed that five derivatives displayed potency below 10 µM (**168aa**, GI_{50}= 6.9 µM). Interestingly, other five derivatives showed selectivity (more than 2-fold) towards MDA-MB-231, with compound **168k** showing a selectivity index of 6.1 (GI_{50}= 3.5 µM). In addition three compounds were selective toward cancer cell lines over Hek293T. Unfortunately lack of selectivity between the isogenic pair of cell lines HCT116 $p53^{(+/+)}$ and $p53^{(-/-)}$ was observed for all compounds. However, docking studies suggested that spirotriazolines oxindoles were still capable of disrupting the p53-MDM2 interaction, and that was obtained for compound **168h** in the live-cell bimolecular fluorescence complementation assay. Compound **168h** also promoted apoptosis as observed by the dose-dependent increase of PARP cleavage and dose-dependent activation of caspases 3 and 7, detected by Western blotting and by a luminescent caspase 3/7 activity assay, respectively. Moreover, compounds **168h** and **168z** showed good stability in plasma, and great susceptibility towards NADPH-dependent rat microsomal enzymes.

Chapter 8

GENERAL CONCLUSIONS AND FUTURE PERSPECTIVES

Restoring p53 function in cancer cells represents a valuable anticancer approach. Several strategies are being developed, and in particular targeting p53-MDM2 interaction has emerged as a promising viable approach when dealing with cancers that retain wild type p53 function. p53-MDM2 interaction inhibitors share common structural features: a rigid heterocyclic scaffold with three lipophilic groups that mimic the three pivotal p53 amino acids (Phe19, Trp23 and Leu26) that interact with MDM2. Furthermore, seven compounds have already entered clinical trials.

The main goal of this PhD thesis was to develop new anticancer agents containing a spirooxindole scaffold with different spiro five-membered rings: isoxazoline, oxadiazoline, and triazolines. The spirocycle can potentially function as the rigid heterocyclic scaffold, from which the three lipophilic groups can be projected to mimic the p53 amino acids.

The PhD thesis included three major strategies: synthesis of spirooxindole derivatives by 1,3 dipolar cycloaddition; biological evaluation of the compounds synthesized and stability assessment.

Chapters three to five were dedicated to the synthesis and biological evaluation of spiroisoxazoline oxindoles. In chapter three, the synthesis of spiroisoxazoline oxindoles containing ester groups at position 4' and aromatic or ester groups at position 3' of the isoxazoline ring was reported. The synthetic methodology developed represents the first time that zinc is used as the dehydrochlorinating agent in 1,3-dipolar cycloadditions. In chapter four the synthetic scope was increased, in order to obtain also spiroisoxazoline oxindole derivatives with alquilic and aromatic groups in position 4' of the isoxazoline ring. Furthermore, it also reports the evaluation of all thirty three derivatives synthesized as anticancer agents. Seven compounds showed an antiproliferative profile superior to the p53-MDM2 interaction inhibitor nutlin-3. The most active derivative showed a GI_{50} of 29.11 μM in HepG2 cell line. Chapter five reports the attempts to synthesize enantioselectively the most active derivative, achieving an ee of 50%. It also describes experiments developed for the enantioselective synthesis of a spiropyrroline oxindole derivative (ee of 72%) performed in parallel to the main objectives of the PhD.

Chapters six and seven describe the synthesis, biological evaluation and stability assessment of the spirooxadiazoline and spirotriazoline oxindole libraries, respectively. It was synthesized and evaluated thirty two spirooxadiazoline oxindoles as anticancer agents. Nine compounds showed an antiproliferative activity below 10 μM, with four compounds more active than the positive control nutlin-3a in HCT116 $p53^{(+/+)}$. It was also synthesized and evaluated twenty seven spirotriazoline oxindoles as anticancer agents. Five compounds showed an antiproliferative activity below 10 μM in MCF-7 cell line. Interestingly, other five derivatives were at least 2-fold more active in MDA-MB-231 than MCF-7. In addition three compounds showed selectivity toward cancer cell lines over Hek293T.

Moreover, proof-of-concept for the three series of compounds was demonstrated by inhibition of the interaction between p53 and MDM2 in a live-cell bimolecular fluorescence complementation assay and by the induction of apoptosis in HCT116 *p53*$^{(+/+)}$ cell line.

Docking studies suggested that the spirooxindoles tested are capable of mimicking the three pivotal p53 amino acids. For spirotriazoline oxindoles *in silico* studies also revealed that an increase in potency can potentially be achieved by modifications in R^3 (ring B), as observed for published spiropyrrolidine oxindoles. Therefore future SAR studies should encompass modifications at this position in an attempt to find derivatives capable of stablishing hydrogen bonds with MDM2 Lys94 and specially His96, as observed for several reported p53-MDM2 interaction inhibitors. Moreover, since p53 independent effects are also observed, a more in depth cellular understanding should be pursued, to assess which signaling pathways and proteins are being affected. This study will be of particular interest for the five spirotriazolines oxindoles that showed at least a 2-fold selectivity toward mutated p53 MDA-MB-231 cell line. Furthermore, *in vivo* efficacy should also be evaluated for the best derivatives.

Overall this PhD thesis contributed with three new families of spirooxindoles with *in vitro* anti-cancer activities that are capable of disrupting the p53-MDM2 interaction in cells. The most active derivative possessed a GI_{50} of 1.72 µM in HCT116 *p53*$^{(+/+)}$ cell line.

Chapter 9

EXPERIMENTAL SECTION

9.1. EXPERIMENTAL SECTION: CHEMISTRY

All chemical and solvents were obtained from commercial suppliers and were normally used without further purification. When used as reaction solvents, CH_2Cl_2 and $CHCl_3$ were dried over $CaCl_2$ and distilled; THF and ether were distilled from sodium-benzophenone system. Et_3N was dried over KOH, distilled and stored with molecular sieves. In chapter 5, dry CH_2Cl_2, toluene, THF, and Et_2O solvents were dispensed from a solvent purification system that passes them through two columns of dry neutral alumina.

Thin layer chromatography was performed using Merck Silica Gel 60 F254 aluminium plates and visualized by UV light. Flash column chromatography was performed on Merck Silica Gel (200-400 mesh ASTM) and CombiFlash Rf from Teledyne ISCO (columns RediSep Rf, silica). Preparative TLC was performed on Merck Silica Gel 60 GF_{254} over glass plates with 0.5 and 1 mm thickness.

In chapter 5, all reactions were performed in oven-dried and argon-purged glassware (including 8- and 4-mL Fisher Scientific vials fitted with PTFE closure). Molecular sieves (4Å) < 50 μm were activated in a vacuum chamber by heating them with a heat gun for 15 min.

^1H and ^{13}C NMR spectra were recorded on a Bruker 400 Ultra-Shield at 400 MHz (^1H NMR) and 100 MHz (^{13}C NMR) or on a Bruker 300 Avance at 300 MHz (^1H NMR) and 75 MHz (^{13}C NMR). In chapter 5, NMR spectra were recorded at 600, 400 or 300 MHz and 150, 100, or 75 MHz, respectively, using a Bruker Avance 600 MHz NMR spectrometer, Varian VNMRS 600 (600 MHz), Varian Mercury 300 (300 MHz), MercuryPlus 300 (300 MHz), or Varian Inova 400 (400 MHz) spectrometers. ^1H and ^{13}C chemical shifts (δ) are expressed in parts per million (ppm) using the solvent as internal reference, and proton coupling constants (J) in hertz (Hz). ^1H spectral data are reported as follows: chemical shift, multiplicity (s, singlet; d, doublet; t, triplet; q, quartet; m, multiplet; dd, doublet of doublets; dt, doublet of triplets, and br, broadened), coupling constant, and integration.

The infrared spectra were collected on a Shimadzu FTIR Affinity-1 spectrophotometer. The spectra were determined using KBr disks or thin films between NaCl plates. Only the most significant absorption bands are reported.

Elemental analysis (C, H, and N) were performed in a Flash 2000 CHNS-O analyzer (ThermoScientific, UK) at Liquid Chromatography and Mass Spectrometry Laboratory, Faculty of Pharmacy of Lisbon University; or in a LECO model CHNS-932 elemental analyzer at the Unit Elemental Analysis, University of Santiago de Compostela, Spain. The results were within ± 0.4% of the theoretical values.

Melting points were determined using a Kofler camera Bock monoscope M and are uncorrected.

All chiral HPLC analyses were performed on a Shimadzu LC-20AB system with a Daicel CHIRALPAK® AD-H column (4.6 x 250 mm, 5 μm), Daicel CHIRALPAK® AS-H column (4.6 x 250 mm, 5 μm), or Daicel CHIRALCEL® OD-H column (4.6 x 250 mm, 5 μm), each attached to a guard column, at a constant flow rate (isopropanol/hexanes isocratic system) using Shimadzu SPD-M20A photodiode array detector and 40 °C column oven temperature.

Compound ***epi*-163** was analyzed for LRMS in the positive ion mode by an Applied Biosystems Qtrap (Foster City, CA). Source parameters were 5 kV spray voltage, with a curtain plate temperature of 275 °C and sheath gas setting of 15. Samples were analyzed via flow injection analysis, by injecting 20 μL samples into a stream of 80 % MeOH/20 % aqueous solution of 0.1% formic acid, flowing at 200 μL per minute.

High resolution mass spectra (HMRS-ESI$^+$) were obtained in a FTICR Bruker Apex Ultra from Faculty of Sciences of Lisbon University, Portugal.

9.1.2. General procedure for the synthesis of 3-methylene indoline-2-ones.

9.1.2.1. Method A- Wittig reaction.

A mixture of the indoline-2-one (1.0 equiv) and phosphonium ylide derivative (1.0 equiv) in toluene was heated to 80 ºC for 5-6 h, under nitrogen atmosphere. After the reaction was complete, the solvent was removed under reduced pressure and the residue was dissolved in EtOAc. The organic phase was washed with brine (2x), dried over anhydrous Na_2SO_4 and concentrated by rotary evaporation. The residue was purified by flash chromatography on silica gel using *n*-hexane/EtOAc (4:1) as the eluent to afford the final product (adapted from [270]).

(*E*)-ethyl 2-(*N*-methyl-2-oxoindolin-3-ylidene)acetate (121a).

Synthesized according to the general procedure (method A), this compound was obtained as an orange solid (467.9 mg, 94 % yield).

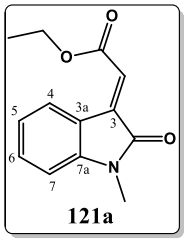

121a

Mp: 90-91 ºC (mp lit. 74-76 ºC [361], 83-85 ºC [274]); **IR** (KBr, selected peaks): 1714.89 (C=O), 1612.77 (C=O) cm^{-1}; **^{1}H NMR** (400 MHz, $CDCl_3$) δ (ppm): 8.56 (d, *J* = 7.7 Hz, 1H, H-4), 7.37 (td, *J* = 7.8, 1.0 Hz, 1H, H-6), 7.07 (td, *J* = 7.7, 0.8 Hz, 1H, H-5), 6.91 (s, 1H, C=CH), 6.80 (d, *J* = 7.8 Hz, 1H, H-7), 4.33 (q, *J* = 7.1 Hz, 2H, CH_2), 3.23 (s, 3H, NCH_3), 1.37 (t, *J* = 7.1 Hz, 3H, CH_3); **^{13}C NMR** (100 MHz, $CDCl_3$) δ (ppm): 167.64 (NC=O), 165.78 (CO_2), 146.06 (Cq-7a), 137.97 (Cq-3), 132.52 (CH-6), 128.85 (CH-4), 122.92 (CH-5), 122.56 (C=CH), 119.95 (Cq-3a), 108.22 (CH-7), 61.29 (CH_2), 26.34 (NCH_3), 14.30 (CH_3) [277].

(*E*)-ethyl 2-(2-oxoindolin-3-ylidene)acetate (121b).

Synthesized according to the general procedure (method A), this compound was obtained as an orange solid (286.6 mg, 97 % yield).

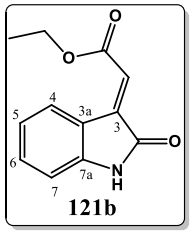

121b

Mp: 170-172 ºC (mp lit. 169-170 ºC [278, 362]; **^{1}H NMR** (400 MHz, $CDCl_3$) δ (ppm): 8.56 (d, *J* = 7.7 Hz, 1H, H-4), 7.85 (br s, 1H, NH), 7.32 (td, *J* = 7.7, 1.1 Hz, 1H, H-6), 7.06 (td, *J* = 7.7, 0.9 Hz, 1H, H-5), 6.88 (s, 1H, C=CH), 6.85 (d, *J* = 7.7 Hz, 1H, H-7), 4.33 (q, *J* = 7.1 Hz, 2H, CH_2), 1.37 (t, *J* = 7.1 Hz, 3H, CH_3) [278].

(*E*)-methyl 2-(*N*-methyl-2-oxoindolin-3-ylidene)acetate (CR121c).

Synthesized according to the general procedure (method A), this compound was obtained as a dark orange solid (309.2 mg, 93 % yield).

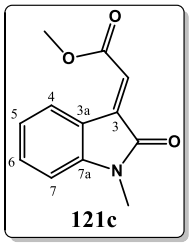

121c

Mp: 136-138 ºC (mp. lit.[274] 137-138ºC); **^{1}H NMR** (400 MHz, $CDCl_3$) δ (ppm): 8.56 (d, J = 7.7 Hz, 1H, H-4), 7.38 (td, J = 7.7, 1.0 Hz, 1H, H-6), 7.08 (td, J = 7.7, 0.8 Hz, 1H, H-5), 6.92 (s, 1H, C=CH), 6.80 (d, J = 7.8 Hz, 1H, H-7), 3.87 (s, 3H, OCH_3), 3.24 (s, 3H, NCH_3) [274].

(*E*)-methyl 2-(2-oxoindolin-3-ylidene)acetate (121d).

Synthesized according to the general procedure (method A), this compound was obtained as an orange solid (272.2 mg, 98 % yield).

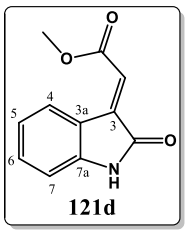

121d

Mp: 180-182 ºC (mp. lit. 181-182ºC [363], 178-180ºC [279]); **^{1}H NMR** (400 MHz, $CDCl_3$) δ (ppm): 8.55 (d, J = 7.8 Hz, 1H, H-4), 7.92 (br s, 1H, NH), 7.33 (t, J = 7.8 Hz, 1H, H-6), 7.06 (t, J = 7.8 Hz, 1H, H-5), 6.88 (s, 1H, C=CH), 6.85 (d, J = 7.8 Hz, 1H, H-7), 3.88 (s, 3H, OCH_3) [279].

9.1.2.2. Method B- Aldolic Condensation.

A mixture of the indoline-2-one derivative (1.0 equiv), aldehyde (1.2 equiv) and piperidine (0.1 equiv) in ethanol was refluxed for a period of 3-8 hours, under nitrogen atmosphere. After the reaction was complete, the solvent was removed under reduced pressure and the residue was purified by flash chromatography on silica gel using as eluent a gradient from *n*-hexane/EtOAc (4:1) to *n*-hexane/EtOAc (2:1) to afford the final product, as a mixture of *E*/*Z* isomers (adapted from [297]).

For most cases only traces of minor *Z* isomer was detected, and therefore for those derivatives only ^{1}H NMR description for the major *E* isomer will be given.

(*E*)-3-benzylideneindolin-2-one (121e).

Synthesized according to the general procedure (method B), this compound was obtained as a yellow solid (1232.6 mg, 99 % yield).

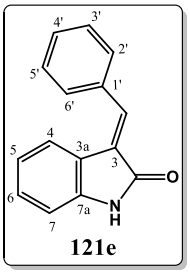

121e

^{1}H NMR (400 MHz, $CDCl_3$) major (*E*) isomer δ (ppm): 8.81 (br s, 1H NH), 7.86 (s, 1H, C=CH), 7.70 – 7.66 (m, 2H, H-2',6'), 7.65 (d, J = 7.7 Hz, 1H, H-4), 7.51 – 7.43 (m, 3H, H-3',4',5'), 7.22 (td, J = 7.7, 1.0 Hz, 1H, H-6), 6.93 (d, J = 7.8 Hz, 1H, H-7), 6.88 (td, J = 7.7, 0.9 Hz, 1H, H-

5) [302, 303].

(*E*)-3-(4-methoxybenzylidene)indolin-2-one (121f).

Synthesized according to the general procedure (method B), this compound was obtained as a yellow solid (1068.8 mg, 76 % yield).

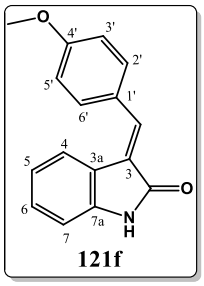

^{1}H NMR (400 MHz, $CDCl_3$) major (*E*) isomer δ (ppm): 8.48 (br s, 1H, NH), 7.80 (s, 1H, C=CH), 7.76 (d, *J* = 7.7 Hz, 1H, H-4), 7.68 (d, *J* = 8.8 Hz, 2H, H-2',6'), 7.21 (td, *J* = 7.7, 1.0 Hz, 1H, H-6), 7.00 (d, *J* = 8.8 Hz, 2H, H-3',5'), 6.93 – 6.88 (m, H-5, H-7), 3.89 (s, 3H, OCH_3); minor (*Z*) isomer: 8.37 (d, *J* = 8.8 Hz, 2H, H-2',6'), 8.18 (br s, 1H, NH), 7.53 – 7.48 (m, 2H, H-4, C=CH), 7.20 (td, *J* = 7.6, 1.0 Hz, 1H, H-6), 7.04 (td, *J* = 7.6, 0.8 Hz, 1H, H-5), 6.98 (d, *J* = 8.8 Hz, 2H, H-3',5'), 6.87 (d, *J* = 7.7 Hz, 1H, H-7), 3.89 (s, 3H, OCH_3) [303, 304].

(*E*)-3-(4-methoxybenzylidene)indolin-2-one (121g).

Synthesized according to the general procedure (method B), this compound was obtained as a pale yellow solid (161.1 mg, 89 % yield).

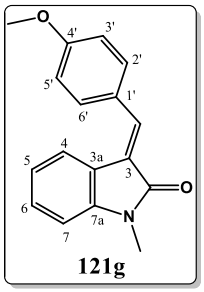

^{1}H NMR (400 MHz, $CDCl_3$) major (*E*) isomer δ (ppm): 7.81 (s, 1H, C=CH), 7.76 (d, *J* = 7.6 Hz, 1H, H-4), 7.65 (d, *J* = 8.7 Hz, 2H, H-2',6'), 7.29 – 7.23 (m, 1H, H-6), 6.99 (d, *J* = 8.8 Hz, H-3',5'), 6.92 (t, *J* = 7.6 Hz, 1H, H-5), 6.82 (d, *J* = 7.8 Hz, 1H, H-7), 3.88 (s, 3H, OCH_3), 3.27 (s, 3H, NCH_3); minor (*Z*) isomer: 8.40 (d, *J* = 8.8 Hz, 2H, H-2',6'), 7.48 (d, *J* = 7.6 Hz, 1H, H-4), 7.46 (s, 1H, C=CH), 7.29 – 7.23 (m, 1H, H-6), 7.04 (t, *J* = 7.6, 1H, H-5), 6.96 (d, *J* = 8.8 Hz, 2H, H-3',5'), 6.79 (d, *J* = 7.9 Hz, 1H, H-7), 3.87 (s, 3H, OCH_3), 3.27 (s, 3H, NCH_3) [305].

(*E*)-3-butylideneindolin-2-one (121h).

Synthesized according to the general procedure (method B), this compound was obtained as a pale yellow solid (223.1 mg, 96 % yield).

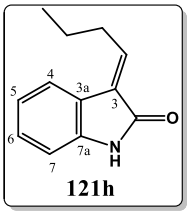

^{1}H NMR (400 MHz, $CDCl_3$) major (*E*) isomer δ (ppm): 8.53 (s, 1H, NH), 7.55 (d, *J* = 7.6 Hz, 1H, H-4), 7.22 (t, *J* = 7.6 Hz, 1H, H-6), 7.08 – 7.00 (m, 2H, H-5, C=CH), 6.90 (d, *J* = 7.8 Hz, 1H, H-7), 2.67 (q, *J* = 7.5 Hz, 2H, $CHC\underline{H}_2$), 1.74 – 1.64 (m, 2H, $C\underline{H}_2CH_3$), 1.05 (t, *J* = 7.4 Hz, 3H, CH_3); minor (*Z*) isomer: 8.27 (br s, 1H, NH), 7.38 (d, *J* = 7.6 Hz, 1H, H-4), 7.19 (t, *J* = 7.7 Hz, 1H, H-6), 6.99 (t, *J* = 7.6 Hz, 1H, H-5), 6.93 – 6.87 (m, 1H, C=CH, overlap with major

isomer) 6.84 (d, *J* = 7.8 Hz, 1H, H-7), 2.98 (q, *J* = 7.6 Hz, 2H, CHC<u>H</u>$_2$), 1.65 – 1.55 (m, 2H, C<u>H</u>$_2$CH$_3$), 1.03 (t, *J* = 7.4 Hz, 3H, CH$_3$) [306].

(*E*)-3-benzylidene-5-nitroindolin-2-one (121i).

Synthesized according to the general procedure (method B), this compound was obtained as a yellow solid (348.7 mg, 93 % yield).

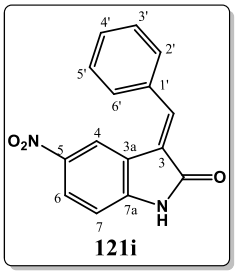

121i

^{1}H NMR (400 MHz, CDCl$_3$) major (*E*) isomer δ (ppm): 8.81 (s, 1H NH), 7.86 (s, 1H, C=CH), 7.70 – 7.66 (m, 2H, H-2',6'), 7.65 (d, *J* = 7.7 Hz, 1H, H-4), 7.51 – 7.43 (m, 3H, H-3',4',5'), 7.22 (td, *J* = 7.7, 1.0 Hz, 1H, H-6), 6.93 (d, *J* = 7.8 Hz, 1H, H-7), 6.88 (td, *J* = 7.7, 0.9 Hz, 1H, H-5) [301].

(*E*)-3-benzylidene-7-chloroindolin-2-one (121j).

Synthesized according to the general procedure (method B), this compound was obtained as a yellow solid (377.0 mg, 99 % yield).

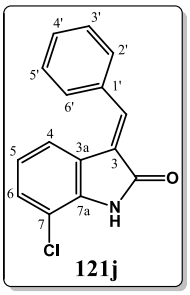

121j

^{1}H NMR (400 MHz, CDCl$_3$) major (*E*) isomer δ (ppm): 7.89 (br s, 1H, NH), 7.79 (s, 1H, C=CH), 7.67 – 7.61 (m, 2H, H-2',6'), 7.54 (d, *J* = 7.8 Hz, 1H, H-4), 7.50 – 7.45 (m, 3H, H-3',4',5'), 7.22 (d, *J* = 7.8 Hz, 1H, H-6), 6.83 (t, *J* = 7.8 Hz, 1H, H-5).

(*E*)-3-benzylidene-6-chloroindolin-2-one (121k).

Synthesized according to the general procedure (method B), this compound was obtained as a yellow solid (363.7 mg, 95 % yield).

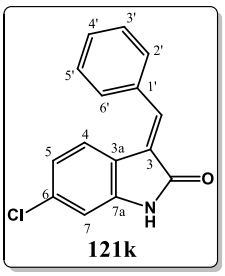

121k

^{1}H NMR (400 MHz, CDCl$_3$) major (*E*) isomer δ (ppm): 8.43 (br s, 1H, NH), 7.85 (s, 1H, C=CH), 7.66 – 7.62 (m, 2H, H-2',6'), 7.56 (d, *J* = 8.3 Hz, 1H, H-4), 7.51 – 7.44 (m, 3H, H-3',4',5'), 6.93 (d, *J* = 1.9 Hz, 1H, H-7), 6.85 (dd, *J* = 8.3, 1.9 Hz, 1H, H-5) [307].

(*E*)-6-chloro-3-(4-methoxybenzylidene)indolin-2-one (121l).

Synthesized according to the general procedure (method B), this compound was obtained as a yellow solid (422.3 mg, 99 %).

^{1}H NMR (400 MHz, CDCl$_3$) major (*E*) isomer δ (ppm): 8.13 (br s, 1H NH), 7.79 (s, 1H, C=CH), 7.67 (d, *J* = 8.2 Hz, 1H, H-4), 7.64 (d, *J* = 8.6 Hz, 2H, H-2',6'), 7.00 (d, *J* = 8.7 Hz, 2H, H-3',5'), 6.90 (s, 1H, H-7), 6.87 (dd, *J* = 8.2, 1.8 Hz, 1H, H-5), 3.89 (s, 3H,

OCH_3); minor (*Z*) isomer: 8.35 (d, *J* = 8.8 Hz, 2H, H-2',6'), 7.98 (br s, 1H, NH), 7.48 (s, 1H, C=CH), 7.41 (d, *J* = 8.2 Hz, 1H, H-4), 7.05 – 6.96 (m, 3H, H-5, H-3',5', obscured by major isomer), 6.91 – 6.85 (m, 1H, H-7, obscured by major isomer), 3.89 (s, 3H, OCH_3) [307].

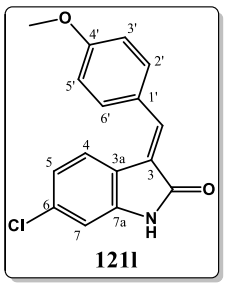

1211

(*E*)-3-benzylidene-6-bromoindolin-2-one (121m).

Synthesized according to the general procedure (method B), this compound was obtained as a yellow solid (324.9 mg, 93 % yield).

^{1}H NMR (400 MHz, $CDCl_3$) major (*E*) isomer δ (ppm): 8.42 (br s, 1H NH), 7.87 (s, 1H, C=CH), 7.66 – 7.61 (m, 2H, H-2',6'), 7.51 – 7.44 (m, 4H, H-4, H-3',4',5'), 7.08 (d, *J* = 1.8 Hz, 1H, H-7), 7.01 (dd, *J* = 8.3, 1.8 Hz, 1H).

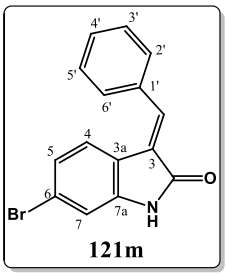

121m

(*E*)-bromo-3-(3-chlorobenzylidene)indolin-2-one (121r).

Synthesized according to the general procedure (method B), this compound was obtained as a yellow solid (369.2 mg, 94 % yield).

^{1}H NMR (300 MHz, $CDCl_3$) major (*E*) isomer δ (ppm): 7.84 (br s, 1H, NH), 7.79 (s, 1H, C=CH), 7.69 (d, *J* = 1.8 Hz, 1H, H-4), 7.61 (d, *J* = 0.9 Hz, 1H, H-2'), 7.56 – 7.51 (m, 1H, H_{Ar}), 7.48 – 7.44 (m, 2H, H_{Ar}), 7.38 (dd, *J* = 8.3, 1.8 Hz, 1H, H-6), 6.79 (d, *J* = 8.3 Hz, 1H, H-7).

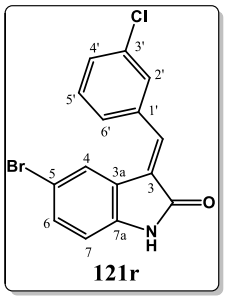

121r

(*E*)-ethyl 2-(*N*-acetyl-5-fluoro-2-oxoindolin-3-ylidene)acetate (121p).

To a round bottom flask with a stir bar charged with phosphonium ylide derivative (1.0 equiv, 18.17 mmol, 6.33 g) in 36 mL THF was added 5-fluoroindoline-2,3-dione (1.0 equiv, 18.17 mmol, 3.00 g). After 10 h at reflux the reaction was concentrated *in vacuo*, and product was purified by flash chromatography on silica gel using as eluent a gradient from hexanes/EtOAc (9:1) to hexanes/EtOAc (4:1) to afford the *N*-H alkylidene product (**121q**).

To a round bottom flask equipped with a stir bar under inert atmosphere and charged with the alkylidene purified in the prior step was added CH_2Cl_2 (91 mL). Subsequently acetic anhydride (7.0 equiv, 127.19 mmol, 12 mL) and pyridine (1.0 equiv, 18.17 mmol, 1.5 mL) were added, followed immediately by *N*,*N*-dimethyl-aminopyridine (0.1 equiv, 1.82 mmol, 222 mg). After the reaction was complete as judged by thin layer chromatography, sat. aq. $NaHCO_3$ (91 mL) was added. The reaction was stirred for 2 h until the evolution of gas ceased, and the organic layer was collected. The organic layer

was washed with sat. aq. $CuSO_4$ (3x), recollected and dried over Na_2SO_4, and concentrated *in vacuo*. The sample was filtered through a pad of silica in 20% EtOAc/hexanes, and the product recrystallized in EtOH (adapted from [330]), affording **121p** as an orange solid (2,52 g, 50% yield).

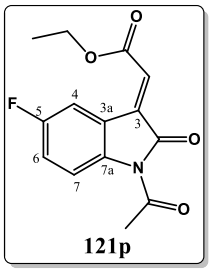

^{1}H-NMR (300 MHz, $CDCl_3$) δ (ppm): 8.49 (dd, J = 9.1, 2.8 Hz, 1H), 8.30 (dd, J = 9.0, 4.8 Hz, 1H), 7.16 (td, J = 8.7, 2.8 Hz, 1H), 6.97 (s, 1H, C=CH), 4.36 (q, J = 7.1 Hz, 2H, CH_2), 2.71 (s, 3H, $NCOCH_3$), 1.39 (t, J = 7.1 Hz, 3H, $CH_2C\underline{H}_3$).

(*E*)-*N*-acetyl-3-benzylidene-6-chloroindolin-2-one (121n).

To a round bottom flask equipped with a stir bar under inert atmosphere and charged with the alkylidene **121k** (1.0 equiv, 1 mmol, 255.7 mg) was added CH_2Cl_2 (10 mL). Subsequently acetic anhydride (7.0 equiv, 7 mmol, 660 µL) and pyridine (1.0 equiv, 1 mmol, 81 µL) were added, followed immediately by *N*,*N*-dimethyl-aminopyridine (0.1 equiv, 0.1 mmol, 12.2 mg). After the reaction was complete as judged by thin layer chromatography (2 h), sat. aq. $NaHCO_3$ (10 mL) was added. The reaction was stirred for 2 h until the evolution of gas ceased, and the organic layer was collected. The organic layer was washed with sat. aq. $CuSO_4$ (3x), recollected, dried over Na_2SO_4, and concentrated *in vacuo*. The product was purified by flash chromatography on silica gel using as eluent hexanes/EtOAc (9:1) (adapted from [330]), affording **121n** as a yellow solid (275.7 g, 93% yield).

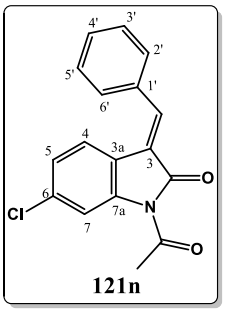

^{1}H NMR (300 MHz, $CDCl_3$) major (*E*) isomer δ (ppm): 7.90 (s, 1H, C=CH), 7.64 – 7.59 (m, 2H, H-2',6'), 7.55 (d, J = 8.4 Hz, 1H, H-4), 7.51 – 7.44 (m, 3H, H-3',4',5'), 7.29 (d, J = 2.0 Hz, 1H, H-7), 7.02 (dd, J = 8.4, 2.0 Hz, 1H, H-5), 2.77 (s, 3H, CH_3).

9.1.3. Synthesis of indolin-2,3-diones and 5-bromoindolin-2-one.

6-chloroindolin-2,3-dione.

A mixture of indolin-2-one (1.0 equiv, 8.35 mmol, 1.40 g) and $CuBr_2$ (4.0 equiv, 33.40 mmol, 7.46 g) in EtOAc (66 mL) was heated at reflux. After 6 h the solvent was removed under reduce pressure and a mixture of MeOH:H_2O (4:1 v/v, 23 mL) was added. The mixture was heated at reflux for 3 h and, after removal of the solvent, the residue was purified by flash chromatography on silica gel using as eluent a gradient from *n*-hexane to

n-hexane:EtOAc (1:1) (adapted from [341, 342]). This compound was obtained as a yellow solid (835.1 mg, 55 % yield).

^{1}H NMR (400 MHz, DMSO-d_6) δ (ppm): 11.18 (br s, 1H, NH), 7.52 (d, *J* = 8.0 Hz, 1H, H-4), 7.11 (d, *J* = 8.0 Hz, 1H, H-5), 6.94 (s, 1H, H-7) [364].

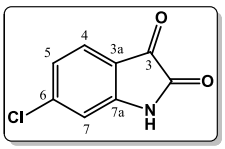

***N*-methyl indolin-2,3-dione.**

CH_3I (1.1 equiv, 7.48 mmol, 465 µL) was added to a stirred suspension of indolin-2-one (1.0 equiv, 6.80 mmol, 1.00 g) and K_2CO_3 (1.3 equiv, 8.84 mmol, 1.22 g) in DMF (15 mL). The mixture was heated at 70 ºC for 2 h, under nitrogen atmosphere. The reaction mixture was quenched with water and extracted with EtOAc (3x). The combined extracts were dried over anhydrous Na_2SO_4. After evaporation of the solvent under reduced pressure, the crude product was purified by flash chromatography on silica gel using as eluent DCM:EtOAc (12:1) (adapted from [271]). This compound was obtained as a white solid (1061.9 mg, 96 % yield).

Mp: 130-131 ºC (mp lit. 131ºC [271]; 129-130ºC [365]; **^{1}H NMR** (400MHz, $CDCl_3$) δ (ppm): 7.61 (t, *J* = 7.6 Hz, 1H, H-6), 7.60 (d, *J* = 7.6 Hz, 1H, H-4), 7.13 (t, *J* = 7.6 Hz, 1H, H-5), 6.89 (d, *J* = 7.8 Hz, 1H, H-7), 3.25 (s, 3H, NCH_3) [365].

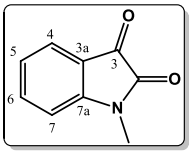

5-bromoindolin-2-one (147a).

$TiCl_4$ (3.0 equiv, 6.63 mmol, 729 µL) was added to a stirred suspension of Zn powder (6 equiv, 13.26 mmol, 867.0 mg) in freshly distilled anhydrous THF (15 mL) at r.t. under nitrogen atmosphere. The mixture was refluxed for 2 h, and then allowed to cool to rt. A solution of 5-bromoindolin-2-one (1 equiv, 2.21 mmol, 500.0 mg) in anhydrous THF (10 mL) was added dropwise, and the mixture was stirred for 10 min under nitrogen atmosphere. The reaction mixture was quenched with 3% HCl solution and extracted with DCM (3x). The combined extracts were washed with water and dried over anhydrous Na_2SO_4. After evaporation of the solvent under reduced pressure, the crude product was purified by flash chromatography on silica gel using as eluent a gradient from 100% *n*-hexane to *n*-hexane:EtOAc (1:1) (adapted from [366]). This compound was obtained as a white solid (304.4 mg, 65 % yield).

^{1}H NMR (300 MHz, $CDCl_3$) δ (ppm): 8.23 (br s, 1H, NH), 7.38 – 7.30 (m, 2H, H-4, H-6), 6.76 (d, *J* = 8.9 Hz, 1H, H-7), 3.54 (s, 2H, CH_2) [364].

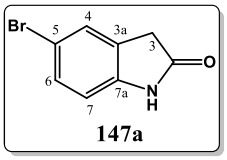

147a

9.1.4. General procedure for the synthesis of 3-imino-indoline-2-ones.

A mixture of indoline-2,3-dione derivative (1.0 equiv), aniline derivative (1.0 equiv), and acetic acid (0.1 equiv) in ethanol (4.0 mL/mmol of indoline-2,3-dione derivative) was heated at reflux for 3-5h, under nitrogen atmosphere. If after 5 hours the reaction was not completed an additional 0.5 equiv of aniline derivative was added and refluxed to maximum reaction duration of 24h. The reaction mixture was allowed to cool to room temperature, and the residue was filtrated. The solid obtained was washed with cold ethanol. The final product was obtained as a mixture of *E*/*Z* isomers (adapted from [340]).

In some cases only traces of minor *Z* isomer was detected, and therefore for those derivatives only ^{1}H NMR description for the major *E* isomer will be given.

3-(phenylimino)indolin-2-one (166a).

Synthesized according to the general procedure, this compound was obtained as a yellow solid (1038.5 mg, 69 % yield).

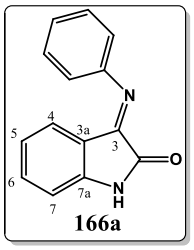

166a

^{1}H NMR (400 MHz, $CDCl_3$) major (*E*) isomer δ (ppm): 9.16 (br s, 1H, NH), 7.44 (t, *J* = 7.8 Hz, 2H, H_{Ar}), 7.31 (t, *J* = 7.8 Hz, 1H, H-6), 7.28 – 7.22 (m, 1H, H_{Ar}), 7.03 (d, *J* = 7.8 Hz, 2H, H_{Ar}), 6.93 (d, *J* = 7.8 Hz, 1H, H-7), 6.75 (t, *J* = 7.8 Hz, 1H, H-5), 6.66 (d, *J* = 7.8 Hz, 1H, H-4) [343, 367].

3-((3-chlorophenyl)imino)indolin-2-one (166b).

Synthesized according to the general procedure, this compound was obtained as a yellow solid (1517.9 mg, 87 % yield).

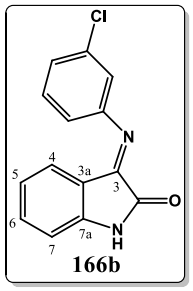

166b

^{1}H NMR (400 MHz, $CDCl_3$) major (*E*) isomer δ (ppm): 9.17 (br s, 1H, NH), 7.40 – 7.31 (m, 2H, H-6, H_{Ar}), 7.24 (d, *J* = 8.1 Hz, 1H, H_{Ar}), 7.04 (s, 1H, H_{Ar}), 6.97 – 6.89 (m, 2H, H-7, H_{Ar}), 6.80 (t, *J* = 7.7 Hz, 1H, H-5), 6.67 (d, *J* = 7.8 Hz, 1H, H-4); minor (*Z*) isomer δ (ppm): 8.86 (br s, 1H, NH), 7.61 (d, *J* = 7.5 Hz, 1H, H-4), 7.56 (t, *J* = 7.7 Hz, 1H, H-6), 7.12 (t, *J* = 7.5 Hz, 1H, H-5), 7.06 (t, *J* = 8.0 Hz, 1H, H_{Ar}), 6.97 – 6.89 (m, 1H, H-7, obscured by major isomer), 6.73 (d, *J* = 8.0 Hz, 1H, H_{Ar}), 6.69 (s, 1H, H_{Ar}), 6.57 (d, *J* = 8.0 Hz, 1H, H_{Ar}) [345]; **^{13}C NMR** (75 MHz, $CDCl_3$) major (*E*) isomer δ (ppm): 165.13 (C=O), 155.37 (C=N), 151.34 (Cq_{Ar}), 145.91 (Cq-7a), 135.35 (CqAr), 135.01 (CH-6), 130.84 (CH_{Ar}), 126.65 (CH-4), 125.53 (CH_{Ar}), 123.18 (CH-5), 118.13 (CH_{Ar}), 116.21 (CH_{Ar}), 116.04 (Cq-3a), 112.07 (CH-7).

3-((4-chlorophenyl)imino)indolin-2-one (166c).

Synthesized according to the general procedure, this compound was obtained as a yellow solid (1408.9 mg, 81 % yield).

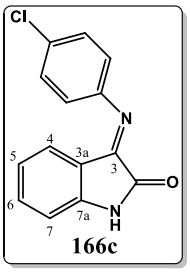

166c

^{1}H NMR (400 MHz, $CDCl_3$) major (*E*) isomer δ (ppm): 8.89 (br s, 1H, NH), 7.42 (d, *J* = 8.4 Hz, 2H, H_{Ar}), 7.34 (t, *J* = 7.6 Hz, 1H, H-6), 6.99 (d, *J* = 8.5 Hz, 2H, H_{Ar}), 6.92 (d, *J* = 7.8 Hz, 1H, H-7), 6.80 (t, *J* = 7.6 Hz, 1H, H-5), 6.75 (d, *J* = 7.6 Hz, 1H, H-4); minor (*Z*) isomer δ (ppm): 8.58 (br s, 1H, NH), 7.62 (d, *J* = 7.6 Hz, 1H, H-4), 7.56 (t, *J* = 7.7 Hz, 1H, H-6), 7.15 – 7.08 (m, 3H, H-5, 2H_{Ar}), 6.92 (d, *J* = 7.8 Hz, 1H, H-7), 6.66 (d, *J* = 8.5 Hz, 2H, H_{Ar}); **^{13}C NMR** (75 MHz, $CDCl_3$) major (*E*) isomer δ (ppm): 164.93 (C=O), 154.99 (C=N), 148.53 (Cq_{Ar}), 145.78 (Cq-7a), 134.88 (CH-6), 131.11 (Cq_{Ar}), 129.81 (2CH_{Ar}), 126.51 (CH-4), 123.10 (CH-5), 119.66 (2CH_{Ar}), 116.16 (Cq-3a), 111.95 (CH-7) [346].

3-((3-chloro-4-fluorophenyl)imino)indolin-2-one (166d).

Synthesized according to the general procedure, this compound was obtained as an orange solid (1671.4 mg, 90 % yield).

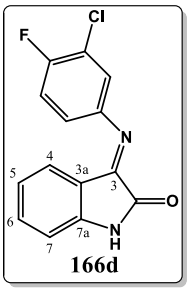

166d

^{1}H NMR (400 MHz, $CDCl_3$) major (*E*) isomer δ (ppm): 8.34 (br s, 1H, NH), 7.37 (t, *J* = 7.6 Hz, 1H, H-6), 7.26 – 7.20 (m, 1H, H_{Ar}), 7.12 (d, *J* = 6.9 Hz, 1H, H_{Ar}), 6.95 – 6.88 (m, 2H, H-7, H_{Ar}), 6.83 (t, *J* = 7.6 Hz, 1H, H-5), 6.76 (d, *J* = 7.7 Hz, 1H, H-4) [347].

3-((4-fluorophenyl)imino)indolin-2-one (166e).

Synthesized according to the general procedure, this compound was obtained as a brown solid (498.0 mg, 61 % yield).

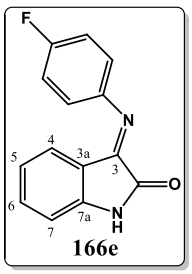

166e

^{1}H NMR (400 MHz, $CDCl_3$) major (*E*) isomer δ (ppm): 9.43 (br s, 1H, NH), 7.32 (t, *J* = 7.6 Hz, 1H, H-6), 7.18 – 7.11 (m, 2H, H_{Ar}), 7.06 – 7.01 (m, 2H, H_{Ar}), 6.94 (d, *J* = 7.8 Hz, 1H, H-7), 6.82 – 6.74 (m, 2H, H-4, H-5) [345].

5-chloro-3-(phenylimino)indolin-2-one (166f).

Synthesized according to the general procedure, this compound was obtained as a dark yellow solid (1187.6 mg, 84 % yield).

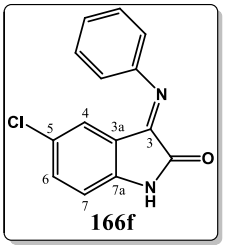

166f

^{1}H NMR (400 MHz, $CDCl_3$) major (*E*) isomer δ (ppm): 9.18 (br s, 1H, NH), 7.47 (t, *J* = 7.8 Hz, 2H, H_{Ar}), 7.33 – 7.27 (m, 2H, H-6, H_{Ar}), 7.02

(d, *J* = 7.8 Hz, 2H, H_{Ar}), 6.88 (d, *J* = 8.3 Hz, 1H, H-7), 6.64 (d, *J* = 1.4 Hz, 1H, H-4).

5-chloro-3-((3-chlorophenyl)imino)indolin-2-one (166g).

Synthesized according to the general procedure, this compound was obtained as a dark orange solid (1096.8 mg, 68 % yield).

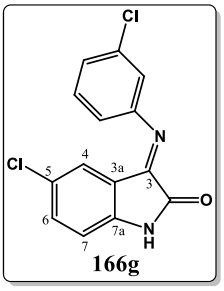

166g

^{1}H NMR (400 MHz, $CDCl_3$) major (*E*) isomer *δ* (ppm): 8.43 (br s, 1H, NH), 7.40 (t, *J* = 7.9 Hz, 1H, H_{Ar}), 7.33 (dd, *J* = 8.4, 1.6 Hz, 1H, H-6), 7.28 (d, *J* = 7.8 Hz, 1H, H_{Ar}), 7.04 (s, 1H, H_{Ar}), 6.91 – 6.86 (m, 2H, H-7, H_{Ar}), 6.67 (s, 1H, H-4); minor (*Z*) isomer *δ* (ppm): 8.19 (br s, 1H, NH), 7.59 (d, *J* = 1.8 Hz, 1H, H-4), 7.54 (dd, *J* = 8.4, 2.0 Hz, 1H, H-6), 7.07 (t, *J* = 8.0 Hz, 1H, H_{Ar}), 6.91 – 6.86 (m, 1H, H-7, partially obscured by major isomer), 6.75 (d, *J* = 8.0 Hz, 1H, H_{Ar}), 6.72 (s, 1H, H_{Ar}), 6.59 (d, *J* = 8.0 Hz, 1H, H_{Ar}).

5-chloro-3-((4-chlorophenyl)imino)indolin-2-one (166h).

Synthesized according to the general procedure, this compound was obtained as an orange solid (1330.8 mg, 83 % yield).

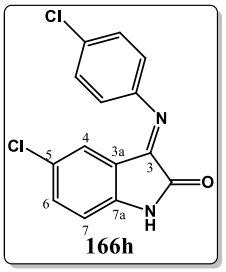

166h

^{1}H NMR (400 MHz, $CDCl_3$) major (*E*) isomer *δ* (ppm): 8.58 (br s, 1H, NH), 7.44 (d, *J* = 8.4 Hz, 2H, H_{Ar}), 7.33 (d, *J* = 8.2 Hz, 1H, H-6), 6.99 (d, *J* = 8.4 Hz, 2H, H_{Ar}), 6.88 (d, *J* = 8.2 Hz, 1H, H-7), 6.78 (s, 1H, H-4); minor (*Z*) isomer *δ* (ppm): 8.34 (br s, 1H, NH), 7.59 (s, 1H, H-4), 7.53 (dd, *J* = 8.2, 1.9 Hz, 1H, H-6), 7.11 (d, *J* = 8.4 Hz, 2H, H_{Ar}), 6.89 (d, *J* = 8.2 Hz, 1H, H-7), 6.65 (d, *J* = 8.4 Hz, 2H, H_{Ar}) [348].

5-bromo-3-(phenylimino)indolin-2-one (166i).

Synthesized according to the general procedure, this compound was obtained as a yellow solid (1071.4 mg, 80 % yield).

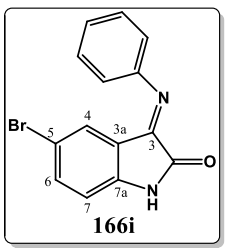

166i

^{1}H NMR (400 MHz, $CDCl_3$) major (*E*) isomer *δ* (ppm): 8.44 (br s, 1H, NH), 7.50 -7.42 (m, 3H, H-6, 2H_{Ar}), 7.30 (t, *J* = 7.6 Hz, 1H, H_{Ar}), 7.02 (d, *J* = 7.5 Hz, 2H, H_{Ar}), 6.81 (d, *J* = 8.4 Hz, 1H, H-7), 6.78 (s, 1H, H-4); minor (*Z*) isomer *δ* (ppm): 8.21 (br s, 1H, NH), 7.73 (s, 1H, H-4), 7.68 (d, *J* = 8.2 Hz, 1H, H-6), 7.21 (t, *J* = 7.0 Hz, 2H, H_{Ar}), 6.93 – 6.86 (m, 3H, H_{Ar}), 6.84 (d, *J* = 8.2 Hz, 1H, H-7).

5-bromo-3-((3-chlorophenyl)imino)indolin-2-one (166j).

Synthesized according to the general procedure, this compound was obtained as a dark orange solid (698.3 mg, 93 % yield).

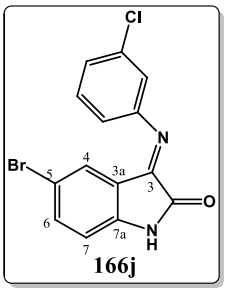

166j

^{1}H NMR (400 MHz, $CDCl_3$) major (*E*) isomer δ (ppm): 8.19 (br s, 1H, NH), 7.48 (d, *J* = 8.1 Hz, 1H, H-6), 7.40 (t, *J* = 7.9 Hz, 1H, H_{Ar}), 7.30 – 7.25 (m, 1H, H_{Ar}), 7.04 (s, 1H, H_{Ar}), 6.89 (d, *J* = 7.6 Hz, 1H, H_{Ar}), 6.86 – 6.79 (m, 2H, H-4, H-7); minor (*Z*) isomer δ (ppm): 8.01 (br s, 1H, NH), 7.74 (s, 1H, H-4), 7.69 (d, *J* = 8.4 Hz, 1H, H-6), 7.07 (t, *J* = 7.8 Hz, 1H, H_{Ar}), 6.86 – 6.79 (m, 1H, H-7, partially obscured by major isomer), 6.78 – 6.72 (m, 1H, H_{Ar}), 6.71 (s, 1H, H_{Ar}), 6.58 (d, *J* = 8.0 Hz, 1H, H_{Ar}).

5-bromo-3-((4-chlorophenyl)imino)indolin-2-one (166k).

Synthesized according to the general procedure, this compound was obtained as an orange solid (637.2 mg, 86 % yield).

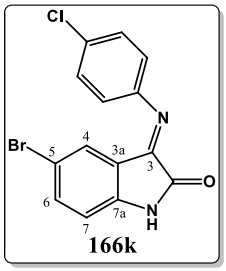

166k

^{1}H NMR (400 MHz, $CDCl_3$) major (*E*) isomer δ (ppm): 8.07 (br s, 1H, NH), 7.50 – 7.40 (m, 3H, H-6, 2H_{Ar}), 7.05 – 6.96 (m, 2H, H_{Ar}), 6.93 (s, 1H, H-4), 6.86 – 6.78 (m, 1H, H-7); minor (*Z*) isomer δ (ppm): 7.94 (br s, 1H, NH), 7.74 (s, 1H, H-4), 7.68 (d, *J* = 7.6 Hz, 1H, H-6), 7.18 – 7.11 (m, 2H, H_{Ar}), 6.86 – 6.78 (m, 1H, H-7, partially obscured by major isomer), 6.75 (d, *J* = 8.1 Hz, 2H, H_{Ar}).

5-bromo-3-((3-chloro-4-fluorophenyl)imino)indolin-2-one (166l).

Synthesized according to the general procedure, this compound was obtained as an orange solid (641.3 mg, 82 % yield).

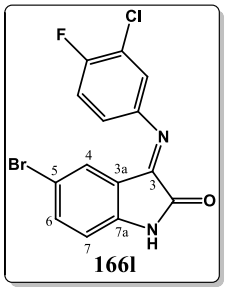

166l

^{1}H NMR (400 MHz, $CDCl_3$) major (*E*) isomer δ (ppm): 8.34 (br s, 1H, NH), 7.50 (d, *J* = 8.4 Hz, 1H, H-6), 7.29 – 7.23 (m, 1H, H_{Ar}), 7.16 – 7.10 (m, 1H, H_{Ar}), 6.96 – 6.88 (m, 2H, H-4, H_{Ar}), 6.84 (d, *J* = 8.2 Hz, 1H, H-7); minor (*Z*) isomer δ (ppm): 8.16 (br s, 1H, NH), 7.74 (d, *J* = 1.5 Hz, 1H, H-4), 7.69 (d, *J* = 8.2, 1.5 Hz, 1H, H-6), 6.96 – 6.88 (m, 1H, H_{Ar}), 6.84 (d, *J* = 8.2 Hz, 1H, H-7), 6.73 – 6.69 (m, 1H, H_{Ar}), 6.55 – 6.49 (s, 1H, H_{Ar}).

5-bromo-3-((3-chloro-2-fluorophenyl)imino)indolin-2-one (166m).

Synthesized according to the general procedure, this compound was obtained as an orange solid (664.5 mg, 85 % yield).

^{1}H NMR (400 MHz, DMSO-d_6) *E* isomer δ (ppm):11.24 (br s, 1H, NH), 7.61 (d, *J* = 8.4 Hz, 1H, H-6), 7.54 (t, *J* = 7.7 Hz, 1H, H_{Ar}), 7.39 – 7.27 (m, 1H, $H_{Ar,}$ partially obscured by *Z* isomer), 7.22 – 7.15 (m, 1H, H_{Ar}, partially obscured by *Z* isomer), 6.91 (d, *J* = 8.4 Hz, 1H, H-7), 6.52 (s, 1H, H-4); *Z* isomer δ (ppm): 11.16 (br s, 1H, NH), 7.79 (s, 1H, H-4), 7.68 (d, *J* = 8.4 Hz, 1H, H-6), 7.39 – 7.27 (m, 1H, H_{Ar}, partially obscured by *E* isomer), 7.22 – 7.15 (m, 1H, H_{Ar}, partially obscured by *E* isomer), 7.10 (t, *J* = 7.6 Hz, 1H, H_{Ar}), 6.88 (d, *J* = 8.4 Hz, 1H, H-7).

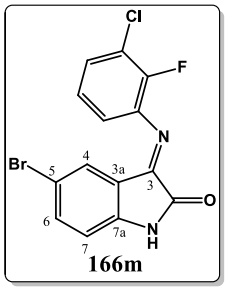

166m

5-bromo-3-((3-bromophenyl)imino)indolin-2-one (166n).

Synthesized according to the general procedure, this compound was obtained as a dark orange solid (723.5 mg, 86 % yield).

^{1}H NMR (400 MHz, DMSO-d_6) major (*E*) isomer δ (ppm): 11.13 (br s, 1H, NH), 7.56 (d, *J* = 8.0 Hz, 1H, H-6), 7.53 – 7.41 (m, 2H, H_{Ar}), 7.32 – 7.22 (m, 1H, H_{Ar}), 7.04 (d, *J* = 7.0 Hz, 1H, H_{Ar}), 6.88 (d, *J* = 8.2 Hz, 1H, H-7), 6.37 (s, 1H, H-4); minor (*Z*) isomer δ (ppm): 11.13 (br s, 1H, NH), 7.70 (s, 1H, H-4), 7.64 (d, *J* = 8.0 Hz, 1H, H-6), 7.53 – 7.41 (m, 1H, H_{Ar}, partially obscured by major), 7.32 – 7.22 (m, 2H, H_{Ar}, partially obscured by major), 7.00 (d, *J* = 6.8 Hz, 1H, H_{Ar}), 6.85 (d, *J* = 8.2 Hz, 1H, H-7).

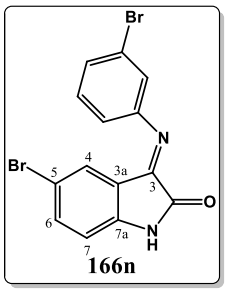

166n

6-chloro-3-(phenylimino)indolin-2-one (166p).

Synthesized according to the general procedure, this compound was obtained as a yellow solid (159.0 mg, 75 % yield).

^{1}H NMR (400 MHz, $CDCl_3$) major (*E*) isomer δ (ppm): 9.11 (br s, 1H, NH), 7.44 (t, *J* = 7.7 Hz, 2H, H_{Ar}), 7.30 – 7.24 (m, 1H, H_{Ar}), 7.02 (d, *J* = 7.6 Hz, 2H, H_{Ar}), 6.95 (s, 1H, H-7), 6.73 (d, *J* = 8.3 Hz, 1H, H-5), 6.59 (d, *J* = 8.3 Hz, 1H, H-4).

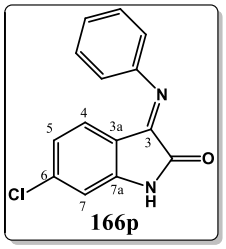

166p

6-chloro-3-((4-chlorophenyl)imino)indolin-2-one (166q).

Synthesized according to the general procedure, this compound was obtained as a yellow solid (262.5 mg, 82% yield).

^{1}H NMR (300 MHz, $CDCl_3$) major (*E*) isomer δ (ppm): 8.02 (br s, 1H, NH), 7.38 (t, *J* = 8.0 Hz, 1H, H_{Ar}), 7.28 – 7.21 (m, 1H, H_{Ar}), 7.03 – 7.00 (m, 1H, H_{Ar}), 6.92 (d, *J* = 1.7 Hz, 1H, H-7), 6.91 – 6.86 (m, 1H, H_{Ar}), 6.78 (dd, *J* = 8.3, 1.8 Hz, 1H, H-5), 6.61 (d, *J* = 8.3 Hz, 1H, H-4).

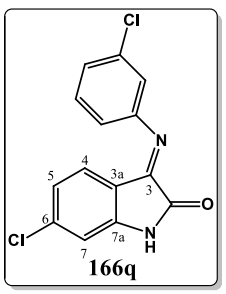

166q

6-chloro-3-((4-chlorophenyl)imino)indolin-2-one (166r).

Synthesized according to the general procedure, this compound was obtained as a yellow solid in (449.2 mg, 80% yield).

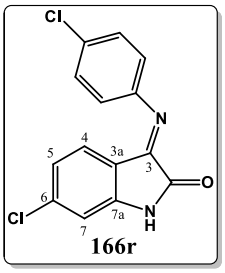

166r

^{1}H NMR (400 MHz, $CDCl_3$) major (*E*) isomer δ (ppm): 8.77 (br s, 1H, NH), 7.42 (d, *J* = 8.3 Hz, 2H, H_{Ar}), 7.00 – 6.93 (m, 3H, H-7, 2H_{Ar}), 6.78 (d, *J* = 8.3 Hz, 1H, H-5), 6.70 (d, *J* = 8.3 Hz, 1H, H-4).

7-chloro-3-(phenylimino)indolin-2-one (166s).

Synthesized according to the general procedure. However, the compound did not precipitate after cooling to room temperature, and even overnight at 5ºC. Therefore, the solvent was removed under reduced pressure and the residue was purified by flash chromatography on silica gel using as eluent a gradient from DCM to DCM:EtOAc (90:10). This compound was obtained as a yellow solid (308.0 mg, 87 % yield).

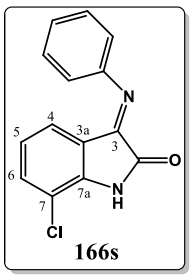

166s

^{1}H NMR (400 MHz, $CDCl_3$) major (*E*) isomer δ (ppm): 8.25 (br s, 1H, NH), 7.44 (t, *J* = 7.8 Hz, 2H, H_{Ar}), 7.32 (d, *J* = 8.1 Hz, 1H, H-6), 7.30 – 7.24 (m, 1H, H_{Ar}), 7.00 (d, *J* = 7.8 Hz, 2H, H_{Ar}), 6.72 (t, *J* = 8.0 Hz, 1H, H-5), 6.57 (d, *J* = 7.8 Hz, 1H, H-4).

7-bromo-3-(phenylimino)indolin-2-one (166t).

Synthesized according to the general procedure. However, the compound did not precipitate after cooling to room temperature, and even overnight at 5ºC. Therefore, the solvent was removed under reduced pressure and the residue was purified by flash chromatography on silica gel using as eluent a gradient from 100% DCM to DCM:EtOAc (90:10). This compound was obtained as a yellow solid (245.0 mg, 80 % yield).

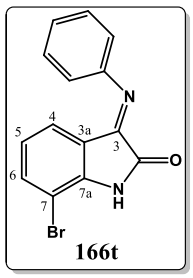

166t

^{1}H NMR (400 MHz, $CDCl_3$) major (*E*) isomer δ (ppm): 8.04 (br s, 1H, NH), 7.48 – 7.41 (m, 3H, H-6, 2H_{Ar}), 7.30 – 7.24 (m, 1H, H_{Ar}), 7.00 (d, *J* = 8.0 Hz, 2H, H_{Ar}), 6.67 (t, *J* = 7.7 Hz, 1H, H-5), 6.61 (d, *J* = 7.6 Hz, 1H, H-4).

3-(*tert*-butylimino)-5-chloroindolin-2-one (166o).

A mixture of 5-indoline-2,3-dione (1.0 equiv, 5.51 mmol, 1.00 g), *tert*-butylamine (2.0 equiv, 11.02 mmol, 1.16 mL), and acetic acid (0.1 equiv, 0.55 mmol, 31 µL) in 22 mL ethanol was stirred at room temperature for 24 h and at reflux for 24 h, under nitrogen

atmosphere. *tert*-Butylamine (2.0 equiv, 11.02 mmol, 1.16 mL) was added and refluxed for another 24h. The reaction mixture was allowed to cool to room temperature, and the residue was filtrated. The yellow solid obtained was washed with cold ethanol (706.0 mg, 54 % yield).

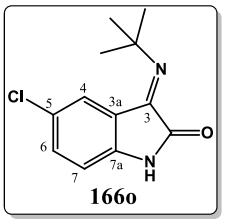

^{1}H NMR (400 MHz, $CDCl_3$) major (*E*) isomer δ (ppm): 7.93 (br s, 1H, NH), 7.54 (d, *J* = 1.9 Hz, 1H, H-4), 7.28 (dd, *J* = 8.2, 2.0 Hz, 1H, H-6), 6.72 (d, *J* = 8.2 Hz, 1H, H-7), 1.53 (s, 9H, $C(CH_3)_3$); minor (*Z*) isomer δ (ppm): 7.93 (br s, 1H, NH), 7.69 (d, *J* = 1.6 Hz, 1H, H-4), 7.36 (dd, *J* = 8.4, 1.7 Hz, 1H, H-6), 6.89 (d, *J* = 8.3 Hz, 1H, H-7), 1.59 (s, 9H, $C(CH_3)_3$).

9.1.5. GENERAL PROCEDURE FOR THE SYNTHESIS OF ALDOXIMES.

A mixture of benzaldehyde derivative (1.0 equiv), hydroxylamine hydrochloride (1.3 equiv) and Na_2CO_3 (0.7 equiv) in water (2.9 mL/mmol of aldehyde) was refluxed for 2-5 h. After cooling to room temperature the reaction mixture was extracted with dichloromethane (3x), and the organic fractions were combined, dried over anhydrous Na_2SO_4 and concentrated by rotary evaporation (adapted from [276]).

Benzaldehyde oxime (129a).

Synthesized according to the general procedure, this compound was obtained as brown oil (1106.3 mg, 97 %).

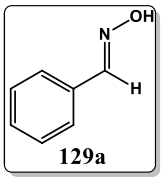

^{1}H NMR (400 MHz, $CDCl_3$) δ (ppm): 10.06 (br s, 1H, OH), 8.26 (s, 1H, CH=N), 7.71 – 7.58 (m, 2H, H_{Ar}), 7.47 – 7.35 (m, 3H, H_{Ar}) [281, 308].

4-Methoxybenzaldehyde oxime (129b).

Synthesized according to the general procedure, this compound was obtained as an off white solid (994.3 mg, 89 %).

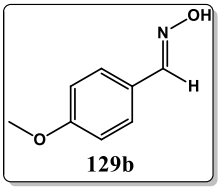

Mp: 58-60 ºC (mp lit. 134 ºC [368], 128-130 ºC [369]); **^{1}H NMR** (400 MHz, $CDCl_3$) δ (ppm): 9.37 (br s, 1H, OH), 8.14 (s, 1H, N=CH), 7.53 (d, *J* = 8.8 Hz, 2H, H_{Ar}), 6.91 (d, *J* = 8.8 Hz, 2H, H_{Ar}), 3.82 (s, 3H, OCH_3) [281, 309].

2-Methoxybenzaldehyde oxime (129c).

Synthesized according to the general procedure, this compound was obtained as a white solid (2159.9 mg, 97 %).

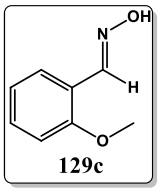

129c

Mp: 80-83 ºC (mp lit. 88 ºC [368], 95 ºC [310]); **^{1}H NMR** (400 MHz, $CDCl_3$) δ (ppm): 9.25 (br s, 1H, OH), 8.48 (s, 1H, N=CH), 7.65 (dd, J = 7.6, 1.6 Hz, 1H, H_{Ar}), 7.39 – 7.32 (m, 1H, H_{Ar}), 6.97 (t, J = 7.6 Hz, 1H, H_{Ar}), 6.93 (d, J = 8.3 Hz, 1H, H_{Ar}), 3.87 (s, 3H, OCH_3) [310, 311].

4-Methylbenzaldehyde oxime (129d).

Synthesized according to the general procedure, this compound was obtained as a white solid (975.0 mg, 87 %).

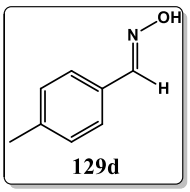

129d

Mp: 72-74 ºC (mp lit. 70 ºC [368], 74-76 ºC [369]); **^{1}H NMR** (400 MHz, $CDCl_3$) δ (ppm): 8.21 (br s, 1H, OH), 8.12 (s, 1H, N=CH), 7.47 (d, J = 8.0 Hz, 2H, H_{Ar}), 7.20 (d, J = 8.0 Hz, 2H, H_{Ar}), 2.37 (s, 3H, CH_3) [308, 309].

4-Nitrobenzaldehyde oxime (129e).

Synthesized according to the general procedure, this compound was obtained as an off-white solid (1080.9 mg, 98 %).

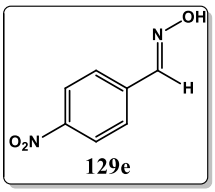

129e

Mp: 132-134 ºC (mp lit. 132-134 ºC [369], 131.3-132 ºC [370]); **^{1}H NMR** (400 MHz, $CDCl_3$) δ (ppm): 8.25 (d, J = 8.8 Hz, 2H, H_{Ar}), 8.20 (s, 1H, OH), 7.91 (s, 1H, N=CH), 7.75 (d, J = 8.8 Hz, 2H, H_{Ar}) [281, 312].

9.1.6. GENERAL PROCEDURE FOR THE SYNTHESIS OF CHLOROOXIMES.

9.1.6.1. Aromatic derivatives

A mixture of the aldehyde (1.0 equiv), hydroxylamine hydrochloride (1.3 equiv) and Na_2CO_3 (0.7 equiv) in water (2.9 mL/mmol of aldehyde) was refluxed for 3-5 h. After cooling to room temperature the reaction mixture was extracted with dichloromethane (3x), and the organic fractions were combined, dried over anhydrous Na_2SO_4 and concentrated by rotary evaporation. The residue was dissolved in DCM (2.9 mL/mmol of aldehyde) and pyridine (0,1 equiv) was added. After 5 min, *N*-chlorosuccinimide (1.0 equiv) was added portionwise to the stirring reaction mixture. After 24 h, the solvent was removed under reduced pressure and the residue was purified by flash chromatography on silica gel using

as eluent a gradient from 100% *n*-hexane to *n*-hexane/EtOAc (85:15) to afford the final product (adapted from [276]).

***N*-Hydroxybenzimidoyl chloride (123b)**.

Synthesized according to the general procedure, this compound was obtained as yellow semi-solid (2592.0 mg, 85 %).

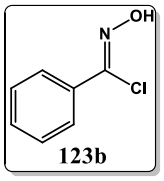

123b

^{1}H NMR (400 MHz, $CDCl_3$) δ (ppm): 9.38 (s, 1H, OH), 7.84 (d, J = 8.0 Hz, 2H, H_{Ar}), 7.46 – 7.38 (m, 3H, H_{Ar}) [276, 280].

***N*-Hydroxy-4-methoxybenzimidoyl chloride (123d)**.

Synthesized according to the general procedure, this compound was obtained as a light brown semi-solid (963.8 mg, 71 %).

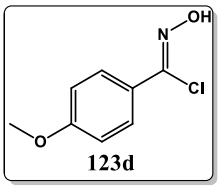

123d

^{1}H NMR (400 MHz, $CDCl_3$) δ (ppm): 7.47 (dd, J = 8.8, 7.9 Hz, 2H, H_{Ar}), 6.95 (dd, J = 9.0, 2.6 Hz, 2H, H_{Ar}), 3.85 (d, J = 4.0 Hz, 3H, OCH_3) [281, 282].

***N*-Hydroxy-4-methylbenzimidoyl chloride (123e)**.

Synthesized according to the general procedure, this compound was obtained as an off-white semi-solid (782.0 mg, 83 %).

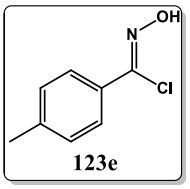

123e

^{1}H NMR (400 MHz, $CDCl_3$) δ (ppm): 7.98 (br s, 1H, OH), 7.73 (d, J = 8.2 Hz, 2H, H_{Ar}), 7.21 (d, J = 8.2 Hz, 2H, H_{Ar}), 2.39 (s, 3H, CH_3) [371, 372].

3-chloro-*N*-hydroxybenzimidoyl chloride (123f).

Synthesized according to the general procedure, this compound was obtained as a white solid (2999.0 mg, 90 %).

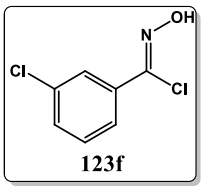

123f

Mp: 63-65 ºC (mp lit. 65-67 ºC [373]); **^{1}H NMR** (400 MHz, $CDCl_3$) δ (ppm): 9.48 (br s, 1H, OH), 7.83 (s, 1H, H_{Ar}), 7.73 (d, J = 7.9 Hz, 1H, H_{Ar}), 7.39 (d, J = 7.9 Hz, 1H, H_{Ar}), 7.32 (t, J = 7.9 Hz, 1H, H_{Ar}); **^{13}C NMR** (75 MHz, $CDCl_3$) δ (ppm): 138.99 (C=N), 134.77 (Cq_{Ar}), 134.21 (Cq_{Ar}), 130.89 (CH_{Ar}), 129.89 (CH_{Ar}), 127.36 (CH_{Ar}), 125.43 (CH_{Ar}).

4-chloro-*N*-hydroxybenzimidoyl chloride (123g).

Synthesized according to the general procedure, this compound was obtained as a white solid (2221.3 mg, 82 %).

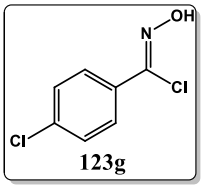

123g

Mp: 70-73 ºC (mp lit. 76-77 ºC [349], 87.5-89 ºC [373]); **^{1}H NMR** (400 MHz, $CDCl_3$) δ (ppm): 8.90 (br s, 1H, OH), 7.77 (d, J = 8.4 Hz, 2H, H_{Ar}), 7.37 (d, J = 8.4 Hz, 2H, H_{Ar}) [281, 349].

3-bromo-*N*-hydroxybenzimidoyl chloride (123h).

Synthesized according to the general procedure, this compound was obtained as a white solid (1112.7 mg, 88 %)

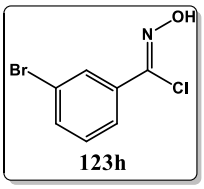

123h

Mp: 62-64ºC; **^{1}H NMR** (400 MHz, $CDCl_3$) δ (ppm): 7.87 (br s, 1H, OH), 7.23 (d, J = 1.6 Hz, 1H, H_{Ar}), 7.01 (d, J = 7.9 Hz, 1H, H_{Ar}), 6.80 (d, J = 7.9 Hz, 1H, H_{Ar}), 6.51 (t, J = 7.9 Hz, 1H, H_{Ar}).

3-chloro-2-fluoro-*N*-hydroxybenzimidoyl chloride (123i).

Synthesized according to the general procedure, this compound was obtained as a white solid (359.3 mg, 91 %)

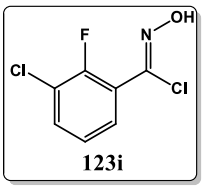

123i

Mp: 92-94 ºC; **^{1}H NMR** (400 MHz, $CDCl_3$) δ (ppm): 8.70 (br s, 1H, OH), 7.58 – 7.46 (m, 2H, H_{Ar}), 7.16 (t, J = 8.0 Hz, 1H, H_{Ar}).

9.1.6.2. Ester derivatives

Glycine ester hydrochloride (2000 mg, 1.0 equiv) was dissolved in 2.5 mL of water, and the solution was cooled to -5 ºC. Hydrochloric acid 37% (d = 1.19, 1.0 equiv) was added, and then a solution of sodium nitrite (1 equiv) in 1.5 mL of water was added dropwise. After 5 minutes, a second equivalent of hydrochloric acid and a second equivalent of sodium nitrite were added in the same manner. The mixture was left 1 h at -5 ºC. The reaction mixture was extracted with ethyl ether (3x), and the extracts were dried over anhydrous Na_2SO_4 and concentrated by rotary evaporation. The crude product was recrystallized from *n*-hexane to afford the final product (adapted from [275]).

Ethyl chlorooximidoacetate (123a).

Synthesized according to the general procedure, this compound was obtained as a white solid (1604.0 mg, 74 %).

Mp: 77-78 ºC (mp lit. 80ºC [275]); **^{1}H NMR** (400 MHz, $CDCl_3$) δ (ppm): 9.15 (br s, 1H, OH), 4.40 (q, J = 7.2 Hz, 2H, CH_2), 1.39 (t, J = 7.2 Hz, 3H, CH_3) [275].

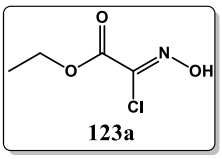

123a

Methyl chlorooximidoacetate (123c).

Synthesized according to the general procedure, this compound was obtained as a white solid (1117.0 mg, 51 %).

Mp: 51-52 ºC (mp lit. 61-63 ºC) [283]; **^{1}H NMR** (400 MHz, $CDCl_3$) δ (ppm): 10.06 (br s, 1H, OH), 3.95 (s, 3H, CH_3); **^{13}C NMR** (100 MHz, $CDCl_3$) δ (ppm): 159.46 (C=O), 132.69 (N=C-Cl), 54.40 (OCH_3) [283].

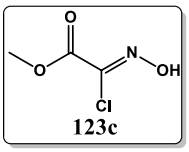

123c

9.1.7. GENERAL PROCEDURE FOR THE SYNTHESIS OF HYDRAZONES

A mixture of phenylhydrazine derivative (1.0 equiv), and benzaldehyde derivative (1.2 equiv) in aqueous ethanol 20% (2mL/mmol of phenylhydrazine) was stirred at room temperature in the dark for 2-3 hours. The precipitate formed was filtered and washed with aqueous ethanol 20%. Due to the fact that for compounds **171f**, **171g**, and **171i**, the starting phenylhydrazine is in chloridrate form, triethylamine (1.0 equiv) was added 15 minutes before adding the corresponding benzaldehyde (adapted from [352]).

1-benzylidene-2-phenylhydrazine (171a).

Synthesized according to the general procedure, this compound was obtained as a brown solid (1612.2 g, 81 % yield).

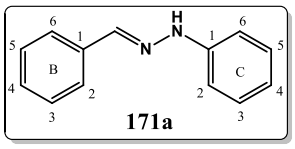

171a

Mp: 157-159 ºC (mp lit. 154 ºC [355], 158-160 ºC [374]), **^{1}H NMR** (400 MHz, $CDCl_3$) δ (ppm): 7.71 – 7.63 (m, 3H, CH=N, H-$B_{2,6}$), 7.60 (br s, 1H, NH), 7.44 – 7.35 (m, 2H, H-$B_{3,5}$), 7.35 – 7.23 (m, 3H, H-B_4, H-$C_{3,5}$), 7.13 (dd, J = 8.6, 1.0 Hz, 2H, H-$C_{2,6}$), 6.95 – 6.85 (m, 1H, H-C_4).; **^{13}C NMR** (75 MHz, $CDCl_3$) δ (ppm): 144.76 (Cq-C_1), 137.41 (CH=N), 135.41 (Cq-B_1), 129.44 (CH-$C_{3,5}$), 128.74 (CH-$B_{3,5}$), 128.55 (CH-B_4), 126.31 (CH-$B_{2,6}$), 120.22 (CH-C_4), 112.86 (CH-$C_{2,6}$) [355, 356].

1-(3-chlorobenzylidene)-2-phenylhydrazine (171b).

Synthesized according to the general procedure, this compound was obtained as an off-white solid (4227.2 mg, 99 % yield).

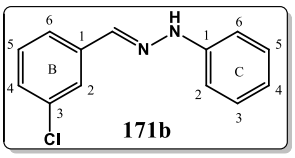

Mp: 134-136 ºC (mp lit. 134ºC [375], 136ºC [376]; **^{1}H NMR** (300 MHz, $CDCl_3$) δ (ppm): 7.70 – 7.61 (m, 2H, NH, H-B_2), 7.55 (s, 1H, CH=N), 7.51 – 7.44 (m, 1H, H-B_6), 7.35 – 7.23 (m, 4H, 2H-$B_{4,5}$, H-$C_{3,5}$), 7.16 – 7.08 (m, 2H, H-$C_{2,6}$), 6.95 – 6.87 (m, 1H, H-C_4); **^{13}C NMR** (75 MHz, $CDCl_3$) δ (ppm): 144.36 (Cq-C_1), 137.32 (Cq-B_1), 135.50 (CH=N), 134.77 (Cq-B_3), 129.95 (CH-B_5), 129.49 (CH-$C_{3,5}$), 128.33 (CH-B_4), 125.85 (CH-B_2), 124.49 (CH-B_6), 120.60 (CH-C_4), 112.96 (CH-$C_{2,6}$) [357].

1-(4-chlorobenzylidene)-2-phenylhydrazine (171c).

Synthesized according to the general procedure, this compound was obtained as an off-white solid (4058.7 mg, 95 % yield).

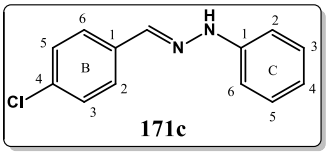

Mp: 127-128 ºC (mp lit. 126 ºC [355], 129 ºC [376]); **^{1}H NMR** (300 MHz, $CDCl_3$) δ (ppm): 7.63 (br s, 1H, NH), 7.62 – 7.55 (m, 3H, N=CH, H-$B_{2,6}$), 7.37 – 7.24 (m, 4H, H-$B_{3,5}$, H-$C_{3,5}$), 7.15 – 7.06 (m, 2H, H-$C_{2,6}$), 6.94 – 6.86 (m, 2H, H-C_4); **^{13}C NMR** (75 MHz, $CDCl_3$) δ (ppm): 144.50 (Cq-C_1), 135.93 (CH=N), 134.07 and 133.97 (Cq-B_1 and Cq-B_4), 129.48 (CH-$C_{3,5}$), 128.95 (CH-$B_{3,5}$), 127.39 (CH-$B_{2,6}$), 120.47 (CH-C_4), 112.90 (CH-$C_{2,6}$) [355, 357].

1-(4-methoxybenzylidene)-2-phenylhydrazine (171d).

Synthesized according to the general procedure, this compound was obtained as a light pink solid (3592.3 mg, 86 % yield).

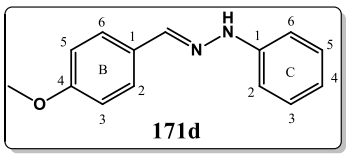

Mp: 117-119 ºC (mp lit. 115 ºC [377], 120 ºC [374]; **^{1}H NMR** (300 MHz, $CDCl_3$) δ (ppm): 7.66 – 7.56 (m, 3H, CH=N, H-$B_{2,6}$), 7.48 (br s, 1H, NH), 7.32 – 7.24 (m, 2H H-$C_{3,5}$), 7.14 – 7.07 (m, 2H, H-$C_{2,6}$), 6.95 – 6.90 (m, 2 H-$B_{3,5}$), 6.89 – 6.81 (m, 1H, H-C_4), 3.84 (s, 3H, OCH_3); **^{13}C NMR** (75 MHz, $CDCl_3$) δ (ppm): 160.10 (Cq-B_4), 145.07 (Cq-C_1), 137.52 (CH=N), 129.40 (CH-$C_{3,5}$), 128.24 (Cq-B_1), 127.69 (CH-$C_{2,6}$), 119.90 (CH-C_4), 114.22 (CH-$B_{3,5}$), 112.75 (CH-$C_{2,6}$), 55.45 (OCH_3) [355, 358].

1-benzylidene-2-(2-chlorophenyl)hydrazine (171e).

Synthesized according to the general procedure, this compound was obtained as a light pink solid (2380.1g, 92 %).

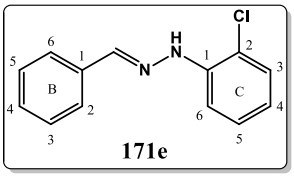

Mp: 70-72 ºC (mp lit. 155 ºC [378]); **^{1}H NMR** (300 MHz, $CDCl_3$) δ (ppm): 8.08 (br s, 1H, NH), 7.84 (s, 1H, CH=N), 7.73 – 7.66 (m, 2H, H-$B_{2,6}$), 7.64 (dd, J = 8.2, 1.4 Hz, 1H, H-C_6), 7.44 –

7.31 (m, 3H, H-$B_{3,4,5}$), 7.31 – 7.21 (m, 2H, H-$C_{3,5}$), 6.87 – 6.75 (m, 1H, H-C_4); **^{13}C NMR** (75 MHz, $CDCl_3$) δ (ppm): 140.68 (Cq-C_1), 139.64 (CH=N), 135.05 (Cq-B_1), 129.23 (CH-C_3), 129.00 (CH-B_4), 128.80 (CH-$B_{3,5}$), 128.09 (CH-C_5), 126.55 (CH-$B_{2,6}$), 120.14 (CH-C_4), 117.01 (Cq-C_2), 114.33 (CH-C_6).

1-benzylidene-2-(3-chlorophenyl)hydrazine (171f).

Synthesized according to the general procedure, this compound was obtained as an off-white solid (2487.4 mg, 84 % yield).

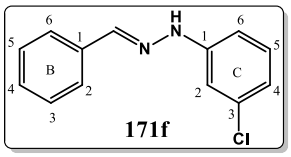

Mp: 132-133 ºC (mp lit. 133 ºC [376]); **^{1}H NMR** (300 MHz, $CDCl_3$) δ (ppm): 7.70 – 7.62 (m, 3H, CH=N, H-$B_{2,6}$), 7.59 (br s, 1H, NH), 7.45 – 7.28 (m, 3H, H-$B_{3,4,5}$), 7.23 – 7.11 (m, 2H, H-$C_{2,5}$), 6.91 (dd, J = 8.2, 1.2 Hz, 1H, H-C_6), 6.84 (dd, J = 7.9, 1.0 Hz, 1H, H-C_4); **^{13}C NMR** (75 MHz, $CDCl_3$) δ (ppm): 145.86 (Cq-C_1), 138.48 (CH=N), 135.28 (Cq-C_3), 134.98 (Cq-B_1), 130.39 (CH-C_5), 128.93 (CH-B_4), 128.79 (CH-$B_{3,5}$), 126.48 (CH-$B_{2,6}$), 120.03 (CH-C_4), 112.85 (CH-C_2), 111.00 (CH-C_6).

1-benzylidene-2-(4-chlorophenyl)hydrazine (171g).

Synthesized according to the general procedure, this compound was obtained as an off-white solid (2375.7 mg, 92 % yield).

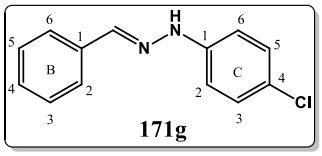

Mp: 128-130 ºC (mp lit. 129 ºC [376], 129-130 ºC [379]); **^{1}H NMR** (300 MHz, $CDCl_3$) δ (ppm): 7.70 – 7.62 (m, 3H, CH=N, CH-$B_{2,6}$), 7.59 (br s, 1H, NH), 7.43 – 7.28 (m, 3H, H-$B_{3,4,5}$), 7.26 – 7.19 (m, 2H, H-$C_{3,5}$), 7.09 – 7.01 (m, 2H, H-$C_{2,6}$); **^{13}C NMR** (75 MHz, $CDCl_3$) δ (ppm): 143.38 (Cq-C_1), 138.07 (CH=N), 135.12 (Cq-B_1), 129.32 (CH-$C_{3,5}$), 128.81 (CH-B_4), 128.79 (CH-$B_{3,5}$), 126.39 (CH-$B_{2,6}$), 124.72 (Cq-C_4), 113.98 (CH-$C_{2,6}$) [358].

1-(3-chlorobenzylidene)-2-(2-chlorophenyl)hydrazine (171h).

Synthesized according to the general procedure, this compound was obtained as a white solid (2657.2 mg, 90 % yield).

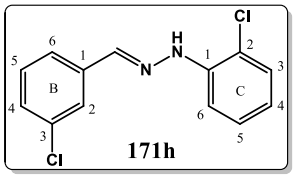

Mp: 119-121 ºC; **^{1}H NMR** (300 MHz, $CDCl_3$) δ (ppm): 8.15 (br s, 1H, NH), 7.76 (s, 1H, C=CH), 7.71 (s, 1H, H-B_2), 7.63 (dd, J = 8.2, 1.4 Hz, 1H, H-C_6), 7.53 – 7.47 (m, 1H, H-B_6), 7.35 – 7.22 (m, 4H, H-$B_{4,5}$, H-$C_{3,5}$), 6.87 – 6.77 (m, 1H, H-C_4); **^{13}C NMR** (75 MHz, $CDCl_3$) δ (ppm): 140.30 (Cq-C_1), 137.74 (CH=N), 136.91 (Cq-B_1), 134.83 (Cq-B_3), 129.99 (CH-B_5), 129.26

(CH-C_3), 128.77 (CH-B_4), 128.12 (CH-C_5), 126.01 (CH-B_2), 124.80 (CH-B_6), 120.51 (CH-C_4), 117.12 (Cq-C_2), 114.40 (CH-C_6).

1-(3-chlorobenzylidene)-2-(3-chlorophenyl)hydrazine (171i).

Synthesized according to the general procedure, this compound was obtained as a light pink solid (2612.9 mg, 88 % yield).

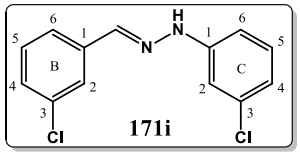

171i

Mp: 99-101 ºC; **^{1}H NMR** (300 MHz, $CDCl_3$) δ (ppm):7.74 (br s, 1H, NH), 7.66 (s, 1H, H-B_2), 7.63 (s, 1H, CH=N), 7.53 – 7.47 (m, 1H, H-B_6), 7.32 – 7.23 (m, 2H, H-$B_{4,5}$), 7.22 – 7.14 (m, 2H, H-$C_{2,5}$), 6.93 (ddd, J = 8.3, 2.1, 0.9 Hz, 1H, H-C_6), 6.85 (ddd, J = 7.9, 2.0, 0.9 Hz, 1H, H-C_4); **^{13}C NMR** (75 MHz, $CDCl_3$) δ (ppm): 145.48 (Cq-C_1), 136.87 (Cq-B_1), 136.62 (CH=N), 135.34 (Cq-C_3), 134.85 (Cq-B_3), 130.45 (CH-C_5), 130.02 (CH-B_5), 128.74 (CH-B_4), 126.06 (CH-B_2), 124.66 (CH-B_6), 120.44 (CH-C_4), 112.97 (CH-C_2), 111.11 (CH-C_6).

9.1.8. General procedure for the synthesis of hydrazonoyl chlorides.

To NCS (3.0 equiv) in CH_2Cl_2 (3.5 mL/mmol of hydrazone) at 0 °C was added methyl sulfide (6.0 equiv) over 5 minutes. After stirring for 15 minutes, the reaction was further cooled to –78 °C. Then the corresponding hydrazone (1.0 equiv) dissolved in CH_2Cl_2 (1 mL/mmol of hydrazone) was added. The reaction was stirred at –78°C for 1h, and then slowly allowed to warm to room temperature over 3 h. The reaction was quenched by addition of cold water. The organic layer was then washed with brine (1x), saturated sodium sulfite aqueous solution (2x), and water. The organic layer was dried over anhydrous Na_2SO_4, filtered, and concentrated to afford the corresponding hydrazonoyl halide (adapted from [353, 354].

***N*'-phenylbenzohydrazonoyl chloride (170a).**

Synthesized according to the general procedure, this compound was obtained as a brown solid (1612.2 mg, 81 % yield).

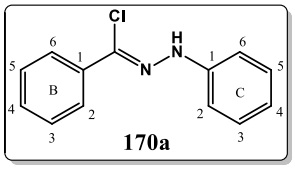

170a

Mp: 127-130 ºC (mp. lit 129-130 ºC [380] 129-131 ºC [381]; **^{1}H NMR** (400 MHz, $CDCl_3$) δ (ppm): 8.05 (br s, 1H, NH), 7.93 (d, J = 7.9 Hz, 2H, H-$B_{2,6}$), 7.45 – 7.37 (m, 3H, H-$B_{3,4,5}$), 7.32 (t, J = 7.6 Hz, 2H, H-$C_{3,5}$), 7.19 (d, J = 8.4 Hz, 2H, H-$C_{2,6}$), 6.95 (t, J = 7.3 Hz, 1H, H-C_4).

3-chloro-*N'*-phenylbenzohydrazonoyl chloride (170b).

Synthesized according to the general procedure, this compound was obtained as a pink-red semi-solid (1635.6 mg, 71 %).

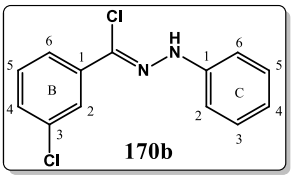

^{1}H NMR (400 MHz, $CDCl_3$) δ (ppm): 8.84 (br s, 1H, NH), 7.90 (dd, J = 2.4, 1.2 Hz, 1H, H-B_2), 7.83 – 7.77 (m, 1H, H-B_6), 7.35 – 7.27 (m, 4H, 2H-$B_{4,5}$, H-$C_{3,5}$), 7.23 – 7.15 (m, 2H, H-$C_{2,6}$), 6.97 – 6.90 (m, 1H, H-C_4); **^{13}C NMR** (75 MHz, $CDCl_3$) δ (ppm): 143.76 (Cq-C_1), 138.61 (Cq-B_1), 134.70 (Cq-B_3), 129.80 (CH-B_5), 129.51 (CH-$C_{3,5}$), 128.31(CH-B_4), 127.12 (CH-B_2), 125.39 (CH-B_6), 123.11 (CCl=N), 121.19 (CH-C_4), 113.61 (CH-$C_{2,6}$) [354].

4-chloro-*N'*-phenylbenzohydrazonoyl chloride (170c).

Synthesized according to the general procedure, this compound was obtained as a light pink solid (1551.2 mg, 67 % yield).

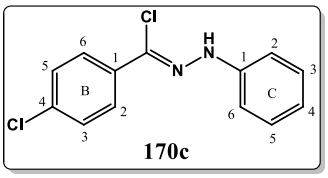

Mp: 145-147 ºC (mp lit. 142-144 ºC [354], 148-149.5 ºC [382]); **^{1}H NMR** (400 MHz, $CDCl_3$) δ (ppm): 8.04 (s, 1H, NH), 7.89 – 7.82 (m, 2H, H-$B_{2,6}$), 7.41 – 7.35 (m, 2H, H-$B_{3,5}$), 7.34 – 7.27 (m, 2H, H-$C_{3,5}$), 7.22 – 7.15 (m, 2H, H-$C_{2,6}$), 7.00 – 6.89 (m, 1H, H-C_4); **^{13}C NMR** (75 MHz, $CDCl_3$) δ (ppm): 143.90 (Cq-C_1), 135.20 and 134.23 (Cq-B_1 and Cq-B_4), 129.50 (CH-$C_{3,5}$), 128.81 (CH-$B_{3,5}$), 128.51 (CH-$B_{2,6}$), 123.61 (CCl=N), 121.04 (CH-C_4), 113.52 (CH-$C_{2,6}$) [354].

4-methoxy-*N'*-phenylbenzohydrazonoyl chloride (170d).

Synthesized according to the general procedure, this compound was obtained as a dark brown semi-solid (1431.2 mg, 62 % yield).

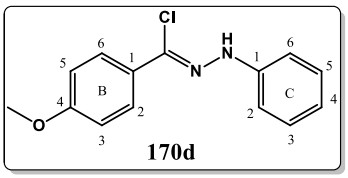

^{1}H NMR (300 MHz, $CDCl_3$) δ (ppm): 8.66 (br s, 1H, NH), 7.90 – 7.78 (m, 2H, H-$B_{2,6}$), 7.35 – 7.25 (m, 2H, H-$C_{3,5}$), 7.22 – 7.12 (m, 2H, H-$C_{2,6}$), 6.99 – 6.85 (m, 3H, H-$B_{3,5}$, H-C_4), 3.85 (s, 3H, OCH_3) [354].

***N'*-(2-chlorophenyl)benzohydrazonoyl chloride (170e).**

Synthesized according to the general procedure, this compound was obtained was obtained as a pink solid (1920.5 mg, 84% yield).

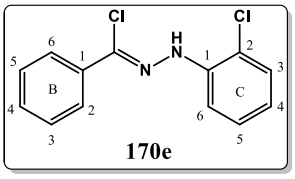

Mp: 82-84 ºC (mp lit. 84-85 ºC [382], 80-81 ºC [378]); **^{1}H NMR** (300 MHz, $CDCl_3$) δ (ppm): 8.57 (br s, 1H, NH), 7.98 -7.91 (m,

H-$B_{2,6}$), 7.60 (dd, *J* = 8.2, 1.5 Hz, 1H, H-C_6), 7.47 – 7.37 (m, 3H, H-$B_{3,4,5}$), 7.33 (dd, *J* = 8.0, 1.4 Hz, 1H, H-C_3), 7.30 – 7.22 (m, 1H, H-C_5), 6.87 (ddd, *J* = 7.9, 7.5, 1.5 Hz, H, H-C_4); **^{13}C NMR** (75 MHz, $CDCl_3$) δ (ppm): 139.52 (Cq-C_1), 134.31 (Cq-B_1), 129.71 (CH-B_4), 129.42 (CH-C_3), 128.59 (CH-$B_{3,5}$), 128.12 (CH-C_5), 127.37 (CCl=N), 126.74 (CH-$B_{2,6}$), 121.23 (CH-C_4), 118.14 (Cq-C_2), 114.75 (CH-C_6).

***N'*-(3-chlorophenyl)benzohydrazonoyl chloride (170f).**

Synthesized according to the general procedure, this compound was obtained as a brown solid (1839.7 mg, 80 % yield).

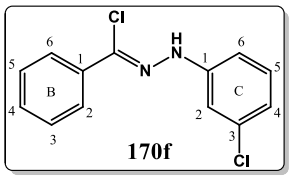

Mp: 83-85 ºC (mp lit. 96-98 ºC [354], 84-85 ºC [382]); **^{1}H NMR** (400 MHz, $CDCl_3$) δ (ppm): 8.03 (br s, 1H, NH), 7.98 – 7.90 (m, 2H, H-$B_{2,6}$), 7.48 – 7.38 (m, 3H, H-$B_{3,4,5}$), 7.26 – 7.18 (m, 2H, H-$C_{2,5}$), 7.00 (ddd, *J* = 8.2, 2.1, 0.9 Hz, 1H, H-C_6), 6.91 (ddd, *J* = 7.9, 2.0, 0.9 Hz, 1H, H-C_4); **^{13}C NMR** (75 MHz, $CDCl_3$) δ (ppm): 144.56 (Cq-C_1), 135.39 (Cq-C_3), 134.21 (Cq-B_1), 130.49 (CH-C_5), 129.68 (CH-B_4), 128.60 (CH-$B_{3,5}$), 126.67 (CH-$B_{2,6}$), 126.06 (CCl=N), 121.16 (CH-C_4), 113.63 (CH-C_2), 111.73 (CH-C_6) [354].

***N'*-(4-chlorophenyl)benzohydrazonoyl chloride (170g).**

Synthesized according to the general procedure, this compound was obtained as a pink-brown solid (2025.0 mg, 88%).

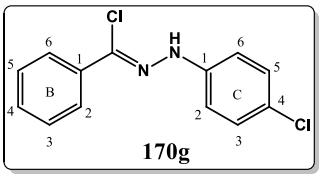

Mp: 105-107 ºC (Lit 107-108.5 ºC [382], 105- 107°C [381]); **^{1}H NMR** (400 MHz, $CDCl_3$) δ (ppm): 8.03 (br s, 1H, NH), 7.95 – 7.88 (m, 2H, H-$B_{2,6}$), 7.47 – 7.35 (m, 3H, H-$B_{3,4,5}$), 7.30 – 7.23 (m, 2H, H-$C_{3,5}$), 7.14 – 7.08 (m, 2H, H-$C_{2,6}$); **^{13}C NMR** (75 MHz, $CDCl_3$) δ (ppm): 142.07 (Cq-C_1), 134.30 (Cq-B_1), 129.56 (CH-B_4), 129.43 (CH-$C_{3,5}$), 128.58 (CH-$B_{3,5}$), 126.57 (CH-$B_{2,6}$), 125.92 (Cq-C_4), 125.59 (CCl=N), 114.69 (CH-$C_{2,6}$).

3-chloro-*N'*-(2-chlorophenyl)benzohydrazonoyl chloride (170h).

Synthesized according to the general procedure, this compound was obtained as a dark pink-reddish solid (1646.9 mg, 73 % yield).

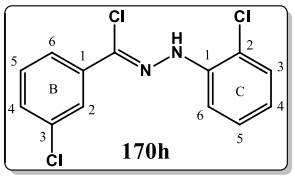

Mp: 92-94 ºC; **^{1}H NMR** (300 MHz, $CDCl_3$) δ (ppm): 8.59 (br s, 1H, NH), 7.94 – 7.92 (m, 1H, H-B_2), 7.85 – 7.79 (m, 1H, H-B_6), 7.59 (dd, *J* = 8.2, 1.5 Hz, 1H, H-C_6), 7.37 – 7.24 (m, 4H, H-$B_{4,5}$, 2H-$C_{3,5}$), 6.93 – 6.85 (m, 1H, H-C_4); **^{1}H NMR** (300 MHz, $CDCl_3$) δ (ppm): 139.17 (Cq-C_1), 136.00 (Cq-B_1), 134.71 (Cq-B_3), 129.79 (CH-B_5), 129.59 (CH-B_4), 129.47 (CH-C_3),

128.17 (CH-C_5), 126.55 (CH-B_2), 125.70 (CCl=N), 124.78 (CH-B_6), 121.61 (CH-C_4), 118.29 (Cq-C_2), 114.83 (CH-C_6).

3-chloro-*N*'-(3-chlorophenyl)benzohydrazonoyl chloride (170i).

Synthesized according to the general procedure, this compound was obtained as a dark brown-reddish solid (1648.7 mg, 73 % yield).

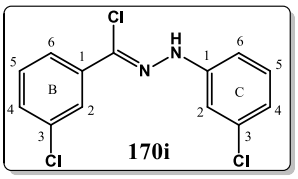

170i

Mp: 53-55 ºC; **^{1}H NMR** (300 MHz, $CDCl_3$) δ (ppm): 8.08 (br s, 1H, NH), 7.91 – 7.88 (m, 1H, H-B_2), 7.83 – 7.77 (m, 1H, H-B_6), 7.38 – 7.34 (m, 2H, H-$B_{4,5}$), 7.24 – 7.19 (m, 2H, H-$C_{2,5}$), 7.01 (ddd, *J* = 8.3, 2.2, 0.9 Hz, 1H, H-C_6), 6.93 (ddd, *J* = 8.0, 1.9, 0.9 Hz, 1H, H-C_4); **^{13}C NMR** (75 MHz, $CDCl_3$) δ (ppm): 144.20 (Cq-C_1), 135.92 (Cq-B_1), 135.44 (Cq-C_3), 134.72 (Cq-B_3), 130.56 (CH-B_5), 129.80 (CH-C5), 129.57 (CH-B_4), 126.52 (CH-B_2), 124.71 (CH-B_6), 124.41 (CCl=N), 121.54 (CH-C_4), 113.74 (CH-C_2), 111.85 (CH-C_6).

9.1.9. GENERAL PROCEDURE FOR THE SYNTHESIS OF 4'*H*-SPIRO[INDOLINE-3,5'-ISOXAZOL]-2-ONES.

9.1.9.1. Method A (Et_3N).

A solution of the appropriate chlorooxime (3.0 equiv) was added, dropwise at 0 ºC, to a solution of the appropriate indolin-2-one (1.0 equiv) and Et_3N (3.0 equiv). The resulting solution was stirred at room temperature under nitrogen atmosphere. The solvent was removed under reduced pressure, and the residue was dissolved in EtOAc. The organic solution was washed with brine, dried over anhydrous Na_2SO_4, and concentrated. The residue was purified by flash chromatography on silica gel using as eluent mixtures of *n*-hexane/EtOAc and recrystallized from ether to afford the final product.

Ethyl *N*-methyl-2-oxo-3'-phenyl-4'*H*-spiro[indoline-3,5'-isoxazole]-4'-carboxylate (119b).

Synthesized according to the general procedure (method A), this compound was obtained as a white solid (24.6 mg, 80 % yield).

Mp: 137-138ºC; **IR** (NaCl, selected peaks): 1727 (C=O) cm^{-1}; **^{1}H NMR** (400 MHz, $CDCl_3$) δ (ppm): 7.69 – 7.64 (m, 2H, H-$B_{2,6}$), 7.45 – 7.34 (m, 5H, H-4, H-6, H-$B_{3,4,5}$), 7.06 (t, *J* = 7.6 Hz, 1H, H-5), 6.86 (d, *J* = 7.6 Hz, 1H, H-7), 4.90 (s, 1H, H-4'), 3.99 – 3,87 (m,

2H, CH_2), 3.24 (s, 3H, NCH_3), 0.89 (t, *J* = 7.2 Hz, 3H, CH_3); **^{13}C NMR** (100 MHz, $CDCl_3$) δ (ppm): 173.95 (NC=O), 166.57 (CO_2), 154.76 (C=N), 144.57 (Cq-7a), 131.57 (CH-6), 130.66 (CH-B_4), 128.95 (CH-$B_{3,5}$), 128.42 (Cq-B_1), 127.16 (CH-$B_{2,6}$), 126.16 (CH-4), 123.54 (Cq-3a), 123.45 (CH-5), 108.85 (CH-7), 86.97 (Cspiro), 62.07 (CH_2), 60.93 (CH-4'), 26.77 (NCH_3), 13.76 (CH_3); **HRMS:** Exact mass calculated for $C_{20}H_{18}N_2O_4Na$ $[M+Na]^+$ 373.1159, found 373.1165.

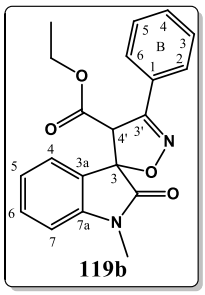

Methyl *N*-methyl-2-oxo-3'-phenyl-4'*H*-spiro[indoline-3,5'-isoxazole]-4'-carboxylate (119c).

Synthesized according to the general procedure (method A), this compound was obtained as a white solid (24.0 mg, 94 % yield).

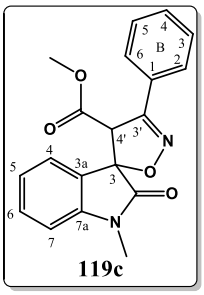

Mp: 200-201ºC; **IR** (KBr, selected peaks): 1740 (C=O), 1726 (C=O) cm^{-1}; **^{1}H NMR** (400 MHz, $CDCl_3$) δ (ppm): 7.69 – 7.64 (m, 2H, H-$B_{2,6}$), 7.45 – 7.41 (m, 3H, H-$B_{3,4,5}$), 7.40 – 7.37 (m, 1H, H-6), 7.33 (d, *J* = 7.6 Hz, 1H, H-4), 7.07 (td, *J* = 7.6, 0.8 Hz, 1H, H-5), 6.87 (d, *J* = 8.0 Hz, 1H, H-7), 4.89 (s, 1H, H-4'), 3.48 (s, 3H, OCH_3), 3.23 (s, 3H, NCH_3); **^{13}C NMR** (100 MHz, $CDCl_3$) δ (ppm): 173.82 (NC=O), 167.12 (CO_2), 154.65 (C=N), 144.59 (Cq-7a), 131.65 (CH-6), 130.72 (CH-B_4), 129.00 (CH-$B_{3,5}$), 128.29 (Cq-B_1), 127.07 (CH-$B_{2,6}$), 125.85 (CH-4), 123.47 (CH-5), 123.22 (Cq-3a), 109.01 (CH-7), 86.96 (Cspiro), 60.71 (CH-4'), 52.88 (OCH_3), 26.71 (NCH_3); **HRMS:** Exact mass calculated for $C_{19}H_{16}N_2O_4Na$ $[M+Na]^+$ 359.1002, found 359.1006.

Ethyl 2-oxo-3'-phenyl-4'*H*-spiro[indoline-3,5'-isoxazole]-4'-carboxylate (119d).

Synthesized according to the general procedure (method A), this compound was obtained as a white solid (64.9 mg, 89 % yield).

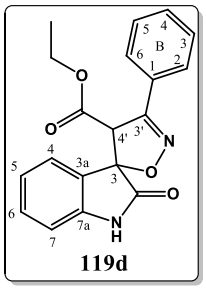

Mp: 198-199ºC; **IR** (KBr, selected peaks): 3158 (N-H), 1749 (C=O), 1730 (C=O) cm^{-1}; **^{1}H NMR** (400 MHz, $CDCl_3$) δ (ppm): 8.18 (br s, 1H, NH), 7.70 – 7.65 (m, 2H, H-$B_{2,6}$), 7.40 – 7.47 (m, 3H, H-$B_{3,4,5}$), 7.36 – 7.29 (m, 2H, H-4, H-6), 7.04 (t, *J* = 7.6 Hz, 1H, H-5), 6.90 (d, *J* = 7.6 Hz, 1H, H-7), 4.93 (s, 1H, H-4'), 3.99 – 3.90 (m, 2H, CH_2), 0.90 (t, *J* = 7.0 Hz, 3H, CH_3); **^{13}C NMR** (100 MHz, $CDCl_3$) δ (ppm): 175.84 (NHC=O), 166.46 (CO_2), 154.80 (C=N), 141.52 (Cq-7a), 131.59 (CH-6), 130.76 (CH-B_4), 128.99 (CH-$B_{3,5}$), 128.30 (Cq-B_1), 127.19 (CH-$B_{2,6}$), 126.58 (CH-4), 123.86 (Cq-3a), 123.52 (CH-5), 110.74 (CH-7), 87.18 (Cspiro), 62.20 (CH_2), 61.00 (CH-4'), 13.77 (CH_3); **HRMS:** Exact mass calculated for $C_{19}H_{16}N_2O_4Na$ $[M+Na]^+$ 359.1002, found 359.1009.

Methyl 2-oxo-3'-phenyl-4'*H*-spiro[indoline-3,5'-isoxazole]-4'-carboxylate (119e).

Synthesized according to the general procedure (method A), this compound was obtained as a white solid (73.0 mg, 92 % yield).

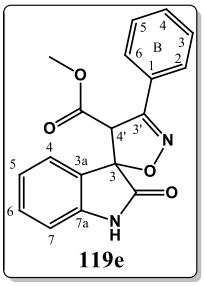

Mp: 200-201ºC; **IR** (KBr, selected peaks): 3098 (NH), 1742 (C=O), 1733 (C=O) cm^{-1}; **^{1}H NMR** (400 MHz, $CDCl_3$) δ (ppm): 8.01 (br s, 1H, NH), 7.70 – 7.65 (m, 2H, H-$B_{2,6}$), 7.47 – 7.40 (m, 3H, H-$B_{3,4,5}$), 7.31 – 7,35 (m, 2H, H-4, H-6), 7.06 (t, *J* = 7.6 Hz, 1H, H-5), 6.91 (d, *J* = 8.0 Hz, 1H, H-7), 4.92 (s, 1H, H-4'), 3.50 (s, 3H, OCH_3); **^{13}C NMR** (100 MHz, $CDCl_3$) δ (ppm): 175.59 (NHC=O), 167.02 (CO_2), 154.72 (C=N), 141.54 (Cq-7a), 131.68 (CH-6), 130.84 (CH-B_4), 129.07 (CH-$B_{3,5}$), 128.21 (Cq-B_1), 127.15 (CH-$B_{2,6}$), 126.34 (CH-4), 123.61 (Cq-3a), 123.58 (CH-5), 110.84 (CH-7), 87.17 (Cspiro), 60.85 (CH-4'), 52.96 (OCH_3); **HRMS:** Exact mass calculated for $C_{18}H_{14}N_2O_4Na$ $[M+Na]^+$ 345.0846, found 345.0854.

9.1.9.2. Method B (Zn).

A mixture of the appropriate indolin-2-one (1.0 equiv), the appropriate chlorooxime (3.0 equiv) and zinc (3.0 equiv) in the proper solvent (27 µL/µmol indolin-2-one) was stirred at room temperature under nitrogen atmosphere. The solvent was removed under reduced pressure, and the residue was dissolved in EtOAc. After filtered through Celite, the organic solution was washed with brine, dried over anhydrous Na_2SO_4, and concentrated. The residue was purified by flash chromatography on silica gel using as eluent mixtures of *n*-hexane/EtOAc, and recrystallized from ether to afford the final product.

Diethyl *N*-methyl-2-oxo-4'*H*-spiro[indoline-3,5'-isoxazole]-3',4'-dicarboxylate (119a).

Synthesized according to the general procedure (method B), this compound was obtained as a white solid (23.7 mg, 79 % yield).

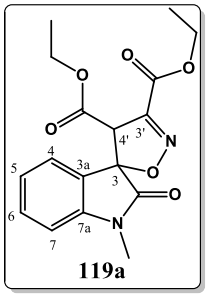

Mp: 117-118ºC; **IR** (KBr, selected peaks): 1751 (C=O), 1721 (C=O) cm^{-1}; **^{1}H NMR** (400 MHz, $CDCl_3$) δ (ppm): 7.39 (td, *J* = 8.0, 1.2 Hz, H-6), 7.27 (d, *J* = 7.8 Hz, H-4), 7.06 (td, *J* = 7.8, 0.8 Hz, H-5), 6.85 (d, *J* = 8.0 Hz, H-7), 4.76 (s, 1H, H-4'), 4.39 (qd, *J* = 7.2, 1.2 Hz, 2H, CH_2), 3.98 – 3,89 (m, 2H, CH_2), 3.23 (s, 3H, NCH_3), 1.38 (t, *J* = 7.2 Hz, 3H, CH_3), 0.90 (t, *J* = 7.2 Hz, 3H, CH_3); **^{13}C NMR** (100 MHz, $CDCl_3$) δ (ppm): 172.60

(NC=O), 165.70 (CO_2), 159.26 (CO_2), 149.48 (C=N), 144.43 (Cq-7a), 131.98 (CH-6), 125.95 (CH-4), 123.61 (CH-5), 122.80 (Cq-3a), 109.01 (CH-7), 88.47 (Cspiro), 62.75 (CH_2), 62.20 (CH_2), 59.46 (CH-4'), 26.87 (NCH_3), 14.19 (CH_3), 13.74 (CH_3); **HRMS:** Exact mass calculated for $C_{17}H_{18}N_2O_6Na$ $[M+Na]^+$ 369.1057, found 369.1067.

3'-ethyl 4'-methyl *N*-methyl-2-oxo-4'*H*-spiro[indoline-3,5'-isoxazole]-3',4'-dicarboxylate (119f).

Synthesized according to the general procedure (method B), this compound was obtained as a white solid (114.8 mg, 75 % yield).

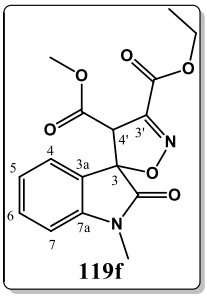

119f

Mp: 124-125 ºC; **IR** (KBr, selected peaks): 1751 (C=O), 1744 (C=O), 1721 (C=O) cm^{-1}; **^{1}H NMR** (400 MHz, $CDCl_3$) δ (ppm): 7.40 (td, J = 7.8, 1.2 Hz, 1H, H-6), 7.26 (d, J = 7.6 Hz, 1H, H-4), 7.07 (td, J = 7.8, 0.4 Hz, 1H, H-5), 6.86 (d, J = 8.0 Hz, 1H, H-7), 4.77 (s, 1H, H-4'), 4.45 – 4.36 (m, 2H, CH_2), 3.49 (s, 3H, OCH_3), 3.23 (s, 3H, NCH_3), 1.39 (t, J = 7.2 Hz, 3H, CH_3); **^{13}C NMR** (100 MHz, $CDCl_3$) δ (ppm): 172.51 (NC=O), 166.24 (CO_2), 159.21 (CO_2), 149.36 (C=N), 144.45 (Cq-7a), 132.05 (CH-6), 125.72 (CH-4), 123.64 (CH-5), 122.58 (Cq-3a), 109.15 (CH-7), 88.49 (Cspiro), 62.77 (CH_2), 59.21 (CH-4'), 52.93 (OCH_3), 26.83 (NCH_3), 14.18 (CH_3); **HRMS:** Exact mass calculated for $C_{16}H_{16}N_2O_6Na$ $[M+Na]^+$ 355.0901, found 355.0904.

4'-ethyl 3'-methyl *N*-methyl-2-oxo-4'*H*-spiro[indoline-3,5'-isoxazole]-3',4'-dicarboxylate (119g).

Synthesized according to the general procedure (method B), this compound was obtained as a white solid (21.3 mg, 74 % yield).

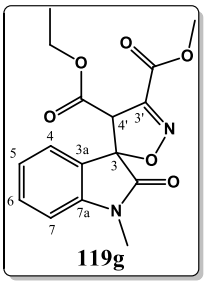

119g

Mp: 106-107ºC; **^{1}H NMR** δ (ppm): (400 MHz, $CDCl_3$): 7.40 (t, J =8.0 Hz, 1H, H-6), 7.27 (d, J = 7.6 Hz, 1H, H-4), 7.06 (t, J = 7.6 Hz, 1H, H-5), 6.86 (d, J = 7.6 Hz, 1H, H-7), 4.76 (s, 1H, H-4'), 3.97 – 3.92 (m, 5H, CH_2, OCH_3), 3.24 (s, 3H, NCH_3), 0.90 (t, J=7.2 Hz, 3H, CH_3); **^{13}C NMR** (100 MHz, $CDCl_3$) δ (ppm): 172.56 (NC=O), 165.68 (CO_2), 159.75 (CO_2), 149.26 (C=N), 144.47 (Cq-7a), 132.03 (CH-6), 125.97 (CH-4), 123.64 (CH-5), 122.75 (Cq-3a), 109.03 (CH-7), 88.56 (Cspiro), 62.25 (CH_2), 59.36 (CH-4'), 53.34 (OCH_3), 26.89 (NCH_3), 13.75 (CH_3).

Diethyl 2-oxo-4'*H*-spiro[indoline-3,5'-isoxazole]-3',4'-dicarboxylate (119h).

Synthesized according to the general procedure (method B), this compound was obtained as a white solid (58.9 mg, 77 % yield).

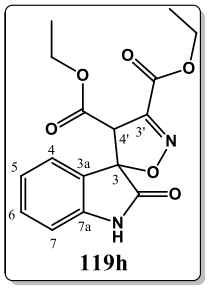

Mp: 129-130 ºC; **IR** (KBr, selected peaks): 3215 (N-H), 1751 (C=O), 1736 (C=O), 1719 (C=O) cm^{-1}. **^{1}H NMR** (400 MHz, $CDCl_3$) δ (ppm): 8.66 (br s, 1H, NH), 7.33 (t, *J* = 7.6 Hz, 1H, H-6), 7.26 (d, *J* = 7.6 Hz, 1H, H-4), 7.04 (t, *J* = 7.6 Hz, 1H, H-5), 6.92 (d, *J* = 7.6 Hz, 1H, H-7), 4.80 (s, 1H, H-4'), 4.40 (q, *J* = 7.2 Hz, 2H, CH_2), 3.99 – 3.90 (m, 2H, CH_2), 1.39 (t, *J* = 7.2 Hz, 3H, CH_3), 0.90 (t, *J* = 7.2 Hz, 3H, CH_3); **^{13}C NMR** (100 MHz, $CDCl_3$) δ (ppm): 174.78 (NHC=O), 165.63 (CO_2Et), 159.25 (CO_2Et), 149.53 (C=N), 141.49 (Cq-7a), 132.04 (CH-6), 126.31 (CH-4), 123.69 (CH-5), 123.16 (Cq-3a), 111.04 (CH-7), 88.79 (Cspiro), 62.86 (CH_2), 62.34 (CH_2), 59.58 (CH-4'), 14.20 (CH_3), 13.73 (CH_3); **HRMS:** Exact mass calculated for $C_{16}H_{16}N_2O_6Na$ $[M+Na]^+$ 355.0901, found 355.0903.

3'-ethyl 4'-methyl 2-oxo-4'*H*-spiro[indoline-3,5'-isoxazole]-3',4'-dicarboxylate (119i)

Synthesized according to the general procedure (method B), this compound was obtained as a white solid (58.9 mg, 76 % yield).

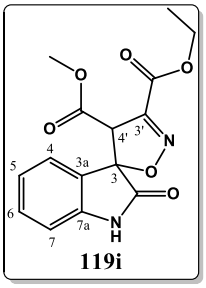

Mp: 167-168 ºC; **IR** (NaCl, selected peaks): 1751 (C=O), 1736 (C=O), 1724 (C=O) cm^{-1}; **^{1}H NMR** (400 MHz, $CDCl_3$) δ (ppm): 8.58 (br s, 1H, NH), 7.34 (td, *J* = 7.6, 0.9 Hz, 1H, H-6), 7.24 (d, *J* = 7.6 Hz, 1H, H-4), 7.05 (t, *J* = 7.6 Hz, 1H, H-5), 6.92 (d, *J* = 7.6 Hz, 1H, H-7), 4.80 (s, 1H, H-4'), 4.45 – 4.35 (m, 2H, CH_2), 3.49 (s, 3H, OCH_3), 1.39 (t, *J* = 7.0 Hz, 3H, CH_3); **^{13}C NMR** (100 MHz, $CDCl_3$) δ (ppm): 174.61 (NHC=O), 166.16 (CO_2), 159.22 (CO_2), 149.44 (C=N), 141.50 (Cq-7a), 132.12 (CH-6), 126.11 (CH-4), 123.74 (CH-5), 122.96 (Cq-3a), 111.16 (CH-7), 88.81 (Cspiro), 62.89 (CH_2), 59.38 (CH-4'), 53.02 (OCH_3), 14.20 (CH_3); **HMRS:** Exact mass calculated for $C_{15}H_{14}N_2O_6Na$ $[M+Na]^+$ 341.0744, found 341.0753.

4'-ethyl 3'-methyl 2-oxo-4'*H*-spiro[indoline-3,5'-isoxazole]-3',4'-dicarboxylate (119j).

Synthesized according to the general procedure (method B), this compound was obtained as a white solid (52.3 mg, 71 % yield).

Mp: 147-148ºC; **IR** (KBr, selected peaks): 3213 (N-H), 1751 (C=O), 1736 (C=O), 1724 (C=O) cm^{-1}; **^{1}H NMR** (400 MHz, $CDCl_3$) δ (ppm): 8.79 (br s, 1H, NH), 7.33 (t, *J* = 8.0 Hz,

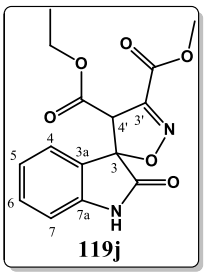

1H, H-6), 7.25 (d, *J* = 7.6 Hz, 1H, H-4), 7.04 (t, *J* = 7.6 Hz, 1H, H-5), 6.93 (d, *J* = 8.0 Hz, 1H, H-7), 4.80 (s, 1H, H-4'), 3.98 – 3.91 (m, 5H, CH_2, OCH_3), 0.90 (t, *J* = 7.0 Hz, 3H, CH_3); **^{13}C NMR** (100 MHz, $CDCl_3$) *δ* (ppm): 174.81 (NHC=O), 165.59 (CO_2), 159.72 (CO_2), 149.31 (C=N), 141.54 (Cq-7a), 132.09 (CH-6), 126.27 (CH-4), 123.70 (CH-5), 123.04 (Cq-3a), 111.12 (CH-7), 88.89 (Cspiro), 62.39 (CH_2), 59.43 (CH-4'), 53.42 (OCH_3), 13.71 (CH_3); **HRMS:** Exact mass calculated for $C_{15}H_{14}N_2O_6Na$ $[M+Na]^+$ 341.0744, found 341.0750.

Ethyl 3'-(4-methoxyphenyl)-2-oxo-4'*H*-spiro[indoline-3,5'-isoxazole]-4'-carboxylate (119k).

Synthesized according to the general procedure (method B), this compound was obtained as a white solid (29.4 mg, 87 % yield).

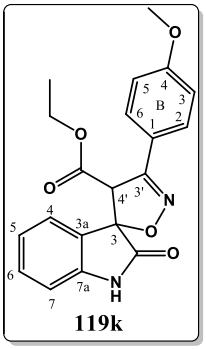

Mp: 210-211ºC; **IR** (KBr, selected peaks): 3446.79 (N-H), 1749 (C=O), 1732 (C=O) cm^{-1}; **^{1}H NMR** (400 MHz, $CDCl_3$) *δ* (ppm): 8.49 (br s, 1H, NH), 7.61 (d, *J* = 8.8 Hz, 2H, H-$B_{2,6}$), 7.34 (d, *J* = 7.6 Hz, 1H, H-4), 7.30 (td, *J* = 8.0, 1.2 Hz, 1H, H-6), 7.03 (t, *J* = 7.6 Hz, 1H, H-5), 6.93 (d, *J* = 8.8 Hz, 2H, H-$B_{3,5}$), 6.90 (d, *J* = 8.0 Hz, 1H, H-7), 4.89 (s, 1H, H-4'), 3.98 – 3.91 (m, 2H, CH_2), 3.84 (s, 3H, OCH_3), 0.91 (t, *J* = 7.2 Hz, 3H, CH_3); **^{13}C NMR** (100 MHz, $CDCl_3$) *δ* (ppm): 176.32 (NHC=O), 166.61 (CO_2), 161.55 (Cq-B_4), 154.39 (C=N), 141.62 (Cq-7a), 131.52 (CH-6), 128.79 (CH-$B_{2,6}$), 126.52 (CH-4), 123.92 (Cq-3a), 123.46 (CH-5), 120.80 (Cq-B_1), 114.44 (CH-$B_{3,5}$), 110.84 (CH-7), 87.04 (Cspiro), 62.15 (CH_2), 61.17 (CH-4'), 55.52 (OCH_3), 13.79 (CH_3); **HRMS**: Exact mass calculated for $C_{20}H_{18}N_2O_5Na$ $[M+Na]^+$ 389.1108, found 389.1102.

Ethyl 3'-(4-methoxyphenyl)-*N*-methyl-2-oxo-4'*H*-spiro[indoline-3,5'-isoxazole]-4'-carboxylate (119l).

Synthesized according to the general procedure (method B), this compound was obtained as a white solid (29.4 mg, 89 % yield).

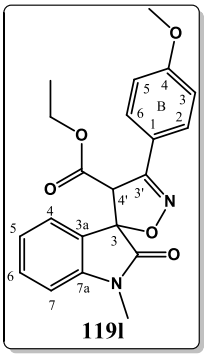

Mp: 136-137ºC; **IR** (KBr, selected peaks): 1725 (C=O) cm^{-1}; **^{1}H NMR** (400 MHz, $CDCl_3$) *δ* (ppm): 7.59 (d, *J* = 9.2 Hz, 2H, H-$B_{2,6}$), 7.40 – 7.34 (m, 2H, H-4, H-6), 7.05 (t, *J* = 7.6 Hz, 1H, H-5), 6.92 (d, *J* = 8.8 Hz, 2H, H-$B_{3,5}$), 6.85 (d, *J* = 8.0 Hz, 1H, H-7), 4.85 (s, 1H, H-4'), 3.98 – 3.89 (m, 2H, CH_2), 3.83 (s, 3H, OCH_3), 3.23 (s, 3H, NCH_3), 0.90 (t, *J* = 7.0 Hz, 3H, CH_3); **^{13}C NMR** 100 MHz, $CDCl_3$) *δ* (ppm): 174.09 (NC=O), 166.68 (CO_2), 161.45 (Cq-B_4), 154.29 (C=N), 144.55 (Cq-7a), 131.48 (CH-6), 128.72 (CH-$B_{2,6}$), 126.14 (CH-4), 123.60 (Cq-3a), 123.39 (CH-5), 120.90 (Cq-B_1),

114.37 (CH-$B_{3,5}$), 108.81 (CH-7), 86.73 (Cspiro), 62.01 (CH_2), 61.12 (CH-4'), 55.48 (OCH_3), 26.72 (NCH_3), 13.78 (CH_3); **HRMS:** Exact mass calculated for $C_{21}H_{20}N_2O_5Na$ $[M+Na]^+$ 403.1264, found 403.1263.

Ethyl 2-oxo-4'-phenyl-4'*H*-spiro[indoline-3,5'-isoxazol]-3'-carboxylate (119m).

Synthesized according to the general procedure (method B), this compound was obtained as a white solid (63.8 mg, 42 % yield).

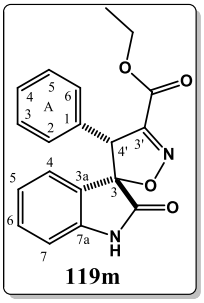

^{1}H NMR (400 MHz, Acetone-d_6) δ (ppm): 9.61 (br s, 1H, NH), 7.39 – 7.30 (m, 3H, H-$A_{3,4,5}$), 7.21 – 7.12 (m, 3H, H-6, H-$A_{2,6}$), 6.89 (d, J = 7.6 Hz, 1H, H-7), 6.63 (t, J = 7.6 Hz, 1H, H-5), 6.32 (d, J = 7.6 Hz, 1H, H-4), 5.11 (s, 1H, H-4'), 4.31 – 4.19 (m, 2H, CH_2), 1.22 (t, J = 7.1 Hz, 3H, CH_3); **^{13}C NMR** (100 MHz, Acetone-d_6) δ (ppm): 175.86 (NHC=O), 160.08 (CO_2Et), 154.90 (C=N), 144.20 (Cq-7a), 134.47 (Cq-A_1), 131.77 (CH-6), 129.70 (CH-$A_{2,6}$), 129.41 (CH-$A_{3,5}$), 129.22 (CH-A_4), 127.84 (CH-4), 122.85 (Cq-3a), 122.64 (CH-5), 111.03 (CH-7), 91.14 (Cspiro), 62.59 (CH_2), 59.02 (CH-4'), 14.20 (CH_3). Anal. Calcd for $C_{19}H_{16}N_2O_4 \cdot 0.7H_2O$: C, 65.39; H, 5,04; N, 8.03. Found: C, 65.12; H, 4.75; N, 7.97.

Ethyl 4'-(4-methoxyphenyl)-2-oxo-4'*H*-spiro[indoline-3,5'-isoxazol]-3'-carboxylate (119n).

Synthesized according to the general procedure (method B), this compound was obtained as a white solid (56.1 mg, 38 % yield).

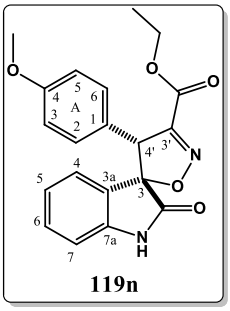

^{1}H NMR (400 MHz, Acetone-d_6) δ (ppm): 9.59 (s, 1H, NH), 7.19 (td, J = 7.7, 1.2 Hz, 1H, H-6), 7.06 (d, J = 8.7 Hz, 2H, H-$A_{2,6}$), 6.93 – 6.87 (m, 3H, H-7, H-$A_{3,5}$), 6.67 (td, J = 7.6, 1.0 Hz, 1H, H-5), 6.39 (d, J = 7.6 Hz, 1H, H-4), 5.04 (s, 1H, H-4'), 4.31 – 4.19 (m, 2H, CH_2), 3.78 (s, 3H, OCH_3), 1.23 (t, J = 7.1 Hz, 3H, CH_3); **^{13}C NMR** (100 MHz, Acetone-d_6) δ (ppm): 175.98 (NHC=O), 160.69 (Cq-A_4), 160.16 (CO_2Et), 155.18 (C=N), 144.30 (Cq-7a), 131.74 (CH-6), 130.65 (CH-$A_{2,6}$), 128.02 (CH-4), 126.23 (Cq-A_1), 123.01 (Cq-3a), 122.68 (CH-5), 115.03 (CH-$A_{3,5}$), 111.01 (CH-7), 91.05 (Cspiro), 62.55 (CH_2), 58.44 (CH-4'), 55.56 (OCH_3), 14.24 (CH_3).

3'-phenyl-4'-propyl-4'*H*-spiro[indoline-3,5'-isoxazol]-2-one (119o).

Synthesized according to the general procedure (method B), this compound was obtained as a white solid (71.7 mg, 44 % yield).

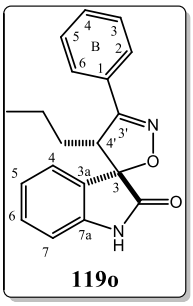

^{1}H NMR (400 MHz, $CDCl_3$) δ (ppm): 8.98 (s br, 1H, NH), 7.71 – 7.65 (m, 2H, H-$B_{2,6}$), 7.48 – 7.43 (m, 3H, H-$B_{3,4,5}$), 7.39 (d, *J* = 7.6 Hz, 1H, H-4), 7.29 (t, *J* = 7.6 Hz, 1H, H-6), 7.06 (t, *J* = 7.6 Hz, 1H, H-5), 6.93 (d, *J* = 7.6 Hz, 1H, H-7), 4.10 (dd, *J* = 10.0, 4.1 Hz, 1H, C-4'), 1.78 – 1.65 (m, 2H, $C\underline{H}_2CH_2CH_3$), 1.13 – 1.00 (m, 1H, $CH_2C\underline{H}_2CH_3$), 0.90 – 0.77 (m, 1H, $CH_2C\underline{H}_2CH_3$), 0.68 (t, *J* = 7.3 Hz, 3H, CH_3); **^{13}C NMR** (100 MHz, $CDCl_3$) δ (ppm): 178.30 (C=O), 160.54 (C=N), 141.56 (Cq-7a), 130.89 (CH-6), 130.37 (CH-B_4), 128.99 (CH-$B_{3,5}$), 128.79 (Cq-B_1), 127.72 (CH-$B_{2,6}$), 126.45 (CH-4), 124.76 (Cq-3a), 123.09 (CH-5), 111.12 (CH-7), 88.67 (Cspiro), 54.52 (CH-4'), 30.39 ($\underline{C}H_2CH_2CH_3$), 20.94 ($CH_2\underline{C}H_2CH_3$), 13.74 (CH_3).

4'-(4-methoxyphenyl)-1-methyl-3'-phenyl-4'*H*-spiro[indoline-3,5'-isoxazol]-2-one (119p).

Synthesized according to the general procedure (method B), this compound was obtained as a white solid (18.7 mg, 22 % yield).

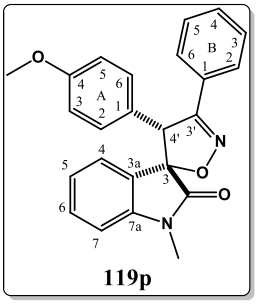

Mp: 195-196ºC; **IR** (KBr, selected peaks): 1730 (C=O), 1250 cm^{-1}; **^{1}H NMR** (400 MHz, $CDCl_3$) δ (ppm): 7.68 – 7.62 (m, 2H, H-$B_{2,6}$), 7.37 – 7.27 (m, 3H, H-$B_{3,4,5}$), 7.22 (t, *J* = 7.6 Hz, 1H, H-6), 6.99 (d, *J* = 8.4 Hz, 2H, H-$A_{2,6}$), 6.81 – 6.74 (m, 3H, H-7, H-$A_{3,5}$), 6.71 (t, *J* = 7.6 Hz, 1H, H-5), 6.33 (d, *J* = 7.6 Hz, 1H, H-4), 4.99 (s, 1H, H-4'), 3.75 (s, 3H, OCH_3), 3.20 (s, 3H, NCH_3); **^{13}C NMR** (100 MHz, $CDCl_3$) δ (ppm): 175.22 (C=O), 159.57 and 159.54 (C=N and Cq-A_4), 144.78 (Cq-7a), 130.60 (CH-B_4), 130.31 (CH-6), 130.23 (CH-$A_{2,6}$), 128.73 (CH-$B_{3,5}$), 128.69 (Cq-B_1), 127.88 (CH-$B_{2,6}$), 127.16 (CH-4), 125.69 (Cq-A_1), 122.78 (CH-5), 122.69 (Cq-3a), 114.43 (CH-$A_{3,5}$), 108.33 (CH-7), 88.68 (Cspiro), 59.59 (CH-4'), 55.36 (OCH_3), 26.39 (NCH_3); Anal. Calcd for $C_{24}H_{20}N_2O_3 \cdot 0.25H_2O$: C, 74.11; H, 5,32; N, 7,20. Found: C, 73,85; H, 5.35; N, 7.12.

9.1.9.3. Method C (synthesis directly from aldoxime).

To a stirred solution of *N*-chlorosuccinimide (3.0 equiv) and pyridine (0.3 equiv) in chloroform (2.5 mL/0.1 mmol of 3-methylene indolin-2-one) was added the appropriate aldoxime (3.0 equiv). The reaction mixture was stirred for 24 h at room temperature before addition of the appropriate 3-methylene indolin-2-one. The mixture was then heated to 50 ºC and triethylamine (3.5 equiv) was added in a dropwise manner. After heating at reflux for 26 h, the mixture was washed with brine (2x) and the aqueous phase extracted with DCM or EtOAc depending on the solubility of the product. The combined organic extracts were dried over anhydrous Na_2SO_4 and the solvent was removed under reduced pressure. The residue was purified by flash chromatography on silica gel using as eluent a gradient

from *n*-hexane/EtOAc (4:1) to 100% EtOAc and recrystallized from EtOAc/*n*-hexane to afford the final product (adapted from [287]).

3',4'-diphenyl-4'*H*-spiro[indoline-3,5'-isoxazol]-2-one (119q).

Synthesized according to the general procedure (method C), this compound was obtained as a white solid (16.4 mg, 53 % yield).

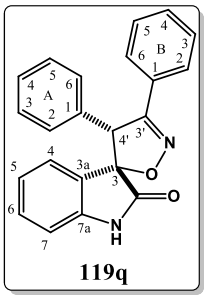

^{1}H NMR (400 MHz, $CDCl_3$) δ (ppm): 7.95 (br s, 1H, NH), 7.70 – 7.65 (m, 2H, H-$B_{2,6}$), 7.38 – 7.29 (m, 3H, H-$B_{3,4,5}$), 7.28 – 7.23 (m, 3H, H-$A_{3,4,5}$, partially obscured by $CDCl_3$ signal), 7.12 (td, J = 7.7, 1.1 Hz, 1H, H-6), 7.09 – 7.04 (m, 2H, H-$A_{2,6}$), 6.80 (d, J = 7.7 Hz, 1H, H-7), 6.63 (t, J = 7.7 Hz, 1H, H-5), 6.25 (d, J = 7.7 Hz, 1H, H-4), 5.08 (s, 1H, H-4'); **^{13}C NMR** (100 MHz, $CDCl_3$) δ (ppm): 177.08 (C=O), 159.19 (C=N), 141.62 (Cq-7a), 133.68 (Cq-A_1), 130.65 (CH-B_4), 130.45 (CH-6), 129.15 (CH-$A_{2,6}$), 129.09 (CH-$A_{3,5}$), 128.82 (CH-$B_{3,5}$), 128.58 (CH-A_4), 128.55 (Cq-B_1), 127.92 (CH-$B_{2,6}$), 127.40 (CH-4), 123.03 (Cq-3a), 122.72 (CH-5), 110.21 (CH-7), 89.05 (Cspiro), 60.41 (H-4'). Anal. Calcd for $C_{22}H_{16}N_2O_2 \cdot 0.5H_2O$: C, 75.63; H, 4.91; N, 8.02. Found: C, 75.36; H, 4.91; N, 7.82 [287].

3'-(4-nitrophenyl)-4'-phenyl-4'*H*-spiro[indoline-3,5'-isoxazol]-2-one (119r).

Synthesized according to the general procedure (method C), this compound was obtained as a light yellow solid (98.6 mg, 57 % yield).

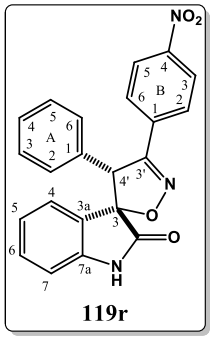

Mp: 274-276 ºC; **IR** (KBr, selected peaks): 3198 (NH), 1712 (C=O), 1522, 1337 cm^{-1}; **^{1}H NMR** (400 MHz, Acetone-d_6) δ (ppm): 9.58 (br s, 1H, NH), 8.25 (d, J = 8.8 Hz, 2H, H-$B_{3,5}$), 7.98 (d, J = 8.8 Hz, 2H, H-$B_{2,6}$), 7.39 – 7.29 (m, 3H, H-$A_{3,4,5}$), 7.27 – 7.21 (m, 2H, H-$A_{2,6}$), 7.10 (t, J = 7.7 Hz, 1H, H-6), 6.91 (d, J = 7.7 Hz, 1H, H-7), 6.63 (t, J = 7.7 Hz, 1H, H-5), 6.29 (d, J = 7.7 Hz, 1H, H-4), 5.46 (s, 1H, H-4'); **^{13}C NMR** (100 MHz, Acetone-d_6) δ (ppm): 176.47 (C=O), 158.92 (C=N), 149.47 (Cq-B_4), 144.24 (Cq-7a), 135.85 (Cq-B_1), 134.40 (Cq-A_1), 131.62 (C-6), 130.05 (CH-$A_{2,6}$), 129.90 (CH-$A_{3,5}$), 129.38 (CH-A_4), 129.35 (CH-$B_{2,6}$), 127.80 (CH-4), 124.79 (CH-$B_{3,5}$), 123.40 (Cq-3a), 122.59 (CH-5), 110.95 (CH-7), 90.45 (Cspiro), 59.56 (CH-4').

3'-(4-methoxyphenyl)-4'-phenyl-4'*H*-spiro[indoline-3,5'-isoxazol]-2-one (119s).

Synthesized according to the general procedure (method C), this compound was obtained as a white solid (117.40 mg, 70 % yield).

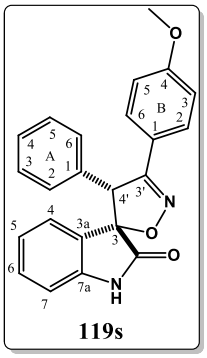

Mp: 267-269 ºC; **IR** (KBr, selected peaks): 3198 (NH), 1712 (C=O), 1522, 1337 cm^{-1}; **^{1}H NMR** (400 MHz, Acetone-d_6) δ (ppm): 9.51 (br s, 1H, NH), 7.64 (d, J = 8.9 Hz, 2H, H-$B_{2,6}$), 7.34 – 7.25 (m, 3H, H-$A_{3,4,5}$), 7.22 – 7.18 (m, 2H, H-$A_{2,6}$), 7.15 (t, J = 7.7 Hz, 1H, H-6), 6.91 (d, J = 8.9 Hz, 2H, H-$B_{3,5}$), 6.88 (d, J = 7.7 Hz, 1H, H-7), 6.60 (t, J = 7.7 Hz, 1H, H-5), 6.24 (d, J = 7.7 Hz, 1H, H-4), 5.27 (s, 1H, H-4'), 3.79 (s, 3H, OCH_3); **^{13}C NMR** (100 MHz, Acetone-d_6) δ (ppm): 177.07 (C=O), 162.07 (Cq-B_4), 159.43 (C=N), 144.14 (Cq-7a), 135.41 (Cq-A_1), 131.21 (CH-6), 130.05 (CH-$A_{2,6}$), 129.96 (CH-$B_{2,6}$), 129.63 (CH-$A_{3,5}$), 128.96 (CH-A_4), 127.72 (CH-4), 124.18 (Cq-3a), 122.37 (CH-5), 122.28 (Cq-B_1), 114.96 (CH-$B_{3,5}$), 110.71 (CH-7), 89.33 (Cspiro), 60.49 (CH-4'), 55.66 (OCH_3); Anal. Calcd for $C_{23}H_{18}N_2O_3 \cdot 0.4H_2O$: C, 73.15; H, 5.03; N, 7.42. Found: C, 72.84; H, 4.90; N, 7.36.

4'-(4-methoxyphenyl)-3'-phenyl-4'*H*-spiro[indoline-3,5'-isoxazol]-2-one (119t).

Synthesized according to the general procedure (method C), this compound was obtained as a white solid (35.2 mg, 57 % yield).

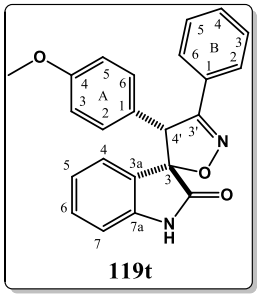

^{1}H NMR (400 MHz, $CDCl_3$) δ (ppm): 8.60 (br s, 1H, NH), 7.70 – 7.65 (m, 2H, H-$B_{2,6}$), 7.38 – 7.29 (m, 3H, H-$B_{3,4,5}$), 7.10 (td, J = 7.8, 1.2 Hz, 1H, H-6), 6.99 (d, J = 8.4 Hz, 2H, H-$A_{2,6}$), 6.82 – 6.76 (m, 3H, H-7, H-$A_{3,5}$), 6.66 (td, J = 7.8, 0.8 Hz, 1H, H-5), 6.31 (d, J = 7.8 Hz, 1H, H-4), 5.03 (s, 1H, H-4'), 3.76 (s, 3H, OCH_3); **^{13}C NMR** (100 MHz, $CDCl_3$) δ (ppm): 177.64 (C=O), 159.61 and 159.50 (C=N and Cq-A_4), 141.84 (Cq-7a), 130.58 (CH-B_4), 130.38 (CH-6), 130.24 (CH-$A_{2,6}$), 128.79 (CH-$B_{3,5}$), 128.65 (Cq-B_1), 127.91 (CH-$B_{2,6}$), 127.40 (CH-4), 125.59 (Cq-A_1), 123.07 (Cq-3a), 122.72 (CH-5), 114.46 (CH-$A_{3,5}$), 110.46 (CH-7), 89.16 (Cspiro), 59.69 (CH-4'), 55.36 (OCH_3) [287].

3',4'-bis(4-methoxyphenyl)-4'*H*-spiro[indoline-3,5'-isoxazol]-2-one (119u).

Synthesized according to the general procedure (method C), this compound was obtained as a white solid (114.4 mg, 72 % yield).

Mp: 219-221 ºC; **IR** (KBr, selected peaks): 3169 (NH), 1717 (C=O), 1260, 1246 cm^{-1}; **^{1}H NMR** (400 MHz, Acetone-d_6) δ (ppm): 9.45 (br s, 1H, NH), 7.64 (d, J = 9.0 Hz, 2H, H-$B_{2,6}$), 7.16 (td, J = 7.6, 1.2 Hz, 1H, H-6), 7.12 (d, J = 8.7 Hz, 2H, H-$A_{2,6}$), 6.91 (d, J = 9.0 Hz, 2H, H-$B_{3,5}$), 6.89 – 6.84 (m, 3H, H-7, H-$A_{3,5}$), 6.64 (td, J = 7.6, 1.0 Hz, 1H, H-5), 6.32

(d, *J* = 7.6 Hz, 1H, H-4), 5.21 (s, 1H, H-4'), 3.79 (s, 3H, B-OCH_3), 3.75 (s, 3H, A-OCH_3); **^{13}C NMR** (100 MHz, Acetone-d_6) δ (ppm): 177.16 (C=O), 162.03 (Cq-B_4), 160.45 (Cq-A_4), 159.62 (C=N), 144.16 (Cq-7a), 131.20 (CH-$A_{2,6}$), 131.16 (CH-6), 129.95 (CH-$B_{2,6}$), 127.89 (CH-4), 127.15 (Cq-A_1), 124.36 (Cq-3a), 122.41 (CH-5), 122.39 (Cq-B_1), 114.93 (CH-$A_{3,5}$, CH-$B_{3,5}$), 110.67 (CH-7), 89.28 (Cspiro), 59.90 (CH-4'), 55.66 (B-OCH_3), 55.49 (A-OCH_3). Anal. Calcd for $C_{24}H_{20}N_2O_4 \cdot 0.1C_4H_{10}O$: C, 71.85; H, 5.20; N, 6.87. Found: C, 72.07; H, 5.58; N, 7.14.

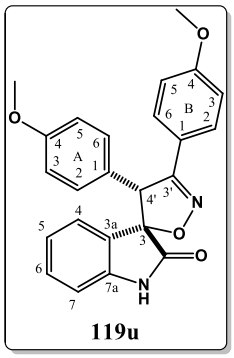

5-nitro-3',4'-diphenyl-4'*H*-spiro[indoline-3,5'-isoxazol]-2-one (119v)

Synthesized according to the general procedure (method C), this compound was obtained as a light yellow solid (74.9 mg, 52 % yield).

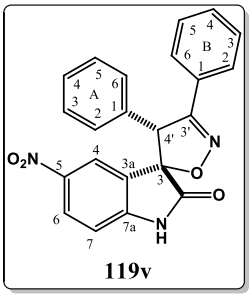

Mp: >320ºC; **IR** (KBr, selected peaks): 3181 (NH), 1726 (C=O), 1528, 1339 cm^{-1}. **^{1}H NMR** (400 MHz, Acetone-d_6) δ (ppm): 10.15 (br s, 1H, NH), 8.17 (dd, *J* = 8.7, 2.3 Hz, 1H, H-6), 7.78 – 7.73 (m, 2H, H-$B_{2,6}$), 7.48 – 7.31 (m, 6H, H-$A_{3,4,5}$, H-$B_{3,4,5}$), 7.30 – 7.26 (m, 2H, H-$A_{2,6}$), 7.14 (d, *J* = 8.7 Hz, 1H, H-7), 7.05 (d, *J* = 2.3 Hz, 1H, H-4), 5.51 (s, 1H, H-4'). **^{13}C NMR** (100 MHz, Acetone-d_6) δ (ppm): 176.80 (C=O), 160.01 (C=N), 150.17 (Cq-7a), 143.45 (Cq-5), 134.39 (Cq-A_1), 131.34 (CH-B_4), 130.04 (CH-$A_{2,6}$), 129.86 (CH-$A_{3,5}$), 129.71 (CH-$B_{3,5}$), 129.59 (CH-A_4), 129.45 (Cq-B_1), 128.49 (CH-$B_{2,6}$), 128.14 (CH-6), 124.87 (Cq-3a), 123.30 (CH-4), 111.08 (CH-7), 88.67 (Cspiro), 60.51 (CH-4'). Anal. Calcd for $C_{22}H_{15}N_3O_4 \cdot 0.4\ H_2O$: C, 67.30; H, 4.06; N, 10.71. Found: C, 67.14; H, 4.13; N, 10.37.

3'-(4-methoxyphenyl)-5-nitro-4'-phenyl-4'*H*-spiro[indoline-3,5'-isoxazol]-2-one (119w).

Synthesized according to the general procedure (method C), this compound was obtained as a light yellow solid (116.5 mg, 72 % yield).

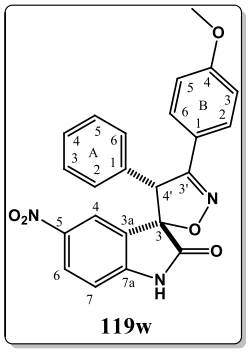

Mp: 299-302 ºC; **IR** (KBr, selected peaks): 3188 (NH), 1734 (C=O), 1526, 1337, 1260 cm^{-1}; **^{1}H NMR** (400 MHz, Acetone-d_6) δ (ppm): 10.14 (br s, 1H, NH), 8.16 (dd, *J* = 8.7, 2.4 Hz, 1H, H-6), 7.68 (d, *J* = 8.9 Hz, 2H, H-$B_{2,6}$), 7.39 – 7.30 (m, 3H, H-$A_{3,4,5}$), 7.28 – 7.24 (m, 2H, H-$A_{2,6}$), 7.13 (d, *J* = 8.7 Hz, 1H, H-7), 7.03 (d, *J* = 2.4 Hz, 1H, H-4), 6.94 (d, *J* = 8.9 Hz, 2H, H-$B_{3,5}$), 5.45 (s, 1H, H-4'), 3.80 (s, 3H, OCH_3);**^{13}C NMR** (100 MHz, Acetone-d_6) δ (ppm): 176.95 (C=O), 162.34 (Cq-B_4), 159.51 (C=N), 150.14 (Cq-7a), 143.43 (Cq-5), 134.62 (Cq-A_1), 130.11 (CH-$B_{2,6}$), 129.98 (CH-

$A_{2,6}$), 129.87 (CH-$A_{3,5}$), 129.50 (CH-A_4), 128.05 (CH-6), 125.08 (Cq-3a), 123.28 (CH-4), 121.75 (Cq-B_1), 115.10 (CH-$B_{3,5}$), 111.01 (CH-7), 88.41 (Cspiro), 60.79 (CH-4'), 55.71 (OCH_3). Anal. Calcd for $C_{23}H_{17}N_3O_5 \cdot 0.9H_2O$: C, 64.00; H, 4.40; N, 9.74. Found: C, 63.67; H, 4.01; N, 9.67.

7-chloro-3'-(4-nitrophenyl)-4'-phenyl-4'*H*-piro[indoline-3,5'-isoxazol]-2-one (119x).

Synthesized according to the general procedure (method C), this compound was obtained as a white solid (76.2 mg, 46 % yield).

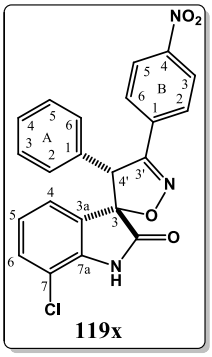

119x

Mp: 240-241 ºC; **IR** (KBr, selected peaks): 3177 (NH), 1734 (C=O), 1518, 1342 cm^{-1}; **^{1}H NMR** (400 MHz, Acetone-d_6) δ (ppm): 9.93 (br s, 1H, NH), 8.26 (d, J = 8.8 Hz, 2H, H-$B_{3,5}$), 7.98 (d, J = 8.8 Hz, 2H, H-$B_{2,6}$), 7.38 – 7.30 (m, 3H, H-$A_{3,4,5}$), 7.28 – 7.22 (m, 3H, H-6, H-$A_{2,6}$), 6.67 (t, J = 7.8 Hz, 1H, H-5), 6.24 (d, J = 7.8 Hz, 1H, H-4), 5.54 (s, 1H, H-4'); **^{13}C NMR** (100 MHz, Acetone-d_6) δ (ppm): 176.04, (C=O), 158.97 (C=N), 149.57 (Cq-B_4), 141.85 (Cq-7a), 135.59 (Cq-B_1), 134.02 (C-A_1), 131.54 (CH-6), 130.06 (CH-$A_{2,6}$), 130.00 (CH-$A_{3,5}$) 129.55 (CH-A_4), 129.43 (CH-$B_{2,6}$), 126.30 (CH-4), 125.24 (C-3a), 124.83 (CH-$B_{3,5}$), 123.73 (CH-5), 115.61 (Cq-7), 90.72 (Cspiro), 59.88 (CH-4').

7-chloro-3'-(4-methoxyphenyl)-4'-phenyl-4'*H*-spiro[indoline-3,5'-isoxazol]-2-one (119y).

Synthesized according to the general procedure (method C), this compound was obtained as a white solid (104.6 mg, 66 % yield).

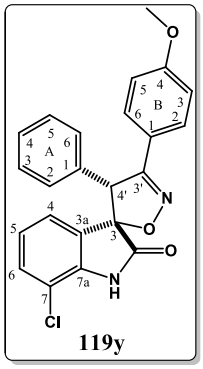

119y

Mp: 218-219 ºC; **IR** (KBr, selected peaks): 3167 (NH), 1724 (C=O), 1252 cm^{-1}; **^{1}H NMR** (400 MHz, Acetone-d_6) δ (ppm): 9.80 (br s, 1H, NH), 7.65 (d, J = 8.7 Hz, 2H, H-$B_{2,6}$), 7.36 – 7.27 (m, 3H, H-$A_{3,4,5}$), 7.26 – 7.20 (m, 3H, H-6, H-$A_{2,6}$), 6.92 (d, J = 8.7 Hz, 2H, H-$B_{3,5}$), 6.64 (t, J = 7.8 Hz, 1H, H-5), 6.19 (d, J = 7.8 Hz, 1H, H-4), 5.36 (s, 1H, H-4'), 3.80 (s, 3H, OCH_3); **^{13}C NMR** (100 MHz, Acetone-d_6) δ (ppm): 176.59 (C=O), 162.20 (Cq-B_4), 159.48 (C=N), 141.74 (Cq-7a), 135.04 (Cq-A_1), 131.14 (CH-6), 130.06 (CH-$B_{2,6}$), 130.02 (CH-$A_{2,6}$), 129.74 (CH-$A_{3,5}$), 129.13 (CH-A_4), 126.22 (CH-4), 126.04 (Cq-3a), 123.51 (CH-5), 122.04 (Cq-B_1), 115.39 (Cq-7), 115.02 (CH-$B_{3,5}$), 89.67 (Cspiro), 60.79 (CH-4'), 55.68 (OCH_3). Anal. Calcd for $C_{23}H_{17}ClN_2O_3 \cdot 1.1H_2O$: C, 65.05; H, 4.52; N, 6.60. Found: C, 65.40; H, 4.68; N, 6.22.

6-chloro-3',4'-diphenyl-4'*H*-spiro[indoline-3,5'-isoxazol]-2-one (119z).

Synthesized according to the general procedure (method C), this compound was obtained as an off-white solid (77.7 mg, 55 % yield).

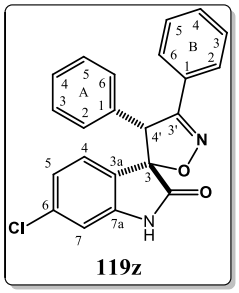

Mp: 271-273 ºC; **IR (**KBr, selected peaks): 3186 (NH), 1732 (C=O) cm^{-1}; **^{1}H NMR** (400 MHz, Acetone-d_6) δ (ppm): 9.67 (br s, 1H, NH), 7.74 – 7.70 (m, 2H, H-$B_{2,6}$), 7.43 – 7.35 (m, 3H, H-$A_{3,4,5}$), 7.35 – 7.27 (m, 3H, H-$B_{3,4,5}$), 7.25 – 7.20 (m, 2H, H-$A_{2,6}$), 6.94 (d, J = 2.0 Hz, 1H, H-7), 6.65 (dd, J = 8.2, 2.0 Hz, 1H, H-5), 6.21 (d, J = 8.2 Hz, 1H, H-4), 5.38 (s, 1H, H-4'); **^{13}C NMR** (100 MHz, Acetone-d_6) δ (ppm): 176.71 (C=O), 159.93 (C=N), 145.58 (Cq-7a), 136.59 (Cq-6), 134.91 (Cq-A_1), 131.10 (CH-B_4), 129.99 (CH-$A_{2,6}$), 129.82 (CH-$A_{3,5}$), 129.75 (Cq-B_1), 129.61 (CH-$B_{3,5}$), 129.22 (CH-A_4), 128.95 (CH-4), 128.40 (CH-$B_{2,6}$), 122.78 (Cq-3a), 122.29 (CH-5), 111.19 (CH-7), 89.10 (Cspiro), 60.24 (CH-4'). Anal. Calcd for $C_{22}H_{15}ClN_2O_2$: C, 70.49; H, 4.04; N, 7.48. Found: C, 70.38; H, 4.27; N, 7.25.

6-chloro-3'-(4-methoxyphenyl)-4'-phenyl-4'*H*-spiro[indoline-3,5'-isoxazol]-2-one (119aa).

Synthesized according to the general procedure (method C), this compound was obtained as a white solid (76.9 mg, 49 % yield).

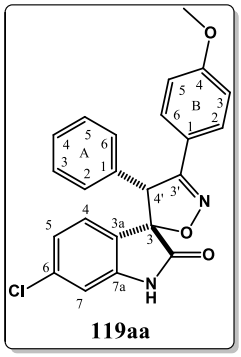

Mp 148-150 ºC; **IR (**KBr, selected peaks): 3186 (NH), 1748 (C=O) 1265 cm^{-1}; **^{1}H NMR** (400 MHz, Acetone-d_6) δ (ppm): 9.65 (br s, NH, 1H), 7.64 (d, J = 8.9 Hz, 2H, H-$B_{2,6}$), 7.36 – 7.27 (m, 3H, H-$A_{3,4,5}$), 7.24 – 7.18 (m, 2H, H-$A_{2,6}$), 6.95 – 6.88 (m, 3H, H-7, H-$B_{3,5}$), 6.64 (dd, J = 8.1, 1.8 Hz, 1H, H-5), 6.19 (d, J = 8.1 Hz, 1H, H-4), 5.31 (s, 1H, H-4'), 3.79 (s, 3H, OCH_3); **^{13}C NMR** (100 MHz, Acetone-d_6) δ (ppm): 176.87 (C=O), 162.17 (Cq-B_4), 159.45 (C=N), 145.56 (Cq-7a), 136.49 (Cq-6), 135.14 (Cq-A_1), 130.00 (CH-$A_{2,6}$, CH-$B_{2,6}$), 129.78 (CH-$A_{3,5}$), 129.14 (CH-A_4), 128.93 (CH-4), 122.98 (Cq-3a), 122.24 (CH-5), 122.07 (Cq-B_1), 115.01 (CH-$B_{3,5}$), 111.13 (CH-7), 88.82 (Cspiro), 60.52 (CH-4'), 55.67 (OCH_3). Anal. Calcd for $C_{23}H_{17}ClN_2O_3 \cdot 0.6H_2O$: C, 66.46; H, 4.42; N, 6.74. Found: C, 66.25; H, 4.34; N, 6.54.

6-chloro-3'-(4-nitrophenyl)-4'-phenyl-4'*H*-spiro[indoline-3,5'-isoxazol]-2-one (119ab).

Synthesized according to the general procedure (method C), this compound was obtained as a light yellow solid (70.1 mg, 43%).

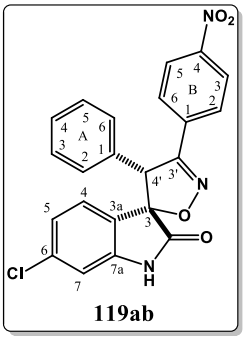

Mp: 255-256 ºC; **IR (**KBr, selected peaks): 3169 (NH), 1721 (C=O), 1522, 1342 cm^{-1}; **^{1}H NMR** (400 MHz, Acetone-d_6) δ (ppm): 9.78 (br s, 1H, NH), 8.26 (d, J = 9.0 Hz, 2H, H-$B_{3,5}$), 7.98 (d, J = 9.0 Hz, 2H, H-$B_{2,6}$), 7.39 – 7.32 (m, 3H, H-$A_{3,4,5}$), 7.26 – 7.22 (m, 2H, H-$A_{2,6}$), 6.96 (d, J = 1.9 Hz, 1H, H-7), 6.67 (dd, J = 8.2, 1.9 Hz, 1H, H-5), 6.25 (d, J = 8.2 Hz, 1H, H-4), 5.49 (s, 1H, H-4'); **^{13}C NMR** (100 MHz, Acetone-d_6) δ (ppm): 176.32 (C=O), 158.93 (C=N), 149.56 (Cq-B_4), 145.67 (Cq-7a), 136.91 (Cq-6), 135.64 (Cq-B_1), 134.13 (Cq-A_1), 130.04 (CH-$A_{2,6}$), 130.00 (CH-$A_{3,5}$), 129.55 (CH-A_4), 129.41 (CH-$B_{2,6}$), 129.02 (CH-4), 124.83 (CH-$B_{3,5}$), 122.46 (CH-5), 122.21 (Cq-3a), 111.39 (CH-7), 89.94 (Cspiro), 59.62 (CH-4'). Anal. Calcd for $C_{22}H_{14}ClN_3O_4 \cdot 1.0H_2O$: C, 60.35; H, 3.69; N, 9.60. Found: C, 60.13; H, 3.41; N, 9.22.

6-chloro-4'-phenyl-3'-(*p*-tolyl)-4'*H*-spiro[indoline-3,5'-isoxazol]-2-one (119ac).

Synthesized according to the general procedure (method C), this compound was obtained as a white solid (107.4 mg, 71% yield).

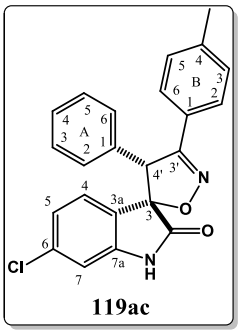

Mp: 136-138 ºC; **IR (**KBr, selected peaks): 3177 (NH), 1744 (C=O) cm^{-1}; **^{1}H NMR** (400 MHz, Acetone-d_6) δ (ppm): 9.65 (br s, 1H, NH), 7.60 (d, J = 8.2 Hz, 2H, H-$B_{2,6}$), 7.35 – 7.28 (m, 3H, H-$A_{3,4,5}$), 7.23 – 7.16 (m, 4H, H-$A_{2,6}$, H-$B_{3,5}$), 6.93 (d, J = 1.9 Hz, 1H, H-7), 6.64 (dd, J = 8.2, 1.9 Hz, 1H, H-5), 6.21 (d, J = 8.2 Hz, 1H, H-4), 5.34 (s, 1H, H-4'), 2.30 (s, 3H, CH_3); **^{13}C NMR** (100 MHz, Acetone-d_6) δ (ppm): 176.77 (C=O), 159.80 (C=N), 145.53 (Cq-7a), 141.34 (Cq-B_4), 136.53 (Cq-6), 135.04 (Cq-A_1), 130.22 (CH-$B_{3,5}$), 129.99 (CH-$A_{2,6}$), 129.78 (CH-$A_{3,5}$), 129.15 (CH-A_4), 128.94 (CH-4), 128.37 (CH-$B_{2,6}$), 126.94 (Cq-B_1), 122.89 (Cq-3a), 122.26 (CH-5), 111.14 (CH-7), 88.94 (Cspiro), 60.39 (CH-4'), 21.32 (CH_3); Anal. Calcd for $C_{23}H_{17}ClN_2O_2 \cdot 0.3H_2O$: C, 70.06; H, 4.51; N, 7.11. Found: C, 69.79; H, 4.30; N, 6.79.

6-chloro-3'-(2-methoxyphenyl)-4'-phenyl-4'*H*-spiro[indoline-3,5'-isoxazol]-2-one (119ad).

Synthesized according to the general procedure (method C), this compound was obtained as a white solid (121.1 mg, 76 % yield).

Mp: 128-130 ºC; **IR (**KBr, selected peaks): 3173 (NH), 1724 (C=O), 1248 cm^{-1}; **^{1}H NMR** (400 MHz, Acetone-d_6) δ (ppm): 9.65 (br s, 1H, NH), 7.93 (dd, J = 7.5, 1.7 Hz, 1H, H-B_6), 7.38 (ddd, J = 8.5, 7.5, 1.7 Hz, 1H, H-B_4), 7.25 – 7.15 (m, 3H, H-$A_{3,4,5}$), 7.13 – 7.08 (m, 2H, H-$A_{2,6}$), 7.02 (td, J = 7.5, 0.9 Hz, 1H, H-B_5), 6.96 (d, J = 8.5 Hz, 1H, H-B_3), 6.89 (d, J = 1.9 Hz, 1H, H-7), 6.67 (dd, J = 8.1, 1.9 Hz, 1H, H-5), 6.47 (d, J = 8.1 Hz, 1H, H-4), 5.66

(s, 1H, H-4'), 3.63 (s, 3H, OCH_3); **^{13}C NMR** (100 MHz, Acetone-d_6) δ (ppm): 177.00 (C=O), 158.84 (C=N), 158.40 (Cq-B_2), 145.13 (Cq-7a), 136.27 (Cq-6), 135.31 (Cq-A_1), 132.69 (CH-B_4), 130.91 (CH-B_6), 129.90 (CH-$A_{2,6}$), 129.29 (CH-$A_{3,5}$), 128.94 (CH-4), 128.60 (CH-A_4), 123.86 (Cq-3a), 122.23 (CH-5), 121.62 (CH-B_5), 118.72 (Cq-B_1), 113.09 (CH-B_3), 111.10 (CH-7), 89.17 (Cspiro), 63.03 (CH-4'), 55.85 (OCH_3); Anal. Calcd for $C_{23}H_{17}ClN_2O_3 \cdot 0.7H_2O$: C, 66.17; H, 4.45; N, 6.71. Found: C, 66.41; H, 4.73; N, 6.33.

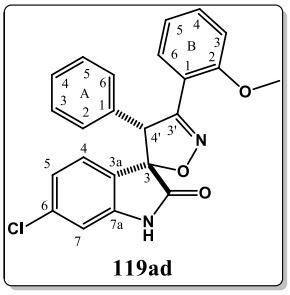

6-chloro-3',4'-bis(4-methoxyphenyl)-4'*H*-spiro[indoline-3,5'-isoxazol]-2-one (119ae).

Synthesized according to the general procedure (method C), this compound was obtained as a white solid (107.0 mg, 70 % yield).

Mp 231-232 ºC; **IR (**KBr, selected peaks): 3219 (NH), 1748 (C=O) 1261 cm^{-1}; **^{1}H NMR** (400 MHz, Acetone-d_6) δ (ppm): 9.61 (s br, 1H, NH), 7.63 (d, J = 8.9 Hz, 2H, H-$B_{2,6}$), 7.12 (d, J = 8.7 Hz, 2H, H-$A_{2,6}$), 6.95 – 6.85 (m, 5H, H-7, H-$A_{3,5}$, H-$B_{3,5}$), 6.68 (dd, J = 8.1, 1.9 Hz, 1H, H-5), 6.28 (d, J = 8.1 Hz, 1H, H-4), 5.25 (s, 1H, H-4'), 3.79 (s, 3H, B-OCH_3), 3.76 (s, 3H, A-OCH_3); **^{13}C NMR** (100 MHz, Acetone-d_6) δ (ppm): 176.94 (C=O), 162.12 (Cq-B_4), 160.56 (Cq-A_4), 159.64 (C=N), 145.54 (Cq-7a), 136.44 (Cq-6), 131.15 (CH-$A_{2,6}$), 129.99 (CH-$B_{2,6}$), 129.10 (CH-4), 126.83 (Cq-A_1), 123.15 (Cq-3a), 122.28 (CH-5), 122.18 (Cq-B_1), 115.08 and 114.98 (CH-$A_{3,5}$ and CH-$B_{3,5}$), 111.08 (CH-7), 88.79 (Cspiro), 59.95 (CH-4'), 55.67 (B-OCH_3), 55.53 (A-OCH_3); Anal. Calcd for $C_{23}H_{19}ClN_2O_4$: C, 66.28; H, 4.41; N, 6.44. Found: C, 65.93; H, 4.71; N, 6.28.

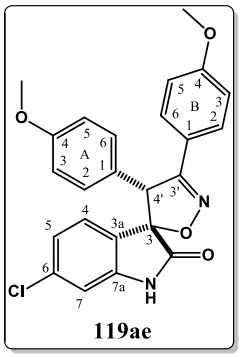

6-bromo-3',4'-diphenyl-4'*H*-spiro[indoline-3,5'-isoxazol]-2-one (119af).

Synthesized according to the general procedure (method C), this compound was obtained as a light yellow solid (61.6 mg, 44 % yield).

MP: 288-290 ºC. **IR** (KBr, selected peaks): 3204 (NH), 1728 (C=O) cm^{-1}; **^{1}H NMR** (400 MHz, Acetone-d_6) δ (ppm): 9.68 (br s, 1H, NH), 7.74 – 7.69 (m, 2H, H-$B_{2,6}$), 7.41 – 7.36 (m, 3H, H-$B_{3,4,5}$), 7.36 – 7.29 (m, 3H, H-$A_{3,4,5}$), 7.24 – 7.20 (m, 2H, H-$A_{2,6}$), 7.08 (d, J = 1.7 Hz, 1H, H-7), 6.81 (dd, J = 8.0, 1.7 Hz, 1H, H-5), 6.15 (d, J = 8.0 Hz, 1H, H-4), 5.37 (s, 1H, H-4'); **^{13}C NMR** (100 MHz, Acetone-d_6) δ (ppm): 176.62 (C=O), 159.94 (C=N), 145.70 (Cq-7a), 134.89 (Cq-A_1), 131.11 (CH-B_4), 129.99 (CH-$A_{2,6}$), 129.83 (CH-$A_{3,5}$), 129.74 (Cq-B_1), 129.62 (CH-$B_{3,5}$), 129.23 (CH-4, CH-A_4), 128.41 (CH-$B_{2,6}$),

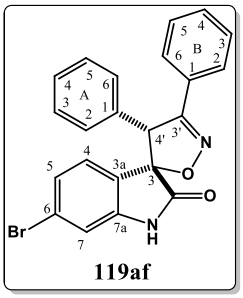

125.27 (CH-5), 124.70 (Cq-6), 123.28 (Cq-3a), 114.05 (CH-7), 89.17 (Cspiro), 60.25 (CH-4'). Anal. Calcd for $C_{22}H_{15}BrN_2O_2 \cdot 0.05H_2O$: C, 62.88; H, 3.63; N, 6.67. Found: C, 62.53; H, 3.79; N, 6.61.

6-bromo-3'-(4-methoxyphenyl)-4'-phenyl-4'*H*-spiro[indoline-3,5'-isoxazol]-2-one (119ag).

Synthesized according to the general procedure (method C), this compound was obtained as a white solid (109.3 mg, 73%).

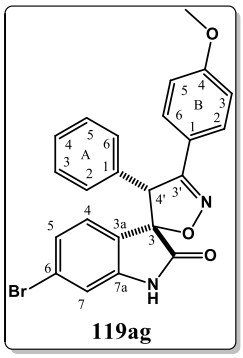

119ag

Mp: 247-248 ºC; **IR** (KBr, selected peaks): 3210 (NH), 1746 (C=O), 1265 cm^{-1}; **^{1}H NMR** (400 MHz, Acetone-d_6) δ (ppm): 9.67 (br s, NH), 7.64 (d, J = 8.9 Hz, 2H, H-$B_{2,6}$), 7.36 – 7.27 (m, 3H, H-$A_{3,4,5}$), 7.24 – 7.18 (m, 2H, H-$A_{2,6}$), 7.08 (d, J = 1.6 Hz, 1H, H-7), 6.91 (d, J = 8.9 Hz, 2H, H-$B_{3,5}$), 6.80 (dd, J = 8.1, 1.7 Hz, 1H, H-5), 6.13 (d, J = 8.1 Hz, 1H, H-4), 5.32 (s, 1H, H-4'), 3.79 (s, 3H, OCH_3); **^{13}C NMR** (100 MHz, Acetone-d_6) δ (ppm): 176.78 (C=O), 162.17 (Cq-B_4), 159.44 (C=N), 145.66 (Cq-7a), 135.11 (Cq-A_1), 130.00 (CH-$A_{2,6}$, CH-$B_{2,6}$), 129.77 (CH-$A_{3,5}$), 129.20 and 129.13 (CH-4 and CH-A_4), 125.21 (CH-5), 124.59 (Cq-6), 123.48 (Cq-3a), 122.05 (Cq-B_1), 115.01 (CH-$B_{3,5}$), 114.00 (CH-7), 88.90 (Cspiro), 60.52 (CH-4'), 55.68 (OCH_3). Anal. Calcd for $C_{23}H_{17}BrN_2O_3 \cdot 0.6H_2O$: C, 60.04; H, 4.00; N, 6.09. Found: C, 59.73; H, 3.71; N, 5.72.

9.1.9.5. Synthesis of compound *N*-acetyl-6-chloro-4'-phenyl-3'-(*p*-tolyl)-4'*H*-spiro[indoline-3,5'-isoxazol]-2-one (119ah).

A 4 mL scintillation vial filled with 20 mg of 4 Å molecular sieves and magnetic stir bar was dried under vacuum with a heat gun for 15 minutes, and then 3-methylene indolin-2-one **121n** (1.0 equiv, 0.1 mmol, 29.8 mg), chlorooxime **123e** (3.0 equiv, 0.3 mmol, 50.9 mg), and CH_2Cl_2 (0.5 mL) were added. The reaction was then sealed under argon atmosphere and stirred for 3 days. The reaction was concentrated *in vacuo* and the diastereomeric ratio was obtained using ^{1}H NMR analysis of the unpurified reaction mixture. Next the mixture was purified by flash chromatography, using as eluent a gradient from 100% hexanes to hexanes:EtOAc (85:15) to yield the compound **119ah** as a white solid (6.9 mg, 16 % yield). Enantiomeric ratio was determined by HPLC with a Daicel CHIRALPAK® AD-H column (5% IPA/hexanes), 1.0 mL/min, tR = 32.0 min and 37.9 min, 50:50 er.

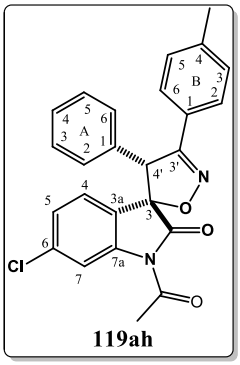

119ah

^{1}H NMR (400 MHz, acetone-d_6) δ (ppm): 8.22 (d, J = 2.0 Hz, 1H, H-

7), 7.60 (d, *J* = 8.3 Hz, 2H, H-$B_{2,6}$), 7.36 – 7.29 (m, 3H, H-$A_{3,4,5}$), 7.24 – 7.15 (m, 4H, H-$A_{2,6}$, H-$B_{3,5}$), 6.90 (dd, *J* = 8.3, 2.0 Hz, 1H, H-5), 6.34 (d, *J* = 8.2 Hz, 1H, H-4), 5.56 (s, 1H, H-4'), 2.63 (s, 3H,$COCH_3$), 2.32 (s, 3H, CH_3).

9.1.9.6. Synthesis of enantioenriched compound 6-chloro-4'-phenyl-3'-(*p*-tolyl)-4'*H*-spiro[indoline-3,5'-isoxazol]-2-one (119ac).

A 4 mL scintillation vial filled with 20 mg of 4 Å molecular sieves and magnetic stir bar was dried under vacuum with a heat gun for 15 minutes, and then (*R*,*S*)-indapybox (0.22 equiv, 0.044 mmol 17.3 mg), NaBArF (0.2 equiv, 0.04 mmol, 35.5 mg), and $Sc(OTf)_3$ (0.2 equiv, 0.04 mmol, 19.7 mg) were added, followed by dichloroethane (1.0 mL). The mixture was allowed to stir at room temperature for 1 h to allow complexation of the ligand and metal. Then the 3-methylene indolin-2-one **121k** (1.0 equiv, 0.2 mmol, 51.2 mg) was added. After 5 min the chlorooxime **123e** (3.0 equiv, 0.6 mmol, 101.8 mg) was added. The reaction was then sealed under argon atmosphere and stirred for 4 days. When reaction conditions were being tested a partially purification was performed by applying part of the mixture on a "mini"-preparative (5 cm x 5 cm, silica gel over glass plate), and eluting two times with hexanes:EtOAC (3:1). With exception of the application point and the nitrile oxide dimer (and/or excess of chlorooxime) bands, all silica was removed, and the mixture extracted with EtOAc, and concentrated *in vacuo*. The diastereomeric ratio was obtained using ^{1}H NMR analysis of the partially purified reaction mixture. The enantiomeric ratio was measured using HPLC with a chiral stationary phase, and compared to a racemic standard that was prepared without ligand. For the best reaction conditions (presented in this procedure), the mixture was also purified by flash chromatography, using as eluent a gradient from 100% hexanes to hexanes:EtOAc (85:15) to yield the compound enantioenriched **119ac** as a white solid (17.0 mg, 23 % yield, 96:4 dr based on ^{1}H NMR, 75:25 er). Enantiomeric ratio was determined by HPLC with a Daicel CHIRALPAK® AD-H column (15% IPA/hexanes), 1.0 mL/min, tR (major) = 16.1 min, tR (minor) = 39.9 min, 75:25 er.

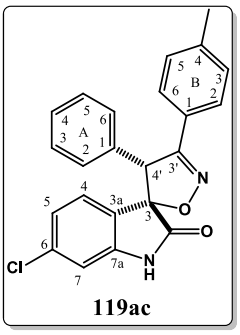

119ac

9.1.10. Synthesis of 4'-ethyl 5'-methyl (3*S*,4'*R*,5'*S*)-*N*-acetyl-5-fluoro-2'-(4-methoxyphenyl)-2-oxo-4',5'-dihydrospiro[indoline-3,3'-pyrrole]-4',5'-dicarboxylate (*epi*-163).

A 4 mL scintillation vial filled with 20 mg of 4 Å molecular sieves and magnetic stir bar was dried under vacuum with a heat gun for 15 minutes, and then (*R*,*S*)-indapybox (0.22 equiv, 0.044 mmol, 17.3 mg), NaBArF (0.2 equiv, 0.04 mmol, 35.5 mg), and

$Sc(OTf)_3$ (0.2 equiv, 0.04 mmol, 19.7 mg) were added, followed by toluene (1.0 mL). The mixture was allowed to stir at room temperature for 1 h to allow complexation of the ligand and metal. Then the 3-methylene indolin-2-one **121p** (1.5 equiv, 0.3 mmol, 83.2 mg) was added. After 5 min the oxazole **161** (1.0 equiv, 0.2 mmol, 41.0 mg) was added. The reaction was then sealed under argon atmosphere and stirred until complete as judged by TLC (10% EtOAc/DCM), which was approximately 12 h. When judged to be complete, the reaction was concentrated *in vacuo* and the diastereomeric ratio was obtained using ^{1}H NMR analysis of the unpurified reaction mixture. A reversal in diastereoselectivity was observed when using the pybox ligand compared to conditions without a ligand. Next the mixture was purified by flash chromatography, using as eluent a gradient from 100% DCM to DCM:EtOAc (90:10) to yield the compound ***epi*-163**. The enantioselectivity of the product was measured using HPLC with a chiral stationary phase, and compared to a racemic standard that was prepared using the Sc(III)-catalyzed procedure without ligand.

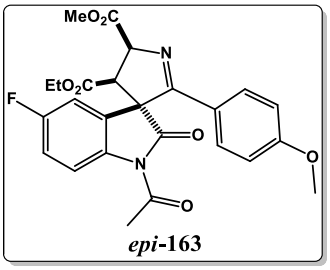

epi-163

Compound ***epi*-3a** was obtained as a white foam (95.4 mg, 99% yield, 9:91 dr based on ^{1}H NMR, 86:14 er). Enantiomeric ratio was determined by HPLC with a Daicel CHIRALPAK® AD-H column (15% IPA/hexanes), 1.0 mL/min, tR (major) = 49.8 min, tR (minor) = 16.7 min, 86:14 er; **^{1}H NMR** (500 MHz, $CDCl_3$) δ (ppm): 8.31 (dd, J = 9.0, 4.7 Hz, 1H), 7.63 (dd, J = 8.3, 2.8 Hz, 1H), 7.30 (d, J = 9.0 Hz, 2H), 7.10 (ddd, J = 8.8, 8.8, 2.8 Hz, 1H), 6.74 (d, J = 9.0 Hz, 2H), 5.40 (d, J = 9.2 Hz, 1H), 4.28 (d, J = 9.3 Hz, 1H), 3.90 (s, 3H), 3.79 – 3.73 (m, 2H), 3.75 (s, 3H), 2.69 (s, 3H), 0.79 (t, J = 7.2 Hz, 3H); **^{13}C NMR** (150 MHz, $CDCl_3$) δ (ppm): 177.1, 171.0, 170.5, 169.3, 167.1, 162.2, 160.5 (d, J_{FC} = 246.0 Hz), 136.2, 129.6, 128.1 (d, J_{FCCC} = 8.9 Hz), 123.9, 117.9 (d, J_{FCCC} = 7.8 Hz), 116.5 (d, J_{FCC} = 22.8 Hz), 114.3, 114.0 (d, J_{FCC} = 26.0 Hz), 73.4, 67.9, 61.5, 58.2, 55.4, 52.8, 26.6, 13.5. LRMS calculated for $C_{25}H_{24}FN_2O_7$ $[M + H]^+$ 483.2, found 483.4.

9.1.11. General procedure for the synthesis of spiro[indoline-3,5'-[1,2,4]oxadiazoline]-2-ones.

Triethylamine (2.0 equiv) was added dropwise to a mixture of 3-imino-indolin-2-one derivative (1.0 equiv), and hydroximoyl chloride derivative (2.0 equiv) in dry DCM (1mL/0.1mmol of 3-imino-indolin-2-one) under nitrogen atmosphere. The reaction was stirred at room temperature for 5-12 h. The mixture was then washed with brine (2x) and the aqueous phase extracted with DCM. The combined organic extracts were dried over anhydrous Na_2SO_4 and the solvent was removed under reduce pressure. The residue was purified by flash chromatography on silica gel using as eluent a gradient from *n*-

hexane/EtOAc (95:5) to *n*-hexane/EtOAc (60:40) and recrystallized from diethyl ether/*n*-hexane or just washed with diethyl ether, to afford the final product.

4'-(4-fluorophenyl)-3'-phenyl-4'*H*-spiro[indoline-3,5'-[1,2,4]oxadiazol]-2-one (165a).

Synthesized according to the general procedure, this compound was obtained as a white solid (119.7 mg, 80 % yield).

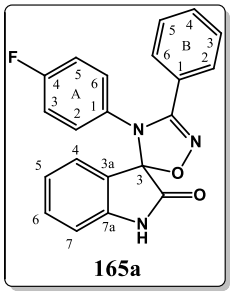

Mp: 168-169 ºC; **IR** (KBr, selected peaks): 3211 (NH), 1726 (C=O), 1626 (C=N), 1506, 1473, 1386, 1208, 842, 749 cm^{-1}; **^{1}H NMR** (400 MHz, Acetone-d_6) δ (ppm): 9.47 (br s, 1H, NH), 7.65 (d, J = 7.5 Hz, 1H, H-4), 7.52 – 7.42 (m, 3H, H-$B_{2,4,6}$), 7.42 – 7.32 (m, 3H, H-6, H-$B_{3,5}$), 7.12 (t, J = 7.5 Hz, 1H, H-5), 7.00 – 6.93 (m, 4H, 4H-A), 6.91 (d, J = 7.8 Hz, 1H, H-7); **^{13}C NMR** (100 MHz, Acetone-d_6) δ (ppm): 172.88 (C=O), 161.91 (d, J_{FC} = 244.0 Hz, Cq-A_4), 156.03 (C=N), 143.81 (Cq-7a), 134.18 (d, J_{FCCCC} = 3.0 Hz, Cq-A_1), 133.05 (CH-6), 131.41 (CH-B_4), 130.30 (d, J_{FCCC} = 9.0 Hz, CH-$A_{2,6}$), 129.48 (CH-$B_{3,5}$), 129.04 (CH-$B_{2,6}$), 127.44 (CH-4), 125.67 (Cq-B_1), 125.46 (Cq-3a), 123.92 (CH-5), 116.69 (d, J_{FCC} = 22.0 Hz, CH-$A_{3,5}$), 111.73 (CH-7), 99.02 (Cspiro). Anal. Calcd for $C_{21}H_{14}FN_3O_2 \cdot 0.2H_2O$: C 69.49, H 4.01, N 11.58, Found: C 69.22, H 3.79, N 11.38.

4'-(3-chlorophenyl)-3'-phenyl-4'*H*-spiro[indoline-3,5'-[1,2,4]oxadiazol]-2-one (165b).

Synthesized according to the general procedure, this compound was obtained as a white solid (120.0 mg, 82 % yield).

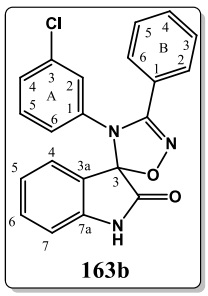

Mp: 186-187 ºC; **IR** (KBr, selected peaks): 3242 (NH), 1729 (C=O), 1624 (C=N), 1587, 1470, 1385, 1206, 847 cm^{-1}; **^{1}H NMR** (400 MHz, Acetone-d_6) δ (ppm): 9.56 (br s, 1H, NH), 7.63 (d, J = 7.6 Hz, 1H, H-4), 7.55 – 7.46 (m, 3H, H-$B_{2,4,6}$), 7.45 – 7.35 (m, 3H, H-6, H-$B_{3,5}$), 7.22 – 7.15 (m, 2H, H-$A_{4,5,}$), 7.12 (t, J = 7.6 Hz, 1H, H-5), 6.96 (d, J = 7.6 Hz, 1H, H-7), 6.86 (s, 1H, H-A_2), 6.81 (d, J = 7.2 Hz, 1H, H-A_6); **^{13}C NMR** (100 MHz, Acetone-d_6) δ (ppm): 172.60 (C=O), 155.54 (C=N), 143.78 (Cq-7a), 139.58 (Cq-A_1), 134.68 (Cq-A_3), 133.23 (CH-6), 131.61 (CH-B_4), 131.29 (CH-A_5), 129.61 (CH-$B_{3,5}$), 129.06 (CH-$B_{2,6}$), 127.60 (CH-4), 127.40 (CH-A_4), 127.08 (CH-A_2), 125.85 (CH-A_6), 125.58 (Cq-B_1), 125.24 (Cq-3a), 124.04 (CH-5), 111.86 (CH-7), 98.84 (Cspiro). Anal. Calcd for $C_{21}H_{14}ClN_3O_2 \cdot 0.2H_2O$: C 66.47, H 3.83, N 11.08, Found: C 66.11, H 3.62, N 10.94.

4'-(4-chlorophenyl)-3'-phenyl-4'*H*-spiro[indoline-3,5'-[1,2,4]oxadiazol]-2-one (163c).

Synthesized according to the general procedure, this compound was obtained as a white solid (127.4 mg, 87 % yield).

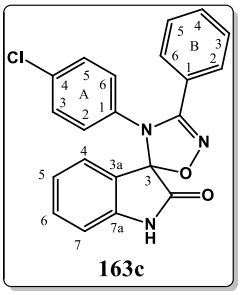

Mp: 161-163 ºC; **IR** (KBr, selected peaks): 3216 (NH), 1725 (C=O), 1622 (C=N), 1490, 1471, 1381, 1209, 588 cm^{-1}; **^{1}H NMR** (400 MHz, Acetone-d_6) δ (ppm): 9.51 (br s, 1H, NH), 7.62 (d, J = 7.6 Hz, 1H, H-4), 7.53 – 7.45 (m, 3H, H-$B_{2,4,6}$), 7.44 – 7.33 (m, 3H, H-6, H-$B_{3,5}$), 7.20 (d, J = 8.6 Hz, 2H, H-$A_{3,5}$), 7.11 (t, J = 7.6 Hz, 1H, H-5), 6.93 (d, J = 7.8 Hz, 1H, H-7), 6.87 (d, J = 8.6 Hz, 2H, H-$A_{2,6}$); **^{13}C NMR** (100 MHz, Acetone-d_6) δ (ppm): 172.67 (C=O), 155.74 (C=N), 143.81 (Cq-7a), 137.04 (Cq-A_1), 133.15 (CH-6), 132.69 (Cq-A_4), 131.53 (CH-B_4), 129.98 (CH-$A_{3,5}$), 129.58 (CH-$B_{3,5}$), 129.16 (CH-$A_{2,6}$), 129.05 (CH-$B_{2,6}$), 127.41 (CH-4), 125.65 (Cq-B_1), 125.35 (Cq-3a), 123.98 (CH-5), 111.82 (CH-7), 98.90 (Cspiro). Anal. Calcd for $C_{21}H_{14}ClN_3O_2 \cdot 0.2H_2O$: C 66.47, H 3.83, N 11.08, Found: C 66.11, H 3.64, N 10.87.

3',4'-bis(3-chlorophenyl)-4'*H*-spiro[indoline-3,5'-[1,2,4]oxadiazol]-2-one (165d).

Synthesized according to the general procedure, this compound was obtained as a white solid (135.1 mg, 85 % yield).

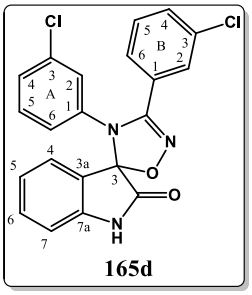

Mp: 143-145 ºC; **IR** (KBr, selected peaks): 3215 (NH), 1726 (C=O), 1622 (C=N), 1558, 1471, 1384, 1207, 788 cm^{-1}; **^{1}H NMR** (400 MHz, Acetone-d_6) δ (ppm): 9.56 (br s, 1H, NH), 7.66 (d, J = 7.4 Hz, 1H, H-4), 7.57 (s, 1H, H-B_2), 7.54 (d, J = 7.5 Hz, 1H, H-B_4), 7.48 – 7.41 (m, 2H, H-$B_{5,6}$), 7.39 (t, J = 7.7 Hz, 1H, H-6), 7.26 – 7.16 (m, 2H, H-$A_{4,5}$), 7.12 (t, J = 7.6 Hz, 1H, H-5), 6.96 (d, J = 7.8 Hz, 1H, H-7), 6.91 (s, 1H, H-A_2), 6.86 (d, J = 7.3 Hz, 1H, H-A_6); **^{13}C NMR** (100 MHz, Acetone-d_6) δ (ppm): 172.44 (C=O), 154.57 (C=N), 143.83 (Cq-7a), 139.20 (Cq-A_1), 134.96 and 134.84 (Cq-A_3 and Cq-B_3), 133.37 (CH-6), 131.62 (CH-B_5), 131.46 (CH-B_4), 131.43 (CH-A_5), 128.81 (CH-B_2), 127.96 (CH-A_4), 127.59 (Cq-B_1), 127.58 (CH-4), 127.54 (CH-B_6), 127.19 (CH-A_2), 126.05 (CH-A_6), 124.95 (Cq-3a), 124.07 (CH-5), 111.90 (CH-7), 99.12 (Cspiro). Anal. Calcd for $C_{21}H_{13}Cl_2N_3O_2 \cdot 0.1H_2O$: C 61.21, H 3.24, N 10.20, Found: C 60.88, H 3.22, N 9.90.

3'-(4-chlorophenyl)-4'-(3-chlorophenyl)-4'*H*-spiro[indoline-3,5'-[1,2,4] oxadiazol] -2-one (165e).

Synthesized according to the general procedure, this compound was obtained as a white solid (127.9 mg, 80 % yield).

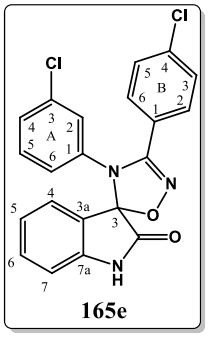

MP: 173-174 ºC; **IR** (KBr, selected peaks): 3228 (NH), 1727 (C=O), 1624 (C=N), 1472, 1379, 1206, 825, 761, 692 cm^{-1}; **^{1}H NMR** (400 MHz, Acetone-d_6) δ (ppm): 9.56 (br s, 1H, NH), 7.63 (d, J = 7.4 Hz, 1H, H-4), 7.53 (d, J = 8.6 Hz, 2H, H-$B_{2,6}$), 7.48 (d, J = 8.6 Hz, 2H, H-$B_{3,5}$), 7.39 (t, J = 7.7 Hz, 1H, H-6), 7.25 – 7.15 (m, 2H, H-$A_{4,5}$), 7.12 (t, J = 7.6 Hz, 1H, H-5), 6.95 (d, J = 7.8 Hz, 1H, H-7), 6.88 (s, 1H, H-A_2), 6.83 (d, J = 7.3 Hz, 1H, H-A_6); **^{13}C NMR** (100 MHz, Acetone-d_6) δ (ppm) 172.50 (C=O), 154.78 (C=N), 143.83 (Cq-7a), 139.33 (Cq-A_1), 137.10 (Cq-B_4), 134.82 (Cq-A_3), 133.34 (CH-6), 131.44 (CH-A_5), 130.74 (CH-$B_{2,6}$), 129.87 (CH-$B_{3,5}$), 127.87 (CH-A_4), 127.48 (CH-4), 127.14 (CH-A_2), 126.04 (CH-A_6), 125.03 (Cq-3a), 124.40 (Cq-B_1), 124.06 (CH-5), 111.89 (CH-7), 99.03 (Cspiro). Anal. Calcd for $C_{21}H_{13}Cl_2N_3O_2 \cdot 0.15H_2O$: C 61.07, H 3.25, N 10.18, Found: C 60.71, H 3.22, N 9.92.

3'-(3-chlorophenyl)-4'-(4-chlorophenyl)-4'*H*-spiro[indoline-3,5'-[1,2,4] oxadiazol]-2-one (165f).

Synthesized according to the general procedure, this compound was obtained as a white solid (134.2 mg, 84 % yield).

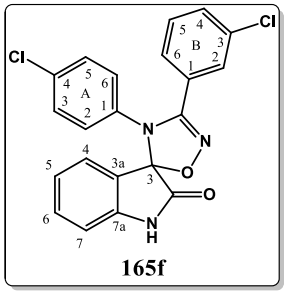

Mp: 176-178 ºC; **IR** (KBr, selected peaks): 3190 (NH), 1725 (C=O), 1624 (C=N), 1554, 1491, 1473, 1377, 1211, 749 cm^{-1}; **^{1}H NMR** (400 MHz, Acetone-d_6) δ (ppm): 9.53 (br s, 1H, NH), 7.64 (d, J = 7.5 Hz, 1H, H-4), 7.55 (s, 1H, H-B_2), 7.54 – 7.50 (m, 1H, H-B_4), 7.43 (t, J = 7.7 Hz, 1H, H-B_5), 7.41 – 7.35 (m, 2H, H-6, H-B_6), 7.23 (d, J = 8.7 Hz, 2H, H-$A_{3,5}$), 7.11 (t, J = 7.5 Hz, 1H, H-5), 6.96 – 6.88 (m, 3H, H-7, H-$A_{2,6}$); **^{13}C NMR** (100 MHz, Acetone-d_6) δ (ppm): 172.51 (C=O), 154.77 (C=N), 143.83 (Cq-7a), 136.63 (Cq-A_1), 134.93 (Cq-B_3), 133.28 (CH-6), 133.03 (Cq-A_4), 131.54 (CH-B_5), 131.40 (CH-B_4), 130.14 (CH-$A_{3,5}$), 129.25 (CH-$A_{2,6}$), 128.77 (CH-B_2), 127.63 (Cq-B_1), 127.54 (CH-4), 127.52 (CH-B_6), 125.03 (Cq-3a), 124.02 (CH-5), 111.86 (CH-7), 99.15 (Cspiro). Anal. Calcd for $C_{21}H_{13}Cl_2N_3O_2 \cdot 0.45H_2O$: C 60.29, H 3.36, N 10.05, Found: C 59.97, H 3.06, N 9.95.

3',4'-bis(4-chlorophenyl)-4'*H*-spiro[indoline-3,5'-[1,2,4]oxadiazol]-2-one (165g).

Synthesized according to the general procedure, this compound was obtained as a white solid (135.8 mg, 85 % yield).

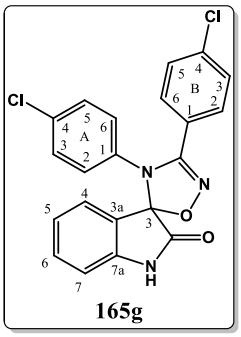

Mp: 104-106 ºC; **IR** (KBr, selected peaks): 3251 (NH), 1735 (C=O), 1621 (C=N), 1492, 1473, 1364, 1203, 1093, 828 cm^{-1}; **^{1}H NMR** (400 MHz, Acetone-d_6) δ (ppm): 9.53 (br s, 1H, NH), 7.61 (d, J = 7.4 Hz, 1H, H-4), 7.54 – 7.43 (m, 4H, H-B), 7.38 (t, J = 7.7 Hz, 1H, H-6), 7.23 (d, J = 8.6 Hz, 2H, H-$A_{3,5}$), 7.11 (t, J = 7.5 Hz, 1H, H-5), 6.93 (d, J = 7.8 Hz, 1H, H-7), 6.88 (d, J = 8.6 Hz, 2H, H-$A_{2,6}$); **^{13}C NMR** (100 MHz, Acetone-d_6) δ (ppm): 172.62 (C=O), 154.98 (C=N), 143.88 (Cq-7a), 137.02 (Cq-B_4), 136.74 (Cq-A_1), 133.24 (CH-6), 132.92 (Cq-A_4), 130.71 (CH-$B_{2,6}$), 130.11 (CH-$A_{3,5}$), 129.83 (CH-$B_{3,5}$), 129.21 (CH-$A_{2,6}$), 127.46 (CH-4), 125.11 (Cq-3a), 124.42 (Cq-B_1), 124.00 (CH-5), 111.87 (CH-7), 99.07 (Cspiro). Anal. Calcd for $C_{21}H_{13}Cl_2N_3O_2 \cdot 0.5H_2O \cdot 0.05Et_2O$: C 60.20, H 3.46, N 9.94, Found: C 60.33, H 3.57, N 9.54.

5-chloro-3',4'-diphenyl-4'*H*-spiro[indoline-3,5'-[1,2,4]oxadiazoline]-2-one (165h).

Synthesized according to the general procedure, this compound was obtained as a white solid (111.0 mg, 76 % yield).

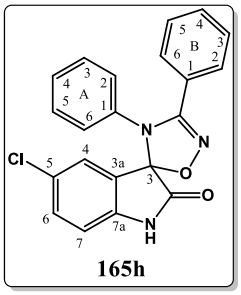

Mp: 232-234 ºC; **IR** (KBr, selected peaks): 3242 (NH), 1743 (C=O), 1620 (C=N), 1498, 1474, 1394, 1213, 828, 752 cm^{-1}; **^{1}H NMR** (400 MHz, Acetone-d_6) δ (ppm): 9.59 (br s, 1H, NH), 7.70 (d, J = 1.6 Hz, 1H, H-4), 7.51 – 7.43 (m, 3H, H-$B_{2,4,6}$), 7.40 – 7.34 (m, 3H, H-6, H-$B_{3,5}$), 7.22 – 7.11 (m, 3H, H-$A_{3,4,5}$), 6.96 – 6.90 (m, 3H, H-7, H-$A_{2,6}$); **^{13}C NMR** (100 MHz, Acetone-d_6) δ (ppm): 172.69 (C=O), 155.96 (C=N), 142.49 (C-7a), 137.74 (Cq-A_1), 132.86 (CH-6), 131.42 (CH-B_4), 130.02 (CH-$A_{3,5}$), 129.41 (CH-$B_{3,5}$), 129.13 (CH-$B_{2,6}$), 128.59 (Cq-5), 127.94 (CH-A_4), 127.78 (CH-$A_{2,6}$), 127.64 (Cq-3a), 127.47 (CH-4), 125.69 (Cq-B_1), 113.21 (CH-7), 98.73 (Cspiro). Anal. Calcd for $C_{21}H_{14}ClN_3O_2 \cdot 0.6H_2O$: C 65.23, H 3.97, N 10.87, Found: C 64.88, H 3.71, N 10.66.

5-chloro-4'-(3-chlorophenyl)-3'-phenyl-4'*H*-spiro[indoline-3,5'-[1,2,4] oxadiazol]-2-one (165i).

Synthesized according to the general procedure, this compound was obtained as a white solid (78.6 mg, 56 % yield).

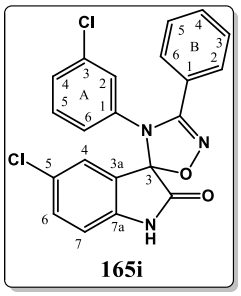

Mp: 186-188 ºC; **IR** (KBr, selected peaks): 3213 (NH), 1743 (C=O), 1620 (C=N), 1589, 1476, 1385, 1266, 760, 692 cm^{-1}; **^{1}H NMR** (400 MHz, Acetone-d_6) δ (ppm): 9.67 (br s, 1H, NH), 7.75 (s, 1H, H-4), 7.52 (d, J = 7.4 Hz, 2H, H-$B_{2,6}$), 7.49 (d, J = 7.2 Hz, 1H, H-B_4), 7.46 – 7.37 (m, 3H, H-6, H-$B_{3,5}$), 7.26 – 7.15 (m, 2H, H-$A_{4,5}$), 6.99 (d, J = 8.3 Hz, 1H, H-7), 6.93 (s, 1H, H-A_2), 6.87 (d, J = 7.4 Hz, 1H, H-A_6); **^{13}C NMR** (100 MHz, Acetone-d_6) δ (ppm): 172.33 (C=O), 155.57 (C=N), 142.43 (Cq-7a), 139.24 (Cq-A_1), 134.79 (Cq-A_3), 133.13 (CH-6), 131.69 (CH-B_4), 131.43 (CH-A_5), 129.59 (CH-$B_{3,5}$), 129.17 (CH-$B_{2,6}$), 128.79 (Cq-5), 127.90 (CH-A_4), 127.50 (CH-4), 127.28 (CH-A_2), 127.18 (Cq-3a), 125.95 (CH-A_6), 125.29 (Cq-B_1), 113.39 (CH-7), 98.61 (Cspiro). Anal. Calcd for $C_{21}H_{13}Cl_2N_3O_2 \cdot 0.15H_2O$: C 61.07, H 3.25, N 10.18, Found: C 60.78, H 3.15, N 10.06.

5-chloro-3',4'-bis(3-chlorophenyl)-4'*H*-spiro[indoline-3,5'-[1,2,4]oxadiazol]-2-one (165j).

Synthesized according to the general procedure, this compound was obtained as a white solid (82.2 mg, 54 % yield).

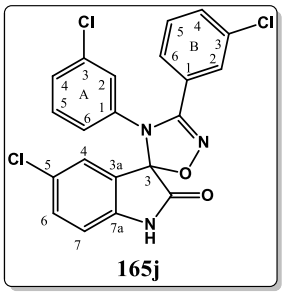

Mp: 215-217 ºC; **IR** (KBr, selected peaks): 3211 (NH), 1735 (C=O), 1617 (C=N), 1593, 1560, 1476, 1373, 854, 819 cm^{-1}; **^{1}H NMR** (400 MHz, Acetone-d_6) δ (ppm): 9.69 (br s, 1H, NH), 7.78 (d, J = 1.6 Hz, 1H, H-4), 7.58 (d, J = 0.8 Hz, 1H-B_2), 7.56 – 7.50 (m, 1H, H-B_4), 7.47 – 7.40 (m, 3H, H-6, H-$B_{5,6}$), 7.28 – 7.19 (m, 2H, H-$A_{4,5}$), 7.01 – 6.96 (m, 2H, H-7, H-A_2), 6.92 (d, J = 7.6 Hz, 1H, H-A_6); **^{13}C NMR** (100 MHz, Acetone-d_6) δ (ppm): 172.18 (C=O), 154.59 (C=N), 142.47 (Cq-7a), 138.84 (Cq-A_1), 134.94 (Cq-A_3 and Cq-B_3), 133.26 (CH-6), 131.70 (CH-B_5), 131.60 (CH-B_4), 131.40 (CH-A_5), 128.95 (CH-B_2), 128.83 (Cq-5), 128.26 (CH-A_4), 127.69 (CH-4), 127.65 (CH-B_6), 127.38 (CH-A_2), 127.30 (Cq-3a), 126.93 (Cq-B_1), 126.16 (CH-A_6), 113.44 (CH-7), 98.87 (Cspiro). Anal. Calcd for $C_{21}H_{12}Cl_3N_3O_2 \cdot 0.15H_2O$: C 56.37, H 2.78, N 9.39, Found: C 56.00, H 2.70, N 9.15.

5-chloro-4'-(3-chlorophenyl)-3'-(4-chlorophenyl)-4'*H*-spiro[indoline-3,5'-[1,2,4]oxadiazol]-2-one (165k).

Synthesized according to the general procedure, this compound was obtained as a white solid (88.4 mg, 58 % yield).

Mp: 241-243 ºC; **IR** (KBr, selected peaks): 3178 (NH), 1744 (C=O), 1616 (C=N), 1590, 1475, 1384, 1197, 760, 690 cm^{-1}; **^{1}H NMR** (400 MHz, Acetone-d_6) δ (ppm): 9.69 (br s, 1H, NH), 7.75 (d, J = 1.7 Hz, 1H, H-4), 7.54 (d, J = 8.5 Hz, 2H, H-$B_{2,6}$), 7.48 (d, J = 8.5

Hz, 2H, H-$B_{3,5}$), 7.42 (dd, *J* = 8.3, 1.7 Hz, 1H, H-6), 7.27 – 7.19 (m, 2H, H-$A_{4,5}$), 6.99 (d, *J* = 8.3 Hz, 1H, H-7), 6.95 (s, 1H, H-A_2), 6.89 (d, *J* = 7.5 Hz, 1H, H-A_6); **^{13}C NMR** (100 MHz, Acetone-d_6) δ (ppm): 172.24 (C=O), 154.81 (C=N), 142.50 (Cq-7a), 138.99 (Cq-A_1), 137.20 (Cq-B_4), 134.93 (Cq-A_3), 133.23 (CH-6), 131.59 (CH-A_5), 130.87 (CH-$B_{2,6}$), 129.86 (CH-$B_{3,5}$), 128.82 (Cq-5), 128.17 (CH-A_4), 127.59 (CH-4), 127.33 (CH-A_2), 127.01 (Cq-3a), 126.16 (CH-A_6), 124.13 (Cq-B_1), 113.44 (CH-7), 98.79 (Cspiro). Anal. Calcd for $C_{21}H_{12}Cl_3N_3O_2 \cdot 0.15H_2O$: C 56.37, H 2.78, N 9.39, Found: C 56.00, H 2.83, N 9.04.

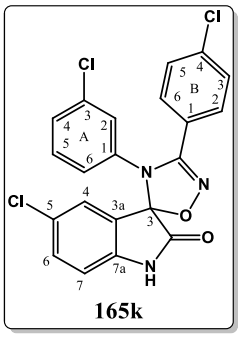

5-chloro-4'-(4-chlorophenyl)-3'-phenyl-4'*H*-spiro[indoline-3,5'-[1,2,4] oxadiazol]-2-one (165l).

Synthesized according to the general procedure, this compound was obtained as a white solid (97.5 mg, 69% yield).

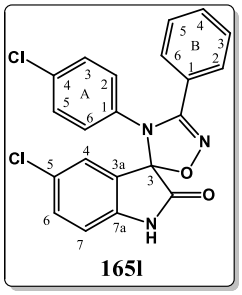

Mp: 274-276 ºC; **IR** (KBr, selected peaks): 3176 (NH), 1748 (C=O), 1617 (C=N), 1491, 1385, 1248, 1198, 1089, 696 cm^{-1}; **^{1}H NMR** (400 MHz, Acetone-d_6) δ (ppm): 9.61 (br s, 1H, NH), 7.73 (d, *J* = 1.7 Hz, 1H, H-4), 7.53 – 7.45 (m, 3H, H-$B_{2,4,6}$), 7.44 – 7.37 (m, 3H, H-6, H-$B_{3,5}$), 7.24 (d, *J* = 8.6 Hz, 2H, H-$A_{3,5}$), 6.97 (d, *J* = 8.4 Hz, 1H, H-7), 6.93 (d, *J* = 8.6 Hz, 2H, H-$A_{2,6}$); **^{13}C NMR** (100 MHz, Acetone-d_6) δ (ppm): 172.38 (C=O), 155.78 (C=N), 142.49 (Cq-7a), 136.69 (Cq-A_1), 133.07 (CH-6), 133.01 (Cq-A_4), 131.62 (CH-B_4), 130.12 (CH-$A_{3,5}$), 129.56 (CH-$B_{3,5}$), 129.34 (CH-$A_{2,6}$), 129.16 (CH-$B_{2,6}$), 128.75 (Cq-5), 127.48 (CH-4), 127.36 (Cq-3a), 125.36 (Cq-B_1), 113.36 (CH-7), 98.69 (Cspiro). Anal. Calcd for $C_{21}H_{13}Cl_2N_3O_2 \cdot 0.15H_2O$: C 61.07, H 3.25, N 10.18, Found: C 60.75, H 3.22, N 10.25.

5-chloro-3'-(3-chlorophenyl)-4'-(4-chlorophenyl)-4'*H*-spiro[indoline-3,5'-[1,2,4]oxadiazol]-2-one (165m).

Synthesized according to the general procedure, this compound was obtained as a white solid (100.9 mg, 66 % yield).

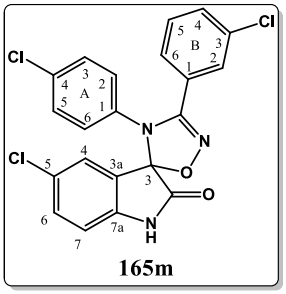

Mp: 206-208 ºC; **IR** υ_{max} (KBr, selected peaks): 3176 (NH), 1747 (C=O), 1620 (C=N), 1493, 1478, 1385, 1198, 1096, 828 cm^{-1}; **^{1}H NMR** (400 MHz, Acetone-d_6) δ (ppm): 9.65 (br s, 1H, NH), 7.77 (s, 1H, H-4), 7.56 (s, 1H, H-B_2), 7.52 (d, *J* = 7.5 Hz, 1H, H-B_4), 7.46 – 7.38 (m, 3H, H-6, H-$B_{5,6}$), 7.27 (d, *J* = 8.6 Hz, 2H, H-$A_{3,5}$), 7.00 – 6.95 (m, 3H, H-7, H-$A_{2,6}$); **^{13}C NMR** (100 MHz, Acetone-d_6) δ (ppm): 172.20 (C=O), 154.80 (C=N), 142.48 (Cq-7a), 136.28 (Cq-A_1), 134.91 (Cq-B_3), 133.33 (Cq-A_4),

133.19 (CH-6), 131.62 (CH-B_5), 131.39 (CH-B_4), 130.28 (CH-$A_{3,5}$), 129.43 (CH-$A_{2,6}$), 128.92 (CH-B_2), 128.79 (Cq-5), 127.66 (CH-4), 127.61 (CH-B_6), 127.36 (Cq-3a), 127.07 (Cq-B_1), 113.41 (CH-7), 98.92 (Cspiro). Anal. Calcd for $C_{21}H_{12}Cl_3N_3O_2 \cdot 0.7H_2O$: C 55.14, H 2.96, N 9.19, Found: C 54.82, H 2.63, N 8.99.

5-chloro-3',4'-bis(4-chlorophenyl)-4'*H*-spiro[indoline-3,5'-[1,2,4]oxadiazol]-2-one (165n).

Synthesized according to the general procedure, this compound was obtained as a white solid (98.2 mg, 64 % yield).

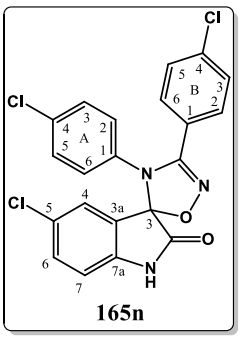

Mp: 218-220 ºC; **IR** (KBr, selected peaks): 3179 (NH), 1747 (C=O), 1616 (C=N), 1492, 1414, 1388, 1194, 1090, 829 cm^{-1}; **^{1}H NMR** (400 MHz, Acetone-d_6) δ (ppm): 9.62 (br s, 1H, NH), 7.73 (d, J = 1.7 Hz, 1H, H-4), 7.51 (d, J = 8.5 Hz, 2H, H-$B_{2,6}$), 7.46 (d, J = 8.6 Hz, 2H, H-$B_{3,5}$), 7.41 (dd, J = 8.3, 1.8 Hz, 1H, H-6), 7.26 (d, J = 8.6 Hz, 2H, H-$A_{3,5}$), 6.97 (d, J = 8.3 Hz, 1H, H-7), 6.95 (d, J = 8.6 Hz, 2H, H-$A_{2,6}$); **^{13}C NMR** (100 MHz, Acetone-d_6) δ (ppm): 172.27 (C=O), 155.00 (C=N), 142.51 (Cq-7a), 137.13 (Cq-B_4), 136.41 (Cq-A_1), 133.24 (Cq-A_4), 133.16 (CH-6), 130.82 (CH-$B_{2,6}$), 130.26 (CH-$A_{3,5}$), 129.82 (CH-$B_{3,5}$), 129.37 (CH-$A_{2,6}$), 128.77 (Cq-5), 127.55 (CH-4), 127.16 (Cq-3a), 124.16 (Cq-B_1), 113.41 (CH-7), 98.85 (Cspiro). Anal. Calcd for $C_{21}H_{12}Cl_3N_3O_2$: C 56.71, H 2.73, N 9.45, Found: C 56.97, H 2.75, N 9.31.

4'-(*tert*-butyl)-5-chloro-3'-(4-chlorophenyl)-4'*H*-spiro[indoline-3,5'-[1,2,4] oxadiazol]-2-one (165o).

Synthesized according to the general procedure, this compound was obtained as a white solid (90.5 mg, 55 % yield).

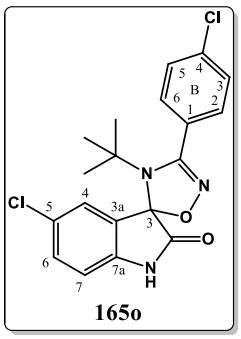

Mp: 275-277 ºC; **IR** (KBr, selected peaks): 3338 (NH), 1763 (C=O), 1619 (C=N), 1473, 1385, 1190, 1262, 1190, 826 cm^{-1}; **^{1}H NMR** (400 MHz, Acetone-d_6) δ (ppm): 9.71 (br s, 1H, NH), 7.77 (d, J = 1.8 Hz, 1H, H-4), 7.75 (d, J = 8.4 Hz, 2H, H-$B_{2,6}$), 7.59 (d, J = 8.4 Hz, 2H, H-$B_{3,5}$), 7.43 (dd, J = 8.3, 1.7 Hz, 1H, H-6), 7.03 (d, J = 8.3 Hz, 1H, H-7), 1.14 (s, 9H, C(CH_3)$_3$); **^{13}C NMR** (100 MHz, Acetone-d_6) δ (ppm): 174.76 (C=O), 156.34 (C=N), 141.05 (Cq-7a), 136.61 (Cq-B_4), 133.61 (CH-$B_{2,6}$), 132.26 (CH-6), 131.28 (Cq-3a), 129.29 (CH-$B_{3,5}$), 128.64 (Cq-5), 127.69 (Cq-B_1), 126.73 (CH-4), 113.48 (CH-7), 98.12 (Cspiro), 55.94 ($\underline{C}$(CH_3)$_3$), 31.13 (C($\underline{C}$$H_3$)$_3$). Anal. Calcd for $C_{19}H_{17}Cl_2N_3O_2 \cdot 1.35H_2O$: C 55.04, H 4.80, N 10.14, Found: C 54.71 H 4.82, N 9.90.

6-chloro-3',4'-diphenyl-4'*H*-spiro[indoline-3,5'-[1,2,4]oxadiazol]-2-one (165p).

Synthesized according to the general procedure, this compound was obtained as a white solid (118.1 mg, 81 % yield).

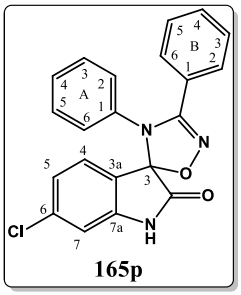

Mp: 245-247 ºC; **IR** (KBr, selected peaks): 3201 (NH), 1748 (C=O), 1621 (C=N), 1595, 1494, 1385, 1213, 756, 690 cm^{-1}; **^{1}H NMR** (400 MHz, Acetone-d_6) δ (ppm): 9.62 (br s, 1H, NH), 7.63 (d, J = 8.0 Hz, 1H, H-4), 7.50 – 7.42 (m, 3H, H-$B_{2,4,6}$), 7.41 – 7.34 (m, 2H, H-$B_{3,5}$), 7.21 – 7.13 (m, 3H, H-$A_{3,4,5}$), 7.11 (d, J = 8.0 Hz, 1.6 Hz, 1H, H-5), 6.95 (d, J = 1.6 Hz, 1H, H-7), 6.92 – 6.87 (m, 2H, H-$A_{2,6}$); **^{13}C NMR** (100 MHz, Acetone-d_6) δ (ppm): 172.84 (C=O), 155.99 (C=N), 145.14 (Cq-7a), 137.98 (Cq-6), 137.87 (Cq-A_1), 131.44 (Cq-B_4), 130.03 (CH-$A_{3,5}$), 129.45 (CH-$B_{3,5}$), 129.06 (CH-$B_{2,6}$), 128.88 (CH-4), 127.91 (CH-A_4), 127.79 (CH-$A_{2,6}$), 125.78 (Cq-B_1), 124.36 (Cq-3a), 123.78 (CH-5), 112.08 (CH-7), 98.47 (Cspiro). Anal. Calcd for $C_{21}H_{14}ClN_3O_2 \cdot 0.6H_2O$: C 65.23, H 3.97, N 10.87, Found: C 64.88 H 3.71, N 10.66.

6-chloro-3'-(4-methylphenyl)-4'-phenyl-4'*H*-spiro[indoline-3,5'-[1,2,4] oxadiazol]-2-one (165q).

Synthesized according to the general procedure, this compound was obtained as a white solid (106.3 mg, 70 % yield).

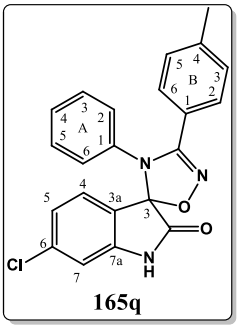

Mp: 269-271 ºC; **IR** (KBr, selected peaks): 3277 (NH), 1737 (C=O), 1614 (C=N), 1385, 1316, 1203, 1143, 812, 751 cm^{-1}; **^{1}H NMR** (400 MHz, Acetone-d_6) δ (ppm): 9.59 (br s, 1H, NH), 7.61 (d, J = 8.0 Hz, 1H, H-4), 7.34 (d, J = 7.9 Hz, 2H, H-$B_{2,6}$), 7.21 – 7.13 (m, 5H, H-$B_{3,5}$, H-$A_{3,4,5}$), 7.11 (d, J = 8.0 Hz, 1H, H-5), 6.94 (s, 1H, H-7), 6.89 (d, J = 7.6 Hz, 2H, H-$A_{2,6}$), 2.32 (s, 3H, CH_3); **^{13}C NMR** (100 MHz, Acetone-d_6) δ (ppm): 172.95 (C=O), 155.95 (C=N), 145.20 (Cq-7a), 141.70 (Cq-B_4), 138.02 (Cq-6), 137.93 (Cq-A_1), 130.06 and 130.01 (CH-$B_{3,5}$ and CH-$A_{3,5}$), 129.00 (CH-$B_{2,6}$), 128.86 (CH-4), 127.86 (CH-A_4), 127.83 (CH-$A_{2,6}$), 124.49 (Cq-3a), 123.76 (CH-5), 122.87 (Cq-B_1), 112.07 (CH-7), 98.39 (Cspiro) 21.34 (CH_3). Anal. Calcd for $C_{22}H_{16}ClN_3O_2 \cdot 0.3H_2O$: C 66.85, H 4.24, N 10.63, Found: C 66.51, H 4.17, N 10.41.

6-chloro-3'-(4-chlorophenyl)-4'-phenyl-4'*H*-spiro[indoline-3,5'-[1,2,4] oxadiazol]-2-one (165r).

Synthesized according to the general procedure, this compound was obtained as a white solid (131.1 mg, 82 % yield).

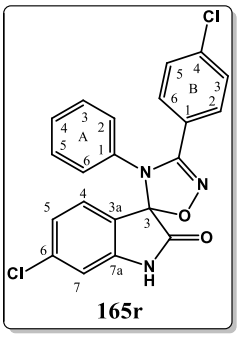

Mp: 125-127 ºC; **IR** (KBr, selected peaks): 3234 (NH), 1735 (C=O), 1616 (C=N), 1446, 1406, 1384, 1207, 1142, 701 cm^{-1}; **^{1}H NMR** (400 MHz, Acetone-d_6) δ (ppm): 9.60 (br s, 1H, NH), 7.65 (d, *J* = 8.0 Hz, 1H, H-4), 7.49 (d, *J* = 8.6 Hz, 2H, H-$B_{2,6}$), 7.45 (d, *J* = 8.6 Hz, 2H, H-$B_{3,5}$), 7.26 – 7.17 (m, 3H, H-$A_{3,4,5}$), 7.14 (d, *J* = 8.0 Hz, 1H, H-5), 6.97 (s, 1H, H-7), 6.92 (d, *J* = 7.6 Hz, 2H, H-$A_{2,6}$); **^{13}C NMR** (100 MHz, Acetone-d_6) δ (ppm): 172.76 (C=O), 155.21 (C=N), 145.23 (Cq-7a), 138.08 (Cq-6), 137.59 (Cq-A_1), 136.93 (Cq-B_4), 130.70 (CH-$B_{2,6}$), 130.17 (CH-$A_{3,5}$), 129.71 (CH-$B_{3,5}$), 128.94 (CH-4), 128.13 (CH-A_4), 127.83 (CH-$A_{2,6}$), 124.58 (Cq-3a), 124.15 (Cq-B_1), 123.81 (CH-5), 112.15 (CH-7), 98.63 (Cspiro). Anal. Calcd for $C_{21}H_{13}Cl_2N_3O_2 \cdot 0.55H_2O$: C 60.03, H 3.39, N 10.00, Found: C 59.71, H 3.27, N 9.62.

6-chloro-3',4'-bis(3-chlorophenyl)-4'*H*-spiro[indoline-3,5'-[1,2,4]oxadiazoline]-2-one (165s).

Synthesized according to the general procedure, this compound was obtained as a white solid (114.3 mg, 75 % yield).

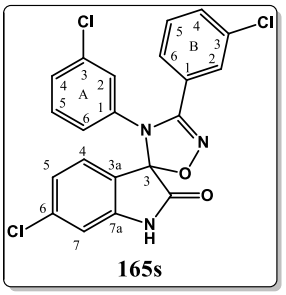

Mp: 209-211 ºC; **IR** (KBr, selected peaks): 3186 (NH), 1731 (C=O), 1617 (C=N), 1484, 1384, 1267, 1205, 821 cm^{-1}; **^{1}H NMR** (400 MHz, Acetone-d_6) δ (ppm): 9.74 (br s, 1H, NH), 7.69 (d, *J* = 8.0 Hz, 1H, H-4), 7.56 (s, 1H, H-B_2), 7.54 (d, *J* = 7.7 Hz, 1H, H-B_4), 7.48 – 7.39 (m, 2H, H-$B_{5,6}$), 7.28 – 7.19 (m, 2H, H-$A_{4,5}$), 7.15 (d, *J* = 8.0 Hz, 1H, H-5), 7.00 (s, 1H, H-7), 6.94 (s, 1H, H-A_2), 6.89 (d, *J* = 7.4 Hz, 1H, H-A_6); **^{13}C NMR** (100 MHz, Acetone-d_6) δ (ppm): 172.39 (C=O), 154.63 (C=N), 145.21 (Cq-7a), 138.97 (Cq-A_1), 138.41 (Cq-6), 134.97 (Cq-B_3), 134.95 (Cq-A_3), 131.71 (CH-B_5), 131.63 (CH-A_5), 131.45 (CH-B_4), 129.02 (CH-4), 128.84 (CH-B_2), 128.23 (CH-A_4), 127.61 (CH-B_6), 127.39 (CH-A_2), 127.37 (Cq-B_1), 126.14 (CH-A_6), 124.01 (CH-5), 123.61 (Cq-3a), 112.35 (CH-7), 98.62 (Cspiro). Anal. Calcd for $C_{21}H_{12}Cl_3N_3O_2$: C 56.71, H 2.73, N 9.45, Found: C 56.42, H 2.70, N 9.27.

6-chloro-4'-(3-chlorophenyl)-3'-(4-chlorophenyl)-4'*H*-spiro[indoline-3,5'-[1,2,4]oxadiazoline]-2-one (165t).

Synthesized according to the general procedure, this compound was obtained as a white solid (119.0 mg, 78 % yield).

Mp: 229-231 C; **IR** (KBr, selected peaks): 3267 (NH), 1736 (C=O), 1617 (C=N), 1405, 1384, 1142, 1099, 693 cm^{-1}; **^{1}H NMR** (400 MHz, Acetone-d_6) δ (ppm): 9.65 (br s, 1H, NH), 7.66 (d, *J* = 8.0 Hz, 1H, H-4), 7.52 (d, *J* = 8.4 Hz, 2H, H-$B_{2,6}$), 7.47 (d, *J* = 8.4 Hz, 2H, H-$B_{3,5}$), 7.29 – 7.18 (m, 2H, H-$A_{4,5}$), 7.14 (d, *J* = 8.0 Hz, 1H, H-5), 7.00 (s, 1H, H-7),

6.91 (s, 1H, H-A_2), 6.86 (d, *J* = 7.1 Hz, 1H, H-A_6); **^{13}C NMR** (100 MHz, Acetone-d_6) *δ* (ppm): 172.44 (C=O), 154.84 (C=N), 145.21 (Cq-7a), 139.10 (Cq-A_1), 138.37 (Cq-6), 137.20 (Cq-B_4), 134.92 (Cq-A_3), 131.60 (CH-A_5), 130.77 (CH-$B_{2,6}$), 129.89 (CH-$B_{3,5}$), 128.96 (CH-4), 128.14 (CH-A_4), 127.34 (CH-A_2), 126.13 (CH-A_6), 124.18 (Cq-B_1), 124.00 (CH-5), 123.68 (Cq-3a), 112.33 (CH-7), 98.54 (Cspiro). Anal. Calcd for $C_{21}H_{12}Cl_3N_3O_2 \cdot 0.9H_2O$: C 54.72, H 3.02, N 9.12, Found: C 54.78 H 2.65, N 8.72.

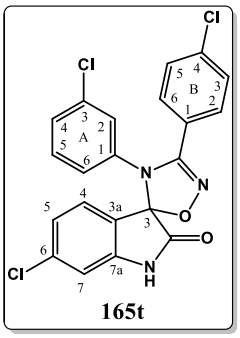

165t

6-chloro-4'-(4-chlorophenyl)-3'-phenyl-4'*H*-spiro[indoline-3,5'-[1,2,4] oxadiazol]-2-one (165u).

Synthesized according to the general procedure, this compound was obtained as a white solid (112.2 mg, 80 % yield).

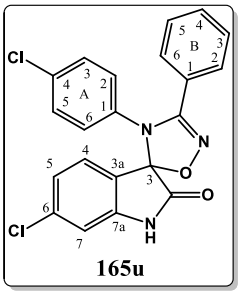

165u

Mp: 226-228 ºC; **IR** (KBr, selected peaks): 3231 (NH), 1731 (C=O), 1617 (C=N), 1384, 1211, 1141, 821, 692 cm^{-1}; **^{1}H NMR** (400 MHz, Acetone-d_6) *δ* (ppm): 9.62 (br s, 1H, NH), 7.65 (d, *J* = 8.0 Hz, 1H, H-4), 7.52 – 7.45 (m, 3H, H-$B_{2,4,6}$), 7.44 – 7.38 (m, 2H, H-$B_{3,5}$), 7.23 (d, *J* = 8.6 Hz, 2H, H-$A_{3,5}$), 7.15 (d, *J* = 8.0 Hz, 1H, H-5), 6.98 (s, 1H, H-7), 6.89 (d, *J* = 8.6 Hz, 2H, H-$A_{2,6}$); **^{13}C NMR** (100 MHz, Acetone-d_6) *δ* (ppm): 172.57 (C=O), 155.81 (C=N), 145.21 (Cq-7a), 138.20 (Cq-6), 136.84 (Cq-A_1), 132.96 (Cq-A_4), 131.64 (CH-B_4), 130.14 (CH-$A_{3,5}$), 129.61 (CH-$B_{3,5}$), 129.30 (CH-$A_{2,6}$), 129.10 (CH-$B_{2,6}$), 128.90 (CH-4), 125.46 (Cq-B_1), 124.08 (Cq-3a), 123.95 (CH-5), 112.27 (CH-7), 98.43 (Cspiro). Anal. Calcd for $C_{21}H_{13}Cl_2N_3O_2 \cdot 0.55H_2O$: C 60.03, H 3.39, N 10.00, Found: C 59.71 H 3.07, N 9.82.

6-chloro-3'-(3-chlorophenyl)-4'-(4-chlorophenyl)-4'*H*-spiro[indoline-3,5'-[1,2,4]oxadiazol]-2-one (165v).

Synthesized according to the general procedure, this compound was obtained as a white solid (122.5 mg, 80 % yield).

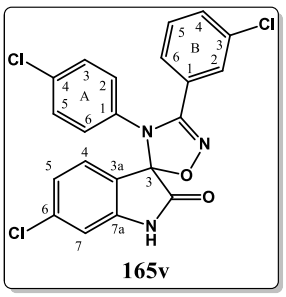

165v

Mp: 214-216 ºC; **IR** (KBr, selected peaks): 3261 (NH), 1733 (C=O), 1617 (C=N), 1492, 1431, 1384, 830, 749 cm^{-1}; **^{1}H NMR** (400 MHz, Acetone-d_6) *δ* (ppm): 9.71 (br s, 1H, NH), 7.68 (d, *J* = 8.0 Hz, 1H, H-4), 7.56 – 7.50 (m, 2H, H-$B_{2,4}$), 7.44 (t, *J* = 7.6 Hz, 1H, H-B_5), 7.39 (d, *J* = 7.6 Hz, 1H, H-B_6), 7.26 (d, *J* = 8.7 Hz, 2H, H-$A_{3,5}$), 7.15 (dd, *J* = 8.0, 1.7 Hz, 1H, H-5), 6.98 (d, *J* = 1.6 Hz, 1H, H-7), 6.94 (d, *J* = 8.7 Hz, 2H H-$A_{2,6}$); **^{13}C NMR** (100 MHz, Acetone-d_6) *δ* (ppm): 172.42 (C=O), 154.83 (C=N), 145.25 (Cq-7a), 138.33 (Cq-6), 136.42 (Cq-A_1), 134.95 (Cq-B_3), 133.28 (Cq-A_4), 131.64

(CH-B_5), 131.44 (CH-B_4), 130.30 (CH-$A_{3,5}$), 129.38 (CH-$A_{2,6}$), 129.01 (CH-4), 128.82 (CH-B_2), 127.59 (CH-B_6), 127.45 (Cq-B_1), 123.98 (CH-5), 123.78 (Cq-3a), 112.33 (CH-7), 98.67 (Cspiro) ppm. Anal. Calcd for $C_{21}H_{12}Cl_3N_3O_2 \cdot 0.10H_2O$: C 56.49, H 2.76, N 9.41, Found: C 56.11, H 2.83, N 9.20.

6-chloro-3',4'-bis(4-chlorophenyl)-4'*H*-spiro[indoline-3,5'-[1,2,4]oxadiazol]-2-one (165w).

Synthesized according to the general procedure, this compound was obtained as a white solid (120.7 mg, 79 % yield).

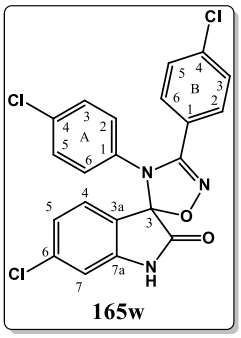

Mp: 222-224 ºC; **IR** (KBr, selected peaks): 3242 (NH), 1736 (C=O), 1616 (C=N), 1496, 1383, 1207, 1139, 830 cm^{-1}; **^{1}H NMR** (400 MHz, Acetone-d_6) δ (ppm): 9.62 (br s, 1H, NH), 7.65 (d, J = 8.0 Hz, 1H, H-4), 7.50 (d, J = 8.6 Hz, 2H, H-$B_{2,6}$), 7.46 (d, J = 8.6 Hz, 2H, H-$B_{3,5}$), 7.25 (d, J = 8.6 Hz, 2H, H-$A_{3,5}$), 7.14 (d, J = 8.0 Hz, 1H, H-5), 6.98 (s, 1H, H-7), 6.91 (d, J = 8.6 Hz, 2H, H-$A_{2,6}$); **^{13}C NMR** (100 MHz, Acetone-d_6) δ (ppm): 172.45 (C=O), 155.02 (C=N), 145.22 (Cq-7a), 138.29 (Cq-6), 137.13 (Cq-B_4), 136.53 (Cq-A_1), 133.17 (Cq-A_4), 130.73 (CH-$B_{2,6}$), 130.26 (CH-$A_{3,5}$), 129.86 (CH-$B_{3,5}$), 129.31 (CH-$A_{2,6}$), 128.95 (CH-4), 124.22 (Cq-B_1), 123.97 (CH-5), 123.83 (Cq-3a), 112.30 (CH-7), 98.57 (Cspiro). Anal. Calcd for $C_{21}H_{12}Cl_3N_3O_2 \cdot 0.5H_2O$: C 55.59, H 2.89, N 9.26, Found: C 55.48 H 2.81, N 8.88.

5-bromo-3',4'-diphenyl-4'*H*-spiro[indoline-3,5'-[1,2,4]oxadiazol]-2-one (165x).

Synthesized according to the general procedure, this compound was obtained as a white solid (101.9 mg, 73 % yield).

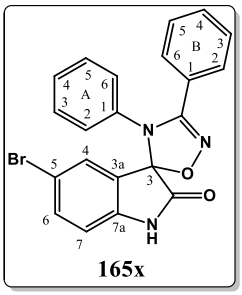

Mp: 246-248 ºC; **IR** (KBr, selected peaks): 3250 (NH), 1735 (C=O), 1617 (C=N), 1444, 1385, 1142, 1068, 823 cm^{-1}; **^{1}H NMR** (400 MHz, Acetone-d_6) δ (ppm): 9.61 (br s, 1H, NH), 7.82 (d, J = 1.7 Hz, 1H, H-4), 7.53 (dd, J = 8.3, 1.8 Hz, 1H, H-6), 7.51 – 7.43 (m, 3H, H-$B_{2,4,6}$), 7.41 – 7.34 (m, 2H, H-$B_{3,5}$), 7.22 – 7.11 (m, 3H, H-$A_{3,4,5}$), 6.96 – 6.86 (m, 3H, H-7, H-$A_{2,6}$); **^{13}C NMR** (100 MHz, Acetone-d_6) δ (ppm): 172.51 (C=O), 155.97 (C=N), 142.96 (Cq-7a), 137.76 (Cq-A_1), 135.78 (CH-6), 131.43 (CH-B_4), 130.29 (CH-4), 130.04 (CH-$A_{3,5}$), 129.42 (CH-$B_{3,5}$), 129.15 (CH-$B_{2,6}$), 128.02 (Cq-3a), 127.96 (CH-A_4), 127.80 (CH-$A_{2,6}$), 125.71 (Cq-B_1), 115.72 (Cq-5), 113.67 (CH-7), 98.68 (Cspiro). Anal. Calcd for $C_{21}H_{14}BrN_3O_2$: C 60.01, H 3.36, N 10.00, Found: C 60.09, H 3.18, N 10.28.

5-bromo-4'-(4-chlorophenyl)-3'-phenyl-4'*H*-spiro[indoline-3,5'-[1,2,4] oxadiazol]-2-one (165y).

Synthesized according to the general procedure, this compound was obtained as a white solid (92.1 mg, 68 % yield).

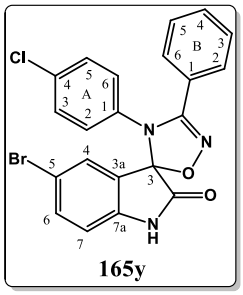

165y

Mp: 290-292 ºC; **IR** (KBr, selected peaks): 3174 (NH), 1748 (C=O), 1619 (C=N), 1491, 1473, 1392, 1253, 1197, 694 cm^{-1}; **^{1}H NMR** (400 MHz, Acetone-d_6) δ (ppm): 10.00 (br s, 1H, NH), 7.82 (s, 1H, H-4), 7.54 (d, J = 7.9 Hz, 1H, H-6), 7.51 – 7.44 (m, 3H, H-$B_{2,4,6}$), 7.43 – 7.36 (m, 2H, H-$B_{3,5}$), 7.22 (d, J = 8.0 Hz, 2H, H-$A_{3,5}$), 6.95 – 6.88 (m, 3H, H-7, H-$A_{2,6}$); **^{13}C NMR** (100 MHz, Acetone-d_6) δ (ppm): 172.21 (C=O), 155.79 (C=N), 142.94 (Cq-7a), 136.70 (Cq-A_1), 135.98 (CH-6), 133.02 (Cq-A_4), 131.63 (CH-B_4), 130.30 (CH-4), 130.13 (CH-$A_{3,5}$), 129.57 (CH-$B_{3,5}$), 129.34 (CH-$A_{2,6}$), 129.18 (CH-$B_{2,6}$), 127.72 (Cq-3a), 125.37 (Cq-B_1), 115.87 (Cq-5), 113.81 (CH-7), 98.63 (Cspiro). Anal. Calcd for $C_{21}H_{13}BrClN_3O_2 \cdot 0.25H_2O$: C 54.92, H 2.97, N 9.15, Found: C 54.54, H 2.87, N 8.88.

5-bromo-4'-(3-chlorophenyl)-3'-phenyl-4'*H*-spiro[indoline-3,5'-[1,2,4] oxadiazol]-2-one (165z).

Synthesized according to the general procedure, this compound was obtained as a white solid (84.0 mg, 62 % yield).

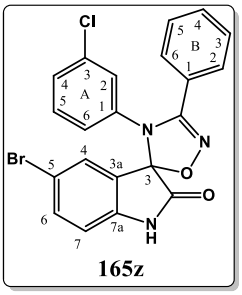

165z

Mp: 208-210 ºC; **IR** (KBr, selected peaks): 3132 (NH), 1749 (C=O), 1617 (C=N), 1590, 1475, 1384, 1195, 687 cm^{-1}; **^{1}H NMR** (400 MHz, Acetone-d_6) δ (ppm): 9.66 (br s, 1H, NH), 7.87 (d, J = 1.6 Hz, 1H, H-4), 7.56 (dd, J = 8.3 Hz, 1.6 Hz, 1H, H-6) 7.54 – 7.46 (m, 3H, H-$B_{2,4,6}$), 7.45 – 7.38 (m, 2H, H-$B_{3,5}$), 7.25 – 7.15 (m, 2H, H-$A_{4,5}$), 6.94 (d, J = 8.4 Hz, 1H, H-7), 6.93 (s, 1H, H-A_2), 6.87 (d, J = 7.6 Hz, 1H, H-A_6); **^{13}C NMR** (100 MHz, Acetone-d_6) δ (ppm): 172.15 (C=O), 155.57 (C=N), 142.86 (Cq-7a), 139.24 (Cq-A_1), 136.04 (CH-6), 134.79 (Cq-A_3), 131.69 (CH-B_4), 131.43 (CH-A_5), 130.31 (CH-4), 129.59 (CH-$B_{3,5}$), 129.18 (CH-$B_{2,6}$), 127.91 (CH-A_4), 127.54 (Cq-3a), 127.29 (CH-A_2), 125.95 (CH-A_6), 125.29 (Cq-B_1), 115.92 (Cq-5), 113.82 (CH-7), 98.55 (Cspiro). Anal. Calcd for $C_{21}H_{13}BrClN_3O_2$: C 55.47, H 2.89, N 9.24, Found: C 55.52, H 2.91, N 9.07.

5-bromo-3'-(4-chlorophenyl)-4'-(3-chlorophenyl)-4'*H*-spiro[indoline-3,5'-[1,2,4]oxadiazol]-2-one (165aa).

Synthesized according to the general procedure, this compound was obtained as a white solid (87.5 mg, 60 % yield).

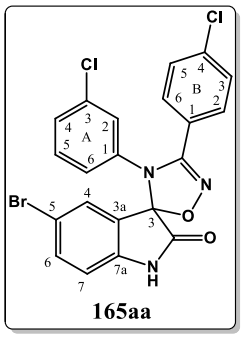

Mp: 256-258 ºC; **IR** (KBr, selected peaks): 3173 (NH), 1745 (C=O), 1617 (C=N), 1590, 1474, 1384, 1197, 760, 690 cm^{-1}; **^{1}H NMR** (400 MHz, Acetone-d_6) δ (ppm): 9.70 (s, 1H, NH), 7.87 (s, 1H, H-4), 7.59 – 7.55 (m, 1H, H-6), 7.54 (d, J = 8.7 Hz, 2H, H-$B_{2,6}$), 7.47 (d, J = 8.7 Hz, 2H, H-$B_{3,5}$), 7.28 – 7.17 (m, 2H, H-$A_{4,5}$), 6.96 – 6.92 (m, 2H, H-7, H-A_2), 6.89 (d, J = 7.6 Hz, 1H, H-A_6); **^{13}C NMR** (100 MHz, Acetone-d_6) δ (ppm): 172.07 (C=O), 154.81 (C=N), 142.94 (Cq-7a), 138.99 (Cq-A_1), 137.20 (Cq-B_4), 136.14 (CH-6), 134.93 (Cq-A_3), 131.59 (CH-A_5), 130.87 (CH-$B_{2,6}$), 130.40 (CH-4), 129.85 (CH-$B_{3,5}$), 128.17 (CH-A_4), 127.36 (Cq-3a), 127.33 (CH-A_2), 126.14 (CH-A_6), 124.12 (Cq-B_1), 115.93 (Cq-5), 113.87 (CH-7), 98.73 (Cspiro). Anal. Calcd for $C_{21}H_{12}BrCl_2N_3O_2 \cdot 0.4H_2O$: C 50.81, H 2.60, N 8.47, Found: C 50.43, H 2.48, N 8.23.

5-bromo-3',4'-bis(3-chlorophenyl)-4'*H*-spiro[indoline-3,5'-[1,2,4]oxadiazol]-2-one (165ab).

Synthesized according to the general procedure, this compound was obtained as a white solid (88.9 mg, 61 % yield).

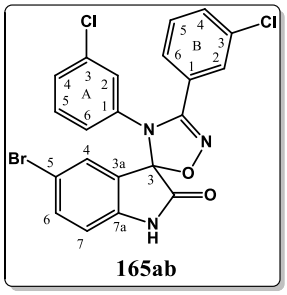

Mp: 246-248 ºC; **IR** (KBr, selected peaks): 3210 (NH), 1734 (C=O), 1617 (C=N), 1592, 1474, 1437, 1375, 818 cm^{-1}; **^{1}H NMR** (400 MHz, Acetone-d_6) δ (ppm): 9.74 (br s, 1H, NH), 7.90 (s, 1H, H-4), 7.60 – 7.50 (m, 2H, H-6, H-B_4), 7.58 (s, 1H, H-B_2), 7.48 – 7.41 (m, 2H, H-$B_{5,6}$), 7.29 – 7.19 (m, 2H, H-$A_{4,5}$), 6.99 – 6.89 (m, 3H, H-7, H-$A_{2,6}$); **^{13}C NMR** (100 MHz, Acetone-d_6) δ (ppm): 172.06 (C=O), 154.60 (C=N), 142.96 (Cq-7a), 138.84 (Cq-A_1), 136.17 (CH-6), 134.94 and 134.93 (Cq-B_3 and Cq-A_3), 131.70 (CH-B_5), 131.61 (CH-A_5), 131.41 (CH-B_4), 130.45 (CH-4), 128.96 (CH-B_2), 128.27 (CH-A_4), 127.71 (CH-B_6), 127.40 (CH-A_2), 127.30 and 127.28 (Cq-B_1 and Cq-3a), 126.15 (CH-A_6), 115.94 (Cq-5), 113.89 (CH-7), 98.81 (Cspiro). Anal. Calcd for $C_{21}H_{12}BrCl_2N_3O_2 \cdot 0.2H_2O$: C 51.18, H 2.54, N 8.53, Found: C 50.81, H 2.48, N 8.31.

5-bromo-3',4'-bis(3-bromophenyl)-4'*H*-spiro[indoline-3,5'-[1,2,4]oxadiazol]-2-one (165ac).

Synthesized according to the general procedure, this compound was obtained as a white solid (102.2 mg, 67 % yield).

Mp: 207-209 ºC; **IR** (KBr, selected peaks): 3230 (NH), 1734 (C=O), 1616 (C=N), 1589, 1473, 1438, 1372, 1199, 819 cm^{-1}; **^{1}H NMR** (400 MHz, Acetone-d_6) δ (ppm): 9.75 (br s, 1H, NH), 7.91 (d, J = 1.5 Hz, 1H, H-4), 7.74 (s, 1H, H-B_2), 7.69 (d, J = 8.0 Hz, 1H, H-B_4), 7.57 (dd, J = 8.3, 1.5 Hz, 1H, H-6), 7.47 (d, J = 7.8 Hz, 1H, H-B_6), 7.41 – 7.34 (m, 2H, H-

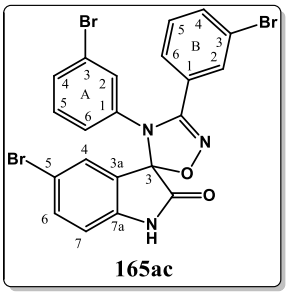

165ac

B_5, H-A_4), 7.19 (t, *J* = 8.1 Hz, 1H, H-A_5), 7.13 (s, 1H, H-A_2), 6.99 – 6.92 (m, 2H, H-A_6, H-7); **^{13}C NMR** (100 MHz, Acetone-d_6) δ (ppm): 172.03 (C=O), 154.44 (C=N), 142.92 (Cq-7a), 138.92 (Cq-A_1), 136.17 (CH-6), 134.65 (CH-B_4), 131.87 (CH-A_5), 131.83 (CH-B_2), 131.59 and 131.20 (CH-A_4 and CH-B_5), 130.48 (CH-4), 130.31 (CH-A_2), 128.10 (CH-B_6), 127.49 (Cq-B_1), 127.26 (Cq-3a), 126.56 (CH-A_6), 122.87 (Cq-B_3), 122.81 (Cq-A_3), 115.95 (Cq-5), 113.87 (CH-7), 98.82 (Cspiro). Anal. Calcd for $C_{21}H_{12}Br_3N_3O_2 \cdot 0.05H_2O$: C 43.56, H 2.11, N 7.26, Found: C 43.16, H 1.89, N 7.04.

5-bromo-4'-(3-chloro-4-fluorophenyl)-3'-(3-chlorophenyl)-4'*H*-spiro[indoline-3,5'-[1,2,4]oxadiazol]-2-one (165ad).

Synthesized according to the general procedure, this compound was obtained as a white solid (78.8 mg, 55 % yield).

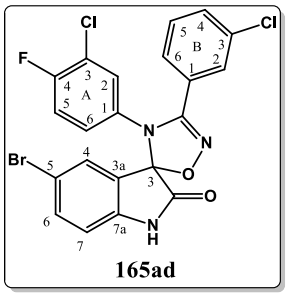

165ad

Mp: 214-216 ºC; **IR** (KBr, selected peaks): 3174 (NH), 1745 (C=O), 1617 (C=N), 1500, 1473, 1384, 1193, 825, 760 cm^{-1}; **^{1}H NMR** (400 MHz, Acetone-d_6) δ (ppm): 9.70 (br s, 1H, NH), 7.94 (d, *J* = 1.6 Hz, 1H, H-4), 7.59 (s, 1H, H-B_2), 7.57 (dd, *J* = 8.3, 1.6 Hz, 1H, H-6), 7.56 – 7.50 (m, 1 H, H-B_4) 7.49 – 7.39 (m, 2H, H-$B_{5,6}$), 7.22 (t, *J* = 8.9 Hz, 1H, H-A_5), 7.17 (dd, *J* = 6.5, 2.4 Hz, 1H, H-A_2), 7.06 – 7.00 (m, 1H, H-A_6), 6.94 (d, *J* = 8.3 Hz, 1H, H-7); **^{13}C NMR** (100 MHz, Acetone-d_6) δ (ppm): 172.02 (C=O), 157.62 (d, J_{FC} = 247.0 Hz, Cq-A_4), 154.74 (C=N), 142.98 (Cq-7a), 136.23 (CH-6), 134.96 (Cq-B_3), 134.36 (d, J_{FCCCC} = 4.0 Hz, Cq-A_1), 131.75 (CH-B_5), 131.44 (CH-B_4), 130.51 (CH-4), 130.37 (CH-A_2), 129.02 (CH-B_2), 128.99 (d, J_{FCCC} = 7.0 Hz, CH-A_6), 127.75 (CH-B_6), 127.13 (Cq-3a), 127.06 (Cq-B_1), 121.57 (d, J_{FCC} = 19.0 Hz, Cq-A_3), 118.24 (d, J_{FCC} = 22.0 Hz, CH-A_5), 115.99 (Cq-5), 113.92 (CH-7), 98.92 (Cspiro). Anal. Calcd for $C_{21}H_{11}BrCl_2FN_3O_2$: C 49.73, H 2.19, N 8.29, Found: C 50.03, H 2.49, N 8.11.

5-bromo-4'-(3-chloro-2-fluorophenyl)-3'-(3-chlorophenyl)-4'*H*-spiro[indoline-3,5'-[1,2,4]oxadiazol]-2-one (165ae).

Synthesized according to the general procedure, this compound was obtained as a white solid (81.6 mg, 57 % yield).

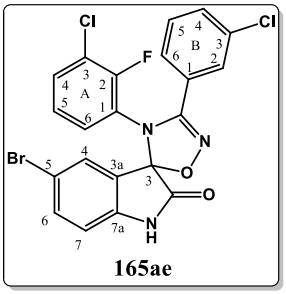

Mp: 242-244 ºC; **IR** (KBr, selected peaks): 3289 (NH), 1742 (C=O), 1618 (C=N), 1560, 1484, 1474, 1436, 1369, 1096, 747 cm^{-1}; **^{1}H NMR** (400 MHz, Acetone-d_6) δ (ppm): 9.74 (br s, 1H, NH), 7.65 (s, 1H, H-4), 7.61 (s, 1H, H-B_2), 7.58 – 7.51 (m, 2H, H-6, H-B_4), 7.48 – 7.43 (m, 2H, H-$B_{5,6}$), 7.43 – 7.37 (m, 1H, H-A_5), 7.19 – 7.09 (m, 2H, H-$A_{4,6}$), 6.94 (d, J = 8.3 Hz, 1H, H-7); **^{13}C NMR** (100 MHz, Acetone-d_6) δ (ppm): 172.03 (C=O), 154.79 (C=N), 154.58 (d, J_{FC} = 249.0 Hz, Cq-A_2), 143.25 (Cq-7a), 136.27 (CH-6), 135.06 (Cq-B_3), 131.96 (CH-B_5), 131.58 (CH-B_4), 131.04 (CH-A_5), 130.28 (CH-4), 128.75 (CH-A_4), 128.38 (CH-B_2), 127.27 (Cq-B_1), 127,25 (d, J_{FCC} = 12 Hz, Cq-A_1), 127.13 (CH-B_6), 126.21 (d, J_{FCCC} = 5 Hz, CH-A_6), 126.09 (Cq-3a), 122.34 (d, J_{FCC} = 16 Hz, Cq-A_3), 115.53 (Cq-5), 113.83 (CH-7), 98.34 (Cspiro). Anal. Calcd for $C_{21}H_{11}BrCl_2FN_3O_2 \cdot 0.2H_2O$: C 49.38, H 2.25, N 8.23, Found: C 48.99, H 1.87, N 8.12.

5-bromo-3'-(3-chloro-2-fluorophenyl)-4'-(3-chlorophenyl)-4'*H*-spiro[indoline-3,5'-[1,2,4]oxadiazol]-2-one (165af).

Synthesized according to the general procedure, this compound was obtained as a white solid (87.1 mg, 61 % yield).

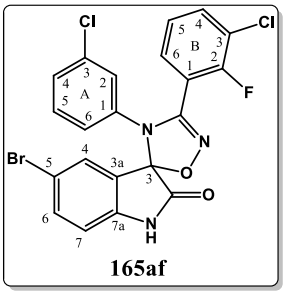

Mp: 242-244 ºC; **IR** (KBr, selected peaks): 3171 (NH), 1748 (C=O), 1619 (C=N), 1476, 1455, 1395, 1194, 826, 687 cm^{-1}; **^{1}H NMR** (400 MHz, Acetone-d_6) δ (ppm): 9.77 (br s, 1H), 7.90 (d, J = 1.6 Hz, 1H, H-4), 7.75 – 7.68 (m, 2H, H-$B_{4,6}$), 7.58 (dd, J = 8.3, 1.6 Hz, 1H, H-6) 7.37 (t, J = 7.9 Hz, 1H, H-B_5), 7.26 – 7.15 (m, 2H, H-$A_{4,5}$), 6.96 (d, J = 8.3 Hz, 1H, H-7), 6.94 (s, 1H, H-A_2), 6.90 (d, J = 7.5 Hz, 1H, H-A_6); **^{13}C NMR** (100 MHz, Acetone-d_6) δ (ppm): 171.80 (C=O), 156.15 (d, J_{FC} = 227.0 Hz, Cq-B_2), 151.35 (C=N), 142.91 (Cq-7a), 138.29 (Cq-A_1), 136.32 (CH-6), 134.94 (Cq-A_3), 134.49 (CH-B_6), 131.68 (CH-A_4), 130.91 (d, J_{FCCC} = 1 Hz, CH-B_4), 130.20 (CH-4), 128.19 (CH-A_5), 127.10 (Cq-3a), 126.69 (CH-B_5), 126.25 (CH-A_2), 125.04 (CH-A_6), 122.34 (d, J_{FCC} = 17 Hz, Cq-B_3), 116.03 (Cq-5), 115.26 (d, J_{FCC} = 14 Hz, Cq-B_1), 114.02 (CH-7), 98.54 (Cspiro). Anal. Calcd for $C_{21}H_{11}BrCl_2FN_3O_2$: C 49.73, H 2.19, N 8.29, Found: C 49.63, H 1.99, N 8.01.

9.1.12. General procedure for the synthesis of 2',4'-dihydrospiro[indoline-3,3'-[1,2,4]triazol]-2-ones.

Triethylamine (2.0 equiv) was added dropwise to a mixture of 3-imino indolin-2-one derivative (1.0 equiv), and hydrazonyl chloride derivative (2.0 equiv) in dry DCM (1

mL/ 0.1 mmol of 3-iminoidolin-2-one) under nitrogen atmosphere. The reaction was stirred at room temperature for 24 hours. The mixture was then washed with brine (2x) and the aqueous phase extracted with DCM. The combined organic extracts were dried over anhydrous Na_2SO_4 and the solvent was removed under reduce pressure. The residue was purified by flash chromatography on silica gel using as eluent a gradient of *n*-hexane/EtOAc (95:5) to *n*-hexane/EtOAc (75:25), preparative thin layer chromatography (PTLC) on silica gel using as eluent *n*-hexane:EtOAc (2:1 or 3:1), and recrystallized from diethyl ether/*n*-hexane to afford the final product.

2',4',5'-triphenyl-2',4'-dihydrospiro[indoline-3,3'-[1,2,4]triazol]-2-one (168a).

Synthesized according to the general procedure, this compound was obtained as a yellow solid (151.2 mg, 81 % yield).

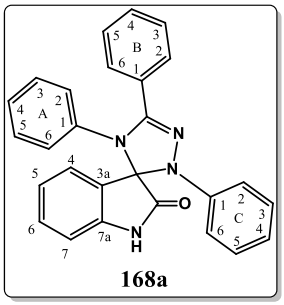

Mp: 203-204 ºC; **IR** (KBr, selected peaks): 3245 (NH), 1735 (C=O), 1594 (C=N), 1493, 1472, 1385, 1320, 1203, 751, 694 cm^{-1}; **^{1}H NMR** (400 MHz, Acetone-d_6) δ (ppm): 7.55 (d, J = 7.4 Hz, 1H, H-4), 7.48 (d, J = 7.0 Hz, 2H, H-$B_{2,6}$), 7.38 – 7.27 (m, 4H, H-6, H-$B_{3,4,5}$), 7.18 – 7.03 (m, 6H, H-5, H-$A_{3,4,5}$, H-$C_{3,5}$), 6.97 – 6.89 (m, 3H, H-7, H-$C_{2,6}$), 6.87 – 6.79 (m, 2H, H-$A_{2,6}$), 6.73 (t, J = 7.3 Hz, 1H, H-C_4); **^{13}C NMR** (100 MHz, Acetone-d_6) δ (ppm): 173.49 (C=O), 148.51 (C=N), 144.43 (Cq-C_1), 143.06 (Cq-7a), 139.18 (Cq-A_1), 132.31 (CH-6), 130.07 (CH-B_4), 129.67 and 129.61 (CH-$A_{3,5}$ and CH-$C_{3,5}$), 129.03 (CH-$B_{3,5}$), 128.88 (Cq-B_1), 128.62 and 128.61 (CH-$A_{2,6}$ and CH-$B_{2,6}$), 127.72 (CH-A_4), 127.34 (Cq-3a), 127.26 (CH-4), 123.99 (CH-5), 120.33 (CH-C_4), 114.54 (CH-$C_{2,6}$), 111.73 (CH-7), 88.46 (Cspiro). Anal. Calcd for $C_{27}H_{20}N_4O{\cdot}0.25H_2O$: C 77.03, H 4.92, N 13.31, Found: C 76.63, H 4.99, N 13.05.

4'-(4-chlorophenyl)-2',5'-diphenyl-2',4'-dihydrospiro[indoline-3,3'-[1,2,4] triazol]-2-one (168b).

Synthesized according to the general procedure, this compound was obtained as a yellow solid (146.9 mg, 84 % yield).

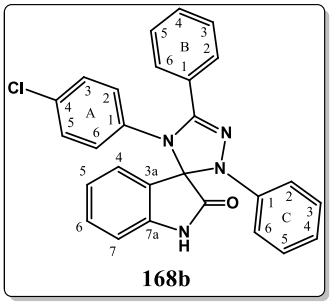

Mp: 185-187 ºC. **IR** (KBr, selected peaks): 3243 (NH), 1738 (C=O), 1597 (C=N), 1491, 1471, 1385, 1320, 1200, 745, 691 cm^{-1}; **^{1}H NMR** (400 MHz, Acetone-d_6) δ (ppm): 9.68 (br s, 1H, NH), 7.56 (d, J = 7.4 Hz, 1H, H-4), 7.49 (d, J = 8.0 Hz, 2H, H-$B_{2,6}$), 7.40 – 7.30 (m, 4H, H-6, H-$B_{3,4,5}$), 7.18 (d, J = 8.6 Hz, 2H, H-$A_{3,5}$), 7.13 – 7.07 (m, 3H, H-5, H-$C_{3,5}$), 6.97 – 6.90 (m, 3H, H-7, H-$C_{2,6}$), 6.82 (d, J = 8.6 Hz, 2H, H-$A_{2,6}$), 6.74 (t, J = 7.3 Hz, 1H, H-C_4); **^{13}C NMR** (100 MHz, Acetone-d_6) δ (ppm): 173.21 (C=O), 148.15 (C=N), 144.30 (Cq-C_1), 142.98 (Cq-7a), 138.14 (Cq-A_1),

132.73 (Cq-A_4), 132.51 (CH-6), 130.26 (CH-B_4), 130.04 (CH-$A_{2,6}$), 129.76 (CH-$A_{3,5}$), 129.65 (CH-$C_{3,5}$), 129.18 (CH-$B_{3,5}$), 128.61 (CH-$B_{2,6}$), 128.52 (Cq-B_1), 127.26 (CH-4), 127.06 (Cq-3a), 124.16 (CH-5), 120.55 (CH-C_4), 114.62 (CH-$C_{2,6}$), 111.88 (CH-7), 88.42 (Cspiro). Anal. Calcd for $C_{27}H_{19}ClN_4O \cdot 0.65H_2O$: C 70.09, H 4.43, N 12.11, Found: C 69.67, H 4.27, N 11.69.

4'-(3-chlorophenyl)-2',5'-diphenyl-2',4'-dihydrospiro[indoline-3,3'-[1,2,4] triazol]-2-one (168c).

Synthesized according to the general procedure, this compound was obtained as a yellow solid (158.2 mg, 90 % yield).

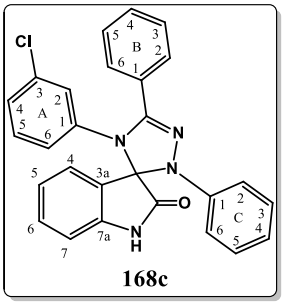

168c

Mp: 208-209 C; **IR** (KBr, selected peaks): 3255 (NH), 1735 (C=O), 1591 (C=N), 1494, 1470, 1384, 1320, 1198, 753, 689 cm^{-1}; **^{1}H NMR** (400 MHz, Acetone-d_6) δ (ppm): 9.72 (br s, 1H, NH), 7.57 (d, J = 7.3 Hz, 1H, H-4), 7.51 (d, J = 8.0 Hz, 2H, H-$B_{2,6}$), 7.43 – 7.32 (m, 4H, H-6, H-$B_{3,4,5}$), 7.20 – 7.14 (m, 2H, H-$A_{4,5}$), 7.13 – 7.08 (m, 3H, H-5, H-$C_{3,5}$), 6.98 (d, J = 7.8 Hz, 1H, H-7), 6.94 (d, J = 7.9 Hz, 2H, H-$C_{2,6}$), 6.81 (s, 1H, H-A_2), 6.80 – 6.71 (m, 2H, H-A_6, H-C_4); **^{13}C NMR** (100 MHz, Acetone-d_6) δ (ppm): 173.11 (C=O), 147.91 (C=N), 144.25 (Cq-C_1), 142.92 (Cq-7a), 140.71 (Cq-A_1), 134.49 (Cq-A_3), 132.59 (CH-6), 131.02 (CH-A_5), 130.34 (CH-B_4), 129.67 (CH-$C_{3,5}$), 129.23 (CH-$B_{3,5}$), 128.62 (CH-$B_{2,6}$), 128.51 (Cq-B_1), 127.97 (CH-A_2), 127.61 (CH-A_4), 127.28 (CH-4), 126.90 (Cq-3a), 126.86 (CH-A_6), 124.20 (CH-5), 120.67 (CH-C_4), 114.73 (CH-$C_{2,6}$), 111.87 (CH-7), 88.36 (Cspiro). Anal. Calcd for $C_{27}H_{19}ClN_4O \cdot 0{,}6H_2O$: C 70.23, H 4.42, N 12.14, Found: C 69.96, H 4.32, N 11.92.

4'-(3-chloro-4-fluorophenyl)-2',5'-diphenyl-2',4'-dihydrospiro[indoline-3,3'-[1,2,4]triazol]-2-one (168d).

Synthesized according to the general procedure, this compound was obtained as a yellow solid (119.5 mg, 70 % yield).

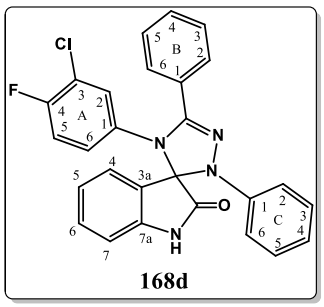

168d

Mp: 203-205 ºC; **IR** (KBr, selected peaks): 3246 (NH), 1731 (C=O), 1597 (C=N), 1493, 1470, 1385, 1325, 1203, 746, 690 cm^{-1}; **^{1}H NMR** (400 MHz, Acetone.d_6) δ (ppm): 9.72 (br s, 1H, NH), 7.61 (d, J = 7.3 Hz, 1H, H-4), 7.52 (d, J = 8.0 Hz, 2H, H-$B_{2,6}$), 7.44 – 7.32 (m, 4H, H-6, H-$B_{3,4,5}$), 7.17 – 7.07 (m, 4H, H-5, H-A_5, H-$C_{3,5}$), 6.98 (d, J = 7.8 Hz, 1H, H-7), 6.96 – 6.90 (d, J = 8.0 Hz, 3H, H-A_2, H-$C_{2,6}$), 6.87 – 6.80 (m, 1H, H-A_6), 6.76 (t, J = 7.3 Hz, 1H, H-C_4); **^{13}C NMR** (100 MHz, Acetone-d_6) δ (ppm): 173.13 (C=O), 157.26 (d, J_{FC} = 247.0 Hz, Cq-A_4), 147.92 (C=N), 144.26 (Cq-C_1), 142.98 (Cq-7a), 136.29 (d, J_{FCCCC} = 3.0 Hz, Cq-A_1), 132.67 (CH-6),

130.59 (CH-B_4), 130.41 (CH-A_2), 129.69 (CH-$C_{3,5}$), 129.37 (d, J_{FCCC} = 8.0 Hz, CH-A_6) 129.28 (CH-$B_{3,5}$), 128.67 (CH-$B_{2,6}$), 128.27 (Cq-B_1), 127.33 (CH-4), 126.83 (Cq-3a), 124.27 (CH-5), 121.02 (d, J_{FCC} = 19.0 Hz, Cq-C_3), 120.71 (CH-C_4), 117.66 (d, J_{FCC} = 22.0 Hz, CH-A_5), 114.68 (CH-$C_{2,6}$), 111.96 (CH-7), 88.52 (Cspiro). Anal. Calcd for $C_{27}H_{18}ClFN_4O \cdot 0.3H_2O$: C 68.37, H 3.96, N 11.81, Found: C 68.75, H 3.62, N 11.42.

5-chloro-2',4',5'-triphenyl-2',4'-dihydrospiro[indoline-3,3'-[1,2,4]triazol]-2-one (168e).

Synthesized according to the general procedure, this compound was obtained as a yellow solid (153.3 mg, 87 % yield).

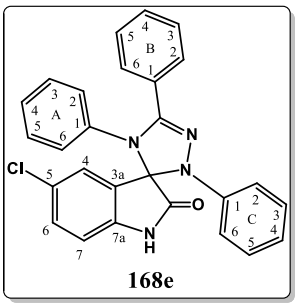

Mp: 218-220 ºC; **IR** (KBr, selected peaks): 3244 (NH), 1742 (C=O), 1595 (C=N), 1493, 1476, 1384, 1320, 1201, 764, 693 cm^{-1}; **^{1}H NMR** (400 MHz, Acetone-d_6) δ (ppm): 9.74 (br s, 1H, NH), 7.64 (s, 1H, H-4), 7.50 (d, J = 7.7 Hz, 2H, H-$B_{2,6}$), 7.42 – 7.29 (m, 4H, H-6, H-$B_{3,4,5}$), 7.21 – 7.11 (m, 5H, H-$A_{3,4,5}$), 6.99 – 6.93 (m, 3H, H-7, H-$C_{2,6}$), 6.91 (d, J = 7.2 Hz, 2H,H-$A_{2,6}$), 6.78 (t, J = 7.2 Hz, 1H, H-C_4); **^{13}C NMR** (100 MHz, Acetone-d_6) δ (ppm): 173.33 (C=O), 148.59 (C=N), 144.20 (Cq-C_1), 141.76 (Cq-7a), 138.93 (Cq-A_1), 132.27 (CH-6), 130.18 (CH-B_4), 129.82 and 129.74 (CH-$A_{3,5}$ and CH-$C_{3,5}$), 129.20 (Cq-3a or Cq-5), 129.04 (CH-$B_{3,5}$), 128.82 (Cq-3a or Cq-5), 128.69 (CH-$A_{2,6}$, CH-$B_{2,6}$), 128.63 (Cq-B_1), 127.99 (CH-A_4), 127.33 (CH-4), 120.65 (CH-C_4), 114.58 (CH-$C_{2,6}$), 113.22 (CH-7), 88.38 (Cspiro). Anal. Calcd for $C_{27}H_{19}ClN_4O \cdot 0.75H_2O$: C 69.69, H 4.47, N 12.04, Found: C 69.82, H 4.46, N 12.07.

5-chloro-4'-(3-chlorophenyl)-2',5'-diphenyl-2',4'-dihydrospiro[indoline-3,3'-[1,2,4]triazol]-2-one (168f).

Synthesized according to the general procedure, this compound was obtained as a yellow solid (148.4 mg, 89 % yield).

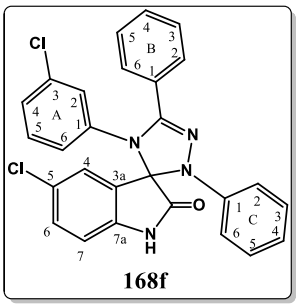

Mp: 172-173 ºC. **IR** (KBr, selected peaks): 3252 (NH), 1741 (C=O), 1590 (C=N), 1495, 1477, 1385, 1323, 1199, 745, 689 cm^{-1}; **^{1}H NMR** (400 MHz, Acetone-d_6) δ (ppm): 9.86 (br s, 1H, NH), 7.65 (d, J = 1.7 Hz, 1H, H-4), 7.56 – 7.48 (m, 2H, H-$B_{2,6}$), 7.44 – 7.32 (m, 4H, H-6, H-$B_{3,4,5}$), 7.25 – 7.16 (m, 2H, H-$A_{4,5}$), 7.13 (t, J = 8.0 Hz, 2H, H-$C_{3,5}$), 7.01 (d, J = 8.2 Hz, 1H, H-7), 6.94 (d, J = 8.0 Hz, 2H, H-$C_{2,6}$), 6.89 (s, 1H, H-A_2), 6.86 – 6.81 (m, 1H, H-A_6), 6.78 (t, J = 7.3 Hz, 1H, H-C_4); **^{13}C NMR** (100 MHz, Acetone-d_6) δ (ppm): 173.05 (C=O), 148.01 (C=N), 144.04 (Cq-C_1), 141.73 (Cq-7a), 140.48 (Cq-A_1), 134.62 (Cq-A_3), 132.54 (CH-6), 131.18 (CH-A_5), 130.43 (CH-B_4), 129.80 (CH-$C_{3,5}$), 129.22 (CH-$B_{3,5}$), 129.03 and 128.79 (Cq-3a and Cq-5), 128.72 (CH-$B_{2,6}$),

128.30 (Cq-B_1), 128.14 (CH-A_4), 127.91 (CH-A_2), 127.39 (CH-4), 126.96 (CH-A_6), 120.97 (CH-C_4), 114.77 (CH-$C_{2,6}$), 113.40 (CH-7), 88.28 (Cspiro). Anal. Calcd for $C_{27}H_{18}Cl_2N_4O \cdot 0{,}14C_6H_{14}$: C 67.18, H 4.08, N 11.26, Found: C 67.35, H 4.23, N 10.86.

4'-(tert-butyl)-5-chloro-2',5'-diphenyl-2',4'-dihydrospiro[indoline-3,3'-[1,2,4] triazol]-2-one (168g).

Synthesized according to the general procedure, this compound was obtained as a yellow solid (144.0 mg, 79 % yield).

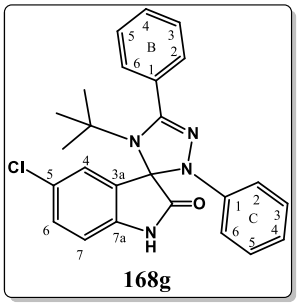

Mp: 195-197 ºC. **IR** (KBr, selected peaks): 3320 (NH), 1751 (C=O), 1596 (C=N), 1495, 1468, 1385, 1314, 1224, 751, 709 cm^{-1}; **^{1}H NMR** (400 MHz, Acetone-d_6) δ (ppm): 9.87 (br s, 1H, NH), 7.74 – 7.69 (m, 2H, H-$B_{2,6}$), 7.67 (d, J = 1.8 Hz, 1H, H-4), 7.54 – 7.49 (m, 3H, H-$B_{3,4,5}$), 7.39 (dd, J = 8.3, 1.6 Hz, 1H, H-6), 7.05 – 6.98 (m, 3H, H-7, H-$C_{3,5}$), 6.85 (d, J = 8.3 Hz, 2H, H-$C_{2,6}$), 6.71 (t, J = 7.2 Hz, 1H, H-C_4), 1.14 (s, 9H, C(CH_3)$_3$); **^{13}C NMR** (100 MHz, Acetone-d_6) δ (ppm): 176.34 (C=O), 151.36 (C=N), 145.00 (Cq-C_1), 141.06 (Cq-7a), 133.34 (Cq-B_1), 131.98 (Cq-3a or Cq-5), 131.90 (CH-$B_{2,6}$), 131.78 (CH-6), 130.07 (CH-B_4), 129.22 (CH-$C_{3,5}$), 128.72 (CH-$B_{3,5}$), 128.70 (Cq-3a or Cq-5), 127.28 (CH-4), 121.32 (CH-C_4), 117.16 (CH-$C_{2,6}$), 113.20 (CH-7), 88.15 (Cspiro), 56.77 (<u>C</u>(CH_3)$_3$), 31.51 (C(<u>C</u>H_3)$_3$). Anal. Calcd for $C_{25}H_{23}ClN_4O \cdot 0.3CH_2Cl_2$: C 66.57, H 5.22, N 12.28, Found: C 66.65, H 5.06, N 12.20.

5-bromo-2',4',5'-triphenyl-2',4'-dihydrospiro[indoline-3,3'-[1,2,4]triazol]-2-one (168h).

Synthesized according to the general procedure, this compound was obtained as a yellow solid (155.7 mg, 95 % yield).

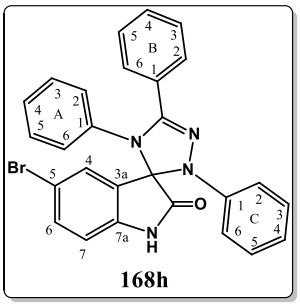

Mp: 212-214ºC. **IR** (KBr, selected peaks): 3211 (NH), 1741 (C=O), 1595 (C=N), 1493, 1473, 1385, 1320, 1200, 766, 693 cm^{-1}; **^{1}H NMR** (400 MHz, Acetone-d_6) δ (ppm): 9.74 (br s, 1H, NH), 7.75 (s, 1H, H-4), 7.52 (d, J = 8.6 Hz, 1H, H-6), 7.48 (d, J = 7.6 Hz, 2H, H-$B_{2,6}$), 7.38 – 7.27 (m, 3H, H-$B_{3,4,5}$), 7.20 – 7.10 (m, 5H, H-$A_{3,4,5}$, H-$C_{3,5}$), 6.96 – 6.85 (m, 5H, H-7, H-$A_{2,6}$, H-$C_{2,6}$), 6.76 (t, J = 7.3 Hz, 1H, H-C_4); **^{13}C NMR** (100 MHz, Acetone-d_6) δ (ppm): 173.13 (C=O), 148.59 (C=N), 144.18 (Cq-C_1), 142.19 (Cq-7a), 138.92 (Cq-A_1), 135.18 (CH-6), 130.18 (CH-B_4), 130.12 (CH-4), 129.83 and 129.76 (CH-$A_{3,5}$ and CH-$C_{3,5}$), 129.56 (Cq-3a), 129.04 (CH-$B_{3,5}$), 128.70 (CH-$A_{2,6}$ and CH-$B_{2,6}$), 128.62 (Cq-B_1), 128.01 (CH-A_4), 120.65 (CH-C_4), 116.04 (Cq-C5), 114.56 (CH-$C_{2,6}$), 113.68 (CH-7), 88.32 (Cspiro). Anal. Calcd for $C_{27}H_{19}BrN_4O$: C 65.46, H 3.87, N 11.31, Found: C 65.31, H 3.97, N 11.05.

5-bromo-4'-(4-chlorophenyl)-2',5'-diphenyl-2',4'-dihydrospiro[indoline-3,3'-[1,2,4]triazol]-2-one (168i).

Synthesized according to the general procedure, this compound was obtained as a yellow solid (146.1 mg, 93 % yield).

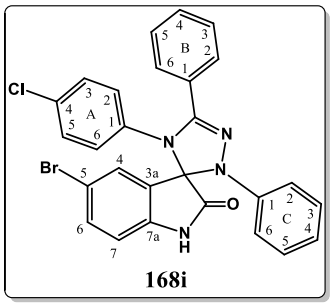

Mp: 140-142 ºC; **IR** (KBr, selected peaks): 3186 (NH), 1730 (C=O), 1598 (C=N), 1490, 1473, 1385, 1307, 1205, 747, 690 cm^{-1}; **^{1}H NMR** (400 MHz, $CDCl_3$) δ (ppm): 8.09 (br s, 1H, NH), 7.70 (s, 1H, H-4), 7.50 – 7.41 (m, 3H, H-6, H-$B_{2,6}$), 7.37 – 7.22 (m, 3H, H-$B_{3,4,5}$), 7.12 (t, J = 7.7 Hz, 2H, H-$C_{3,5}$), 7.05 (d, J = 8.4 Hz, 2H, H-$A_{3,5}$), 6.90 (d, J = 8.0 Hz, 2H, H-$C_{2,6}$), 6.83 (t, J = 7.4 Hz, 1H, H-C_4), 6.69 (d, J = 8.4 Hz, 2H, H-$A_{2,6}$), 6.64 (d, J = 8.3 Hz, 1H, H-7); **^{13}C NMR** (100 MHz, $CDCl_3$) δ (ppm): 173.21 (C=O), 147.96 (C=N), 143.10 (Cq-C_1), 139.72 (Cq-7a), 136.41 (Cq-A_1), 134.63 (CH-6), 133.04 (Cq-A_4), 129.78 (CH-B_4), 129.58 (CH-4), 129.42 (CH-$A_{2,6}$), 129.29 (CH-$C_{3,5}$), 129.05 (Cq-B_1), 128.83 (CH-$A_{3,5}$), 128.49 (CH-$B_{3,5}$), 128.03 (CH-$B_{2,6}$), 126.91 (Cq-3a), 120.99 (CH-C_4), 116.85 (Cq-5), 114.49 (CH-$C_{2,6}$), 113.07 (CH-7), 88.09 (Cspiro). Anal. Calcd for $C_{27}H_{18}BrClN_4O{\cdot}0.05H_2O$: C 61.10, H 3.44, N 10.56, Found: C 60.71, H 3.50, N 10.23.

5-bromo-4'-(3-chloro-4-fluorophenyl)-2',5'-diphenyl-2',4'-dihydrospiro [indoline-3,3'-[1,2,4]triazol]-2-one (168j).

Synthesized according to the general procedure, this compound was obtained as a yellow solid (138.9 mg, 90 % yield).

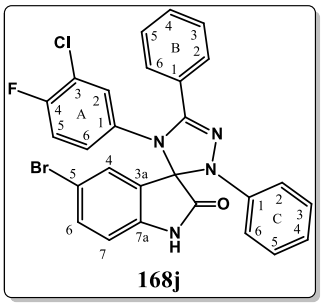

MP: 135-137 ºC; **IR** (KBr, selected peaks): 3242 (NH), 1735 (C=O), 1597 (C=N), 1492, 1473, 1384, 1261, 1194, 764, 691 cm^{-1}; **^{1}H NMR** (400 MHz, Acetone-d_6) δ (ppm): 9.75 (br s, 1H, NH), 7.82 (s, 1H, H-4), 7.56 (d, J = 8.4 Hz, 1H, H-6), 7.52 (d, J = 7.2 Hz, 2H, H-$B_{2,6}$), 7.42 – 7.32 (m, 3H, H-$B_{3,4,5}$), 7.20 – 7.10 (m, 3H, H-A_5, H-$C_{3,5}$), 7.03 (dd, J = 6.5, 2.2 Hz, 1H, H-A_2), 6.96 (d, J = 8.4 Hz, 1H, H-7), 6.95 – 6.88 (m, 3H, H-A_6, H-$C_{2,6}$), 6.78 (t, J = 7.3 Hz, 1H, H-C_4); **^{13}C NMR** (100 MHz, Acetone-d_6) δ (ppm): 172.84 (C=O), 157.42 (d, J_{FC} = 247.0 Hz, CH-A_4), 148.03 (C=N), 144.02 (Cq-C_1), 142.14 (Cq-7a), 136.02 (d, J_{FCCCC} = 4.0 Hz, Cq-A_1), 135.51 (CH-6), 130.83 (CH-B_4), 130.49 (CH-A_2), 130.22 (CH-4), 129.82 (CH-$C_{3,5}$), 129.48 (d, J_{FCCC} = 7.0 Hz, CH-A_6), 129.27 (CH-$B_{3,5}$), 129.04 (Cq-3a), 128.78 (CH-$B_{2,6}$), 128.04 (Cq-B_1), 121.17 (d, J_{FCC} = 18.0 Hz, Cq-A_3), 120.99 (CH-C_4), 117.82 (d, J_{FCC} = 23.0 Hz CH-A_5), 116.29 (Cq-5), 114.70 (CH-$C_{2,6}$), 113.91 (CH-7), 88.35 (Cspiro). Anal. Calcd for $C_{27}H_{18}BrClFN_4O{\cdot}0.1H_2O$: C 59.00, H 3.16, N 10.20, Found: C 58.67, H 3.52, N 10.17.

5-bromo-4'-(3-chlorophenyl)-2',5'-diphenyl-2',4'-dihydrospiro[indoline-3,3'-[1,2,4]triazol]-2-one (168k).

Synthesized according to the general procedure, this compound was obtained as a yellow solid (144.8 mg, 92 % yield).

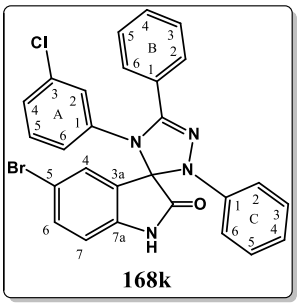

Mp: 143-145 ºC; **IR** (KBr, selected peaks): 328 (NH), 1738 (C=O), 1597 (C=N), 1493, 1385, 1325, 1201, 745, 687 cm^{-1}; **^{1}H NMR** (400 MHz, Acetone-d_6) δ (ppm): 9.88 (br s, 1H, NH), 7.78 (d, J = 1.7 Hz, 1H, H-4), 7.56 (dd, J = 8.4, 1.7 Hz, 1H, H-6), 7.52 (d, J = 8.2 Hz, 2H, H-$B_{2,6}$), 7.42 – 7.33 (m, 3H, H-$B_{3,4,5}$), 7.24 – 7.17 (m, 2H, H-$A_{4,5}$), 7.14 (t, J = 7.8 Hz, 2H, H-$C_{3,5}$), 6.97 (d, J = 8.4 Hz, 1H, H-7), 6.93 (d, J = 7.8 Hz, 2H, H-$C_{2,6}$), 6.89 (s, 1H, H-A_2), 6.86 – 6.81 (m, 1H, H-A_6), 6.78 (t, J = 7.6 Hz, 1H, H-C_4); **^{13}C NMR** (75 MHz, Acetone-d_6) δ (ppm): 172.90 (C=O), 148.04 (C=N), 144.04 (Cq-C_1), 142.19 (Cq-7a), 140.49 (Cq-A_1), 135.47 (CH-6), 134.64 (Cq-A_3), 131.20 (CH-A_5), 130.45 (CH-B_4), 130.21 (CH-4), 129.82 (CH-$C_{3,5}$), 129.24 (CH-$B_{3,5}$), 129.15 (Cq-3a), 128.74 (CH-$B_{2,6}$), 128.31 (Cq-B_1), 128.18 (CH-A_4), 127.94 (CH-A_2), 126.98 (CH-A_6), 120.98 (CH-C_4), 116.24 (Cq-5), 114.77 (CH-$C_{2,6}$), 113.85 (CH-7), 88.23 (Cspiro). Anal. Calcd for $C_{27}H_{18}BrClN_4O{\cdot}0.15H_2O$: C 60.89, H 3.47, N 10.52, Found: C 60.76, H 3.87, N 10.19.

7-chloro-2',4',5'-triphenyl-2',4'-dihydrospiro[indoline-3,3'-[1,2,4]triazol]-2-one (168l).

Synthesized according to the general procedure, this compound was obtained as a yellow solid (159.6 mg, 91 % yield).

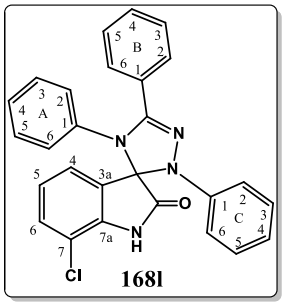

Mp: 186-188 ºC; **IR** (KBr, selected peaks): 3059 (NH), 1750 (C=O), 1594 (C=N), 1494, 1475, 1337, 1177, 1154, 749, 694 cm^{-1}; **^{1}H NMR** (400 MHz, $CDCl_3$) δ (ppm): 7.53 – 7.44 (m, 3H, H-4, H-$B_{2,6}$), 7.32 (d, J = 8.2 Hz, 1H, H-6), 7.29 (d, J = 7.2 Hz, 1H, H-B_4), 7.27 – 7.21 (m, 2H, H-$B_{3,5}$), 7.19 – 7.02 (m, 6H, H-5, $A_{3,4,5}$, $C_{3,5}$), 6.91 (d, J = 8.0 Hz, 2H, H-$C_{2,6}$), 6.82 (t, J = 7.3 Hz, 1H, H-C_4), 6.80 – 6.72 (m, 2H, H-$A_{2,6}$); **^{13}C NMR** (100 MHz, $CDCl_3$) δ (ppm): 172.37 (C=O), 148.38 (C=N), 143.34 (Cq-C_1), 138.47 (Cq-7a), 137.86 (Cq-A_1), 131.27 (CH-6), 129.48 (CH-B_4), 129.20 and 129.17 (CH-$A_{3,5}$ and CH-$C_{3,5}$), 128.87 (Cq-B_1), 128.27 (CH-$B_{3,5}$), 128.07 (CH-$B_{2,6}$), 127.77 (CH-$A_{2,6}$), 127.38 (Cq-3a), 127.32 (CH-A_4), 125.02 (CH-4), 124.74 (CH-5), 120.86 (CH-C_4), 116.08 (Cq-7), 114.80 (CH-$C_{2,6}$), 88.97 (Cspiro). Anal. Calcd for $C_{27}H_{19}ClN_4O{\cdot}0{,}65H_2O$: C 69.69, H 4.47, N 12.04, Found: C 69.37, H 4.31, N 11.73.

7-bromo-2',4',5'-triphenyl-2',4'-dihydrospiro[indoline-3,3'-[1,2,4]triazol]-2-one (168m).

Synthesized according to the general procedure, this compound was obtained as a yellow solid (154.1 mg, 94 % yield).

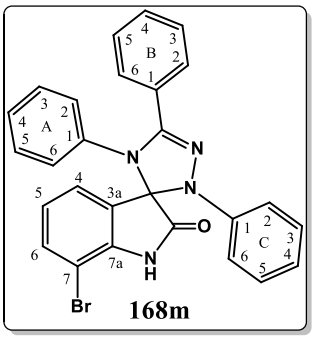

Mp: 220-222ºC; **IR** (KBr, selected peaks): 3057 (NH), 1741 (C=O), 1594 (C=N), 1494, 1472, 1385, 1337, 1178, 761, 694 cm^{-1}; **^{1}H NMR** (400 MHz, Acetone-d_6) δ (ppm): 9.86 (br s, 1H, NH), 7.58 (d, J = 7.4 Hz, 1H, H-4), 7.55 (d, J = 8.0 Hz, 1H, H-6), 7.47 (d, J = 7.1 Hz, 2H, H-$B_{2,6}$), 7.38 – 7.28 (m, 3H, H-$B_{3,4,5}$), 7.20 – 7.09 (m, 5H, H-$A_{3,4,5}$, H-$C_{3,5}$), 7.06 (t, J = 7.7 Hz, 1H, H-5), 6.92 (d, J = 8.0 Hz, 2H, H-$C_{2,6}$), 6.87 – 6.81 (m, 2H, H-$A_{2,6}$), 6.76 (t, J = 7.3 Hz, 1H, H-C_4); **^{13}C NMR** (100 MHz, Acetone-d_6) δ (ppm): 173.40 (C=O), 148.62 (C=N), 144.22 (Cq-C_1), 142.26 (Cq-7a), 138.87 (Cq-A_1), 135.10 (CH-6), 130.21 (CH-B_4), 129.84 and 129.76 (CH-$A_{3,5}$ and CH-$C_{3,5}$), 129.25 (Cq-3a), 129.07 (CH-$B_{3,5}$), 128.70 (CH-$A_{2,6}$), 128.64 (CH-$B_{2,6}$), 128.59 (Cq-B_1), 128.07 (CH-A_4), 126.36 (CH-4), 125.56 (CH-5), 120.73 (CH-C_4), 114.70 (CH-$C_{2,6}$), 104.43 (Cq-7), 89.29 (Cspiro). Anal. Calcd for $C_{27}H_{19}BrN_4O$: C 65.46, H 3.87, N 11.31, Found: C 65.36, H 3.99, N 11.18.

5'-(3-chlorophenyl)-4'-(4-chlorophenyl)-2'-phenyl-2',4'-dihydrospiro [indoline-3,3'-[1,2,4]triazol]-2-one (168n).

Synthesized according to the general procedure, this compound was obtained as a yellow solid (169.0 mg, 89 % yield).

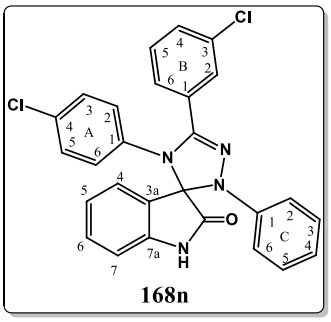

Mp: 98-100 ºC. **IR** (KBr, selected peaks): 3244 (NH), 1733 (C=O), 1593 (C=N), 1491, 1471, 1318, 1197, 1093, 746, 688 cm^{-1}; **^{1}H NMR** (300 MHz, Acetone-d_6) δ (ppm): 9.72 (br s, 1H, NH), 7.61 – 7.54 (m, 2H, H-4, H-B_2), 7.44 – 7.31 (m, 4H, H-6, H-$B_{4,5,6}$), 7.24 – 7.16 (m, 2H, H-$A_{3,5}$), 7.15 – 7.05 (m, 3H, H-5, H-$C_{3,5}$), 6.98 – 6.91 (m, 3H, H-7, H-$C_{2,6}$), 6.89 – 6.82 (m, 2H, H-$A_{2,6}$), 6.81 – 6.73 (m, 1H, H-C_4); **^{13}C NMR** (75 MHz, Acetone-d_6) δ (ppm): 173.08 (C=O), 146.87 (C=N), 144.01 (Cq-C_1), 142.93 (Cq-7a), 137.75 (Cq-A_1), 134.59 (Cq-B_3), 133.01 (Cq-A_4), 132.61 (CH-6), 130.92 (CH-B_5), 130.49 (Cq-B_1), 130.11 (CH-B_4), 130.02 (CH-$A_{2,6}$), 129.91 (CH-$A_{3,5}$), 129.70 (CH-$C_{3,5}$), 128.23 (CH-4), 127.33 (CH-B_2), 126.89 (CH-B_6), 126.75 (Cq-3a), 124.20 (CH-5), 120.87 (CH-C_4), 114.72 (CH-$C_{2,6}$), 111.93 (CH-7), 88.60 (Cspiro). Anal. Calcd for $C_{21}H_{14}ClN_3O_2 \cdot 0.9H_2O$: C 64.65, H 3.99, N 11.17, Found: C 64.43, H 3.83, N 11.47.

4',5'-bis(4-chlorophenyl)-2'-phenyl-2',4'-dihydrospiro[indoline-3,3'-[1,2,4] triazol]-2-one (168o).

Synthesized according to the general procedure, this compound was obtained as a yellow solid (163.5 mg, 86 % yield).

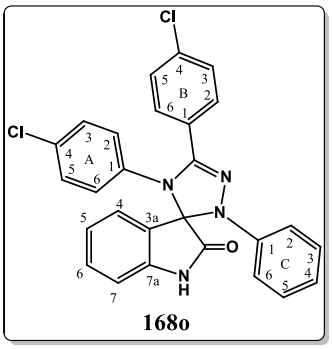

Mp: 155-157 ºC;. **IR** (KBr, selected peaks): 3205 (NH), 1731 (C=O), 1600 (C=N), 1492, 1474, 1319, 1203, 1014, 835, 746 cm^{-1}; **^{1}H NMR** (300 MHz, Acetone-d_6) δ (ppm): 9.68 (br s, 1H, NH), 7.56 (d, J = 7.4 Hz, 1H, H-4), 7.53 – 7.46 (m, 2H, H-$B_{2,6}$), 7.43 – 7.34 (m, 3H, H-6, H-$B_{3,5}$), 7.24 – 7.17 (m, 2H, H-$A_{3,5}$), 7.15 – 7.05 (m, 3H, H-5, H-$C_{3,5}$), 7.00 – 6.89 (m, 3H, H-7, H-$C_{2,6}$), 6.88 – 6.80 (m, 2H, H-$A_{2,6}$), 6.79 – 6.71 (m, 1H, H-C_4); **^{13}C NMR** (75 MHz, Acetone-d_6) δ (ppm): 173.13 (C=O), 147.20 (C=N), 144.15 (Cq-C_1), 143.02 (Cq-7a), 137.89 (Cq-A_1), 135.58 (Cq-B_4), 132.96 (Cq-A_4), 132.61 (CH-6), 130.17 and 130.04 (CH-$A_{2,6}$ and CH-$B_{2,6}$), 129.91 (CH-$A_{3,5}$), 129.70 (CH-$C_{3,5}$), 129.41 (CH-$B_{3,5}$), 127.32 (CH-4 and Cq-B_1), 126.90 (Cq-3a), 124.20 (CH-5), 120.78 (CH-C_4), 114.70 (CH-$C_{2,6}$), 111.94 (CH-7), 88.56 (Cspiro). Anal. Calcd for $C_{21}H_{14}ClN_3O_2 \cdot 0.75H_2O$: C 65.00, H 3.95, N 11.23, Found: C 64.64, H 3.90, N 11.50.

2'-(2-chlorophenyl)-4'-(4-chlorophenyl)-5'-phenyl-2',4'-dihydrospiro [indoline-3,3'-[1,2,4]triazol]-2-one (168p).

Synthesized according to the general procedure, this compound was obtained as a white solid (146.7 mg, 76 % yield).

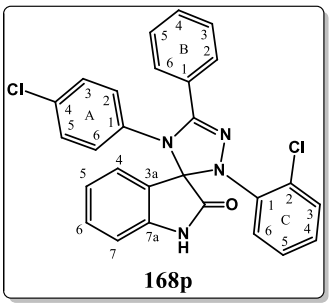

Mp: 212-214 ºC; **IR** (KBr, selected peaks): 3261 (NH), 1739 (C=O), 1616 (C=N), 1492, 1472, 1384, 1202, 756, 697 cm^{-1}; **^{1}H NMR** (300 MHz, Acetone-d_6) δ (ppm): 9.31 (br s, 1H, NH), 7.70 (dd, J = 8.1, 1.5 Hz, 1H, H-C_6), 7.58 – 7.50 (m, 2H, H-$B_{2,6}$), 7.45 – 7.32 (m, 3H, H-$B_{3,4,5}$), 7.29 (ddd, J = 8.1, 7.3, 1.5 Hz, 1H, H-C_5) 7.21 – 7.08 (m, 4H, H-6, H-$A_{3,5}$, H-C_3), 7.04 (ddd, J = 8.0, 7.3, 1.5 Hz, 1H, H-C_4), 6.95 (d, J = 7.0 Hz, 1H, H-4), 6.84 – 6.69 (m, 4H, H-5, H-7, H-$A_{2,6}$); **^{13}C NMR** (75 MHz, Acetone-d_6) δ (ppm): 173.99 (C=O), 152.73 (C=N), 144.20 and 144.15 (Cq-7a and Cq-C_1), 138.61 (Cq-A_1), 132.44 (Cq-A_4), 132.03 (CH-6), 130.59 (CH-C_3), 130.28 (CH-B_4), 129.93 (CH-$A_{2,6}$), 129.65 (CH-$A_{3,5}$), 129.65 (Cq-C_2) 129.21 (CH-$B_{3,5}$), 129.00 (CH-$B_{2,6}$), 128.72 (Cq-B_1), 128.48 (CH-4), 127.82 (CH-$C_{5,6}$), 126.76 (CH-C_4), 124.92 (Cq-3a), 122.59 (CH-5), 111.27 (CH-7), 89.65 (Cspiro). Anal. Calcd for $C_{27}H_{18}Cl_2N_4O \cdot 0{,}3H_2O$ $0{,}2H_2O$: C 66.07, H 3.83, N 11.42, Found: C 65.77, H 3.81, N 11.17.

2'-(3-chlorophenyl)-4'-(4-chlorophenyl)-5'-phenyl-2',4'-dihydrospiro [indoline-3,3'-[1,2,4]triazol]-2-one (168q).

Synthesized according to the general procedure, this compound was obtained as a yellow solid (172.0 mg, 91 % yield).

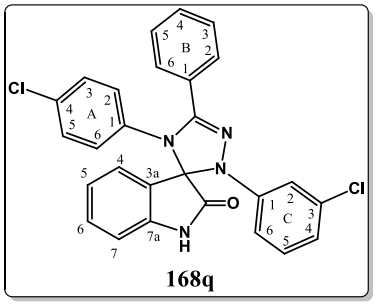

Mp: 120-122 ºC; **IR** (KBr, selected peaks): 3255 (NH), 1735 (C=O), 1591 (C=N), 1491, 1474, 1385, 1324, 1196, 1092, 754 cm^{-1}; **^{1}H NMR** (300 MHz, Acetone-d_6) δ (ppm): 9.79 (br s, 1, NH), 7.59 (dd, J = 7.6, 0.7 Hz, 1H, H-4), 7.55 – 7.47 (m, 2H, H-$B_{2,6}$), 7.45 – 7.31 (m, 4H, H-6, H-$B_{3,4,5}$), 7.23 – 7.17 (m, 2H, H-$A_{3,5}$), 7.12 (td, J = 7.6, 1.0 Hz, 1H, H-5), 7.11 - 7.04 (m, 2H, H-$C_{2,5}$), 6.98 (d, J = 7.7 Hz, 1H, H-7), 6.87 – 6.80 (m, 2H, H-$A_{2,6}$), 6.75 (ddd, J = 8.0, 2.0, 0.9 Hz, 1H, H-C_4), 6.67 (ddd, J = 8.4, 2.3, 0.9 Hz, 1H, H-C_6); **^{13}C NMR** (75 MHz, Acetone-d_6) δ (ppm): 172.86 (C=O), 149.09 (C=N), 145.34 (Cq-C_1), 143.01 (Cq-7a), 137.78 (Cq-A_1), 135.19 (Cq-C_3), 133.08 (Cq-A_4), 132.87 (CH-6), 131.14 (CH-B_4), 130.61 (CH-C_5), 130.22 (CH-$A_{2,6}$), 129.90 (CH-$A_{3,5}$), 129.28 (CH-$B_{3,5}$), 128.83 (CH-$B_{2,6}$), 128.16 (Cq-B_1), 127.36 (CH-4), 126.33 (Cq-3a), 124.40 (CH-5), 119.99 (CH-C_4), 114.39 (CH-C_2), 112.27 (CH-C_6), 112.06 (CH-7), 88.12 (Cspiro). Anal. Calcd for $C_{27}H_{18}Cl_2N_4O{\cdot}0{,}4H_2O$: C 65.83, H 3.85, N 11.38, Found: C 65.51, H 3.76, N 11.12.

2',4'-bis(4-chlorophenyl)-5'-phenyl-2',4'-dihydrospiro[indoline-3,3'-[1,2,4] triazol]-2-one (168r).

Synthesized according to the general procedure, this compound was obtained as a yellow solid (159.3 mg, 84 % yield).

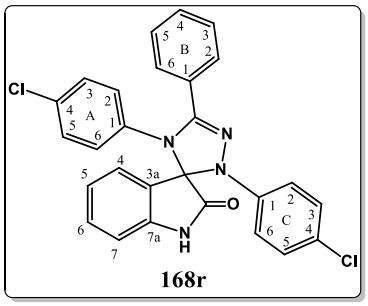

MP: 130-132 ºC; **IR** (KBr, selected peaks): 3208 (NH), 1731 (C=O), 1595 (C=N), 1490, 1385, 1320, 1194, 1014, 820, 746 cm^{-1}; **^{1}H NMR** (300 MHz, Acetone-d_6) δ (ppm): 9.68 (br s, 1H, NH), 7.57 (d, J = 7.4 Hz, 1H, H-4), 7.53 – 7.46 (m, 2H, H-$B_{2,6}$), 7.42 – 7.30 (m, 4H, H-6, H-$B_{3,4,5}$), 7.22 – 7.16 (m, 2H, H-$A_{3,5}$), 7.16 – 7.07 (m, 3H, H-5, H-$C_{3,5}$), 6.96 (d, J = 7.8 Hz, 1H, H-7), 6.94 – 6.86 (m, 2H, H-$C_{2,6}$), 6.86 – 6.78 (m, 2H, H-$A_{2,6}$); **^{13}C NMR** (75 MHz, Acetone-d_6) δ (ppm): 172.93 (C=O), 148.85 (C=N), 143.19 (Cq-C_1), 143.03 (Cq-7a), 137.95 (Cq-A_1), 132.98 (Cq-A_4), 132.75 (CH-6), 130.50 (CH-B_4), 130.15 (CH-$A_{2,6}$), 129.86 and 129.56 (CH-$A_{3,5}$ and CH-$C_{3,5}$), 129.25 (CH-$B_{3,5}$), 128.76 (CH-$B_{2,6}$), 128.32 (Cq-B_1), 127.35 (CH-4), 126.56 (Cq-3a), 124.87 (Cq-C_4), 124.32 (CH-5), 116.05 (CH-$C_{2,6}$), 112.07 (CH-7), 88.41 (Cspiro). Anal. Calcd for $C_{21}H_{14}ClN_3O_2$: C 66.81, H 3.75, N 11.55, Found: C 66.60, H 3.76, N 11.36.

2'-(2-chlorophenyl)-5'-(3-chlorophenyl)-4'-(4-chlorophenyl)-2',4'-dihydro spiro[indoline-3,3'-[1,2,4]triazol]-2-one (168s).

Synthesized according to the general procedure, this compound was obtained as a white solid (173.8 mg, 86 % yield).

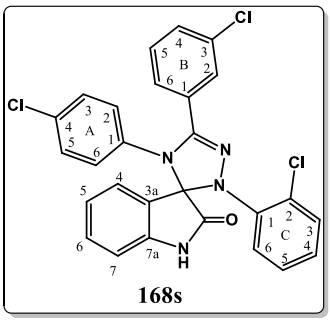

168s

Mp: 244-245ºC. **IR** (KBr, selected peaks): 3284 (NH), 1745 (C=O), 1605 (C=N), 1492, 1473, 1427, 1375, 1195, 753, 688 cm^{-1}. **^{1}H NMR** (300 MHz, Acetone-d_6) δ (ppm): 9.37 (br s, 1H, NH), 7.70 (dd, J = 8.1, 1.5 Hz, 1H, H-C_6), 7.65 – 7.60 (m, 1H, H-B_2), 7.46 – 7.33 (m, 3H, H-$B_{4,5,6}$), 7.29 (ddd, J = 8.1, 7.2, 1.6 Hz, 1H, H-C_5), 7.20 – 7.11 (m, 4H, H-6, H-$A_{3,5}$, H-C_3), 7.05 (ddd, J = 8.0, 7.2, 1.6 Hz, 2H, H-C_4), 6.97 (dd, J = 7.5, 1.5Hz, 1H, H-4), 6.88 – 6.81 (m, 2H, H-$A_{2,6}$), 6.80 – 6.70 (m, 2H, H-5, H-7); **^{13}C NMR** (75 MHz, Acetone-d_6) δ (ppm): 173.93 (C=O), 151.35 (C=N), 144.14 (Cq-7a), 143.77 (Cq-C_1), 138.27 (Cq-A_1), 134.65 (Cq-B_3), 132.71 (Cq-A_4), 132.15 (CH-6), 130.98 (CH-B_5), 130.74 (Cq-C_2), 130.48 (CH-C_3), 130.34 (CH-B_4), 129.91 (CH-$A_{2,6}$), 129.82 (CH-$A_{3,5}$), 129.70 (Cq-B_1), 128.69 (CH-C_5), 128.57 (CH-B_2), 127.97 (CH-4), 127.88 (CH-B_6), 127.35 (CH-C_4), 127.01 (CH-C_6), 124.55 (Cq-3a), 122.63 (CH-5), 111.30 (CH-7), 89.83 (Cspiro). Anal. Calcd for $C_{27}H_{17}Cl_3N_4O$: C 62.38, H 3.30, N 10.78, Found: C 62.78, H 3.41, N 10.65.

5-bromo-4',5'-bis(3-chlorophenyl)-2'-phenyl-2',4'-dihydrospiro[indoline-3,3'-[1,2,4]triazol]-2-one (168t).

Synthesized according to the general procedure, this compound was obtained as a yellow solid (142.5 mg, 85 % yield).

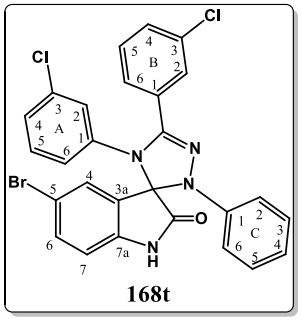

168t

Mp: 104-106 ºC; **IR** (KBr, selected peaks): 3251 (NH), 1738 (C=O), 1590 (C=N), 1474, 1434, 1384, 1314, 1197, 748, 689 cm^{-1}; **^{1}H NMR** (300 MHz, Acetone-d_6) δ (ppm): 9.91 (br s, 1H, NH), 7.81 (d, J = 2.0 Hz, 1H, H-4), 7.61 (d, J = 0.9 Hz, 1H, H-B_2), 7.55 (dd, J = 8.3, 2.0 Hz, 1H, H-6), 7.45 – 7.34 (m, 3H, H-$B_{4,5,6}$), 7.26 – 7.20 (m, 2H, H-$A_{4,5}$), 7.15 (t, J = 8.0 Hz, 2H, H-$C_{3,5}$), 7.00 – 6.91 (m, 4H, H-7, H-A_2, H-$C_{2,6}$), 6.90 – 6.85 (m, 1H, H-A_6), 6.80 (t, J = 7.3 Hz, 1H, H-C_4); **^{13}C NMR** (75 MHz, Acetone-d_6) δ (ppm): 172.79 (C=O), 146.77 (C=N), 143.77 (Cq-C_1), 142.16 (Cq-7a), 140.13 (Cq-A_1), 135.56 (CH-6), 134.79 (Cq-A_3), 134.64 (Cq-B_3), 131.36 (CH-A_5), 130.97 (CH-B_5), 130.32 (CH-4 and CH-B_4), 130.30 (Cq-B_1), 129.87 (CH-$C_{3,5}$), 128.82 (Cq-3a), 128.42 (CH-B_2), 128.22 and 128.19 (CH-A_4 and CH-A_2), 127.06 and 127.04 (CH-A_6 and CH-B_6), 121.27 (CH-C_4), 116.29 (Cq-5), 114.87 (CH-$C_{2,6}$), 113.88 (CH-7), 88.42 (Cspiro). Anal. Calcd for $C_{27}H_{17}BrCl_2N_4O$: C 57.47, H 3.04, N 9.93, Found: C 57.80, H 3.23, N 9.72.

5-bromo-4'-(3-chlorophenyl)-5'-(4-chlorophenyl)-2'-phenyl-2',4'-dihydro spiro[indoline-3,3'-[1,2,4]triazol]-2-one (168u).

Synthesized according to the general procedure, this compound was obtained as a yellow solid (138.6 mg, 82 % yield).

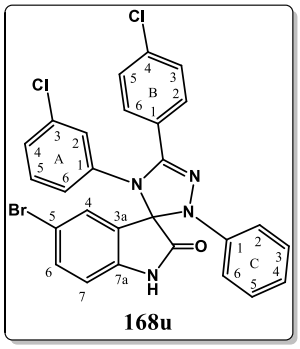

Mp: 116-118 ºC; **IR** (KBr, selected peaks): 3251 (NH), 1735 (C=O), 1590 (C=N), 1491, 1474, 1384, 1315, 1092, 821, 689 cm^{-1}; **^{1}H NMR** (300 MHz, Acetone-d_6) δ (ppm): 9.89 (br s, 1H, NH), 7.78 (d, J = 2.0 Hz, 1H, H-4), 7.58 – 7.50 (m, 3H, H-6, H-$B_{2,6}$), 7.41 (d, J = 8.6 Hz, 2H, H-$B_{3,5}$), 7.25 – 7.19 (m, 2H, H-$A_{4,5}$), 7.15 (t, J = 8.0 Hz, 2H, H-$C_{3,5}$), 7.00 – 6.92 (m, 3H, H-7, H-$C_{2,6}$), 6.91 (d, J = 1.0 Hz, 1H, H-A_2) 6.88 – 6.83 (m, 1H, H-A_6), 6.80 (t, J = 7.3 Hz, 1H, H-C_4); **^{13}C NMR** (75 MHz, Acetone-d_6) δ (ppm): 172.86 (C=O), 147.07 (C=N), 143.86 (Cq-C_1), 142.27 (Cq-7a), 140.24 (Cq-A_1), 135.74 (Cq-B_4), 135.52 (CH-6), 134.76 (Cq-A_3), 131.32 (CH-A_5), 130.30 (CH-$B_{2,6}$), 130.23 (CH-4), 129.85 (CH-$C_{3,5}$), 129.44 (CH-$B_{3,5}$), 128.98 (Cq-3a), 128.13 (CH-$A_{2,4}$), 127.13 (Cq-B_1), 127.03 (CH-A_6), 121.15 (CH-C_4), 116.21 (Cq-5), 114.82 (CH-$C_{2,6}$), 113.91 (CH-7), 88.37 (Cspiro). Anal. Calcd for $C_{27}H_{17}BrCl_2N_4O$: C 57.47, H 3.04, N 9.93, Found: C 57.87, H 2.84, N 9.77.

5-bromo-4'-(3-chlorophenyl)-5'-(4-methoxyphenyl)-2'-phenyl-2',4'-dihydro spiro[indoline-3,3'-[1,2,4]triazol]-2-one (168v).

Synthesized according to the general procedure, this compound was obtained as a yellow solid (50.2 mg, 60 % yield).

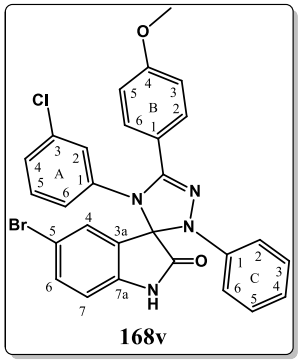

Mp: 123-125 ºC; **IR** (KBr, selected peaks): 3259 (NH), 1746 (C=O), 1590 (C=N), 1498, 1475, 1385, 1255, 1177, 1032, 689 cm^{-1}; **^{1}H NMR** (300 MHz, Acetone-d_6) δ (ppm): 9.86 (br s, 1H, NH), 7.75 (d, J = 2.0 Hz, 1H, H-4), 7.54 (dd, J = 8.3, 2.0 Hz, 1H, H-6), 7.47 – 7.41 (m, 2H, H-$B_{2,6}$), 7.25 – 7.17 (m, 2H H-$A_{4,5}$), 7.16 – 7.09 (m, 2H, H-$C_{3,5}$), 6.96 (d, J = 8.3 Hz, 1H, H-7), 6.93 – 6.87 (m, 5H, H-A_2, H-$B_{3,5}$, H-$C_{2,6}$), 6.85 – 6.80 (m, 1H, H-A_6), 6.76 (t, J = 7.3 Hz, 1H, H-C_4), 3.80 (s, 3H, OCH_3); **^{13}C NMR** (75 MHz, Acetone-d_6) δ (ppm): 173.00 (C=O), 161.68 (Cq-B_4), 147.92 (C=N), 144.21 (Cq-C_1), 142.16 (Cq-7a), 140.64 (Cq-A_1), 135.38 (CH-6), 134.60 (Cq-A_3), 131.16 (CH-A_5), 130.31 (CH-$B_{2,6}$), 130.16 (CH-4), 129.78 (CH-$C_{3,5}$), 129.25 (Cq-3a), 128.27 (CH-A_4), 127.89 (CH-A_2), 127.10 (CH-A_6), 120.74 (CH-C_4), 120.38 (Cq-B_1), 116.19 (Cq-5), 114.68 and 114.64 (CH-$B_{3,5}$ and CH-$C_{2,6}$), 113.80 (CH-7), 88.10 (Cspiro), 55.67 (OCH_3). Anal. Calcd for $C_{28}H_{20}BrClN_4O_2 \cdot 0{,}3H_2O$: C 59.49, H 3.68, N 9.91, Found: C 59.17, H 3.34, N 10.08.

5-bromo-2'-(2-chlorophenyl)-4'-(3-chlorophenyl)-5'-phenyl-2',4'-dihydro spiro[indoline-3,3'-[1,2,4]triazol]-2-one (168w).

Synthesized according to the general procedure, this compound was obtained as a white solid (105.2 mg, 63 % yield).

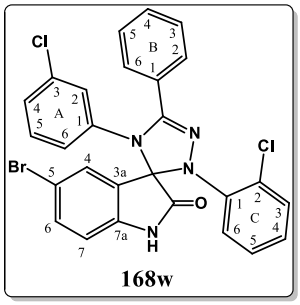

168w

Mp: 244-246 ºC; **IR** (KBr, selected peaks): 3168 (NH), 1747 (C=O), 1588 (C=N), 1474, 1384, 1196, 828, 761, 690 cm^{-1}; **^{1}H NMR** (300 MHz, Acetone-d_6) δ (ppm): 9.53 (br s, 1H, NH), 7.77 (dd, J = 8.1, 1.5 Hz, 1H, H-C_6), 7.59 – 7.54 (m, 2H, H-$B_{2,6}$), 7.46 – 7.30 (m, 5H, H-6, H-$B_{3,4,5}$, H-C_5), 7.22 – 7.06 (m, 4H, H-4, H-$A_{4,5}$, H-$C_{3,4}$), 6.90 – 6.86 (m, 1H, H-A_2), 6.85 – 6.81 (m, 1H, H-A_6), 6.77 (d, J = 8.3 Hz, 1H, H-7); **^{13}C NMR** (75 MHz, Acetone-d_6) δ (ppm): 173.60 (C=O), 152.48 (C=N), 143.75 (Cq-C_1), 143.26 (Cq-7a), 140.86 (Cq-A_1), 134.91 (CH-6), 134.57 (Cq-A_3), 131.40 (CH-A_5), 131.06 (CH-B_4), 130.75 (CH-4), 130.38 (CH-C_3), 129.59 (Cq-C_2), 129.24 (CH-$B_{3,5}$), 129.11 (CH-$B_{2,6}$), 128.44 (Cq-B_1), 128.31 (CH-A_4), 128.10 (CH-C_6), 127.96 (CH-C_5), 127.63 (CH-C_4), 127.26 (CH-A_2), 126.99 (Cq-3a), 126.75 (CH-A_6), 114.64 (Cq-5), 113.10 (CH-7), 89.48 (Cspiro). Anal. Calcd for $C_{27}H_{17}BrCl_2N_4O \cdot 0{,}55H_2O$: C 56.48, H 3.18, N 9.76, Found: C 56.21, H 3.32, N 9.37.

5-bromo-2',4'-bis(3-chlorophenyl)-5'-phenyl-2',4'-dihydrospiro[indoline-3,3'-[1,2,4]triazol]-2-one (168x).

Synthesized according to the general procedure, this compound was obtained as a yellow solid (147.4 mg, 88 % yield).

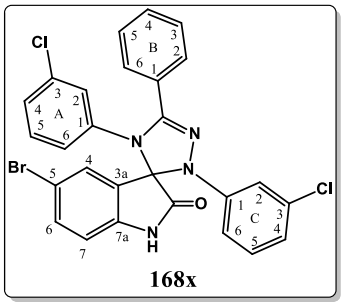

168x

Mp: 118-120ºC; **IR** (KBr, selected peaks): 3245 (NH), 1735 (C=O), 1589 (C=N), 1474, 1384, 1328, 1197, 773, 691 cm^{-1}; **^{1}H NMR** (300 MHz, Acetone-d_6) δ (ppm): 7.83 (d, J = 2.0 Hz, 1H, H-4), 7.57 (dd, J = 8.4, 2.0 Hz, 1H, H-6), 7.55 – 7.51 (m, 2H, H-$B_{2,6}$), 7.43 – 7.35 (m, 3H, H-$B_{3,4,5}$), 7.23 – 7.19 (m, 2H, H-$A_{4,5}$), 7.14 – 7.06 (m, 2H, H-$C_{2,5}$), 6.99 (d, J = 8.4 Hz, 1H, H-7), 6.90 (dd, J = 2.4, 1.3 Hz, 1H, H-A_2), 6.88 – 6.82 (m, 1H, H-A_6), 6.78 (ddd, J = 7.9, 2.0, 0.6 Hz, 1H, H-C_4), 6.65 (ddd, J = 8.3, 2.2, 0.6 Hz, 1H, H-C_6); **^{13}C NMR** (75 MHz, Acetone-d_6) δ (ppm): 172.54 (C=O), 148.91 (C=N), 145.04 (Cq-C_1), 142.19 (Cq-7a), 140.09 (Cq-A_1), 135.78 (CH-6), 135.31 (Cq-C_3), 134.72 (Cq-A_3), 131.30 (CH-B_4 and CH-C_5), 130.75 (CH-A_5), 130.30 (CH-4), 129.29 (CH-$B_{3,5}$), 128.92 (CH-$B_{2,6}$), 128.39 (Cq-3a), 128.34 (CH-A_4), 128.22 (CH-A_2), 127.91 (Cq-B_1), 127.11 (CH-A_6), 120.38 (CH-C_4), 116.44 (Cq-5), 114.56 (CH-C_2), 114.00 (CH-7), 112.25 (CH-C_6) 87.88 (Cspiro). Anal. Calcd for $C_{27}H_{17}BrCl_2N_4O \cdot 0{,}85H_2O$: C 55.95, H 3.26, N 9.67, Found: C 55.61, H 3.13, N 9.39.

5-bromo-4'-(3-chlorophenyl)-2'-(4-chlorophenyl)-5'-phenyl-2',4'-dihydro spiro[indoline-3,3'-[1,2,4]triazol]-2-one (168y).

Synthesized according to the general procedure, this compound was obtained as a yellow solid (149.4 mg, 89 % yield).

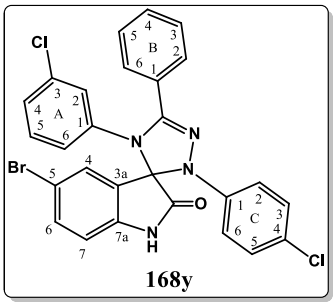

168y

Mp: 203-205 ºC; **IR** (KBr, selected peaks): 3085 (NH), 1746 (C=O), 1590 (C=N), 1491, 1475, 1385, 1199, 776, 694 cm^{-1}; **^{1}H NMR** (300 MHz, Acetone-d_6) δ (ppm): 7.79 (d, J = 2.0 Hz, 1H, H-4), 7.58 – 7.49 (m, 3H, H-6, H-$B_{2,6}$), 7.42 – 7.31 (m, 3H, H-$B_{3,4,5}$), 7.24 – 7.17 (m, 2H, H-$A_{4,5}$), 7.15 (d, J = 9.0 Hz, 2H, H-$C_{3,5}$), 6.96 (d, J = 8.2 Hz, 1H, H-7), 6.92 (d, J = 9.0 Hz, 2H, H-$C_{2,6}$), 6.89 (dd, J = 2.3, 1.2 Hz, 1H, H-A_2), 6.87 – 6.80 (m, 1H, H-A_6); **^{13}C NMR** (75 MHz, Acetone-d_6) δ (ppm): 172.60 (C=O), 148.66 (C=N), 142.87 (Cq-C_1), 142.27 (Cq-7a), 140.27 (Cq-A_1), 135.65 (CH-6), 134.70 (Cq-A_3), 131.25 (CH-A_5), 130.64 (CH-B_4), 130.23 (CH-4), 129.71 (CH-$C_{3,5}$), 129.27 (CH-$B_{3,5}$), 128.85 (CH-$B_{2,6}$), 128.62 (Cq-3a), 128.26 (CH-A_4), 128.09 (CH-A_2), 128.08 (Cq-B_1) 127.02 (CH-A_6), 125.23 (Cq-C_4), 116.32 (Cq-5), 116.14 (CH-$C_{2,6}$), 114.02 (CH-7), 88.18 (Cspiro). Anal. Calcd for $C_{27}H_{17}BrCl_2N_4O{\cdot}0{,}15H_2O$: C 57.19, H 3.08, N 9.88, Found: C 56.86, H 3.27, N 9.70.

5-bromo-2'-(2-chlorophenyl)-4',5'-bis(3-chlorophenyl)-2',4'-dihydrospiro [indoline-3,3'-[1,2,4]triazol]-2-one (168z).

Synthesized according to the general procedure, this compound was obtained as a white solid (143.1 mg, 80 % yield).

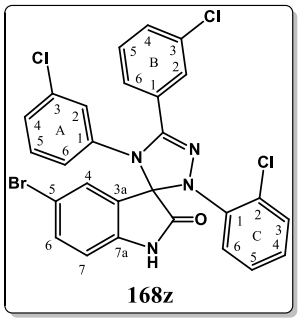

168z

Mp: 239-240ºC; **IR** (KBr, selected peaks): 3242 (NH), 1747 (C=O), 1589 (C=N), 1474, 1431, 1384, 1195, 1077, 764, 695 cm^{-1}; **^{1}H NMR** (300 MHz, Acetone-d_6) δ (ppm): 9.57 (br s, 1H, NH), 7.77 (dd, J = 8.1, 1.5 Hz, 1H, H-C_6), 7.67 – 7.64 (m, 1H, H-B_2), 7.48 – 7.30 (m, 5H, H-6, H-$B_{4,5,6}$, H-C_5), 7.24 (d, J = 2.0 Hz, 1H, H-4), 7.23 – 7.14 (m, 3H, H-$A_{4,5,}$ H-C_3), 7.11 (ddd, J = 8.0, 7.3, 1.6 Hz, 1H, H-C_4), 6.96 – 6.92 (m, 1H, H-A_2), 6.91 – 6.86 (m, 1H, H-A_6), 6.77 (d, J = 8.3 Hz, 1H, H-7); **^{13}C NMR** (75 MHz, Acetone-d_6) δ (ppm): 173.54 (C=O), 151.10 (C=N), 143.44 and 143.19 (Cq-7a and Cq-C_1), 140.53 (Cq-A_1), 135.03 (CH-6), 134.74 (Cq-A_3), 134.67 (Cq-B_3), 131.53 and 131.24 (CH-C_3 and CH-A_5), 131.00 and 130.65 (CH-4 and CH-B_5), 130.49 (Cq-C_2), 130.44 (CH-B_4), 129.64 (Cq-B_1), 128.86, 128.48, 128.11, 128.01 and 127.93 (CH-$A_{2,4}$, CH-B_2, CH-$C_{5,6}$), 127.48 (CH-B_6 and CH-C_4), 126.82 (CH-A_6), 126.67 (Cq-3a), 114.70 (Cq-5), 113.12 (CH-7), 89.69 (Cspiro). Anal. Calcd for $C_{27}H_{16}BrCl_3N_4O$: C 54.16, H 2.70, N 9.36, Found: C 54.54, H 2.80, N 9.29.

5-bromo-2',4',5'-tris(3-chlorophenyl)-2',4'-dihydrospiro[indoline-3,3'-[1,2,4] triazol]-2-one (168aa)

Synthesized according to the general procedure, this compound was obtained as a yellow solid (156.3 mg, 88 % yield).

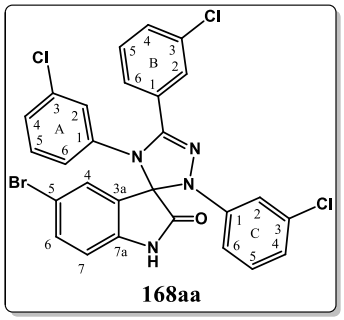

168aa

Mp: 113-115 ºC; **IR** (KBr, selected peaks): 3240 (NH), 1740 (C=O), 1589 (C=N), 1475, 1430, 1385, 1326, 1195, 768, 691 cm^{-1}.**^{1}H NMR** (300 MHz, Acetone-d_6) δ (ppm): 10.02 (br s, 1H, NH), 7.87 (d, J = 2.0 Hz, 1H, H-4), 7.64 – 7.60 (m, 1H, H-B_2), 7.58 (dd, J = 8.3, 2.0 Hz, 1H, H-6), 7.46 – 7.33 (m, 3H, H-$B_{4,5,6}$), 7.27 – 7.22 (m, 2H, H-$A_{4,5}$), 7.16 – 7.08 (m, 2H, H-$C_{2,5}$), 6.99 (d, J = 8.3 Hz, 1H, H-7), 6.96 (dd, J = 2.5, 1.3 Hz, 1H, H-A_2), 6.92 – 6.87 (m, 1H, H-A_6), 6.81 (ddd, J = 8.0, 2.0, 0.8 Hz, 1H, H-C_4), 6.68 (ddd, J = 8.4, 2.3, 0.8 Hz, 1H, H-C_6); **^{13}C NMR** (75 MHz, Acetone-d_6) δ (ppm): 172.38 (C=O), 147.63 (C=N), 144.79 (Cq-C_1), 142.08 (Cq-7a), 139.70 (Cq-A_1), 135.87 (CH-6), 135.34 (Cq-C_3), 134.86 (Cq-A_3), 134.68 (Cq-B_3), 131.43 and 131.34 (CH-C_5 and CH-A_5), 131.01 (CH-B_5), 130.61 and 130.41 (CH-4 and CH-B_4), 129.90 (Cq-B_1), 128.60 and 128.49 (CH-B_2 and CH-A_4), 128.33 (CH-A_2), 128.07 (Cq-3a), 127.26 (CH-B_6), 127.15 (CH-A_6), 120.69 (CH-C_4), 116.50 (Cq-5), 114.65 (CH-C_2), 114.00 (CH-7), 112.39 (CH-C_6), 88.05 (Cspiro). Anal. Calcd for $C_{27}H_{16}BrCl_3N_4O$: C 54.16, H 2.70, N 9.36, Found: C 54.51, H 2.79, N 9.22.

9.1.12. SYNTHESIS OF 5-BROMO-4'-(3-CHLOROPHENYL)-2',5'-DIPHENYL-2',4'-DIHYDROSPIRO[INDOLINE-3,3'-PYRAZOL]-2-ONE (167F).

Triethylamine (2.0 equiv, 0.3 mmol, 42 µL) was added dropwise to a mixture of 3-methylene indolin-2-one **121r** (1.0 equiv, 0.15 mmol, 50.0 mg), and hydrazonyl chloride **170a** (2.0 equiv, 0.3 mmol, 69.2 mg) in dry DCM (1.5 mL) under nitrogen atmosphere. The reaction was stirred at room temperature for 5 hours. The mixture was then washed with brine (2x) and the aqueous phase extracted with DCM. The combined organic extracts were dried over anhydrous Na_2SO_4 and the solvent was removed under reduce pressure. The residue was purified by flash chromatography on silica gel using as eluent a gradient of 100% *n*-hexane to *n*-hexane/EtOAc (60:40), and recrystallized from diethyl ether to afford compound **167f** as a white solid (59.3 mg, 75%).

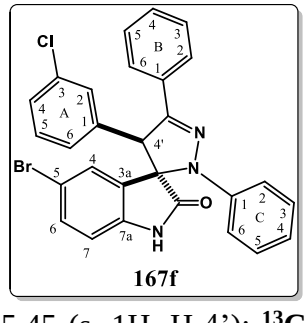

167f

Mp: 185-187 ºC; **IR** (KBr, selected peaks): 3215 (NH), 1726 (C=O), 1705, 1596, 1492, 1473, 1384, 1194, 751, 689 cm^{-1}; **^{1}H NMR** (400 MHz, Acetone-d_6) δ (ppm): 9.92 (br s, 1H, NH), 7.81 – 7.71 (m, 2H, H-$B_{2,6}$), 7.40 – 7.26 (m, 6H, H-6, H-$B_{3,4,5}$, H-$A_{4,5}$), 7.18 – 7.07 (m, 4H, H-$A_{2,6}$, H-$C_{3,5}$), 6.98 – 6.91 (m, 3H, H-7, H-$C_{2,6}$), 6.86 – 6.78 (m, 1H, H-C_4), 6.54 (d, J = 2.0 Hz, 1H, H-4), 5.45 (s, 1H, H-4'); **^{13}C**

NMR (100 MHz, Acetone-d_6) δ (ppm): 176.76 (C=O), 149.40 (C=N), 145.06 (Cq-C_1), 141.67 (Cq-7a), 138.24 (Cq-A_1), 135.00 (Cq-A_3), 133.32 (CH-6), 132.37 (Cq-B_1), 131.17 (CH-B_4), 130.05 (CH-4), 129.89 and 129.84 (CH-A_4 and CH-A_5), 129.74 (CH-$C_{3,5}$), 129.44 (CH-$B_{3,5}$), 129.04 (CH-A_2), 128.65 (CH-A_6), 128.40 (Cq-3a), 127.55 (CH-$B_{2,6}$), 121.80 (CH-C_4), 115.90 (CH-$C_{2,6}$), 114.67 (Cq-5), 112.95 (CH-7), 77.22 (Cspiro), 62.34 (CH-4'). Anal. Calcd for $C_{28}H_{19}BrClN_3O \cdot 0.2H_2O$: C 63.16, H 3.68, N 7.89, Found: C 62.76, H 4.07, N 7.99.

9.2. EXPERIMENTAL SECTION: BIOLOGY.

HCT116 cells were grown in McCoy's 5A supplemented with 10% fetal bovine serum (FBS) (Invitrogen, Grand Island, NY, USA), 1% GlutaMAX™ (Invitrogen) and 1% penicillin/streptomycin solution (Sigma-Aldrich, St Louis, MO, USA). SW620 cells were grown in DMEM (Invitrogen) supplemented with 10% FBS and 1% antibiotic/antimycotic solution (Sigma-Aldrich). HepG2 human hepatoma cells were grown in DMEM (Invitrogen) supplemented with 10% FBS, 1% non-essential amino acids and 1% antibiotic/antimycotic solution (Sigma-Aldrich). HEK293T (ATCC CRL-11268), MCF-7 (ATCC HTB-22™) and MDA-MB-231 (ATCC HTB-26™) were cultivated in RPMI 1640 culture medium supplemented with 10% fetal bovine serum, 100 units of penicillin G (sodium salt), 100 mg of streptomycin sulfate and 2 mM L-glutamine. Cells were maintained at 37 ºC in a humidified atmosphere of 5% CO_2. For cell viability assays cells were seeded at 1 x 10^5 cells/mL (HCT116, HepG2, SW620) and 2x10^5 cells/mL (MCF-7, MDA-MB-231, Hek293T); for Western blot cells were seeded at 3 × 10^5 cells/mL (HCT116, HepG2, SW620) and 2x10^5 cells/mL (MCF-7, MDA-MB-231, and Hek293T); and for flow cytometry analysis cells were seeded at 3 × 10^5 cells/mL. HCT116 human colorectal carcinoma cells rendered p53-null by somatic knockout [383] were a kind gift from Dr. Bert Vogelstein (Johns Hopkins University, Baltimore, MD).

9.2.1. *In vitro* anti-proliferative assay.

The cellular growth inhibitory activity was evaluated in seven cell lines: human hepatocellular carcinoma cell line [HepG2 (wild-type p53)], an isogenic matched pair of wild type p53 and deleted human colorectal cancer cell lines [HCT116 $p53^{(+/+)}$ and $p53^{(-/-)}$], human colorectal adenocarcinoma cell lines [SW620 (mut p53)], human embryonic kidney epithelial cell line (Hek-273T), two breast cancer cell lines MCF-7 (estrogen receptor positive (ER+) and human epidermal growth factor receptor 2 negative (HER2-) and MDA-MB-231 (ER-, and HER2-).

HepG2, HCT116, SW620 cells were incubated with vehicle or the compounds approximately 24 h after plating. For the assays with these cell lines, the compounds were dissolved in DMSO and diluted in culture medium to a range of concentrations from 0.5 to 200 µM (at least twelve concentrations were used). The final concentration of DMSO in culture medium during treatment did not exceed 0.8% (v/v) and the same concentration of DMSO was added to the control. Each compound concentration and DMSO was tested in duplicate in a single experiment which was repeated at least 3 times. Cells were incubated at 37 ºC in humidified 5% CO_2 atmosphere. Cell viability was assessed 24 h or 72 h after compound incubation by using the CellTiter96® AQueous Non-Radioactive Cell Proliferation Assay (Promega), according to the manufacturer's protocol. The method is based on the reduction of MTS tetrazolium compound by viable cells to generate a colored

formazan product that is soluble in cell culture media. The absorbance was measured at 490 nm using Bio-Rad microplate reader Model 680 (Bio-Rad, Hercules, CA, USA). Nutlin-3 or nutlin-3a was used as positive control.

Cytotoxicity assays in Hek273T, MCF-7 and MDA-MB-231 were performed by Lídia M. Gonçalves (iMed.ULisboa), and were assessed using 3-(4,5-dimethyl-2-thiazolyl)-2,5-diphenyl-2H-tetrazolium bromide (MTT), a yellow, water-soluble tetrazolium dye that is converted by mitochondrial dehydrogenases in viable cells to a water-insoluble, purple formazan [384]. For these cell lines, tested compounds were dissolved in DMSO, serially diluted in the culture medium and added to the cells. The final concentration of DMSO in culture medium during treatment did not exceed 0.5% (v/v), and the same concentration of DMSO was added to the control. Each compound concentration and DMSO were tested in triplicate in a single experiment which was repeated at least 3 times, Cells were incubated at 37 ºC in humidified 5% CO_2 atmosphere. After 72 h, cell media was removed and replaced with fresh medium, the MTT dye solution was added to each well (5 mg/mL in 10 mM phosphate buffer solution at pH 7.4), and after 3 h of incubations the media was removed and intracellular formazan crystals were solubilized and extracted with DMSO. After 15 min at room temperature absorbance was measured at 570 nm in a microplate reader (FLUOstar Omega, BMG Labtech, Germany), and the percentage of viable cells was determined for each compound concentration as described previously [385]. Nutlin-3a was used as a positive control.

The concentrations of the compounds that inhibited cell growth by 50% (IC_{50}) were determined by non-linear regression using GraphPad PRISM software.

9.2.2. Western blot analysis.

Total protein extracts from HCT116 $p53^{(+/+)}$ cells incubated with vehicle, compound **119aa**, **119ac**, or nutlin-3 at 25 and 50 µM, and compound **165aa**, **165ad**, **168h**, and nutlin-3a at 10 and 20 µM for 24 h, were prepared following standard protocols [386]. Protein concentrations were determined using the Bio-Rad protein assay kit, according to the manufacturer's specifications. 60 µg of total protein extracts were separated on 8 and 14% (w/v) sodium dodecyl sulphate (SDS)-polyacrylamide gel electrophoresis. After electrophoretic transfer onto nitrocellulose membranes, and blocking with a 5% (w/v) non-fat dry milk solution, membranes were incubated overnight at 4-8 ºC with primary mouse caspase 3 (H-277, sc-7148, 1:100) (Santa Cruz Biotechnology, Santa Cruz, CA) and rabbit polyclonal antibody reactive to PARP-1/2 (H-250, sc-7150, 1:1000) (Santa Cruz Biotechnology, Santa Cruz, CA). Finally, a secondary goat anti-mouse or anti-rabbit IgG antibody conjugated with horseradish peroxidase (BioRad Laboratories, Hercules, CA, USA) was added for 3 h at room temperature. The membranes were processed for protein detection using the SuperSignal substrate (Pierce Biotechnology, Rockford, IL, USA) or

the Immobilon Western Chemiluminescent HRP substrate (Millipore Corporation, Billerica, MA, USA). β-Actin (AC-15; Sigma-Aldrich; 1:8000) was used as a loading control. The relative intensities of protein bands were analyzed using the QuantityOne Version 4.6 or ImageLab 5.1 densitometric analysis program (Bio-Rad) and normalized to the corresponding loading control. Western blot analyses were performed by Joana D. Amaral (Cellular Function and Therapeutic Targeting, iMed.ULisboa).

9.2.3. Evaluation of caspase-3/7 activity

Caspase-3 and -7 activities were measured using the Caspase-Glo 3/7 Assay (Promega). This assay is based on the cleavage of a pro luminescent substrate containing the specific DEVD sequence recognized by caspase-3 and -7 to release aminoluciferin in cell lysates. The subsequent luciferase cleavage of the unconjugated aminoluciferin generates a luminescent signal directly proportional to the amount of caspase activity present in the sample. Equal volumes of total protein extracts and caspase-Glo 3/7 reagent were incubated on a 96-well plate and mixed by orbital shaking for 30 s, as previously described [387, 388]. Subsequently the mixture was incubated at room temperature for 30 min, leading to stabilization of substrate cleavage by caspases, and accumulation of luminescent signal. The resulting luminescence was measured using the GloMax-Multi^{+} Detection System (Promega). Caspase 3/7 activity assays were performed by Joana D. Amaral (Cellular Function and Therapeutic Targeting group, iMed.ULisboa).

9.2.4. Bimolecular Fluorescence Complementation (BiFC) assay.

HCT116 p53$^{(-/-)}$ cells were co-transfected using 1 μg of each BiFC pair plasmid and Lipofectamine 2000 (Invitrogen). 4–6 h after transfection, the medium was replaced with fresh medium and derivatives **119z**, nutlin-3 were added to a final concentration of 25 and 50 μM; and derivatives **165ab**, **168h**, and nutlin-3a to a final concentration of 5, 10 and 20 μM. The same concentrations of DMSO were tested as control. Cells were washed twice with Ca^{2+}- and Mg^{2+}-free phosphate buffered saline (PBS) (Invitrogen Corp.), treated with accutase and harvested with culture medium. Cell suspensions were centrifuged, supernatants discarded, and cell pellets resuspended in PBS [260]. Fluorescence was measured using a FACSCalibur (compound **119z** and nutlin-3) and Guava® easyCyte™ 5HT Flow Cytometer (**165ab**, **168h**, and nutlin 3a).

9.3. EXPERIMENTAL SECTION: STABILITY.

9.3.1. HPLC analysis.

High-performance liquid chromatography (HPLC) measurements were carried out using a VWR HITACHI assembly equipped with a UV detector L-2400, a column oven L-2300, and a pump L-2130. An injection valve equipped with 20 µL sample loop was used. The separation was performed on a LichroCART® RP-18 (5 µm, 250-4 mm) analytical column (Merck). Acetonitrile: H_2O (70:30, v:v) was used as eluent system for compounds **119aa** and **119ag**. Methanol:H_2O with 1% HCOOH was used as eluent system for compound **165x (**72.5:27.5), **165ae**, **168h**, and **168z** (82.5:17.5). Elution was performed at a solvent flow rate of 1 mL/min. Chromatograms were monitored by UV detection at 260 nm. All analyses were performed at 25 ºC. Acquisition and treatment of data were done using Ezchrom Elite software.

9.3.2. Stability in pH 7.4 phosphate buffer.

12.5 µL of a 10^{-3} M stock solutions of tested compounds in DMSO were added to 2.5 mL of potassium phosphate buffer solution (pH 7.4, 0.5M) at 37ºC. At appropriate intervals, samples (100 µL) were removed and added to acetonitrile (200 µL), and analyzed by HPLC using the methodology previously described. The stability was assessed for a period of 72 h.

9.3.3. Stability in human plasma.

Human plasma was obtained from the pooled, heparinized blood of healthy donors, and was frozen and stored at -20 ºC prior to use. 12.5 µL of a 10^{-3} M stock solutions of tested compounds in DMSO were incubated at 37 °C in 2.5 mL of human plasma diluted to 80% (v/v) with potassium phosphate buffer (pH 7.4, 0.5M). At appropriate intervals, aliquots (100 µL) were removed and added to acetonitrile (200 µL) to quench the reaction and precipitate plasma proteins. These samples were vortexed, centrifuged and the supernatant was analyzed by HPLC using the methodology previously described. The stability was assessed for a period of 72 h.

9.3.4. Stability in rat microsomes.

Male Rat Pooled Liver Microsomes (Sprague-Dawley) BD Gentest™ were used. A mixture of 570 µL purified water, 160 µL potassium phosphate (pH 7.4, 0.5 M), 40 µL NADPH Regenerating System Solution A (BD Biosciences Cat. No. 451220), 8 µL

NADPH Regenerating System Solution B (BD Biosciences Cat. No. 451200), and 20 µL of microsomes was incubated 5 minutes at 37 ºC in a water bath before addition of 8 µL of a 10^{-3} M stock solution of the tested compounds in DMSO. At appropriate intervals, aliquots (50 µL) were removed and added to acetonitrile (50 µL). These samples were mixed, centrifuged and the supernatant was analyzed by HPLC using the methodology previously described. The half-life was determined applying the pseudo-first-order reaction equation: $t_{1/2}$= ln(2)/k. The viability of the rat microsomes was verified by evaluating their CYP2E1-catalyzed *p*-nitrophenol hydroxylation capacity [389].

9.4. EXPERIMENTAL SECTION: DOCKING STUDIES

All computational calculations were performed on the scientific cluster of the Faculty of Pharmacy, University of Lisbon by Sara Silva (Medicinal Chemistry group, iMed.ULisboa).

The binding mode of the synthesized spirooxindole derivatives was predicted by performing docking calculations, using GOLD 5.1.0 software [390], with the MDM2 crystal structure (PDB 4WT2, [98]).

The docking procedure with the selected MDM2 structure was validated through a series of previous exhaustive docking calculations. It was tested the ability to correctly predict the binding poses of a series of known MDM2 inhibitors (using inhibitors with different ranges of biological activity) on a variety of MDM2 crystal structures available. Initially, four MDM2 crystal structures (PDB 3LBL[123], 4MDN [391], 40BA [99] and 4WT2 [98]) were retrieved from Protein Data Bank, protonated (using the function Protonate 3D, a temperature of 300K and defining a pH of 7.4) and prepared on MOE 2014.09 [392]. It was only considered the MDM2 monomer, excluding additional chains present on the crystal structure, water molecules, ions and other molecules originated from the crystallographic procedure were excluded. Chemical structures of synthesized inhibitors were built, protonated and the energy minimized on MOE by using the MMFF94x forcefield with a RMS gradient of 0.1 kcal mol^{-1}.

In all docking calculations the defined binding site was centred on His96 residue (considered well suited by preliminary testing of other possible binding sites) and encompassing an interaction radius for ligands of 12 Å. The efficiency of the search algorithm was set to 100%, which attempts all optimal settings for each ligand, and the scoring function employed was CHEMPLP (selected following a series of preliminary calculations with other existing functions) on a total of 500 runs.

All MDM2 crystal structures revealed good ability to correctly predict the binding poses of the tested ligands.

Chapter 10

REFERENCES

1. Levine, A.J. and Oren, M., The first 30 years of p53: growing ever more complex. *Nat Rev Cancer*, **2009**. *9*(10): p. 749-758.
2. Bieging, K.T., Mello, S.S., and Attardi, L.D., Unravelling mechanisms of p53-mediated tumour suppression. *Nat Rev Cancer*, **2014**. *14*(5): p. 359-70.
3. Brown, C.J., Lain, S., Verma, C.S., Fersht, A.R., and Lane, D.P., Awakening guardian angels: drugging the p53 pathway. *Nat Rev Cancer*, **2009**. *9*(12): p. 862-873.
4. Vousden, K.H. and Lane, D.P., p53 in health and disease. *Nat Rev Mol Cell Biol*, **2007**. *8*(4): p. 275-283.
5. Meek, D.W., Tumour suppression by p53: a role for the DNA damage response? *Nat Rev Cancer*, **2009**. *9*(10): p. 714-723.
6. Brady, C.A. and Attardi, L.D., p53 at a glance. *J Cell Sci*, **2010**. *123*(15): p. 2527-2532.
7. Vousden, K.H. and Prives, C., Blinded by the Light: The Growing Complexity of p53. *Cell*, **2009**. *137*(3): p. 413-431.
8. Christophorou, M.A., Martin-Zanca, D., Soucek, L., Lawlor, E.R., Brown-Swigart, L., Verschuren, E.W., and Evan, G.I., Temporal dissection of p53 function in vitro and in vivo. *Nat Genet*, **2005**. *37*(7): p. 718-726.
9. Kastan, M.B., Wild-type p53: Tumors can't stand it. *Cell*, **2007**. *128*(5): p. 837-840.
10. Shangary, S. and Wang, S., *Small-Molecule inhibitors of the MDM2-p53 protein-protein interaction to reactivate p53 function: a novel approach for cancer therapy*, in *Annu Rev Pharmacol Toxicol*. **2009**. p. 223-241.
11. Cheok, C.F., Verma, C.S., Baselga, J., and Lane, D.P., Translating p53 into the clinic. *Nat Rev Clin Oncol*, **2011**. *8*(1): p. 25-37.
12. Selivanova, G., Therapeutic targeting of p53 by small molecules. *Semin Cancer Biol*, **2010**. *20*(1): p. 46-56.
13. Wang, Z. and Sun, Y., Targeting p53 for novel anticancer therapy. *Transl Oncol*, **2010**. *3*(1): p. 1-12.
14. Athar, M., Elmets, C.A., and Kopelovich, L., Pharmacological activation of p53 in cancer cells. *Curr Pharm Des*, **2011**. *17*(6): p. 631-639.
15. Kim, S.-H. and Dass, C.R., p53-targeted cancer pharmacotherapy: Move towards small molecule compounds. *J Pharm Pharmacol*, **2011**. *63*(5): p. 603-610.
16. Essmann, F. and Schulze-Osthoff, K., Translational approaches targeting the p53 pathway for anti-cancer therapy. *Br J Pharmacol*, **2012**. *165*(2): p. 328-344.
17. Stegh, A.H., Targeting the p53 signaling pathway in cancer therapy - the promises, challenges and perils. *Expert Opin Ther Targets*, **2012**. *16*(1): p. 67-83.
18. Golubovskaya, V.M. and Cance, W.G., Targeting the p53 pathway. *Surg Oncol Clin N Am*, **2013**. *22*(4): p. 747-764.

19. Duffy, M.J., Synnott, N.C., McGowan, P.M., Crown, J., O'Connor, D., and Gallagher, W.M., p53 as a target for the treatment of cancer. *Cancer Treat Rev*, **2014**. *40*(10): p. 1153-1160.
20. Hoe, K.K., Verma, C.S., and Lane, D.P., Drugging the p53 pathway: Understanding the route to clinical efficacy. *Nat Rev Drug Discov*, **2014**. *13*(3): p. 217-236.
21. Hong, B., van den Heuvel, A.P.J., Prabhu, V.V., Zhang, S., and El-Deiry, W.S., Targeting tumor suppressor p53 for cancer therapy: Strategies, challenges and opportunities. *Curr Drug Targets*, **2014**. *15*(1): p. 80-89.
22. Selivanova, G., Wild type p53 reactivation: From lab bench to clinic. *FEBS Lett*, **2014**. *588*(16): p. 2628-2638.
23. Yu, X., Narayanan, S., Vazquez, A., and Carpizo, D.R., Small molecule compounds targeting the p53 pathway: are we finally making progress? *Apoptosis*, **2014**. *19*(7): p. 1055-1068.
24. Zawacka-Pankau, J. and Selivanova, G., Pharmacological reactivation of p53 as a strategy to treat cancer. *J Intern Med*, **2015**. *277*(2): p. 248-59.
25. Tazawa, H., Kagawa, S., and Fujiwara, T., Advances in adenovirus-mediated p53 cancer gene therapy. *Expert Opin Biol Ther*, **2013**. *13*(11): p. 1569-1583.
26. Chene, P., Inhibition of the p53-MDM2 interaction: Targeting a protein-protein interface. *Mol Cancer Res*, **2004**. *2*(1): p. 20-28.
27. Buolamwini, J.K., Addo, J., Kamath, S., Patil, S., Mason, D., and Ores, M., Small molecule antagonists of the MDM2 oncoprotein as anticancer agents. *Curr Cancer Drug Targets*, **2005**. *5*(1): p. 57-68.
28. Fotouhi, N. and Graves, B., Small molecule inhibitors of p53/MDM2 interaction. *Curr Top Med Chem*, **2005**. *5*(2): p. 159-165.
29. Deng, J.X., Dayam, R., and Neamati, N., Patented small molecule inhibitors of p53-MDM2 interaction. *Expert Opin Ther Patents*, **2006**. *16*(2): p. 165-188.
30. Fischer, P.M., Peptide, peptidomimetic, and small-molecule antagonists of the p53-HDM2 protein-protein interaction. *Int J Pept Res Ther*, **2006**. *12*(1): p. 3-19.
31. Dudkina, A.S. and Lindsley, C.W., Small molecule protein-protein inhibitors for the p53-MDM2 interaction. *Curr Top Med Chem*, **2007**. *7*(10): p. 952-960.
32. Hardcastle, I.R., Inhibitors of the MDM2-p53 interaction as anticancer drugs. *Drug Future*, **2007**. *32*(10): p. 883-896.
33. Vassilev, L.T., MDM2 inhibitors for cancer therapy. *Trends Mol Med*, **2007**. *13*(1): p. 23-31.
34. Hu, C.-Q. and Hu, Y.-Z., Small molecule inhibitors of the p53-MDM2. *Curr Med Chem*, **2008**. *15*(17): p. 1720-1730.

35. Patel, S. and Player, M.R., Small-molecule inhibitors of the p53-HDM2 interaction for the treatment of cancer. *Expert Opin Investig Drugs*, **2008**. *17*(12): p. 1865-1882.
36. Shangary, S. and Wang, S., Targeting the MDM2-p53 interaction for cancer therapy. *Clin Cancer Res*, **2008**. *14*(17): p. 5318-5324.
37. Dickens, M.P., Fitzgerald, R., and Fischer, P.M., Small-molecule inhibitors of MDM2 as new anticancer therapeutics. *Semin Cancer Biol*, **2010**. *20*(1): p. 10-18.
38. Weber, L., Patented inhibitors of p53-Mdm2 interaction (2006-2008). *Expert Opin Ther Patents*, **2010**. *20*(2): p. 179-191.
39. Millard, M., Pathania, D., Grande, F., Xu, S., and Neamati, N., Small-molecule inhibitors of p53-MDM2 interaction: the 2006-2010 update. *Curr Pharm Des*, **2011**. *17*(6): p. 536-559.
40. Shen, H. and Maki, C.G., Pharmacologic activation of p53 by small-molecule MDM2 antagonists. *Curr Pharm Des*, **2011**. *17*(6): p. 560-568.
41. Kamal, A., Mohammed, A.A., and Shaik, T.B., p53-Mdm2 inhibitors: patent review (2009-2010). *Expert Opin Ther Patents*, **2012**. *22*(2): p. 95-105.
42. Khoury, K. and Doemling, A., P53 Mdm2 inhibitors. *Curr Pharm Des*, **2012**. *18*(30): p. 4668-4678.
43. Carry, J.-C. and Garcia-Echeverria, C., Inhibitors of the p53/hdm2 protein-protein interaction-path to the clinic. *Bioorg Med Chem Lett*, **2013**. *23*(9): p. 2480-2485.
44. Nag, S., Zhang, X., Srivenugopal, K.S., Wang, M.H., Wang, W., and Zhang, R., Targeting MDM2-p53 interaction for cancer therapy: are we there yet? *Curr Med Chem*, **2014**. *21*(5): p. 553-574.
45. Zhao, Y., Aguilar, A., Bernard, D., and Wang, S., Small-molecule inhibitors of the MDM2-p53 protein-protein interaction (MDM2 inhibitors) in clinical trials for cancer treatment. *J Med Chem*, **2015**. *58*(3): p. 1038-52.
46. Wu, X.W., Bayle, J.H., Olson, D., and Levine, A.J., The p53 MDM-2 autoregulatory feedback loop. *Genes Dev*, **1993**. *7*(7A): p. 1126-1132.
47. Zhao, Y., Yu, H., and Hu, W., The regulation of MDM2 oncogene and its impact on human cancers. *Acta Biochim Biophys Sin*, **2014**. *46*(3): p. 180-189.
48. Kussie, P.H., Gorina, S., Marechal, V., Elenbaas, B., Moreau, J., Levine, A.J., and Pavletich, N.P., Structure of the MDM2 oncoprotein bound to the p53 tumor suppressor transactivation domain. *Science*, **1996**. *274*(5289): p. 948-953.
49. *Clinical Trial.gov USNIH.* [June 30, 2015]; Available from: http://clinicaltrials.gov/.
50. Vassilev, L.T., Vu, B.T., Graves, B., Carvajal, D., Podlaski, F., Filipovic, Z., Kong, N., Kammlott, U., Lukacs, C., Klein, C., Fotouhi, N., and Liu, E.A., In vivo activation of the p53 pathway by small-molecule antagonists of MDM2. *Science*, **2004**. *303*(5659): p. 844-848.

51. Popowicz, G.M., Doemling, A., and Holak, T.A., The structure-based design of Mdm2/Mdmx-p53 inhibitors gets serious. *Angew Chem Int Ed*, **2011**. *50*(12): p. 2680-2688.
52. Stuhmer, T., Chatterjee, M., Hildebrandt, M., Herrmann, P., Gollasch, H., Gerecke, C., Theurich, S., Cigliano, L., Manz, R.A., Daniel, P.T., Bommert, K., Vassilev, L.T., and Bargou, R.C., Nongenotoxic activation of the p53 pathway as a therapeutic strategy for multiple myeloma. *Blood*, **2005**. *106*(10): p. 3609-3617.
53. Tovar, C., Rosinski, J., Filipovic, Z., Higgins, B., Kolinsky, K., Hilton, H., Zhao, X.L., Vu, B.T., Qing, W.G., Packman, K., Myklebost, O., Heimbrook, D.C., and Vassilev, L.T., Small-molecule MDM2 antagonists reveal aberrant p53 signaling in cancer: Implications for therapy. *Proc Natl Acad Sci U S A*, **2006**. *103*(6): p. 1888-1893.
54. Drakos, E., Thomaides, A., Medeiros, L.J., Li, J., Leventaki, V., Konopleva, M., Andreeff, M., and Rassidakis, G.Z., Inhibition of p53-murine double minute 2 interaction by nutlin-3A stabilizes p53 and induces cell cycle arrest and apoptosis in Hodgkin lymphoma. *Clin Cancer Res*, **2007**. *13*(11): p. 3380-3387.
55. Gu, L., Zhu, N., Findley, H.W., and Zhou, M., MDM2 antagonist nutlin-3 is a potent inducer of apoptosis in pediatric acute lymphoblastic leukemia cells with wild-type p53 and overexpression of MDM2. *Leukemia*, **2008**. *22*(4): p. 730-739.
56. Zheng, T., Wang, J., Song, X., Meng, X., Pan, S., Jiang, H., and Liu, L., Nutlin-3 cooperates with doxorubicin to induce apoptosis of human hepatocellular carcinoma cells through p53 or p73 signaling pathways. *J Cancer Res Clin Oncol*, **2010**. *136*(10): p. 1597-1604.
57. Ohnstad, H.O., Paulsen, E.B., Noordhuis, P., Berg, M., Lothe, R.A., Vassilev, L.T., and Myklebost, O., MDM2 antagonist Nutlin-3a potentiates antitumour activity of cytotoxic drugs in sarcoma cell lines. *BMC Cancer*, **2011**. *11*: p. 11.
58. Vu, B., Wovkulich, P., Pizzolato, G., Lovey, A., Ding, Q.J., Jiang, N., Liu, J.J., Zhao, C.L., Glenn, K., Wen, Y., Tovar, C., Packman, K., Vassilev, L., and Graves, B., Discovery of RG7112: A small-molecule MDM2 inhibitor in clinical development. *ACS Med Chem Lett*, **2013**. *4*(5): p. 466-469.
59. Ray-Coquard, I., Blay, J.-Y., Italiano, A., Le Cesne, A., Penel, N., Zhi, J., Heil, F., Rueger, R., Graves, B., Ding, M., Geho, D., Middleton, S.A., Vassilev, L.T., Nichols, G.L., and Binh Nguyen, B., Effect of the MDM2 antagonist RG7112 on the p53 pathway in patients with MDM2-amplified, well-differentiated or dedifferentiated liposarcoma: An exploratory proof-of-mechanism study. *Lancet Oncol*, **2012**. *13*(11): p. 1133-1140.
60. Tovar, C., Graves, B., Packman, K., Filipovic, Z., Higgins, B., Xia, M., Tardell, C., Garrido, R., Lee, E., Kolinsky, K., To, K.-H., Linn, M., Podlaski, F., Wovkulich, P., Vu, B., and Vassilev, L.T., MDM2 small-molecule antagonist RG7112 activates

p53 signaling and regresses human tumors in preclinical cancer models. *Cancer Res*, **2013**. *73*(8): p. 2587-2597.

61. Hu, C., Li, X., Wang, W., Zhang, L., Tao, L., Dong, X., Sheng, R., Yang, B., and Hu, Y., Design, synthesis, and biological evaluation of imidazoline derivatives as p53-MDM2 binding inhibitors. *Bioorg Med Chem*, **2011**. *19*(18): p. 5454-5461.
62. Hu, C., Dou, X., Wu, Y., Zhang, L., and Hua, Y., Design, synthesis and CoMFA studies of N1-amino acid substituted 2,4,5-triphenyl imidazoline derivatives as p53-MDM2 binding inhibitors. *Bioorg Med Chem*, **2012**. *20*(4): p. 1417-1424.
63. Guan, X. and Hu, Y., Imidazoline derivatives: a patent review (2006-present). *Expert Opin Ther Patents*, **2012**. *22*(11): p. 1353-1365.
64. Zak, K., Pecak, A., Rys, B., Wladyka, B., Doemling, A., Weber, L., Holak, T.A., and Dubin, G., Mdm2 and MdmX inhibitors for the treatment of cancer: a patent review (2011-present). *Expert Opin Ther Patents*, **2013**. *23*(4): p. 425-448.
65. Miyazaki, M., Kawato, H., Naito, H., Ikeda, M., Miyazaki, M., Kitagawa, M., Seki, T., Fukutake, S., Aonuma, M., and Soga, T., Discovery of novel dihydroimidazothiazole derivatives as p53-MDM2 protein-protein interaction inhibitors: Synthesis, biological evaluation and structure-activity relationships. *Bioorg Med Chem Lett*, **2012**. *22*(20): p. 6338-6342.
66. Miyazaki, M., Uoto, K., Sugimoto, Y., Naito, H., Yoshida, K., Okayama, T., Kawato, H., Miyazaki, M., Kitagawa, M., Seki, T., Fukutake, S., Aonuma, M., and Soga, T., Discovery of DS-5272 as a promising candidate: A potent and orally active p53-MDM2 interaction inhibitor. *Bioorg Med Chem*, **2015**. *23*(10): p. 2360-7.
67. Ding, K., Lu, Y., Nikolovska-Coleska, Z., Qiu, S., Ding, Y.S., Gao, W., Stuckey, J., Krajewski, K., Roller, P.P., Tomita, Y., Parrish, D.A., Deschamps, J.R., and Wang, S.M., Structure-based design of potent non-peptide MDM2 inhibitors. *J Am Chem Soc*, **2005**. *127*(29): p. 10130-10131.
68. Ding, K., Lu, Y., Nikolovska-Coleska, Z., Wang, G., Qiu, S., Shangary, S., Gao, W., Qin, D., Stuckey, J., Krajewski, K., Roller, P.P., and Wang, S., Structure-based design of spiro-oxindoles as potent, specific small-molecule inhibitors of the MDM2-p53 interaction. *J Med Chem*, **2006**. *49*(12): p. 3432-3435.
69. Ding, K., Wang, G.P., Deschamps, J.R., Parrish, D.A., and Wang, S.M., Synthesis of spirooxindoles via asymmetric 1,3-dipolar cycloaddition. *Tetrahedron Lett*, **2005**. *46*(35): p. 5949-5951.
70. Yu, S., Qin, D., Shangary, S., Chen, J., Wang, G., Ding, K., McEachern, D., Qiu, S., Nikolovska-Coleska, Z., Miller, R., Kang, S., Yang, D., and Wang, S., Potent and orally active small-molecule inhibitors of the MDM2-p53 interaction. *J Med Chem*, **2009**. *52*(24): p. 7970-7973.

71. Shangary, S., Qin, D., McEachern, D., Liu, M., Miller, R.S., Qiu, S., Nikolovska-Coleska, Z., Ding, K., Wang, G., Chen, J., Bernard, D., Zhang, J., Lu, Y., Gu, Q., Shah, R.B., Pienta, K.J., Ling, X., Kang, S., Guo, M., Sun, Y., Yang, D., and Wang, S., Temporal activation of p53 by a specific MDM2 inhibitor is selectively toxic to tumors and leads to complete tumor growth inhibition. *Proc Natl Acad Sci U S A*, **2008**. *105*(10): p. 3933-3938.

72. Zhao, Y., Yu, S., Sun, W., Liu, L., Lu, J., McEachern, D., Shargary, S., Bernard, D., Li, X., Zhao, T., Zou, P., Sun, D., and Wang, S., A potent small-molecule inhibitor of the MDM2-p53 interaction (MI-888) achieved complete and durable tumor regression in mice. *J Med Chem*, **2013**. *56*(13): p. 5553-5561.

73. Wang, S., Sun, W., Zhao, Y., McEachern, D., Meaux, I., Barriere, C., Stuckey, J.A., Meagher, J.L., Bai, L., Liu, L., Hoffman-Luca, C.G., Lu, J., Shangary, S., Yu, S., Bernard, D., Aguilar, A., Dos-Santos, O., Besret, L., Guerif, S., Pannier, P., Gorge-Bernat, D., and Debussche, L., SAR405838: An optimized inhibitor of MDM2-p53 interaction that induces complete and durable tumor regression. *Cancer Res*, **2014**. *74*(20): p. 5855-5865.

74. Zhao, Y., Liu, L., Sun, W., Lu, J., McEachern, D., Li, X., Yu, S., Bernard, D., Ochsenbein, P., Ferey, V., Carry, J.-C., Deschamps, J.R., Sun, D., and Wang, S., Diastereomeric spirooxindoles as highly potent and efficacious MDM2 inhibitors. *J Am Chem Soc*, **2013**. *135*(19): p. 7223-7234.

75. Aguilar, A., Sun, W., Liu, L., Lu, J., McEachern, D., Bernard, D., Deschamps, J.R., and Wang, S., Design of chemically stable, potent, and efficacious MDM2 inhibitors that exploit the retro-Mannich ring-opening-cyclization reaction mechanism in spiro-oxindoles. *J Med Chem*, **2014**. *57*(24): p. 10486-10498.

76. Zhang, Z., Ding, Q., Liu, J.-J., Zhang, J., Jiang, N., Chu, X.-J., Bartkovitz, D., Luk, K.-C., Janson, C., Tovar, C., Filipovic, Z.M., Higgins, B., Glenn, K., Packman, K., Vassilev, L.T., and Graves, B., Discovery of potent and selective spiroindolinone MDM2 inhibitor, RO8994, for cancer therapy. *Bioorg Med Chem*, **2014**. *22*(15): p. 4001-4009.

77. Shu, L.H., Li, Z.Z., Gu, C., and Fishlock, D., Synthesis of a spiroindolinone pyrrolidinecarboxamide MDM2 antagonist. *Org Process Res Dev*, **2013**. *17*(2): p. 247-256.

78. Zhang, Z., Chu, X.-J., Liu, J.-J., Ding, Q., Zhang, J., Bartkovitz, D., Jiang, N., Karnachi, P., So, S.-S., Tovar, C., Filipovic, Z.M., Higgins, B., Glenn, K., Packman, K., Vassilev, L., and Graves, B., Discovery of potent and orally active p53-MDM2 inhibitors RO5353 and RO2468 for potential clinical development. *ACS Med Chem Lett*, **2014**. *5*(2): p. 124-127.

79. Kumar, A., Gupta, G., Bishnoi, A.K., Saxena, R., Saini, K.S., Konwar, R., Kumar, S., and Dwivedi, A., Design and synthesis of new bioisosteres of spirooxindoles

(MI-63/219) as anti-breast cancer agents. *Bioorg Med Chem*, **2015**. *23*(4): p. 839-48.

80. Ivanenkov, Y.A., Vasilevski, S.V., Beloglazkina, E.K., Kukushkin, M.E., Machulkin, A.E., Veselov, M.S., Chufarova, N.V., Chernyaginab, E.S., Vanzcool, A.S., Zyk, N.V., Skvortsov, D.A., Khutornenko, A.A., Rusanov, A.L., Tonevitsky, A.G., Dontsova, O.A., and Majouga, A.G., Design, synthesis and biological evaluation of novel potent MDM2/p53 small-molecule inhibitors. *Bioorg Med Chem Lett*, **2015**. *25*(2): p. 404-409.
81. Gomez-Monterrey, I., Bertamino, A., Porta, A., Carotenuto, A., Musella, S., Aquino, C., Granata, I., Sala, M., Brancaccio, D., Picone, D., Ercole, C., Stiuso, P., Campiglia, P., Grieco, P., Ianelli, P., Maresca, B., and Novellino, E., Identification of the spiro(oxindole-3,3 '-thiazolidine)-based derivatives as potential p53 activity modulators. *J Med Chem*, **2010**. *53*(23): p. 8319-8329.
82. Costa, B., Bendinelli, S., Gabelloni, P., Da Pozzo, E., Daniele, S., Scatena, F., Vanacore, R., Campiglia, P., Bertamino, A., Gomez-Monterrey, I., Sorriento, D., Del Giudice, C., Iaccarino, G., Novellino, E., and Martini, C., Human glioblastoma multiforme: p53 reactivation by a novel MDM2 inhibitor. *PLoS One*, **2013**. *8*(8).
83. Bertamino, A., Soprano, M., Musella, S., Rusciano, M.R., Sala, M., Vernieri, E., Di Sarno, V., Limatola, A., Carotenuto, A., Cosconati, S., Grieco, P., Novellino, E., Illario, M., Campiglia, P., and Gomez-Monterrey, I., Synthesis, in vitro, and in cell studies of a new series of indoline-3,2 '-thiazolidine - based p53 modulators. *J Med Chem*, **2013**. *56*(13): p. 5407-5421.
84. Sorriento, D., Del Giudice, C., Bertamino, A., Ciccarelli, M., Gomez-Monterrey, I., Campiglia, P., Novellino, E., Illario, M., Trimarco, B., De Luca, N., and Iaccarino, G., New small molecules, ISA27 and SM13, inhibit tumour growth inducing mitochondrial effects of p53. *Br J Cancer*, **2015**. *112*(1): p. 77-85.
85. Ding, Q., Zhang, Z., Liu, J.-J., Jiang, N., Zhang, J., Ross, T.M., Chu, X.-J., Bartkovitz, D., Podlaski, F., Janson, C., Tovar, C., Filipovic, Z.M., Higgins, B., Glenn, K., Packman, K., Vassilev, L.T., and Graves, B., Discovery of RG7388, a potent and selective p53-MDM2 inhibitor in clinical development. *J Med Chem*, **2013**. *56*(14): p. 5979-5983.
86. Higgins, B., Glenn, K., Walz, A., Tovar, C., Filipovic, Z., Hussain, S., Lee, E., Kolinsky, K., Tannu, S., Adames, V., Garrido, R., Linn, M., Meille, C., Heimbrook, D., Vassilev, L., and Packman, K., Preclinical optimization of MDM2 antagonist scheduling for cancer treatment by using a model-based approach. *Clin Cancer Res*, **2014**. *20*(14): p. 3742-3752.
87. de Turiso, F.G.-L., Sun, D., Rew, Y., Bartberger, M.D., Beck, H.P., Canon, J., Chen, A., Chow, D., Correll, T.L., Huang, X., Julian, L.D., Kayser, F., Lo, M.-C., Long, A.M., McMinn, D., Oliner, J.D., Osgood, T., Powers, J.P., Saiki, A.Y.,

Schneider, S., Shaffer, P., Xiao, S.-H., Yakowec, P., Yan, X., Ye, Q., Yu, D., Zhao, X., Zhou, J., Medina, J.C., and Olson, S.H., Rational design and binding mode duality of MDM2-p53 inhibitors. *J Med Chem*, **2013**. *56*(10): p. 4053-4070.

88. Rew, Y., Sun, D., De Turiso, F.G.-L., Bartberger, M.D., Beck, H.P., Canon, J., Chen, A., Chow, D., Deignan, J., Fox, B.M., Gustin, D., Huang, X., Jiang, M., Jiao, X., Jin, L., Kayser, F., Kopecky, D.J., Li, Y., Lo, M.-C., Long, A.M., Michelsen, K., Oliner, J.D., Osgood, T., Ragains, M., Saiki, A.Y., Schneider, S., Toteva, M., Yakowec, P., Yan, X., Ye, Q., Yu, D., Zhao, X., Zhou, J., Medina, J.C., and Olson, S.H., Structure-based design of novel inhibitors of the MDM2-p53 interaction. *J Med Chem*, **2012**. *55*(11): p. 4936-4954.
89. Michelsen, K., Jordan, J.B., Lewis, J., Long, A.M., Yang, E., Rew, Y., Zhou, J., Yakowec, P., Schnier, P.D., Huang, X., and Poppe, L., Ordering of the N-terminus of human MDM2 by small molecule inhibitors. *J Am Chem Soc* **2012**. *134*(41): p. 17059-17067.
90. Rew, Y. and Sun, D., Discovery of a small molecule MDM2 inhibitor (AMG 232) for treating cancer. *J Med Chem*, **2014**. *57*(15): p. 6332-6341.
91. Lucas, B.S., Fisher, B., McGee, L.R., Olson, S.H., Medina, J.C., and Cheung, E., An expeditious synthesis of the MDM2-p53 inhibitor AM-8553. *J Am Chem Soc* **2012**. *134*(30): p. 12855-12860.
92. Bernard, D., Zhao, Y., and Wang, S., AM-8553: A novel MDM2 inhibitor with a promising outlook for potential clinical development. *J Med Chem*, **2012**. *55*(11): p. 4934-4935.
93. Sun, D., Li, Z., Rew, Y., Gribble, M., Bartberger, M.D., Beck, H.P., Canon, J., Chen, A., Chen, X., Chow, D., Deignan, J., Duquette, J., Eksterowicz, J., Fisher, B., Fox, B.M., Fu, J., Gonzalez, A.Z., De Turiso, F.G.-L., Houze, J.B., Huang, X., Jiang, M., Jin, L., Kayser, F., Liu, J., Lo, M.-C., Long, A.M., Lucas, B., McGee, L.R., McIntosh, J., Mihalic, J., Oliner, J.D., Osgood, T., Peterson, M.L., Roveto, P., Saiki, A.Y., Shaffer, P., Toteva, M., Wang, Y., Wang, Y.C., Wortman, S., Yakowec, P., Yan, X., Ye, Q., Yu, D., Yu, M., Zhao, X., Zhou, J., Zhu, J., Olson, S.H., and Medina, J.C., Discovery of AMG 232, a potent, selective, and orally bioavailable MDM2-p53 inhibitor in clinical development. *J Med Chem*, **2014**. *57*(4): p. 1454-1472.
94. Wang, Y., Zhu, J., Liu, J., Chen, X., Mihalic, J., Deignan, J., Yu, M., Sun, D., Kayser, F., McGee, L.R., Lo, M.-C., Chen, A., Zhou, J., Ye, Q., Huang, X., Long, A.M., Yakowec, P., Oliner, J.D., Olson, S.H., and Medina, J.C., Optimization beyond AMG 232: Discovery and SAR of sulfonamides on a piperidinone scaffold as potent inhibitors of the MDM2-p53 protein-protein interaction. *Bioorg Med Chem Lett*, **2014**. *24*(16): p. 3782-3785.

95. Yu, M., Wang, Y., Zhu, J., Bartberger, M.D., Canon, J., Chen, A., Chow, D., Eksterowicz, J., Fox, B., Fu, J., Gribble, M., Huang, X., Li, Z., Liu, J., Lo, M.-c., McMinn, D., Oliner, J.D., Osgood, T., Rew, Y., Saiki, A.Y., Shaffer, P., Yan, X., Ye, Q., Yu, D., Zhao, X., Zhou, J., Olson, S.H., Medina, J.C., and Sun, D., Discovery of potent and simplified piperidinone-based inhibitors of the MDM2-p53 interaction. *ACS Med Chem Lett*, **2014**. *5*(8): p. 894-899.

96. Canon, J., Osgood, T., Olson, S.H., Saiki, A.Y., Robertson, R., Yu, D., Eksterowicz, J., Ye, Q., Jin, L., Chen, A., Zhou, J., Cordover, D., Kaufman, S., Kendall, R., Oliner, J.D., Coxon, A., and Radinsky, R., The MDM2 Inhibitor AMG 232 Demonstrates Robust Antitumor Efficacy and Potentiates the Activity of p53-Inducing Cytotoxic Agents. *Mol Cancer Ther*, **2015**.

97. Gonzalez, A.Z., Li, Z.H., Beck, H.P., Canon, J., Chen, A., Chow, D., Duquette, J., Eksterowicz, J., Fox, B.M., Fu, J.S., Huang, X., Houze, J., Jin, L.X., Li, Y.H., Ling, Y., Lo, M.C., Long, A.M., McGee, L.R., McIntosh, J., Oliner, J.D., Osgood, T., Rew, Y., Saiki, A.Y., Shaffer, P., Wortman, S., Yakowec, P., Yan, X.L., Ye, Q.P., Yu, D.Y., Zhao, X.N., Zhou, J., Olson, S.H., Sun, D.Q., and Medina, J.C., Novel inhibitors of the MDM2-p53 interaction featuring hydrogen bond acceptors as carboxylic acid isosteres. *J Med Chem* **2014**. *57*(7): p. 2963-2988.

98. Rew, Y., Sun, D.Q., Yan, X.L., Beck, H.P., Canon, J., Chen, A., Duquette, J., Eksterowicz, J., Fox, B.M., Fu, J.S., Gonzalez, A.Z., Houze, J., Huang, X., Jiang, M., Jin, L.X., Li, Y.H., Li, Z.H., Ling, Y., Lo, M.C., Long, A.M., McGee, L.R., McIntosh, J., Oliner, J.D., Osgood, T., Saiki, A.Y., Shaffer, P., Wang, Y.C., Wortman, S., Yakowec, P., Ye, Q.P., Yu, D.Y., Zhao, X.N., Zhou, J., Medina, J.C., and Olson, S.H., Discovery of AM-7209, a potent and selective 4-amidobenzoic acid inhibitor of the MDM2-p53 interaction. *J Med Chem*, **2014**. *57*(24): p. 10499-10511.

99. Gonzalez, A.Z., Eksterowicz, J., Bartberger, M.D., Beck, H.P., Canon, J., Chen, A., Chow, D., Duquette, J., Fox, B.M., Fu, J., Huang, X., Houze, J.B., Jin, L., Li, Y., Li, Z., Ling, Y., Lo, M.-C., Long, A.M., McGee, L.R., McIntosh, J., McMinn, D.L., Oliner, J.D., Osgood, T., Rew, Y., Saiki, A.Y., Shaffer, P., Wortman, S., Yakowec, P., Yan, X., Ye, Q., Yu, D., Zhao, X., Zhou, J., Olson, S.H., Medina, J.C., and Sun, D., Selective and potent morpholinone inhibitors of the MDM2-p53 protein-protein interaction. *J Med Chem*, **2014**. *57*(6): p. 2472-2488.

100. Grasberger, B.L., Lu, T.B., Schubert, C., Parks, D.J., Carver, T.E., Koblish, H.K., Cummings, M.D., LaFrance, L.V., Milkiewicz, K.L., Calvo, R.R., Maguire, D., Lattanze, J., Franks, C.F., Zhao, S.Y., Ramachandren, K., Bylebyl, G.R., Zhang, M., Manthey, C.L., Petrella, E.C., Pantoliano, M.W., Deckman, I.C., Spurlino, J.C., Maroney, A.C., Tomczuk, B.E., Molloy, C.J., and Bone, R.F., Discovery and

cocrystal structure of benzodiazepinedione HDM2 antagonists that activate p53 in cells. *J Med Chem* **2005**. *48*(4): p. 909-912.

101. Parks, D.J., LaFrance, L.V., Calvo, R.R., Milkiewicz, K.L., Gupta, V., Lattanze, J., Ramachandren, K., Carver, T.E., Petrella, E.C., Cummings, M.D., Maguire, D., Grasberger, B.L., and Lu, T.B., 1,4-benzodiazepine-2,5-diones as small molecule antagonists of the HDM2-p53 interaction: discovery and SAR. *Bioorg Med Chem Lett*, **2005**. *15*(3): p. 765-770.
102. Cummings, M.D., Schubert, C., Parks, D.J., Calvo, R.R., LaFrance, L.V., Lattanze, J., Milkiewicz, K.L., and Lu, T.B., Substituted 1,4-benzodiazepine-2,5-diones as alpha-helix mimetic antagonists of the HDM2-p53 protein-protein interaction. *Chem Biol Drug Des*, **2006**. *67*(3): p. 201-205.
103. Bissantz, C., Kuhn, B., and Stahl, M., A medicinal chemist's guide to molecular interactions. *J Med Chem*, **2010**. *53*(14): p. 5061-5084.
104. Raboisson, P., Marugan, J.J., Schubert, C., Koblish, H.K., Lu, T.B., Zhao, S.Y., Player, M.R., Maroney, A.C., Reed, R.L., Huebert, N.D., Lattanze, J., Parks, D.J., and Cummings, M.D., Structure-based design, synthesis, and biological evaluation of novel 1,4-diazepines as HDM2 antagonists. *Bioorg Med Chem Lett*, **2005**. *15*(7): p. 1857-1861.
105. Parks, D.J., LaFrance, L.V., Calvo, R.R., Milkiewicz, K.L., Marugan, J.J., Raboisson, P., Schubert, C., Koblish, H.K., Zhao, S.Y., Franks, C.F., Lattanze, J., Carver, T.E., Cummings, M.D., Maguire, D., Grasberger, B.L., Maroney, A.C., and Lu, T.B., Enhanced pharmacokinetic properties of 1,4-benzodiazepine-2,5-dione antagonists of the HDM2-p53 protein-protein interaction through structure-based drug design. *Bioorg Med Chem Lett*, **2006**. *16*(12): p. 3310-3314.
106. Leonard, K., Marugan, J.J., Raboisson, P., Calvo, R., Gushue, J.M., Koblish, H.K., Lattanze, J., Zhao, S.Y., Cummings, M.D., Player, M.R., Maroney, A.C., and Lu, T.B., Novel 1,4-benzodiazepine-2,5-diones as Hdm2 antagonists with improved cellular activity. *Bioorg Med Chem Lett*, **2006**. *16*(13): p. 3463-3468.
107. Marugan, J.J., Leonard, K., Raboisson, P., Gushue, J.M., Calvo, R., Koblish, H.K., Lattanze, J., Zhao, S.Y., Cummings, M.D., Player, M.R., Schubert, C., Maroney, A.C., and Lu, T.B., Enantiomerically pure 1,4-benzodiazepine-2,5-diones as Hdm2 antagonists. *Bioorg Med Chem Lett*, **2006**. *16*(12): p. 3115-3120.
108. Koblish, H.K., Zhao, S.Y., Franks, C.F., Donatelli, R.R., Tominovich, R.M., LaFrance, L.V., Leonard, K.A., Gushue, J.M., Parks, D.J., Calvo, R.R., Milkiewicz, K.L., Marugan, J.J., Raboisson, P., Cummings, M.D., Grasberger, B.L., Johnson, D.L., Lu, T.B., Molloy, C.J., and Maroney, A.C., Benzodiazepinedione inhibitors of the Hdm2 : p53 complex suppress human tumor cell proliferation in vitro and sensitize tumors to doxorubicin in vivo. *Mol Cancer Ther*, **2006**. *5*(1): p. 160-169.

109. Huang, Y., Wolf, S., Bista, M., Meireles, L., Camacho, C., Holak, T.A., and Doemling, A., 1,4-Thienodiazepine-2,5-diones via MCR (I): Synthesis, virtual space and p53-Mdm2 activity. *Chem Biol Drug Des*, **2010**. *76*(2): p. 116-129.

110. Zhuang, C., Miao, Z., Zhu, L., Zhang, Y., Guo, Z., Yao, J., Dong, G., Wang, S., Liu, Y., Chen, H., Sheng, C., and Zhang, W., Synthesis and biological evaluation of thio-benzodiazepines as novel small molecule inhibitors of the p53-MDM2 protein-protein interaction. *Eur J Med Chem*, **2011**. *46*(11): p. 5654-5661.

111. Guo, Z., Zhuang, C., Zhu, L., Zhang, Y., Yao, J., Dong, G., Wang, S., Liu, Y., Chen, H., Sheng, C., Miao, Z., and Zhang, W., Structure-activity relationship and antitumor activity of thio-benzodiazepines as p53-MDM2 protein-protein interaction inhibitors. *Eur J Med Chem*, **2012**. *56*: p. 10-16.

112. Yu, Z., Zhuang, C., Wu, Y., Guo, Z., Li, J., Dong, G., Yao, J., Sheng, C., Miao, Z., and Zhang, W., Design, synthesis and biological evaluation of sulfamide and triazole benzodiazepines as novel p53-MDM2 inhibitors. *Int J Mol Sci*, **2014**. *15*(9): p. 15741-15753.

113. Hardcastle, I.R., Ahmed, S.U., Atkins, H., Calvert, A.H., Curtin, N.J., Farnie, G., Golding, B.T., Griffin, R.J., Guyenne, S., Hutton, C., Kallbad, P., Kemp, S.J., Kitching, M.S., Newell, D.R., Norbedo, S., Northen, J.S., Reid, R.J., Saravanan, K., Willems, H.M.G., and Lunec, J., Isoindolinone-based inhibitors of the MDM2-p53 protein-protein interaction. *Bioorg Med Chem Lett*, **2005**. *15*(5): p. 1515-1520.

114. Hardcastle, I.R., Ahmed, S.U., Atkins, H., Farnie, G., Golding, B.T., Griffin, R.J., Guyenne, S., Hutton, C., Kallblad, P., Kemp, S.J., Kitching, M.S., Newell, D.R., Norbedo, S., Northen, J.S., Reid, R.J., Saravanan, K., Willems, H.M.G., and Lunec, J., Small-molecule inhibitors of the MDM2-p53 protein-protein interaction based on an isoindolinone scaffold. *J Med Chem*, **2006**. *49*(21): p. 6209-6221.

115. Riedinger, C., Endicott, J.A., Kemp, S.J., Smyth, L.A., Watson, A., Valeur, E., Golding, B.T., Griffin, R.J., Hardcastle, I.R., Noble, M.E., and McDonnell, J.M., Analysis of chemical shift changes reveals the binding modes of isoindolinone inhibitors of the MDM2-p53 interaction. *J Am Chem Soc*, **2008**. *130*(47): p. 16038-16044.

116. Hardcastle, I.R., Liu, J., Valeur, E., Watson, A., Ahmed, S.U., Blackburn, T.J., Bennaceur, K., Clegg, W., Drummond, C., Endicott, J.A., Golding, B.T., Griffin, R.J., Gruber, J., Haggerty, K., Harrington, R.W., Hutton, C., Kemp, S., Lu, X., McDonnell, J.M., Newell, D.R., Noble, M.E.M., Payne, S.L., Revill, C.H., Riedinger, C., Xu, Q., and Lunec, J., Isoindolinone inhibitors of the murine double minute 2 (MDM2)-p53 protein-protein interaction: Structure-activity studies leading to improved potency. *J Med Chem*, **2011**. *54*(5): p. 1233-1243.

117. Riedinger, C., Noble, M.E., Wright, D.J., Mulks, F., Hardcastle, I.R., Endicott, J.A., and McDonnell, J.M., Understanding small-molecule binding to MDM2:

Insights into structural effects of isoindolinone inhibitors from NMR spectroscopy. *Chem Biol Drug Des*, **2011**. *77*(5): p. 301-308.

118. Watson, A.F., Liu, J., Bennaceur, K., Drummond, C.J., Endicott, J.A., Golding, B.T., Griffin, R.J., Haggerty, K., Lu, X., McDonnell, J.M., Newell, D.R., Noble, M.E.M., Revill, C.H., Riedinger, C., Xu, Q., Zhao, Y., Lunec, J., and Hardcastle, I.R., MDM2-p53 protein-protein interaction inhibitors: A-ring substituted isoindolinones. *Bioorg Med Chem Lett*, **2011**. *21*(19): p. 5916-5919.
119. Soares, J., Pereira, N.A.L., Monteiro, A., Leao, M., Bessa, C., dos Santos, D., Rairnundo, L., Queiroz, G., Bisio, A., Inga, A., Pereira, C., Santos, M.M.M., and Saraiva, L., Oxazoloisoindolinones with in vitro antitumor activity selectively activate a p53-pathway through potential inhibition of the p53-MDM2 interaction. *Eur J Pharm Sci* **2015**. *66*: p. 138-147.
120. Allen, J.G., Bourbeau, M.P., Wohlhieter, G.E., Bartberger, M.D., Michelsen, K., Hungate, R., Gadwood, R.C., Gaston, R.D., Evans, B., Mann, L.W., Matison, M.E., Schneider, S., Huang, X., Yu, D., Andrews, P.S., Reichelt, A., Long, A.M., Yakowec, P., Yang, E.Y., Lee, T.A., and Oliner, J.D., Discovery and optimization of chromenotriazolopyrimidines as potent inhibitors of the mouse double minute 2-tumor protein 53 protein-protein interaction. *J Med Chem*, **2009**. *52*(22): p. 7044-7053.
121. Beck, H.P., DeGraffenreid, M., Fox, B., Allen, J.G., Rew, Y., Schneider, S., Saiki, A.Y., Yu, D.Y., Oliner, J.D., Salyers, K., Ye, Q.P., and Olson, S., Improvement of the synthesis and pharmacokinetic properties of chromenotriazolopyrimidine MDM2-p53 protein-protein inhibitors. *Bioorg Med Chem Lett*, **2011**. *21*(9): p. 2752-2755.
122. Czarna, A., Beck, B., Srivastava, S., Popowicz, G.M., Wolf, S., Huang, Y., Bista, M., Holak, T.A., and Doemling, A., Robust generation of lead compounds for protein-protein interactions by computational and MCR chemistry: p53/Hdm2 antagonists. *Angew Chem Int Ed*, **2010**. *49*(31): p. 5352-5356.
123. Popowicz, G.M., Czarna, A., Wolf, S., Wang, K., Wang, W., Domling, A., and Holak, T.A., Structures of low molecular weight inhibitors bound to MDMX and MDM2 reveal new approaches for p53-MDMX/MDM2 antagonist drug discovery. *Cell Cycle*, **2010**. *9*(6): p. 1104-1111.
124. Huang, Y.J., Wolf, S., Koes, D., Popowicz, G.M., Camacho, C.J., Holak, T.A., and Domling, A., Exhaustive Fluorine Scanning toward Potent p53-Mdm2 Antagonists. *ChemMedChem*, **2012**. *7*(1): p. 49-52.
125. Stoll, R., Renner, C., Hansen, S., Palme, S., Klein, C., Belling, A., Zeslawski, W., Kamionka, M., Rehm, T., Muhlhahn, P., Schumacher, R., Hesse, F., Kaluza, B., Voelter, W., Engh, R.A., and Holak, T.A., Chalcone derivatives antagonize

interactions between the human oncoprotein MDM2 and p53. *Biochemistry*, **2001**. *40*(2): p. 336-344.

126. Kumar, S.K., Hager, E., Pettit, C., Gurulingappa, H., Davidson, N.E., and Khan, S.R., Design, synthesis, and evaluation of novel boronic-chalcone derivatives as antitumor agents. *J Med Chem*, **2003**. *46*(14): p. 2813-2815.
127. Jandial, D.D., Blair, C.A., Zhang, S., Krill, L.S., Zhang, Y.-B., and Zi, X., Molecular targeted approaches to cancer therapy and prevention using chalcones. *Curr Cancer Drug Targets*, **2014**. *14*(2): p. 181-200.
128. Gessier, F., Kallen, J., Jacoby, E., Chène, P., Stachyra-Valat, T., Ruetz, S., Jeay, S., Holzer, P., Masuya, K., and Furet, P., Discovery of dihydroisoquinolinone derivatives as novel inhibitors of the p53-MDM2 interaction with a distinct binding mode. *Bioorg Med Chem Lett*, **2015**, http://dx.doi.org/10.1016/j.bmcl.2015.06.058.
129. Chen, L.H., Yin, H., Farooqi, B., Sebti, S., Hamilton, A.D., and Chen, J.D., p53 alpha-helix mimetics antagonize p53/MDM2 interaction and activate p53. *Mol Cancer Ther* **2005**. *4*(6): p. 1019-1025.
130. Yin, H., Lee, G.I., Park, H.S., Payne, G.A., Rodriguez, J.M., Sebti, S.M., and Hamilton, A.D., Terphenyl-based helical mimetics that disrupt the p53/HDM2 interaction. *Angew Chem Int Ed*, **2005**. *44*(18): p. 2704-2707.
131. Lawrence, H.R., Li, Z., Yip, M.L.R., Sung, S.-S., Lawrence, N.J., McLaughlin, M.L., McManus, G.J., Zaworotko, M.J., Sebti, S.M., Chen, J., and Guida, W.C., Identification of a disruptor of the MDM2-p53 protein-protein interaction facilitated by high-throughput in silico docking. *Bioorg Med Chem Lett*, **2009**. *19*(14): p. 3756-3759.
132. Zhuang, C., Miao, Z., Zhu, L., Dong, G., Guo, Z., Wang, S., Zhang, Y., Wu, Y., Yao, J., Sheng, C., and Zhang, W., Discovery, synthesis, and biological evaluation of orally active pyrrolidone derivatives as novel inhibitors of p53-MDM2 protein-protein interaction. *J Med Chem*, **2012**. *55*(22): p. 9630-9642.
133. Li, J., Wu, Y., Guo, Z., Zhuang, C., Yao, J., Dong, G., Yu, Z., Min, X., Wang, S., Liu, Y., Wu, S., Zhu, S., Sheng, C., Miao, Z., and Zhang, W., Discovery of 1-arylpyrrolidone derivatives as potent p53-MDM2 inhibitors based on molecule fusing strategy. *Bioorg Med Chem Lett*, **2014**. *24*(12): p. 2648-2650.
134. Zhuang, C., Miao, Z., Wu, Y., Guo, Z., Li, J., Yao, J., Xing, C., Sheng, C., and Zhang, W., Double-edged swords as cancer therapeutics: Novel, orally active, small molecules simultaneously inhibit p53-MDM2 interaction and the NF-kappa B pathway. *J Med Chem*, **2014**. *57*(3): p. 567-577.
135. Zhuang, C., Sheng, C., Shin, W.S., Wu, Y., Li, J., Yao, J., Dong, G., Zhang, W., Sham, Y.Y., Miao, Z., and Zhang, W., A novel drug discovery strategy: Mechanistic investigation of an enantiomeric antitumor agent targeting dual p53 and NF-kappa B pathways. *Oncotarget*, **2014**. *5*(21): p. 10830-10839.

136. Ma, Y., Lahue, B.R., Shipps, G.W., Jr., Brookes, J., and Wang, Y., Substituted piperidines as HDM2 inhibitors. *Bioorg Med Chem Lett*, **2014**. *24*(4): p. 1026-1030.

137. Pan, W., Lahue, B.R., Ma, Y., Nair, L.G., Shipps, G.W., Jr., Wang, Y., Doll, R., and Bogen, S.L., Core modification of substituted piperidines as Novel inhibitors of HDM2-p53 protein-protein interaction. *Bioorg Med Chem Lett*, **2014**. *24*(8): p. 1983-1986.

138. Ma, Y., Lahue, B.R., Gibeau, C.R., Shipps, G.W., Bogen, S.L., Wang, Y.L., Guo, Z.Y., and Guzi, T.J., Pivotal role of an aliphatic side chain in the development of an HDM2 inhibitor. *ACS Med Chem Lett*, **2014**. *5*(5): p. 572-575.

139. Zheng, G.-h., Shen, J.-j., Zhan, Y.-c., Yi, H., Xue, S.-t., Wang, Z., Ji, X.-y., and Li, Z.-r., Design, synthesis and in vitro and in vivo antitumour activity of 3-benzylideneindolin-2-one derivatives, a novel class of small-molecule inhibitors of the MDM2-p53 interaction. *Eur J Med Chem*, **2014**. *81*: p. 277-288.

140. Galatin, P.S. and Abraham, D.J., A nonpeptidic sulfonamide inhibits the p53-mdm2 interaction and activates p53-dependent transcription in mdm2-overexpressing cells. *J Med Chem*, **2004**. *47*(17): p. 4163-4165.

141. Zhao, J.H., Wang, M.J., Chen, J., Luo, A.P., Wang, X.Q., Wu, M., Yin, D.L., and Liu, Z.H., The initial evaluation of non-peptidic small-molecule HDM2 inhibitors based on p53-HDM2 complex structure. *Cancer Lett*, **2002**. *183*(1): p. 69-77.

142. Lu, Y.P., Nikolovska-Coleska, Z., Fang, X.L., Gao, W., Shangary, S., Qiu, S., Qin, D.G., and Wang, S.M., Discovery of a nanomolar inhibitor of the human murine double minute 2 (MDM2)-p53 interaction through an integrated, virtual database screening strategy. *J Med Chem*, **2006**. *49*(13): p. 3759-3762.

143. Bowman, A.L., Nikolovska-Coleska, Z., Zhong, H., Wang, S., and Carlson, H.A., Small molecule inhibitors of the MDM2-p53 interaction discovered by ensemble-based receptor models. *J Am Chem Soc*, **2007**. *129*(42): p. 12809-12814.

144. Wang, W.S., Zhu, X.L., Hong, X.Q., Zheng, L., Zhu, H., and Hu, Y.Z., Identification of novel inhibitors of p53-MDM2 interaction facilitated by pharmacophore-based virtual screening combining molecular docking strategy. *MedChemComm*, **2013**. *4*(2): p. 411-416.

145. Vasilevich, N.I., Afanasyev, I.I., Rastorguev, E.A., Genis, D.V., and Kochubey, V.S., Dual mode of action of phenyl-pyrazole-phenyl (6-5-6 system)-based PPI inhibitors: alpha-helix backbone versus alpha-helix binding epitope. *MedChemComm*, **2013**. *4*(12): p. 1597-1603.

146. Christner, S., Clausen, D., Beumer, J., Parise, R., Guo, J., Huang, Y., Dömling, A., and Eiseman, J., In vitro cytotoxicity and in vivo efficacy, pharmacokinetics, and metabolism of pyrazole-based small molecule inhibitors of Mdm2/4–p53 interaction. *Cancer Chemother Pharmacol*, **2015**: p. 1-13.

147. Vasilevich, N.I., Afanasyev, I.I., Kovalskiy, D.A., Genis, D.V., and Kochubey, V.S., A Re-examination of the MDM2/p53 interaction leads to revised design criteria for novel inhibitors. *Chem Biol Drug Des*, **2014**. *84*(5): p. 585-92.

148. Vaupel, A., Bold, G., De Pover, A., Stachyra-Valat, T., Hergovich-Lisztwan, J., Kallen, J., Masuya, K., and Furet, P., Tetra-substituted imidazoles as a new class of inhibitors of the p53-MDM2 interaction. *Bioorg Med Chem Lett*, **2014**. *24*(9): p. 2110-2114.

149. Gureev, M.A., Davidovich, P.B., Tribulovich, V.G., and Garabadzhiu, A.V., Natural compounds as a basis for the design of modulators of p53 activity. *Russ Chem Bull*, **2014**. *63*(9): p. 1963-1975.

150. Duncan, S.J., Gruschow, S., Williams, D.H., McNicholas, C., Purewal, R., Hajek, M., Gerlitz, M., Martin, S., Wrigley, S.K., and Moore, M., Isolation and structure elucidation of chlorofusin, a novel p53-MDM2 antagonist from a Fusarium sp. *J Am Chem Soc*, **2001**. *123*(4): p. 554-560.

151. Duncan, S.J., Cooper, M.A., and Williams, D.H., Binding of an inhibitor of the p53/MDM2 interaction to MDM2. *Chem Commun* **2003**(3): p. 316-317.

152. Clark, R.C., Lee, S.Y., Searcey, M., and Boger, D.L., The isolation, total synthesis and structure elucidation of chlorofusin, a natural product inhibitor of the p53-MDM2 protein-protein interaction. *Nat Prod Rep*, **2009**. *26*(4): p. 465-477.

153. Tsukamoto, S., Yoshida, T., Hosono, H., Ohta, T., and Yokosawa, H., Hexylitaconic acid: A new inhibitor of p53-HDM2 interaction isolated from a marine-derived fungus, Arthrinium sp. *Bioorg Med Chem Lett*, **2006**. *16*(1): p. 69-71.

154. Malloy, K.L., Choi, H., Fiorilla, C., Valeriote, F.A., Matainaho, T., and Gerwick, W.H., Hoiamide D, a marine cyanobacteria-derived inhibitor of p53/MDM2 interaction. *Bioorg Med Chem Lett*, **2012**. *22*(1): p. 683-688.

155. Nakamura, Y., Kato, H., Nishikawa, T., Iwasaki, N., Suwa, Y., Rotinsulu, H., Losung, F., Maarisit, W., Mangindaan, R.E.P., Morioka, H., Yokosawa, H., and Tsukamoto, S., Siladenoserinols A-L: New sulfonated serinol derivatives from a Tunicate as inhibitors of p53-Hdm2 interaction. *Org Lett*, **2013**. *15*(2): p. 322-325.

156. Leao, M., Pereira, C., Bisio, A., Ciribilli, Y., Paiva, A.M., Machado, N., Palmeira, A., Fernandes, M.X., Sousa, E., Pinto, M., Inga, A., and Saraiva, L., Discovery of a new small-molecule inhibitor of p53-MDM2 interaction using a yeast-based approach. *Biochem Pharmacol*, **2013**. *85*(9): p. 1234-1245.

157. Leao, M., Gomes, S., Pedraza-Chaverri, J., Machado, N., Sousa, E., Pinto, M., Inga, A., Pereira, C., and Saraiva, L., alpha-Mangostin and gambogic acid as potential inhibitors of the p53-MDM2 interaction revealed by a yeast approach. *J Nat Prod*, **2013**. *76*(4): p. 774-778.

158. Froufe, H.J.C., Abreu, R.M.V., and Ferreira, I.C.F.R., Virtual screening of low molecular weight mushrooms compounds as potential Mdm2 inhibitors. *J Enzym Inhib Med Chem*, **2013**. *28*(3): p. 569-575.
159. Liu, J., Shaik, S., Dai, X.P., Wu, Q., Zhou, X.X., Wang, Z.W., and Wei, W.Y., Targeting the ubiquitin pathway for cancer treatment. *Biochim Biophys Acta-Rev Cancer*, **2015**. *1855*(1): p. 50-60.
160. Stintzing, S. and Lenz, H.J., Molecular pathways: Turning proteasomal protein degradation into a unique treatment approach. *Clin Cancer Res*, **2014**. *20*(12): p. 3064-3070.
161. Macchiarulo, A., Giacche, N., Mancini, F., Puxeddu, E., Moretti, F., and Pellicciari, R., Alternative strategies for targeting mouse double minute 2 activity with small molecules: novel patents on the horizon? *Expert Opin Ther Patents*, **2011**. *21*(3): p. 287-294.
162. Lai, Z.H., Yang, T., Kim, Y.B., Sielecki, T.M., Diamond, M.A., Strack, P., Rolfe, M., Caligiuri, M., Benfield, P.A., Auger, K.R., and Copeland, R.A., Differentiation of Hdm2-mediated p53 ubiquitination and Hdm2 autoubiquitination activity by small molecular weight inhibitors. *Proc Natl Acad Sci U S A*, **2002**. *99*(23): p. 14734-14739.
163. Davydov, I.V., Woods, D., Safiran, Y.J., Oberoi, P., Fearnhead, H.O., Fang, S., Jensen, J.P., Weissman, A.M., Kenten, J.H., and Vousden, K.H., Assay for ubiquitin ligase activity: High-throughput screen for inhibitors of HDM2. *J Biomol Screen* **2004**. *9*(8): p. 695-703.
164. Yang, Y.L., Ludwig, R.L., Jensen, J.P., Pierre, S.A., Medaglia, M.V., Davydov, I.V., Safiran, Y.J., Oberoi, P., Kenten, J.H., Phillips, A.C., Weissman, A.M., and Vousden, K.H., Small molecule inhibitors of HDM2 ubiquitin ligase activity stabilize and activate p53 in cells. *Cancer Cell*, **2005**. *7*(6): p. 547-559.
165. Kitagaki, J., Agama, K.K., Pommier, Y., Yang, Y.L., and Weissman, A.M., Targeting tumor cells expressing p53 with a water-soluble inhibitor of Hdm2. *Mol Cancer Ther*, **2008**. *7*(8): p. 2445-2454.
166. Sasiela, C.A., Stewart, D.H., Kitagaki, J., Safiran, Y.J., Yang, Y.L., Weissman, A.M., Oberoi, P., Davydov, I.V., Goncharova, E., Beutler, J.A., McMahon, J.B., and O'Keefe, B.R., Identification of inhibitors for MDM2 ubiquitin ligase activity from natural product extracts by a novel high-throughput electrochemiluminescent screen. *J Biomol Screen* **2008**. *13*(3): p. 229-237.
167. Clement, J.A., Kitagaki, J., Yang, Y., Saucedo, C.J., O'Keefe, B.R., Weissman, A.M., McKee, T.C., and McMahon, J.B., Discovery of new pyridoacridine alkaloids from Lissoclinum cf. badium that inhibit the ubiquitin ligase activity of Hdm2 and stabilize p53. *Bioorg Med Chem*, **2008**. *16*(23): p. 10022-8.

168. Weissman, A.M., Yang, Y., Kitagaki, J., Sasiela, C.A., Beutler, J.A., and O'Keefe, B.R., Inhibiting Hdm2 and ubiquitin-activating enzyme: targeting the ubiquitin conjugating system in cancer. *Ernst Schering Found Symp Proc*, **2008**(1): p. 171-90.

169. Herman, A.G., Hayano, M., Poyurovsky, M.V., Shimada, K., Skouta, R., Prives, C., and Stockwell, B.R., Discovery of Mdm2-MdmX E3 ligase inhibitors using a cell-based ubiquitination assay. *Cancer Discov*, **2011**. *1*(4): p. 312-325.

170. Chargari, C., Leteur, C., Angevin, E., Bashir, T., Schoentjes, B., Arts, J., Janicot, M., Bourhis, J., and Deutsch, E., Preclinical assessment of JNJ-26854165 (Serdemetan(1)), a novel tryptamine compound with radiosensitizing activity in vitro and in tumor xenografts. *Cancer Letters*, **2011**. *312*(2): p. 209-218.

171. Tabernero, J., Dirix, L., Schoffski, P., Cervantes, A., Lopez-Martin, J.A., Capdevila, J., van Beijsterveldt, L., Platero, S., Hall, B., Yuan, Z.L., Knoblauch, R., and Zhuang, S.H., A phase I first-in-human pharmacokinetic and pharmacodynamic study of Serdemetan in patients with advanced solid tumors. *Clin Cancer Res*, **2011**. *17*(19): p. 6313-6321.

172. Kojima, K., Burks, J.K., Arts, J., and Andreeff, M., The novel tryptamine derivative JNJ-26854165 induces wild-type p53-and E2F1-mediated apoptosis in acute myeloid and lymphoid leukemias. *Mol Cancer Ther*, **2010**. *9*(9): p. 2545-2557.

173. Jones, R.J., Gu, D., Bjorklund, C.C., Kuiatse, I., Remaley, A.T., Bashir, T., Vreys, V., and Orlowski, R.Z., The novel anticancer agent JNJ-26854165 induces cell death through inhibition of cholesterol transport and degradation of ABCA1. *J Pharmacol Exp Ther*, **2013**. *346*(3): p. 381-92.

174. Shvarts, A., Steegenga, W.T., Riteco, N., vanLaar, T., Dekker, P., Bazuine, M., vanHam, R.C.A., vanOordt, W.V., Hateboer, G., vanderEb, A.J., and Jochemsen, A.G., MDMX: A novel p53-binding protein with some functional properties of MDM2. *EMBO J*, **1996**. *15*(19): p. 5349-5357.

175. Marine, J.C. and Jochemsen, A.G., Mdmx as an essential regulator of p53 activity. *Biochem Biophys Res Commun*, **2005**. *331*(3): p. 750-760.

176. Wade, M., Li, Y.-C., and Wahl, G.M., MDM2, MDMX and p53 in oncogenesis and cancer therapy. *Nat Rev Cancer*, **2013**. *13*(2): p. 83-96.

177. Garcia, D., Warr, M.R., Martins, C.P., Swigart, L.B., Passegue, E., and Evan, G.I., Validation of MdmX as a therapeutic target for reactivating p53 in tumors. *Genes Dev* **2011**. *25*(16): p. 1746-1757.

178. Reed, D., Shen, Y., Shelat, A.A., Arnold, L.A., Ferreira, A.M., Zhu, F., Mills, N., Smithson, D.C., Regni, C.A., Bashford, D., Cicero, S.A., Schulman, B.A., Jochemsen, A.G., Guy, R.K., and Dyer, M.A., Identification and characterization of

the first small molecule inhibitor of MDMX. *J Biol Chem*, **2010**. *285*(14): p. 10786-10796.

179. Bista, M., Smithson, D., Pecak, A., Salinas, G., Pustelny, K., Min, J., Pirog, A., Finch, K., Zdzalik, M., Waddell, B., Wladyka, B., Kedracka-Krok, S., Dyer, M.A., Dubin, G., and Guy, R.K., On the mechanism of action of SJ-172550 in inhibiting the interaction of MDM4 and p53. *PLoS One*, **2012**. *7*(6).
180. Berkson, R.G., Hollick, J.J., Westwood, N.J., Woods, J.A., Lane, D.P., and Lain, S., Pilot screening programme for small molecule activators of p53. *Int J Cancer*, **2005**. *115*(5): p. 701-710.
181. Wang, H. and Yan, C., A Small-Molecule p53 Activator Induces Apoptosis through Inhibiting MDMX Expression in Breast Cancer Cells. *Neoplasia*, **2011**. *13*(7): p. 611-U58.
182. Roh, J.-L., Park, J.Y., and Kim, E.H., XI-011 enhances cisplatin-induced apoptosis by functional restoration of p53 in head and neck cancer. *Apoptosis*, **2014**. *19*(11): p. 1594-1602.
183. Vogel, S.M., Bauer, M.R., Joerger, A.C., Wilcken, R., Brandt, T., Veprintsev, D.B., Rutherford, T.J., Fersht, A.R., and Boeckler, F.M., Lithocholic acid is an endogenous inhibitor of MDM4 and MDM2. *Proc Natl Acad Sci U S A*, **2012**. *109*(42): p. 16906-16910.
184. Blackburn, T.J., Ahmed, S., Coxon, C.R., Liu, J., Lu, X., Golding, B.T., Griffin, R.J., Hutton, C., Newell, D.R., Ojo, S., Watson, A.F., Zaytzev, A., Zhao, Y., Lunec, J., and Hardcastle, I.R., Diaryl- and triaryl-pyrrole derivatives: inhibitors of the MDM2-p53 and MDMX-p53 protein-protein interactions. *MedChemComm*, **2013**. *4*(9): p. 1297-1304.
185. Qin, L., Yang, F., Zhou, C., Chen, Y., Zhang, H., and Su, Z., Efficient reactivation of p53 in cancer cells by a dual MdmX/Mdm2 inhibitor. *J Am Chem Soc*, **2014**. *136*(52): p. 18023-18033.
186. Graves, B., Thompson, T., Xia, M., Janson, C., Lukacs, C., Deo, D., Di Lello, P., Fry, D., Garvie, C., Huang, K.-S., Gao, L., Tovar, C., Lovey, A., Wanner, J., and Vassilev, L.T., Activation of the p53 pathway by small-molecule-induced MDM2 and MDMX dimerization. *Proc Natl Acad Sci U S A*, **2012**. *109*(29): p. 11788-11793.
187. Rubbi, C.P. and Milner, J., Disruption of the nucleolus mediates stabilization of p53 in response to DNA damage and other stresses. *EMBO J*, **2003**. *22*(22): p. 6068-77.
188. Bursac, S., Brdovcak, M.C., Pfannkuchen, M., Orsolic, I., Golomb, L., Zhu, Y., Katz, C., Daftuar, L., Grabusic, K., Vukelic, I., Filic, V., Oren, M., Prives, C., and Volarevic, S., Mutual protection of ribosomal proteins L5 and L11 from

degradation is essential for p53 activation upon ribosomal biogenesis stress. *Proc Natl Acad Sci U S A*, **2012**. *109*(50): p. 20467-20472.

189. Hein, N., Hannan, K.M., George, A.J., Sanij, E., and Hannan, R.D., The nucleolus: An emerging target for cancer therapy. *Trends Mol Med*, **2013**. *19*(11): p. 643-654.
190. Choong, M.L., Yang, H., Lee, M.A., and Lane, D.P., Specific activation of the p53 pathway by low dose actinomycin D: a new route to p53 based cyclotherapy. *Cell Cycle*, **2009**. *8*(17): p. 2810-8.
191. Peltonen, K., Colis, L., Liu, H., Jaamaa, S., Moore, H.M., Enback, J., Laakkonen, P., Vaahtokari, A., Jones, R.J., af Hallstrom, T.M., and Laiho, M., Identification of novel p53 pathway activating small-molecule compounds reveals unexpected similarities with known therapeutic agents. *PLoS One*, **2010**. *5*(9): p. e12996.
192. Peltonen, K., Colis, L., Liu, H., Trivedi, R., Moubarek, M.S., Moore, H.M., Bai, B., Rudek, M.A., Bieberich, C.J., and Laiho, M., A targeting modality for destruction of RNA polymerase I that possesses anticancer activity. *Cancer Cell*, **2014**. *25*(1): p. 77-90.
193. Haddach, M., Schwaebe, M.K., Michaux, J., Nagasawa, J., O'Brien, S.E., Whitten, J.P., Pierre, F., Kerdoncuff, P., Darjania, L., Stansfield, R., Drygin, D., Anderes, K., Proffitt, C., Bliesath, J., Siddiqui-Jain, A., Omori, M., Huser, N., Rice, W.G., and Ryckman, D.M., Discovery of CX-5461, the first direct and selective inhibitor of RNA polymerase I, for cancer therapeutics. *ACS Med Chem Lett*, **2012**. *3*(7): p. 602-606.
194. Bywater, M.J., Poortinga, G., Sanij, E., Hein, N., Peck, A., Cullinane, C., Wall, M., Cluse, L., Drygin, D., Anderes, K., Huser, N., Proffitt, C., Bliesath, J., Haddach, M., Schwaebe, M.K., Ryckman, D.M., Rice, W.G., Schmitt, C., Lowe, S.W., Johnstone, R.W., Pearson, R.B., McArthur, G.A., and Hannan, R.D., Inhibition of RNA polymerase I as a therapeutic strategy to promote cancer-specific activation of p53. *Cancer Cell*, **2012**. *22*(1): p. 51-65.
195. Lu, W., Chen, L., Peng, Y., and Chen, J., Activation of p53 by roscovitine-mediated suppression of MDM2 expression. *Oncogene*, **2001**. *20*(25): p. 3206-16.
196. MacCallum, D.E., Melville, J., Frame, S., Watt, K., Anderson, S., Gianella-Borradori, A., Lane, D.P., and Green, S.R., Seliciclib (CYC202, R-Roscovitine) induces cell death in multiple myeloma cells by inhibition of RNA polymerase II-dependent transcription and down-regulation of Mcl-1. *Cancer Res*, **2005**. *65*(12): p. 5399-407.
197. Gasparian, A.V., Burkhart, C.A., Purmal, A.A., Brodsky, L., Pal, M., Saranadasa, M., Bosykh, D.A., Commane, M., Guryanova, O.A., Pal, S., Safina, A., Sviridov, S., Koman, I.E., Veith, J., Komar, A.A., Gudkov, A.V., and Gurova, K.V., Curaxins: Anticancer compounds that simultaneously suppress NF-kappa B and activate p53 by targeting FACT. *Sci Transl Med*, **2011**. *3*(95).

198. Di Bussolo, V. and Minutolo, F., Curaxins: A new family of non-genotoxic multitargeted anticancer agents. *ChemMedChem*, **2011**. *6*(12): p. 2133-2136.
199. Mutka, S.C., Yang, W.Q., Dong, S.D., Ward, S.L., Craig, D.A., Timmermans, P.B., and Murli, S., Identification of nuclear export inhibitors with potent anticancer activity in vivo. *Cancer Res*, **2009**. *69*(2): p. 510-517.
200. Sakakibara, K., Saito, N., Sato, T., Suzuki, A., Hasegawa, Y., Friedman, J.M., Kufe, D.W., VonHoff, D.D., Iwami, T., and Kawabe, T., CBS9106 is a novel reversible oral CRM1 inhibitor with CRM1 degrading activity. *Blood*, **2011**. *118*(14): p. 3922-3931.
201. Senapedis, W.T., Baloglu, E., and Landesman, Y., Clinical translation of nuclear export inhibitors in cancer. *Semin Cancer Biol*, **2014**. *27*: p. 74-86.
202. Love, I.M. and Grossman, S.R., It takes 15 to tango: Making sense of the many ubiquitin ligases of p53. *Genes Cancer*, **2012**. *3*(3-4): p. 249-63.
203. Soucy, T.A., Smith, P.G., Milhollen, M.A., Berger, A.J., Gavin, J.M., Adhikari, S., Brownell, J.E., Burke, K.E., Cardin, D.P., Critchley, S., Cullis, C.A., Doucette, A., Garnsey, J.J., Gaulin, J.L., Gershman, R.E., Lublinsky, A.R., McDonald, A., Mizutani, H., Narayanan, U., Olhava, E.J., Peluso, S., Rezaei, M., Sintchak, M.D., Talreja, T., Thomas, M.P., Traore, T., Vyskocil, S., Weatherhead, G.S., Yu, J., Zhang, J., Dick, L.R., Claiborne, C.F., Rolfe, M., Bolen, J.B., and Langston, S.P., An inhibitor of NEDD8-activating enzyme as a new approach to treat cancer. *Nature*, **2009**. *458*(7239): p. 732-U67.
204. Blank, J.L., Liu, X.J., Cosmopoulos, K., Bouck, D.C., Garcia, K., Bernard, H., Tayber, O., Hather, G., Liu, R., Narayanan, U., Milhollen, M.A., and Lightcap, E.S., Novel DNA damage checkpoints mediating cell death induced by the NEDD8-activating enzyme inhibitor MLN4924. *Cancer Res*, **2013**. *73*(1): p. 225-34.
205. Saito, N., Sakakibara, K., Sato, T., Friedman, J.M., Kufe, D.W., VonHoff, D.D., and Kawabe, T., CBS9106-induced CRM1 degradation is mediated by cullin ring ligase activity and the neddylation pathway. *Mol Cancer Ther*, **2014**. *13*(12): p. 3013-3023.
206. Vaziri, H., Dessain, S.K., Eagon, E.N., Imai, S.I., Frye, R.A., Pandita, T.K., Guarente, L., and Weinberg, R.A., hSIR2(SIRT1) functions as an NAD-dependent p53 deacetylase. *Cell*, **2001**. *107*(2): p. 149-159.
207. Dai, C. and Gu, W., p53 post-translational modification: Deregulated in tumorigenesis. *Trends Mol Med*, **2010**. *16*(11): p. 528-536.
208. Grozinger, C.M., Chao, E.D., Blackwell, H.E., Moazed, D., and Schreiber, S.L., Identification of a class of small molecule inhibitors of the sirtuin family of NAD-dependent deacetylases by phenotypic screening. *J Biol Chem*, **2001**. *276*(42): p. 38837-38843.

209. Mai, A., Massa, S., Lavu, S., Pezzi, R., Simeoni, S., Ragno, R., Mariotti, F.R., Chiani, F., Camilloni, G., and Sinclair, D.A., Design, synthesis, and biological evaluation of sirtinol analogues as class III histone/protein deacetylase (sirtuin) inhibitors. *J Med Chem*, **2005**. *48*(24): p. 7789-7795.

210. Lara, E., Mai, A., Calvanese, V., Altucci, L., Lopez-Nieva, P., Martinez-Chantar, M.L., Varela-Rey, M., Rotili, D., Nebbioso, A., Ropero, S., Montoya, G., Oyarzabal, J., Velasco, S., Serrano, M., Witt, M., Villar-Garea, A., Inhof, A., Mato, J.M., Esteller, M., and Fraga, M.F., Salermide, a Sirtuin inhibitor with a strong cancer-specific proapoptotic effect. *Oncogene*, **2009**. *28*(6): p. 781-791.

211. Rotili, D., Tarantino, D., Nebbioso, A., Paolini, C., Huidobro, C., Lara, E., Mellini, P., Lenoci, A., Pezzi, R., Botta, G., Lahtela-Kakkonen, M., Poso, A., Steinkuehler, C., Gallinari, P., De Maria, R., Fraga, M., Esteller, M., Altucci, L., and Mai, A., Discovery of salermide-related sirtuin inhibitors: Binding mode studies and antiproliferative effects in cancer cells including cancer stem cells. *J Med Chem*, **2012**. *55*(24): p. 10937-10947.

212. Heltweg, B., Gatbonton, T., Schuler, A.D., Posakony, J., Li, H.Z., Goehle, S., Kollipara, R., DePinho, R.A., Gu, Y.S., Simon, J.A., and Bedalov, A., Antitumor activity of a small-molecule inhibitor of human silent information regulator 2 enzymes. *Cancer Res*, **2006**. *66*(8): p. 4368-4377.

213. Medda, F., Russell, R.J.M., Higgins, M., McCarthy, A.R., Campbell, J., Slawin, A.M.Z., Lane, D.P., Lain, S., and Westwood, N.J., Novel cambinol analogs as sirtuin inhibitors: Synthesis, biological evaluation, and rationalization of activity. *J Med Chem*, **2009**. *52*(9): p. 2673-2682.

214. Medda, F., Joseph, T.L., Pirrie, L., Higgins, M., Slawin, A.M.Z., Lain, S., Verma, C., and Westwood, N.J., N1-Benzyl substituted cambinol analogues as isozyme selective inhibitors of the sirtuin family of protein deacetylases. *MedChemComm*, **2011**. *2*(7): p. 611-615.

215. Mahajan, S.S., Scian, M., Sripathy, S., Posakony, J., Lao, U., Loe, T.K., Leko, V., Thalhofer, A., Schuler, A.D., Bedalov, A., and Simon, J.A., Development of pyrazolone and isoxazol-5-one cambinol analogues as sirtuin inhibitors. *J Med Chem*, **2014**. *57*(8): p. 3283-3294.

216. Bedalov, A., Gatbonton, T., Irvine, W.P., Gottschling, D.E., and Simon, J.A., Identification of a small molecule inhibitor of Sir2p. *Proc Natl Acad Sci U S A*, **2001**. *98*(26): p. 15113-15118.

217. Posakony, J., Hirao, M., Stevens, S., Simon, J.A., and Bedalov, A., Inhibitors of Sir2: Evaluation of splitomicin analogues. *J Med Chem*, **2004**. *47*(10): p. 2635-2644.

218. Neugebauer, R.C., Uchiechowska, U., Meier, R., Hruby, H., Valkov, V., Verdin, E., Sippl, W., and Jung, M., Structure-activity studies on splitomicin derivatives as

sirtuin inhibitors and computational prediction of binding mode. *J Med Chem*, **2008**. *51*(5): p. 1203-1213.

219. Freitag, M., Schemies, J., Larsen, T., El Gaghlab, K., Schulz, F., Rumpf, T., Jung, M., and Link, A., Synthesis and biological activity of splitomicin analogs targeted at human NAD(+)-dependent histone deacetylases (sirtuins). *Bioorg Med Chem*, **2011**. *19*(12): p. 3669-3677.
220. Napper, A.D., Hixon, J., McDonagh, T., Keavey, K., Pons, J.F., Barker, J., Yau, W.T., Amouzegh, P., Flegg, A., Hamelin, E., Thomas, R.J., Kates, M., Jones, S., Navia, M.A., Saunders, J., DiStefano, P.S., and Curtis, R., Discovery of indoles as potent and selective inhibitors of the deacetylase SIRT1. *J Med Chem*, **2005**. *48*(25): p. 8045-8054.
221. Zhao, X., Allison, D., Condon, B., Zhang, F., Gheyi, T., Zhang, A., Ashok, S., Russell, M., MacEwan, I., Qian, Y., Jamison, J.A., and Luz, J.G., The 2.5 angstrom crystal structure of the SIRT1 catalytic domain bound to nicotinamide adenine dinucleotide (NAD^+) and an indole (EX527 analogue) reveals a novel mechanism of histone deacetylase inhibition. *J Med Chem*, **2013**. *56*(3): p. 963-969.
222. Lain, S., Hollick, J.J., Campbell, J., Staples, O.D., Higgins, M., Aoubala, M., McCarthy, A., Appleyard, V., Murray, K.E., Baker, L., Thompson, A., Mathers, J., Holland, S.J., Stark, M.J.R., Pass, G., Woods, J., Lane, D.P., and Westwood, N.J., Discovery, in vivo activity, and mechanism of action of a small-molecule p53 activator. *Cancer Cell*, **2008**. *13*(5): p. 454-463.
223. Zhang, Q., Zeng, S.Y.X., Zhang, Y., Zhang, Y.W., Ding, D.R., Ye, Q.Z., Meroueh, S.O., and Lu, H., A small molecule Inauhzin inhibits SIRT1 activity and suppresses tumour growth through activation of p53. *EMBO Mol Med*, **2012**. *4*(4): p. 298-312.
224. Yuan, H.F., Su, L.L., and Chen, W.Y., The emerging and diverse roles of sirtuins in cancer: a clinical perspective. *Oncotargets Ther*, **2013**. *6*: p. 1399-1416.
225. Dang, W., The controversial world of sirtuins. *Drug Discov Today Technol*, **2014**. *12*: p. e9-e17.
226. Lin, J., Yang, Q.Y., Yan, Z., Markowitz, J., Wilder, P.T., Carrier, F., and Weber, D.J., Inhibiting S100B restores p53 levels in primary malignant melanoma cancer cells. *J Biol Chem*, **2004**. *279*(32): p. 34071-34077.
227. Hartman, K.G., McKnight, L.E., Liriano, M.A., and Weber, D.J., The evolution of S100B inhibitors for the treatment of malignant melanoma. *Future Med Chem*, **2013**. *5*(1): p. 97-109.
228. Markowitz, J., Chen, J., Gitti, R., Baldisseri, D.M., Pan, Y.P., Udan, R., Carrier, F., MacKerell, A.D., and Weber, D.J., Identification and characterization of small molecule inhibitors of the calcium-dependent S100B-p53 tumor suppressor interaction. *J Med Chem*, **2004**. *47*(21): p. 5085-5093.

229. Charpentier, T.H., Wilder, P.T., Liriano, M.A., Varney, K.M., Zhong, S., Coop, A., Pozharski, E., MacKerell, A.D., Jr., Toth, E.A., and Weber, D.J., Small molecules bound to unique sites in the target protein binding cleft of calcium-bound S100B as characterized by nuclear magnetic resonance and X-ray crystallography. *Biochemistry*, **2009**. *48*(26): p. 6202-6212.

230. Yoshimura, C., Miyafusa, T., and Tsumoto, K., Identification of small-molecule inhibitors of the human S100B-p53 interaction and evaluation of their activity in human melanoma cells. *Bioorg Med Chem*, **2013**. *21*(5): p. 1109-1115.

231. Cavalier, M.C., Pierce, A.D., Wilder, P.T., Alasady, M.J., Hartman, K.G., Neau, D.B., Foley, T.L., Jadhav, A., Maloney, D.J., Simeonov, A., Toth, E.A., and Weber, D.J., Covalent small molecule inhibitors of Ca^{2+}-bound S100B. *Biochemistry*, **2014**. *53*(42): p. 6628-6640.

232. Issaeva, N., Bozko, P., Enge, M., Protopopova, M., Verhoef, L., Masucci, M., Pramanik, A., and Selivanova, G., Small molecule RITA binds to p53, blocks p53-HDM-2 interaction and activates p53 function in tumors. *Nat Med*, **2004**. *10*(12): p. 1321-1328.

233. Krajewski, M., Ozdowy, P., D'Silva, L., Rothweiler, U., and Holak, T.A., NMR indicates that the small molecule RITA does not block p53-MDM2 binding in vitro. *Nat Med*, **2005**. *11*(11): p. 1135-1136.

234. Zhao, C.Y., Grinkevich, V.V., Nikulenkov, F., Bao, W., and Selivanova, G., Rescue of the apoptotic-inducing function of mutant p53 by small molecule RITA. *Cell Cycle*, **2010**. *9*(9): p. 1847-1855.

235. Burmakin, M., Shi, Y., Hedstrom, E., Kogner, P., and Selivanova, G., Dual targeting of wild-type and mutant p53 by small molecule RITA results in the inhibition of N-Myc and key survival oncogenes and kills neuroblastoma cells in vivo and in vitro. *Clin Cancer Res*, **2013**. *19*(18): p. 5092-5103.

236. Spinnler, C., Hedstrom, E., Li, H., de Lange, J., Nikulenkov, F., Teunisse, A.F.A.S., Verlaan-de Vries, M., Grinkevich, V., Jochemsen, A.G., and Selivanova, G., Abrogation of Wip1 expression by RITA-activated p53 potentiates apoptosis induction via activation of ATM and inhibition of HdmX. *Cell Death Differ*, **2011**. *18*(11): p. 1736-1745.

237. Lin, J., Jin, X., Bu, Y., Cao, D., Zhang, N., Li, S., Sun, Q., Tan, C., Gao, C., and Jiang, Y., Efficient synthesis of RITA and its analogues: derivation of analogues with improved antiproliferative activity via modulation of p53/miR-34a pathway. *Org Biomol Chem*, **2012**. *10*(48): p. 9734-9746.

238. Jiang, J., Ding, C., Li, L., Gao, C., Jiang, Y., Tan, C., and Hua, R., Synthesis and antiproliferative activity of RITA and its analogs. *Tetrahedron Lett*, **2014**. *55*(49): p. 6635-6638.

239. Muller, P.A.J. and Vousden, K.H., Mutant p53 in cancer: New functions and therapeutic opportunities. *Cancer Cell*, **2014**. *25*(3): p. 304-317.
240. Bykov, V.J.N. and Wiman, K.G., Mutant p53 reactivation by small molecules makes its way to the clinic. *FEBS Lett*, **2014**. *588*(16): p. 2622-2627.
241. Boeckler, F.M., Joerger, A.C., Jaggi, G., Rutherford, T.J., Veprintsev, D.B., and Fersht, A.R., Targeted rescue of a destabilized mutant of p53 by an in silico screened drug. *Proc Natl Acad Sci U S A*, **2008**. *105*(30): p. 10360-10365.
242. Wilcken, R., Liu, X., Zimmermann, M.O., Rutherford, T.J., Fersht, A.R., Joerger, A.C., and Boeckler, F.M., Halogen-enriched fragment libraries as leads for drug rescue of mutant p53. *J Am Chem Soc*, **2012**. *134*(15): p. 6810-6818.
243. Liu, X., Wilcken, R., Joerger, A.C., Chuckowree, I.S., Amin, J., Spencer, J., and Fersht, A.R., Small molecule induced reactivation of mutant p53 in cancer cells. *Nucleic Acids Res*, **2013**. *41*(12): p. 6034-6044.
244. Bykov, V.J.N., Issaeva, N., Shilov, A., Hultcrantz, M., Pugacheva, E., Chumakov, P., Bergman, J., Wiman, K.G., and Selivanova, G., Restoration of the tumor suppressor function to mutant p53 by a low-molecular-weight compound. *Nat Med*, **2002**. *8*(3): p. 282-288.
245. Lambert, J.M.R., Gorzov, P., Veprintsev, D.B., Soderqvist, M., Segerback, D., Bergman, J., Fersht, A.R., Hainaut, P., Wiman, K.G., and Bykov, V.J.N., PRIMA-1 reactivates mutant p53 by covalent binding to the core domain. *Cancer Cell*, **2009**. *15*(5): p. 376-388.
246. Bykov, V.J.N., Issaeva, N., Zache, N., Shilov, A., Hultcrantz, M., Bergman, J., Selivanova, G., and Wiman, K.G., Reactivation of mutant p53 and induction of apoptosis in human tumor cells by maleimide analogs. *J Biol Chem*, **2005**. *280*(34): p. 30384-30391.
247. Zache, N., Lambert, J.M.R., Rokaeus, N., Shen, J., Hainaut, P., Bergman, J., Wiman, K.G., and Bykou, V.N., Mutant p53 targeting by the low molecular weight compound STIMA-1. *Mol Oncol*, **2008**. *2*(1): p. 70-80.
248. Wassman, C.D., Baronio, R., Demir, O., Wallentine, B.D., Chen, C.K., Hall, L.V., Salehi, F., Lin, D.W., Chung, B.P., Hatfield, G.W., Chamberlin, A.R., Luecke, H., Lathrop, R.H., Kaiser, P., and Amaro, R.E., Computational identification of a transiently open L1/S3 pocket for reactivation of mutant p53. *Nat Commun*, **2013**. *4*: p. 9.
249. Takimoto, R., Wang, W.G., Dicker, D.T., Rastinejad, F., Lyssikatos, J., and El-Deiry, W.S., The mutant p53-conformation modifying drug, CP-31398, can induce apoptosis of human cancer cells and can stabilize wild-type p53 protein. *Cancer Biol Ther*, **2002**. *1*(1): p. 47-55.

250. Wang, W.G., Takimoto, R., Rastinejad, F., and El-Deiry, W.S., Stabilization of p53 by CP-31398 inhibits ubiquitination without altering phosphorylation at serine 15 or 20 or MDM2 binding. *Mol Cell Biol*, **2003**. *23*(6): p. 2171-2181.

251. Demma, M., Maxwell, E., Ramos, R., Liang, L., Li, C., Hesk, D., Rossman, R., Mallams, A., Doll, R., Liu, M., Seidel-Dugan, C., Bishop, W.R., and Dasmahapatra, B., SCH529074, a small molecule activator of mutant p53, which binds p53 DNA binding domain (DBD), restores growth-suppressive function to mutant p53 and interrupts HDM2-mediated ubiquitination of wild type p53. *J Biol Chem*, **2010**. *285*(14): p. 10198-10212.

252. Yu, X., Vazquez, A., Levine, A.J., and Carpizo, D.R., Allele-specific p53 mutant reactivation. *Cancer Cell*, **2012**. *21*(5): p. 614-625.

253. Yu, X., Blanden, A.R., Narayanan, S., Jayakumar, L., Lubin, D., Augeri, D., Kimball, S.D., Loh, S.N., and Carpizo, D.R., Small molecule restoration of wildtype structure and function of mutant p53 using a novel zinc-metallochaperone based mechanism. *Oncotarget*, **2014**. *5*(19): p. 8879-8892.

254. Li, D., Marchenko, N.D., and Moll, U.M., SAHA shows preferential cytotoxicity in mutant p53 cancer cells by destabilizing mutant p53 through inhibition of the HDAC6-Hsp90 chaperone axis. *Cell Death Differ*, **2011**. *18*(12): p. 1904-1913.

255. Kravchenko, J.E., Ilyinskaya, G.V., Komarov, P.G., Agapova, L.S., Kochetkov, D.V., Strom, E., Frolova, E.I., Kovriga, I., Gudkov, A.V., Feinstein, E., and Chumakov, P.M., Small-molecule RETRA suppresses mutant p53-bearing cancer cells through a p73-dependent salvage pathway. *Proc Natl Acad Sci U S A*, **2008**. *105*(17): p. 6302-6307.

256. Lu, C., Wang, W., and El-Deiry, W.S., Non-genotoxic anti-neoplastic effects of ellipticine derivative NSC176327 in p53-deficient human colon carcinoma cells involve stimulation of p73. *Cancer Biol Ther*, **2008**. *7*(12): p. 2039-2046.

257. Ding, L., Zhang, Z., Liang, G., Yao, Z., Wu, H., Wang, B., Zhang, J., Tariq, M., Ying, M., and Yang, B., SAHA triggered MET activation contributes to SAHA tolerance in solid cancer cells. *Cancer Lett*, **2015**. *356*(2): p. 828-836.

258. Rao, B., Lain, S., and Thompson, A.M., p53-Based cyclotherapy: exploiting the 'guardian of the genome' to protect normal cells from cytotoxic therapy. *Br J Cancer*, **2013**. *109*(12): p. 2954-2958.

259. Santos, M.M.M., Recent advances in the synthesis of biologically active spirooxindoles. *Tetrahedron*, **2014**. *70*(52): p. 9735-9757.

260. Amaral, J.D., Herrera, F., Rodrigues, P.M., Dionisio, P.A., Outeiro, T.F., and Pereira Rodrigues, C.M., Live-cell imaging of p53 interactions using a novel Venus-based bimolecular fluorescence complementation system. *Biochem Pharmacol*, **2013**. *85*(6): p. 745-752.

261. Jager, V. and Colinas, P.A., *Nitrile Oxides*, in *Synthetic applications of 1,3-dipolar cycloaddition chemistry towards heterocycles and natural products*, A. Padwa and W. H. Pearson, Editors. **2002**, John Wiley & Sons, Inc.
262. Belen'kii, L.I., *Nitrile oxides*, in *Nitrile oxides, nitrones, and nitronates in organic synthesis: novel strategies in synthesis*, H. Feuer, Editor. **2008**, John Wiley & Sons, Inc. p. 1-127.
263. Ribeiro, C.J.A., *Síntese de Derivados Spiro-oxindoles via Cicloadição 1,3-Dipolar. Master thesis*. **2010**, University of Lisbon. Lisbon.
264. Cecchi, L., De Sarlo, F., and Machetti, F., Isoxazoline derivatives from activated primary nitrocompounds and tertiary diamines. *Tetrahedron Lett*, **2005**. *46*(46): p. 7877-7879.
265. Cecchi, L., De Sarlo, F., and Machetti, F., 1,4-diazabicyclo[2.2.2]octane (DABCO) as an efficient reagent for the synthesis of isoxazole derivatives from primary nitro compounds and dipolarophiles: the role of the base. *Eur J Org Chem*, **2006**(21): p. 4852-4860.
266. Machetti, F., Cecchi, L., Trogu, E., and De Sarlo, F., Isoxazoles and isoxazolines by 1,3-dipolar cycloaddition: Base-catalysed condensation of primary nitro compounds with dipolarophiles. *Eur J Org Chem*, **2007**(26): p. 4352-4359.
267. Ramachandiran, K., Karthikeyan, K., Muralidharan, D., and Perumal, P.T., Synthesis of isoxazolobenzoxepanes via Michael addition of indoles to nitroalkenes and sequential intramolecular nitrile oxide cycloaddition. *Tetrahedron Lett*, **2010**. *51*(22): p. 3006-3009.
268. Zagozda, M. and Plenkiewicz, J., Optically active nitrile oxides: synthesis and 1,3-dipolar cycloaddition reactions. *Tetrahedron-Asymmetry*, **2007**. *18*(12): p. 1457-1464.
269. Akritopoulou-Zanze, I., Gracias, V., Moore, J.D., and Djuric, S.W., Synthesis of novel fused isoxazoles and isoxazolines by sequential Ugi/INOC reactions. *Tetrahedron Lett*, **2004**. *45*(17): p. 3421-3423.
270. Raunak, Kumar, V., Mukherjee, S., Poonam, Prasad, A.K., Olsen, C.E., Schaeffer, S.J.C., Sharma, S.K., Watterson, A.C., Errington, W., and Parmar, V.S., Microwave-mediated synthesis of spiro-(indoline-isoxazolidines): mechanistic study and biological activity evaluation. *Tetrahedron*, **2005**. *61*(23): p. 5687-5697.
271. Shmidt, M.S., Reverdito, A.M., Kremenchuzky, L., Perillo, I.A., and Blanco, M.M., Simple and efficient microwave assisted *N*-alkylation of isatin. *Molecules*, **2008**. *13*(4): p. 831-840.
272. Morales-Rios, M.S., Garcia-Velgara, M., Cervantes-Cuevas, H., Alvarez-Cisneros, C., and Joseph-Nathan, P., Push-pull and pull-push effects in isatylidenes. *Magn Reson Chem*, **2000**. *38*(3): p. 172-176.

273. Cao, S.-H., Zhang, X.-C., Wei, Y., and Shi, M., Chemoselective Reduction of Isatin-Derived Electron-Deficient Alkenes Using Alkylphosphanes as Reduction Reagents. *Eur J Org Chem*, **2011**(14): p. 2668-2672, S2668/1-S2668/65.

274. Osman, F.H., El-Samahy, F.A., and Farag, I.S.A., A nucleophilic addition of acetone enolate to (*E*)-alkyloxindolylideneacetates. *Monatsh Chem*, **2004**. *135*(7): p. 823-831.

275. Kozikowski, A.P. and Adamczyk, M., Methods for the stereoselective cis cyanohydroxylation and carboxyhydroxylation of olefins. *J Org Chem*, **1983**. *48*(3): p. 366-372.

276. Dubrovskiy, A.V. and Larock, R.C., Synthesis of benzisoxazoles by the 3+2 cycloaddition of in situ generated nitrile oxides and arynes. *Org Lett*, **2010**. *12*(6): p. 1180-1183.

277. Palumbo, C., Mazzeo, G., Mazziotta, A., Gambacorta, A., Loreto, M.A., Migliorini, A., Superchi, S., Tofani, D., and Gasperi, T., Noncovalent organocatalysis: A powerful tool for the nucleophilic epoxidation of alpha-ylideneoxindoles. *Org Lett*, **2011**. *13*(23): p. 6248-6251.

278. Rasmussen, H.B. and MacLeod, J.K., Total synthesis of donaxaridine. *J Nat Prod*, **1997**. *60*(11): p. 1152-1154.

279. Gabriele, B., Salerno, G., Veltri, L., Costa, M., and Massera, C., Stereoselective synthesis of (E)-3-(methoxycarbonyl)methylene-1,3-dihydroindol-2-ones by palladium-catalyzed oxidative carbonylation of 2-ethynylanilines. *Eur J Org Chem*, **2001**(24): p. 4607-4613.

280. Bialecki, J.B., Ruzicka, J., Weisbecker, C.S., Haribal, M., and Attygalle, A.B., Collision-induced dissociation mass spectra of glucosinolate anions. *J Mass Spectrom*, **2010**. *45*(3): p. 272-283.

281. Sanders, B.C., Friscourt, F., Ledin, P.A., Mbua, N.E., Arumugam, S., Guo, J., Boltje, T.J., Popik, V.V., and Boons, G.J., Metal-free sequential 3+2 - dipolar cycloadditions using cyclooctynes and 1,3-dipoles of different reactivity. *J Am Chem Soc*, **2011**. *133*(4): p. 949-957.

282. Castellano, S., Kuck, D., Viviano, M., Yoo, J., Lopez-Vallejo, F., Conti, P., Tamborini, L., Pinto, A., Medina-Franco, J.L., and Sbardella, G., Synthesis and biochemical evaluation of delta(2)-isoxazoline derivatives as DNA methyltransferase 1 inhibitors. *J Med Chem*, **2011**. *54*(21): p. 7663-7677.

283. Abbott, S.D., Lanebell, P., Sidhu, K.P.S., and Vederas, J.C., Synthesis and testing of heterocyclic-analogs of diaminopimelic acid (DAP) as inhibitors of dap dehydrogenase and dap epimerase. *J Am Chem Soc*, **1994**. *116*(15): p. 6513-6520.

284. Kissane, M. and Maguire, A.R., Asymmetric 1,3-dipolar cycloadditions of acrylamides. *Chem Soc Rev*, **2010**. *39*(2): p. 845-883.

285. El-Ahl, A.A.S., 1,3-dipolar cycloaddition reactions in synthesis of spiro 2-oxoindoline derivatives. *Pol J Chem*, **1997**. *71*(1): p. 27-31.
286. Savage, G.P., Spiro isoxazolines via nitrile oxide 1,3-dipolar cycloaddition reactions. *Curr Org Chem*, **2010**. *14*(14): p. 1478-1499.
287. Risitano, F., Grassi, G., Foti, F., Bruno, G., and Rotondo, A., Diastereoselective synthesis and structure of spirooxindole derivatives. *Heterocycles*, **2003**. *60*(4): p. 857-863.
288. Velikorodov, A.V., Poddubnyi, O.Y., Kuanchalieva, A.K., and Krivosheev, O.O., Synthesis of new spiro compounds containing a carbamate group. *Russ J Org Chem*, **2010**. *46*(12): p. 1826-1829.
289. Franke, A., Spirocyclic 2-indolinones by 1,3-dipolar cycloaddition. *Justus Liebigs Ann Chem*, **1978**(5): p. 717-725.
290. Singh, A. and Roth, G.P., A 3+2 dipolar cycloaddition route to 3-hydroxy-3-alkyl oxindoles: An approach to pyrrolidinoindoline alkaloids. *Org Lett*, **2011**. *13*(8): p. 2118-2121.
291. Zheng, Y., Tice, C.M., and Singh, S.B., The use of spirocyclic scaffolds in drug discovery. *Bioorg Med Chem Lett*, **2014**. *24*(16): p. 3673-3682.
292. Galliford, C.V. and Scheidt, K.A., Pyrrolidinyl-spirooxindole natural products as inspirations for the development of potential therapeutic agents. *Angew Chem Int Ed*, **2007**. *46*(46): p. 8748-8758.
293. Veber, D.F., Johnson, S.R., Cheng, H.Y., Smith, B.R., Ward, K.W., and Kopple, K.D., Molecular properties that influence the oral bioavailability of drug candidates. *J Med Chem*, **2002**. *45*(12): p. 2615-2623.
294. Yu, B., Yu, D.Q., and Liu, H.M., Spirooxindoles: Promising scaffolds for anticancer agents. *Eur J Med Chem* **2015**. *96*: p. 673-698.
295. Yu, B., Yu, Z., Qi, P.-P., Yu, D.-Q., and Liu, H.-M., Discovery of orally active anticancer candidate CFI-400945 derived from biologically promising spirooxindoles: Success and challenges. *Eur J Med Chem*, **2015**. *95*(0): p. 35-40.
296. Antonchick, A.P., Gerding-Reimers, C., Catarinella, M., Schuermann, M., Preut, H., Ziegler, S., Rauh, D., and Waldmann, H., Highly enantioselective synthesis and cellular evaluation of spirooxindoles inspired by natural products. *Nat Chem*, **2010**. *2*(9): p. 735-740.
297. Sun, L., Tran, N., Tang, F., App, H., Hirth, P., McMahon, G., and Tang, C., Synthesis and biological evaluations of 3-substituted indolin-2-ones: A novel class of tyrosine kinase inhibitors that exhibit selectivity toward particular receptor tyrosine kinases. *J Med Chem*, **1998**. *41*(14): p. 2588-2603.
298. Sun, L., Tran, N., Liang, C.X., Tang, F., Rice, A., Schreck, R., Waltz, K., Shawver, L.K., McMahon, G., and Tang, C., Design, synthesis, and evaluations of substituted 3- (3-or 4-carboxyethylpyrrol-2-yl)methylidenyl indolin-2-ones as inhibitors of

VEGF, FGF, and PDGF receptor tyrosine kinases. *J Med Chem*, **1999**. *42*(25): p. 5120-5130.

299. Andreani, A., Granaiola, M., Leoni, A., Locatelli, A., Morigi, R., Rambaldi, M., and Garaliene, V., Synthesis and antitumor activity of 1,5,6-substituted E-3-(2-chloro-3-indolylmethylene)-1,3-dihydroindol-2-ones. *J Med Chem*, **2002**. *45*(12): p. 2666-2669.
300. Pandit, B., Sun, Y., Chen, P., Sackett, D.L., Hu, Z., Rich, W., Li, C., Lewis, A., Schaefer, K., and Li, P.K., Structure-activity-relationship studies of conformationally restricted analogs of combretastatin A-4 derived from SU5416. *Bioorg Med Chem*, **2006**. *14*(19): p. 6492-501.
301. Balderamos, M., Ankati, H., Akubathini, S.K., Patel, A.V., Kamila, S., Mukherjee, C., Wang, L., Biehl, E.R., and D'Mello, S.R., Synthesis and structure-activity relationship studies of 3-substituted indolin-2-ones as effective neuroprotective agents. *Exp Biol Med*, **2008**. *233*(11): p. 1395-1402.
302. Cotter, J., Hogan, A.-M.L., and O'Shea, D.F., Development and application of a direct vinyl lithiation of cis-stilbene and a directed vinyl lithiation of an unsymmetrical cis-stilbene. *Org Lett*, **2007**. *9*(8): p. 1493-1496.
303. Zhang, W. and Go, M.-L., Functionalized 3-benzylidene-indolin-2-ones: Inducers of NAD(P)H-quinone oxidoreductase 1 (NQO1) with antiproliferative activity. *Bioorg Med Chem*, **2009**. *17*(5): p. 2077-2090.
304. Hu, Y., Kang, H., Zeng, B.-W., Huang, H., and Wei, P., Facile synthesis of 3-arylidene-1,3-dihydroindol-2-ones catalyzed by Bronsted acidic ionic liquids. *Heterocycl Commun*, **2008**. *14*(4): p. 263-267.
305. Teichert, A., Jantos, K., Harms, K., and Studer, A., One-pot homolytic aromatic substitutions/HWE olefinations under microwave conditions for the formation of a small oxindole library. *Org Lett*, **2004**. *6*(20): p. 3477-3480.
306. Kise, N., Sasaki, K., and Sakurai, T., Reductive coupling of isatins with ketones and aldehydes by low-valent titanium. *Tetrahedron*, **2014**. *70*(51): p. 9668-9675.
307. Khan, M., Yousaf, M., Wadood, A., Junaid, M., Ashraf, M., Alam, U., Ali, M., Arshad, M., Hussain, Z., and Khan, K.M., Discovery of novel oxindole derivatives as potent alpha-glucosidase inhibitors. *Bioorg Med Chem*, **2014**. *22*(13): p. 3441-3448.
308. Abedi, S., Karimi, B., Kazemi, F., Bostina, M., and Vali, H., Amorphous TiO2 coated into periodic mesoporous organosilicate channels as a new binary photocatalyst for regeneration of carbonyl compounds from oximes under sunlight irradiation. *Org Biomol Chem*, **2013**. *11*(3): p. 416-419.
309. Allen, C.L., Davulcu, S., and Williams, J.M.J., Catalytic acylation of amines with aldehydes or aldoximes. *Org Lett*, **2010**. *12*(22): p. 5096-5099.

310. Tyman, J.H.P. and Payne, P.B., The synthesis of phenolic propane-1,2- and 1,3-diols as intermediates in immobilised chelatants for the borate anion. *J Chem Res-S* **2006**(11): p. 691-695.
311. Ramirez-Monroy, A. and Swager, T.M., Metal chelates based on isoxazoline[60]fullerenes. *Organometallics*, **2011**. *30*(9): p. 2464-2467.
312. Tavares, A., Schneider, P.H., and Merlo, A.A., 3,5-Disubstituted Isoxazolines as Potential Molecular Kits for Liquid-Crystalline Materials. *Eur J Org Chem*, **2009**(6): p. 889-897.
313. Germain, M., Affar, E.B., D'Amours, D., Dixit, V.M., Salvesen, G.S., and Poirier, G.G., Cleavage of automodified poly(ADP-ribose) polymerase during apoptosis - Evidence for involvement of caspase-7. *J Biol Chem*, **1999**. *274*(40): p. 28379-28384.
314. Gothelf, K.V. and Jorgensen, K.A., Asymmetric 1,3-dipolar cycloaddition reactions. *Chem Rev*, **1998**. *98*(2): p. 863-909.
315. Curran, D.P., Jeong, K.S., Heffner, T.A., and Rebek, J., New chiral auxiliaries for thermal cycloadditions. *J Am Chem Soc*, **1989**. *111*(26): p. 9238-9240.
316. Kanemasa, S., Nishiuchi, M., Kamimura, A., and Hori, K., 1st successful metal coordination control in 1,3-dipolar cycloadditions - High-rate acceleration and regiocontrol and stereocontrol of nitrile oxide cycloadditions to the magnesium alkoxides of allylic and homoallylic alcohols. *J Am Chem Soc*, **1994**. *116*(6): p. 2324-2339.
317. Yamamoto, H., Watanabe, S., Kadotani, K., Hasegawa, M., Noguchi, M., and Kanemasa, S., Metal ion-mediated diastereoface-selective 1,3-dipolar cycloaddition of nitrile oxides with dipolarophiles bearing an oxazolidinone chiral auxiliary. *Tetrahedron Lett*, **2000**. *41*(17): p. 3131-3136.
318. Faita, G., Paio, A., Quadrelli, P., Rancati, F., and Seneci, P., Solid supported chiral auxiliaries in asymmetric synthesis. Part 2: Catalysis of 1,3-dipolar cycloadditions by Mg(II) cation. *Tetrahedron*, **2001**. *57*(39): p. 8313-8322.
319. Rasmussen, B.S., Elezcano, U., and Skrydstrup, T., Synthesis and binding properties of chiral macrocyclic barbiturate receptors: application to nitrile oxide cyclizations. *J Chem Soc, Perkin Trans 1*, **2002**(14): p. 1723-1733.
320. Yamamoto, H., Hayashi, S., Kubo, M., Harada, M., Hasegawa, M., Noguchi, M., Sumimoto, M., and Hori, K., Asymmetric 1,3-dipolar cycloaddition reactions of benzonitrile oxide mediated by a chiral Lewis acid. *Eur J Org Chem*, **2007**(17): p. 2859-2864.
321. Serizawa, M., Ukaji, Y., and Inomata, K., Preparation of novel N-sulfonylated (S,S)-2,3-diaminosuccinate-type chiral auxiliaries and application to an asymmetric 1,3-dipolar cycloaddition reaction of nitrile oxides to allyl alcohol. *Tetrahedron-Asymmetry*, **2006**. *17*(22): p. 3075-3083.

322. Sibi, M.P., Itoh, K., and Jasperse, C.P., Chiral Lewis acid catalysis in nitrile oxide cycloadditions. *J Am Chem Soc*, **2004**. *126*(17): p. 5366-5367.
323. Brinkmann, Y., Madhushaw, R.J., Jazzar, R., Bernardinelli, G., and Kuendig, E.P., Chiral ruthenium Lewis acid-catalyzed nitrile oxide cycloadditions. *Tetrahedron*, **2007**. *63*(35): p. 8413-8419.
324. Gucma, M. and Golebiewski, W.M., Enantioselective 1,3-dipolar cycloaddition reactions using complexes of (-)-sparteine. *J Heterocyclic Chem*, **2008**. *45*(1): p. 241-245.
325. Golebiewski, W.M. and Gucma, M., Enantioselective 1,3-dipolar cycloaddition reactions using chiral lanthanide catalysts. *J Heterocyclic Chem*, **2008**. *45*(6): p. 1687-1693.
326. Suga, H., Adachi, Y., Fujimoto, K., Furihata, Y., Tsuchida, T., Kakehi, A., and Baba, T., Asymmetric 1,3-dipolar cycloaddition reactions of nitrile oxides catalyzed by chiral binaphthyldiimine-Ni(II) complexes. *J Org Chem*, **2009**. *74*(3): p. 1099-1113.
327. Ono, F., Ohta, Y., Hasegawa, M., and Kanemasa, S., Molecular sieve 4 angstrom generates nitrile oxides from hydroximoyl chlorides. Development of catalyzed enantioselective nitrile oxide cycloadditions to monosubstituted alkenes. *Tetrahedron Lett*, **2009**. *50*(18): p. 2111-2114.
328. Sibi, M.P., Ma, Z.H., Itoh, K., Prabagaran, N., and Jasperse, C.P., Enantioselective cycloadditions with alpha,beta-disubstituted acrylimides. *Org Lett*, **2005**. *7*(12): p. 2349-2352.
329. Evans, D.A., Fandrick, K.R., Song, H.J., Scheidt, K.A., and Xu, R.S., Enantioselective Friedel-Crafts alkylations catalyzed by bis(oxazolinyl)pyridine-scandium(III) triflate complexes. *J Am Chem Soc*, **2007**. *129*(32): p. 10029-10041.
330. Ball-Jones, N.R., Badillo, J.J., Tran, N.T., and Franz, A.K., Catalytic enantioselective carboannulation with allylsilanes. *Angew Chem Int Ed*, **2014**. *53*(36): p. 9462-9465.
331. MacDonald, J.P., Shupe, B.H., Schreiber, J.D., and Franz, A.K., Counterion effects in the catalytic stereoselective synthesis of 2,3 '-pyrrolidinyl spirooxindoles. *Chem Commun*, **2014**. *50*(40): p. 5242-5244.
332. Shupe, B.H., Allen, E.E., MacDonald, J.P., Wilson, S.O., and Franz, A.K., Synthesis of spirocarbamate oxindoles via intramolecular trapping of a beta-silyl carbocation by an *N*-Boc group. *Org Lett*, **2013**. *15*(13): p. 3218-3221.
333. Hanhan, N.V., Ball-Jones, N.R., Tran, N.T., and Franz, A.K., Catalytic asymmetric 3+2 annulation of allylsilanes with isatins: synthesis of spirooxindoles. *Angew Chem Int Ed*, **2012**. *51*(4): p. 989-992.

334. Hanhan, N.V., Tang, Y.C., Tran, N.T., and Franz, A.K., Scandium(III)-catalyzed enantioselective allylation of isatins using allylsilanes. *Org Lett*, **2012**. *14*(9): p. 2218-2221.
335. Badillo, J.J., Arevalo, G.E., Fettinger, J.C., and Franz, A.K., Titanium-catalyzed stereoselective synthesis of spirooxindole oxazolines. *Org Lett*, **2011**. *13*(3): p. 418-421.
336. Badillo, J.J., Silva-Garcia, A., Shupe, B.H., Fettinger, J.C., and Franz, A.K., Enantioselective Pictet-Spengler reactions of isatins for the synthesis of spiroindolones. *Tetrahedron Lett*, **2011**. *52*(43): p. 5550-5553.
337. Gutierrez, E.G., Wong, C.J., Sahin, A.H., and Franz, A.K., Enantioselective and regioselective indium(III)-catalyzed addition of pyrroles to isatins. *Org Lett*, **2011**. *13*(21): p. 5754-5757.
338. Hanhan, N.V., Sahin, A.H., Chang, T.W., Fettinger, J.C., and Franz, A.K., Catalytic asymmetric synthesis of substituted 3-hydroxy-2-oxindoles. *Angew Chem Int Ed*, **2010**. *49*(4): p. 744-747.
339. Badillo, J.J., Ribeiro, C.J.A., Olmstead, M.M., and Franz, A.K., Titanium(IV)-catalyzed stereoselective synthesis of spirooxindole-1-pyrrolines. *Org Lett*, **2014**. *16*(24): p. 6270-6273.
340. Abadi, A.H., Abou-Seri, S.M., Abdel-Rahman, D.E., Klein, C., Lozach, O., and Meijer, L., Synthesis of 3-substituted-2-oxoindole analogues and their evaluation as kinase inhibitors, anticancer and antiangiogenic agents. *Eur J Med Chem*, **2006**. *41*(3): p. 296-305.
341. Rossiter, S., A convenient synthesis of 3-methyleneoxindoles: cytotoxic metabolites of indole-3-acetic acids. *Tetrahedron Lett*, **2002**. *43*(26): p. 4671-4673.
342. Kraynack, E.A., Dalgard, J.E., and Gaeta, F.C.A., An improved procedure for the regiospecific synthesis of electron deficient 4- and 6-substituted isatins. *Tetrahedron Lett*, **1998**. *39*(42): p. 7679-7682.
343. Vine, K.L., Locke, J.M., Ranson, M., Pyne, S.G., and Bremner, J.B., In vitro cytotoxicity evaluation of some substituted isatin derivatives. *Bioorg Med Chem*, **2007**. *15*(2): p. 931-938.
344. Gonzalez, A., Quirante, J., Nieto, J., Almeida, M.R., Saraiva, M.J., Planas, A., Arsequell, G., and Valencia, G., Isatin derivatives, a novel class of transthyretin fibrillogenesis inhibitors. *Bioorg Med Chem Lett*, **2009**. *19*(17): p. 5270-5273.
345. Panda, J., Patro, V.J., Sahoo, B., and Mishra, J., Green Chemistry Approach for Efficient Synthesis of Schiff Bases of Isatin Derivatives and Evaluation of Their Antibacterial Activities. *J Nanopart*, **2013**. *2013*.
346. De, T. and Kumar, S., Synthesis and antimicrobial activity of Mannich bases of isatin derivatives. *Pharmanest*, **2013**. *4*(5): p. 1054-1061, 8 pp.

347. Karki, S.S., Kulkarni, A.A., Thota, S., Nikam, S., Kamble, A.S., and Dhawale, N.D., Synthesis, antimicrobial screening and beta lactamase inhibitory activity of 3-(3-chloro-4-fluorophenylimino)indolin-2-one and 5-chloroindolin-2-one derivatives. *Turk J Pharm Sci*, **2012**. *9*(3): p. 353-358.
348. Sridhar, S.K., Saravanan, M., and Ramesh, A., Synthesis and antibacterial screening of hydrazones, Schiff and Mannich bases of isatin derivatives. *Eur J Med Chem*, **2001**. *36*(7-8): p. 615-625.
349. Ismail, T., Shafi, S., Singh, P.P., Qazi, N.A., Sawant, S.D., Ali, I., Khan, I.A., Kumar, H.M.S., Qazi, G.N., and Alam, M.S., Biologically active hydroxymoyl chlorides as antifungal agents. *Indian J Chem Sect B-Org Chem Incl Med Chem*, **2008**. *47*(5): p. 740-747.
350. Azizian, J., Jadidi, K., Mehrdad, M., and Sarrafi, Y., One pot synthesis of some new spiro 3H-indol-3,5 '(4 ' H)- 1,2,4 oxadiazol -2-ones and bis spiro 3H-indol-3,5 '(4 ' H)- 1,2,4 oxadiazol -2-ones. *Synthetic Commun*, **2000**. *30*(13): p. 2309-2315.
351. Monteiro, A., Goncalves, L.M., and Santos, M.M.M., Synthesis of novel spiropyrazoline oxindoles and evaluation of cytotoxicity in cancer cell lines. *Eur J Med Chem*, **2014**. *79*: p. 266-272.
352. Hwu, J.R., Lin, C.C., Chuang, S.H., King, K.Y., Sue, T.R., and Tsay, S.C., Aminyl and iminyl radicals from arylhydrazones in the photo-induced DNA cleavage. *Bioorg Med Chem*, **2004**. *12*(10): p. 2509-2515.
353. Patel, H.V., Vyas, K.A., Pandey, S.P., and Fernandes, P.S., Facile synthesis of hydrazonyl halides by reaction of hydrazones with N-halosuccinimide-dimethyl sulfide complex. *Tetrahedron*, **1996**. *52*(2): p. 661-668.
354. Wang, G., Liu, X., Huang, T., Kuang, Y., Lin, L., and Feng, X., Asymmetric catalytic 1,3-dipolar cycloaddition reaction of nitrile imines for the synthesis of chiral spiro-pyrazoline-oxindoles. *Org Lett*, **2013**. *15*(1): p. 76-79.
355. Yadav, U.N. and Shankarling, G.S., Room temperature ionic liquid choline chloride-oxalic acid: A versatile catalyst for acid-catalyzed transformation in organic reactions. *J Mol Liq* **2014**. *191*: p. 137-141.
356. Turbiak, A.J. and Showalter, H.D.H., A new route to substituted pyrimido 5,4-e -1,2,4-triazine-5,7(1H,6H)-diones and facile extension to 5,7(6H,8H) isomers. *Synthesis-Stuttgart*, **2009**(23): p. 4022-4026.
357. Toeroek, B., Sood, A., Bag, S., Tulsan, R., Ghosh, S., Borkin, D., Kennedy, A.R., Melanson, M., Madden, R., Zhou, W., LeVine, H., III, and Toeroek, M., Diaryl hydrazones as multifunctional inhibitors of amyloid self-assembly. *Biochemistry*, **2013**. *52*(7): p. 1137-1148.
358. Hu, J.R., Zhang, W.J., and Zheng, D.G., A one-pot synthesis of bisarylhydrazones by Cu(I)-catalyzed aerobic oxidation. *Tetrahedron*, **2013**. *69*(46): p. 9865-9869.

359. Azizian, J., Soozangarzadeh, S., and Jadidi, K., Microwave-induced one-pot synthesis of some new spiro 3H-indole-3,5 '(4 ' H)- 1,2,4 -triazoline -2-ones. *Synthetic Commun*, **2001**. *31*(7): p. 1069-1073.

360. Singh, A., Loomer, A.L., and Roth, G.P., Synthesis of oxindolyl pyrazolines and 3-amino oxindole building blocks via a nitrile imine [3 + 2] cycloaddition strategy. *Org Lett*, **2012**. *14*(20): p. 5266-5269.

361. Fang, C.L., Horne, S., Taylor, N., and Rodrigo, R., Dimerization of a 3-substituted oxindole at C-3 and its application to the synthesis of (+/-)-folicanthine. *J Am Chem Soc*, **1994**. *116*(21): p. 9480-9486.

362. Julian, P.L., Printy, H.C., Ketcham, R., and Doone, R., Studies in the indole series.14. Oxindole-3-acetic acid. *J Am Chem Soc*, **1953**. *75*(21): p. 5305-5309.

363. Suarez-Castillo, O.R., Sanchez-Zavala, M., Melendez-Rodriguez, M., Castelan-Duarte, L.E., Morales-Rios, M.S., and Joseph-Nathan, P., Preparation of 3-hydroxyoxindoles with dimethyldioxirane and their use for the synthesis of natural products. *Tetrahedron*, **2006**. *62*(13): p. 3040-3051.

364. Tingare, Y.S., Shen, M.-T., Su, C., Ho, S.-Y., Tsai, S.-H., Chen, B.-R., and Li, W.-R., Novel oxindole based sensitizers: Synthesis and application in dye-sensitized solar cells. *Org Lett*, **2013**. *15*(17): p. 4292-4295.

365. Esmaili, A.A. and Bodaghi, A., New and efficient one-pot synthesis of functionalized gamma-spirolactones mediated by vinyltriphenylphosphonium salts. *Tetrahedron*, **2003**. *59*(8): p. 1169-1171.

366. Lin, W., Hu, M.H., Feng, X., Fu, L., Cao, C.P., Huang, Z.B., and Shi, D.Q., Selective reduction of carbonyl groups in the presence of low-valent titanium reagents. *Tetrahedron Lett*, **2014**. *55*(14): p. 2238-2242.

367. Banerji, J., Lai, T.K., Basak, B., Neuman, A., Prange, T., and Chatterjee, A., A novel route to anticonvulsant imesatins and an approach to cryptolepine, the alkaloid from Cryptolepis Sp. *Indian J Chem Sect B-Org Chem Incl Med Chem*, **2005**. *44*(2): p. 426-429.

368. Moghadam, M., Tangestaninejad, S., Mirkhani, V., Mohammadpoor-Baltork, I., and Moosavifar, M., Host (nanocavity of dealuminated zeolite Y)-guest (12-molybdophosphoric acid) nanocomposite material: An efficient and reusable catalyst for oximation of aldehydes. *Appl Catal A-Gen.*, **2009**. *358*(2): p. 157-163.

369. Mokhtari, J., Naimi-Jamal, M.R., Hamzeali, H., Dekamin, M.G., and Kaupp, G., Kneading ball-milling and stoichiometric melts for the quantitative derivatization of carbonyl compounds with gas-solid recovery. *ChemSusChem*, **2009**. *2*(3): p. 248-254.

370. Yoshimura, A., Zhu, C.J., Middleton, K.R., Todora, A.D., Kastern, B.J., Maskaev, A.V., and Zhdankin, V.V., Hypoiodite mediated synthesis of isoxazolines from

aldoximes and alkenes using catalytic KI and Oxone as the terminal oxidant. *Chem Commun* **2013**. *49*(42): p. 4800-4802.

371. Di Nunno, L., Vitale, P., Scilimati, A., Simone, L., and Capitellib, F., Stereoselective dimerization of 3-arylisoxazoles to cage-shaped bis-beta-lactams syn 2,6-diaryl-3,7-diazatricyclo 4.2.0.0(2,5) octan-4,8-diones induced by hindered lithium amides. *Tetrahedron*, **2007**. *63*(50): p. 12388-12395.
372. Toth, M., Kun, S., Bokor, E., Benltifa, M., Tallec, G., Vidal, S., Docsa, T., Gergely, P., Somsak, L., and Praly, J.P., Synthesis and structure-activity relationships of C-glycosylated oxadiazoles as inhibitors of glycogen phosphorylase. *Bioorg Med Chem*, **2009**. *17*(13): p. 4773-4785.
373. Liu, K.C., Shelton, B.R., and Howe, R.K., A particularly convenient preparation of benzohydroximinoyl chlorides (nitrile oxide precursors). *J Org Chem*, **1980**. *45*(19): p. 3916-3918.
374. N., R., Singh, M., Jangra, S., Rohilla, A., Kaur, R., and Malik, P., In-vitro studies of various carbonyl derivatives on liver alkaline phosphatase. *J Chem Pharm Res*, **2010**. *2*(4): p. 801-807.
375. Beech, W.F., Preparation of aromatic aldehydes and ketones from diazonium salts. *J Chem Soc*, **1954**(APR): p. 1297-1302.
376. Lynch, B.M. and Pausacker, K.H., The oxidation of phenylhydrazones. Part II. *J Chem Soc*, **1954**(MAR): p. 1131-1134.
377. Metwally, S.A.M., Mohamed, T.A., Moustafa, O.S., and El-Ossaily, Y.A., Reactions of 4-alkylidene(arylidene)-1-phenylpyrazolidine-3,5-dione. *Chem Heterocycl Compd* **2007**(9): p. 1335-1341.
378. Barnish, I.T., Transitional activation phenomena : Synthesis of the 4H-Benzo[e] [1,3 ,4]-thiadiazine ring. *J Chem SOC (C)*, **1970**(6): p. 854-&.
379. Tsuge, O. and Kanemasa, S., Studies of acyl and thioacyl isocyanates .14. Reactions of benzoyl and thiobenzoyl isocyanates with hydrazones. *Bull Chem Soc Jpn*, **1974**. *47*(11): p. 2676-2681.
380. Buzykin, B.I., Titova, Z.S., Cherepinskiimalov, V.D., Gazetdinova, N.G., Stolyarov, A.P., Litvinov, I.A., Struchkov, Y.T., and Kitaev, Y.P., Spectral characteristics, molecular-structure, and hydrogen-bonding in arylhydrazones of benzoyl chlorides and aromatic-aldehydes. *B Acad Sci USSR Ch*, **1983**. *32*(3): p. 485-491.
381. Attanasi, O., Battistoni, P., and Fava, G., Effect of metal-ions in organic-synthesis .15. Reaction of (arylazo) alkenes and copper(II) chloride in dienophiles or acetone - synthesis of some N-(alpha-chlorobenzylidene)-N'-arylhydrazines. *Can J Chem-Rev Can Chim*, **1983**. *61*(12): p. 2665-2668.
382. Kaugars, G., Gemrich, E.G., and Rizzo, V.L., Miticidal activity of benzoyl chloride phenylhydrazones. *J Agr Food Chem*, **1973**. *21*(4): p. 647-650.

383. Bunz, F., Dutriaux, A., Lengauer, C., Waldman, T., Zhou, S., Brown, J.P., Sedivy, J.M., Kinzler, K.W., and Vogelstein, B., Requirement for p53 and p21 to sustain G(2) arrest after DNA damage. *Science*, **1998**. *282*(5393): p. 1497-1501.

384. Mosmann, T., Rapid colorimetric assay for cellular growth and survival - Application to proliferation and cyto-toxicity assays. *J Immunol Methods*, **1983**. *65*(1-2): p. 55-63.

385. Cadete, A., Figueirede, L., Lopes, R., Calado, C.C.R., Almeida, A.J., and Goncalves, L.M.D., Development and characterization of a new plasmid delivery system based on chitosan-sodium deoxycholate nanoparticles. *Eur J Pharm Sci*, **2012**. *45*(4): p. 451-458.

386. Sola, S., Castro, R.E., Kren, B.T., Steer, C.J., and Rodrigues, C.M.P., Modulation of nuclear steroid receptors by ursodeoxycholic acid inhibits TGF-beta 1-Induced E2F-1/p53-mediated apoptosis of rat hepatocytes. *Biochemistry*, **2004**. *43*(26): p. 8429-8438.

387. Liu, D.Y., Li, C.S., Chen, Y.L., Burnett, C., Liu, X.Y., Doens, S., Collins, R.D., and Hawiger, J., Nuclear import of proinflammatory transcription factors is required for massive liver apoptosis induced by bacterial lipopolysaccharide. *J Biol Chem*, **2004**. *279*(46): p. 48434-48442.

388. Ferreira, D.M., Afonso, M.B., Rodrigues, P.M., Simao, A.L., Pereira, D.M., Borralho, P.M., Rodrigues, C.M., and Castro, R.E., c-Jun N-terminal kinase 1/c-Jun activation of the p53/microRNA 34a/sirtuin 1 pathway contributes to apoptosis induced by deoxycholic acid in rat liver. *Mol Cell Biol*, **2014**. *34*(6): p. 1100-20.

389. Chang, T.K.H., Crespi, C.L., and Waxman, D.J., Spectrophotometric analysis of human CYP2E1-catalyzed p-nitrophenol hydroxylation. *Methods Mol Biol (Clifton, N.J.)*, **2006**. *320*: p. 127-31.

390. Verdonk, M.L., Cole, J.C., Hartshorn, M.J., Murray, C.W., and Taylor, R.D., Improved protein-ligand docking using GOLD. *Proteins*, **2003**. *52*(4): p. 609-623.

391. Bista, M., Wolf, S., Khoury, K., Kowalska, K., Huang, Y., Wrona, E., Arciniega, M., Popowicz, G.M., Holak, T.A., and Domling, A., Transient Protein States in Designing Inhibitors of the MDM2-p53 Interaction. *Structure*, **2013**. *21*(12): p. 2143-2151.

392. Molecular Operating Environment (MOE), 2014.09; Chemical Computing Group Inc.,1010 Sherbooke St. West, Suite #910, Montreal, QC, Canada, H3A 2R7, 2013